

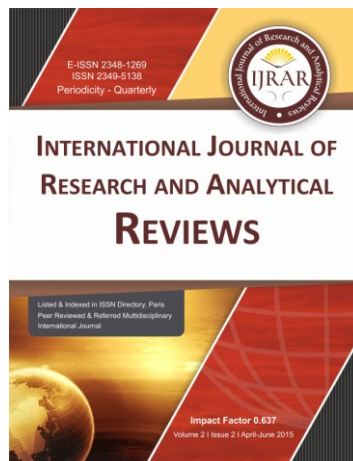
# International Journal of Research and Analytical Reviews

UGC Approved Research Journal

Periodicity - Quarterly



Atman Publishing Academy



International Journal of Research and Analytical Reviews

Atman Publishing Academy

2061-C/2/B, Nr. Adhyatma Vidya Mandir, Sanskar Mandal, Bhavnagar-364002.

Contact : 9427903033 E mail : [editorsijrar@gmail.com](mailto:editorsijrar@gmail.com), [ijrar1@gmail.com](mailto:ijrar1@gmail.com)



# International Journal of Research and Analytical Reviews

ijrar.com

© IJRAR - All rights reserved. Reproduction in any form is strictly prohibited.  
**This work is licenced under Creative Commons International Licence Attribution 4.0 E-version.**

Rs. 900

Subscription	1 year	2 years	5 years
Individual	3,000	6,000	15,000
Institutional	4,000	8,000	40,000
Advertisement	1000/Black	3000/colour	Per Page

**Send your Paper(s)/Article(s) and Contact us on any one of following**

**E mail: (1) [editorsijrar@gmail.com](mailto:editorsijrar@gmail.com) (2) [ijrar1@gmail.com](mailto:ijrar1@gmail.com) (3) [drbjoshi@ijrar.com](mailto:drbjoshi@ijrar.com)**

**Contact No.: +91 9427903033**

1. Thoughts, language vision and example in published research paper are entirely of author of research paper. It is not necessary that both editor and editorial board are satisfied by the research paper. The responsibility of the matter of research paper/article is entirely of author.
2. Editing of the IJRAR is processed without any remittance. The selection and publication is done after recommendations of at least two subject expert referees.
3. In any condition if any National/International University denies accepting the research paper/article published in IJRAR, than it is not the responsibility of Editor, Publisher and Management.
4. Only the first author is entitle to receive the copies of all co-author.
5. Before re-use of published research paper in any manner, it is compulsory to take written permission from the Editor – IJRAR, unless it will be assumed as disobedience of copyright rules.
6. All the legal undertakings related to IJRAR is subject to Bhavnagar Jurisdiction.

---

**Editor**

**International Journal of Research and Analytical Reviews**

Atman Publishing Academy

2061-C/2/B, Nr. Adhyatma Vidya Mandir, Sanskar Mandal, Bhavnagar-364002.

Contact : 9427903033 E mail : [editorsijrar@gmail.com](mailto:editorsijrar@gmail.com), [ijrar1@gmail.com](mailto:ijrar1@gmail.com)

**Editor in chief****Dr. R. B. Joshi****Senior Advisory Board**

<b>Dr. H. O. Joshi</b> Retd. Prof. & Head, Department of Education, Saurashtra University, Rajkot, Gujarat.	<b>Dr. Bhavesh Joshi</b> Associate Professor College of Food Processing Technology & Bioenergy, Agricultural University, Anand – 388110, Gujarat	<b>Vasantkumar Pathak</b> Director, Pathak Group of Schools & College, Rajkot.
---	---	---

**Editorial Board**

<b>Prof. (Dr.) Ami Upadhyay</b> Director, Department of Humanities And Social Sciences, Dr. Babasaheb Ambedkar Uni. A'Bad.	<b>Dr. Awa Shukla</b> Asst. Professor & Director, Social Sciences Dept. Babasaheb Ambedkar Open University, Ahmedabad.	<b>Dr. Dushyant Nimavat</b> Associate Professor Department of English, Gujarat University, Gujarat, India
<b>Dr. A. Heidari</b> Faculty of Chemistry California South University (CSU) Irvine, California, U. S. A.	<b>Dr. Bharat Ramanuj</b> Professor & Head, Department of Education, Saurashtra University, Rajkot.	<b>Dr. Nahla Mohammed Abd El-Aziz</b> Assistant professor - Entomology Department, Faculty of Science Cairo University, <b>Egypt.</b>
<b>Dr. Manahar Thaker</b> Principal G. H. Sanghavi college of Education, Bhavnagar, Gujarat.	<b>Dr. K. S. Meenakshisundaram</b> Director, C. A. A., Great Lakes Institute of Management, Chennai	<b>Dr. J. D. Dave</b> I/c Principal P.D. Malviya Graduate Teachers' College, Rajkot, Gujarat.
<b>Dr. M. B. Gaijan</b> Associate Professor, Shamaldas Arts College, Bhavnagar.	<b>Dr. A. K. Lodi</b> H.O.D. Faculty of Education, Integral University, Lucknow(UP)	<b>Dr. Trupti Pathak</b> Assistant Vice President(Tech.) Claris life Sciences, Ahmedabad. Gujarat.
<b>Dr. K. Ramadevi</b> Associate Professor Department of Civil Engineering Kumaraguru College of Technology, Coimbatore, Tamilnadu.	<b>Dr. Jayant Vyas</b> Professor & Head, Department of Education, M. K. Bhavnagar University, Bhavnagar	<b>Dr. Dilip D. Bhatt</b> Associate Prof. & Head, Department of English, V. D. K. Arts college, Savarkundla, Gujarat.
<b>K. S. Dave</b> Lecturer J. H. Bhalodia Women's College Rajkot, Gujarat.	<b>Dr. Anil Ambasana</b> Retd. Prof. & Head, Department of Education, Saurashtra University, Rajkot. Gujarat.	<b>Dr. Sandeep R. Sirsat</b> Associate Professor & Head, Department of Computer Science, Shri Shivaji Science & Arts College, Chikhli, Dist: Buldana (M.S.-India)

## Review Committee

### Editor & Head of Review Committee

**Dr. S. Chelliah**

Professor & Head,

Dept. of English and Comparative Literature,  
Madurai Kamraj University, Madurai-21, **India.**

<p><b>Mr. Zeeshan Shah</b> Senior Lecturer, Department of Multimedia and Communication, University College of Bahrain, <b>Kingdom of Bahrain.</b></p>	<p><b>Dr. Samira Shahbazi</b> Plant Protection &amp; Biotechnology Research Group, Nuclear Agricultural Research School, Nuclear Science &amp; Technology Research Institute (NSTRI), <b>Iran</b></p>	<p><b>Dr. Belal Mahmoud Al-Wadi</b> Lecturer, University of Dammam (Saudi Arabia), Founder &amp; Vice President of the Jordanian Society for Business Entrepreneurship <b>(Jordan)</b></p>
<p><b>Harish Mahuvakar</b> Associate Professor &amp; Head, Dept. of English, Sir P. P. Institute of Science, Bhavnagar, Gujarat, <b>India.</b></p>	<p><b>Dr. Mainu Devi</b> Assistant Professor (Sr. Grade) in Zoology, Diphu Govt. college, Karbi Anglong – Assam <b>India.</b></p>	<p><b>Asim Gokhan YETGIN</b> Assistant Professor, Faculty of Engineering, Dumlupinar University, Kutahya, <b>Turkey.</b></p>
<p><b>Dr. A. Kusuma</b> Assistant Professor, Department of Social Work, Vikramasimhapuri University, Nellore.(AP)</p>	<p><b>Prof. Rajeshkumar N. Joshi</b> I/C Dean, Faculty of Arts &amp; Humanities, C. U. Shah University, Gujarat, <b>India.</b></p>	<p><b>Sunita. B. Nimavat</b> Assistant Professor of English, N.P.College of Computer &amp; Mgt., Kadi (North Gujarat).</p>
<p><b>Nahla Mohammed Abdelazez</b> Assistant Professor Faculty of Science, Cairo University, Giza Governorate, <b>Egypt.</b></p>	<p><b>Dr. Riyad Awad</b> Associate professor, Structural Engineering, An - Najah National University, Nablus, <b>Palestine.</b></p>	<p><b>Dr. Amer A. Taqa</b> Professor Dept. of Dental Basic Science, College of Dentistry, Mosul University, Masul, <b>Iraq.</b></p>

**4<sup>th</sup> International Conference on Trends  
in Information, Management,  
Engineering and Science**

**(ICTIMES 2018)**

Website: <http://mrce.in/ictimes2018.html>

Conference Dates:  
**December 28<sup>th</sup>& 29<sup>th</sup> 2018,**

Organised by  
**Malla Reddy College of Engineering**  
Secunderabad-500100

---

# International Journal of Research and Analytical Reviews

---

## **About MRGI:**

Malla Reddy group of Institutions is one of the biggest conglomerates of hi-tech professional educational institutions in the state of Telangana, established in 2001 sprawling over 200 acres of land. The group is dedicated to impart quality professional education like pharmacy, Engineering & Technology, MCA, MBA courses. Our sole objective is to turn out high caliber professionals from those students who join us

## **About MRCE:**

Malla Reddy group of Engineering (Formerly CM Engineering College) has been established under the aegis of the Malla Reddy Group of Institutions in the year 2005, a majestic empire, founded by chairman Sri Ch.Malla Reddy Garu. He has been in the field of education for the last 23 years with the intention of spearheading quality education among children from the school level itself. Malla Reddy College of Engineering has been laid upon a very strong foundation and has ever since been excelling in every aspect. The bricks of this able institute are certainly the adept management, the experienced faculty, the selfless non-teaching staff and of course the students.

## **About ICTIMES:**

In this emerging world, to confer benefits upon mankind, it is essential for all students, academic staff and researchers of all nations to keep themselves abreast with the latest innovations in technology and methods of all areas of Engineering, Management and Sciences. The International Conference on Trends in Information, Management, Engineering and Sciences (ICTIMES) is being organized by Malla Reddy College of Engineering, to provide an opportunity for students, academic staff and researchers to present their research work and also a platform for exchanging knowledge in the fields of Engineering, Management and Sciences.

## **Department of ECE- (ICLTEC- 2018)**

Under the banner of ICTIMES, the Department of Electronics and Communication Engineering at MRCE organizes the – International Conference on Latest Trends in Electronics and Communication (ICLTEC-2018) to provide a scholarly platform to ignite the spirit of Research and bring out the latent potential in teaching fraternity and student community. ICLTEC accommodates major areas like, signal processing, Embedded systems, Network Security, Green Technology, Digital signal processing, Communication systems.

## **Department of CSE- (ICETCS - 2018)**

Under the banner of ICTIMES, the Department of Computer Science and Engineering at MRCE organizes the – International Conference on Emerging Technologies in Computer Science (ICETCS-2018) to provide a scholarly platform to ignite the spirit of Research and bring out the latent potential in teaching fraternity and student community. ICETCS accommodates major areas like, Big Data, Data mining, Information Retrieval, Neural Networks, Data Security, etc.

## **Department of Mechanical - (ICFTME - 2018)**

Under the banner of ICTIMES, the Department of Mechanical Engineering at MRCE organizes the – International Conference on Future Technologies in Mechanical Engineering (ICFTME-2018) to provide a scholarly platform to ignite the spirit of Research and bring out the latent potential in teaching fraternity and student community. ICFTME accommodates major areas like, Applied Mechanics, Tribology, Advanced Manufacturing Process, Fluid Dynamics etc.

---

# International Journal of Research and Analytical Reviews

---

## **Department of Humanities & Sciences - (ICASHM - 2018)**

Under the banner of ICTIMES, the Department of Humanities Sciences and Management at MRCE organizes the – International Conference on Advances in Humanities Sciences and Management (ICAHSM-2018) to provide a scholarly platform to ignite the spirit of Research and bring out the latent potential in teaching fraternity and student community. ICAHSM accommodates major areas like, English Language, Literature, Phonetics, Mathematics, Physics, Chemistry and Management Sciences

## Dignitaries

### **Chief Patron:**

#### **Sri. Ch. Malla Reddy**

Founder Chairman, MRGI

MLA (Medchal Constituency)

Minister, Labour & Employment, Factories, Women & Child Welfare and Skill Development, Telangana

### **Patrons:**

#### **Sri Ch. Mahender Reddy**

Secretary, MRGI

#### **Dr. Ch. Bhadra Reddy**

President, MRGI

### **Co-Patrons:**

**Coln. Sri. G. Ram Reddy**, Director - Admin, MRGI

### **Conference Chair:**

#### **Dr. P. John Paul,**

Principal, MRCE

### **International Advisory Committee**

#### **Dr. Mohammad Alam,**

Texas A&M University, Texas USA

#### **Dr. Angappa Gunasekaran**

State University, Bakersfield

#### **Dr. Mohd Sapuan Salit**

University of Putra Malaysia, Malaysia

#### **Dr. R. Darwin Joseph**

MDIS Business School, Singapore

#### **Dr. Ooi Kim Tiow**

NTU, Malaysia

---

# International Journal of Research and Analytical Reviews

---

## National Advisory Committee:

**Dr. C. Krishna Mohan**

Professor, IIT Hyderabad

**Dr. P. N. Girija**

Professor, Hyderabad Central Univ.

**Dr. B. SudheerPrem Kumar**

Professor, JNTU Hyderabad

**Dr. T. Kishore Kumar**

Professor, NIT Warangal

**Dr. K. Shyamala**

Associate Professor, Osmania Univ.

**Dr. D. Rama Krishna**

Associate Professor, Osmania Univ.

## Organising Committee:

**Dr. T. V. Reddy**, Vice Principal, MRCE

**Dr. T. Sunil**, Dean Academics

**Dr. Nikhil Raj**, Dean R&D

**Dr. V. Bhoopathy**, Dean Placement

**Dr. M. Narayanan**, IQAC Coordinator& HOD-CSE

**Dr. A. Karthikeyan**, Dean Student Affair& HOD-MECH

**Dr. N. Muthu Kumar**, Dean EDC & HOD-MBA

**Dr. R. P. Naik**, Dean Task NSS & HOD-ECE

**Dr. J. Gladson Britto**, Dean Prof. Bodies

## PROGRAM Committee:

**Dr. A. Kannagi**, Dean WDC

**Dr. S. Ananth**, COE MRCE

**Dr. Moses Dian**, Dean ICT

**Dr. P. Velmurugan**, Dean Industry & Internship

---

## Contents

Sr.	Title & Author(s)	Subject	Page No.
01	<b>A New Text Mining Approach for Web Content Search</b> Thayyaba Khatoon Mohammed & Chandrasekar V & A Govardhan	CSE	01 – 04
02	<b>A Comprehensive review on Density-Based clustering algorithm in data mining</b> R. Sujatha & V Chandrasekar & Dr. G. Britto	CSE	05 – 09
03	<b>An Efficient Feature Selection Technique for Keystroke Authentication Based on Low Impact Biometric Verification</b> V Chandrasekar & Sujatha Dandu & Dr. V. Bhoopathy	CSE	10 – 14
04	<b>Design of Chaotic Behavior for programmable cellular automata based Symmetric Key Encryption Algorithm for Wireless Sensor Networks</b> Shanthi S & Chandrasekar V & Dr. V. Bhoopathy	CSE	15 – 19
05	<b>THE VEHICLE NETWORK ARCHITECTURE IN SMART CITY WITH BLOCKCHAIN TECHNOLOGY</b> R.JAHNAVI & Rajasekar Rangasamy	CSE	20 – 25
06	<b>KEYSTROKE DYNAMICS USER IDENTIFICATION USING PAIRWISE CLIENT COUPLING</b> D.Tejaswi & Rajasekar Rangasamy	CSE	26 - 32
07	<b>Aggressive and Community Auditing System with Clear Agreement for Cloud Data</b> Naveena Vemula & Subhashini Peneti	CSE	33 – 38
08	<b>Different Types of Machine Learning Techniques in Python programming</b> Mr Naveen Kumar R & Ms Adepu Aravinda & Mrs Subhashini Peneti	CSE	39 – 43
09	<b>DESIGN OF DYNAMIC ACCURACY CONFIGURABLE MULTIPLIER USING DUAL QUALITY 4:2 COMPRESSOR</b> Ancychristabel S.C & Nimmy Lazer & G.Selva Malar	ECE	44 - 48
10	<b>DESIGN AND IMPLEMENTATION OF HIGH PERFORMANCE MAC UNIT CARRY SKIP ADDER</b> M. Josphine Sheela & G.V. Soni Meera	ECE	49 – 52
11	<b>ARCHITECTURE DEVELOPMENT OF COST-EFFICIENT MICRO CONTROL UNIT FOR WBSN</b> Ms.S. Sajini & Mr.E.Sherjin Tintu	ECE	53 – 58
12	<b>VLSI ARCHITECTURE FOR CDMA TECHNOLOGY USING WALSH CODE GENERATOR</b> S. Akhila & H.Christal Beni	ECE	59 – 66

# International Journal of Research and Analytical Reviews

---

13	<b>TEMPLATES FOR ARITHMETIC OPERATION IN DSP</b> Sherin Thomas & M. Joselin Kavitha	ECE	67 – 72
14	<b>AN EFFICIENT APPROXIMATE RECONFIGURABLE ADDER USING SIMPLE CARRY PREDICTION</b> J.B.Abisha Jey & S.Amutha	ECE	73 – 77
15	<b>The Fault Tolerant Parallel Filters Implementation Based on Error Correction Codes</b> N.Saibaba & P.Venkatapathi	ECE	78 – 81
16	<b>Design of Chaotic Behavior for programmable cellular automata based Symmetric Key Encryption Algorithm for Wireless Sensor Networks</b> Shanathi S & Chandrasekar V	ECE	82 - 86
17	<b>CENTRIFUGE CONTROL SYSTEM IN SUGAR WASHING PROCESS USING PLC</b> Ms.M.Brindha , Ms.P.Poovizhi , N.Kayalvizhi , K.Praveenkumar , K.F.Felvin	ECE	87 - 90
18	<b>High Frequency AC Link Dual Active Bridge Isolated Bidirectional Dc-Dc Converter for PV Application</b> DRK. Mahesh & P. Manikya Rao & P. Poushya	ECE	91 – 94
19	<b>INTEND INNOVATIVE TECHNOLOGY FOR RECOGNITION OF SEAT VACANCY IN BUS</b> Gudipelly Mamatha & B.Manjula & P.Venkatapathi	ECE	95 – 100
20	<b>OBSERVING OPERATING ACTIVITIES OF WORK VEHICLES BY USING ZIGBEE NETWORK SYSTEM</b> ASHOK BHUKYA & Mr.G.Sanjeev	ECE	101 – 107
21	<b>VLSI DESIGN OF N x N BIT HIGH PERFORMANCE MULTIPLIER WITH REDUNDANT BINARY ENCODING</b> BHUVANESWARI K & Dr . R.PURUSHOTHAM NAIK & MOSES CH	ECE	108 - 115
22	<b>Design of Nano-Calculator Using Quantum Dot Cellular Automata (QCA)</b> FARHEEN BEGUM & P.VENKATAPATHI	ECE	116 – 121
23	<b>THE DEVELOPMENT OF A REMOTELY CONTROLLED HOME AUTOMATION SYSTEM FOR ENERGY SAVING</b> G.Naveen & B.Manjulai	ECE	122 – 128
24	<b>IOT BASED CHILD SAFETY WEARABLE DEVICE</b> Poonam Gupta & Ms.P.Anitha	ECE	129 – 136
25	<b>BOOKING SYSTEM OF A VEHICLHLE PARK USING IOT TECHNOLOGY</b> M.Prudhvi Raj & N.Naresh & Vijayalakshmi Ch	ECE	137 – 140
26	<b>An Energy-Efficient Cooperative Spectrum Sensing for Cognitive Radio: A Review</b> P.Venkatapathi, R Krishna Chaitany, Dr.Habibulla Khan, Dr.S.Srinivasa Rao	ECE	141 – 146

---

# International Journal of Research and Analytical Reviews

---

- 27 **Resource Allocation Strategies in Cognitive Radio Systems:A Survey** ECE 147 – 151  
P.Rajeshwari , P.Venkatapathi , , Dr.Habibulla Khan , Dr.S.Srinivasa Rao
- 28 **SUPER ACTIVE MATRIX OLED** ECE 152 - 155  
Y.ROJA RANI & Dr .R.PURUSHOTHAM NAIK & B.SAMATHA
- 29 **THE FinFET TECHNOLOGY** ECE 156 – 161  
B.SAMATHA & Dr .R.PURUSHOTHAM NAIK & Y.ROJA RANI
- 30 **DESIGN OF BUS TRACKING AND FUEL MONITORING SYSTEM** ECE 162 – 164  
Vasam shirisha & Dr. P. John Paul
- 31 **IMPLEMENTATION OF AUTOMATIC DRIVER DROWSINESS ALERT SYSTEM BY USING IOT** ECE 165 – 170  
Suresh kumar Perumalla & Vijaya Lakshmi Chintamaneni
- 32 **OPTIMIZING THE CONVOLUTION OPERATION TO ACCELERATE DEEP NEURAL NETWORKS ON FPGA** ECE 171 – 177  
GODUGU SWATHI & Mrs. B. MANJULA
- 33 **An Approach to reduce Self Transitions with Quadro Coding Technique in Very Large Scale Integration** ECE 178 – 182  
Pasupula Tansy Melina & Mrs. P. Anitha reddy
- 34 **DESIGN OF POWER AND AREA EFFICIENT APPROXIMATE MULTIPLIERS** ECE 183 – 188  
B.VIJAYA & Dr .R.PURUSHOTHAM NAIK
- 35 **EFFECT OF DIFFERENT PROCESS PARAMETERS ON THE SYNTHESIS AND CHARACTERIZATION OF CARBON NANOTUBES** Physics 189 - 195  
Gidla Rabecca Rani
- 36 **PERFORMANCE ANALYSIS OF BOILER IN THERMAL POWER PLANT** Mechanical 196 – 203  
P.Papireddy & Dr. S. Ananth & Mr. Vikash Kumar
- 37 **DESIGN OF ABSORPTION REFRIGERATION SYSTEM DRIVEN BY ENGINE EXHAUST GAS FOR VEHICLES** Mechanical 204 – 211  
P.Pavan Kumar & Dr. S. Ananth & Mr. Vikash Kumar
- 38 **Improvement of an Automobile Radiator using Thermal Analysis** Mechanical 212 – 216  
S. Vinay & Dr. A. Karthikeyan & Mr. Vikash Kumar
- 39 **IMPROVING THE HEAT TRANSFER RATE OF AC CONDENSER BY OPTIMISING THE MATERIAL** Mechanical 217 – 227  
Md. Abdul Raheem & Dr. A. Karthikeyan & Mr. Vikash Kumar
- 40 **Thermal performance and analysis of a solar water heating system with heat pipe evacuated tube collector** Mechanical 228 – 231  
Md Nizam Raza & Dr. Velmurugan P. & Mr. Vikash Kumar
-

# International Journal of Research and Analytical Reviews

---

- 41 **ANALYSIS OF HEAT TRANSFER RATE BY VARYING COOLING FLUID FOR ENGINE CYLINDER FINS** Mechanical 232 – 240  
Mr.RANJITH AAVULA & Mr.VIKASH KUMAR
- 42 **DESIGN AND ANALYSIS OF PRESSURE VESSEL WITH FRP MATERIAL** Mechanical 241 – 243  
Sukruthi Priya & P .Ravi Chandra & Mr. V. Ravinder
- 43 **DESIGN AND CFD ANALYSIS OF HAIR PIN HEAT EXCHANGER AT DIFFERENT NANO FLUIDS** Mechanical 244 – 249  
M.Renuka & Dr. Velmurugan P. & Mr. Vikash Kumar
- 44 **DESIGN AND HEAT TRANSFER ANALYSIS OF A PARABOLIC SHAPED DISH COLLECTOR** Mechanical 250 - 258  
N.Sriveni & Dr. Karthikeyan A. & Mr. Vikash Kumar
- 45 **NATURAL CONVECTIVE HEAT TRANSFER FROM INCLINED NARROW PLATES** Mechanical 259 - 265  
R. Swapna & Dr. T.V. Reddy & Mr. Vikash Kumar
- 46 **Basic Design of An Anthropomorphic Robotic Arm** Mechanical 266 – 279  
Pradeep.S, Hari shankar.S.P, Nandha Kumar.M, Rajeshwaran.T, Karthik.V
- 47 **Domestic Oil Extraction Machine** Mechanical 280 – 282  
Anand.M, Manimaran R, Praveen Kumar.M, Sujith Bhrathi.S
- 48 **Autonomous Swarm Robots** Mechanical 283 – 287  
T.Kousalya, K.M. Aarsha Suresh, K.Nivethithaan, Terrin J. Mario Pereria, Dilshad Bin Mohammed Iqbal
- 49 **POULTRY FARM MONITORING AND CONTROLLING USING PLC WITH INTERNET OF THINGS** Mechanical 288 – 292  
Mr. A Vishnu, Sheshaghiri N , Joeresh Julius A, Sathish Kumar A, Satharth Noorul Hassan
- 50 **HEAT TRANSFER ALONG VERTICAL CHIMNEY** Mechanical 293 – 302  
K. Rajanikanth & Dr. T.V. Reddy & Mr. Vikash Kumar
- 51 **EFFECT OF BIODIESEL BLENDS AND NANO-PARTICLES ON ENGINE PERFORMANCE** Mechanical 303 – 312  
Md. Ashfaque Alam & Dr. A. K. Prasad
- 52 **Application of Optimization Algorithm for Composite Laminate Optimization** Mechanical 313 – 321  
A.Karthikeyan & Dr. A.Karthikeyan & Dr.K.Venkatesh Raja & Dr.K.Venkatesh
- 53 **Traveling Salesman Problem for Visiting 10 Tamil Nadu Cities Using Genetic Algorithm** Mechanical 322 - 328  
A.Karthikeyan & Dr. A.Karthikeyan & Dr.K.Venkatesh Raja & Dr.K.Venkatesh
- 54 **WEAR BEHAVIOUR OF ALUMINIUM MATRIX COMPOSITES** Mechanical 329 – 333  
Vijayakumar.K
-

# International Journal of Research and Analytical Reviews

---

- 55 **THERMAL ANALYSIS OF VARIOUS FRICTION SURFACING MATERIALS USING ANSYS** Mechanical 334 – 338  
Sivanesh A R & Aravind Kumar R & Arivazhakan.D & Ananth.S
- 56 **CHANGING TRENDS AND GROWTH OF SORGHUM IN SELECTED DISTRICTS OF TAMILNADU – INDIA** Mechanical 339 – 342  
Mrs. M. Jayashree & Dr. E.G. Wesely
- 57 **COLOR IMAGE RETREIVAL SYSTEM USING FUZZY SIMILARITY MEASURE** Mechanical 343 – 348  
Poornima N & Aravind Kumar R & Sivanesh A R
- 58 **Investigation of Design, Analysis and Manufacturing of GFRP composite leaf spring by VARTM process** Mechanical 349 – 352  
P. Manuneethi Arasu & A. Karthikeyan & R.Venkatachalam
- 59 **Effect of Geometrical and Roughness Parameters on Artificially Roughened Solar Air Heater** Mechanical 353 - 365  
Ahmad Kamal Hassan & Dr. Mohammad Emran Khan & Dr. M. Muzaffarul Hasan
- 





## A New Text Mining Approach for Web Content Search

Thayyaba Khatoon Mohammed<sup>1</sup> & Chandrasekar V<sup>2</sup> & A Govardhan<sup>3</sup>

<sup>1,2</sup>Malla Reddy College of Engineering and Technology, Hyderabad, Telangana State,

<sup>3</sup>Rector, JNTUH, Kukatpally, Hyderabad-500085, India

---

**ABSTRACT:** Text-mining (TM) refers generally to the practice of extracting attractive and non-trivial information and facts from unstructured text. TM includes several computer science (CS) regulations with a strong direction towards artificial intelligence (AI) in general, including but not limited to pattern recognition (PR), neural networks (NN), natural language processing (NLP), information retrieval (IR) and machine learning (ML). A significant variation with search is that search requires a user to identify what he or she is looking for while TM attempts to realize information in a model that is not known earlier. TM is mainly motivating in domains where users have to invent new information. This is the case, for e.g., in criminal enquiries and legal findings. Such examinations require 100% evoke, i.e., users can not meet the expense of missing relevant data. In distinction, a user searching the internet for background information using a benchmark search engine (SE) simply requires any data as long as it is reliable. A different technique is to combine standard significance ranking with adaptive filtering (AF) and interactive visualization (IV) that is based on characteristics that have been mined earlier.

**Keywords:** Artificial intelligence, Neural networks, Machine learning, Interactive Visualization, Search Engine, Adaptive Filtering, Text Mining.

---

### I. Introduction

Within the area of expertise of TM, now and then called text analytics, several attractive technologies such as computers, IT, PR, statistics, advanced mathematical techniques, AI, visualization, and IR. The information bang of modern times will persist at the same rate [1, 2]. TM techniques play a crucial role in the upcoming years in this lifelong process. Due to continuing globalization there is also much interest in multi-language text mining (MLTM) TM: the attaining of insights in ML collections. MLTM is much more difficult that it appears as in addition to differences in words and character sets, TM makes concentrated use of data as well as the linguistic properties of a language. There are many essential hypotheses about capitalization and tokenization that would not work for other languages. When TM methods are used on non-English data collections supplementary challenges have to be concentrated [4, 5].

TM is about investigating unstructured information and extracting relevant patterns or models and uniqueness. Using these models and characteristics better search results and deeper data analysis is possible; giving quick IR otherwise it would remain hidden. The field of data mining (DM) is better known than that of TM. A good e.g., of DM is the analyzing of operational details contained in relational databases, such as debit card transactions or credit card payments. To such

operational diverse supplementary information can be provided: date, location, age of card holder, salary, etc. With support of this information patterns of behavior can be determined However, 95% of all information is unstructured information, and both the proportion and the total amount of unstructured information raise daily.

Only a small amount of information is stored in a structured format in a relational database. The greater part of information that users work on every day is in the form of text documents (TD), E-Mails/ multimedia files (speech, video and photos). Searching analysis using database (DB) or DM methods of this information is not possible, as these procedures work only on structured information (SI). It is easier to manage, share, search, organize, and to generate reports so on, for computers as well as users, therefore the wish is to give structure to unstructured information. This allows computers and public to better manage the data, and allow known procedures and methods to be used.

TM, using manual procedures, was use first during the 1980s. It hastily became obvious that these manual procedures were labor demanding and therefore costly [6]. It also cost too much time to manually process the already-growing amount of information. Over time there was growing success in creating applications to mechanically process the data, and in the previous ten years much development has seen.

Currently the study of TM worries the growth of various mathematical, statistical, and methods which allow mechanical analysis of unstructured information as well as the extraction of high quality and appropriate data, and to make the text as a whole better searchable. High excellence refers here, irrelevance and the obtaining of new and interesting approaches. A TD contains characters that jointly form words, which can be pooled to structure phrases. They are all syntactic assets or properties that collectively symbolize defined categories, concepts, meanings. TM must distinguish, extract and use all this information. Using TM, instead of searching for words, we can search for linguistic (scientific study of language) word patterns and this is therefore searching at a higher level.

## II. Searching Unstructured Information

What turns out exactly when somebody uses a computer program to search unstructured text? Computers are digital apparatus with limited capabilities. Computers manage best with figures, especially complete (whole) numbers, also known as integers, if it has to be really fast. Public are analogue, and individual language is also analogue, full of irregularity, obstruction, errors and exceptions. If public search for something then they often think in concepts and semantics, all regions in which a machine can't straightly transact with. For machines to be able to make a computationally proficient search in a huge amount of text, the difficulty needs first to be transformed to a numerical problem that a computer can associate with. This directs to very large storages containing many numbers in which numbers characterizing search terms are compared with numbers characterizing information and documents. This is the basic standard that our field concerns itself with: translation of information that users can work with into information that a computer can work with, and then convert the result back into a form that public can understand.

This expertise exists ever since 1960's. One of the initial experts working in this field was Gerard Salton who was an expert in earlier days; both jointly with other experts complete one of the initial texts SE. Each incident of a word in the text was entered in a keyword index. Searching was then done in the index, analogous to the index at the back of a book but with many more words and much earlier.. With procedures such as B-trees and hashing, it was probable to speedily and proficiently make a list from all documents

containing a word or a Boolean combination of words [7].

Documents and search terms were transformed to vectors and contrasted using the cosine distance among them: how lesser the cosine distance, how additional the search term and the document communicated. This was an efficient technique to decide the relevance of a document from the search expression. This was called the vector space model, and is still used today by some applications. Later on, a variety of other techniques used for searching and particular, to the combination of the relevance.

There are many search procedures with good-sounding names such as: directed and non-directed proximity, fuzzy, wildcards, semantically, taxonomies, conceptual, etc. Examples of normally known relevance defining procedures are: term-based frequency ranking (TBFR), the page-rank algorithm (PRA), and probabilistic ranking (PR). Because these days there is so much information digitally available and because it is now often crucial to directly react on present activities, new procedures are necessary to keep up with the continuously rising amount of unstructured information. In addition, people will have different causes for searching large amount of data and different goals to find, and those distinctions require an alternative advances.

## III. Searching and Finding

Fraud researchers or public prosecutors don't only want the best documents; they want all probable appropriate documents. In addition, in an internet SE everyone does their best to get to the top of the results list; search engine optimization has in itself become a skill. This is done by using synonyms and code names, and relatively often these are common words that are used so often that a search cannot be done without returning millions of knocks (hits). TM can offer a solution to find the appropriate information.

Fraud researchers also have another frequent difficulty: at the beginning of the analysis they do not know accurately what they must search for. They do not know the code names or synonyms, or they do not exactly know which companies, account numbers, persons, or amounts must be searched for. Using TM it is likely to recognize all these types of properties from their linguistic role, and then to categorize them in a structured manner to present them to the user. It then becomes very simple to investigate the found companies further.

Sometimes the difficulties facing by a researcher go a little deeper: they are searching without really

knowing what they are searching for. TM can be used to discover the words and subjects important for the examination; the computer searches for specified patterns in the text: "who paid to whom", "who talked to whom", etc. These types of patterns can be predictable using language technology and TM, and extracted from the text and presented to the researcher, who can then quickly decide the legal transactions from the suspect ones.

An example: If the HDFC bank transfers money to the AXIS then that is a normal transaction. But if "Norman" transfers money to Kumaran Enterprises Inc. then that may be doubtful. TM can recognize these natures of patterns, and further searches can be made on the words in those patterns using normal search procedures to further recognize and examine details. The obtaining of new insights is also called fortune. TM can be custom-made very efficiently to obtain new but often vital insights necessary to progress in an examination.

Therefore, the TM helps in the search for data by using models for which the values of the elements are not exactly known earlier. This is analogous with mathematical functions in which the variables and the statistical distribution of the variables are not always known. Here the heart of the difficulty can be seen as a conversion problem from human language to mathematics. The better the mathematical conversion, the better excellence of the TM will be.

**IV. INFORMATION VISUALIZATION**

TM is often stated as information visualisation (IV). This is because visualisation is one of the practical possibilities after unstructured information has been structured. To be able to make these sorts of visualizations the features must be structured or planned, and that is accurately the area in which TM expertise can help: by structuring unstructured information it is possible to visualise the data and more rapidly obtain new insights [8]

Washington, The Pacific Northwest, July 16th, 2001 - ZyLAB, the developer of document imaging and full-text retrieval software, has donated a PACS system to the government of U.S [3]. "We have been working closely with the World Health Organization, US International for the last 4 years now," said, CEO of ZyLAB Technologies. "The USA government faced hard job with the ZyLAB system will be of tremendous assistance to them. Unfortunately, the U.S has scarce resources to procure advanced imaging and archiving systems to help them in this job, full operational PACS system was donated to them."

An example is the following text:  
 In that text, the following entities and attributes can be found in the Table - 1:

Table - 1: Entities and Attributes of Above Text

<b>Places</b>	Washington
<b>Countries</b>	The <u>Pacific Northwest</u> , U.S
<b>Persons</b>	Gerald Gahima, David
<b>Function titles</b>	CEO
<b>Data</b>	July 16th, 2001
<b>Organisations</b>	Government of U.S, WHO, Criminal Justice Source Center, American-Canadian (AC) helper group
<b>Companies</b>	ZyLAB, ZyLAB Technologies BV
<b>Products</b>	PACS

Let's assume that there are various documents containing this type of automatically found structured properties; then the documents could not only be presented in tabular form, but also for e.g., in a tree structure in which the document could be structured on occurrences per land and then on occurrences per administration. The principle can also be used to dynamically imagine a tree structure, which would then appear as shown in the Fig - 1.

With the assist from these kinds of visualization methods it is possible to gain a quicker and better insight into difficult data collections, particularly if it involves large groups of unstructured information that can be mechanically structured using DM.

With the assist from these kinds of visualization methods it is possible to gain a quicker and better insight into difficult data collections, particularly if it involves large groups of unstructured information that can be mechanically structured using DM



Fig 1: Hyperbolic Tree visualisation of a tree structure

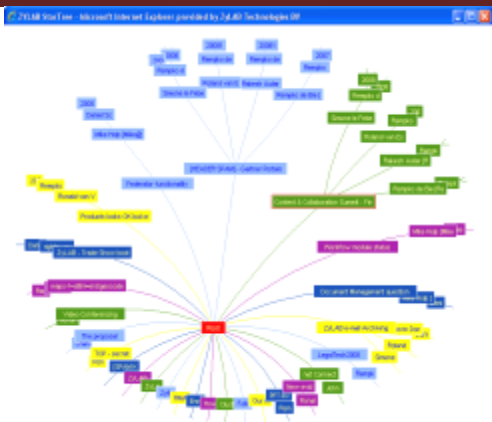


Fig 2: E-mail visualisation using a Hyperbolic Tree

### Advantages of Structured and Analysed Data

In addition to the visualization, various other search extensions are possible when the data has been structured and has Meta details.

Here is a concise list:

Details are easier to organize in folders. It is easier to filter data on specified Meta details, when searching Details can be contrasted, and linked using the Meta details. It is probable to sort, group and prioritize the documents using any of the attributes. Particulars can be grouped using the Meta elements. With the assist of Meta details duplicates and almost-duplicates can be sensed. These can then be deleted. Categorizations can be copied from the Meta elements. It is feasible to search the Meta details from already found documents. Statistical reports can be made on the basis of the Meta details.

### V. Conclusion

Although changes in the authorized world are always evolutions, there is definitely a probable function for TM in Electronic-Discovery and Electronic-Disclosure. Data sets are just reaching large and must be re-examined serially. Groups need to be pre-examined and pre-documented. Re-examinations can be implemented more efficiently and goals can be made easier. The challenge will be to encourage courts of the rightness of these new tools. Therefore, a hybrid advance is recommended where computers make the initial selection and classification of documents and research directions and human reviewers and researchers implement quality control and value the survey suggestions. By doing so, computers can focus on recall and human being can focus on accuracy. There are many other applications where this approach has led to both more

competence but also to acceptance of the technology by the public.

### References

- [1] Allan, James (Editor), (2002). Kluwer Academic Publishers.
- [2] Andrews, Whit and Knox, Rita (2008). Gartner Research Report, ID Number: G00161178. Gartner, Inc
- [3] Baron, Jason R. (2005). Sedona Conference Journal. Vol. 6, 2005
- [4] Berry, M.W., Editor (2004). Springer-Verlag.
- [5] Berry, M. W. and Castellanos, M. Editors (2006). Springer-Verlag.
- [6] Bilisoly, Roger (2008). Wiley Series on Methods Applications in Data Mining. Applications in Data Mining.
- [7] Blair, D.C. and Maron, M.E. (1985). Communications of the ACM, Vol. 28, No. 3, pp. 289-299.
- [8] Card, Stuart K., Mackinlay, Jock D., and Shneiderman, Ben, Editors (1999). Morgan Kaufmann Publishers.
- [9] [http://www.mimuw.edu.pl/~son/datamining/materials/search\\_engine.pdf](http://www.mimuw.edu.pl/~son/datamining/materials/search_engine.pdf)
- [10] Hwee-Leng Ong, Ah-Hwee Tan, Jamie Ng, Hong Pan and Qiu-Xiang Li.(2001),“FOCI : Flexible Organizer for Competitive Intelligence”, In Proceedings, Tenth International Conference on Information and Knowledge Management (CIKM’01), p p. 523-525, Atlanta, USA, 5-10
- [11] XiQuan Yang, DiNa Guo, XueYa Cao and JianYuan Zhou (2008), “Research on Ontology-based Text Clustering”, Third International Workshop on Semantic Media Adaptation and Personalization China,, IEEE Computer Society , 141-146.
- [12] Emilio Sanchis, Davide Buscaldi, Sergio Grau, Lluís Hurtado and David Griol (2006),“ SPOKEN QA BASED ON A PASSAGE RETRIEVAL ENGINE”, Proceedings of IEEE international conference, Spain, 62-65.
- [13] Pak Chung Wong, Paul Whitney and Jim Thomas,“ Visualizing Association Rules for Text Mining”, , International Conference, Pacific Northwest National Laboratory, USA, 1-5
- [14] Journal of Universal Computer Science, vol. 19, no. 3 (2013), 406-427 submitted: 22/9/11, accepted: 28/1/13, appeared: 1/2/13 © J.UCS
- [15] Maziarz M., Piasecki M., Szpakowicz S.: Approaching pWordNet 2.0. In Proc. of the 6th Global WordNet Conference, Matsue, Japan, January 2012.
- [16] Amr Ahmed and Eric P. Xing. Timeline: A Dynamic Hierarchical Dirichlet Process Model for Recovering Birth/Death and Evolution of Topics in Text Stream. In UAI, pages 20–29, 2010.

# A Comprehensive review on Density-Based clustering algorithm in data mining

R. Sujatha & V Chandrasekar & Dr. G. Britto  
MRCET, Hyderabad, Telangana State, India

**ABSTRACT:** The problem of detecting clusters of points in data is challenging when the clusters are of different size, density and shape. Many of these issues become even more significant when the data is of very high dimensionality and when it includes noise and outliers. Clusters are identified by looking at the density of points. This paper gives an overview on various density based cluster algorithms –DBSCAN, OPTICS, and DENCLUE. These algorithms are particularly suited to deal with large datasets, with noise, and are able to identify clusters with different sizes and shapes. In machine learning and data analytics clustering methods are useful tools that help us visualize and understand data better.

**Keywords:** Density, Clustering, Minpoints, DBSCAN, OPTICS, DENCLUE

## 1. Introduction

DBSCAN is a density based clustering algorithm, it is focused on finding neighbors by density (MinPts) on an 'n-dimensional sphere' with radius  $\epsilon$ . A cluster can be defined as the maximal set of 'density connected points' in the feature space.[1] DBSCAN algorithm is that, for each point of a cluster, the neighborhood of a given radius has to contain at least a minimum number of points, that is, the density in the neighborhood has to exceed some predefined threshold.[2] This algorithm needs three input parameters:

- k, the neighbour list size
- Eps, the radius that delimitate the neighborhood area of a point (Epsneighbourhood)
- MinPts, the minimum number of points that must exist in the Eps-neighbourhood.

### 1.1 Parameter estimation

The parameter estimation is a problem for every data mining task. To choose good parameters we need to understand how they are used and have at least a basic previous knowledge about the data set that will be used.[3]

**eps:** if the eps value chosen is too small, a large part of the data will not be clustered. It will be considered outliers because don't satisfy the number of points to create a dense region. The eps should be chosen based on the distance of the dataset (we can use a k-distance graph to find it), but in general small eps values are preferable.

**minPoints:** As a general rule, a minimum minPoints can be derived from a number of dimensions (D) in the data set, as  $\text{minPoints} \geq D + 1$ . Larger values are usually better for data sets with noise and will form more significant clusters.

The minimum value for the minPoints must be 3, but the larger the data set, the larger the minPoints value that should be chosen.

To clusters a dataset, our DBSCAN implementation starts by identifying the k nearest neighbors of each point and identify the farthest k nearest neighbor (in terms of Euclidean distance) . [4] The average of all this distance is then calculated. After that, for each point of the dataset the algorithm identifies the directly density-reachable points and classifies the points into core or border points.

The clustering process is based on the classification of the points in the dataset as core points, border points and noise points, and on the use of density relations between points to form the clusters.[5]

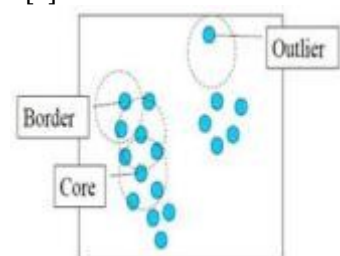


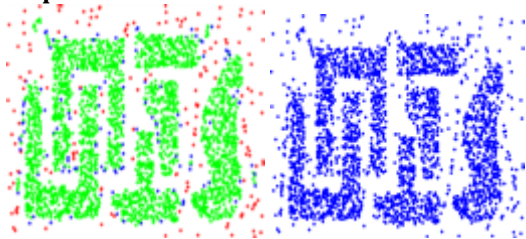
Fig.1 Diagram Representation of classification points

A point is a core point show in figure.1 if it has more than a specified number of points (MinPts) within Eps—these are points that are at the interior of a cluster.

A border point has fewer than MinPts within Eps, but is in the neighborhood of a core point.

A noise point is any point that is neither a core point nor a border point

**Example:**



**Original data Point types: core, border and Outliers**

Fig.2 Representation of classification points

**Density-based clustering Algorithms mainly include three techniques:**

- DBSCAN which grows clusters according to a density-based connectivity analysis.
- OPTICS extends DBSCAN to produce a cluster ordering obtained from a wide range of parameters settings.
- DENCLUE Clusters objects based on a set of density distribution functions.[7]

## 2. Density Based Clusters

Clusters may be looked at as dense regions in the data space; where clusters are separated by a sparse region containing “relatively few” data. Given this assumption, a cluster can either be of “regular” or “arbitrary” shape. Density based clustering is to detect clusters of non-spherical or arbitrary shapes.

Some of the common density based clustering techniques are DBSCAN, OPTICS, VDBSCAN, DVBSCAN, DBCLASD, ST-DBSCAN and DENCLUE. One of the earliest density based clustering methods is **Density-Based Spatial Clustering of Applications with Noise (DBSCAN)**. [8]

DBSCAN discovers high density regions in spatial databases with noise and creates clusters out of them. It uses the concept of density reachability and density connectivity.

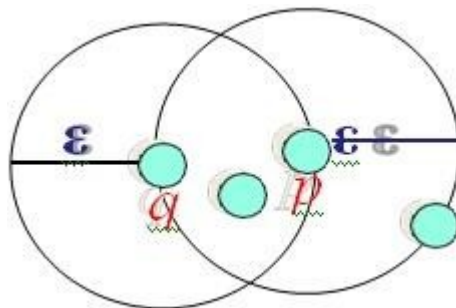
**Density Reachability** - A point "p" is said to be density reachable from a point "q" if point "p" is within  $\epsilon$  distance from point "q" and "q" has sufficient number of points in its neighbors who are within distance  $\epsilon$ .

**Density Connectivity** - A point "p" and "q" are said to be density connected if there exist a point "r" which has sufficient number of points in its neighbors and both the points "p" and "q" are within the  $\epsilon$  distance. This is chaining process. So, if "q" is neighbor of "r", "r" is neighbor of "s", "s" is neighbor of "t" which in turn is neighbor of "p" implies that "q" is neighbor of "p".

## Density reachability

Directly density-reachable An object q as shown in figure.3 is directly density-reachable from object p if q is within the  $\epsilon$ -neighborhood of p and p is a core object. [9]

- q is directly density-reachable from p
- p is not directly density-reachable from q



MinPts = 4

Fig.3 Directly density-reachable

## Density-Reachable (directly and indirectly):

**Density-Reachable:** An object p as shown in figure.4 is density-reachable from q w.r.t  $\epsilon$  and MinPts if there is a chain of objects  $p_1, \dots, p_n$ , with  $p_1 = q$ ,  $p_n = p$  such that  $p_{i+1}$  is directly density-reachable from  $p_i$  w.r.t  $\epsilon$  and MinPts for all  $1 \leq i \leq n$

A point p is directly density-reachable from  $p_2$

$p_2$  is directly density-reachable from  $p_1$

$p_1$  is directly density-reachable from q

$p \square p_2 \square p_1 \square q$  form a chain

p is (indirectly) density-reachable from q

q is not density-reachable from p

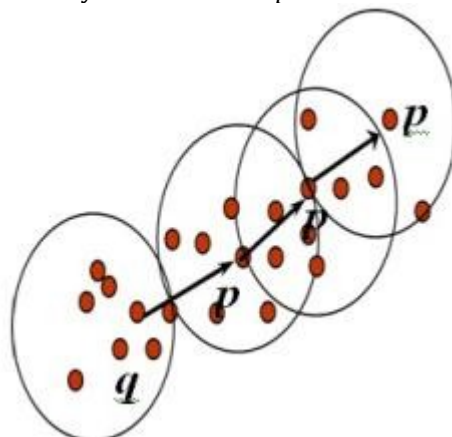


Fig.4 Representation of Density-Reachability

## 3. DBSCAN ALGORITHM:

- Select a point p.
- Retrieve all points density-reachable

from  $p$  with respect to  $\epsilon$  and  $\text{MinPts}$ .

- If  $p$  is a core point, a cluster is formed.
- If  $p$  is a border point, no points are density-reachable from  $p$  and it visits the next point of the database.
- Continue the process until all the points have been processed.[10]

#### Advantages of DBSCAN

Clusters of arbitrary shape can be detected  
 No prior knowledge about the number of clusters is required

There is a notion of noise (objects not belonging to any cluster)

Only two (2) input parameters ( $\epsilon$  - radius and  $\text{MinPts}$  - minimum number of points) and is mostly insensitive to the ordering of the points in the database

#### Disadvantages of DBSCAN

Proper determination of the initial values of the parameters  $\epsilon$  and  $\text{MinPts}$  is difficult

For  $n$  data objects, without any special structure or spatial indexing, the computational complexity is  $O(n^2)$ ; with spatial indexing it is  $O(n \log n)$ . [11]

#### 4. OPTICS

While the partitioning density-based clustering algorithm DBSCAN can only identify a flat clustering, the newer algorithm OPTICS computes an ordering of the points augmented by additional information, i.e. the reachability distance, representing the intrinsic hierarchical (nested) cluster structure. [11]

**Core-distance:** Let  $p$  be an object from a database  $DB$ , let  $N_\epsilon(p)$  be the  $\epsilon$ -neighborhood of  $p$ , let  $\text{MinPts}$  be a natural number and let  $\text{MinPts-dist}(p)$  be the distance of  $p$  to its  $\text{MinPts}$ -neighbor. Then, the *core-distance* of  $p$ , denoted as  $\text{core-dist}_\epsilon, \text{MinPts}(p)$  is defined as  $\text{MinPts-dist}(p)$  if  $|N_\epsilon(p)| \geq \text{MinPts}$  and INFINITY otherwise.

**Reachability-distance:** Let  $p$  and  $o$  be objects from a database  $DB$ , let  $N_\epsilon(o)$  be the  $\epsilon$ -neighborhood of  $o$ , let  $\text{dist}(o, p)$  be the distance between  $o$  and  $p$ , and let  $\text{MinPts}$  be a natural number. Then the *reachability distance* of  $p$  w.r.t.  $o$  as shown in fig.5, denoted as  $\text{reachability-dist}_\epsilon, \text{MinPts}(p, o)$ , is defined as  $\max(\text{core-dist}_\epsilon, \text{MinPts}(o), \text{dist}(o, p))$ . [13]

The OPTICS algorithm creates an ordering of a database, along with a reachability-value for each object. Its main data structure is a *seedlist*, containing tuples of points and reachability-distances. The seedlist is organized ascending reachability-distances. Initially the seedlist is empty and all points are marked as *not-done*. [12]

Advantages

- It solves the problem of finding good clusters if data has changeable density
  - It outcomes the objects in a particular ordering.
- Disadvantages
- It expects some kind of density decline to find cluster borders.
  - It is less sensitive to erroneous data.

**5. DENCLUE** (Density based clustering) Main concepts are used here i.e. influence and density functions. Influence of each data point can be modeled as mathematical function and resulting function is called Influence Function. Influence function describes the impact of data point within its neighborhood. Second factor is Density function which is sum of influence of all data points. According to DENCLUE two types of clusters are defined i.e. Centre defined and multi Centre defined clusters. [13].

In Centre defined cluster a density attractor. The influence function of a data objects  $y \in F$  is a function. Which is defined in terms of a basic influence function  $F, F(x) = -F(x, y)$ . The density function is defined as the sum of the influence functions of all data points. DENCLUE also generalizes other clustering methods such as Density based clustering; partition based clustering, hierarchical clustering.

In density based clustering DBSCAN is the example and square wave influence function is used and multicenter defined clusters are here which uses two parameter  $\sigma = \text{Eps}, \xi = \text{MinPts}$ . In partition based clustering example of k-means clustering is taken where Gaussian Influence function is discussed. Here in center defined clusters  $\xi=0$  is taken and  $\sigma$  is determined. In hierarchical clustering center defined clusters hierarchy is formed for different value of  $\sigma$ .

#### 5.1 Algorithm

- Take Data set in Grid whose each side is of  $2\sigma$
- Find highly densed cells i.e. Find out the mean of highly populated cells If  $d(\text{mean}(c1), \text{mean}(c2)) < 4a$  then two cubes are connected.
- Now highly populated or cubes that are connected to highly populated cells will be considered in determining clusters.
- Find Density Attractors using a Hill Climbing procedure.
- Randomly pick point  $r$ . Compute Local  $4\sigma$  density Pick another point  $(r+1)$  close to previous computed density. If  $\text{den}(r) < \text{den}(r+1)$  climb.
- Put points within  $(\sigma/2)$  of path into cluster.

- Connect the density attractor based cluster.[14]

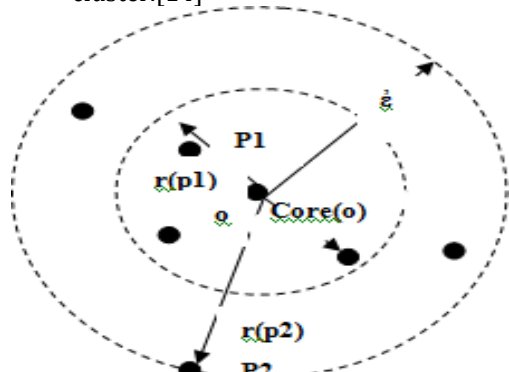


Fig.5 Core-distance (o), reachability-distances  $r(p1,o)$ ,  $r(p2,o)$  for  $MinPts=4$

**Advantages:**

- It detects erroneous data very well.
- It allows a brief description of non-spherical shaped clusters in high-dimensional data sets.
- Its processing is much faster than DBSCAN.

**Disadvantages**

- It needs many constants.
- It is less sensitive to outliers

**Table.1 Comparison of Density-Based Clustering Methods[15]**

Name	Noise	Variable Density	Primary Input Required	Complexity	Data Type	Cluster Type	Data Set
DBSCAN	Yes	No	Cluster radius, Minimum no. of Objects	$O(n \log n)$	Numerical	arbitrary	High-Dimensional
OPTICS	Yes	Yes	Density Threshold	$O(n \log n)$	Numerical	arbitrary	High-Dimensional
DENC LUE	Yes	Yes	Radius	$O(n^2)$	Numerical	arbitrary	High-Dimensional

**5. Conclusion**

Clustering algorithms are attractive for the task of class identification in spatial databases. In this paper, several densities based clustering algorithms proposed for clustering have been discussed with its advantages and disadvantages. And also it gives a comparative analysis of three density-based clustering algorithms i.e. DBSCAN, OPTICS and DENCLUE.

**References**

1. RashiChauhan, PoojaBatra, "A Survey of Density Based Clustering Algorithms" IJCST Vol. 5, ISSue 2, April - June 2014
2. PoojaBatraNagpal, "Comparative Study of Density based Clustering Algorithms", International Journal of Computer Applications (0975 - 8887) Volume 27- No.11, August 2011
3. International Journal of Computer Applications (0975 - 8887) Volume 27- No.11, August 2011 44 Comparative Study of Density based Clustering Algorithms PoojaBatraNagpal Department Of Computer Science NIT KurukshetraPriyankaAhlawat Mann Department Of Computer Science NIT Kurukshetra
4. Fast density clustering strategies based on the  $k$ -means algorithm, Elsevier, Volume 71, November 2017, Pages 375-386
5. B.G. Obula Reddy, Dr. MaligelaUssenaiah, "Literature Survey On Clustering Techniques", IOSR Journal of Computer Engineering, Vol. 3, Issue 1, July 2012
6. HenrikBäcklund, Anders Hedblom, NiklasNeijman, "DBSCAN A Density-Based Spatial Clustering of Application with Noise", 2011
7. Density-ratio based clustering for discovering clusters with varying densities, pattern recognition, Elsevier, Volume 60, December 2016, Pages 983-997
8. Yong-Feng Zhou, Qing-Bao Liu, S. Deng, Q. Yang, An Incremental Outlier Factor Based Clustering Algorithm, Proceedings of First International Conference on Machine Learning and Cybernetics, Beijing, 4-5 Nov 2002
9. [DBCAN] Ester M., Kriegel H.-P., Sander J., Xu X.: "A DensityBased Algorithm for Discovering Clusters in Large Spatial Databases with Noise", Proc. 2nd Int. Conf. on Knowledge Discovery and Data Mining, Portland, OR, AAAI Press, 1996, pp.226- 231.
10. S.Chakraborty, Prof.N.K.Nagwani, Analysis and Study of Incremental DBSCAN Clustering Algorithm, International Journal of Enterprise Computing And Business Systems, Vol. 1, July 2011
11. [OPTICS] Ankerst, M., Breunig, M., Kriegel, H.-P., and Sander, J. 1999. OPTICS: Ordering points to identify clustering structure. In Proceedings of the ACM SIGMOD Conference, 49-60, Philadelphia, PA.
12. M. Ankerst, M. M. Breunig, H. P. Kriegel and J. Sander, OPTICS: Ordering Points To Identify Clustering Structure, at International Conference on Management of Data, Philadelphia, ACM 1999
13. Aastha Joshi et.al., "A Review: Comparative Study of Various Clustering Techniques in Data Mining", International Journal of

Advanced Research in Computer Science and Software Engineering, Vol. 3, Issue 3, March 2013.

14. Hinneburg and D. Keim, "An efficient approach to clustering Large multimedia databases with noise," in Proc. 4th Int. Conf. Knowledge Discovery and Data Mining (KDD'98), 1998, pp. 58-65.
15. An Empirical Evaluation of Density-Based Clustering Techniques Glory H. Shah, C. K. Bhensdadia, Amit P. Ganatra, International Journal of Soft Computing and Engineering (IJSCE) ISSN: 2231-2307, Volume-2, Issue-1, March 2012

# An Efficient Feature Selection Technique for Keystroke Authentication Based on Low Impact Biometric Verification

V Chandrasekar & Sujatha Dandu & Dr. V. Bhoopathy

Malla Reddy College of Engineering and Technology, Hyderabad, Telangala State, India

**ABSTRACT:** *Advances in the field of Computer science and Technology also make Information Security an inseparable part of it. In order to deal with security, Authentication plays an important role. This paper presents a review on the biometric authentication techniques and some future possibilities in this field. In biometrics, a human being needs to be identified based on some characteristic physiological parameters. A wide variety of systems require reliable personal recognition schemes to either confirm or determine the identity of an individual requesting their services. The purpose of such schemes is to ensure that the rendered services are accessed only by a legitimate user, and not anyone else. By using biometrics, it is possible to confirm or establish an individual's identity. The position of biometrics in the current field of Security has been depicted in this work. We have also outlined opinions about the usability of biometric authentication systems, comparison between different techniques and their advantages and disadvantages in this paper.*

**Keywords:**

## 1. Introduction

Computer systems and networks are now used in almost all technical, industrial, and business applications. The dependence of people on computers has increased tremendously in recent years and many businesses rely heavily on the effective operations of their computer systems and networks. The total number of computer systems installed in most organizations has been increasing at a phenomenal rate. Corporations store sensitive information on manufacturing process, marketing, credit records, driving records, income tax, classified military data, and the like. There are many other examples of sensitive information that if accessed by unauthorized users, may entail loss of money or releasing confidential information to unwanted parties [1- 9].

Many incidents of computer security problems have been reported in the popular media [1]. Among these is the recent incident at Rice University where intruders were able to gain high level of access to the university computer systems which forced the administration to shut down the campus computer network and cut its link with the Internet for one week in order to resolve the problem. Other institutions such as Bard College of the University of Texas Health Science centre reported similar

breaches. Parker [10] reported that one basic problem with computer security is that the pace of the technology of data processing equipment has

outstripped capability to protect the data and information from intentional misdeeds. Attacks on computer systems and networks can be divided into active and passive attacks [11-12].

1. Active attacks: These attacks involve altering of data stream or the creation of a fraudulent stream. They can be divided into four subclasses: masquerade, replay, modification of messages, and denial of service. A masquerade occurs when one entity fakes to be a different entity. For example, authentication sequence can be collected and replayed after a valid authentication sequence has taken place. Replay involves the passive capture of data unit and its subsequent retransmission to construct an unapproved access. Modification of messages simply means that some portion of a genuine message is changed, or that messages are delayed or recorded, to produce an unauthorized result.

2. Passive attacks: These are inherently eavesdropping on, or snooping on, transmission. The goal of the attacker is to access information that is being transmitted. Here, there are two subclasses: release of message contents, and traffic analysis. In the first subclass, the attack occurs, for example, on an e-mail message, or a transferred file that may contain sensitive information. In traffic analysis, which is more sophisticated, the attacker could discover the location and identity of communicating hosts and could observe the frequency and length of encrypted messages being exchanged. Such

information could be useful in guessing the nature of information/data.

## 2. Keystroke Dynamics

The system is based upon the concept that the coordination of a person's fingers is neurophysiological determined and unique for a given genotype. A user typing or keystroke characteristics can be measured by examining the timing of the keystrokes or the pressure of the keystrokes. Vectors is used to represent the data. The vector was constructed using interleaved hold times and digraph latency times. The hold time of a key time is obtained by subtracting the press time of the key from the release time of the key. A digraph is a two keystroke combination. The digraph latency is obtained by subtracting a first key's release time from a second key's press time. The ordering elements of the vector is not important but the vectors should be constructed such that the samples relating to a user are constructed in the same manner so that they can be properly compared. The components of the vectors are physical characteristics of a person's keystroke characteristics. These physical characteristics are used to construct vectors which are processed, transmitted and stored within the system as signals. The vector can be made up of data pertaining to the key press time, key release times, digraph latency times, key hold times, keystroke pressure, keystroke acceleration or deceleration, or any features relating to the user's keystroke characteristics. Once the data is collected and placed in vector format, the vectors can be analysed to determine if the user is authorized or an imposter. The data was normalized using the transformation linear method which is shown below;

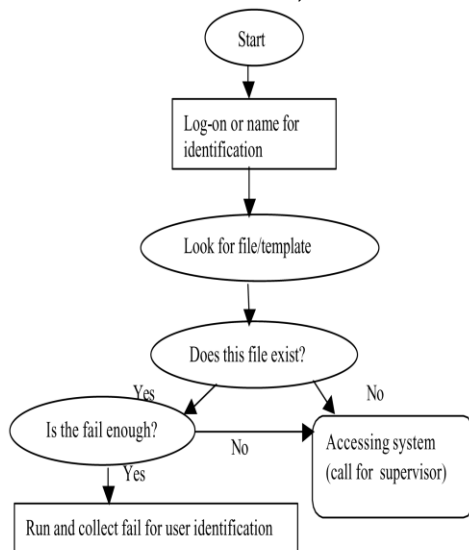


Fig. 1 Algorithm for keystroke dynamics method

## 3. Neural Networks Method

The main concern of this research was to find the best method to discriminate/purify the data collected. In this study, two kinds of neural network model and architecture was used to perform as the basic data or methodology. This paper describes the application of neural networks to the problem of identifying specific users through the typing characteristics exhibited when typing their own names. The network was chosen based on the problem to be solved. First of all, the previous study was done to compare two kind of methods to discriminate the data which are geometric distance and Euclidean distance. The system under investigation was then tested using two kind of neural network architecture and model. There are ADALINE and Backpropagation network. The network was chosen based on network model, architecture, data and the type of problem. The choice of network model depends heavily on the type of problems you would like to solve. The nature of the problem usually restricts the choice of network to one or two model. Sometimes the choice of network comes down to personal preference or familiarity. In this case, the problem to be solved is a pattern classifier problem since it needs to determine which pattern belongs to the authorised or non-authorised user. The input layer consists of 27 nodes, which is equivalent to the number of the input elements. Whereas for the middle layer, it is a single middle layer with 24 nodes, which is 90% of the input nodes. There will be two output nodes, 1 for the authorised user and 0 for the nonauthorised user. The availability and integrity of data constitute the most important factor for training neural networks. The data should fully represent all possible states of the problem being tackled and there should be sufficient data to allow test and validation data sets to be extracted. The right preparation of data is needed to ensure the accurateness of the output. Since the sigmoid activation function is used as the transfer function, it generates its output between 0 and 1. It is important for us to perform normalisation to scale the data so it will fall between this range. During the experiment, the number of input nodes, learning rate value, number of hidden nodes, momentum value and performance goal value was changed to find the most suitable parameter values. The appropriate parameter values are chosen based from trial and error performed during experiment and on the convergence and goal performance result.

## 4. Experimental Results

### 4.1 Data Sets

We collected the data sets from 16 participants. Each participant was requested to type the 10 passwords in Table 1 repeatedly. The 10 participants among them were each considered as the legitimate user for one password, each played the role of an imposter for the passwords. For each password, the other 15 participants were considered as imposters except the legitimate user. The passwords 1 to 5 are the Korean words on the English keyboard, and the passwords 6 to 9 are the English words. The password 10 is a random string including upper-cases, lower-cases, and numbers. The password strings were chosen carefully with regard to the familiarity and the typing difficulty on our own. The dimensions of the passwords and the numbers of samples are shown in Table 1. We used 20 samples of a legitimate user in making a hypothesis space, and the rest of the samples were used for test.

Table 1: Password strings used in the experiments

No	Password	Dimension	Number of Timing Vectors
1	qlalfqjsgh	23	340
2	rhdWkdudghk	20	320
3	rntk1tod	15	350
4	tjdnf1945	20	338
5	j6kbkeakd	14	325
6	transaction	16	319
7	DoItYourself	12	340

8	money4nothing	18	329
9	Sk8erBoi	25	335
10	FvVohx7x9P	22	320
<b>Ave.</b>		<b>18.5</b>	<b>331.6</b>
<b>Min.</b>		<b>12</b>	<b>319</b>
<b>Max.</b>		<b>25</b>	<b>350</b>

### 4.2 The Shapes of the Hypothesis Spaces

We proposed the extended p-norm to describe the hypothesis space. As shown in Figure 3, the value of p determines the shape of a hypothesis space. To find the proper shape of a hypothesis space, we tested for the hypothesis spaces of  $p = 1$ ,  $p = 2$ , and  $p = \infty$ . The results of the test is shown in Table 2. Bold faces figures represent the best pair of results with respect to the total error rate in the corresponding row. Each of the extended 1-norm and the extended 2-norm showed the best in 4 cases among the 10 passwords. Especially for the password 5, the extended 1-norm showed nearly zero error rates in the classification. The extended 2-norm showed relatively small error rates for the password 4. We could not find a considerable superiority between the extended 1-norm and the extended 2-norm, but it was observed that the extended infinity-norm performed poor in the test. Choosing the value of  $\gamma$  is another question. If the value of  $\gamma$  is too low (high security level), the FAR is nearly zero, but the FRR is too high. On the other side, if the value of  $\gamma$  is too high (low security level), the FRR is nearly zero, but the FAR is too high. With the current version, the values between 5 and 15 seems to be reasonable.

Table 2: Comparison of the hypothesis spaces

No.	Extended 1-norm				Extended 2-norm				Extended infinity-norm			
	$\gamma = 7.5$		$\gamma = 15$		$\gamma = 7.5$		$\gamma = 15$		$\gamma = 7.5$		$\gamma = 15$	
	FRR <sup>†</sup>	FAR <sup>‡</sup>	FRR	FAR	FRR	FAR	FRR	FAR	FRR	FAR	FRR	FAR
1	34	1	8	0	48	1	32	0	27	0	29	1
2	9	0	21	0	12	1	18	1	4	0	6	1
3	2	0	35	1	14	1	9	1	38	1	30	1
4	22	0	29	0	10	1	31	0	48	0	47	1
5	30	1	49	1	19	1	15	1	29	0	27	1
6	23	1	10	0	27	0	14	1	40	0	46	0
7	26	0	38	0	7	0	19	0	44	0	25	1
8	38	1	44	0	55	0	49	0	4	1	17	0
9	11	0	43	1	53	0	6	1	1	1	33	1
10	16	0	12	1	45	1	35	0	31	1	38	0
<b>Ave.</b>	21	0	29	0	29	1	23	1	27	0	30	1
<b>Min.</b>	2	0	8	0	7	0	6	0	1	0	6	0

<b>Max.</b>	38	1	49	1	55	1	49	1	48	1	47	1
-------------	----	---	----	---	----	---	----	---	----	---	----	---

† False reject rate.  
 ‡ False accept rate.

### 4.3 Effects of Eliminating Outliers

To observe the effects of eliminating outliers, we examined the hypothesis spaces using the extended 2-norm for  $\alpha = \infty$ ,  $\alpha = 2$ , and  $\alpha = 1$ . If the value of  $\alpha$  is infinite in inequality (6), no elimination occurs. The experimental results are shown in Table 3. For the 7 passwords excepting the passwords 2, 4, and 7, the error rates were reduced by eliminating outliers. It was observed that the hypothesis space for  $\alpha = 2$  performed better than the hypothesis space for  $\alpha = 1$  on average. We suspect that it is because most of the elements in the timing vectors were eliminated when  $\alpha = 1$ .

Table 3: The error rates for eliminating outliers

No.	Extended 2-norm					
	$\alpha = \infty$		$\alpha = 2$		$\alpha = 1$	
	FRR†	FAR‡	FRR	FAR	FRR	FAR
1	4.41	3.51	4.41	3.51	<b>2.45</b>	<b>3.51</b>
2	<b>9.76</b>	<b>0.88</b>	10.24	0.88	14.63	3.51
3	7.25	4.81	<b>5.7</b>	<b>5.77</b>	7.25	2.88
4	<b>1.6</b>	<b>0.79</b>	4.26	1.57	3.19	1.57
5	2.94	0.74	0	2.22	<b>0.49</b>	<b>1.48</b>
6	3.68	1.52	<b>3.68</b>	<b>0.76</b>	7.37	0
7	<b>11.27</b>	<b>5.22</b>	13.62	8.7	11.74	8.7
8	3.9	6.09	<b>3.9</b>	<b>5.22</b>	4.39	5.22
9	1.06	7.63	2.65	1.69	<b>1.59</b>	<b>2.54</b>
10	4.5	27.12	<b>2</b>	<b>11.02</b>	1.5	17.8
<b>Ave.</b>	<b>5.04</b>	<b>5.83</b>	<b>5.05</b>	<b>4.13</b>	<b>5.46</b>	<b>4.72</b>
<b>Min.</b>	<b>1.06</b>	<b>0.74</b>	<b>0</b>	<b>0.76</b>	<b>0.49</b>	<b>0</b>
<b>Max.</b>	<b>11.27</b>	<b>27.12</b>	<b>13.62</b>	<b>11.02</b>	<b>14.63</b>	<b>17.8</b>

† False reject rate.  
 ‡ False accept rate.

Table 4: The error rates with the adaptation

No	Extended 2-norm			
	FRR	FAR	FRR	FAR
1	10.5	2.5	<b>2.94</b>	<b>2.63</b>
2	13.6	3.8	<b>7.32</b>	<b>5.26</b>
3	<b>3.8</b>	<b>4.2</b>	5.7	7.69
4	12.8	6.5	<b>2.13</b>	<b>2.36</b>
5	<b>3.9</b>	<b>3.8</b>	1.47	8.89
6	8.5	8.4	<b>3.16</b>	<b>3.03</b>

7	13.5	6.7	<b>6.57</b>	<b>3.48</b>
8	15.9	4.9	<b>6.34</b>	<b>1.74</b>
9	<b>1.89</b>	<b>3.54</b>	3.7	5.08
10	12.5	8.54	<b>4</b>	<b>3.39</b>
<b>Ave.</b>	9.689	5.288	4.333	4.355
<b>Min.</b>	1.89	2.5	1.47	1.74
<b>Max.</b>	15.9	8.54	7.32	8.89

### 4.4 Improvements by the Adaptation

The proposed adaptation mechanism utilizes the results of the classification. The measured timing vector is used in up- dating a hypothesis space, if it is classified as the legitimate user. We tested the hypothesis spaces with the adaptation mechanism using the extended 2-norm. To avoid a heavy load, we executed the adaptation process once whenever 20 samples were collected. The experimental results are shown in Table 4. The adaptation mechanism improved the performance of the system on average. However, it is observed that the error rates for the passwords 3, 5, and 9 were in- creased slightly by the adaptation mechanism. We believe it was because the misclassification in the early stage misled the hypothesis space.

### 5. Conclusions

To conclude, keystroke dynamics are rich with individual mannerism and traits and they can be used to extract features that can be used to authenticate/verify access to computer systems and networks. The keystroke dynamics of a computer user's login string provide a characteristic pattern that can be used for verification of the user's identity. Keystroke patterns combined with other security schemes can provide a very powerful and effective means of authentication and verification of computer users. Neither our work nor any other work we are aware of has dealt with typographical errors. Further research into reliable methods for handling typographical errors is needed in order to make keystroke-based authentication systems non-irritating and widely accepted by the computing and network security community. Finally, it is found that artificial neural network paradigms are more successful than classical pattern recognition algorithms in the classification of users.

**Reference**

1. M. S. Obaidat and B. Sadoun, "Verification of Computer users using Keystroke Dynamics," IEEE Trans. on Systems, Man and Cybernetics, Vol. 27, No. 2, pp. 261-269, April 1997.
2. M. S. Obaidat and B. Sadoun, "An Evaluation Simulation Study of Neural Network Paradigm for Computer Users Identification," Information Sciences Journal-Applications, Elsevier, Vol. 102, No. 1-4, pp. 239-258, November 1997.
3. M. S. Obaidat, "A Methodology for Improving Computer Access Security," Computers & Security, Vol. 12, pp. 657-662, 1993.
4. M. S. Obaidat and D. T. Macchairolo, "An On-line Neural Network System for Computer Access Security," IEEE Trans. Industrial Electronics, Vol. 40, No. 2, pp. 235-241, April 1993.
5. S. Bleha and M. S. Obaidat, "Dimensionality Reduction and Feature Extraction Applications in Identifying Computer Users," IEEE Trans. Systems, Man, and Cybernetics, Vol. 21, No. 2, March/April 1991.
6. S. Bleha and M.S. Obaidat, "Computer User Verification Using the Perceptron," IEEE Trans. Systems, Man, and Cybernetics, Vol. 23, NO. 3, pp. 900-902, May/June, 1993.
7. M. S. Obaidat et al., "An Intelligent Neural Network System for Identifying Computer Users," In Intelligent Engineering Systems through Artificial Neural Networks (C. Dagli et al. editors), pp. 953-959, ASME Press, New York, 1991.
8. M. S. Obaidat and D. T. Macchairolo, "A Multilayer Neural Network System for Computer Access Security," IEEE Trans. on Systems, Man and Cybernetics, Vol. 24, No. 5, pp. 806-813, May 1994.
9. J. A. Adam, "Threats and Countermeasures," IEEE Spectrum, Vol. 29, No. 8, 21-28, August 1992.
10. D. B. Parker, Computer Security Management, Reston Publishing Co., Reston, VA, 1981.
11. W. Satllings, Network and Internetwork Security, Prentice Hall, Upper Saddle River, NJ, 1995.
12. C. P. Pfleeger, Security in Computing, Prentice Hall, Upper Saddle River, NJ, 1997.

# Design of Chaotic Behavior for programmable cellular automata based Symmetric Key Encryption Algorithm for Wireless Sensor Networks

Shanthi S & Chandrasekar V & Dr. V. Bhoopathy

Malla Reddy College of Engineering and Technology, Hyderabad, Telangala State, India

**ABSTRACT:** Cellular automata are highly parallel and distributed systems which are able to perform complex computations. Cryptographic techniques are very important in these times dominated by the growth of digital information storage and transmission. CA are an attractive approach for cryptographic applications. They are simple, modular logic systems that can generate good quality pseudorandom bit streams as required in robust cryptographic systems. Further advantage is that they can be easily and efficiently implemented. This paper focuses on using cellular automata in cryptography, thereby bringing the advantages of using cellular automata in cryptography.

**Keywords:** Cellular automata, types of cellular automata, Cryptography, Advantages of using Cellular automata in cryptography.

## 1. Introduction

In this age of information, communications and electronic connectivity, security is a topic of general interest that should never be underestimated. The security of data bases, of data communications, of Internet connections, of scientific research and of personal e-mail and phone calls are some examples where the encryption of data/information plays a major role. Therefore, cryptography has become an important field of research in theory and applications development.

Because of its importance, cryptography is nowadays a science by itself, strongly related to other modern research fields as complexity theory, chaos, dynamical systems, computing theory etc. The state-of-the art for the field of cryptography is probably classified as it has military applications, but for the public domain a good reference can be found in [1] and [2]. The encryption of a message/data file/other information is a process (algorithm) that modifies this message/data file/information making it completely unintelligible, except for the person who knows the encryption key. The key refers to the encryption algorithm that has been used - in fact, to the reverse algorithm that should be used for decryption - and the particular parameters that have been used during the encryption. The decryption algorithm should render the original message/file/information complete and unaltered. Encryption can be achieved by constructing two different types of ciphers—stream ciphers and block ciphers. A block cipher is one in which a message is broken into successive

blocks that are encrypted using a single key or multiple keys. In a stream cipher the message is broken into successive bits or characters and then the string of characters is encrypted using a key stream. The *cryptographic scheme* refers to the assembly of encryption and decryption algorithms.

An ideal cryptographic scheme or algorithm has not been developed yet, as an ideal cryptographic scheme implies:

- no data expansion during encoding process;
- fast encoding algorithm;
- small dimension key;
- fast decoding algorithm;
- correct and complete rendering of message after encryption/decryption;
- invulnerability to attacks.

The last point is a major issue in cryptography; complex mathematical studies and research have to be done in order to establish the vulnerability of each cryptographic scheme. In simple words, this answers the basic question: how difficult is to break the code? This “difficulty” has to be established in terms of complexity, cost and computing time. Therefore, depending of the particular applications, sometimes it is enough to have a code and cryptographic scheme that requires a long search for the key, although the process is very simple. This is the situation for the briefcases with cipher, where the breaking process is quite simple: one has to try *all* possible numbers in order to find the right one. Cellular automata are applied with success in cryptography mainly because their vast phenomenology and apparently big complexity

require a very long computing time to break well-chosen cryptographic schemes. There are indeed a lot of parameters and factors that can drastically affect the encrypted message (cyphertext) and therefore the complexity of the attack is considerably increased. Cellular automata offer an ideal mathematical model for massive parallel computation, but most research and applications in cellular automata domain are done through simulation. However, it is obvious that only the hardware implementations of this model fully exploit its computing and high-speed possibilities. In particular, cellular automata applications in cryptography are efficient because of the massive parallelism of the model. When implemented by means of other computing systems (simulated in software or emulated with microcontrollers etc.) the parallel processes are in fact executed sequentially. Special cellular automata hardware is the only means to benefit of all the advantages of the model.

## 2. Cryptography with Cellular Automata

### 2.1. The Cellular Automata Model

Basically, cellular automata are parallel systems that consist of a typically large number of finite automata (finite state machines) as elementary “cells”. The cells are locally connected, in other words the global network supports only local connections. The system evolves through local changes: all cells are updated synchronously, depending on their own current state and on the states of the neighbouring cells in the network. The computing task performed by cellular automata is generally conceived as the global evolution of its configuration, starting from the initial configuration (input data) and leading to an intermediate or final configuration or attraction cycle that are interpreted as a result. This almost “visual” perceptible computation is quite an advantage in task like modeling and simulation, image processing and cryptography.

The Cellular Automata formalisms [Wol86] are well-suited to describe some kind of real complex systems with different description levels.

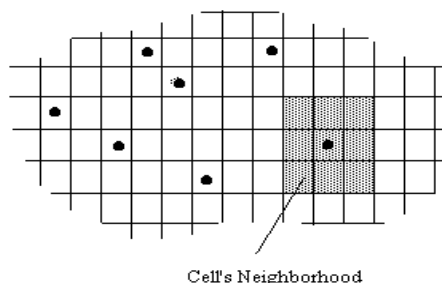


**Figure 1 Sketch of a Cellular Automata**

### 2.1.1 The three fundamental properties of CA

1. *Parallelism*: A system is said to be parallel when its constituents evolve simultaneously and independently. In that case cells updates are performed independently of each other.

2. *Locality*: The new state of a cell only depends on its actual state and on the neighborhood.

3. *Homogeneity*: The laws are universal, that's to say common to the whole space of CA.

Two common two-dimensional neighborhoods are the von Neumann neighborhood, in which each cell has neighbors to the north, south, east and west; and the Moore neighborhood, which adds the diagonal cells to the northeast, southeast, southwest and northwest.

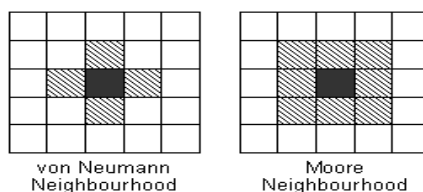


**Figure 2 Types of Neighbourhoods**

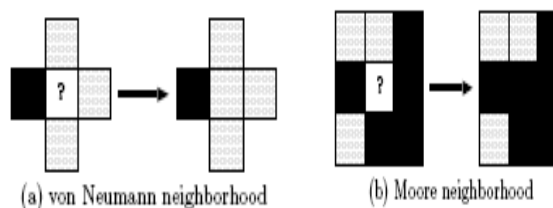


**Figure 3 Two examples of a cell with a one-step update. The center cell examines its neighborhood and applies the update rule**

### 2.1.2 Basic Rules of CA

Rule 1: Survival – a live cell with exactly two or three neighbors stay alive [7][8]

Rule 2: Birth – a dead cell with exactly three live neighbors becomes alive

Rule 3: Death – a cell dies due to ‘loneliness’ if it has only one neighbor or due to ‘crowding’ if it has more than four neighbors

Cellular automata are defined by the following elements:

- topology and dimension of the lattice of cells;
- the set of the neighbours of each cell that are involved in the next state's computation;
- the number of states of each cell (identical for all cells; binary automata, for instance, have only two states per cell: 0/1, visually translated as white/black);

- the local rule that gives the next state of the cells.

In cryptography the main topologies that are applied are linear and two-dimensional, referring to a row or matrix of "cells".

## 2.2 Characteristics of cellular automata.

Cellular automata were first introduced by John Von Neumann (1966), as a means of modeling the nature of self-reproduction in biological systems. The Game of Life constructed by Conway constitutes a famous example of cellular automata which may be easily simulated on a personal computer. Cellular automata are discrete dynamical systems in which the space, time, and states are discrete. Despite their conceptual simplicity, cellular automata may reveal very complex behavior. A cellular automaton is a mechanism for modeling systems with local inter-actions. It consists of a regular array of identically programmed units called cells which interact with their neighbors subject to a finite set of prescribed rules for local transitions. All cells form a regular spatial lattice. Time progresses in discrete steps. The state of a cell at time  $t + 1$  is a function only of its own state and of the states of its neighbors at time  $t$ . All cells states are updated synchronously. In order to establish a rigorous mathematical definition, we need some basic notions. Cellular automata remain very interesting for systems with high complexity. A cellular automaton is a mathematical model which is perfectly suited to complex systems containing a large number of simple identical components with local interactions. Cellular automata have also been considered as a means for symbolic dynamics. Such an approach offers many advantages. In theory, it is a convenient method to represent many discrete or continuous processes conventionally described by partial differential equations. In practice, cellular automata may be viewed as parallel-processing computers of simple construction. Because of this, Cellular automata have been used to study complex systems widely.

## 2.3. Complexity of Cellular Automata

The cellular automata model is inspired from the natural model of complex systems that often consist of a large number of simple basic elements, having only local interactions that lead to a complex global behaviour. This model is an important research and simulation tool in the science of complexity. Strictly speaking, the cellular automata model and also the cellular automata evolution are not complex, as its structure and rules are very regular and simple.

But the huge dimension of the rules and configuration spaces confers to its phenomenology a considerably great *apparent* complexity. In the quite simple example of binary linear cellular automata with 100 cells (a modest dimension) with local rules involving the central cell and two neighbours on each side (binary functions with 5 variables), there are:  $2^{100}$  global configurations, which is approximately  $10^{30}$  and  $2^{32}$  possible local functions, which by a rough approximation means around 4,000,000 functions.

Not all possible functions are of practical interest, but even in this conditions a search in the local functions' space is a very long computing task. This is related to the difficulty of cellular automata synthesis: there is no algorithm that gives the appropriate local function for a specific application. The universality of the cellular automata model is theoretically proven, but the practical applications are still waiting for development tools, since the experiment is, by now, the main means of cellular automata synthesis. The work of S. Wolfram [7] imposed a certain order in the space of local rules of functions, mainly for linear cellular automata, dividing it into four complexity classes (that express how complex is the evolution of the system govern by a certain rule). Class 3 of Wolfram's classification contains the automata that have an apparently chaotic evolution, also strongly depending on the initial global configuration. Such an evolution is illustrated in Fig. 1, where time is on the vertical axis, downwards, and the horizontal bit string is the configuration of a binary linear cellular automata. The *class 3 automata* are ideal for applications like random sequences generation and cryptography.

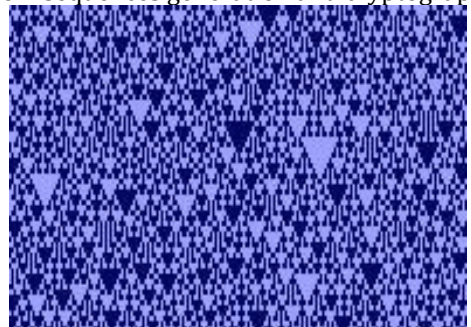


Fig. 1. Evolution of class 3 linear cellular automata

### 2.3.1 Chaos and complexity

Wolfram gives a rough geometrical analogy of behavior of these four classes:

1. **Class 1** - limit points
2. **Class 2** - limit cycle
3. **Class 3** - chaotic - "strange" attractor

**4. Class 4** - more complex behavior, but capable of universal computation[4][5]

#### 2.3.1.1 Class 1 cellular automata

After a finite number of time-steps, class one automata tend to achieve a *unique state* from (nearly) all possible starting conditions.

#### 2.3.1.2 Class 2 cellular automata

This type of automata usually creates patterns that *repeat periodically* (typical with small periods) or are stable. One can understand this type of CA's as a kind of *filter*, which makes them interesting for digital image processing

#### 2.3.1.3 Class 3 cellular automata

From nearly all starting conditions, this type of CA's lead to aperiodic - chaotic patterns. The statistical properties of these patterns and the statistical properties of the starting patterns are almost identical (after a sufficient period of time). The patterns created by this type of CA's (usually one dimensional CA's) are a kind of self-similar fractal curves.

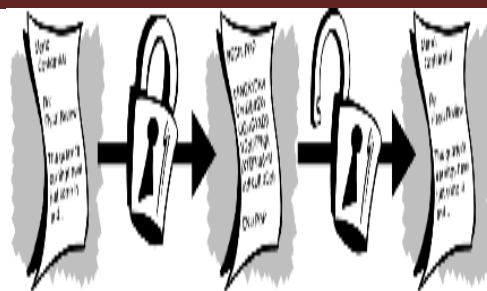
#### 2.3.1.4 Class 4 cellular automata

After finite steps of time, this type of CA's usually "dies" - the state of all cells becomes zero. Nevertheless a few stable (periodic) figures are possible. One popular example of an automaton of this type is the Game of Life. In addition to that Class 4 automata can perform universal computation. This class of CA's show a high irreversibility in their time development.

The first three types can be read as *Cantor sets* with a certain dimensionality, either in countable or in *fractal* dimension. Class 3 is the most frequent class. With increasing  $k$  and  $r$  the probability to find class 3 automaton for an arbitrary selected rule is again increasing.

### 3. Cryptography

Encryption is the science of changing data so that it is unrecognizable and useless to an unauthorized person. Decryption is changing it back to its original form. The most secure techniques use a mathematical algorithm and a variable value known as a 'key'. The selected key (often any random character string) is input on encryption and is integral to the changing of the data. The EXACT same key MUST be input to enable decryption of the data. This is the basis of the protection.... if the key (sometimes called a password) is only known by authorized individual(s), the data cannot be exposed to other parties. Only those who know the key can decrypt it. This is known as 'private key' cryptography, which is the most well known form.



Plaintext encryption cipher text decryption  
plain text

Figure 4 Cryptography basics

Data that can be read and understood without any special measures is called plaintext or cleartext. The method of disguising plaintext in such a way as to hide its substance is called encryption. Encrypting plaintext results in unreadable gibberish called cipher text. You use encryption to make sure that information is hidden from anyone for whom it is not intended, even those who can see the encrypted data. The process of reverting cipher text to its original plaintext is called decryption.

### 4. Cellular Automata in Cryptography

The very large phenomenology of the cellular automata model and its apparently big complexity offer a good basis for applications in cryptography (cellular automata are not the only dynamical systems applied in cryptography, and some of the basic principles of cryptography with cellular automata also stand for other dynamical systems). Massive parallelism is another feature of cellular automata that make this model attractive for cryptography, since lot of computation is often necessary in real-time applications. However, this parallelism, when emulated in software or in sequential hardware, disappears. In the last two decades many results have been obtained in this direction. A good review of some cryptographic schemes and systems with cellular automata proposed in the scientific literature is given in [5] and [6]. In the next section some of these will be discussed as possible basis for hardware implementations, taking as valuable the theoretical results concerning the efficiency and invulnerability of the schemes.

### 5. Other Advantages of Cellular Automata

The design style under VLSI technology prefers the simple, modular and local connected logic circuit structure. Cellular automata are ideal from the hardware designer's point of view. The local connectivity, regularity and the simple basic components make CA very appropriate to

implement low-cost and robust massive parallel machines or application-oriented circuits. The reason why there are not so many cellular-automata inspired electronic circuits is mainly the difficulty of the synthesis for this computing model; however, dedicated circuits for specific applications (signal generators, associative memories, image pre-processing blocks, various simulators for natural phenomena) have been successfully designed and produced [6].

Apart from cryptography cellular automata can be used in variety of applications because of its simpler structure providing solution to the complex problems.

### **6. Conclusion**

This paper has introduced the basic concepts of cellular automata and cryptography and some applications of cellular automata in cryptography. cellular automata along with cryptography can be used to model a wide variety of real world applications.

### **7. References**

1. William Stallings, *Cryptography and Network Security* Prentice-Hall 2003 New Jersey, USA
2. Brian A. LaMacchia, *.NET Framework Security* Addison Wesley 2002, USA [1] Toffoli, T., & Margolus, N. (1987). *Cellular Automata Machines*. MIT Press.
3. S. Wolfram, *Cellular Automata and Complexity*, Addison-Wesley Publishing Company, 1994
4. J. Kari "Reversibility of 2D Cellular Automata is Undecidable", *Physica D*, Vol 45:379-385, 1990
5. H. Gutowitz *Method and Apparatus for Encryption, Decryption and Authentication using Dynamical Systems* US Patent 5365589, 1994
6. P. Chaudhuri, D. Chowdhury, S. Nandi, S. Chattopadhyay, *Additive Cellular Automata: Theory and Applications*, IEEE Computer Society Press, 1997.
7. Wolfram, S. (2002). *A New Kind of Science*. Wolfram Media, Inc., Champaign, IL.
8. 1986. Wolfram, S. (Ed.). *Theory and Applications of Cellular Automata*. Singapore: World Scientific.
9. V. Vemuri, 1978, *modeling of Complex Systems: An introduction*. Chapter 3 pp. 67-88
10. Pidd, M. 1992a. *Computer simulation in management science* 3rd ed, Chichester.: John Wiley & Sons.

# THE VEHICLE NETWORK ARCHITECTURE IN SMART CITY WITH BLOCKCHAIN TECHNOLOGY

R.JAHNAVI\* & Rajasekar Rangasamy\*\*

\* PG Scholar, Department of Computer Science and Engineering,

\*\* Professor, Department of Computer Science and Engineering,  
St. Peter's Engineering College, Hyderabad, Telangana, India.

**ABSTRACT:** The interconnected smart vehicle variety of sophisticated services to vehicle owners, car manufacturers and other providers of services. The rapid growth of the Internet of Vehicles (IoV) has brought the entire system enormous challenges for large data storage, intelligent management and information security. The traditional centralized management approach for IoV is facing the challenge of responding in real time. The block chain has already shown great advantages in the application of Bit coin as an efficient technology for decentralized distributed storage and security management. Block chain technology enables smart data -vehicles to be shared in a decentralized and manipulative manner while maintaining privacy, integrity, resilience and non-repudience. Smart vehicles, both consumers and producers of data smart cities, are increasingly interested. Vehicles can use intelligent city data to make decisions, such as dynamic traffic routing. In this paper, we examine how block chain innovation can be stretched out to vehicle organizing applications, considering the protected and dispersed storage of Big Data.

**Keywords:** Block chain Technology, Local Block Manger(LBM), IOV, OEMs(Original Equipment Manufacturer),Security, Vehicular Network Architecture, VANET, Smart Cities

## INTRODUCTION

Smart cities are areas that support innovation through digital networks and applications (Figure 1). smart towns are often referred to as sustainable, digital or connected towns[1]. The aim of turning a city into an smart environment is to alleviate the problems of urbanization and an increasing urban population. A clever town is an urban area that offers sustainable economic growth and quality of life. Smart solutions, such as avoiding traffic congestion[2], Some of the technologies used are green buildings[3] and modern industrial control systems (ICS)[4] Could make urbanization sustainable today.

A clever city involves smart technology to Enhance how people live, work, travel. A key aspect of a clever city Vehicles of the next generation that incorporate new sensing, communication and social skills The broader concept of the Internet of Things. By providing wireless communication and mobile sensing, Vehicles can facilitate access to data, which is critical to smart cities a reality.

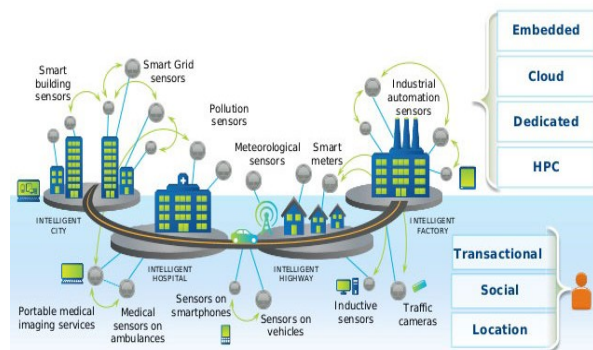


Fig.no: 1 SMART CITY

The characteristic advancement of the Internet (of PCs) to embedded and cyber physical frameworks that PCs themselves, albeit clearly not have computers Within a system of modest sensors and interconnected items, data on our reality and condition can be gathered at an a lot more elevated amount.Smart vehicles are progressively associated with roadside framework, e.g. traffic the executives frameworks, to other close-by vehicles and, all the more for the most part, to the Internet, making vehicles part of the IoT.

Block chain[5] is a promising new technology(Figure 2) that can deal with the challenges mentioned above. It promotes decentralization, security and privacy and is

widely used in various disciplines including finance, law, the IoT and energy[6]. Block chain has a Distributed block ledger that is shared across all nodes. Block chain maintains a distributed block library that is shared across all nodes involved. Every exchange, i.e. the trading of information between hubs, is confirmed by all or a portion of the hubs included, therefore dispensing with the requirement for focal experts.

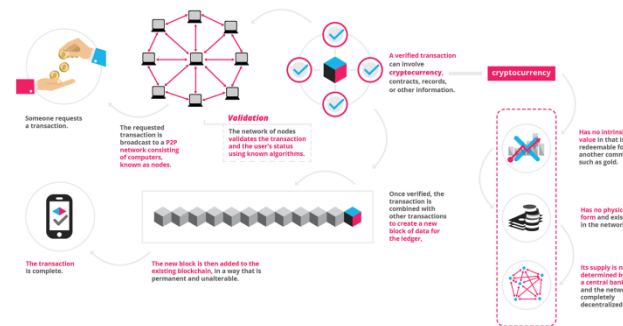


FIG.NO: 2 BLOCK CHAIN TECHNOLOGY

Exchanges are gathered together into squares and connected to the block chain. Adding another block to the block chain, known as mining, includes understanding a riddle or notwithstanding casting a ballot so as to achieve an agreement between the Peer-to-Peer (P2P) organize hubs that deal with the square chain distributively. Sensitive data transmitted between nodes that protect against eavesdropping can be encrypted. To ensure the security of the client, the Bitcoin cryptocurrency[7].

## 2. ADVANTAGES OF BLOCK CHAIN

### 2.1 Greater Transparency

The history of transactions becomes more transparent by using blockchain technology. Since blockchain is a dispersed record type, all members in the system share in distinguishable documentation from each duplicate. This common version can only be updated by consensus, which means that everyone has to agree.

To change a solitary exchange record, every consequent record would should be modified and the whole system would be associated. The blockchain information is in this manner increasingly precise, steady and straight forward Instead of pushing it through paper-substantial procedures.It is also open to all participants who have access.

### 2.2 Enhanced Security

There are a number of ways in which blockchain is safer than other recording systems. Transactions must be agreed in advance of recording. Following endorsement of the exchange, it is encoded and

connected to the past exchange. This makes it extremely trouble some for programmers to bargain exchange information, together with the way that data is put away on a system of PCs rather than on a solitary server. In any industry where the insurance of delicate information is critical money related administrations, government, social insurance—blockchain truly has the chance to change the way critical information is shared by preventing fraud and unauthorized activity.

### 2.3 Improved Traceability

On the off chance that your organization manages items that are exchanged a mind boggling store network, you realize that it is so hard to follow an item back to its starting point. At the point when ware trades are recorded on a blockchain, you wind up with a review trail demonstrating where a benefit originated from and where it stops made on its adventure. This historical transaction data can help check asset authenticity and prevent fraud.

### 2.4 Increased Efficiency And Speed (I should start here)

When using traditional, paper-intensive processes, trade is a time consuming process that is prone to human error and often requires mediation from third parties. Exchanges can be finished speedier and all the more effectively by streamlining and robotizing these procedures with a block chain. Since recording is carried out using a single digital booklet shared between participants, you do not have to reconcile multiple booklets and end up with less clutter. Furthermore, it winds up less demanding to confide in one another without the requirement for various middle people when everybody approaches a similar data. Clearing and settlement can therefore occur much faster.

### 2.5 Reduced Costs

Decreasing expenses is a need for generally organizations. You don't require the same number of outsiders or delegates to make ensures with blockchain on the grounds that it doesn't make a difference whether you can believe your exchanging accomplice. Instead, you just have to confide the blockchain data. You will also not need to review so much documentation to complete a trade, because everyone has access to a single, unchanging version.

## 3. ARCHITECTURE OF SMART VEHICLES

Our BC-based architecture described in this area can satisfy the up to referenced security, protection and versatility prerequisites. The overlay, as appeared in (Figure 3), is involved

unique hubs including keen vehicles, smart structures (that can be keen homes or administration focuses), OEMs(Original Equipment Manufacturer), vehicle mechanical production systems, SW suppliers, cloud stockpiles, and client's cell phones such as cell phones, workstations, or tablets. Each shrewd building is halfway overseen by a believed hub known as Local Block Manager (LBM).

The OBM's are picked by the cluster individuals utilizing techniques, for example, portrayed in [9]. The group individuals can choose another CH on the off chance that an OBM fizzles or is imperiled. In the overlay there are two kinds of exchanges, specifically:

1. Single signature transactions
2. Multi sig transactions

In the vehicle gathering the OEM will store its PK on each amassed vehicle and the vehicle will produce a mystery key combine (e.g., a RSA key match comprising of a private and an open key). Both the PK of the OEM and the key match will be se-curely put away on the WVI in a carefully designed capacity. While a vehicle is gathered it can likewise make a beginning exchange, an underlying exchange required to take part in the BC.

Overlay exchanges are communicated and checked by the OBM's. An OBM checks an exchange by confirming the mark of the exchange members with their PK. Furthermore, the OBM confirms if the past exchange referenced in the second field of every exchange exists in people in general BC and is legitimate. OBM's create new squares and communicate them to other OBM's.

On accepting another square, an OBM confirms the exchanges inside the square before adding it to its own BC and communicate it to different OBM's. A versatile vehicle that changes its group can still speak with other overlay hubs and store exchanges on the general population BC, yet it will be unavailable for overlay hubs as the vehicle PK isn't in the key lists of the new OBM. To make itself open, the vehicle should store its key on the key lists of its new OBM.

#### 4. SMART CONTRACT & SUPPLY CHAIN USING BLOCK CHAIN

Blockchain based on smart contracts is expected to play an important role in the management, control and most importantly the securing of IoT devices in the context of IoT.

Nick Szabo first authored the term Smart Contracts in 1994. (Figure 4) A smart contract is on an exceptionally essential dimension an electronic exchange custom that executes the terms of the assention. In the oversimplified definition, smart contracts are programs composed by clients to be transferred and executed on the blockchain. Smart contracts empower you to exchange money, property, offers or anything of huge worth in a direct, conflict-free way while avoiding a specialist's organizations. The most ideal approach to depict

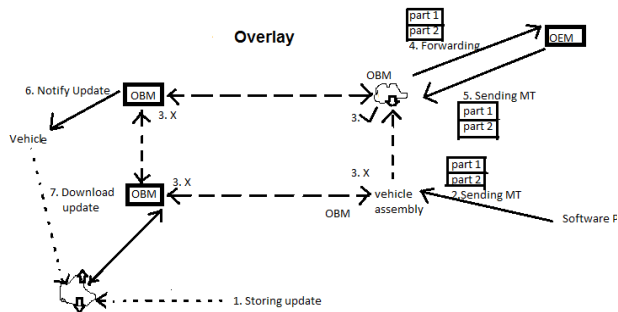


Fig.no: 3 ARCHITECTURE OF SMART VEHICLES

In the proposed design, a vehicle can interface with the overlay either straightforwardly or through the smart building. A vehicle is a piece of a smart building while it is inside the scope of the LBM (e.g., while it is stopped at home). Each smart building has a safe local storage. In an administration focus this storage will be used to gather vehicles-explicit information (e.g., the date of the last vehicle upkeep) and additionally data required by the mechanics to keep up the vehicle (e.g., the most recent accessible SW updates and fix directions). In a smart home, vehicle related information, client information (e.g., originating from brilliant gadgets, for example, cell phones), and information originating from neighborhood sensors and actuators can be gathered in the local storage. A smart vehicle can likewise specifically associate with the overlay arrange.

There are two types of cloud storages in the overlay. The first category is overseen by the OEM or potentially SW refresh supplier and could be utilized to store most recent SW refreshes. The second gathering incorporates storage which vehicle proprietors use for putting away vehicular information to get explicit administrations, e.g. cloud capacity given by vehicle insurance agencies.

The overlay is a clustered network and its groups are kept up by Cluster Heads (CH). The CHs likewise deal with the open BC by checking and putting away exchanges and squares and are thus likewise alluded to as Overlay Block Manager (OBM).

Smart contracts is by contrasting innovation and a merchant.

You would typically go to an attorney or a public accountant and pay them and hang tight for the report. You simply drop a bitcoin into the moving machine with smart contracts (i.e. Record), and your escrow, driver's permit, or any drops to your record.

All the more along these lines, smart contracts not just characterize the guidelines and punishments around an understanding similarly that a customary contract does, yet additionally consequently implement those commitments.

In block chain solidity, which is a JavaScript-like language, is the script or programming language for intelligent contracts. Ethereum Blockchain supplies EVM (Ethereum Virtual Machines) that are essentially the mineral nodes. These nodes are able to carry out and enforce these programs or contracts in a cryptographically reliable manner.

Ethereum supports Ether's own digital currency. As in Bitcoin in Ethereum, users can transfer coins to each other using normal transactions recorded on the booklet and there is no need for a blockchain status in Bitcoin for such transactions.

An intelligent contract has its own account and address and its own executable code and balance of Ether coins is associated with it. EVM storage is moderately costly and another remote, decentralized information store, for example, Bit Torrent, IPFS or Swarm can be utilized to transfer expansive capacity to the blockchain.

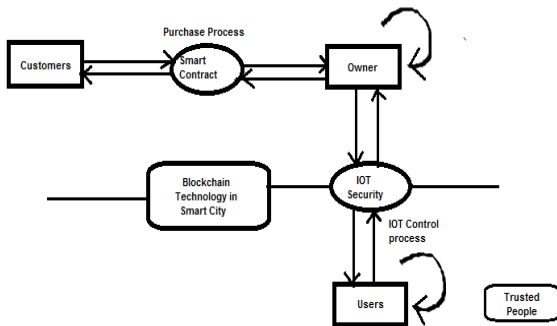


FIG.NO:4 SMART CONTRACTS

**5. CHALLENGES IN VEHICULAR NETWORK**

**5.1 Technical Challenges:**

The highlights of VANETs additionally assume an essential job in the transmission of the packets. The transmission challenges identified during the packet transmission include next hop selection, queuing disciplines and duration of the paths. DSR / GPSR Protocols maintain neighborhood lists for next hop determination. In the event that the rundowns are not right, the best next jump could

be missed or more terrible, a vehicle hub that is as of now out of the scope of transmission could be chosen. The maintenance of updated lists requires the frequent broadcast of " hello " packets between the network nodes.

**5.2 Security Challenges:**

Security has so far gotten less consideration among every one of the difficulties of the VANET. VANET packets may contain life - critical information and it is therefore necessary to ensure that these packets are not attacked by the intruder. Likewise, drivers ' liability is established by informing them of the traffic environment correctly at specified time.

**5.3 Social and Economic Challenges:**

In addition to the technical challenges involved in the use of the VANET, there are social and economic challenges. It is difficult to build a system that transmits a traffic signal violation that can increase production costs that the manufacturer cannot deal with.

**6. SECURITY IN VEHICULAR NETWORK**

**6.1 Inspections:**

In most of the United States States, inspection of all vehicles must pass once a year. This annual trip to the mechanic offers interesting security maintenance options as well as typical maintenance. The inspection process gives the system a chance to return to a known basic state and acts as a firebreak against worms and virus infections. These inspections can also be included in the standard maintenance package whenever a driver enters the vehicle for a tune - up.

**6.2 Honest Majority:**

Another benefit of vehicle networks is that most drivers will probably be honest. This is reinforced by the fact that few people feel comfortable with their vehicles, so that most drivers simply accept the default settings. If vehicles have adequate safeguards<sup>2</sup> against worms and viruses, drivers ' trustworthiness becomes vehicles that correctly adhere to established protocols.

**6.3 Registration central:**

In contrast to ad hoc networks, all nodes in a vehicle network must be registered with a central authority, such as the state (in the US). These institutions have already developed extensive infrastructure to track and manage these registrations, and in the long term, we could use this existing bureaucracy to improve the safety of vehicle applications. However, given the vast nature of the existing infrastructure, it takes years of effort to make changes and requires considerable funding.

**6.4 Access Controlled:**

There are already access control mechanisms for many parts of the transport system. For instance, toll streets and numerous bridges have controlled passage and leave focuses, so it might be down to earth to furnish these areas with the vital foundation to distribute ephemeral identities and/or keys to enable vehicles to communicate while on the controlled road.

**7. APPLICATIONS****7.1 Authenticated Message Origin Location:**

The location will play an important role in many vehicle applications, making it essential to determine whether a message originated at a particular location. It would also prevent an opponent from using another communication medium (e.g. cellular) to replay a message heard in one location as if it originated in another location, thus preventing the types of attacks in sensor networks by wormholes[8].

**7.2 Traffic Congestion Detection**

In this application, vehicles recognize when the quantity of neighboring vehicles surpasses a certain limit (and additionally their normal speed dips under a given edge), and after that hand-off this tally to vehicles moving toward the area of the congestion.

**7.3 Warning System For Deceleration**

In this application, if a vehicle significantly reduces its speed, a warning will be broadcast along to other vehicles with its current position and speed. Beneficiaries will communicate the message to vehicles and any vehicles their d will be alerted directly behind the vehicle in question Alert their drivers by means of visual and/or audio signals.

**8. Conclusion**

In this paper, we proposed a BC-based security architecture for smart connected vehicles capable of supporting a wide range of (future) automotive applications. We evaluated our architecture utilizing a proof-of-idea usage of a remote SW refresh framework and utilize the last to demonstrate the relevance of our design and also its advantages contrasted with a declaration based framework.

The privacy of users is guaranteed through the use of changing public keys (PK). The security of our architecture is largely due to the strong security features of the BC technology underlying it. The OBMs also provide access control for transactions sent to the members of their clusters.

The architecture supports emerging automotive services by providing a safe and reliable way to

exchange data while safeguarding the safety of the end user.

**9. REFERENCES**

1. Xiong, Z.; Sheng, H.; Rong, W.; Cooper, D.E. Intelligent transportation systems for smart cities: A progress review. *Sci. China Inf. Sci.* 2012, 55, 2908–2914.
2. Bowerman, B.; Braverman, J.; Taylor, J.; Todosow, H.; von Wimmersperg, U. The vision of a smart city. In *Proceedings of the 2nd International Life Extension Technology Workshop*, Paris, France, 28 September 2000; Volume 28.
3. Su, K.; Li, J.; Fu, H. Smart city and the applications. In *Proceedings of the 2011 International Conference on Electronics, Communications and Control (ICECC)*, Zhejiang, China, 9–11 September 2011; pp. 1028–1031.
4. Hollands, R.G. Will the real smart city please stand up? *Intelligent, progressive or entrepreneurial? City* 2008, 12, 303–320.
5. A. Dorri, S. S. Kanhere, and R. Jurdak, "Towards an optimized blockchain for iot," in *2nd International Conference on Internet-of-Things Design and Implementation*. ACM, 2017, pp. 173–178.
6. F. Tschorsch and B. Scheuermann, "Bitcoin and beyond: A technical survey on decentralized digital currencies," *IEEE Communications Surveys Tutorials*, vol. 18, no. 3, pp. 2084–2123, 2016.
7. S. Nakamoto, "Bitcoin: A peer-to-peer electronic cash system," <http://bitcoin.org/bitcoin.pdf>, retrieved 25 jun 2018," 2008.
8. Yih-Chun Hu, Adrian Perrig, and David B. Johnson. Packet leashes: A defense against wormhole attacks in wireless networks. In *Proc. of IEEE INFOCOM*, April 2003.
9. Hancke, G.; Silva, B.; Hancke, G., Jr. The Role of Advanced Sensing in Smart Cities. *Sensors* 2012, 13, 393–425. [CrossRef] [PubMed]
10. Kyriazis, D.; Varvarigou, T.; White, D.; Rossi, A.; Cooper, J. Sustainable smart city IoT applications: Heat and electricity management amp; Eco-conscious cruise control for public transportation. In *Proceedings of the 2013 IEEE 14th International Symposium on "A World of Wireless, Mobile and Multimedia Networks" (WoWMoM)*, Madrid, Spain, 4–7 June 2013; pp. 1–5.
11. Zanella, A.; Bui, N.; Castellani, A.; Vangelista, L.; Zorzi, M. Internet of Things for Smart Cities. *IEEE Internet Things J.* 2014, 1, 22–32.
12. Elmangoush, A.; Alhazmi, A.; Magedanz, T.; Schuch, W.; Estevez, C.; Ehijo, A.; Wu, J.; Nguyen, T.; Ventura, N.; Mwangama, J.; et al. Towards Unified Smart City Communication Platforms. In *Proceedings of the Workshop on Research in*

- Information Systems and Technologies, Chillán, Chile, 16 October 2015.
13. Satoshi Nakamoto, "Bitcoin: A peer-to-peer electronic cash system", 2008, [https://s3.amazonaws.com/academia.edu.documents/32413652/Bitcoin\\_P2P\\_electronic\\_cash\\_system.pdf?AWSAccessKeyId=AKIAIWOWYYGZ2Y53UL3A&Expires=1506052605&Signature=ua%2FsjZRbx0wc7Tx35Kl1dwUwmqo%3D&responsecontentdisposition=inline%3B%20filename%3DBitcoin\\_A\\_Peer-toPeer\\_Electronic\\_Cash\\_S.pdf](https://s3.amazonaws.com/academia.edu.documents/32413652/Bitcoin_P2P_electronic_cash_system.pdf?AWSAccessKeyId=AKIAIWOWYYGZ2Y53UL3A&Expires=1506052605&Signature=ua%2FsjZRbx0wc7Tx35Kl1dwUwmqo%3D&responsecontentdisposition=inline%3B%20filename%3DBitcoin_A_Peer-toPeer_Electronic_Cash_S.pdf), accessed on Sep 22, 2017.
  14. Inspiring, <http://www.inspiring.co.uk>, accessed on Sep 20, 2017.
  15. Slock, <https://slock.it>, accessed on Sep 20, 2017.
  16. J.-P. Hubaux, S. Capkun, and J. Luo, "The Security and Privacy of Smart Vehicles," IEEE Security and Privacy Mag., vol. 2, no. 3, May-June 2004, pp. 49-55.
  17. B. Parno and A. Perrig, "Challenges in Securing Vehicular Networks," Wksp. Hot Topics in Networks (HotNetsIV), 2005.
  18. Jean-Pierre Hubaux, Srđan Ćapkun, and Jun Luo. The security and privacy of smart vehicles. IEEE Security & Privacy Magazine, 2(3):49-55, May-June 2004.
  19. T. Bakıcı, E. Almirall, J. Wareham, A smart city initiative: the case of Barcelona, J. Knowl.Econ.(2012),<http://dx.doi.org/10.1007/s13132-012-0084-9>(Available at <http://www.springerlink.com/content/9318pq8q61r06345/>)

# KEYSTROKE DYNAMICS USER IDENTIFICATION USING PAIRWISE CLIENT COUPLING

D.Tejaswi\* & Rajasekar Rangasamy\*\*

\* PG Scholar, Department of Computer Science and Engineering,

\*\* Professor, Department of Computer Science and Engineering, St. Peter's Engineering College, Hyderabad, Telangana, India.

**ABSTRACT:** In this paper due to the increasing vulnerabilities in the internet, security alone isn't sufficient to keep a rupture, however digital crime scene investigation and cyber intelligence is also required to prevent future assaults or to identify the potential attacker. The unpretentious and incognito nature of biometric information gathering of keystroke dynamics has a high potential for use in cyber forensics or cyber intelligence and crime scene investigation or digital knowledge. The keystroke dynamics is a biometric assumption that different people typify in a unique way. The information accessing from computer systems is normally controlled by client accounts with usernames and passwords. If the set of data falls into the wrong hands, such a scheme has little security. For example fingerprints, can be used to strengthen security; however they require very expensive additional hardware. Keystroke dynamics with no additional hardware can be used. Keystroke dynamics is for the most part applicable to verification and identification also possible. In verification it is known who the client is supposed to be and the biometric system should verify if the user is who he claims to be in identification, the biometric The system should identify the client with keystroke dynamics without additional knowledge. This paper examines the usefulness of keystroke dynamics to determine the user's identity. We propose three plans for user identification when entering a keyboard. We use different machine learning algorithms in conjunction with the proposed user coupling technology. In particular, we show that combined user coupling in a bottom - up tree structure scheme provides the best performance in terms of both precision and time complexity. The techniques proposed are validated by keystroke data. Lastly, we also examined the performance of the identification system and demonstrated that the performance was not optimal, as expected.

**Keywords:** Pairwise Client Coupling; Keystroke Dynamics, User Identification, Behavioural Biometrics; Cyber-forensics or cyber intelligence, Biometrics, pattern recognition, computer security.

## 1.INTRODUCTION

Keystroke Dynamics (KD) is a well established behavioral biometric modality due to the unobtrusive nature of biometric data collection, low computational complexity and no special hardware required for data collection [1], [2], [3]. Keystroke dynamics are identified by the writing dynamics of the user or client, which are considered to be unique to a large extent among different people. Keystroke dynamics are known by a few names: keyboard dynamics, keystroke analysis, biometrics typing and rhythm typing. The biometric keystroke dynamics system is very high. The keystroke dynamics are mostly applicable for verification; it is also possible to identify them. It is known who the user should be and the biometric system should verify whether the user is the person he professes to be. When recognizing, the biometric system should recognize the client, using just keystroke dynamics, without any extra information. Most keystroke dynamics applications are in the field of verification.

Keystroke dynamics is a well-explored research domain in authentication, where the research problem is a two class problem i.e. legitimate or imposter user. Finally, an example where identification could be of use is in a chat room, where the behavior of an unknown person is compared to the known profiles.

For instance, if a person is demonstrating pedophile behavior, then his or her typing behavior can be compared to the behavior of a lot of known pedophiles.

This paper's primary commitments are as follows: We propose three distinctive identification schemes in this paper. These schemes are based on the combination of user coupling, Let us consider the Example is multi-class pattern identification problem, it will be divided into several two-class problems. These schemes could be useful for user identification.

Extensive analysis was carried out with a keystroke data set based on the online test; this data set was collected from 64 users with three different typing methods. We have used another

keystroke data set with our optimal settings to approve our research. We analyzed both open-set and close-set settings and showed that our optimal settings outperform state-of - the-art research.

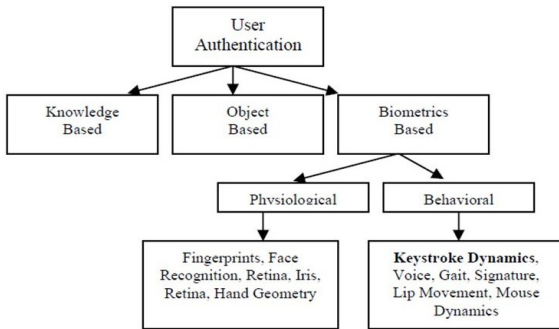


**Fig1: User authentication approach using Keystroke Dynamics**

**2. KEYSTROKE DYNAMICS AUTHENTICATION TECHNIQUES**

**FIELD:**

The invention concerns keystroke dynamics authentication. In Specifically, the invention identifies with data manipulations that offer enhanced performance for authentication systems for keystroke dynamics.

**BACKGROUND**

Computer systems often contain essential and delicate information, control access to or play an integral role in securing physical sites and assets. Computer security depends heavily on secret passwords before. Unfortunately, clients frequently choose passwords that are anything but easy to guess or easy to determine using comprehensive searches or other means. When more complex passwords are allocated, clients may find them difficult to remember, so they can write them down, creating new, different security vulnerability.

Different approaches have been attempted to enhance the security of computer systems. However, an authorized client can still allow an unauthorized client to use a system by simply giving the unauthorized user the token and secret code. The estimation of unique physical characteristics (" biometrics ") of users to identify authorized users depends on other authentication methods. For example, fingerprints, Voice patterns and retinal images have all been used with some Success. However, these strategies typically require special hardware to implement that is keystroke.

In KD, clients are identified or authenticated dependent on the manner in which they type on a keyboard. A KD based authentication or

identification system is low-cost and easy to implement because most of systems are software based. In such a system, the keystroke timing information must be captured for pattern analysis [4]. KD is a well establish biometrics for static, periodic or continuous authentication [5], [6], [7]. Table I shows state-of - the-art KD research depending on the different objectives (e.g. authentication or identification) with different functionalities, i.e. static (user authentication is based on the password or passphrase type rhythm), Periodic (user re-authentication after a fixed amount of data, e.g. after 500 keystrokes) and continuous (user re-authentication based on typing behavior continually).

	Authentication	Identific ation
Static	[6],[7],[16],[17],[18],[19]	[13],[14]
Periodi c	[10],[11],[12]	[15]
Contin uous	[8]	[20]

**Fig2: State-of-the-art Keystroke research**

In [8] has an artificial neural network technique been used for real time user identification using Keystroke dynamics. This approach was validated experimentally based on data of 6 users, each typing a 15 character phrase 20 times. The achieved identification accuracy was 97.8%. In [9] a Euclidean distance based nearest neighbor classifier has been used for personal identification and an accuracy of 99.3% for 36 users was achieved. Several researchers have participated in this competition and proposed different techniques to improve the baseline performance.

**3. CLASSIFIER:**

Client identification by analyzing the client's keystroke behavior profiles is challenging due to limited data, large intra-class variations and the sparse nature of the information. We observed that statistical analysis (i.e. distance based classifiers) is successful for authentication but, fails to achieve good results in the identification. Therefore we have used four different classifiers in our research.

**1) Artificial Neural Network (ANN):**

ANN is a combination of multiple artificial neurons which can be used for classification and regression analysis. We have used the Scaled Conjugate Gradient algorithm which is efficient to optimize the cost function and also it will reduce the ANN training time.

**2) Counter-Propagation Artificial Neural Network (CPANN):**

CPANN is a hybrid learning mechanism dependent on ANN to deal with supervised learning problems. In CPANN, the output layer is added to the Kohonen layer which is very similar to Self Organizing Maps and provides both the advantages of supervised and unsupervised learning.

**3) Support Vector Machine (SVM):**

SVM is a very well-known supervised learning algorithm which can be used for classification problems. The SV is the data point of the various classes closest to the decision line.

**4) Decision Tree (DT):mi**

DT is a predictive learning model based on a tree structure that maps the features of an item's observation to the target objective value where leaves are class labels and branches are combinations of features leading to class labels.

**4.SYSTEM PIPELINE**

To achieve better performance, we applied the combination of User Coupling (CUC) technique using the above mentioned classifiers (in background section).

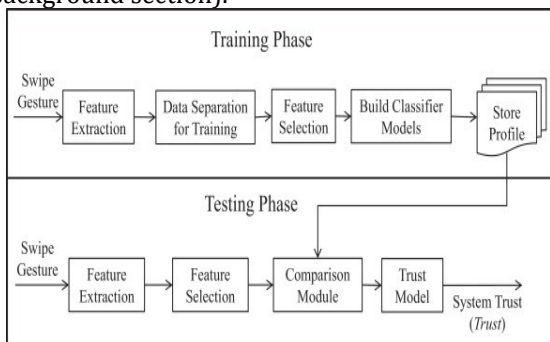


**Fig3: Block diagram of Pipe line**

**Pair wise Client Training Data Preparation:**

Figure4 shows a case of a multi-class (i.e. N class) training dataset for the preparation of conventional training data. In this example,  $FV_i^q$  represents the feature vector of user  $i$  from  $q$ th sample, where  $i = 1, 2, \dots, N$ ,  $q = 1, 2, \dots, n$  and  $n$  is the total number of training samples for user  $i$ . The last column represents the class label i.e. a value between 1 and  $N$ . we came up with a solution called PCC, where the multi-class classification problem will be divided into several two-class classification problems.

Feature Vector	Class Label
$FV^1$	1
1	
...	...
$FV^1$	1

$n$	
$FV^2$	2
1	
...	...
$FV^2$	2
$n$	
...	...
$FVN-1$	N-1
1	
...	...
$FVN-1$	N-1
$n$	
...	...
$N$	N
$FVn$	

**Fig 4: Multi-class (i.e. N class) training Dataset for Conventional Training Data Preparation**

$PM_2^1$	$PM_3^1$	...	$PM_{N-1}^1$	$PM_N^1$
$PM_1^2$	$PM_3^2$	...	$PM_{N-1}^2$	$PM_N^2$
$PM_1^3$	$PM_2^3$	...	$PM_{N-1}^3$	$PM_N^3$
$PM_1^4$	$PM_2^4$	...	$PM_{N-1}^4$	$PM_N^4$
...	...	...	...	...
$PM_{N-1}^N$	$PM_{N-2}^N$	...	$PM_{N-2}^N$	$PM_{N-1}^N$
$PM_1^N$	$PM_2^N$	...	$PM_{N-2}^N$	$PM_{N-1}^N$

**Fig 5: Pairwise training models for multi-class PUC.**

Figure 3 shows a pictorial representation of a pairwise training models for multi-class PUC. In this example, we can see that multiple training models are created (denoted by  $PM^i$ ) for user  $i$  and  $j$ , where  $i = 1, 2, \dots, N$  and  $j = [1, 2, \dots, N]$  [i].

Three different identification systems (i.e. S1, S2 and S3) were developed for the examination and decision module.

In Scheme S1, we will randomly arrange the set of clients into pairs and we will determine for each pair (client  $i$ , client  $j$ ) whether the information fits better with the client  $i$  or client  $j$  profile.

In Scheme S2, we will randomly select  $k$  other clients for each client  $i$  and determine the mean score for client  $i$  when comparing the test data in  $k$  pairwise examinations with the randomly selected other clients.

Scheme S3 depends on twice applying Scheme S2. The first S2 system is used to reduce the number

of potential users from the first N users to c clients only. The remaining c clients are compared in a complete comparison in the second step.

**Scheme (S1):**

*Scheme 1 (S1)* where consider the total number of users is 20 and the required rank is 1, i.e.  $N = 20$  and  $r = 1$ . the pairs are created in increasing order but we have to selected these pairs randomly in each round. Rank depends on average score maximization i.e.  $S_i > S_j$  for m number of keystrokes where the number of T1 comparisons is  $T1(N, r) = N - r$  when it starts with N clients and stops at rank r.

$$S = \frac{1}{m} \sum_{sc} \text{ and } S = 1 - S$$

Algorithm 1: Algorithm for Scheme 1

**Input:**  $PM^i$  The pairwise classifier model for any given classifier, where  $i \in I = \{1, 2, 3, \dots, N\}$  N is the number of users and  $j \in J = I - \{i\}$ ;  $\Gamma$  The set of test keystrokes, where  $|\Gamma| = m$ , i.e. m is the number of performed keystrokes;  $r$  The required rank.

**Output:**  $User_{rat\_score}$

```

1 while |I| > r do
2   k = floor(|I|/2); T = I; SC = {}
3   while |I| >= k do
4     i = random(I); T = T - {i}; j = random(T); T = T - {j}
5     Calculate score sc (i.e.  $sc_p = P(y_p|H)$  where  $y_p$  is the feature vector after feature selection of the performed
        keystroke p and  $H$  is the hypothesis for the user i) for all test keystrokes  $\Gamma$  from the selected pair  $PM^i$  with
        given classifier(s).
6     So,  $S = \frac{1}{m} \sum_{p \in \Gamma} sc_p$ ;  $S_i = 1 - S$ 
7     if  $S_i > S_j$  then
8       I = I - {j}; SC = SC union ({i, S})
9     else
10      I = I - {i}; SC = SC union ({j, S})
11    end
12  end
13 end
14  $User_{rat\_score} = SC$ 
    
```

**Scheme 2 (S2):**

The below Algorithm 2 for *Scheme 2 (S2)* where  $k = 6$  and  $r = 1$ . When comparing the subject and  $i^{th}$  subject, we initially select k pairs from the set  $PM^i$  randomly and calculate the classification scores for each of these pairs. This gives each classifier an aggregate value of k m.

At that point, we get the resulting score for the  $i^{th}$  client by the number of comparisons T2 for this scheme is independent of r, but it depends on N and k. In specifically we have  $T_2(N, k) = N \times k$ .

$$S^i = \frac{1}{m \times k} \sum_{q=1}^k \sum_{p=1}^m sc_p^q$$

Algorithm 2: Algorithm for Scheme 2

**Input:**  $PM^i$  The pairwise classifier model for any given classifier, where  $i \in I = \{1, 2, 3, \dots, N\}$  N is the number of users and  $j \in J = I - \{i\}$ ;  $\Gamma$  The set of test keystrokes, where  $|\Gamma| = m$ , i.e. m is the number of performed keystrokes;  $k$  The number of comparison and  $k < N$ ;  $r$  The required rank.

**Output:**  $User_{rat\_score}$

```

1 SC = {}; T = I
2 while |I| = 0 do
3   i = {i}; I = I - {i}; J = T - {i}; S = 0
4   while k > 0 do
5     j = random(J); J = J - {j}
6     Calculate score sc (i.e.  $sc_p = P(y_p|H)$  where  $y_p$  is the feature vector after feature selection of the performed
        keystroke p and  $H$  is the hypothesis for the user i) for all test keystrokes  $\Gamma$  from the selected pair  $PM^i$  with
        given classifier(s).
7     So,  $S = S + \frac{1}{m \times k} \sum_{p=1}^m sc_p$ ;  $k = k - 1$ 
8   end
9   SC = SC union ({i, S})
10 end
11 X = {i(i, S) in SC}
12  $X_i \in X$  where  $|X_i| = r$ 
13  $User_{rat\_score} = \{(i, S) \min \{S^i \in X_i\} > \max \{S^j \in X - X_i\}\}$ 
    
```

**Scheme3 (S3):**

Below algorithm for Scheme (S3). Let  $\Delta = \{\delta_1, \delta_2, \dots, \delta_c\}$  be the set of the Rank-c clients subsequent to applying S2 with  $r = c$ , where  $\Delta$  subset or equivalent to  $\{1, 2, \dots, N\}$ . Now we repeat S2 with the set of  $\Delta$  users with a fixed value of k, i.e.  $k = c - 1$ . This scheme can be considered as using S2 for a re-ranking process after the initial S2 scheme. For S3 the number of comparisons  $T_3$  depends on N, k and c. To be precise we have  $T_3(N, k, c) = T_2(N, k) + c \times (c - 1)$ .

Algorithm 3: Algorithm for Scheme 3

**Input:**  $PM^i$  The pairwise classifier model for any given classifier, where  $i \in I = \{1, 2, 3, \dots, N\}$  N is the number of users and  $j \in J = I - \{i\}$ ;  $\Gamma$  The set of test keystrokes, where  $|\Gamma| = m$ , i.e. m is the number of performed keystrokes;  $k$  The number of comparison for Algorithm 2 and  $k < N$ ;  $c$  The rank correction;  $r$  The required rank and  $r < c$ .

**Output:**  $User_{rat\_score}$

```

1 T = The set of Rank-c users after applying Algorithm 2
2 SC = {}; I = T
3 while |I| = 0 do
4   i = {i}; I = I - {i}; J = T - {i}; t = J; S = 0
5   while t > 0 do
6     j = {j}
7     Calculate score sc (i.e.  $sc_p = P(y_p|H)$  where  $y_p$  is the feature vector after feature selection of the performed
        keystroke p and  $H$  is the hypothesis for the user i) for all test keystrokes  $\Gamma$  from the selected pair  $PM^i$  with
        given classifier(s).
8     So,  $S = S + \frac{1}{m \times k} \sum_{p=1}^m sc_p$ ;  $t = t - 1$ 
9   end
10  SC = SC union ({i, S})
11 end
12 X = {i(i, S) in SC}
13  $X_i \in X$  where  $|X_i| = r$ 
14  $User_{rat\_score} = \{(i, S) \min \{S^i \in X_i\} > \max \{S^j \in X - X_i\}\}$ 
    
```

ACCURACY(%)				
	AN N	CPAN N	SV M	DT
K=5	31.8	56.5	52	58.6
K=15	41.4	58.4	56.3	61.6
K=25	41.8	58.6	58.8	61.4

fig 6:obtained final results from s3 for different k values.

**5. FEATURES USED WITH KEYSTROKE DYNAMICS**

The keystroke dynamics include various estimates that can be distinguished by pressing keys on the keyboard.

1. Measurement possibilities include:
2. Latency between consecutive keystrokes.
3. Keystroke duration,
4. hold-time.
5. Type speed overall.

Frequency of errors (how often backspace is used by the user). The habit to use additional keys in the keyboard, e.g. write numbers with the number pad. In which order the user presses the keys when writing letters of capital, the letter key is shifted or first released.

Statistics can be global, i.e. combined for all keys, or accumulated independently for each key or keystroke. Most applications only measure latency between successive keystrokes or keystroke durations. In Figure3 an example of writing word "password" several times and measuring latencies between keystrokes. Timings have been measured for three different persons. There are clear deference in latencies and their standard deviations.

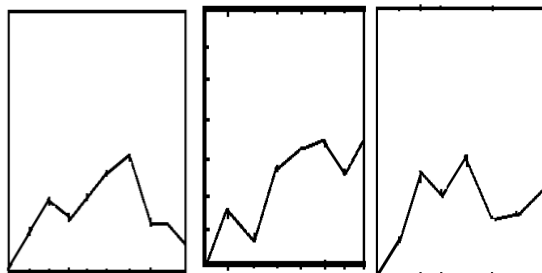


Fig7: Latency between keystrokes when three different people write the word "password" The word has been written repeatedly. The lines represent average latencies, standard deviations are the error bars.

**6. IMPLEMENTATION**

Authentication with keystroke dynamics can be achieved by training a certain algorithm with the typing pattern of a person. In this section, some of the most famous implementations are reviewed and separated into categories depending on their functionality, local or web, and the scope of their development, academic or commercial.

**Local Authentication: (from keystroke pdf)**

Keystroke dynamic local authentication suggests a locally installed program or some sort of mechanism, with all computations and data storage taking place locally, that might authenticate user logins, text typing etc.

Authentication through keystroke dynamics has mostly been achieved with the help of pattern recognition systems, with the most common of them listed bellow.

- Statistical Models [10][11].
- Neural networks [12].
- Fuzzy logic [13][14]
- Support-vector machines [15]

**Web Authentication**

Web keystroke dynamic authentication on the other hand refers to authentication on websites, web applications etc. The data and the computations might take place either on a remote server which can only be contacted through some kind of connection such as a network or the Internet or locally through an installed program.

There have not been as many researches in web authentication as in local authentication. Some of them will be listed bellow, depending on their pattern recognition approach.

- Statistical Models [10]
- Neural Networks

**7. OPERATIONAL PHASES**

Keystroke dynamics; consist of three operational phases, the data gathering, the training and the classification procedure.

**Raw Data Collection:**

Data collection is the first phase of a keystroke dynamic system. It is essentially the phase where the mechanism collects characteristic data and computes the features of one or more individuals. More specifically, in keystroke dynamics, data collection refers to the process of saving keystroke timings, such as the press and release time of a user.

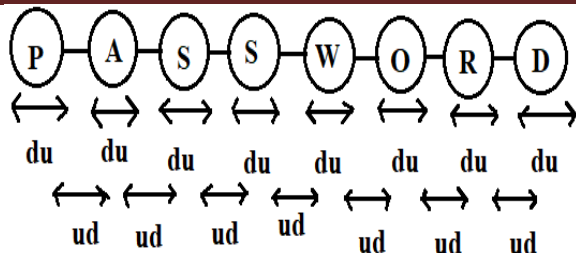


**Fig 8: Some of the most important features of a keystroke sensitive password.**

**Types of Errors in Keystroke Dynamics**

They are always statistical errors in recognition patterns, thus any algorithm used in keystroke dynamic authentication or identification. Those errors rates define the quality of the application of a keystroke dynamic system and a biometric system in general and its electiveness in distinguishing people from each other. A set of metrics have been defined, in order to calculate the accuracy and the efficiency of biometric system. Those types of errors are listed as follows.

**FAR (False Acceptance Rate):**

It represents the probability of an authentication system providing access to an impostor. The probability of that can be very low in physiological biometrics, but in the case of behavioral biometrics such as keystroke dynamics, it is something very common and it relies upon the strictness of the system.

**FRR (False Rejection Rate):**

The false rejection rate represents the probability of an authentication system denying access to the legitimate user. Obviously, it also depends on the strictness of the system.

An important thing that should be mentioned is that FAR, FRR respectively, have inverse relationships.

Biometric	FAR	FRR	Subjects	Comments
Face	1%	10%	37437	Varied light, indoor/outdoor
Finger print	2%	2%	25000	Rotation and exaggerated skin distortion
Hand geometry	2%	2%	129	With rings and improper placement
Iris	.94 %	.99 %	1224	Indoor environment
Keystrokes	7%	.1%	15	During 6 months period
Voice	2%	10%	30	Text dependent and multilingual

**Fig9: Biometric Technique Relation between FAR and FRR**

**8. CONCLUSION**

In this research, Keystrokes dynamic authentication is an underrated authentication mechanism, "As a service" was a basic concept behind the implementation, so that users and websites have the opportunity to access these technologies without any additional infrastructure or costs, in hopes of it being more accessible to the wider public. We have focused on identifying a person based on the person's typing behavior. A comprehensive analysis was carried out in an online test dataset based on keystroke dynamics and achieved approximately 7 percent better identification.

We proposed three identification schemes with combination of user coupling and shown that bottom up tree structure based scheme gives the best results. In the future, we plan to perform an experiment on real world cyber-forensics data and investigate how it can be used as forensics evidence in court. In the future, we will also investigate how well we can improve the performance for one handed typing and the scalability of our proposed schemes.

**9. REFERENCES:**

1. R. V. Yampolskiy and V. Govindaraju, "Behavioural biometrics: a survey and classification," *Int. Journal of Biometrics*, vol. 1, pp. 81-113, 2008.
2. S. Bhatt and T. Santhanam, "Keystroke dynamics for biometric authentication - a survey," in *Int. Conf. on Pattern Recognition, Informatics and Mobile Engineering (PRIME'13)*, 2013, pp. 17-23.
3. M. Karnan, M. Akila, and N. Krishnaraj, "Biometric personal authentication using keystroke dynamics: A review," *Applied Soft Computing*, vol. 11, no. 2, pp. 1565 - 1573, 2011.
4. J. Sucupira, L.H.R., M. Lizarraga, L. Ling, and J. B. T. Yabu- Uti, "User authentication through typing biometrics features," *IEEE Trans. on Signal Processing*, vol. 53, no. 2, pp. 851-855, 2005.
5. F. Bergadano, D. Gunetti, and C. Picardi, "Identity verification through dynamic keystroke analysis," *Intelligent Data Analysis*, vol. 7, no. 5, pp. 469-496, 2003.
6. K. S. Killourhy, "A scientific understanding of keystroke dynamics," Ph.D. dissertation, Carnegie Mellon University, January 2012.
7. P. Bours and S. Mondal, *Continuous Authentication with Keystroke Dynamics*.
8. M. Obaidat and D. Macchiarolo, "An online neural network system for computer access

- security," IEEE Trans. on Industrial Electronics, vol. 40, no. 2, pp. 235-242, 1993.
9. C.C.Tappert, M. Villani, and S.-H. Cha, "Keystroke biometric identification and authentication on long-text input," Behavioral Biometrics for Human Identification: Intelligent Application
  10. G.E. Forsen, M.R. Nelson, R.J. Staron, PATTERN ANALYSIS, and RECOGNITION CORP ROME N Y. Personal Attributes Authentication Techniques. Defense Technical Information Center, 1977. URL <http://books.google.gr/books?id=tbs40AAACAAJ>.
  11. Rick Joyce and Gopal Gupta. Identity authentication based on keystroke latencies. Commun. ACM, 33(2):168-176, 1990. ISSN 0001-0782. URL <http://dx.doi.org/10.1145/75577.75582>.
  12. M. S. Obaidat and B. Sadoun. Verification of computer users using keystroke dynamics. Trans. Sys. Man Cyber. Part B, 27(2):261-269, 1997. ISSN 10834419. doi: 10.1109/3477.558812. URL <http://dx.doi.org/10.1109/3477.558812>.
  13. Bassam Hussien, Robert McLaren, and Saleh Bleha. An application of fuzzy algorithms in a computer access security system. Pattern Recognition Letters, 9(1):39-43, 1989. URL <http://dblp.uni-trier.de/db/journals/prl/prl9.html#HussienMB89>.
  14. Willem G. de Ru and Jan H. P. Eloff. Enhanced password authentication through fuzzy logic. IEEE Expert: Intelligent Systems and Their Applications, 12(6):38-45, November 1997. ISSN 0885-9000. doi: 10.1109/64.642960. URL <http://dx.doi.org/10.1109/64.642960>.

# Aggressive and Community Auditing System with Clear Agreement for Cloud Data

Naveena Vemula\* & Subhashini Peneti\*\*

\*PG Student, Department of CSE, Malla Reddy College of Engineering, Hyderabad, India.

\*\*Assistant Professor, Department of CSE, Malla Reddy College of Engineering, Hyderabad, India.

**ABSTRACT:** Cloud users no longer physically possess their data, so how to ensure the integrity of their outsourced data becomes a Challenging task. Recently proposed schemes such as “provable data possession” and “proofs of retrievability” are designed to address this problem, but they are designed to audit static archive data and therefore lack of data dynamics support. Moreover, threat models in these schemes usually assume an honest data owner and focus on detecting a dishonest cloud service provider despite the fact that clients may also misbehave. This paper proposes a public auditing scheme with data dynamics support and fairness arbitration of potential disputes. In particular, we design an index switcher to eliminate the limitation of index usage in tag computation in current schemes and achieve efficient handling of data dynamics.

**Keywords:** Integrity, auditing, verifiability, arbitration, fairness.

## Introduction

Cloud computing is the use of computing resources (hardware and software) that are delivered as a service over a network (typically the Internet). The name comes from the common use of a cloud-shaped symbol as an abstraction for the complex infrastructure it contains in system diagrams. Cloud computing entrusts remote services with a user's data, software and computation. Cloud computing consists of hardware and software resources made available on the Internet as managed third-party services. These services typically provide access to advanced software applications and high-end networks of server computers.

The goal of cloud computing is to apply traditional supercomputing, or high-performance computing power, normally used by military and research facilities, to perform tens of trillions of computations per second, in consumer-oriented applications such as financial portfolios, to deliver personalized information, to provide data storage or to power large, immersive computer games. The cloud computing uses networks of large groups of servers typically running low-cost consumer PC technology with specialized connections to spread data-processing chores across them. This shared IT infrastructure contains large pools of systems that are linked together. Often, virtualization techniques are used to maximize the power of cloud computing.

A. Characteristics and Services Models:

The salient characteristics of cloud computing based on the definitions provided by the National Institute of Standards and Terminology (NIST) are outlined below:

On-demand self-service: A consumer can unilaterally provision computing capabilities, such as server time and network storage, as needed automatically without requiring human interaction with each service's provider[9].

Broad network access: Capabilities are available over the network and accessed through standard mechanisms that promote use by heterogeneous thin or thick client platforms (e.g., mobile phones, laptops, and PDAs).

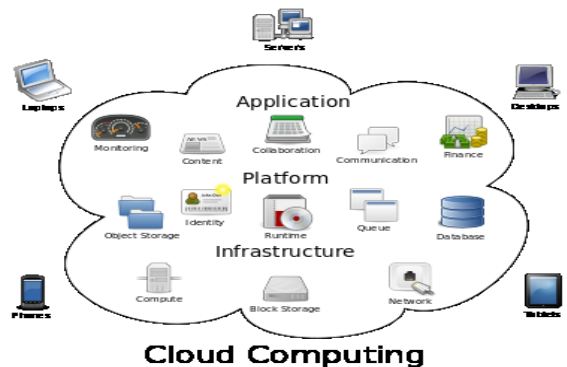


Figure 1. Structure of cloud computing

B. Characteristics and Services Models:

The salient characteristics of cloud computing based on the definitions provided by the National Institute of Standards and Terminology (NIST) are outlined below:

On-demand self-service: A consumer can unilaterally provision computing capabilities, such as server time and network storage, as needed automatically without requiring human interaction with each service's provider.

- Broad network access: Capabilities are available over the network and accessed through standard mechanisms that promote use by heterogeneous thin or thick client platforms (e.g., mobile phones, laptops, and PDAs).
- Resource pooling: The provider's computing resources are pooled to serve multiple consumers using a multi-tenant model, with different physical and virtual resources dynamically assigned and reassigned according to consumer demand. There is a sense of location-independence in that the customer generally has no control or knowledge over the exact location of the provided resources but may be able to specify location at a higher level of abstraction (e.g., country, state, or data center). Examples of resources include storage, processing, memory, network bandwidth, and virtual machines.
- Rapid elasticity: Capabilities can be rapidly and elastically provisioned, in some cases automatically, to quickly scale out and rapidly released to quickly scale in. To the consumer, the capabilities available for provisioning often appear to be unlimited and can be purchased in any quantity at any time.
- Measured service: Cloud systems automatically control and optimize resource use by leveraging a metering capability at some level of abstraction appropriate to the type of service (e.g., storage, processing, bandwidth, and active user accounts). Resource usage can be managed, controlled, and reported providing transparency for both the provider and consumer of the utilized service.

#### C. Services Models:

Cloud Computing comprises three different service models, namely Infrastructure-as-a-Service (IaaS), Platform-as-a-Service (PaaS), and Software-as-a-Service (SaaS). The three service models or layer are completed by an end user layer that encapsulates the end user perspective on cloud services. The model is shown in figure below. If a cloud user accesses services on the

infrastructure layer, for instance, she can run her own applications on the resources of a cloud infrastructure and remain responsible for the support, maintenance, and security of these applications herself. If she accesses a service on the application layer, these tasks are normally taken care of by the cloud service provider.

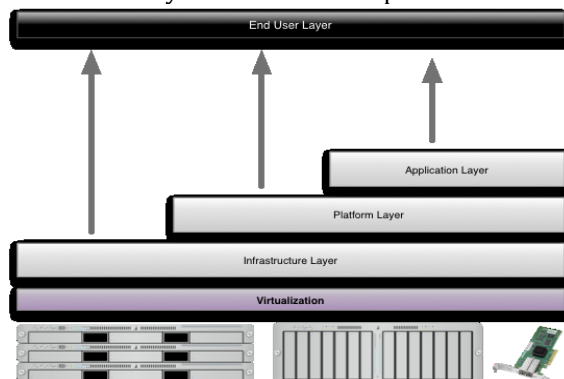


Figure 2. Structure of service models

#### D. Benefits of cloud computing:

1. Achieve economies of scale – increase volume output or productivity with fewer people. Your cost per unit, project or product plummets.
2. Reduce spending on technology infrastructure. Maintain easy access to your information with minimal upfront spending. Pay as you go (weekly, quarterly or yearly), based on demand.
3. Globalize your workforce on the cheap. People worldwide can access the cloud, provided they have an Internet connection.
4. Streamline processes. Get more work done in less time with less people.
5. Reduce capital costs. There's no need to spend big money on hardware, software or licensing fees.
6. Improve accessibility. You have access anytime, anywhere, making your life so much easier!
7. Monitor projects more effectively. Stay within budget and ahead of completion cycle times.
8. Less personnel training is needed. It takes fewer people to do more work on a cloud, with a minimal learning curve on hardware and software issues.
9. Minimize licensing new software. Stretch and grow without the need to buy expensive software licenses or programs.
10. Improve flexibility. You can change direction without serious "people" or "financial" issues at stake.

## II. Literature Survey

This section provides different types of data Integrity auditing schemes:

### A. Data Integrity Auditing Schemes:

1. Remote integrity checking
2. Demonstrating data possessing and uncheatable data transfer
3. Pors: Proofs of retrievability for large file
4. Provable data possession at untrusted stores
5. Compact proofs of retrievability

#### a) Remote integrity checking

This paper analyzes the problem of checking the integrity of files stored on remote servers. Since servers are prone to successful attacks by malicious hackers, the result of simple integrity checks run on the servers cannot be trusted. Conversely, downloading the files from the server to the verifying host is impractical. Two solutions are proposed, based on challenge-response protocols [1].

#### b) Demonstrating data possessing and uncheatable data transfer

We observe that a certain RSA-based secure hash function is homomorphic. We describe a protocol based on this hash function which prevents 'cheating' in a data transfer transaction, while placing little burden on the trusted third party that oversees the protocol. We also describe a cryptographic protocol based on similar principles, through which a prover can demonstrate possession of an arbitrary set of data known to the verifier. The verifier isn't required to have this data at hand during the protocol execution, but rather only a small hash of it. The protocol is also provably as secure as integer factoring[2].

#### c) Pors: Proofs of retrievability for large file

In this paper, we define and explore proofs of retrievability (PORs). A POR scheme enables an archive or back-up service (prover) to produce a concise proof that a user (verifier) can retrieve a target file  $F$ , that is, that the archive retains and reliably transmits file data sufficient for the user to recover  $F$  in its entirety. A POR may be viewed as a kind of cryptographic proof of knowledge (POK), but one specially designed to handle a *large* file (or bit string)  $F$ . We explore POR protocols here in which the communication costs, number of memory accesses for the prover, and storage requirements of the user (verifier) are small parameters essentially independent of the length of  $F$ . In addition to proposing new, practical POR constructions, we explore implementation considerations and

optimizations that bear on previously explored, related schemes. In a POR, unlike a POK, neither the prover nor the verifier need actually have knowledge of  $F$ . PORs give rise to a new and unusual security definition whose formulation is another contribution of our work. We view PORs as an important tool for semi-trusted online archives. Existing cryptographic techniques help users ensure the privacy and integrity of files they retrieve. It is also natural, however, for users to want to verify that archives do not delete or modify files prior to retrieval. The goal of a POR is to accomplish these checks *without users having to download the files themselves*. A POR can also provide quality-of-service guarantees, i.e., show that a file is retrievable within a certain time bound[3][6].

#### d) Provable data possession at untrusted stores

We introduce a model for *provable data possession* (PDP) that allows a client that has stored data at an untrusted server to verify that the server possesses the original data without retrieving it. The model generates probabilistic proofs of possession by sampling random sets of blocks from the server, which drastically reduces I/O costs. The client maintains a constant amount of metadata to verify the proof. The challenge/response protocol transmits a small, constant amount of data, which minimizes network communication. Thus, the PDP model for remote data checking supports large data sets in widely-distributed storage system.

We present two provably-secure PDP schemes that are more efficient than previous solutions, even when compared with schemes that achieve weaker guarantees. In particular, the overhead at the server is low (or even constant), as opposed to linear in the size of the data. Experiments using our implementation verify the practicality of PDP and reveal that the performance of PDP is bounded by disk I/O and not by cryptographic computation[4].

#### e) Compact proofs of retrievability

In a proof-of-retrievability system, a data storage center convinces a verifier that he is actually storing all of a client's data. The central challenge is to build systems that are both efficient and *provably* secure—that is, it should be possible to extract the client's data from any prover that passes a verification check. In this paper, we give the first proof-of-retrievability schemes with full proofs of security against *arbitrary* adversaries in the strongest model, that of Juels and Kaliski. Our first scheme, built from BLS signatures and secure in the random oracle model, has the *shortest query and response* of any proof-of-retrievability with

public verifiability. Our second scheme, which builds elegantly on pseudorandom functions (PRFs) and is secure in the standard model, has the *shortest response* of any proof-of-retrievability scheme with private verifiability (but a longer query). Both schemes rely on homomorphic properties to aggregate a proof into one small authenticator value[5].

#### B. Disadvantages of existing data integrity schemes

- a) Providing data dynamics support is the most challenging. This is because most existing auditing schemes intend to embed a block's index into its tag computation, which serves to authenticate challenged blocks. However, if we insert or delete a block, block indices of all subsequent blocks will change, then tags of these blocks have to be re-computed. This is unacceptable because of its high computation overhead.
- b) Current research usually assumes an honest data owner in their security models, which has an inborn inclination toward cloud users. However, the fact is, not only the cloud, but also cloud users, have the motive to engage in deceitful behaviors.
- c) In Existing System no integrity auditing scheme with public verifiability, efficient data dynamics and fair disputes arbitration.
- d) Existing system has the limitation of index usage in tag computation
- e) In Existing System tag re-computation caused by block update operations
- f) In Existing System both clients and the CSP potentially may misbehave during auditing and data update.

### III. Dynamic public auditing scheme

The public auditing system is designed based on tag index (used for tag computation) and block index (indicate block position), and rely an index switcher to keep a mapping between them. Upon each update operation, we allocate a new tag index for the operating block and update the mapping between tag indices and block indices. Such a layer of indirection between block indices and tag indices enforces block authentication and avoid stag re-computation of blocks after the operation position simultaneously[7][8].

#### A. The public auditing scheme consist of different participants:

1. User

2. Third Party Auditor(TPA)
3. Third Party Arbitrator(TPAR)
4. Cloud Service Provider(CSP)

#### a) user

The data owner performs the following actions:

User performs User registration and user login details.

- Every User need to register while accessing to the cloud.
- Every user will be activated by the Cloud.
- After Cloud activated, every user need to provide public key to login the user home.
- Public key will be provided to the user by third party auditor.
- User can view file details and can insert, modify and delete the file with help of TPAR.
- User will have the TPAR message whenever the user update the file

#### b) Third Party Auditor(TPA)

*It acts as semi-cloud.*

- TPA Provide public key for every user to access the user home page.
- After cloud given auditing proof then only TPA can audit all files

#### c) Third Party Arbitrator(TPAR)

- It acts as fair dispute for users and cloud.
- Intimate the files message, each time user insert, modify, delete files to cloud.
- Send TPAR message to user and cloud.

#### d) Cloud Service Provider(CSP)

- Activate data for user.
- Cloud sends storage auditing proof for all files to TPA.
- Cloud can view the user downloaded files from cloud.
- Cloud will have the TPAR message whenever the user updates the file.

As a result, the efficiency of handling data dynamics is greatly enhanced. Furthermore and important, in a public auditing scenario, a data owner always delegates his auditing tasks to a TPA who is trusted by the owner but not necessarily by the cloud. Our work also adopts the idea of signature exchange to ensure the metadata correctness and protocol fairness, and we concentrate on combining efficient data dynamics support and fair dispute arbitration into a single auditing scheme.

To address the fairness problem in auditing, we introduce a third-party arbitrator (TPAR) into our threat model, which is a professional institute for conflicts arbitration and is trusted and payed by both data owners and the CSP. Since a TPA can be viewed as a delegator of the data owner and is not necessarily trusted by the CSP, we differentiate between the roles of auditor and arbitrator. Moreover, we adopt the idea of signature exchange to ensure metadata correctness and provide dispute arbitration, where any conflict about auditing or data update can be fairly arbitrated. Generally, this paper proposes a new auditing scheme to address the problems of data dynamics support, public verifiability and dispute arbitration simultaneously.

*B. Public Auditing Scheme Architecture*

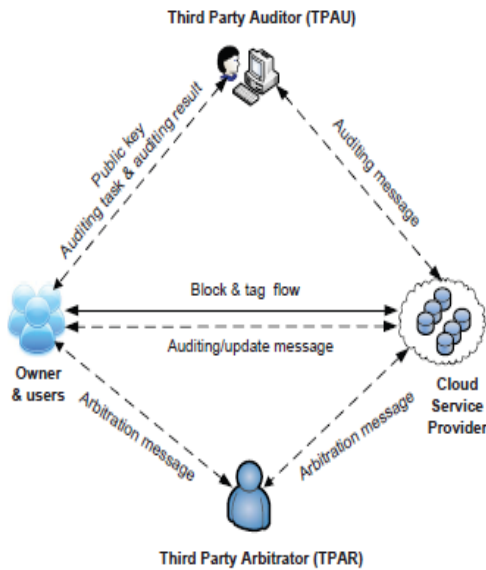


Fig. 1. The system and threat model.

As illustrated in Fig. 1, the system model involves four different entities: the data owner/cloud user, who has a large amount of data to be stored in the cloud, and will dynamically update his data (e.g., insert, delete or modify a data block) in the future; the cloud service provider (CSP), who has massive storage space and computing power that users do not possess, stores and manages user’s data and related metadata (i.e., the tag set and the index switcher); the third party auditor (TPAU) is similar to the role of TPA in existing schemes, who is a public verifier with expertise and capabilities for auditing, and is trusted and payed by the data owner (but not necessarily trusted by the cloud) to assess the integrity of the owner’s remotely stored data; the third party arbitrator (TPAR), who is a professional institute for conflict

arbitration and trusted by both the owner and the CSP, which is different to the role of TPAU. Cloud users rely on the CSP for data storage and maintenance, and they may access and update their data. To alleviate their burden, cloud users can delegate auditing tasks to the TPAU, who periodically performs the auditing and honestly reports the result to users. Additionally, cloud users may perform auditing tasks themselves if necessary. For potential disputes between the auditor and the CSP, the TPAR can fairly settle the disputes on proof verification or data update. Note in following sections, we may use the terms “TPAU” and “auditor” interchangeably, so are the terms “TPAR” and “arbitrator”.

*C. Advantages Of Proposed System*

- ❖ The proposed system solves the data dynamics problem in auditing by introducing an index switcher to keep a mapping between block indices and tag indices, and eliminate the passive effect of block indices in tag computation without incurring much overhead[11].
- ❖ The proposed system extend the threat model in current research to provide dispute arbitration, which is of great significance and practicality for cloud data auditing, since most existing schemes generally assume an honest data owner in their threat models[10].
- ❖ The proposed system provides fairness guarantee and dispute arbitration in our scheme, which ensures that both the data owner and the cloud cannot misbehave in the auditing process or else it is easy for a third-party arbitrator to find out the cheating party[11][12].

**IV. CONCLUSION**

The aim of this paper is to provide an integrity auditing scheme with public verifiability, efficient data dynamic sand fair disputes arbitration. To eliminate the limitation of index usage in tag computation and efficiently support data dynamics, we differentiate between block indices and tag indices, and devise an index switcher to keep block-tag index mapping to avoid tag re-computation caused by block update operations, which incurs limited additional overhead, as shown in our performance evaluation. Meanwhile, since both clients and the CSP potentially may misbehave during auditing and data update, we extend the existing threat model in current research to provide fair arbitration for solving disputes between clients and the CSP, which is of vital significance for the

deployment and promotion of auditing schemes in the cloud environment. We achieve this by designing arbitration protocols based on the idea of exchanging metadata signatures upon each update operation. Our experiments demonstrate the efficiency of our proposed scheme, whose overhead for dynamic update and dispute arbitration are reasonable.

## References

1. Y. Deswarte, J.-J. Quisquater, and A. Saïdane, "Remote integrity checking," in Proc. 5th Working Conf. Integrity and Intl Control in Information Systems, 2004, pp. 1–11.
2. D. L. Gazzoni Filho and P. S. L. M. Barreto, "Demonstrating data possession and uncheatable data transfer." IACR Cryptology ePrint Archive, Report 2006/150, 2006.
3. A. Juels and B. S. Kaliski Jr, "Pors: Proofs of retrievability for large files," in Proc. 14th ACM Conf. Computer and Comm. Security (CCS07), 2007, pp. 584–597.
4. G. Ateniese, R. Burns, R. Curtmola, J. Herring, L. Kissner, Z. Peterson, and D. Song, "Provable data possession at untrusted stores," in Proc. 14th ACM Conf. Computer and Comm. Security (CCS07), 2007, pp. 598–609.
5. H. Shacham and B. Waters, "Compact proofs of retrievability," in Proc. 14th Intl Conf. Theory and Application of Cryptology and Information Security: Advances in Cryptology (ASIACRYPT 08), 2008, pp. 90–107.
6. Q. Wang, C. Wang, J. Li, K. Ren, and W. Lou, "Enabling public verifiability and data dynamics for storage security in cloud computing," in Proc. 14th European Conf. Research in Computer Security (ESORICS 08), 2009, pp. 355–370.
7. M. A. Shah, R. Swaminathan, and M. Baker, "Privacy preserving audit and extraction of digital contents." IACR Cryptology ePrint Archive, Report 2008/186, 2008.
8. C. Wang, K. Ren, W. Lou, and J. Li, "Toward publicly auditable secure cloud data storage services," Network, IEEE, vol. 24, no. 4, pp. 19–24, 2010.
9. C. Erway, A. K. Upc, u, C. Papamanthou, and R. Tamassia, "Dynamic provable data possession," in Proc. 16th ACM Conf. Computer and Comm. Security (CCS 09), 2009, pp. 213–222.
10. Y. Zhu, H. Wang, Z. Hu, G.-J. Ahn, H. Hu, and S. S. Yau, "Dynamic audit services for integrity verification of outsourced storages in clouds," in Proc. ACM Symp. Applied Computing (SAC 11), 2011, pp. 1550–1557.
11. Q. Zheng and S. Xu, "Fair and dynamic proofs of retrievability," in Proc. 1st ACM Conf. Data and Application Security and Privacy (CODASPY 11), 2011, pp. 237–248.
12. A. K. Upc, u, "Official arbitration with secure cloud storage application,"

# Different Types of Machine Learning Techniques in Python programming

Mr Naveen Kumar R<sup>1</sup> & Ms Adepur Aravinda<sup>2</sup> & Mrs Subhashini Peneti<sup>3</sup>

<sup>1,2</sup>M-Tech Student, CSE, Mallareddy College of Engineering

<sup>3</sup>Assistant Professor, CSE, Mallareddy College of Engineering

---

**ABSTRACT:** When we hear "Machine learning", We will probably imagine a robot or something like the deadly Terminator as we see in movies. But, machine learning is involved not only in robotics<sup>1</sup>, but also in many other applications. Now it is not just a futuristic fantasy, its already here. In fact, it has been around for decades in some specialized applications, such as Optical Character Recognition (OCR). But the first Machine Learning application that really became mainstream, improving the lives of hundreds of millions of people, took over the world back in the 1990s. It was the spam<sup>2</sup> filter. It does have all technical qualities to qualify as Machine Learning. It has, learned so well that you seldom need to flag an email as spam anymore. It was followed by hundreds of Machine Learning applications that now quietly power hundreds of products and features that you use regularly, from better recommendations to face recognition and voice search. This paper focuses on Explaining What is Machine Learning, why we need Machine Learning, Types of Machine Learning, Various Technologies available to implement Machine learning and how to use Python<sup>3</sup> as development environment for developing Machine Learning.

**Keywords:** Machine Learning, training set, clustering, reinforcement, python, NumPy, SciPy, Scikit-learn, Python, pip, Spam, OCR, robotics.

---

## I. INTRODUCTION

Machine learning is a subfield of artificial intelligence (AI). The goal of machine learning generally is to understand the structure of data and fit that data into models that can be understood and utilized by people [1]. Although machine learning is a field within computer science, it differs from traditional computational approaches. In traditional computing, algorithms are sets of explicitly programmed instructions used by computers to calculate or problem solve. Machine learning algorithms instead allow for computers to train on data inputs and use statistical analysis to output values that fall within a specific range of given output values. [4] In this age of modern technology, there is one resource that we have in abundance is large amount of structured and unstructured data. In the second half of the twentieth century, machine learning has evolved that involved the development of self-learning algorithms to gain knowledge from that data to make predictions. Instead of requiring humans to manually derive rules and build models from analysing large amounts of data, machine learning offers a more efficient alternative for capturing the knowledge in data to gradually improve the performance of predictive models and make data-driven decisions. Not only is machine learning becoming increasingly important in computer science

research, but it also plays an ever-greater role in our everyday life. Thanks to machine learning, we enjoy robust e-mail spam filters, convenient text and voice recognition software, reliable Web search engines, challenging chess players, and, hopefully soon, safe and efficient self-driving cars.

## II WHAT IS MACHINE LEARNING?

Machine Learning is the science of programming that gives computers the ability to learn without being explicitly programmed. Technically A computer program is said to learn from experience E with respect to some task T and some performance measure P, if its performance on T, as measured by P, improves with experience E. [1] For example, your spam filter is a Machine Learning program that can learn to flag spam given examples of spam emails (e.g., flagged by users) and examples of regular (non-spam or ham) emails. The examples that the system uses to learn are called the training set. Each training example is called a training instance (or sample). In this case, the task T is to flag spam for new emails, the experience E is the training data, and the performance measure P needs to be defined; for example, you can use the ratio of correctly classified emails. This, performance measure is called accuracy and it is often used in classification tasks.

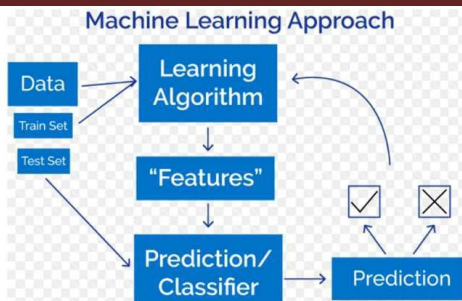


Fig. 2. Flow in Machine Learning

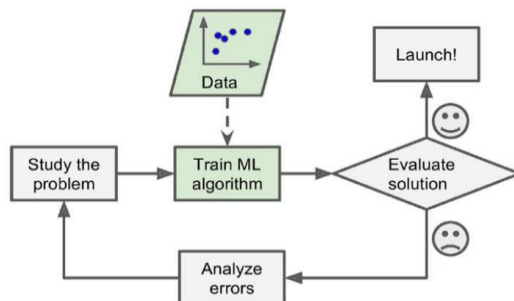


Fig. 4. Machine Learning approach

### III. WHY USE MACHINE LEARNING?

Consider how to write a spam filter using traditional programming techniques.

1. First look at what spam typically looks like. We might notice that some words or phrases (such as “4U”, “credit card”, “free”, and “amazing”) tend to come up a lot in the subject. Perhaps we would also notice a few other patterns<sup>4</sup> in the sender’s name, the email’s body, and so on.[3]
2. We have to write a detection algorithm for each of the patterns that we noticed, and our program would flag emails as spam if a number of these patterns are detected.
3. We have to test the program and repeat steps 1 and 2 until it is good enough.

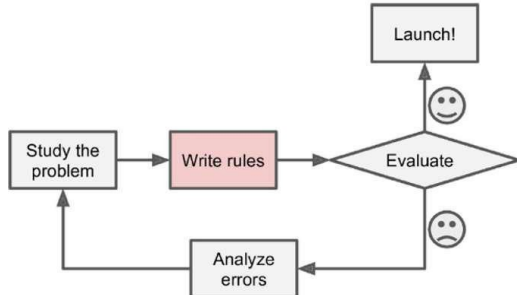


Fig. 3. Traditional approach

Since the problem is not trivial, the program will likely become a long list of complex rules which are hard to maintain.

In contrast, a spam filter based on Machine Learning techniques automatically learns which words and phrases are good predictors of spam by detecting unusually frequent patterns of words in the spam examples compared to the ham examples.

The program is much shorter, easier to maintain, and most likely more accurate. Moreover, if spammers notice that all their emails containing “4U” are blocked, they might start writing “For U” instead. A spam filter using traditional programming techniques would need to be updated to flag “For U” emails. If spammers keep working around the spam filter, we will need to keep writing new rules forever. In contrast, a spam filter based on Machine Learning techniques automatically notices that “For U” has become unusually frequent in spam flagged by users, and it starts flagging them without our intervention.

Another area where Machine Learning shines is for problems that either are too complex for traditional approaches or have no known algorithm. For example, consider speech recognition: say we want to start simple and write a program capable of distinguishing the words “one” and “two.” You might notice that the word “two” starts with a high-pitch sound (“T”), so you could hardcode an algorithm that measures high-pitch sound intensity

Arrangement or words in a format and use that to distinguish ones and twos. Obviously, this technique will not scale to thousands of words spoken by millions of very different people in noisy environments and in dozens of languages. The best solution (at least today) is to write an algorithm that learns by itself, given many example recordings for each word.

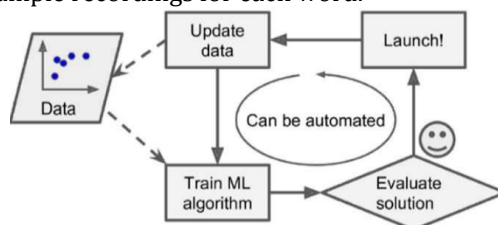


Fig. 5. Automatically adopting to change

<sup>1</sup> Technology dealing with design of robots  
 Irrelevant or unwanted messages.

<sup>3</sup> Python is an interpreted, object-oriented, high-level  
 programming language with dynamic semantics.

<sup>4</sup> Arrangement or words in a format

To summarize, Machine Learning is great for: Problems for which existing solutions require a lot of hand-tuning or long lists of rules: one Machine Learning algorithm can often simplify code and perform better.

Complex problems for which there is no good solution at all using a traditional approach: the best Machine Learning techniques can find a solution.

Fluctuating environments: a Machine Learning system can adapt to new data.

Getting insights about complex problems and large amounts of data.

**IV. HOW DOES MACHINE LEARNING WORK ?**

Machine Learning algorithm is trained using a training data set to create a model. When new input data is introduced to the Machine Learning algorithm, it makes a prediction on the basis of the model. The prediction is evaluated for accuracy and if the accuracy is acceptable, the Machine Learning algorithm is deployed. If the accuracy is not acceptable, the Machine Learning algorithm is trained again and again with an augmented training data set. This is just a very high-level example as there are many factors and other steps involved.[3]

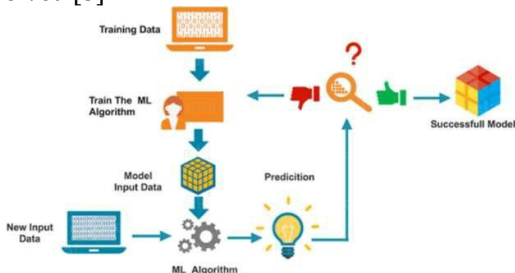


Fig. 6. Machine Learning Flowchart

**V. TYPES OF MACHINE LEARNING**

There are so many different types of Machine Learning systems that it is useful to classify them in broad categories. In this paper, we will look at the three types of machine learning: [4]

Supervised learning, Unsupervised learning, and Reinforcement learning.

We will learn about the fundamental differences between the three different learning types and, using conceptual examples, we will develop an intuition for the practical problem domains where these can be applied.

**A. Supervised Learning:**

Supervised Learning is the one, where you can consider the learning is guided by a teacher. We have a dataset which acts as a teacher and its role is to train the model or the machine. Once the

model gets trained it can start making prediction or decision when new data is given to it. In supervised learning, the training data you feed to the algorithm includes the desired solutions, called labels.[4]

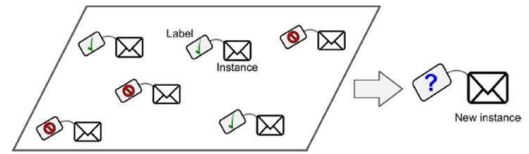


Fig. 7. Supervised Learning - Training set

A typical supervised learning task is classification. The spam filter is a good example of this: it is trained with many example emails along with their class (spam or ham), and it must learn how to classify new emails. Another typical task is to predict a target numeric value, such as the price of a car, given a set of features (mileage, age, brand, etc.) called predictors. To train the system, you need to give it many examples of cars, including both their predictors and their labels (i.e., their prices).

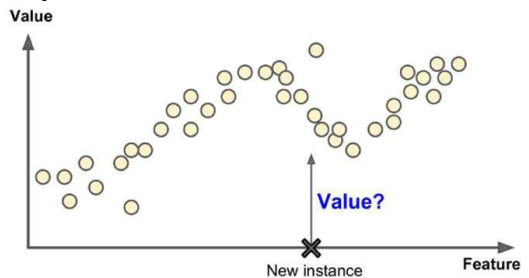


Fig. 8. Supervised Learning ( Feature - Value graph )

Here are some of the most important k-Nearest Neighbours Support Vector Machines (SVMs) Decision Trees and Random Forests Neural networks

**B. Unsupervised Learning**

The model learns through observation and finds structures in the data. Once the model is given a dataset, it automatically finds patterns and relationships in the dataset by creating clusters<sup>5</sup> in it. What it cannot do is add labels to the cluster, like it cannot say this a group of apples or mangoes, but it will separate all the apples from mangoes.[4]

Suppose we presented images of apples, bananas and mangoes to the model, so what it does, based on some patterns and relationships it creates clusters and divides the dataset into those clusters. Now if a new data is fed to the model, it adds it to one of the created clusters. In unsupervised learning, as you might guess, the training data is unlabelled. The system tries to learn without a teacher.

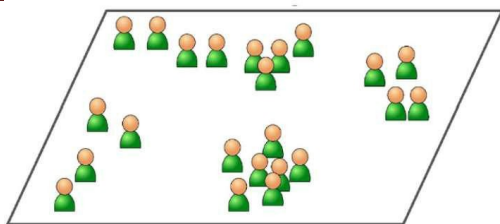


Fig. 9. Unsupervised Learning ( training set )

Here are some of the most important unsupervised learning algorithms

Clustering

Visualization and dimensionality reduction

Association rule learning.

For example, say you have a lot of data about your blog's visitors. You may want to run a clustering algorithm to try to detect groups of similar visitors. At no point do you tell the algorithm which group a visitor belongs to: it finds those connections without your help. For example, it might notice that 40% of your visitors are males who love comic books and generally read your blog in the evening, while 20% are young sci-fi lovers who visit during the weekends, and so on. If you use a hierarchical clustering algorithm, it may also subdivide each group into smaller groups. This may help you target your posts for each group.

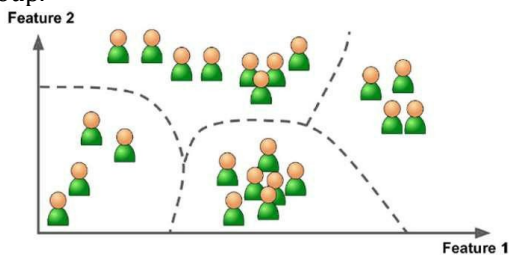


Fig. 10. Clustering in Unsupervised Learning

### C. Reinforcement Learning

It is the ability of an agent to interact with the environment and find out what is the best outcome. It follows the concept of hit and trial method. The agent is rewarded or penalized with a point for a correct or a wrong answer, and on the basis of the positive reward points gained the model trains itself. And again, once trained it gets ready to predict the new data presented to it.[4]

## VI. ROADMAP FOR BUILDING MACHINE LEARNING SYSTEMS

The diagram below shows a typical workflow diagram for using machine learning in predictive modelling.

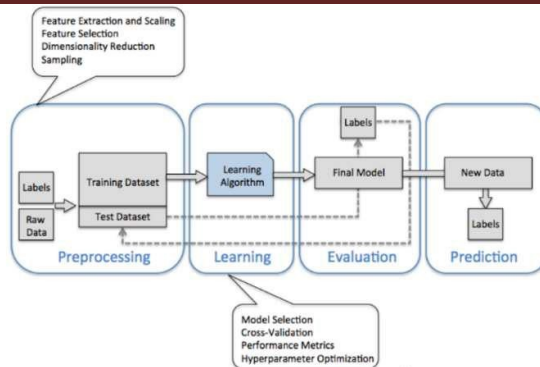


Fig. 11. Machine Learning System - Roadmap

A. Pre-processing - getting data into shape: Raw data rarely comes in the form and shape that is necessary for the optimal performance of a learning algorithm. Thus, the pre- processing of the data is one of the most crucial steps in any machine learning.[5]

B. Training and selecting a predictive model: It is essential to compare at least a handful of different algorithms in order to train and select the best performing model. But before we can compare different models, we first have to decide upon a metric<sup>6</sup> to measure performance. One commonly used metric is classification accuracy, which is defined as the proportion of correctly classified instances.[5]

C. Evaluating models and predicting unseen data instances:

After we have selected a model that has been fitted on the training dataset, we can use the test dataset to estimate how well it performs on this unseen data to estimate the generalization error. If we are satisfied with its performance, we can now use this model to predict new, future data. It is important to note that the parameters for the previously mentioned procedures such as feature scaling and dimensionality reduction are solely obtained from the training dataset, and the same parameters are later re-applied to transform the test dataset, as well as any new data samples the performance measured on the test data may be overoptimistic otherwise.[5]

## VII. USING PYTHON FOR MACHINE LEARNING

Python is one of the most popular programming languages for data science and therefore, enjoys many useful add-on libraries developed by its great community.

Although the performance of interpreted languages, such as Python, for computation-intensive tasks is inferior to lower-level programming languages, extension libraries such as NumPy<sup>7</sup> and SciPy<sup>8</sup> have been developed that build upon lower layer Fortran and C

<sup>5</sup> A group of similar things occurring closely together

implementations for fast and vectorized operations on multidimensional arrays. For machine learning programming tasks, we will mostly refer to the scikit-learn library, which is one of the most popular and accessible open source machine learning libraries as of today. [2]

Installing Python packages

Python is available for all three major operating systems—Microsoft Windows, Mac OS X, and Linux—and the installer, as well as the documentation, can be downloaded from the official Python website: <https://www.python.org>, and it is recommended to use the most recent version of

Python 3 that is currently available, although most of the code examples may also be compatible with the version of Python  $\geq 2.7.10$ .

If you decide to use Python 2.7 to execute the code examples, please make sure that you know about the major differences between the two Python versions. The additional packages that can be installed via the pip installer program, which has been part of the Python standard library since Python 3.3. After we have successfully installed Python, we can execute pip from the command line terminal to install additional Python packages:[2]

```
pip install SomePackage
```

Already installed packages can be updated via the -- upgrade flag:

```
pip install SomePackage -upgrade
```

Another important library is NumPy. we will mainly use NumPy's multi-dimensional arrays to store and manipulate data. Occasionally, we will make use of pandas, which is a library built on top of NumPy that provides additional higher-level data manipulation tools that make working with tabular data even more convenient. To augment our learning experience and visualize quantitative data, which is often extremely useful to intuitively make sense of it, we will use the very customizable matplotlib library.

The example of version numbers of the major Python packages are listed below. Please make sure that the version numbers of your installed packages are equal to, or greater than, those version numbers to ensure the code examples run correctly:

- NumPy 1.9.1
- SciPy 0.14.0

- scikit-learn 0.15.2
- matplotlib 1.4.0
- pandas 0.15.2

## VIII. CONCLUSION

In this paper, we have explored machine learning on a very high level and familiarized ourselves with the big picture and major concepts. We learned about What is Machine Learning, How and where we can use Machine learning, Different types of Machine Learning and that supervised learning is composed of two important subfields: classification and regression. While classification models allow us to categorize objects into known classes, we can use regression analysis to predict the continuous outcomes of target variables. Unsupervised learning not only offers useful techniques for discovering structures in unlabelled data, but it can also be useful for data compression in feature pre-processing steps.

We briefly went over the typical roadmap for applying machine learning to problem tasks, which can be used as a foundation for developing Machine learning systems. Eventually, we also saw how to set up our Python environment and install and updated the required packages to get ready to see machine-learning in action.

## ACKNOWLEDGEMENT

We would like to acknowledge the contribution of all the people who have helped in reviewing this paper. We would like to give sincere thanks to Mrs. Subhashini Peneti, for her guidance and support throughout this paper. We would also like to thank our families and friends who supported us during writing this paper.

## REFERENCES

- [1] Hands-On Machine Learning with Scikit-Learn and TensorFlow, by - Aurélien Géron
- [2] Python Machine Learning, by - Sebastian Raschka
- [3] Machine Learning in Action, by Peter Harrington
- [4] Machine Learning For Dummies, by - John Paul Mueller and Luca Massaron
- [5] <https://www.digitalocean.com/community/tutorials/an-introduction-to-machine-learning#approaches>

---

6 Measurement of a characteristic  
7. Package for scientific calculation in Python

8. Another library for scientific computing in Python

## DESIGN OF DYNAMIC ACCURACY CONFIGURABLE MULTIPLIER USING DUAL QUALITY 4:2 COMPRESSOR

Ancychristabel S.C<sup>1</sup> & Nimmy Lazer<sup>2</sup> & G.Selva Malar<sup>3</sup>

<sup>1,2,3</sup>Department of ECE, Marthandam College of Engineering and Technology, Tamilnadu, India.

**ABSTRACT:** In this paper, four 4:2 compressors with high flexibility of switching between the exact and approximate operating modes is designed. Dual-quality compressors provide higher speeds and lower power consumptions at the cost of lower accuracy in approximate mode. The efficiencies of this compressor can be evaluated using 32-bit Dadda multiplier. Here, a Dadda multiplier is also designed and their results are analysed. Dadda multiplier can be used to evaluate the performance of compressor.

**Keywords:** 4:2 compressor, Dadda multiplier, accuracy, approximate, computing, configurable, delay, power.

### I. INTRODUCTION

Among different arithmetic blocks, the multiplier is one of the main Blocks, which are widely used in different applications especially signal Processing applications[1,2]. There are two general architectures for the multipliers, which are sequential and parallel. While sequential architectures are low power, their latency is very large. On the other hand, parallel architectures (such as Wallace tree and Dadda) are fast while having high-power consumptions. The Parallel multipliers are used in high- performance applications where their large power consumptions may create hot-spot locations on the die. The speed of a processor greatly depends on its multiplier's performance. This in turn increases the demand for high speed multipliers, at the same time keeping in mind low area and moderate power consumption. Over the past few decades, several new architectures of multipliers have been designed and explored. Multipliers based on the Booth's and modified Booth's algorithm is quite popular in modern VLSI design but come along with their own set of disadvantages. [3]In these algorithms, the multiplication process, involves several intermediate operations before arriving at the final answer. In order to address the disadvantages with respect to speed of the above mentioned methods, and explored a new approach to multiplier design based on ancient Vedic Mathematics.

The number of half and full adders count to the total delay in Conventional multiplier [4]. The use of compressor structures which perform more than three bit addition. 4-2 compressor has five inputs and three outputs, as shown in Fig. 1.1 The four inputs X0, X1, X2, and

X3, and the output have the same weight. Cin is the output carry of preceding module and Cout, the carry output of current stage is fed to the next compressor. The output Carry is weighted one binary bit order higher. The compressor is governed by the following basic equation:

$$X_0 + X_1 + X_2 + X_3 + C_{in} = \text{Sum} + 2(\text{Carry} + C_{out})$$

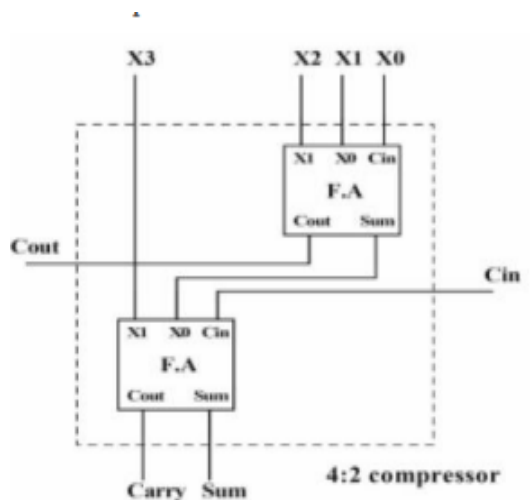


Fig 1.1 Block diagram of a 4:2 compressor

Besides, to accelerate the carry save summation of the partial products, it is imperative that the output Cout be independent of the input Cin. The conventional architecture of a 4:2 compressor consists of two serially connected full adders. This circuit leads to a long critical path delay[5,6]. Also of an even delay profiles of outputs from different inputs.

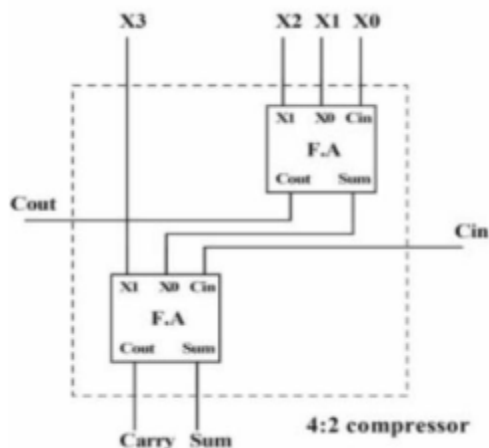


Fig1. 2. Conventional 4-2 compressor scheme

The overall structure of the proposed structure is shown in Figure 1.3.

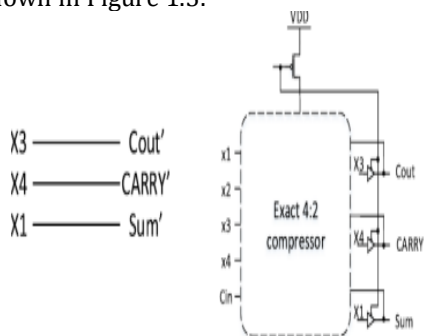


Fig1. 3 Approximate part and overall structure of DQ4:2C2

The previous structures, in the approximate operating mode, had maximum power and delay reductions compared with those of the exact compressor. In some applications, however, a higher accuracy may be needed. In the third structure, the accuracy of the approximate operating mode is improved by increasing the complexity of the approximate part whose internal structure is shown

$$\text{Sum} = x + x + x + x + C$$

.....(i)

$$\text{Carry} = \text{Majority} [(x + x + x), x, C]$$

.....(ii)

$$C = \text{Majority} (x, x, x)$$

.....(iii)

The gate-level and the transistor-level designs are two different approaches for designing blocks such as 4:2 compressors. The major drawback of this approach is its limited optimization capability.

## II. PURPOSED METHOD

To reduce the delay of the partial product summation stage of parallel Multipliers, 4:2 and 5:2 compressors are widely employed. The focus of this paper is on approximate 4:2 compressors. First, some background on the exact 4:2 compressor is presented. This type of compressor, shown schematically in Fig. 3.1, has four inputs ( $x_1-x_4$ ) along with an input carry ( $C_{in}$ ), and two outputs (sum and carry) along with an output  $C_{out}$ . The internal structure of an exact 4:2 compressor is composed of two serially connected full adders, as shown in Fig. 2. In this structure, the weights of all the inputs and the sum output are the same whereas the weights of the carry and  $C_{out}$  outputs are one binary bit position higher.

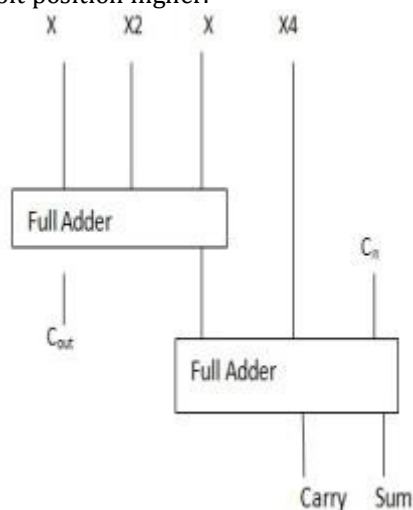


Fig3.1. Conventional 4:2 compressor.

## III. EXISITNG METHOD

The 4:2 compressors has five input signals, including four main inputs and an input carry bit ( $C_{in}$ ), coming from the previous stage, and three output signals including Sum and Carry main outputs and an output carry signal ( $C_{out}$ ) which serves as the  $C_{in}$  of the next neighboring block. It is worth mentioning that the  $C_{out}$  signal is independent of the  $C_{in}$  input due to the elimination of carry propagation through the multiplier tree[14,15,16]. A 4:2 compressor cell generates Sum, Carry and  $C_{out}$  outputs from  $\times 1, \times 2, \times 3, \times 4$  and  $C_{in}$  inputs.

The proposed system of 4:2 compressor consist of Half-adder, full -adder and 4 2 compressors, EXOR gates tend to contribute high amount of area and power. For the process of approximating half-adder, EXOR gate of the Sum is changed with OR gate. This results in one error in the Sum output.

Sum =  $x_1+x_2$ ; Carry =  $x_1.x_2$ . In the process of approximation of full-adder in the multiplier, one of the EXOR gates is replaced with OR gate to reduce hardware complexity. Carry is altered in such a way it has no error. The proposed dual quality 4:2 compressors operate in two accuracy modes. They are Approximate Mode and Exact Mode. Power gating technique is turn off the unused components of approximate part. In the exact operating mode, the delay of this structure is about same as that of the exact 4:2 compressor. The structure of NAND gate of the approximate part is not used during the exact operating mode. The output sum, carry, cout can be obtained from.

$$\text{Sum} = x_1 \oplus x_2 \oplus x_3 \oplus x_4 \oplus C_{in} \dots \dots \dots (iv)$$

$$\text{Carry} = (x_1 \otimes x_2 \oplus x_3 \oplus x_4) C_{in} + x_1 \oplus x_2 \oplus x_3 \oplus x_4$$

$$x_4 \dots (v) \text{ Cout} = (x_1 \oplus x_2) x_3 + (x_1 \oplus x_2) x_1 \dots \dots \dots (vi)$$

Dual-Quality 4:2 Compressors are utilized in the reduction module of four approximate multipliers. In terms of transistor count, the first design has a 46% improvement, while the second design has a 49% improvement. In terms of power dissipation, the first design has a 57% improvement and the second design has a 60% improvement over CMOS implementation at feature sizes of 32 nm. In terms of delay, the second design has a 44% improvement compared to the exact compressor and 35% improvement compared to the first design on average at CMOS feature sizes of 32 nm. The proposed multipliers show a significant improvement in terms of power consumption and transistor count compared to an exact multiplier. Advantages of proposed system includes signal processing and data mining with tolerable error, compressors can also utilize in multimedia signal processing application, reducing the design complication, increase in performance and power efficiency, and reduced power and error rate.

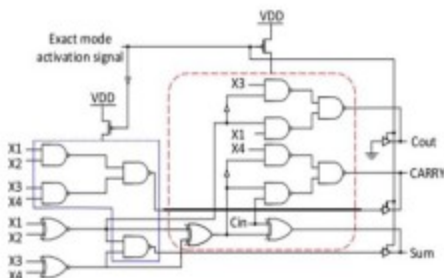


Fig 3.2 Overall Structure of DQ4:2 compressors

Description of the Structure consists of two main parts of approximate and supplementary. During the approximate mode, only the approximate part is exploited while the supplementary part is power

gated. During the exact operating mode, the supplementary and some parts of the approximate parts are utilized.

The language used is Verilog, a hardware description language(HDL). It is a language used for describing a digital system like a network switch or a microprocessor or a memory or a flip-flop. Verilog supports a design at many levels of abstraction. The software used here is Xilinx software controls all aspects of the design flow. Through the Project Navigator interface, you can access all of the design entry and design implementation tools. You can also access the files and documents associated with your projects because implementation is dependent on up-to-date synthesis results.

#### IV. RESULTS AND DISCUSSIONS

In this section, first, the efficacies of the proposed 4:2 compressors in the approximate operating mode are investigated.

DESIGN 1 OUTPUT: The proposed design 1 yielding an error rate of 37.5%. This is less than the error rate using the best approximate full-adder cell. The power consumption is reduced when compared to other proposed system.

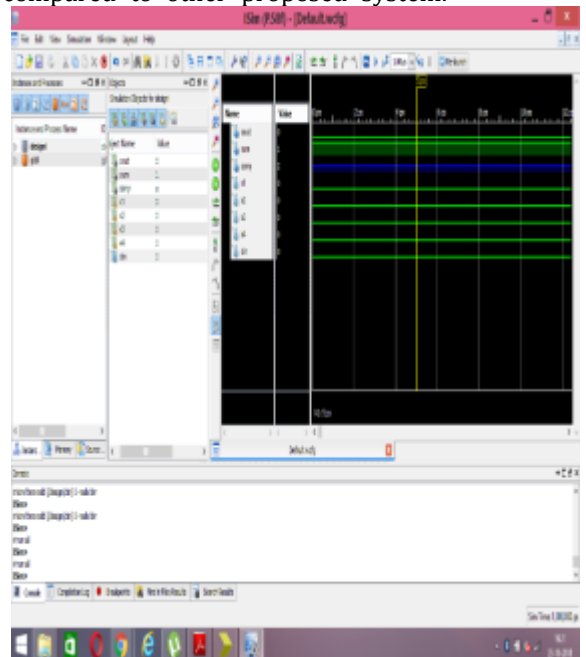


Fig 4.1. Design 1 output

RTL schematic: It models a synchronous digital circuit in terms of the flow of digital signals between hardware registers, and the logical operations performed on those signals. The structural description of design 1 circuit may lead to easy identification of a process. The transistor count is reduced to 48.

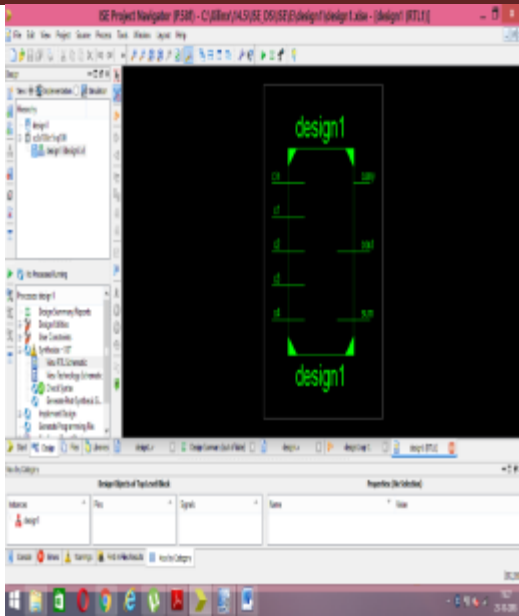


Fig4.2. Design 1 RTL Schematic

Design 2 outputs: A second design of an approximate compressor is proposed to further increase performance as well as reducing the error rate can be ignored in the hardware design. The power dissipation up to 0.010096 in design methodology.

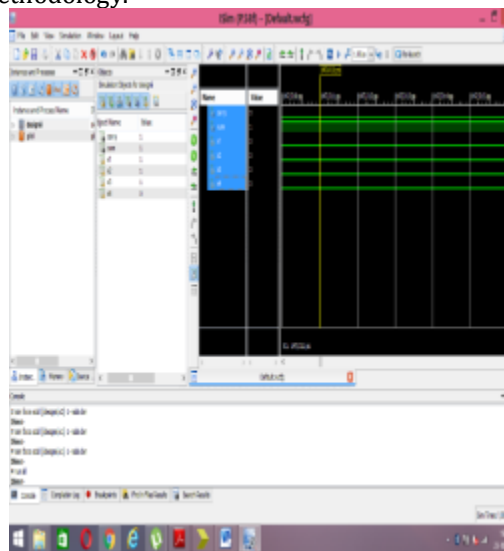


Fig4.3. Design 2 output

RTL schematic: The transistor count is further reduced to 42. In terms of delay, the second design has a 44% improvement compared to the exact compressor and 35% improvement compared to the first design on average at CMOS feature sizes of 32 nm.

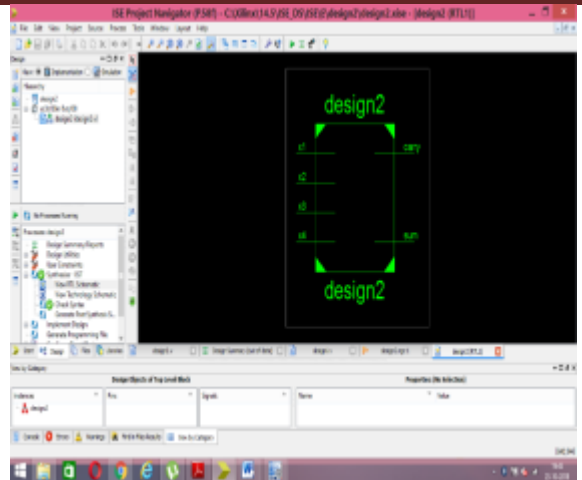


Fig4.4. Design 2 RTL schematic

Output for Approximate part: In the process of approximation of full-adder in the multiplier, one of the EXOR gates is replaced with OR gate to reduce hardware complexity. This results in change of values of output in last two cases out of eight cases. Carry is altered in such a way it has no error.



Fig4.5. Output for approximate part

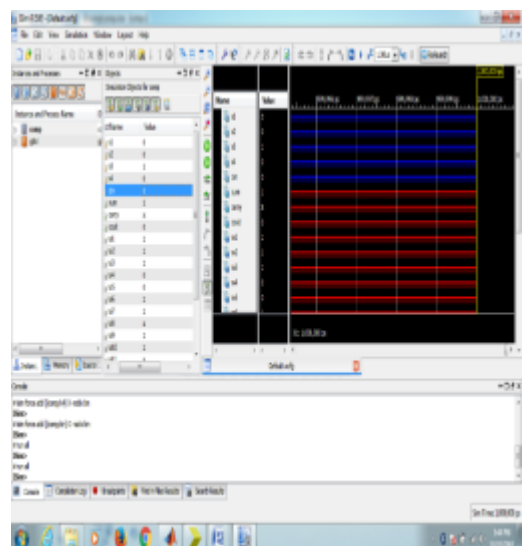


Fig4.6. Simulated output

Implementation of Dadda multiplier for comparative Study: First, the efficacies of the proposed 4:2 compressors in the approximate operating mode are investigated. In the comparative study, which is performed by utilizing them in the Dadda multiplier, the design parameters of the multipliers are compared with the two approximate 4:2 compressors proposed.



Fig4.7: 32 bit dadda multiplier

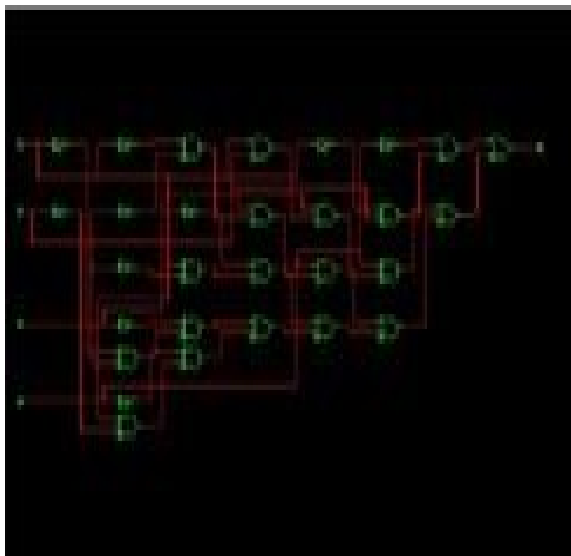


Fig4.8 Technology schematic for dada multiplier

### V. Comparison

Finally, the delay, area and power approximate 32-bit Dadda multipliers using the proposed compressors are lower compared with the exact Dadda multiplier, on average, by 49.3%, 68% and 83.7%, respectively. Also, when compared with the Dadda multiplier realized by the proposed approximate compressors of, the delay, area, power, energy, and EDP of the approximate 32-bit Dadda multipliers realized by our proposed compressors are better, on average, by 29% (69%) and 52% respectively.

### VI. CONCLUSION

In this project, we presented four DQ4:2Cs, which

had the flexibility of switching between the exact and approximate operating modes. In the approximate mode, these compressors provided higher speeds and lower power consumptions at the cost of lower accuracy. Each of these compressors had its own level of accuracy in the approximate mode as well as different delays and powers in the approximate and exact modes. These compressors were employed in the structure of a 32-bit Dadda multiplier to provide a configurable multiplier whose accuracy (as well as its power and speed) could be changed dynamically during the runtime. Our studies revealed that for the

32-bit multiplication, the proposed compressors yielded, on average, 46% and 68% lower delay and power consumption in the approximate mode compared with those of the recently suggested approximate compressors. Also, utilizing the proposed compressors in 32-bit Dadda multiplier provided, on average, about 33% lower NED compared with the state-of-the-art compressor-based approximate multipliers. When comparing with no compressor-based approximate multipliers, the errors of the proposed multipliers were higher while the design parameters were considerably better. Finally, our studies showed that the multipliers realized based on the suggested compressors have, on average, about 93% smaller FOM value compared with the considered approximate multipliers.

### VII. FUTURE WORK

The proposed work developed and designed a new 4:2 compressor. In the future this can be applied in image processing and signal processing applications. It ensures high speeds, low delay and small area of the multipliers.

### REFERENCES

1. P. Kulkarni, P. Gupta, and M. Ercegovac, "Trading accuracy for power with an underdesigned multiplier architecture," in Proc. 24th Int. Conf. VLSI Design, Jan. 2011, pp. 346–351.
2. D. Baran, M. Aktan, and V. G. Oklobdzija, "Multiplier structures for low power applications in deep-CMOS," in Proc. IEEE Int. Symp. Circuits Syst. (ISCAS), May 2011, pp. 1061–1064.
3. S. Ghosh, D. Mohapatra, G. Karakonstantis, and K. Roy, "Voltage scalable high-speed robust hybrid arithmetic units using adaptive clocking," IEEE Trans. Very Large Scale Integr. (VLSI) Syst., vol. 18, no. 9, pp. 1301–1309, Sep. 2010.
4. O. Akbari, M. Kamal, A. Afzali-Kusha, and M. Pedram, "RAP-CLA: A reconfigurable approximate carry look-ahead adder," IEEE

- Trans. Circuits Syst. II, Express Briefs, doi: 10.1109/TCSII.2016.2633307.
5. A. Sampson et al., "EnerJ: Approximate data types for safe and general low-power computation," in Proc. 32nd ACM SIGPLAN Conf. Program. Lang. Design Implement. (PLDI), 2011, pp. 164–174.
  6. A. Raha, H. Jayakumar, and V. Raghunathan, "Input-based dynamic reconfiguration of approximate arithmetic units for video encoding," IEEE Trans. Very Large Scale Integr. (VLSI) Syst., vol. 24, no. 3, pp. 846–857, May 2015.
  7. J. Joven et al., "QoS-driven reconfigurable parallel computing for NoC-based clustered MPSoCs," IEEE Trans. Ind. Informat., vol. 9, no. 3, pp. 1613–1624, Aug. 2013.
  8. R. Ye, T. Wang, F. Yuan, R. Kumar, and Q. Xu, "On reconfiguration oriented approximate adder design and its application," in Proc. IEEE/ACM Int. Conf. Comput. Aided Design (ICCAD), Nov. 2013, pp. 48–54.
  9. M. Shafique, W. Ahmad, R. Hafiz, and J. Henkel, "A low latency generic accuracy configurable adder," in Proc. 52nd ACM/EDAC/IEEE Design Autom. Conf. (DAC), Jun. 2015, pp. 1–6.
  10. S. Narayanamoorthy, H. A. Moghaddam, Z. Liu, T. Park, and N. S. Kim, "Energy-efficient approximate multiplication for digital signal processing and classification applications," IEEE Trans. Very Large Scale Integr. (VLSI) Syst., vol. 23, no. 6, pp. 1180–1184, Jun. 2015.
  11. S. Hashemi, R. I. Bahar, and S. Reda, "DRUM: A dynamic range unbiased multiplier for approximate applications," in Proc. IEEE/ACM Int. Conf. Comput.-Aided Design (ICCAD), Austin, TX, USA, Nov. 2015, pp. 418–425.
  12. K. Y. Kyaw, W. L. Goh, and K. S. Yeo, "Low-power high-speed multiplier for error-tolerant application," in Proc. IEEE Int. Conf. Electron Devices Solid-State Circuits (EDSSC), Dec. 2010, pp. 1–4.
  13. H. R. Mahdiani, A. Ahmadi, S. M. Fakhraie, and C. Lucas, "Bio - inspired imprecise computational blocks for efficient VLSI implementation of soft-computing applications," IEEE Trans. Circuits Syst. I, Reg. Papers, vol. 57, no. 4, pp. 850–862, Apr. 2010.
  14. A. Momeni, J. Han, P. Montuschi, and F. Lombardi, "Design and analysis of approximate compressors for multiplication," IEEE Trans. Comput., vol. 64, no. 4, pp. 984–994, Apr. 2015.
  15. C. H. Lin and I. C. Lin, "High accuracy approximate multiplier with error correction," in Proc. IEEE 31st Int. Conf. Comput. Design (ICCD), Oct. 2013, pp. 33–38.
  16. C. Liu, J. Han, and F. Lombardi, "A low-power, high-performance approximate multiplier with configurable partial error recovery," in Proc. Conf. Design, Autom. Test Eur. (DATE), 2014, Art. no. 95.
  17. R. Zendegani, M. Kamal, M. Bahadori, A. Afzali-Kusha, and M. Pedram, "RoBA multiplier: A rounding-based approximate multiplier for high-speed yet energy-efficient digital signal processing," IEEE Trans. Very Large Scale Integr. (VLSI) Syst., doi: 10.1109/TVLSI.2016.2587696.
  18. [18] C. H. Chang, J. Gu, and M. Zhang, "Ultra low-voltage low-power CMOS 4-2 and 5-2 compressors for fast arithmetic circuits," IEEE Trans Circuits Syst. I, Reg. Papers, vol. 51, no. 10, pp. 1985–1997, Oct. 2004. [19] D. Baran, M. Aktan, and V. G. Oklobdzija, "Energy efficient implementation of parallel CMOS multipliers with improved compressors," in Proc. ACM/IEEE Int. Symp. Low-Power Electron. Design (ISLPED), Aug. 2010, pp. 147–152.
  19. J. Liang, J. Han, and F. Lombardi, "New metrics for the reliability of approximate and probabilistic adders," IEEE Trans. Comput., vol. 62, no. 9, pp. 1760–1771, Sep. 2013.
  20. (2016). NanGate—The Standard Cell Library Optimization Company. [Online]. Available: <http://www.nangate.com/>
  21. M. S. K. Lau, K. V. Ling, and Y. C. Chu, "Energy-aware probabilistic multiplier: Design and analysis," in Proc. Int. Conf. Compil., Archit., Synth. Embedded Syst., 2009, pp. 281–290.
  22. H. R. Myler and A. R. Weeks, The Pocket Handbook of Image Processing Algorithms in C. Englewood Cliffs, NJ, USA: Prentice-Hall, 2009.
  23. Sipi.usc.edu. (2016). SIPI Image Database. [Online]. Available: <http://sipi.usc.edu/database/>
  24. Z. Wang, A. C. Bovik, H. R. Sheikh, and E. P. Simoncelli, "Image quality assessment: From error visibility to structural similarity," IEEE Trans. Image Process., vol. 13, no. 4, pp. 600–612, Apr. 2004.
  25. Trace.eas.asu.edu. (2016). YUV Sequences. [Online]. Available: <http://trace.eas.asu.edu/yuv/>

## DESIGN AND IMPLEMENTATION OF HIGH PERFORMANCE MAC UNIT CARRY SKIP ADDER

M. Josphine Sheela<sup>1</sup> & G.V. Soni Meera<sup>2</sup>

<sup>1</sup>Student, VLSI Design, Marthandam College of Engineering and Technology, Kuttakuzhi

<sup>2</sup>Assistant Professor, ECE, Marthandam College of Engineering and Technology, Kuttakuzhi

**ABSTRACT:** In this paper, we proposed a new architecture of multiplier -and- accumulator (MAC) for high-speed arithmetic and low power consumption. Multiplication occurs frequently infinite impulse response filters, fast Fourier transforms, discrete cosine transforms, convolution, and other important DSP applications. The objective of a good multiplier and accumulator (MAC) is to provide a less area, good speed and low power consuming chip also to consume significant power in VLSI design, and to reduce its dynamic power. The aim of this project is to design and implement the MAC unit for high-speed DSP applications. For designing the MAC unit using carry adders. The MAC unit implementation is done using VHDL, synthesized and simulated using Xilinx ISE.

**Keywords:**

### I.INTRODUCTION

Digital signal processing is one of the important technologies applied in most areas such as wireless communications, audio and video processing, and industrial control. Digital signal processing (DSP) applications constitute the important operations, which usually involve many multiplications and accumulations. The main aim of MAC design has been to enhance its speed, because speed and throughput rate are always important in the digital signal processing systems. Due to the increase of portable electronic products, low power designs have also become major considerations, because the limited battery energy of these portable products restricts the power consumption of the system. Therefore, the motivation behind this project is to investigate various pipelined MAC architectures and circuit and the design techniques which are suitable for the implementation of high throughput signal processing algorithms. The aim of this project is to design the VLSI implementation of pipelined MAC for high speed DSP applications. For designing the MAC, various architectures of carry adder are considered. The total process is coded with Verilog to describe the hardware.

### II.MAC Architecture

A design of high performance 16 bit Multiplier-and-Accumulator is designed. The Multiplier is designed using an array multiplier and the adder is carry skip adder. The attractive feature of the carry skips adder structure is reducing the delay based on the MAC unit. This will increase the

speed and improve the area utilization and power consumption. The total design is coded with Verilog-HDL and the synthesis is done using Xilinx ISE Compiler.

### BLOCK DIAGRAM

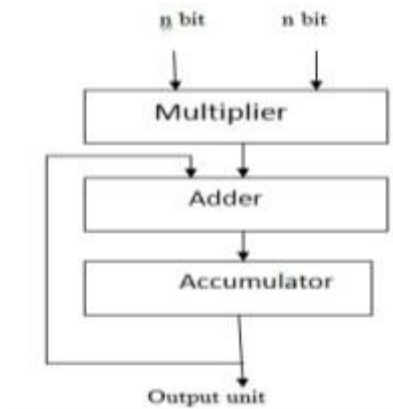


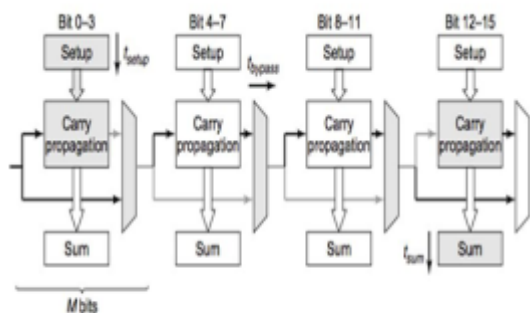
Fig : MAC architecture

MAC Unit is a fundamental block of the computing devices, especially Digital Signal Processor (DSP). The MAC unit performs multiplication and accumulation process. Basic MAC unit consist of multiplier, adding and accumulator .Multiplier circuit is based on adding and shift algorithm .Each partial product is generated using the multiplication of the multiplicand with one multiplier bit. The generated partial product are shifted according to their bit orders and then added. An adder is a digital circuit which performs addition of numbers. In many computers and other kinds of processor adders are used in the arithmetic logic

units or ALU. An accumulator is a registered element used for short-term, intermediate storage of arithmetic and logic data in a computer's CPU(Central Processing Unit) .

**A. Carry skip adder**

A carry-skip adder (also known as a carry-bypass adder) is an adder implementation that improves the delay of a ripple-carry adder compared to other adders. The worst-case delay can be improved by using several carry-skip adders to form a block-carry-skip adder. The critical path of a carry-skip-adder begins at the first full-adder, passes through all adders and ends of the sum-bit .Carry-skip-adders are chained to reduce the overall critical path.



$$t_{adder} = t_{setup} + M_{carry} + (NM-1)t_{bypass} + (M-1)t_{carry} + t_{sum}$$

Fig : Block diagram of carry skip adder

**B.Array Multiplier**

An array multiplier is a digital combinational circuit used for multiplication of two binary numbers by employing an array of half adder and full adders. They are well known for their regular structure. N X M bits are used for the generation of partial product and some area of multiplier are added to the N partial product and they require N-1 bit adders. The shifting of partial product is done by simple routing and they do not require any logic. For the performance optimization first the critical timing path should be identified , which are nontrivial. The critical path expression for the propagation delay can be expressed as

$$T_{multiplier} = [(M-1) + (N-2)]t_{carry} + (N-1) t_{sum} + t_{and}$$

Where t represents the propagation delay between the input and the output carry, tsum represents the delay between the input carry and a sum bit of the full adder, and t is the delay of AND . In order to get the effective processing elements linear pipeline is implemented .The multiplication of the M bit Multiplicand and N bit

multiplier yields N X M matrix of partial product. The reduction of partial product is made by the parallel application partial results in a matrix with a height of two.

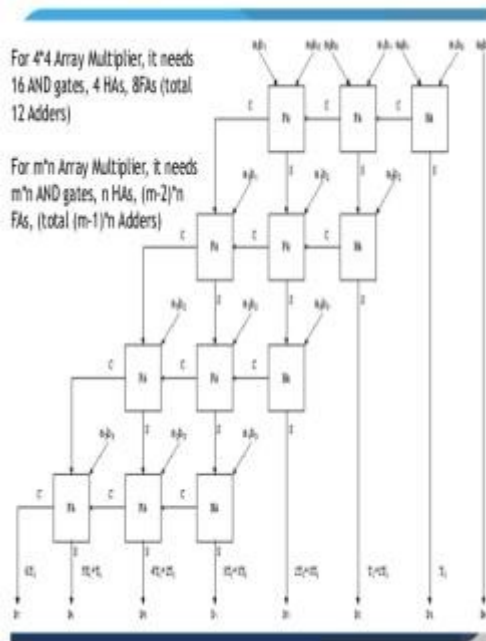


Fig: Array multiplier architecture

**C. Comparison**

The table shows the parameter analysis of area, power and delay comparing the conventional adder and proposed adder.

Parameter	Conventional Adder	Proposed Adder
AREA	88	98
No of LUT	32	18
Transistor count		
DELAY	5.978	4.392
POWER	100 MHZ	100 MHZ
Frequency	1.048	1.024

Fig : Comparison of Area ,Delay and Power

**D. Advantages**

- Less area
- Less delay
- Least gate count

**III.EXPERIMENTAL RESULT**

In this paper, A design of 16 Software Overview The Xilinx software controls all aspects of the design flow. By the Project Navigator interface, we can access all of the design entry and design implementation tools. We can also access the files and documents related to our project. There are four panel sub-windows in the Project Navigator. The top left is the Start, Design, Files, and Libraries panels, which implies display

and access to the source files in the project as well as access to running processes to the currently selected source. The Start panel is used for quick access to open the projects also frequently access reference material, documentation and tutorials. At the bottom of the Project Navigator indicates the Console, Errors, and Warnings panels, which display status messages, errors, and warnings. The right is a multi-document interface (MDI) window which is referred as the Workspace. The Workspace is useful to view design reports, text files, schematics, and simulation waveforms. Windows can also be resized, undocked from Project Navigator, moved to a new location within the main Project Navigator window, tiled, layered, or closed. We can use the View Panels menu commands to open or close the panels. Bit Multiplier-and-Accumulator (MAC) is implemented and a static CMOS CSKA structure called CI-CSKA was proposed with MAC, which implements high speed and consumes less power. The high speed was achieved by altering the structure through the concatenation and instrumentation techniques. The multiplier is designed using an array multiplier and the adder is designed to carry skip adder. Also, AOI and OAI compound gates were exploited for the carry skip logics. Verilog-HDL is used for coding and the synthesis is done using the Cadence RTL compiler.

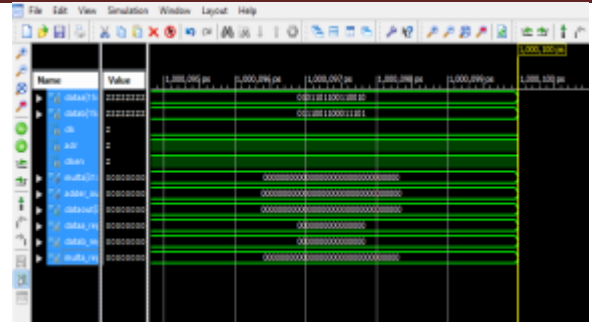


Fig : Output of MAC unit

#### IV.CONCLUSION

In this paper, a design of high performance 16-bit Multiplier-and-Accumulator (MAC) is implemented which exhibits a higher speed and lower energy consumption. The speed enhancement can be modified through the concatenation and Instrumentation technique. The carry skip adder in the middle includes a parallel adder structure to increase the slack time, which reduce the energy consumption by reducing the supply voltage.

#### REFERENCES

1. Avisek Sen , Debarshi Datta , Parha Mitra.,( 2013) "Low power MAC unit using DSP processors," International journal of Recent Technologyand Engineering,, January. ISSN: 2277-3878, volume-6, pp 93-95.
2. Aamir A. Farooqie, Vojin G. Oklobdzija.,( 1998) "General data path organization of MAC unit for VLSI implementation of DSP processors," IEEE Transaction on Circuits and System., pp 260-263.
3. Aapurva Kaul, Abhijeet kumar.,( 2016) "Simulation of 64-bit MAC unit using kogge stone adder and ancient indian mathematics," Int. Journal of Engineering Research and Application., june. ISSN: 2248-9622 vol. 6, pp 01-05.
4. Abdelgawad, Magdy Bayoumi., (2007) "High speed and area efficient multiply accumulate (MAC) unit for digital signal processing application," IEEE Transaction on Circuits and System., pp 3199-3202.
5. Akondi Narayana Kiran, G.Veera Pandu., ( 2012) "Hardware efficient VLSI architecture of parallel MAC for high speed signal processing application." Int. Journal of Engineering Research and Application., August ISSN: 2278-0181 vol. 1 issue 6, pp. 01-05.
6. Anusree T U, Bonifus P L., (2016) "Design and analysis of modified fast compressors for MAC unit," Int. Journal of Computer Trends and Technology., june. vol. 36, pp 213-218.
7. P.Asadee., ( 2009) "A new MAC design using high speed partial product summation tree." IEEE Transaction on Circuits and System., pp 234-231.

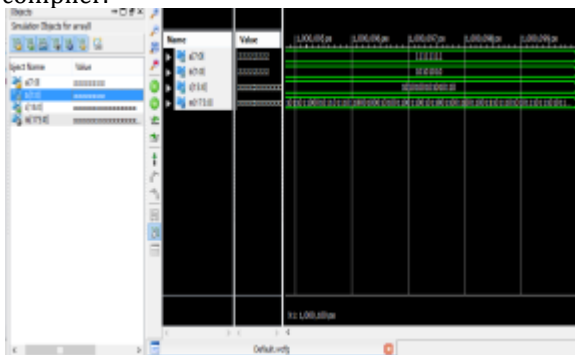


Fig: Output of Array multiplier



Fig: Output of Carry skip Adder

8. Ashish B.Kharate, P.R. Gumble., ( 2009) "VLSI Design and implementation of low power MAC for digital FIR filter," Int. Journal of Electronics and communication and computer Engineering., july. vol. 4, pp 5861.
9. Avisek Sen , Debarshi Datta , Parha Mitra.,( 2013) "Low power MAC unit using DSP processors," International journal of Recent Technology and Engineering., January. ISSN: 2277-3878, volume-6, pp 93-95.
10. Belle W. Y. Wei, Wen- Jung Liu, and Xiaoping Huang.,(1994) "A high-performance CMOS redundant binary Multiplication and accumulation(MAC) unit," IEEE Transaction on Circuits and System.: Fundamental Theory and Application, January. Vol 41, no. 1 pp 33-39.
11. N. Chaumartin, G. Geort, A.Lorenzi, J.M. Troude, G. Vanneuville, and V. Verfaillie., (1991) "VLSI ASIC design for MAC video processing integration in SGS-THOMSON microelectronics chip," IEEE Transaction on Circuits and System., pp 131-134.
12. Cyrill Prassana Raj, Kulkarni S.Y and Shanthala S, ( 2009) "Design and VLSI implementation of pipelined multiply accumulate unit," IEEE Transaction On Second International Conference on Emerging Trends in Engineering and Technology., pp 381-386.
13. Divyanshu Rao, Naveen Khare, and Ravi Mohan., ( 2016) "VLSI implementation of high speed MAC unit using karatsuba multiplication technique," Journal of Network Communications and Emerging Technologies., January. Volume 6, issue 1, pp 24-28.
14. Durga Bhavani. A, and Nagaraj Krishnha naik.,( 2015) "VLSI design of low power MAC unit,"International Journal of Current Engineering and Science Research., January. Volume 2, issue 6, pp 113-118.
15. Ganeshbabu.C, and Santhiya.S., (2016 )"Design and implementation of multiplier using Reversible logic in Multiple Accumulate unit," International Journal of Advanced research in Electronics and Communication Engineering ., April. volume 5, Issue 4, pp 1080-1086.

# ARCHITECTURE DEVELOPMENT OF COST-EFFICIENT MICRO CONTROL UNIT FOR WBSN

Ms.S. Sajini & Mr.E.Sherjin Tintu

VLSI Design, Marthandam College of Engineering and Technology, Kuttakuzhi

**ABSTRACT:** Data transmission of Electrocardiography(ECG) signal over Wireless Body Area Network(WBAN) is currently a widely used system that comes together with challenges in terms of efficiency and affectivity. In this study, an effective Very-Large-Scale Integration(VLSI) circuit design of lossless Electrocardiography(ECG) signal transmission over WBAN. The proposed design was realized based on a novel lossless compression algorithm which consists of an adaptive fuzzy prediction, a voting-based scheme and a tri-stage entropy encoder. The tri-stage entropy encoder is composed of a two-stage Huffman and LFSR(Linear feedback shift register) encoders with static coding table using basic comparator and multiplexer components. A pipelining technique was incorporated to enhance the performance of the proposed design. The proposed design was fabricated using a 0.18 CMOS technology containing 8405 gates with 2.58Mw simulated power consumption under an operating condition of 100MHz clock speed.

**Keywords:** Wireless sensor networks, micro control unit, lossless compression, very large scale integration(VLSI).

## I. INTRODUCTION

In modern days, applications of wireless body sensor networks(WBSNs) have become wider and wider. These applications provide an effective solution for many health care. In future trend of development, such as wireless sensor system for analyzing infectious disease nodes and efficiently protecting sensitive personal data in network security, the usage of WBSNs technique is improved rapidly. As the result of light-weight for wearable and portable application, development of an efficient device to monitor physical signals via the VLSI technique has become an important trend.

The author Lee et.al [8] proposed an efficiency complementary metal-oxide-semiconductor(CMOS) sensor for body

temperature detection. The blood pressure can be detected by a magnetoelastic skin curvature sensor proposed in [9]. The pH value can be measured by an ISFET sensor proposed in [10]. Although all these sensors provided efficient devices to capture the various physical signals, the WBSNs suffered from the limitation of wireless transmission bandwidth, computing resource and energy in batteries.

Several studies concerned hardware-oriented architecture of WBSNs has been presented recently. For saving more power consumption and keep longer using time, an adaptive power controller and adaptive fuzzy controller designed. A multi lossless body-signals compressor was presented in portable monitoring system.

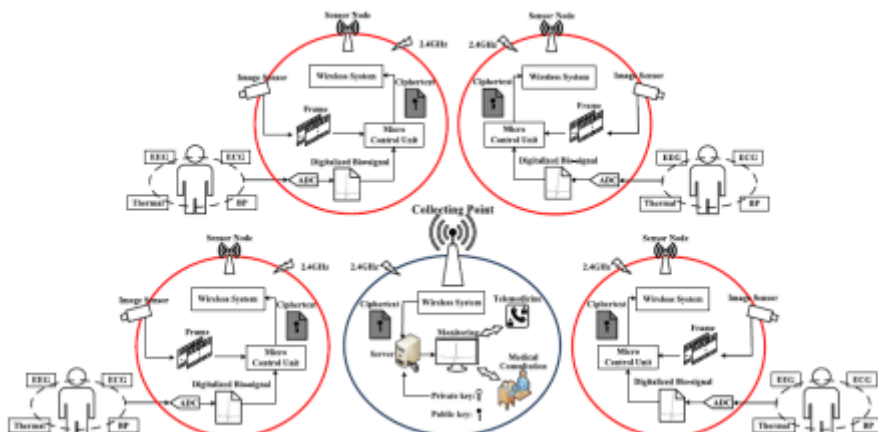


Fig.1 WBSNs system and the architecture of wireless sensor nodes

Recently for handling various bio-signals and processing physical signals in WBSNs, a multi-sensor micro control unit(MCU) was designed [11]. A bio-signal processing technique was used to improve signal quality in medical applications successfully. By using specific mathematical operations the physical signals can be analyzed.

## II. WIRELESS BODY SENSOR NETWORK SYSTEM

Fig.1 shows the WBSNs system and the architecture of wireless sensor nodes. A typical WBSNs composed a bunch of wireless sensor nodes. Each node consists of analog-to-digital converter(ADC), a micro control unit(MCU), and a wireless transceiver with an antenna.

The ever-increasing interest in wireless communications has resulted in the development of new technologies and applications for the personal use of radio frequencies. Technologies advancement in integrated circuits(ICs), coupled with that of wireless technology and physiological sensors, opens up opportunities for developing small, low power, light weight and intelligent physiological monitoring devices. These devices can form a Wireless Body Sensor Network(WBSN), launching a new era of using technology to unobtrusively obtain physiological measurements for improved well-being monitoring. This paper aims to give a comprehensive review on the use of wireless sensor technology for monitoring behavior related to human physiological responses.

In WBSNs are applicable in different physical signals, such as electroencephalography(EEG), Electrocardiogram(ECG), thermal and blood pressure(BP), are captured with the help of different sensors. Now, the MCU needs to process and merge the physical and image data are then sent to processed and merge data to a 2.4 GHz band communication system for transmission.

## III. ARCHITECTURE OF MICRO CONTROL UNIT

The architecture of MCU has been developed in order to develop a MCU design for wireless body sensor networks, a cost-efficient and power-efficient. Fig. 2 shows the architecture of the proposed MCU design. First, the physical data are detected from the four body sensors from human beings. The detected data is in the form of analog and then it can be transformed as digital data by an analog-digital converter (ADC) device. Second, these digital data are processed by the proposed MCU design that consists of an asynchronous interface, a multi-sensor controller,

a register bank, a hardware-sharing filter, a lossless compressor, an encryption encoder, an error correct coding (ECC), a QRS complex detector, a power management. At last, the processed digital data will be sent to the UART interface for transmission. All these operations and functions in the proposed MCU design are of low-complexity, which is suitable for development of WBSNs and implementation with a cost-efficient and high performance architecture via the VLSI technique.

### A. Multi-Sensor Controller

The WBSNs contain sensors that are used for detecting different physical signals from the human body. By generating a control signal to a 4-to-1 multiplexer, the multi-sensor controller can handle four different sensors, such as sensor1, sensor2, sensor3 and sensor4 as shown in Fig. 2. The multi-sensor controller can select one of four signals according to the control signal sent from the MCU. Since the multiplexer selects the sensor properly, with the help of MCU

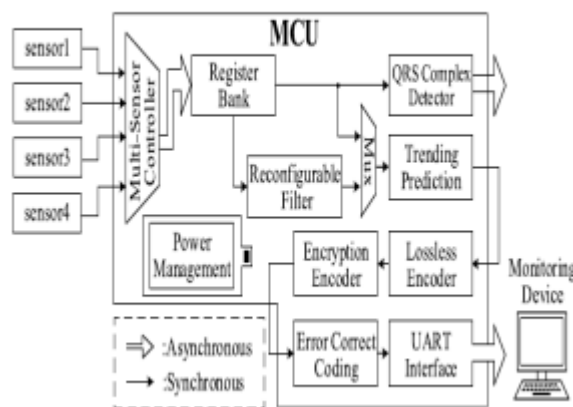


**Fig. 2** Proposed micro control unit successfully. More than one sensor is active at any and sending signals to the MCU simultaneously. In addition, the multi-sensor controller also controls the signals to store the data in one of four-line register buffers in the register bank of the MCU. Therefore, based on the design of the multi-sensor controller, the proposed MCU design can be efficient one and also prevent data from missing.

### B. Register Bank

The register bank was designed in order to process four different signals, in the proposed MCU. In the proposed architecture of the register bank consists of four line buffers  $X_1, X_2, X_3, X_4$ , and one multiplexer. There are 16 shifts-registers are used to store the four values for each channel. The proposed MCU produces a control signal by the finite state machine circuit to classify different

sensor data. Each channel in the register bank stores four values: one current value  $X_i(t)$  and three past values  $X_i(t-1)$ ,  $X_i(t-2)$  and  $X_i(t-3)$  where "i" is the index of line buffer. Each register can receive only one value of physical signal in each time.

C. Reconfigurable Filter

In order to process the signals in different requirements, there are three types of filters which is designed to achieve the abilities of different physical signals filtering: sharpen filter, binomial filter, and average filter. Here the Sharpen filter can be represented by  $G(x)$ , Binomial filter can be represented by  $P(x)$ , Average filter can be represented by  $A(x)$ .

Sharpen filter  $G(x)$  uses Gaussian equation [17] to increase the intensity of high frequency and filter out low frequency parts of the signal. Binomial filter  $P(x)$  can be obtained by Pascal's triangle [18], and the filter can enhance central value and cutoff high and low frequency noises from the signal. Average filter  $A(x)$  uses the same weighting coefficients to calculate average value of the signal stored in register bank. By using these different kinds of filters, the physical signals can be observed apparently.

D. QRS complex detector

In order to achieve the target of the proposed multi control unit for WBSNs, heartbeats are considered by a QRS complex detector. To obtain the heartbeats information in the real time, the proposed QRS complex detection algorithm will detect the information and record the QRS information by analyzing the critical regions of the ECG signal. For example, the R and S points usually appear at the maximum (Max) and minimum (Min) values in the ECG signals respectively. Hence, the critical regions in the heartbeats can be easily detected according to information on the detected R and S points. Two thresholds *High* and *Low* are used to determine whether the values enter into the critical regions while the process is taking place. The R and S points are recorded as *Max* and *Min* values in order to update the values of *High* and *Low* thresholds, respectively. The High threshold can be evaluated by

$$High = (Max - \frac{(Max - Min)}{2^n})$$

The Low threshold can be evaluated by

$$Low = (Max - \frac{(Max - Min)}{2^n})$$

E. Lossless Compressor

In order to reduce the power consumption caused by the wireless communication and maintain the integrity of physical signals, a lossless compressor is used. The lossless compressor includes two and they are, an adaptive trending predictor and a hybrid entropy encoder was created for the WBSNs. Lossless Compressor is a class of data compression algorithms that allows the original data to be perfectly reconstructed from the compressed data. To be able to reduce the data redundancy efficiently, an adaptive three-trending-prediction algorithm was proposed. The current value  $X_i(t)$  was forecasted by the past three values of the  $X_i(t-1)$ ,  $X_i(t-2)$  and  $X_i(t-3)$ .

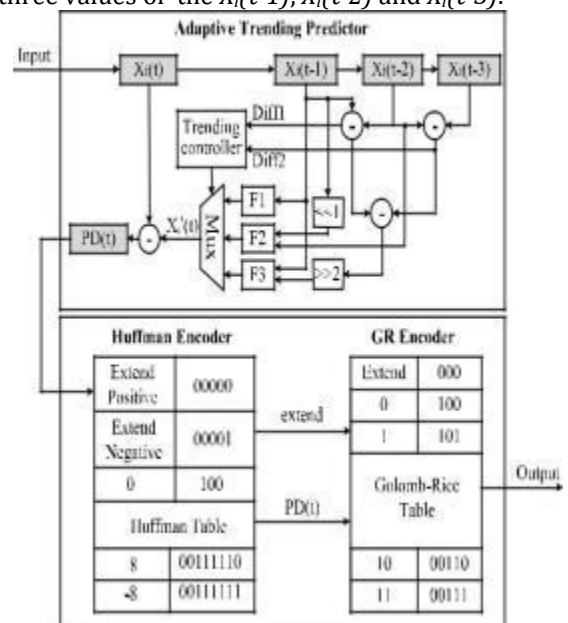


Fig. 3 Architecture of proposed Lossless Compressor

Fig. 3 shows the architecture of the proposed lossless compressor. It consists of an adaptive trending predictor and an hybrid entropy encoder. The predictor contain 1 register, 3 subtractors, 1 multiplexer, 3 prediction function generators, and 1 trending controller. The trending controller produced control signals to select a result of  $X_i^0(t)$  from three predicted function generators  $F1$ ,  $F2$ , and  $F3$ . Finally, the prediction difference ( $PD(t)$ ) can be produced by calculating the difference between  $X_i(t)$  and  $X_i^0(t)$ . The extensible hybrid-entropy encoder consists of a modified Huffman and absolute GR encoder.

F. Huffman Coding

Huffman coding [15] is a classic entropy coding algorithm, it is mainly used for the probability distribution of target values is

centralized. However, the silicon area of a Huffman encoder will be enlarged for the depth of the Huffman coding tree. Hence, a limited Huffman coding technique was selected as the first stage of the proposed entropy coding methodology.

The main idea of Huffman Coding is to assign variable-length codes to input characters, the length of the assigned codes are based on the frequencies of corresponding characters. The most frequent character gets the smallest code and the least frequent character gets the largest code. The variable-length codes assigned to input characters are Prefix Codes, means the codes (bit sequences) are assigned in such a way that the code assigned to one character is not prefix of code assigned to any other character. This is how Huffman Coding makes sure that there is no ambiguity when decoding the generated bit stream.

On the other hand, two extending codes, positive and negative extending codes, were added to encode the values beyond the range of the limited Huffman coding table, which successfully improved the performance by removing a sign bit of Golomb-Rice (GR) codes and reduced half silicon area.

**FLOWCHART OF HUFFMAN ALGORITHM**

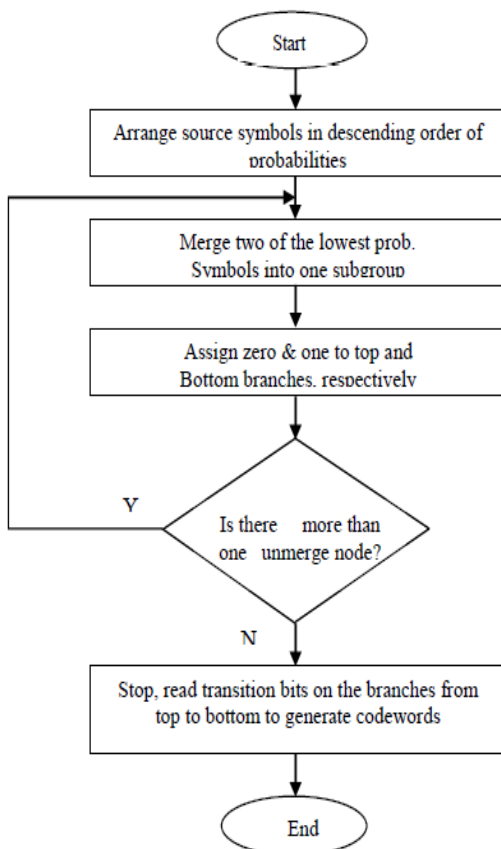


**Fig. 4** Flow chart of Huffman algorithm

**G. Encryption Encoder**

Encryption Encoder prevent the personal information from being cracked. It is a technique used to transfer the plaintext to ciphertext for WBSNs. EEC is based on ElGamal cryptography which is a kind of asymmetric encryption coding. ElGamal algorithm is an efficient way to prevent the personal information by using two key and they are, public key and private key. Public key is a confidential parameter and private key is an open parameter.

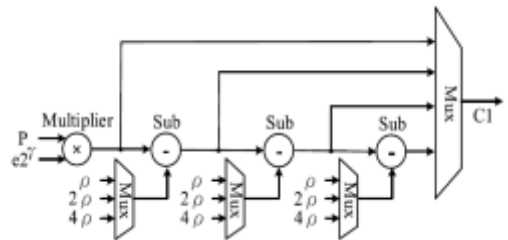


**Fig. 5** Architecture of the proposed encryption encoder

where p is the plaintext,  $e_2^\gamma$  is the public key Fig. 5 shows the architecture of the proposed encryption encoder. It consists of 1 multiplier, 3 subtractors, and 4 multi-plexers. The remainder values ciphertext  $C_1$  were calculated. Finally, the simplified encryption encoder provides both low-cost architecture, and produces better security for the proposed MCU design.

To be able to decrypt the ciphertext which is sent from sensor node, the private key is used. The wireless sensor nodes used public keys to encrypt the personal information, but they cannot use the public key to decrypt the ciphertext. However, the private key set by the administrator is the only one which can decrypt the text

**H. Error Correct Coding**

ECC can used to increase the reliability for wireless transmission. The Encrypted data is given to the block. ECC add an additional bit called redundancy code before transmission. So the receiver can able to check whether transmission data are correct or not before decoding. It is also used to decrease the transmission error.

**H. Universal Asynchronous Receiver/ Transceiver Interface**

UART is used to transmit the bit stream to other devices. It communicate between hardware and PC.

**IV. EXPERIMENTAL RESULT**

This work was synthesized by using a Xilinx ISE software. Xilinx software controls all aspects of the design flow.

Fig 6 shows the Design summary of proposed MCU design. Design Summary provides access to design reports, messages, and summary of results data. Message filtering can also be performed. Design Utilities Provides access to symbol generation, instantiation templates, viewing command line history, and simulation library compilation. User constraints provides access to editing location and timing constraints.

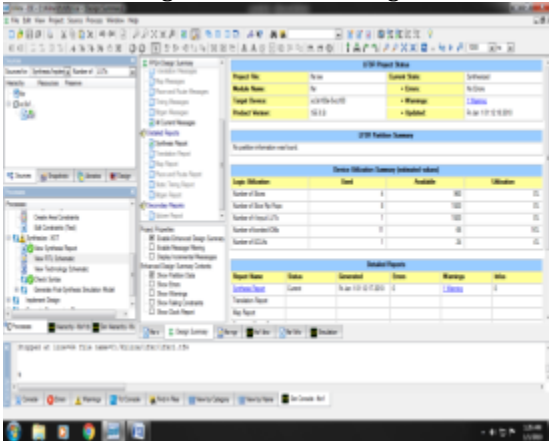


Fig.6 Design Summary of Proposed MCU

Fig.7 shows the coding window of the proposed MCU design. In computing, a linear-feedback shift register (LFSR) is a shift register whose input bit is a linear function of its previous state. However, an LFSR with a well-chosen feedback function can produce a sequence of bits that appears random and has a very long cycle.

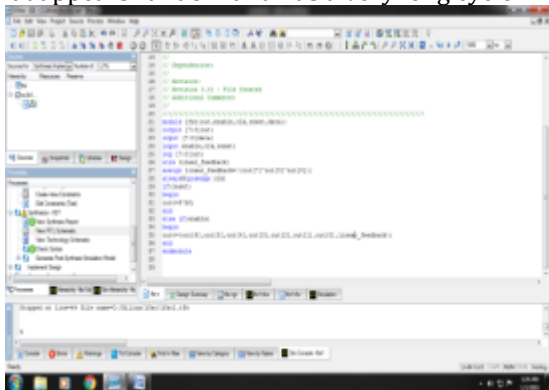


Fig.7 Coding Window of proposed MCU

Fig 8 shows the RTL schematic of proposed MCU. By using this LFSR technique various cryptography applications can be generated by pseudo random numbers. The overall number of random state produced by the LFSR is determined by the feedback polynomial which reduces the delay to an considerable amount compare to that of other methods.

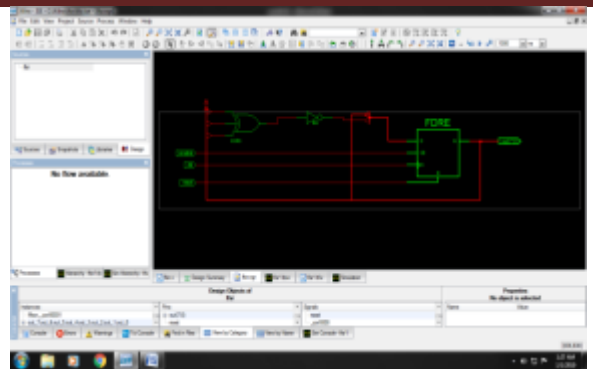


Fig.8 RTL Schematic of proposed MCU

Fig 9 shows the stimulation output of the proposed MCU. When discussing a sequence of random numbers, each number drawn must be statistically independent of the other.

Random number generator is a computational device to generate a sequence of numbers or that lack any pattern. LFSR gives those random pattern generation

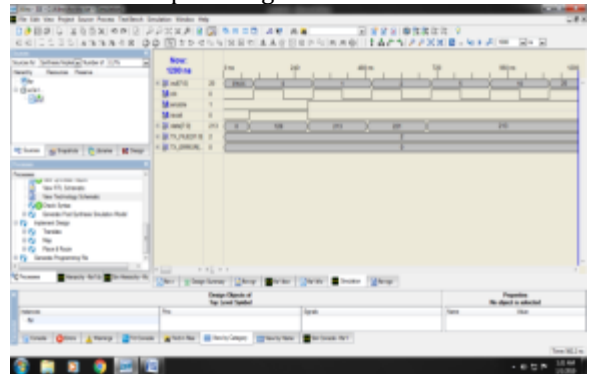


Fig. 10 Stimulated Output

Compared with the previous studies, this work is better in the block of QRS detector and an encryption encoder, but has higher performance, higher security, higher reliability, higher compatibility, more functions, and more exibility than previous designs.

**V.CONCLUSION**

In this paper, a VLSI architecture of a cost-efficient and micro control unit (MCU) design for WBSNs was presented. The novel hardware-sharing reconfigurable filter was design for reducing the chip area. To reduce the possibilities of misdiagnosis and decrease the transmission power, the lossless compressor consist of an adaptive trending predictor and an extensible hybrid entropy encoder was developed. Through adding an asymmetric architecture of encryption encoder (EEC), the personal information can be protected while wireless transmission. On the other hand, an additional architecture of QRS

complex detector was design, which provided more information of physical signals such as heart-beats. The simulation results shows, the proposed MCU design was synthesized by the VLSI technique. Compared with previous designs, this work had better for lower cost, higher compression rate, more functions, and higher security than previous studies.

## REFERANCE

1. M. Naeem, U. Pareek, D. C. Lee, A. S. Khwaja, and A. Anpalagan, "Wireless resource allocation in next generation healthcare facilities," *IEEE Sensors J.*, vol. 15, no. 3, pp. 1463 1474, Mar. 2015.
2. H. C. Chuang, C. Y. Shih, C. H. Chou, J. T. Huang, and C. J. Wu, "The development of a blood leakage monitoring system for the applications in hemodialysis therapy," *IEEE Sensors J.*, vol. 15, no. 3, pp. 1515 1522, Mar. 2015.
3. P. J. F. White, B. W. Podaima, and M. R. Friesen, "Algorithms for smart-phone and tablet image analysis for healthcare applications," *IEEE Access*, vol. 2, pp. 831 840, Aug. 2014.
4. D. Kwon, M. R. Hodkiewicz, J. Fan, T. Shibutani, and M. G. Pecht, "IoT-based prognostics and systems health management for industrial applications," *IEEE Access*, vol. 4, pp. 3659 3670, Jul. 2016.
5. J.-F. Cheng, J.-C. Chou, T.-P. Sun, S.-K. Hsiung, and H.-L. Kao, "Study on a multi-ions sensing system for monitoring of blood electrolytes with wireless home-care system," *IEEE Sensors J.*, vol. 12, no. 5, pp. 967 977, May 2011.
6. X. Sun, Z. Lu, X. Zhang, M. Salathé, and G. Cao, "Infectious disease containment based on a wireless sensor system," *IEEE Access*, vol. 4, pp. 1548 1559, Apr. 2016.
7. L. Xu, C. Jiang, J. Wang, J. Yuan, and Y. Ren, "Information security in big data: Privacy and data mining," *IEEE Access*, vol. 2, pp. 1149 1176, Oct. 2014.
8. H.-Y. Lee, S.-L. Chen, and C.-H. Luo, "A CMOS smart thermal sensor for biomedical application," *Inst. Electron., Inf. Commun. Eng.*, vol. E91-C, no. 1, pp. 96 104, Jan. 2008.
9. E. Kaniusas et al., "Method for continuous nondisturbing monitoring of blood pressure by magnetoelastic skin curvature sensor and ECG," *IEEE Sensors J.*, vol. 6, no. 3, pp. 819 828, Jun. 2006.
10. P. Rai, S. Jung, T. Ji, and V. K. Varadan, "Drain current centric modal-ity: Instrumentation and evaluation of ISFET for monitoring myocardial ischemia like variations in pH and potassium ion concentration," *IEEE Sensors J.*, vol. 9, no. 12, pp. 1987 1995, Dec. 2009.
11. E. Nemati, M. J. Deen, and T. Mondal, "A wireless wearable ECG sen-sor for long-term applications," *IEEE Commun. Mag.*, vol. 50, no. 1, pp. 36 43, Jan. 2012.
12. S.-L. Chen, H.-Y. Lee, C.-A. Chen, H.-Y. Huang, and C.-H. Luo, "Wire-less body sensor network with adaptive low-power design for biometrics and healthcare applications," *IEEE Syst. J.*, vol. 3, no. 4, pp. 398 409, Dec. 2009.
13. S. L. Chen, "A power-ef cient adaptive fuzzy resolution control system for wireless body sensor networks," *IEEE Access*, vol. 3, pp. 743 751, 2015.
14. E. Chua and W.-C. Fang, "Mixed bio-signal lossless data compressor for portable brain-heart monitoring systems," *IEEE Trans. Consum. Electron.*, vol. 57, no. 1, pp. 267 273, Feb. 2011.
15. C.-A. Chen, S.-L. Chen, H.-Y. Huang, and C.-H. Luo, "An asyn-chronous multi-sensor micro control unit for wireless body sensor networks (WBSNs)," *Sensors*, vol. 11, no. 7, pp. 7022 7036, Jul. 2011.

# VLSI ARCHITECTURE FOR CDMA TECHNOLOGY USING WALSH CODE GENERATOR

S. Akhila\* & H.Christal Beni\*\*

\*Student, VLSI Design, Marthandam College of Engineering and Technology, Kuttakuzhi

\*\*Assistant Professor, ECE, Marthandam College of Engineering and Technology, Kuttakuzhi

---

**ABSTRACT:** A Code Division Multiple Access (CDMA) is implemented in an on-chip crossbar due to its fixed latency, reduced arbitration overhead, and higher bandwidth. The overloaded CDMA interconnect (OCI) architecture used is the Walsh code generator to enhance the capacity of CDMA (Network on Chip) NoC by increasing the spreading codes. In the serial OCI crossbar, it can achieve 100% higher bandwidth, 31% less resource utilization, and 45% power saving, while in parallel OCI crossbar it achieves  $N$  times higher bandwidth compared to serial OCI crossbar at the expense of increased area and power consumption

**Keywords:** Code Division Multiple Access (CDMA), Overloaded CDMA Interconnect (OCI), Network on Chip (NoC)

---

## I. INTRODUCTION

System on Chip integrates several intellectual property (IP) blocks into a single chip. All of these IPs need to communicate in the Gbps range. So the on-chip communication requirements for these systems are very demanding. The IP blocks must comprise an interconnection architecture and several interfaces to connect the peripheral devices. The interconnection architecture includes many physical interfaces and communication mechanisms. On-chip data transfer affects the area, performance and the power utilization of the System on Chips (SoC). Developing a suitable high-performance on-chip interconnect architecture has been of supreme significance while considering the high-speed computing technologies. Network on Chips (NoC) provide a way to prevail over the restrictions inherent in regular bus-based interconnection schemes and offers several benefits like high throughput, lower energy dissipation, flexible scalability, and design reusability.

Code-division multiple access (CDMA) is another medium sharing technique that leverages the code space to enable simultaneous medium access. In CDMA channels, each transmit-receive (TX-RX) pair is assigned a unique bipolar spreading code and data spread from all transmitters are summed in an additive communication channel. The spreading codes in classical CDMA systems are orthogonal (cross-correlation between orthogonal codes is zero). These codes enable the CDMA receiver to properly decode the received sum via a correlator decoder.

To enable the medium sharing classical CDMA systems to rely on Walsh–Hadamard orthogonal codes. CDMA has been used as an on-chip interconnect sharing technique for both bus and NoC interconnect architectures. Reduced power consumption, fixed communication latency, and reduced system complexity are the advantages of using CDMA for on-chip interconnects. A CDMA switch has less wiring complexity than SDMA crossbar and less arbitration overhead than a TDMA switch and thus provides a good compromise of both.

Overloaded CDMA is a well-known medium access technique deployed in wireless communications where the number of users sharing the communication channel is boosted by increasing the number of usable spreading codes. To increase the interconnect capacity of on-chip interconnects, overloaded CDMA concept can be used. Multiple Access Interference (MAI) limits the capacity of the CDMA system. By overcoming the MAI problems, interconnect capacity of the CDMA can be significantly increased without degrading the performance or increasing the resource utilization. CDMA channel overloading is a known technique mainly used in wireless communications to increase the communication channel capacity. This technique increases the number of elements sharing the ordinary CDMA bus while keeping the system complexity unchanged by using simple encoding circuitry and relying on the accumulator-based decoder with minimal changes. The conventional method can be advanced by the TDMA OCI (T-OCI) and Parallel-OCI (P-OCI) topologies to increase the bus

capacity by 100%. Code overloading for both topologies relies on exploiting special properties of the used spreading code set, namely Walsh code family to add a set of identifiable non-orthogonal spreading codes. NoCs provide a scalable solution for large SoCs, but they exhibit increased power consumption and large resource overheads. To make the crossbar more efficient, a Parallel Compare and Compress (PCC) based codec can be used in the crossbar architecture. This reduces the surplus area needed to store the message data. Also, it provides a security for the data that transmitted through the crossbar.

The paper is organized as follows Section II Network on Chip and section III covers proposed the method of CDMA and section IV covers Walsh Code Sequence and section V Results and discussion and conclusion is given in section VI.

## II. NETWORK ON CHIP

Network-on-Chip (NoC) is an advanced design method of communication network into System-on-Chip (SoC). It provides a solution to the problems of traditional bus-based SoC. It is widely considered that NoC will take the place of traditional bus-based design and will meet the communication requirements of next SoC design. A router is the key component and known as the communication backbone in NoC. Fig 1 shows the basic structure of NoC.

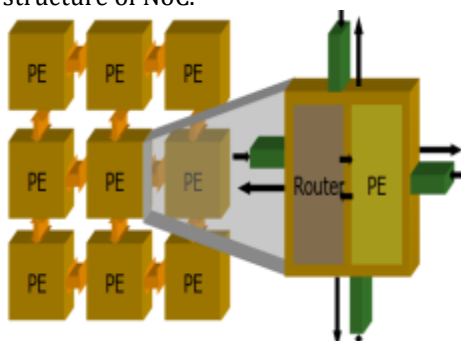


Fig 1: Basic structure of NoC

The NoC is placed on a single chip, which is separated into several regular tiles. A tile is a part of the chip that contains an Intellectual Property (IP) core or Processing Element (PE) and a network router, which is the main component in NoCs. The IP cores are usually heterogeneous in such design because the applications are heterogeneous. The NoC can have general purpose processors, application specific cores, memory modules, input or output devices and so on. The PE performs computation and communicates with other PE by messages, which are sent through the communication network. By using a Network

Adapter (NA), the PE is connected to the network. Its function is to provide an interface between the PE and the network. It also specifies how the communication services are made available to any PE type.

The NA provides mainly two interfaces: one for PEs and another one for the network. It handles the messages generated by the PEs by breaking them into several smaller units called packets. A packet is the logical unit of information that is transmitted through a network route using routers. The packet is composed of the following parts: a header, a data payload, and a tail. The packet header is the front of a packet and it contains the information about the source and destination NoC routers. This helps the NoC to decide the path of the packet. The data payload holds the data transmitted by the PE core across the NoC. The packet tail marks the end of the packet and typically contains codes for error checking and correction.

The communication channel in NoC is the combination of transmitter, physical links, and the receiver. It makes the physical connection between several PEs. The function of the transmitters is to convert digital to analog signals and receivers are used to convert analog signals to digital signal respectively. Analog signals are carried by a set of wires or fibers known as the physical link. Some other important terminals used for communication purpose in NoC's are flit and phit. A packet is made of flow control units, named as flits. A flit is the minimum unit of information that can be transformed across a link and either accepted or rejected. Each flit is made of one or more physical units called phits. The phit is the minimum size datagram that can be transmitted in one link transaction. In most of the cases, both the flit and phit are equal.

The router is the another important NoC component which drives the information through the network. It uses a routing algorithm to determine which of the possible paths, from source to destination are used as routes and which route is taken by each particular packet. Buffers are used at the input ports of the router to store the flits until the router can handle them. The router contains a crossbar switch that provides the means to route the information. A switching mechanism determines how and when the data traverses its route in NoC architectures packet switching is used. That means messages are broken into a sequence of packets and that packets are individually routed.

**III. PROPOSED METHOD OF CDMA**

CDMA is a spread spectrum technique which encodes the information prior to transmission onto a communication medium, permitting simultaneous use of the medium by separate information streams. By using CDMA encoding, the interconnecting wiring can be reduced to a certain extent. It relies on the principle of codeword orthogonality, such that when multiple code words are summed they do not interfere completely with each other at any point in time and can be separated without loss of information. The channel utilization can be increased by spreading the channel bandwidth using the spread spectrum technique. There are two types of mainly used techniques; one is called Frequency Hopping Spread Spectrum (FHSS) and is currently and the second one is called Direct Sequence Spread Spectrum (DSSS) which is generally used in civil application systems. CDMA is a spread spectrum multiple access techniques. A spread spectrum technique is one which spreads the bandwidth of the data uniformly for the same transmitted power. A pseudo-random code which has a narrow ambiguity function, unlike other narrow pulse codes, is known as the Spreading code. In CDMA a locally generated code runs at a much higher rate than the data to be transmitted. The main advantages of CDMA technique are listed below,

- It increases the efficient use of communication media.
- Anti-jam capability.
- Anti-interference capability.
- Low probability of intercept.
- Anti-multipath capability.
- Multi-access capability.

The CDMA technique uses various spreading codes to encode and decode the message sent and received. One of them is Walsh code.

Walsh-Hadamard sequences are used in the CDMA to transmit and receive the signals. Orthogonal codes are those, which provide a zero cross-correlation when there is no offset between the codes. They make use of Orthogonality property, which refers to dot product between the two spreading codes, is equal to zero. Hadamard transform is one of the best-known code expansion techniques to generate orthogonal codes. Walsh sequences are generated by mapping codeword rows of a Hadamard transform. Also, it can be generated by using the Walsh code generator circuit which is shown in Fig 2. The

important property of the Walsh spreading code is that it obeys the balancing property.

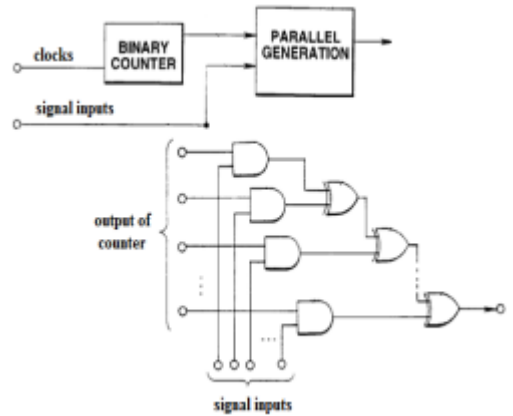


Fig. 2 Walsh code generator circuit.

**IV WALSH CODE SEQUENCE IN CROSSBAR SWITCH**

The Fig.3 illustrates the high-level architecture of a CDMA-based NoC router.

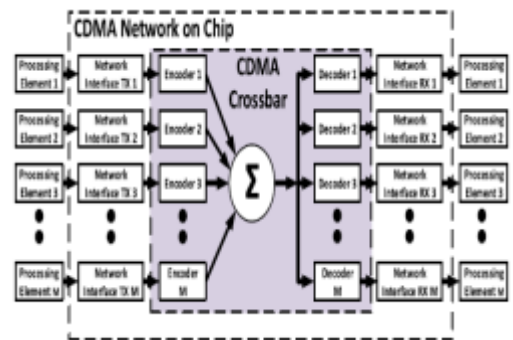


Fig 3 High-Level Architecture of a CDMA-based NoC router

The physical layer of the router is based on the classical CDMA Switch. The classical CDMA crossbar as shown in Fig. 4 consists of three sections. They are the encoder section, channel section, and decoder section. In the encoder part, the spreading code generator module (Walsh spreading code) generates binary orthogonal code which has a chip length of  $N$  is XORed with the transmitted data bit and sent out serially. It indicates that a single bit is spread in a duration of  $N$  clock cycles. The number of TX-RX ports sharing the CDMA router equals  $M = N - 1$  for Walsh spreading codes. Serial streams from all transmit PEs sharing the crossbar are added together and the binary sum is sent to the decoding section, which is connected to the receiving ports.

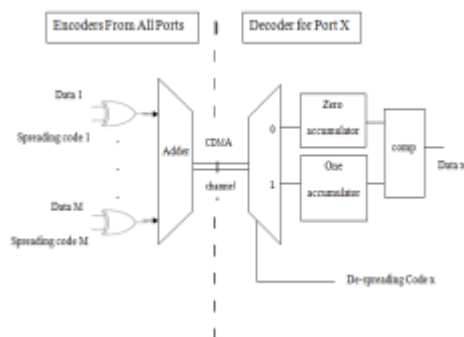


Fig.4 Conventional CDMA Crossbar Switch.

Binary encoding and signalling is multilevel signalling for implementing the channel adder due to its superior performance, reliability, and its inherent support by digital platforms. The decoder is implemented as a wrapper that crosses correlates the serialized channel sum with the signature code assigned to the TX-RX pair. The decoding process is periodic and the decoding cycle lasts for N clock cycles. The spreading operation is realized using a correlator decoder that correlates the received channel sum with the spreading code assigned to the TX-RX pair. Two accumulators are used to realize the correlator decoder. According to the assigned CDMA code, the received sum is passed to the zero accumulator when the current chip value is "0" and to the one accumulator when the chip value is "1," which is equivalent to multiplying the crossbar sum by  $\pm 1$ . At the end of the decoding cycle, the decoder has received the sum of spreading codes or their complements encoded according to the data spread by the transmit ports. Decoding the crossbar sum containing an orthogonal code or its complement using other orthogonal codes (cross-correlation) results in adding the same value to both accumulators. Decoding the crossbar sum containing an orthogonal code or its complement using the same code (autocorrelation) makes the value of one accumulator greater than the other accumulator by the number of ones in the code, which equals  $N/2$  spreading codes. The cross-correlation between orthogonal codes yields zero, while autocorrelation (multiplying the code by itself or its complement) yields  $\pm N/2$ . Therefore, the difference between the one and zero accumulators is always  $\pm N/2$  for orthogonal spreading codes. This can be directly derived for the accumulator decoder using the correlation definition and Walsh code orthogonal property. Overloaded CDMA is a technique used to increase the number of users sharing the communication

channel is boosted by increasing the number of usable spreading codes. This concept can be applied to on-chip interconnects to increase the interconnect capacity. The CDMA router has M transmit/ receive ports. The main difference between the overloaded and classical CDMA routers is that  $M > N - 1$  for the former due to channel overloading. Each Processing Element is connected to two Network Interfaces (Nis), i.e., the transmit and receive Network Interface modules.

During the data transmission from a PE, the packet is divided into flits to be stored in the transmit NI first-input first output (FIFO). The router arbiter then selects M winning flits at most from the top of the Network Interface FIFOs to be transmitted during the current transaction. Each of the selected flits has a destination address to avoid the conflicts and a winner from two conflicting flits is selected. This is done on the basis of the router's priority scheme. The employed priority scheme is the fixed winner that takes all priority schemes; only one of the transmitters is given a spreading code and is acknowledged to start encoding.

Once this process is completed, the router then assigns CDMA codes to each of the transmit and receive Network Interface (NI). Network Interfaces with empty FIFOs or conflicting destinations are assigned all-zero CDMA codes such that they do not contribute Multiple Access Interference (MAI) to the CDMA channel sum. Afterward, flits from each NI are spread by the CDMA codes in the encoder module. The data are spread into N chips, where N is the CDMA code length that equals the number of clock cycles in a single crossbar transaction. Spread data chips from all encoders are summed by the CDMA crossbar adder and the sum is sent out serially to all decoders. The encoding/decoding process lasts for N synchronized via a counter. At each decoder, a code is cross-correlated with the received sum to decode the data from the summed chips. The decoded flits are stored in the receive NI FIFOs until they are read by the PEs.

Two architecture variants of the crossbar can be implemented by using the same structure. They are TDMA Overloaded on CDMA Interconnect (T-OCI) and Parallel Overloaded CDMA Interconnect (P-OCI). The non-orthogonal codes imitate the TDMA signalling scheme. The encoding/decoding scheme used in the architecture provides a novel approach that enables coexistence between CDMA and TDMA signals in the same shared medium. Therefore, the developed encoder is called TDMA overloaded on CDMA interconnect (T-OCI). The

Parallel Overloaded CDMA Interconnect (P-OCI) crossbar employs the same Walsh and Overloaded Codes as the T-OCI crossbar; however, the data spreading and decoding are parallelized.

There are several advantages for the overloaded CDMA crossbar when compared with the conventional CDMA crossbar. They are:

- Increases the channel capacity  
 In Overloaded CDMA the number of users sharing the communication channel is boosted by increasing the number of usable spreading codes. This increases the channel capacity.

- Reduction in area  
 The area can be reduced by using the PCC based architecture. Because the area needed to store the data bits can be reduced by the compression technique.

- Fixed communication latency  
 The CDMA technique only offers fixed communication latency. The conventional CDMA and T-OCI crossbar variants exhibit the same latency, which is N clock cycles because a single data bit is spread in N chips. The latency of the P-OCI crossbar, however, is only one cycle.

**V. RESULTS AND DISCUSSIONS**

**1. SIMULATION OUTPUT FOR CDMA**

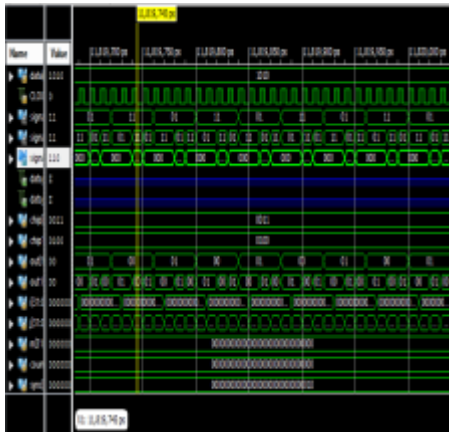


Fig.5 Simulation output for CDMA transmission



Fig.6 Simulation output for CDMA receiver

**2. SIMULATION OUTPUT FOR TRANSMITTER SECTION**

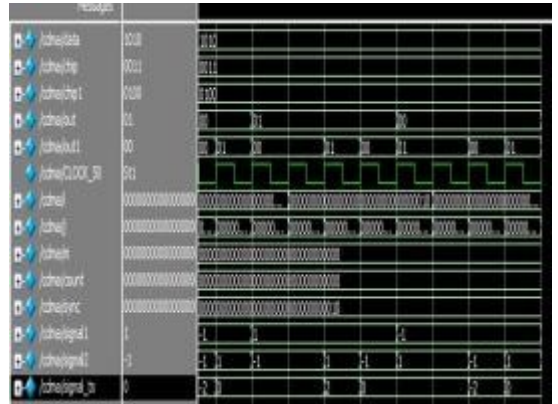


Fig.7 Simulation output for transmitter section

**3. SIMULATION OUTPUT FOR COUNTER**



Fig.8 Simulation output for counter

**4. SIMULATION OUTPUT FOR DEVELOPMENT OF COUNTER IN WALSH CODE GENERATOR**

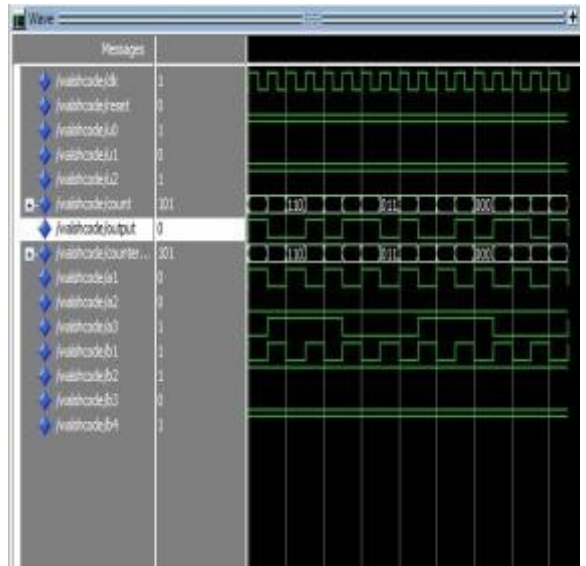


Fig.9 Simulation for counter + walsh code output

5. SIMULATION OUTPUT FOR ORTHOGONAL AND NON-ORTHOGONAL SEQUENCES

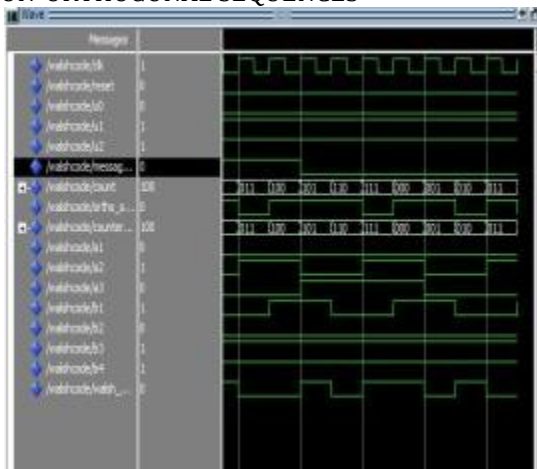


Fig.10 Simulation output for orthogonal sequence

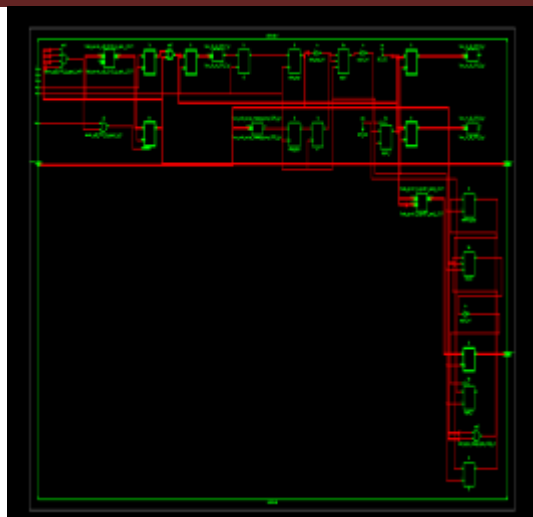


Fig. 13 RTL representation

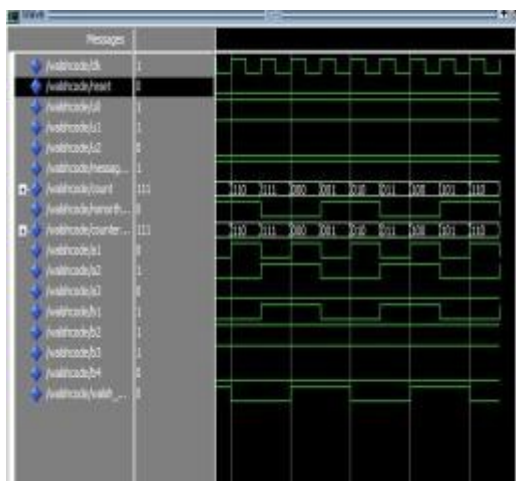


Fig.11 Simulation output for non-orthogonal sequence

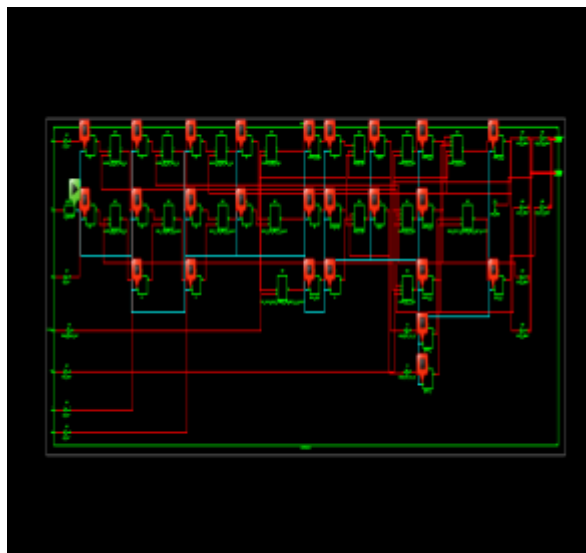


Fig. 14 Technology

6. RTL SCHEMATIC FOR ENCODER

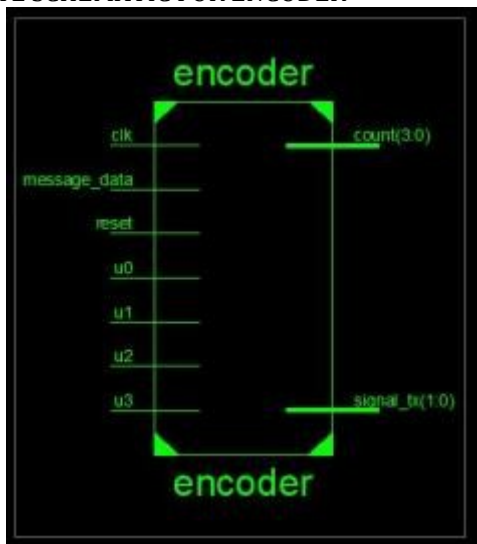


Fig.12 Signal representation

7. SIMULATION OUTPUT FOR ENCODER

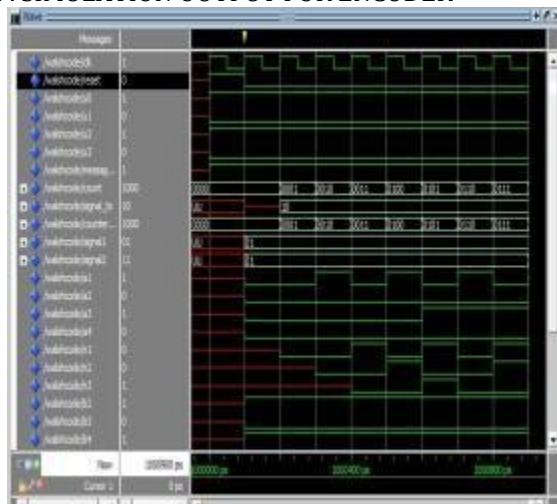


Fig.15 Simulation output for encoder

Table I Hardware Utilization

Device Utilization Summary			
Slice Logic Utilization	Used	Available	Utilization
Number of Slice Registers	25	126,800	1%
Number used as Flip Flops	25		
Number of Slice LUTs	18	63,400	1%
Number used as logic	18	63,400	1%
Number using O6 output only	18		
Number of occupied Slices	8	15,850	1%
Number of LUT Flip Flop pairs used	20		
Number with an unused LUT	2	20	10%
Number of fully used LUT-FF pairs	18	20	90%
Number of unique control sets	1		
Number of slice register sites lost to control set restrictions	7	126,800	1%
Number of bonded IOBs	13	210	6%
Number of BUFG/BUFGCTRLs	1	32	3%
Number used as BUFPGs	1		
Average Fanout of Non-Clock Nets	1.72		

From the table, the number of slice registers used is 25 and the available bits are 126,800 and the utilization is 1%. The total number used as flip-flops is 25. The number used as logic and the number of slice LUTs used is 18 and bits available is 63,400 and the utilization is 1%. The number using O6 output only is 18. The number of occupied slices used is 8 and the available bits are 15,850 and the utilization is 1%. The number of LUT flip-flop pairs used is 20. The number with an unused LUT used is 2 and the available bits are 20 and the utilization is 10%. The number of fully used LUT-FF pairs used is 18, the available bits are 20 and the utilization is 90%. The number of unique control sets used is 1. A number of slice register sites lost to control set restrictions used is 7 and the available bits is 126,800 and the utilization is 1%. The number of bonded IOBs, used in this project is 13 and available IOBs are 210 and utilization is 6%. The numbers of BUFG/BUFGCTRLs used are 1 and the available bits are 32 and the utilization is 3%. The number used as BUFPGs is 1. The average fan-out of non-clock nets is 1.72.

It is clear that power consumption is low compared to the previous works and also TRNG plus digital processor produces high randomness number.

## V. CONCLUSIONS

One of the most important factors which affect the performance of the system on chips is on-chip interconnects. The most suitable interconnection method which is capable of

addressing several high-performance applications is Network on Chip. The widely used method to implement on-chip crossbars is Code Division Multiple Access (CDMA). Overloaded CDMA is used to intensify the capacity of the CDMA based Network on Chip and to overcome the problems due to Multiple Access Interference (MAI). In overloaded CDMA, the communication channel is overloaded with non-orthogonal codes to increase the channel capacity. Two crossbar architectures that leverage the overloaded CDMA concept namely, T-OCI and P-OCI are advanced to increase the CDMA crossbar capacity. To make the crossbar more efficient a PaCC codec is implemented in between the adder and the decoder section. It uses a PRLE scheme and observes the continuous flow of 0/1. If they are all 0 or 1, all the k bits are bypassed in one clock cycle. In addition to the compression of data it also provides security by encrypting the data. The simulation results show that the PaCC based crossbar become more efficient by effectively balance the area and performance.

## REFERENCES

1. Khaled E. Ahmed, Mohamed R. Rizk (2017) "Overloaded CDMA Crossbar for Network-On-Chip" IEEE Transactions on Very Large Scale Integration, vol.24 .pp.1842-1855.
2. R. H. Bell, C. Y. Kang, L. John, and E. E. Swartzlander, (2001) "CDMA as a multiprocessor interconnect strategy," in Proc. Conf. Rec. 35th Asilomar Conf. Signals, Syst. Comput., vol. 2. pp. 1246-1250.
3. D. Kim, M. Kim, and G. E. Sobelman, (2005) "Design of a high-performance scalable CDMA router for on-chip switched networks," in Proc. International SoC Design Conference, pp. 32-35.
4. J. Kim, I. Verbauwhede, and M.-C. F. Chang, (2007) "Design of an interconnect architecture and signaling technology for parallelism in communication," IEEE Transactions on Very Large Scale Integration, (VLSI) Syst., vol. 15, no. 8, pp. 881-894.
5. W. Lee and G. E. Sobelman, (2009) "Mesh-star hybrid NoC architecture with CDMA switch,". IEEE Int. Symp. Circuits Syst. (ISCAS), May, pp. 1349-1352.
6. T. Nikolic, M. Stojcev, and G. Djordjevic, (2009) "CDMA bus-based on-chip interconnect infrastructure," Microelectron. Rel., vol. 49, no. 4, pp. 448-459.
7. B. Halak, T. Ma, and X. Wei, (2014.) "A dynamic CDMA network for multicore systems," Microelectron. J., vol. 45, no. 4, pp. 424-434.
8. Khaled E. Ahmed, Mohamed R. Rizk (2016) "Aggregated CDMA Crossbar for

- Network-On-Chip"IEEE Conference on Very Large Scale Integration, pp.69-75.
9. Yiqun Wang, Yongpan Liu (2015) "PaCC: A Parallel Compare and Compress Codec for Area Reduction in Non-volatile Processors," IEEE Transactions On Very Large Scale Integration, Vol. 22, No. 7.
  10. J. Wang, Z. Lu, Y. Li, (2016)"A New CDMA Encoding/Decoding Method for On-Chip Communication Network," IEEE Trans. Very Large Scale Integr. (VLSI) Syst., vol. 24, no.4, pp. 1607-1611.

## TEMPLATES FOR ARITHMETIC OPERATION IN DSP

Sherin Thomas\* & M. Joselin Kavitha\*\*

\*Student, VLSI Design Marthandam college of Engineering and Technology Kuttakuzhi

\*\*Assistant professor, ECE Marthandam College of Engineering and Technology Kuttakuzhi

**ABSTRACT:** To develop templates so as to do all the combination of mathematical operations occurring DSP is much simpler manner. In this we develop a new architecture so as to develop those combination of templates depending upon the operation of the DSP. These templates can be used whenever the combination of mathematical equations occur such as  $A(X+Y)+k$ , for this equation we can develop template with combination addition and multiplication, the advantage of these templates are, whenever these combination operation occur, we can directly make use of the architecture and make the operation in DSP easy.

**Keywords:** Digital Signal Processing (DSP)

### I. INTRODUCTION

Digital Signal Processing normally consists of lots of addition, multiplication and subtraction operation for it different applications. The multiplication operation is a vast and time consuming process, which consists of partial products. Booth multipliers are used in the architecture to reduce the partial product since in DSP we have multiplication operations also, as in normal multiplication we have  $n$  partial products so by using booth multiplier we can reduce the partial product by  $n/2$ , which is also known as radix-4. Modern systems target high-end application domains requiring efficient implementations of computationally intensive digital signal processing (DSP) functions. The incorporation of heterogeneity through specialized hardware accelerators improves performance, gain and reduces energy consumption. Although application-specific integrated circuits (ASICs) form the ideal acceleration solution in terms of performance and power, their inflexibility leads to increased silicon complexity, as multiple instantiated ASICs are needed to accelerate various kernels

We propose a high-performance architectural scheme for the synthesis of flexible hardware DSP accelerators by combining optimization techniques from both the architecture and arithmetic levels of abstraction. We introduce a flexible datapath architecture that exploits CS optimized templates of chained operations. The proposed architecture comprises flexible computational units (FCUs), which enable the execution of a large set of operation templates found in DSP kernels. The proposed accelerator

architecture delivers average gains of up to 61.91% in area-delay product and 54.43% in energy consumption compared to state-of-art flexible datapaths sustaining efficiency toward scaled technologies. The arithmetic optimizations at higher abstraction levels than the structural circuit one significantly impact on the datapath performance.

In timing-driven optimizations based on carry-save (CS) arithmetic were performed at the post-Register Transfer Level (RTL) design stage. In common sub expression elimination in CS computations is used to optimize linear DSP circuits. Developed transformation techniques on the application's DFG to maximize the use of CS arithmetic prior the actual datapath synthesis. The aforementioned CS optimization approaches target inflexible datapath, i.e., ASIC, implementations. CS representation has been widely used to design fast arithmetic circuits due to its inherent advantage of eliminating the large carry-propagation chains. CS arithmetic optimizations rearrange the application's DFG and reveal multiple input additive operations (i.e., chained additions in the initial DFG), which can be mapped onto CS compressors. The goal is to maximize the range that a CS computation is performed within the DFG.

### II. TEMPLATES

The paper already existing templates consists of either full of addition operation or either multiplication, there was no combination of both multiplication and addition operation in a single template was available. So in this available templates it can only be used for either

addition/subtraction and next template for multiplication, so if in DSP a combination of addition/subtraction and multiplication occurs, we have to make use of two template combination to form that equation, which makes the work and operation complicated. The Booth recorder which is used to reduce or minimize the partial product consists of SMB section for addition of the inputs and then to the output of the same the third input as X is given for multiplication. The CSA is the arithmetic used to do the multiplication process, the main advantage of CSA is that it reduces the carry and the final block used is Carry Look Ahead (CLA).

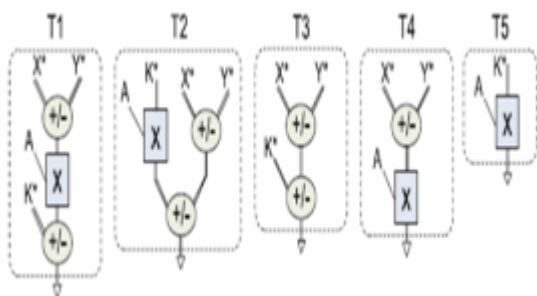


Fig 1:- Block of Combinational Templates

This templates can be used for equation such as  $(A+B) + C-D$ , we have just multiplication operation templates which can be used for equation such as  $(A.B)$ , and for operation such as  $(A+B).(C+D)$  we should make use both the templates which hence results in complication and vast operation. So in order to avoid this we develop new architecture to develop the combination of templates with addition/subtraction and multiplication available in single template which makes the work easy by increasing the performance and reducing the delay and more makes the work simple.

The figure shows the modified templates with combination of addition and multiplication combination. The Modified booth is used to reduce the partial product by  $n/2$  to make the multiplication operation with minimum number of partial product. In the already existing architecture of Booth we have adder for addition of inputs and then the output of it as Y is given to the MB section with a third input X for multiplication. Since the adder used separately for addition causes some amount of delay because of critical path delay. So in order to reduce this delay we develop a new architecture for this MB where we fuse the MB with Sum to get a new section known as SMB, where the inputs for addition is directly given to the SMB and we get an output as Y to which we give a third input X to the SMB

itself. So all the inputs are directly given to SMB, this reduces the critical path delay which was caused because of separate adder used. It shows the already existing MB and shows the Booth with new introduce architecture as SMB.

In the SMB we have three different schemes to the operations which mainly consists of adders such as full adder, half adder, conventional full adder as FA\* and FA\*\* and also conventional half adder as HA\* and HA\*\*. So in order to avoid this we develop new architecture to develop the combination of templates with addition/subtraction and multiplication available in single template which makes the work easy by increasing the performance and reducing the delay and more makes the work simple. Since the adder used separately for addition causes some amount of delay because of critical path delay. So in order to reduce this delay we develop a new architecture for this MB where we fuse the MB with Sum to get a new section known as SMB.

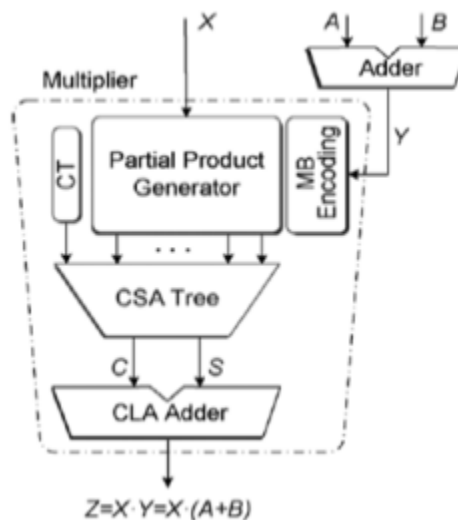


Fig 2 :- Block of existing Modified booth

As in this figure we can see an adder used for addition of two inputs A and B, which thus results in critical path delay at Y, so in order to reduce this we have a new architecture of SMB. Booth multiplication algorithm consists of three major steps as shown in the structure of booth algorithm figure that includes generation of partial product called as recoding, reducing the partial product in two rows, and addition that gives final product.

For a better understanding of modified booth algorithm & for multiplication, we must know about each block of booth algorithm for multiplication process. This modified booth multiplier is used to perform high-speed multiplications using modified booth algorithm.

This modified booth multiplier's computation time and the logarithm of the word length of operands are proportional to each other. We can reduce half the number of partial product. Radix-4 booth algorithm used here increases the speed of multiplier and reduces the area of multiplier circuit. In this algorithm, every second column is taken and multiplied by 0 or +1 or +2 or -1 or -2 instead of multiplying with 0 or 1 after shifting and adding of every column of the booth multiplier.

Thus, half of the partial product can be reduced using this booth algorithm. Based on the multiplier bits, the process of encoding the multiplicand is performed by radix-4 booth encoder. The composition of an array multiplier is, there is a one to one topological correspondence between this hardware structure and the manual multiplication. The generation of n partial products requires N\*M two bit AND gates.

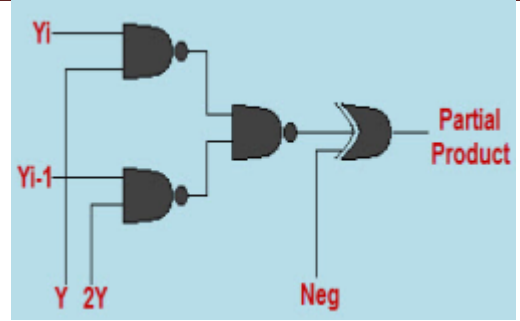


Fig 4:- Partial product generator

Now, every partial product point consists of two inputs (consecutive bits) from multiplicand and, based on the requirement, the output will be generated and its complements also generated in case if required. The 2's complement is taken for negative values of y. There are different types of adders such as conventional adders, ripple-carry adders, carry-look-ahead adders, and carry select adders. The carry select adders (CSLA) and carry-look-ahead adders are considered as fastest adders and are frequently used. The multiplication of y is done by after performing shift operation on y - that is - y is shifted to the left by one bit.

Hence, to design n-bit parallel multipliers only n/2 partial products are generated by using booth algorithm. Thus, the propagation delay to run circuit, complexity of the circuit, and power consumption can be reduced.

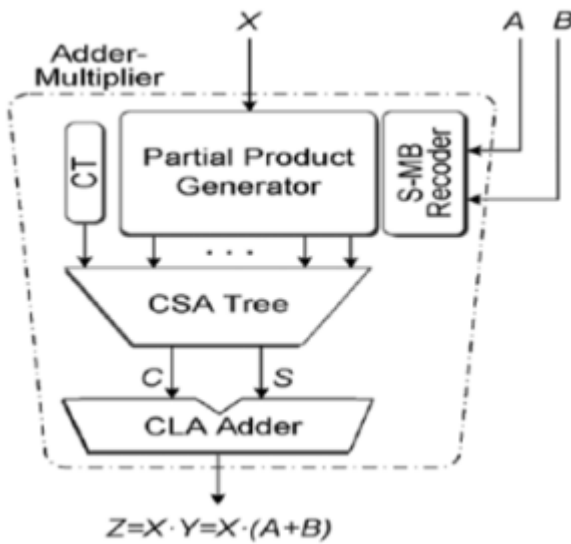


Fig 3:- Block of SMB

### III. RADIX 4 BOOTH ALGORITHM

The steps given below represent the radix-4 booth algorithm:

- Extend the sign bit 1 position if necessary to ensure that n is even.
- Append a 0 to the right of the least significant bit of the booth multiplier.
- According to the value of each vector, each partial product will be 0, +y, -y, +2y or -2y.

If we take the partial product as -2y, -y, 0, y, 2y then, we have to modify the general partial product generator.

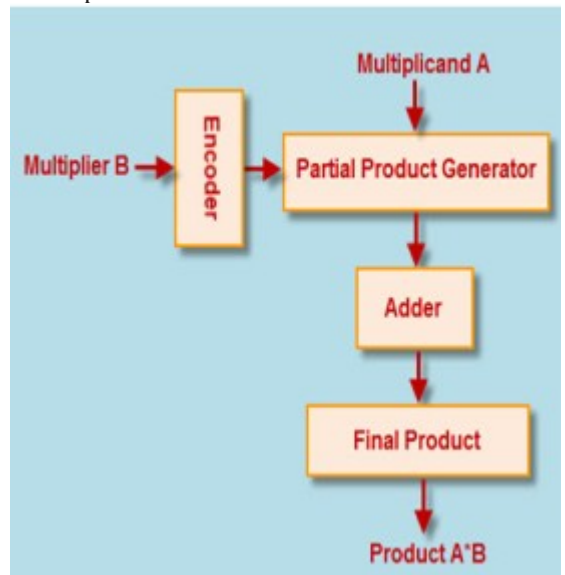


Fig 5:- Modified booth flow chart

Booth multiplication algorithm or Booth algorithm was named after the inventor Andrew Donald Booth. It can be defined as an algorithm or method of multiplying binary numbers in two's complement notation. It is a simple method to multiply binary numbers in which multiplication

is performed with repeated addition operations by following the booth algorithm.

Again this booth algorithm for multiplication operation is further modified and hence, named as modified booth algorithm. Booth's algorithm examines adjacent pairs of bits of the 'N'-bit multiplier  $Y$  in signed two's complement representation, including an implicit bit below the least significant bit,  $y_{-1} = 0$ . For each bit  $y_i$ , for  $i$  running from 0 to  $N - 1$ , the bits  $y_i$  and  $y_{i-1}$  are considered. Where these two bits are equal, the product accumulator  $P$  is left unchanged. Where  $y_i = 0$  and  $y_{i-1} = 1$ , the multiplicand times  $2^i$  is added to  $P$ ; and where  $y_i = 1$  and  $y_{i-1} = 0$ , the multiplicand times  $2^i$  is subtracted from  $P$ . The final value of  $P$  is the signed product. The carry save arithmetic is variety of arithmetic-dominated circuits.

Carry save arithmetic occurs naturally in a variety of DSP applications, and further opportunities to exploit it can be exposed through systematic data flow transformations that can be applied by a hardware compiler. Field-programmable gate arrays (FPGAs), however, are not particularly well suited to carry-save arithmetic. To address this concern, we introduce the "field programmable counter array" (FPCA), an accelerator for carry-save arithmetic intended for integration into an FPGA as an alternative to DSP blocks.

In addition to multiplication and multiply accumulation, the FPCA can accelerate more general carry-save operations, such as multi-input addition (e.g., add integers) and multipliers that have been fused with other adders. Our experiments show that the FPCA accelerates a wide variety of applications than DSP blocks and improves performance, area utilization, and energy consumption compared with soft FPGA logic. The extension for the above project is Multiplier. Experimental results are seen by using Xilinx ISE.

Modern embedded systems target highend application domains requiring efficient implementations of computationally intensive digital signal processing (DSP) functions. The incorporation of heterogeneity through specialized hardware accelerators improves performance and reduces energy consumption. Although application-specific integrated circuits (ASICs) form the ideal acceleration solution in terms of performance and power, their inflexibility leads to increased silicon complexity, as multiple instantiated ASICs are needed to accelerate various kernels. Many researchers have proposed the use of domain specific coarse-

grained reconfigurable accelerators in order to increase ASICs' flexibility without significantly compromising their performance.

High-performance flexible data paths have been proposed to efficiently map primitive or chained operations found in the initial dataflow graph (DFG) of a kernel. The templates of complex chained operations are either extracted directly from the kernel's DFG or specified in a predefined behavioral template library. Design decisions on the accelerator's data path highly impact its efficiency. Existing works on coarse grained reconfigurable data paths mainly exploit architecture-level optimizations, e.g., increased instruction-level parallelism (ILP). The domain specific architecture generation algorithms and vary the type and number of computation units achieving a customized design structure. The flexible architectures were proposed exploiting ILP and operation chaining. Recently aggressive operation chaining is adopted to enable the computation of entire sub expressions using multiple ALUs with heterogeneous arithmetic features.

Field programmable array is The selective use of carry-save arithmetic, where appropriate, can accelerate a variety of arithmetic-dominated circuits. Carry save arithmetic occurs naturally in a variety of DSP applications, and further opportunities to exploit it can be exposed through systematic data flow transformations that can be applied by a hardware compiler. Field-programmable gate arrays (FPGAs), however, are not particularly well suited to carry-save arithmetic. To address this concern, we introduce the "field programmable counter array" (FPCA), an accelerator for carry-save arithmetic intended or integration into an FPGA alternative to DSP blocks. In addition to multiplication and multiply accumulation, the FPCA can accelerate more general carry-save operations, such as multi-input addition (e.g., add  $K > 2$  integers) and multipliers that have been fused with other adders.

#### IV. RESULT AND DISCUSSION

In this section, we present a theoretical analysis and comparative study in terms of area complexity and critical delay among the three recoding schemes that we described in Section III and the three existing recoding techniques. Our analysis is based on the unit gate model. More specifically, for our quantitative comparisons the 2-input primitive gates (NAND, AND, NOR, OR) count as one gate equivalent for both area and delay, whereas the 2-input XOR, XNOR gates count as two gate equivalent.

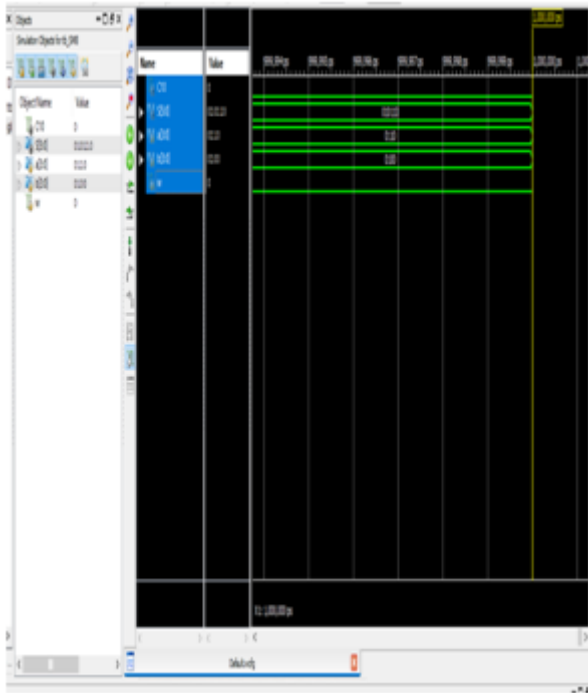


Fig 6:- SMB2 output for four bit numbers

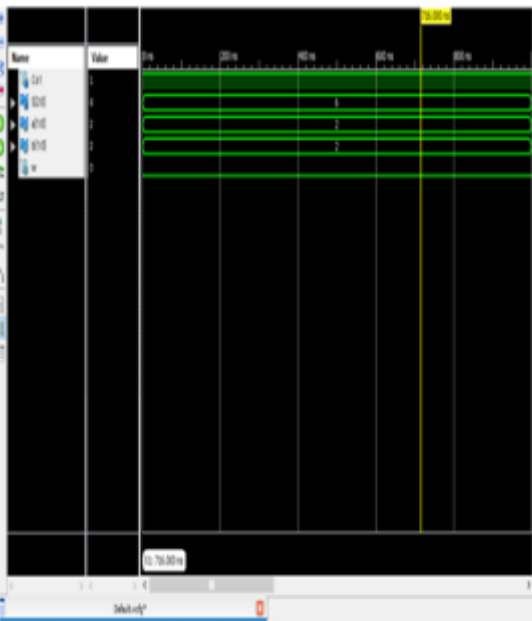


Fig 7: SMB2 output of two bit number in unsigned form

The area of a FA and a HA is 7 and 3 gate equivalents respectively. The delays of the sum and carry outputs of a FA are 4 and 3 gate equivalents respectively, while those of a HA are 2 and 1. The output of the SMB2 for a four bit number is shown in figure 6 and 7 respectively further by this idea we can develop all the other two schemes and also check all the outputs. The output of the Modified booth section is also compared with the already

existing booth and the result of the comparison is that we find less critical path delay and also increased performance in the modified booth with SMB schemes.

### V. CONCLUSIONS

This paper focuses on developing an architecture to produce combinational templates which can do almost all the combinational operation available in DSP. We propose a technique for the direct recoding of the sum of two numbers to its MB form. We make use of alternative designs of the proposed S-MB recoder and use the SMB2 scheme in the MB. The proposed recoding schemes, when they are incorporated in FAM designs, yield considerable performance improvements in comparison with the most efficient recoding schemes. Thus this was a successful architecture to reduce the delay and increase the performance to make the modified booth more effective, and hence the overall performance of this architecture would be high with minimized delay.

### REFERENCES

1. Kostas Tsoumanis, "An Optimized Modified Booth Recoder for Efficient Design of the Add-Multiply Operator" IEEE TRANSACTIONS ON CIRCUITS AND SYSTEMS—I: REGULAR PAPERS, VOL. 61, NO. 4, APRIL 2014
2. P. M. Heysters, G. J. M. Smit, and E. Molenkamp, "A flexible and energy-efficient coarse-grained reconfigurable architecture for mobile systems," J. Supercomput., vol. 26, no. 3, pp. 283–308, 2003.
3. M. D. Galanis, G. Theodoridis, S. Tragoudas, and C. E. Goutis, "A high-performance data path for synthesizing DSP kernels," IEEE Trans. Comput.-Aided Design Integr. Circuits Syst., vol. 25, no. 6, pp. 1154–1162, Jun. 2006.
4. S. Xydis, G. Economakos, and K. Pekmestzi, "Designing coarse-grain reconfigurable architectures by inlining flexibility into custom arithmetic data-paths," Integr., VLSI J., vol. 42, no. 4, pp. 486–503, Sep. 2009.
5. S. Xydis, G. Economakos, D. Soudris, and K. Pekmestzi, "High performance and area efficient flexible DSP datapath synthesis," IEEE Trans. Very Large Scale Integr. (VLSI) Syst., vol. 19, no. 3, pp. 429–442, Mar. 2011.
6. G. Ansaloni, P. Bonzini, and L. Pozzi, "EGRA: A coarse grained reconfigurable architectural template," IEEE Trans. Very Large Scale Integr. (VLSI) Syst., vol. 19, no. 6, pp. 1062–1074, Jun. 2011.
7. R. Kastner, A. Kaplan, S. O. Memik, and E. Bozorgzadeh, "Instruction generation for hybrid reconfigurable systems," ACM Trans. Design Autom. Electron. Syst., vol. 7, no. 4, pp. 605–627, Oct. 2002.

8. T. Kim and J. Um, "A practical approach to the synthesis of arithmetic circuits using carry-save-adders," IEEE Trans. Comput.- Aided Design Integr. Circuits Syst., vol. 19, no. 5, pp. 615-624, May 2000.
9. A. Hosangadi, F. Fallah, and R. Kastner, "Optimizing high speed arithmetic circuits using three-term extraction," in Proc. Design, Autom. Test Eur. (DATE), vol. 1. Mar. 2006, pp. 1-6.
10. A. K. Verma, P. Brisk, and P. Ienne, "Data-flow transformations to maximize the use of carry-save representation in arithmetic circuits," IEEE Trans. Comput.-Aided Design Integr. Circuits Syst., vol. 27, no. 10, pp. 1761-1774, Oct. 2000.

## AN EFFICIENT APPROXIMATE RECONFIGURABLE ADDER USING SIMPLE CARRY PREDICTION

J.B.Abisha Jey & S.Amutha

PG Scholar, Assistant Professor,  
ECE, Marthandam College of Engineering and Technology, Kuttakuzhi.

**ABSTRACT:** With the advent of rapidly increasing adder configuration to precise the adders and power consumption for accurate result. An appropriate computing is a difficult approach for the IC design in low power process. To overcome certain drawbacks the reconfigurable adders is developed. However this design reduces the large area, nearly 39%. We modify the simple accuracy configurable adder design that reduces the error and it is helpful for the error correction. In this paper the proposed simple accuracy configurable adder is used to get accurate accuracy levels. This implementation reduces the complexity to reduce the dynamic level of approximation. Appropriate adder achieves efficient energy system design. In this technique the speed of the system is increased to receive the predicted data quickly. Compared to configurable adder this adders are more efficient and reconfigurable. The MSB value prediction is predicted easily by the reconfigurable adder design. Computing is a recently used process to get research attention. However the system reduce the large area overhead, as they predict the carry and redundant computing. The technique used in this paper is simple accuracy configurable adder to improve the accuracy- power-delay.

**Keywords:** Error detection, Critical path delay, delay adaptive, accurate mode, rectified, truncation error.

### I.INTRODUCTION:

Appropriate computing is a growing technology that has been recently modified design [1]. Low power technology has already launched concept based on the power methodologies. Appropriate computing that enable efficient hardware and software implementation and used in variety of application such as audio, video processing, etc. This technique improves the performance, error correction and error detection if possible by using this process.

The paradigm of appropriate computing fully concentrated on arithmetic logic circuit which enhances and activate as a building blocks for computing circuit design. This process has established modified potential in appropriate computing. Several adders have been developed in the reconfigurable design. Such design gains 60% power reduction for DCT(Discrete Cosine Transform) computation without changing the images in the appropriate circuit. In normal realistic case accuracy requirement vary for different applications in audio, video and mobile computing. Power modes may vary based upon the accuracy. In addition to the SARA (Simple Accuracy Reconfigurable Adder) technique the errors can be eliminated. The important concept designed behind the technique is that accuracy can be adjusted using the methods such as dynamic voltage and frequency scaling to retain the accurate accuracy power tradeoff. The benefit

of this accuracy modification method enhances to reduce the delay and area, where errors occur at the critical path associated with the significant bit.

In early decades appropriate computing cannot be done efficiently and accurately, but the recent techniques enhances appropriate accuracy in computing [1]. By using the design of simple accuracy configurable adder the error detection and correction in the circuit is possible. [2]Dynamic levels of approximation is used to reduce the area and thereby to improve the accuracy by the adder circuit. The baseline of the reconfigurable adder contains the significant redundancy and the error correction/detection circuit moreover increases area overhead. In past few, accuracy configurable adder design has been developed. The error correction value is predicted from the least significant bit and the accuracy improves to enroll the required configuration. To overcome the drawback and to achieve actual accuracy level the error correction circuit uses the reconfigurable adder design.

Few works that establish to focus on appropriate computing in the VLSI design. In this paper the fast reconfigurable adder design is proposed. As longer the error correction/detection can be predicted in simple way. In addition this method support for the degradation process. The reconfigurable adder design composed of CRA (Carry Ripple Adder) and CLA (Carry Lookahead Adder) for extra prediction.

So that quite large area is degraded into smaller area.

## II.SYSTEM STRUCTURE:

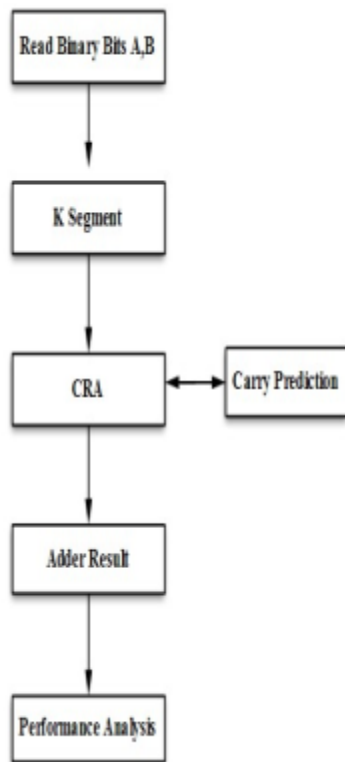


Figure1: System Structure

In this system structure, binary data bit “A and “B”, operates on two operands and the data is loaded using a gate level schematic of the reconfigurable adder. It is composed of a ‘k’, segments by which the k segment more separate the binary bits .In the carry ripple adder the bit is propagated and it computes the sum and carry. Meanwhile the carry prediction circuit predicts the optimal approximation values. A new method simple accuracy reconfigurable adder is designed to stimulate the adder result. Finally the area, power delayed can be analyzed by the performance analysis.

## III. MODULES OF PROPOSED TECHNIQUE:

### 1. Carry Ripple Adder:

Carry Ripple Adder is a extra configurable carry prediction circuitry, similar as the carry look-ahead part of CLA (Carry Look-ahead Adder). Adders are CRA designs while the carry-prediction circuit is similar to the carry look-ahead part of CLA. Further, its carry prediction can be configured to different However, the complicated accuracy levels. carry prediction”

induces large area overhead. The RAP-CLA scheme uses CLA for its baseline where the carry-ahead of each bit is computed directly from the addends of all of its lower bits. Its carry prediction reuses a part of the look- ahead circuit rather than building extra dedicated prediction circuitry, and hence is area-efficient than GDA. Its carry prediction also reuses part of the sub-adders rather than having dedicated prediction circuitry

A ripple carry adder is a digital circuit that produces the arithmetic sum of two binary numbers. It can be constructed with full adders connected in cascaded, with the carry output from each full adder connected to the carry input of the next full adder in the chain. In the ripple carry adder, the output is known after the carry generated by the previous stage. Thus, the sum of the most significant bit is only available after the carry signal has rippled through the adder from the least significant stage to the most significant stage. As a result, the final sum and carry bits will be valid after a considerable delay. All gates are equally loaded for simplicity. All delays are normalized relative to the delay of a simple inverter.

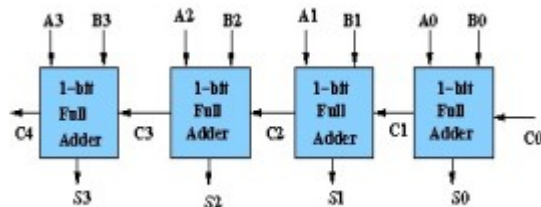


Figure2: Carry Ripple adder

### 2. Carry Prediction:

Prediction methods initialize with an accurate adder and use carry prediction for optional approximation. As such, they no longer need error detection/correction and do not incur any data stall. In addition, they intrinsically support graceful degradation. A new carry-prediction-based accuracy configurable adder design SARA (Simple Accuracy Reconfigurable Adder) is introduced. It is a simple design with significantly less area than CLA, and it has not been achieved in the past in accuracy configurable adders.

### 3. Configurable Adders:

We review a few representative works on accuracy configurable adder design and show the relation with our method. These designs can be generally categorized into two groups: error-correction-based configurations and carry prediction-based configurations.

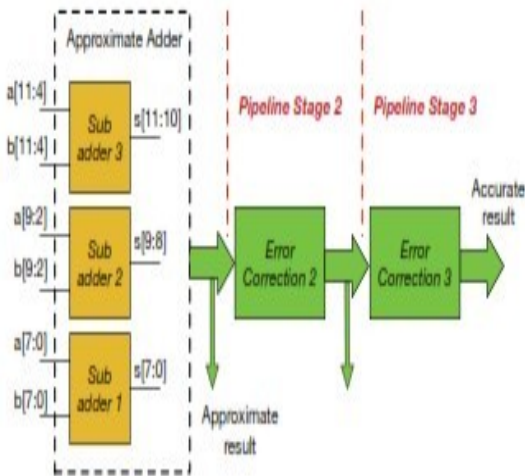


Figure3:Error-correction-based configurable adder.

The main idea of an error-correction-based approach is shown in Figure. The scheme starts with an approximate adder (the dashed box), where the carry chain is shortened by using separated sub-adders with truncated carry-in. In order to reduce the truncation error, the bit-width in some sub-adders contains redundancy. For example, subadder2 calculates the sum for only bit 8 and 9, but it is an 8-bit adder using bit [9:2] of the addends, 6 bits of which are redundant. Even with the redundancy, there is still residual error which is detected and corrected by additional circuits. In Figure, the errors of sub-adder2 must be corrected by error-correction2 before the errors of sub-adder3 are rectified by error-correction3. As such, the configuration progression always starts with small accuracy improvements. The redundancy and error detection/correction reduces large area overhead. Since the error correction circuits are usually pipelined, an accurate computation may take multiple clock cycles and could stall entire data path, depending on the addend values.

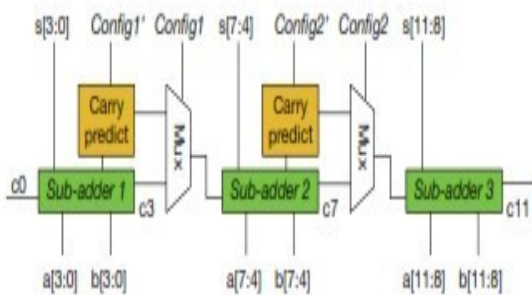


Figure4:Carry-prediction-based configurable adder.

The framework of carry-prediction-based methods shown in Figure. These schemes start with an accurate adder design, which is formed by chaining a set of sub adders. Each sub-adder comes with a fast but approximated carry prediction circuit. By selecting between the carry-out from sub-adder or carry prediction, the overall accuracy can be configured to different levels. Such an approach does not need error detection/correction circuitry. Moreover, the configuration of higher bits is independent of lower bits. This leads to fast convergence or graceful degradation in the progression of configurations. In GDA, the sub-adders in CRA designs by which the carry-prediction circuit is similar to the carry look-ahead part of CLA. Further, its carry prediction can be configured to different accuracy levels. However, the complicated carry prediction induces large area overhead. The RAP-CLA scheme uses CLA for its baseline where the carry-ahead of each bit is computed directly from the addends of all of its lower bits. Its carry prediction reuses a part of the look-ahead circuit rather than building extra dedicated prediction circuitry, and hence is more area-efficient than GDA. However, its baseline is much more expensive than GDA.

**IV.RESULTS AND DISCUSSION:**

Simple Carry Prediction Approximate Adder is a predicted carry look ahead adder, coupled between a lower order adder and a higher order adder. In simple carry Prediction adder, the adder inputs are 7133 and 1244 and the output is 8377.

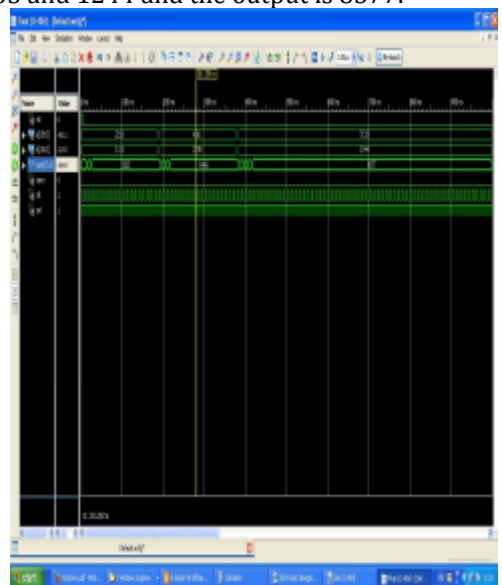


Figure5: Simulation output for Simple Carry Prediction Approximate Adder

**Timing Summary:**

- Speed Grade: -3
- Minimum period: 1.473ns (Maximum Frequency: 678.771MHz)
- Minimum input arrival time before clock: 4.574ns
- Maximum output required time after clock: 4.382ns
- Maximum combinational path delay: 6.056ns

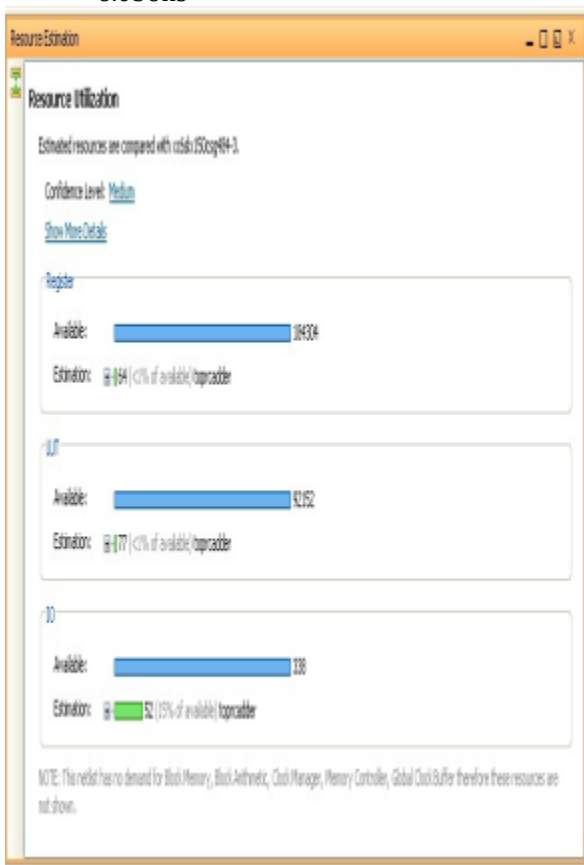


Figure 6: Resource Prediction from Xilinx Synthesizer

For Resource Utilization used both Register and LUT to savings in terms of processing time and retrieving a value from memory is often small amount of fast storage, although some registers have specific hardware functions, and may be read-only or write-only.

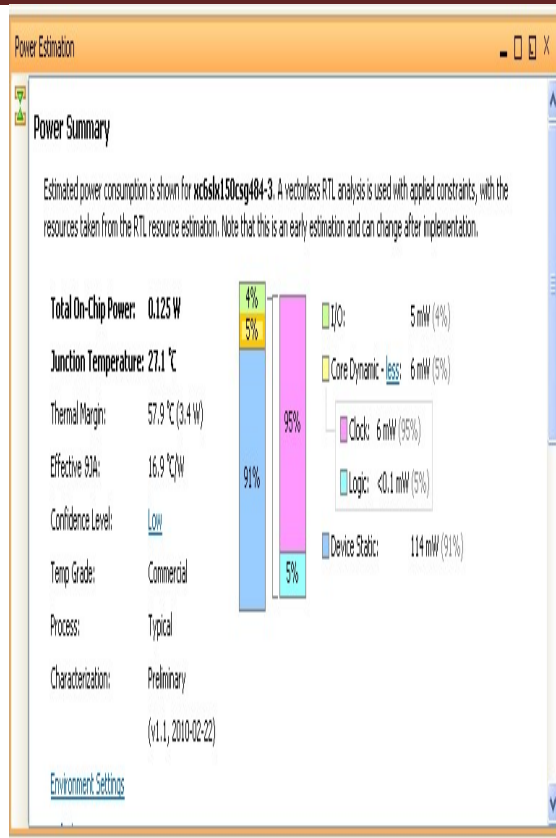


Figure7: Power Estimation from Xilinx Synthesizer

Power summary have both static and dynamic power. Also the power dissipation is estimated by Synopsys PrimeTime considering, including both static and dynamic power. The power-delay tradeoff can be obtained by different accuracy configurations or varying supply voltages.

**4 Comparative Analysis of Parameters**

The comparison here involves the performance of the parameters discussed so far. Table 1 represents Area (%) obtained from different method discussed.

Table : Analysis of Delay, Area and Power

S. No	Delay (ns)	Power (mw)	Energy (pJ)	Area (No of LUTs)
1	13.073	29	379.12	28
2	12.451	27	336.18	28
3	13.691	27	369.66	59
4	14.380	30	431.40	39

**V.CONCLUSION:**

A simple accuracy reconfigurable adder (SARA) design is proposed. It has a reconfigurable adder that reduces the delay and power. The proposed method has significant low power delay product than the previous work. At the same time accuracy

level is somewhat improved. Further optimization of the proposed also done which improves the accuracy. In addition simple accuracy reconfigurable adder has considered lower area. The most important aspect of this

proposed method is that maintaining the accuracy. The accuracy-power-delay efficiency is further improved by a delay-adaptive reconfigurable technique.

#### REFERENCES:

1. J. Han and M. Orshansky, "Approximate computing: An emerging paradigm for energy-efficient design," in IEEE European Test Symposium, pp. 1-6, 2013.
2. V. Chippa, A. Raghunathan, K. Roy, and S. Chakradhar, "Dynamic effort scaling: Managing the quality-efficiency tradeoff," in DAC, pp. 603-608, 2011.
3. V. Gupta, D. Mohapatra, A. Raghunathan, and K. Roy, "Low-power digital signal processing using approximate adders," TCAD, vol. 32, no. 1, pp. 124-137, 2013.
4. S. Venkataramani, K. Roy, and A. Raghunathan, "Substitute-and-simplify: A unified design paradigm for approximate and quality configurable circuits," in DATE, pp. 1367-1372, 2013.
5. K. Du, P. Varman, and K. Mohanram, "High performance reliable variable latency carry select addition," in DATE, pp. 1257- 1262, 2012.
6. N. Zhu, W. L. Goh, and K. S. Yeo, "An enhanced low-power high-speed adder for error-tolerant application," in ISIC, pp. 69- 72, 2009.
7. J. Hu and W. Qian, "A new approximate adder with low relative error and correct sign calculation," in DATE, pp. 1449-1454, 2015.
8. J. Miao, K. He, A. Gerstlauer, and M. Orshansky, "Modeling and synthesis of quality-energy optimal approximate adders," in ICCAD, pp. 728-735, 2012.
9. S. Mazahir, O. Hasan, R. Hafiz, M. Shafique, and J. Henkel, "An area-efficient consolidated configurable error correction for approximate hardware accelerators," in DAC, pp. 1-6, 2016.
10. A. B. Kahng and S. Kang, "Accuracy-configurable adder for approximate arithmetic designs," in DAC, pp. 820-825, 2012.

# The Fault Tolerant Parallel Filters Implementation Based on Error Correction Codes

N.Saibaba<sup>1</sup> & P.Venkatapathi<sup>2</sup>

<sup>1</sup>PG scholar, Department of ECE, Malla Reddy College of Engineering, Hyderabad, Telangana, India

<sup>2</sup>Associate Professor, Department of ECE, Malla Reddy College of Engineering, Hyderabad, Telangana, India

---

**ABSTRACT:** *As the many-sided quality of interchanges and flag handling frameworks increments, thus will the number of squares or parts that they need. As a rule, some of these parts add parallel, playing out a similar preparing on various signs. An average case of those components are computerized channels. The enlargement in unpredictability likewise presents unwavering quality difficulties and makes the necessity for blame tolerant usage. Specifically, it's in contestable that the means that channel sources of information and yields aren't bits however rather numbers empowers a superior security. This diminishes the insurance overhead and makes the number of repetitive channels freed from the number of parallel channels. The proposed plot is initial delineated and afterward diagrammatic with two discourse analyses. At last, each the viability in guaranteeing against blunders and also the expense are assessed for a field-programmable door exhibit usage.*

**Keywords:** *Error correction codes (ECCs), filters, and soft errors.*

---

## I. INTRODUCTION

One established precedent is the utilization of triple measured excess (TMR) in which the outline is tripled and a dominant part vote of the yields are utilized to adjust mistakes. Another precedent is the utilization of blunder adjustment codes (ECCs) to secure the bits put away in memory gadgets [5]. For this situation, various equality checks are processed and put away in the memory so mistakes can be recognized and rectified when the information are perused. At last, for applications that have standard structure and properties, those can be abused to distinguish and remedy mistakes with a lower cost than TMR. This is the situation for some, flag handling circuits [6]. Much of the time, ECCs or particular assurance methods are joined with TMR to accomplish a total security. For instance, the ECC encoders and decoders might be secured with TMR to guarantee that they are not influenced by blunders. In those cases, TMR is utilized to secure a little piece of the circuit that can't be ensured by the ECC or the particular procedure.

The assurance of advanced channels has been generally examined. For instance, blame tolerant usage in light of the utilization of deposit number frameworks or math codes have been proposed [7], [8]. The utilization of decreased exactness replication or word-level insurance has been additionally considered [9], [10]. Another

choice to perform blunder adjustment is to utilize two distinctive channel executions in parallel [11]. Each one of those systems center around the security of a solitary channel.

The assurance of parallel channels has just been as of late considered. In [12], an underlying method to secure two parallel channels was proposed. This plan was summed up in [13], where the utilization of a plan in light of ECCs was introduced. In this work, each channel was dealt with as a bit on an ECC, and extra channels are added to go about as equality check bits. This implies, for single blunder redress, the quantity of repetitive channels required is the same as the quantity of bits required in a customary single mistake revision Hamming code [14]. For instance, for four parallel channels, three excess channels are required, while for eight channels, four repetitive channels are required. This plan along these lines altogether decreases the usage cost contrasted and that of TMR.

This concise investigations the insurance of parallel channels utilizing more broad coding systems. Specifically, a key distinction with ECCs is that both channel sources of info and yields are numbers. Thusly, not just a zero or a one can be utilized for the coding (as finished with ECCs). This can be misused, as appeared in whatever is left of this brief, to give blunder amendment by including just two excess channels paying little mind to the quantity of parallel channels. The

diminished number of repetitive channels does not influence the capacity of the plan to amend mistakes yet decreases the execution cost. In whatever remains of this short, first, the parallel channels and the current ECC-based assurance plot are portrayed. At that point, the proposed coding plan is given and represented a couple of viable contextual investigations. At long last, the contextual analyses are assessed for a field-programmable door cluster (FPGA) usage and contrasted and the already proposed ECC-based procedure

The outcomes demonstrate that the utilization of a more broad coding plan diminishes the security overhead while giving a comparative mistake remedy ability to that of the ECC conspire. The rest of this brief introduces the new scheme by first summarizing the parallel filters considered in Section II. Then, in Section III, the simulation results is presented. Finally, the conclusions are summarized in Section IV.

## II. PARALLEL FILTERS WITH THE SAME RESPONSE

The drive reaction  $h[n]$  totally characterizes a discrete time channel that plays out the accompanying activity on the approaching sign  $x[n]$ :

$$y[n] = \sum_{l=0}^{\infty} x[n-l] \cdot h[l]. \quad (1)$$

The drive reaction can be interminable or be nonzero for a limited number of tests. In the main case, the channel is a boundless drive reaction (IIR) channel, and in the second, the channel is a limited motivation reaction (FIR) channel. In the following, a set of  $k$  parallel filters with the same response and different input signals are considered. illustrated in Fig. 1. This kind of filter is found in some communication systems that use several channels in parallel. In data acquisition and processing applications is also common to filter several signals with the same response.

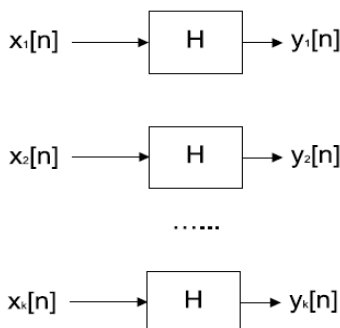


Fig. 1. Parallel filters with the same response.

These parallel filters are In the two cases, the separating activity is straight with the end goal that

$$y_1[n] + y_2[n] = \sum_{l=0}^{\infty} (x_1[n-l] + x_2[n-l]) \cdot h[l]. \quad (2)$$

This property can be abused on account of parallel channels that work on various approaching signs, as appeared on Fig. 2. For this situation, four channels with a similar reaction process the approaching signs  $x_1[n]$ ,  $x_2[n]$ ,  $x_3[n]$ , and  $x_4[n]$  to create four yields  $y_1[n]$ ,  $y_2[n]$ ,  $y_3[n]$ , and  $y_4[n]$ . To distinguish and rectify blunders, each channel can be seen as a bit in an ECC, and repetitive channels can be added to frame equality check bits [13]. This is additionally shown in Fig. 1, where three repetitive channels are utilized to shape the equality check bits of a traditional single mistake amendment Hamming code [14]. Those relate to the yields  $z_1[n]$ ,  $z_2[n]$ , and  $z_3[n]$ . Blunders can be distinguished by checking if

$$\begin{aligned} z_1[n] &= y_1[n] + y_2[n] + y_3[n] \\ z_2[n] &= y_1[n] + y_2[n] + y_4[n] \\ z_3[n] &= y_1[n] + y_3[n] + y_4[n]. \end{aligned} \quad (3)$$

At the point when a portion of those checks come up short, a blunder is identified. The blunder can be remedied in view of which particular checks fizzled. For instance, a blunder on channel  $y_1$  will cause mistakes on the checks of  $z_1$ ,  $z_2$ , and  $z_3$ . Also, blunders on alternate channels will cause mistakes on an alternate gathering of  $z_i$ . Along these lines, similarly as with the conventional ECCs, the mistake can be found. To redress the blunder, the coming up short yield is recreated from the right yields. For instance, when a mistake on  $y_1$  is recognized, it very well may be rectified by making

$$y_{c1}[n] = z_1[n] - y_2[n] - y_3[n]. \quad (4)$$

This ECC-based plan diminishes the assurance overhead contrasted and the utilization of TMR. Table I outlines the quantity of excess channels required for various parallel channel designs. It very well may be seen that the number develops with the logarithm in construct two in light of the quantity of channels. In this way, the expense is considerably littler than TMR, in which the quantity of channels is tripled. The cost decreases were affirmed by some contextual analysis executions in.

In this ECC-based plan, the coding of the repetitive channels depends on basic augmentations that supplant the XOR paired tasks



the ECC method (bring down expenses accomplishing comparable blame tolerant ability). In this way, the proposed procedure is valuable to actualize fault tolerant parallel channels. Future work can contemplate applying the attempt to parallel channels that have an identical information flag none the less extraordinary drive reactions.

## REFERENCES

1. P. P. Vaidyanathan, *Multirate Systems and Filter Banks*, Englewood Cliffs, N.J., USA: Prentice Hall, 1993.
2. C. L. Chen and M. Y. Hsiao, "Blunder redressing codes for semiconductor memory applications: A best in class survey," *IBM J. Res. Create.*, vol. 28, no. 2, pp. 124-134, Mar. 1984.
3. A. Reddy and P. Banarjee "Calculation based blame recognition for flag preparing applications," *IEEE Trans. Comput.*, vol. 39, no. 10, pp. 1304-1308, Oct. 1990.
4. S. Pontarelli, G. C. Cardarilli, M. Re, and A. Salsano, "Thoroughly blame tolerant RNS based FIR channels," in *Proc. IEEE IOLTS*, 2008, pp. 192-194.
5. Z. Gao, W. Yang, X. Chen, M. Zhao and J. Wang, "Blame missing rate examination of the number juggling deposit codes based blame tolerant FIR channel outline," in *Proc. IEEE IOLTS*, 2012, pp. 130-133.
6. B. Shim and N. Shanbhag, "Vitality effective delicate blunder tolerant advanced flag handling," *IEEE Trans. Large Scale Integr. Syst.*, vol. 14, no. 4, pp. 336-348, Apr. 2006.
7. Y.- H. Huang, "High-proficiency delicate mistake tolerant advanced flag preparing utilizing fine-grain subword-identification handling," *IEEE Trans. Large Scale Integr. Syst.*, vol. 18, no 2, pp. 291-304, Feb. 2010.
8. P. Reviriego, C. J. Bleakley, and J. A. Maestro, "Auxiliary DMR: A method for usage of delicate blunder tolerant FIR channels," *IEEE Trans. Circuits Syst. II: Exp. Briefs*, vol. 58, no. 8, pp. 512-516, Aug. 2011.
9. P. Reviriego, S. Pontarelli, C. Bleakley and J. A. Maestro, "Zone effective simultaneous mistake recognition and amendment for parallel channels," *IET Electron. Lett.*, vol. 48, no 20, pp. 1258-1260, Sep. 2012.
10. S. Lin and D. J. Costello, *Error Control Coding*, 2nd ed. Englewood Cliffs, NJ, USA: Prentice-Hall. 2004.
11. R. W. Hamming, "Error correcting and error detecting codes," *Bell Syst. Tech. J.*, vol. 29, pp. 147-160, Apr. 1950.
12. N. Raj and R. K. Sharma, "A High Swing OTA with wide Linearity for design of Self Tuneable Resistor", *International Journal of VLSI design & Communication system (VLSICS)*, Volume 1, No. 3, pp. 1-11, 2010.
13. N. Raj, A.K. Singh, A.K. Gupta, "Modeling of Human Voice Box in VLSI for Low Power Biomedical Applications", *IETE Journal of Research*, Vol. 57, Issue 4, pp. 345-353, 2011.
14. N. Raj, A.K. Singh, and A.K. Gupta, "Low power high output impedance high bandwidth QFGMOS current mirror", *Microelectronics Journal*, Vol. 45, No. 8, pp. 1132-1142, 2014.
15. N. Raj, A.K. Singh, and A.K. Gupta, "Low-voltage bulk-driven self-biased cascode current mirror with bandwidth enhancement", *Electronics Letters*, Vol. 50, No. 1, pp. 23-25, 2014.
16. N. Raj, A.K. Singh, and A.K. Gupta, "Low Voltage High Output Impedance Bulk-driven Quasi-floating Gate Self-biased High-swing Cascode Current Mirror", *Circuit System & Signal Processing Journal*, Vol. 35, No. 8, pp. 2683-2703, 2015.
17. N. Raj, A.K. Singh, and A.K. Gupta, "High performance Current Mirrors using Quasi-floating Bulk", *Microelectronics Journal*, Vol. 52, No. 1, pp. 11-22, 2016.
18. N. Raj, A.K. Singh, and A.K. Gupta, "Low Voltage High Performance Bulk-driven Quasi-floating Gate Self-biased Cascode Current Mirror", *Microelectronics Journal*, Vol. 52, No. 1, pp. 124-133, 2016.
19. N. Raj, A.K. Singh, and A.K. Gupta, "Low Voltage High Bandwidth Self-biased High Swing Cascode Current Mirror", *Indian Journal of Pure and Applied Physics*, Vol. 55, No. 4, pp. 245-253, 2017.
20. Raj N. and Gupta A. K., "Analysis of Operational Transconductance Amplifier using Low Power Techniques", *Journal of Semiconductor Devices and Circuits (STM Journal)*, Vol. 1, No. 3, pp. 1-9, 2015.
21. Raj N. and Gupta A. K., "Multifunction Filter Design using BDQFG Miller OTA", *Journal of Electrical and Electronics Engineering: An International Journal (EEEIJ Journal)*, Vol. 4, No. 3, pp. 55-67, 2015.
22. N. Raj, A.K. Singh, and A.K. Gupta, "Low Power Circuit Design Techniques: A Survey", *International Journal of Computer Theory and Engineering*, Vol. 7, No. 3, pp. 172-176, 2015.

# Design of Chaotic Behavior for programmable cellular automata based Symmetric Key Encryption Algorithm for Wireless Sensor Networks

Shanthi S & Chandrasekar V

Malla Reddy College of Engineering and Technology, Hyderabad, Telangala State, India

**ABSTRACT:** Cellular automata are highly parallel and distributed systems which are able to perform complex computations. Cryptographic techniques are very important in these times dominated by the growth of digital information storage and transmission. CA are an attractive approach for cryptographic applications. They are simple, modular logic systems that can generate good quality pseudorandom bit streams as required in robust cryptographic systems. Further advantage is that they can be easily and efficiently implemented. This paper focuses on using cellular automata in cryptography, thereby bringing the advantages of using cellular automata in cryptography.

**Keywords:** Cellular automata, types of cellular automata, Cryptography, Advantages of using Cellular automata in cryptography.

## 1. Introduction

In this age of information, communications and electronic connectivity, security is a topic of general interest that should never be underestimated. The security of data bases, of data communications, of Internet connections, of scientific research and of personal e-mail and phone calls are some examples where the encryption of data/information plays a major role. Therefore, cryptography has become an important field of research in theory and applications development.

Because of its importance, cryptography is nowadays a science by itself, strongly related to other modern research fields as complexity theory, chaos, dynamical systems, computing theory etc. The state-of-the art for the field of cryptography is probably classified as it has military applications, but for the public domain a good reference can be found in [1] and [2]. The *encryption* of a message/data file/other information is a process (algorithm) that modifies this message/data file/information making it completely unintelligible, except for the person who knows the encryption *key*. The *key* refers to the encryption algorithm that has been used - in fact, to the reverse algorithm that should be used for decryption - and the particular parameters that have been used during the encryption. The *decryption* algorithm should render the original message/file/information complete and unaltered. Encryption can be achieved by constructing two different types of ciphers—stream ciphers and block ciphers. A block cipher is one in which a message is broken into successive

blocks that are encrypted using a single key or multiple keys. In a stream cipher the message is broken into successive bits or characters and then the string of characters is encrypted using a key stream. The *cryptographic scheme* refers to the assembly of encryption and decryption algorithms.

An ideal cryptographic scheme or algorithm has not been developed yet, as an ideal cryptographic scheme implies:

- no data expansion during encoding process;
- fast encoding algorithm;
- small dimension key;
- fast decoding algorithm;
- correct and complete rendering of message after encryption/decryption;
- invulnerability to attacks.

The last point is a major issue in cryptography; complex mathematical studies and research have to be done in order to establish the vulnerability of each cryptographic scheme. In simple words, this answers the basic question: how difficult is to break the code? This “difficulty” has to be established in terms of complexity, cost and computing time. Therefore, depending of the particular applications, sometimes it is enough to have a code and cryptographic scheme that requires a long search for the key, although the process is very simple. This is the situation for the briefcases with cipher, where the breaking process is quite simple: one has to try *all* possible numbers in order to find the right one. Cellular automata are applied with success in cryptography mainly because their vast phenomenology and apparently big complexity

require a very long computing time to break well-chosen cryptographic schemes. There are indeed a lot of parameters and factors that can drastically affect the encrypted message (cyphertext) and therefore the complexity of the attack is considerably increased. Cellular automata offer an ideal mathematical model for massive parallel computation, but most research and applications in cellular automata domain are done through simulation. However, it is obvious that only the hardware implementations of this model fully exploit its computing and high-speed possibilities. In particular, cellular automata applications in cryptography are efficient because of the massive parallelism of the model. When implemented by means of other computing systems (simulated in software or emulated with microcontrollers etc.) the parallel processes are in fact executed sequentially. Special cellular automata hardware is the only means to benefit of all the advantages of the model.

**2. Cryptography with Cellular Automata**  
**2.1. The Cellular Automata Model**

Basically, cellular automata are parallel systems that consist of a typically large number of finite automata (finite state machines) as elementary "cells". The cells are locally connected, in other words the global network supports only local connections. The system evolves through local changes: all cells are updated synchronously, depending on their own current state and on the states of the neighbouring cells in the network. The computing task performed by cellular automata is generally conceived as the global evolution of its configuration, starting from the initial configuration (input data) and leading to an intermediate or final configuration or attraction cycle that are interpreted as a result. This almost "visual" perceptible computation is quite an advantage in task like modeling and simulation, image processing and cryptography.

The Cellular Automata formalisms [Wol86] are well-suited to describe some kind of real complex systems with different description levels.

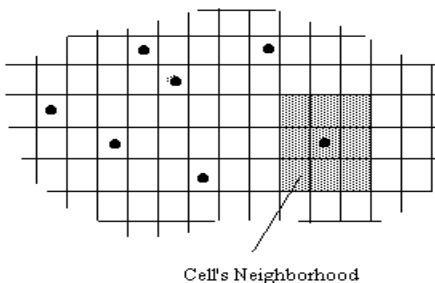


**Figure 1 Sketch of a Cellular Automata**

**2.1.1 The three fundamental properties of CA**

1. **Parallelism:** A system is said to be parallel when its constituents evolve simultaneously and independently. In that case cells updates are performed independently of each other.
2. **Locality:** The new state of a cell only depends on its actual state and on the neighborhood.
3. **Homogeneity:** The laws are universal, that's to say common to the whole space of CA.

Two common two-dimensional neighborhoods are the von Neumann neighborhood, in which each cell has neighbors to the north, south, east and west; and the Moore neighborhood, which adds the diagonal cells to the northeast, southeast, southwest and northwest.

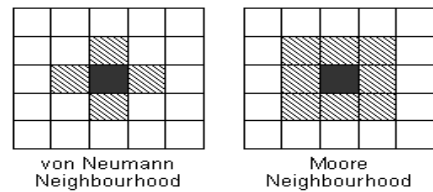


**Figure 2 Types of Neighbourhoods**

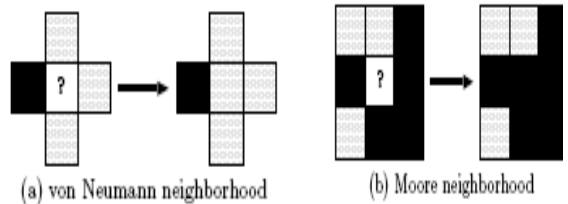


**Figure 3 Two examples of a cell with a one-step update. The center cell examines its neighborhood and applies the update rule**

**2.1.2 Basic Rules of CA**

- Rule 1: Survival – a live cell with exactly two or three neighbors stay alive [7][8]
- Rule 2: Birth – a dead cell with exactly three live neighbors becomes alive
- Rule 3: Death – a cell dies due to 'loneliness' if it has only one neighbor or due to 'crowding' if it has more than four neighbors

Cellular automata are defined by the following elements:

- topology and dimension of the lattice of cells;
- the set of the neighbours of each cell that are involved in the next state's computation;
- the number of states of each cell (identical for all cells; binary automata, for instance, have only two states per cell: 0/1, visually translated as white/black);

- the local rule that gives the next state of the cells.

In cryptography the main topologies that are applied are liner and two-dimensional, referring to a row or matrix of "cells".

## 2.2 Characteristics of cellular automata.

Cellular automata were first introduced by John Von Neumann (1966), as a means of modeling the nature of self-reproduction in biological systems. The Game of Life constructed by Conway constitutes a famous example of cellular automata which may be easily simulated on a personal computer. Cellular automata are discrete dynamical systems in which the space, time, and states are discrete. Despite their conceptual simplicity, cellular automata may reveal very complex behavior. A cellular automaton is a mechanism for modeling systems with local inter-actions. It consists of a regular array of identically programmed units called cells which interact with their neighbors subject to a finite set of prescribed rules for local transitions. All cells form a regular spatial lattice. Time progresses in discrete steps. The state of a cell at time  $t + 1$  is a function only of its own state and of the states of its neighbors at time  $t$ . All cells states are updated synchronously. In order to establish a rigorous mathematical definition, we need some basic notions. Cellular automata remain very interesting for systems with high complexity. A cellular automaton is a mathematical model which is perfectly suited to complex systems containing a large number of simple identical components with local interactions. Cellular automata have also been considered as a means for symbolic dynamics. Such an approach offers many advantages. In theory, it is a convenient method to represent many discrete or continuous processes conventionally described by partial differential equations. In practice, cellular automata may be viewed as parallel-processing computers of simple construction. Because of this, Cellular automata have been used to study complex systems widely.

## 2.3. Complexity of Cellular Automata

The cellular automata model is inspired from the natural model of complex systems that often consist of a large number of simple basic elements, having only local interactions that lead to a complex global behaviour. This model is an important research and simulation tool in the science of complexity. Strictly speaking, the cellular automata model and also the cellular automata evolution are not complex, as its structure and rules are very regular and simple.

But the huge dimension of the rules and configuration spaces confers to its phenomenology a considerably great *apparent* complexity. In the quite simple example of binary linear cellular automata with 100 cells (a modest dimension) with local rules involving the central cell and two neighbours on each side (binary functions with 5 variables), there are:  $2^{100}$  global configurations, which is approximately  $10^{30}$  and  $2^{32}$  possible local functions, which by a rough approximation means around 4,000,000 functions.

Not all possible functions are of practical interest, but even in this conditions a search in the local functions' space is a very long computing task. This is related to the difficulty of cellular automata synthesis: there is no algorithm that gives the appropriate local function for a specific application. The universality of the cellular automata model is theoretically proven, but the practical applications are still waiting for development tools, since the experiment is, by now, the main means of cellular automata synthesis. The work of S. Wolfram [7] imposed a certain order in the space of local rules of functions, mainly for linear cellular automata, dividing it into four complexity classes (that express how complex is the evolution of the system govern by a certain rule). Class 3 of Wolfram's classification contains the automata that have an apparently chaotic evolution, also strongly depending on the initial global configuration. Such an evolution is illustrated in Fig. 1, where time is on the vertical axis, downwards, and the horizontal bit string is the configuration of a binary linear cellular automata. The *class 3 automata* are ideal for applications like random sequences generation and cryptography.

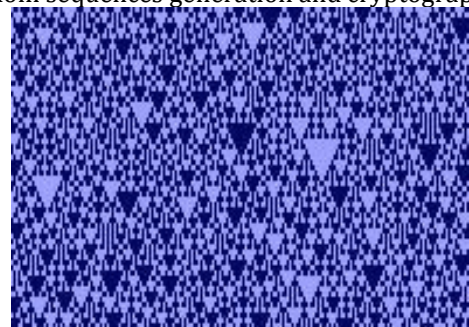


Fig. 1. Evolution of class 3 linear cellular automata

### 2.3.1 Chaos and complexity

Wolfram gives a rough geometrical analogy of behavior of these four classes:

1. **Class 1** - limit points
2. **Class 2** - limit cycle
3. **Class 3** - chaotic - "strange" attractor

**4. Class 4** - more complex behavior, but capable of universal computation[4][5]

#### 2.3.1.1 Class 1 cellular automata

After a finite number of time-steps, class one automata tend to achieve a *unique state* from (nearly) all possible starting conditions.

#### 2.3.1.2 Class 2 cellular automata

This type of automata usually creates patterns that *repeat periodically* (typical with small periods) or are stable. One can understand this type of CA's as a kind of *filter*, which makes them interesting for digital image processing

#### 2.3.1.3 Class 3 cellular automata

From nearly all starting conditions, this type of CA's lead to aperiodic - chaotic patterns. The statistical properties of these patterns and the statistical properties of the starting patterns are almost identical (after a sufficient period of time). The patterns created by this type of CA's (usually one dimensional CA's) are a kind of self-similar fractal curves.

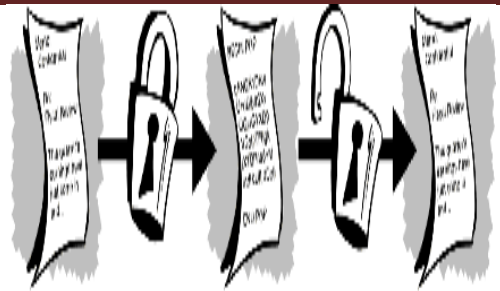
#### 2.3.1.4 Class 4 cellular automata

After finite steps of time, this type of CA's usually "dies" - the state of all cells becomes zero. Nevertheless a few stable (periodic) figures are possible. One popular example of an automaton of this type is the Game of Life. In addition to that Class 4 automata can perform universal computation. This class of CA's show a high irreversibility in their time development.

The first three types can be read as *Cantor sets* with a certain dimensionality, either in countable or in *fractal* dimension. Class 3 is the most frequent class. With increasing  $k$  and  $r$  the probability to find class 3 automaton for an arbitrary selected rule is again increasing.

### 3. Cryptography

Encryption is the science of changing data so that it is unrecognizable and useless to an unauthorized person. Decryption is changing it back to its original form. The most secure techniques use a mathematical algorithm and a variable value known as a 'key'. The selected key (often any random character string) is input on encryption and is integral to the changing of the data. The EXACT same key MUST be input to enable decryption of the data. This is the basis of the protection.... if the key (sometimes called a password) is only known by authorized individual(s), the data cannot be exposed to other parties. Only those who know the key can decrypt it. This is known as 'private key' cryptography, which is the most well known form.



Plaintext encryption cipher text decryption  
plain text

Figure 4 Cryptography basics

Data that can be read and understood without any special measures is called plaintext or cleartext. The method of disguising plaintext in such a way as to hide its substance is called encryption. Encrypting plaintext results in unreadable gibberish called cipher text. You use encryption to make sure that information is hidden from anyone for whom it is not intended, even those who can see the encrypted data. The process of reverting cipher text to its original plaintext is called decryption.

### 4. Cellular Automata in Cryptography

The very large phenomenology of the cellular automata model and its apparently big complexity offer a good basis for applications in cryptography (cellular automata are not the only dynamical systems applied in cryptography, and some of the basic principles of cryptography with cellular automata also stand for other dynamical systems). Massive parallelism is another feature of cellular automata that make this model attractive for cryptography, since lot of computation is often necessary in real-time applications. However, this parallelism, when emulated in software or in sequential hardware, disappears. In the last two decades many results have been obtained in this direction. A good review of some cryptographic schemes and systems with cellular automata proposed in the scientific literature is given in [5] and [6]. In the next section some of these will be discussed as possible basis for hardware implementations, taking as valuable the theoretical results concerning the efficiency and invulnerability of the schemes.

### 5. Other Advantages of Cellular Automata

The design style under VLSI technology prefers the simple, modular and local connected logic circuit structure. Cellular automata are ideal from the hardware designer's point of view. The local connectivity, regularity and the simple basic components make CA very appropriate to

implement low-cost and robust massive parallel machines or application-oriented circuits. The reason why there are not so many cellular-automata inspired electronic circuits is mainly the difficulty of the synthesis for this computing model; however, dedicated circuits for specific applications (signal generators, associative memories, image pre-processing blocks, various simulators for natural phenomena) have been successfully designed and produced [6].

Apart from cryptography cellular automata can be used in variety of applications because of its simpler structure providing solution to the complex problems.

## 6. Conclusion

This paper has introduced the basic concepts of cellular automata and cryptography and some applications of cellular automata in cryptography. cellular automata along with cryptography can be used to model a wide variety of real world applications.

## 7. References

1. William Stallings, Cryptography and Network Security Prentice-Hall 2003 New Jersey, USA
2. Brian A. LaMacchia, .NET Framework Security Addison Wesley 2002, USA [1] Toffoli, T., & Margolus, N. (1987). Cellular Automata Machines. MIT Press.
3. S. Wolfram, Cellular Automata and Complexity, Addison-Wesley Publishing Company, 1994
4. J. Kari "Reversibility of 2D Cellular Automata is Undecidable", Physica D, Vol 45:379-385, 1990
5. H. Gutowitz Method and Apparatus for Encryption, Decryption and Authentication using Dynamical Systems US Patent 5365589, 1994
6. P. Chaudhuri, D. Chowdhury, S. Nandi, S. Chattopadhyay, Additive Cellular Automata: Theory and Applications, IEEE Computer Society Press, 1997.
7. Wolfram, S. (2002). A New Kind of Science. Wolfram Media, Inc., Champaign, IL.
8. 1986. Wolfram, S. (Ed.). Theory and Applications of Cellular Automata. Singapore: World Scientific.
9. V. Vemuri, 1978, modeling of Complex Systems: An introduction. Chapter 3 pp. 67-88
10. Pidd, M. 1992a. Computer simulation in management science 3rd ed, Chichester.: John Wiley & Sons.

## CENTRIFUGE CONTROL SYSTEM IN SUGAR WASHING PROCESS USING PLC

Ms.M.Brindha<sup>1</sup>, Ms.P.Poovizhi<sup>2</sup>, N.Kayalvizhi<sup>3</sup>, K.Praveenkumar<sup>4</sup>, K.F.Felvin<sup>5</sup>

<sup>1</sup>Assistant Professor, Department of EIE, SNS College of Technology, Coimbatore, India

<sup>2</sup>Assistant Professor, Department of IT, SNS College of Engineering, Coimbatore, India

<sup>3,4</sup> UG Scholars, Department of EIE, SNS College of Technology, Coimbatore, India

**ABSTRACT:** *The raw sugar which is in its natural state is converted into white sugar which is used in household and as a ingredients in soft drinks called sugar refining process. The process is carried out by the rotating shaft inside the carbonation tank. In this process chemicals like calcium hydroxide and carbon dioxide is used in the refining process. the mixture is heated in the carbonation tank. After this the calcium hydroxide is neutralized and which the sugar is obtained. In this method only small amount of sugar can be refined at a particular time. PLC and SCADA automates the refining process by this consumption of time is less and it will be secured. Approximately 1300kgs can be refined in short period.*

**Keywords:** PLC (Programmable Logic Controller), SCADA

### INTRODUCTION:

A sugar refinery is a refinery process in which raw sugar is converted into white refined sugar or that processes sugar beet to refined sugar. Many cane sugar mills produce raw sugar, which is sugar that still contains molasses, giving it more color than the white sugar which is normally consumed in households and used as an ingredient in soft drinks and foods. The extraction process is carried out by the rotating shaft inside the cylinder which makes the sugar to deposit on the surface of the cylinder.

The deposited sugar is removed using plough and filtered. The carbonation process is carried out in which is designed to separate sugar and molasses.

In this process the sugarcane syrup is mixed with calcium hydroxide, then the mixture is treated with carbon dioxide gas bubbles. The mixture obtained is heated inside the carbonation tank. Then the calcium hydroxide is neutralized and precipitated as calcium carbonate which is filtered to obtain pure sugar and molasses.

The refined sugar produced is more than 99 percent pure sucrose. The raw sugar is stored in large warehouses and then transported into the sugar refinery by means of transport belts. In the traditional refining process, the raw sugar is first mixed with heavy syrup and move on to the remaining process. As in many other industries factory automation has been promoted heavily in sugar refineries in recent decades. The production process is generally controlled by a

central process control system, which directly controls most of the machines and components.

Only for certain special machines such as the centrifuges in the sugar house decentralized PLC's are used for security reasons. In this project we are using PLC and SCADA technologies for automating centrifugal sugar washing process. It is the last process of sugar production. The process automation is accomplished by PLC. The SCADA shows animated graphical view of process automation and generation reports. The PLC system controls ON-OFF of motor. The whole process is viewed and controlled by SCADA.

### CHALLENGES:

In the carbonation tank the usage of chemicals like calcium hydroxide and carbon dioxide are used. Using this method only less amount of sugar can be refined.

In this method, there is a need of human resource to operate the machines manually. This method consumes more amount of time for sugar refining process. Only small amount of sugar can be refined at a particular time. The refined sugar will have some amount of chemicals, that may have some effects. The safety is at its risk in this process. There is no central control over the process.

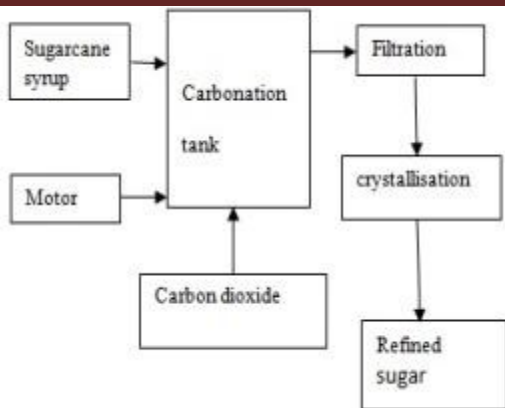


Figure 1. Block Diagram

**BASIC DESIGN:**

The design system is based on the centrifuge control system of sugar refining which sugar and molasses are separated by centrifugally rotating shaft. In this process the sugarcane syrup is stirred in a centrifuge cylinder so that the sugar is succumbed on the surface. The PLC system controls the ON-OFF controller. The whole process is viewed and controlled by SCADA.

**PROPOSED SYSTEM ARCHITECTURE:  
 Centrifuge Control System**

The main objective of the proposed work is to improve the percentage of sugar purity. The Sugar refining process consists of sequence of steps. The major part of proposed system is take place after the final process of sugar refining. The below figure 2 explain about process of the system.

A batch type sugar centrifuge separates the sugar crystals from the mother liquor. These centrifuges have a capacity of up to 1,300 kilograms per cycle. In Centrifuge Control System the sugar and molasses are separated by centrifugally rotating shaft.

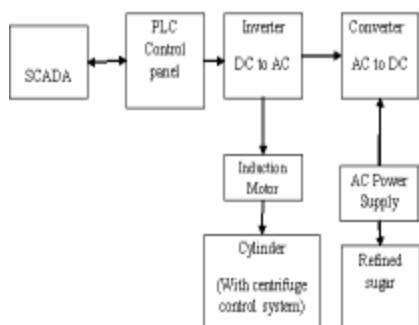


Figure 2. Sugar refining process

In this process the sugarcane syrup is stirred in a centrifuge cylinder so that the sugar is

succumbed on the surface. The sugar from the centrifuges is dried and cooled and then stored in a silo or directly packed into bags for shipment. The PLC system controls the ON-OFF of motor. The whole process is viewed and controlled by SCADA. Entire process is fully automated which automatically save energy of system and process time. The production process is generally controlled by a central process control system, which directly controls most of the machines and components. The proposed system has special machines such as the centrifuges in the sugar house decentralized PLCs are used for security reasons.

**SCADA**

SCADA is an acronym for Supervisory Control and Data Acquisition. SCADA systems are used to monitor and control a plant or equipment in industries such as telecommunications, water and waste control, energy, oil and gas refining and transportation. These systems encompass the transfer of data between a SCADA central host computer and a number of Remote Terminal Units (RTUs) and/or Programmable Logic Controllers (PLCs), and the central host and the operator terminals. A SCADA system gathers information (such as where a leak on a pipeline has occurred), transfers the information back to a central site, then alerts the home station that a leak has occurred, carrying out necessary analysis and control, such as determining if the leak is critical, and displaying the information in a logical and organized fashion.

These systems can be relatively simple, such as one that monitors environmental conditions of a small office building, or very complex, such as a system that monitors all the activity in a nuclear power plant or the activity of a municipal water system. Traditionally, SCADA systems have made use of the Public Switched Network (PSN) for monitoring purposes. Today many systems are monitored using the infrastructure of the corporate Local Area Network (LAN)/Wide Area Network (WAN). Wireless technologies are now being widely deployed for purposes of monitoring. SCADA systems consist of

- One or more field data interface devices, usually RTUs, or PLCs, which interface to field sensing devices and local control switchboxes and valve actuators
- A communications system used to transfer data between field data interface devices and control units and the computers in the SCADA central host. The system can be radio, telephone, cable, satellite, etc.

- A central host computer server or servers (sometimes called a SCADA Center, master station, or Master Terminal Unit (MTU).
- A collection of standard and/or custom software [sometimes called Human Machine Interface (HMI) software or Man Machine Interface (MMI) software] systems used to provide the SCADA central host and operator terminal application, support the communications system, and monitor and control remotely located field data interface devices.

## COMPONENTS SPECIFICATIONS

### INPUT COMPONENTS

There are several input units in centrifugal control system in sugar washing process some of them are as follows.

### MOTOR

The centrifugal control system in sugar washing process uses 3 phase induction motor.

### INDUCTION MOTOR

An induction or asynchronous motor is an AC electric motor in which the electric current in the rotor needed to produce torque is obtained by electromagnetic induction from the magnetic field of the stator winding.

### PRICIPLE OF OPERATION

In both induction and synchronous motors, the AC power supplied to the motor's stator creates a magnetic field that rotates in time with the AC oscillations. Whereas a synchronous motor's rotor turns at the same rate as the stator field, an induction motor's rotor rotates at a slower speed than the stator field. The induction motor stator's magnetic field is therefore changing or rotating relative to the rotor. This induces an opposing current in the induction motor's rotor, in effect the motor's secondary winding, when the latter is short-circuited or closed through external impedance. The rotating magnetic flux induces currents in the windings of the rotor in a manner similar to currents induced in a transformer's secondary winding.

The currents in the rotor windings in turn create magnetic fields in the rotor that react against the stator field. Due to Lenz's law the direction of the magnetic field created will be such as to oppose the change in current through the rotor windings. The cause of induced current in the rotor windings is the rotating stator magnetic field, so to oppose the change in rotor-winding currents the rotor will start to rotate in the direction of the rotating stator magnetic field. The rotor accelerates until the magnitude of induced rotor current and torque balances the applied

load. Since rotation at synchronous speed would result in no induced rotor current, an induction motor always operates slower than synchronous speed. The difference, or "slip," between actual and synchronous speed varies from about 0.5 to 5.0% for standard Design B torque curve induction motors. The induction machine's essential character is that it is created solely by induction instead of being separately excited as in synchronous or DC machines or being self-magnetized as in permanent magnet motors.

### SENSORS

Sensors are used to sense the capacity of the sugar deposition, vibration, oscillation, etc.,

Proximity sensor

- Capacity sensor

### Proximity sensor

Used to sense the vibration of the motor and oscillation of the shaft.

### Capacity sensor

Used to sense the sugar deposition on the surface of the cylinder, which makes the plough to remove the sugar at preset.

### RESULT:

Thus the result of this process is pre viewed in figure using the SCADA software. Using this software it is easy to note the speed of the motor, process time, etc., The hardware toolkit for the sugar refining process is shown in the figure shown below in which uses the PLC and SCADA software. The sugar refined through this process are free of chemicals.

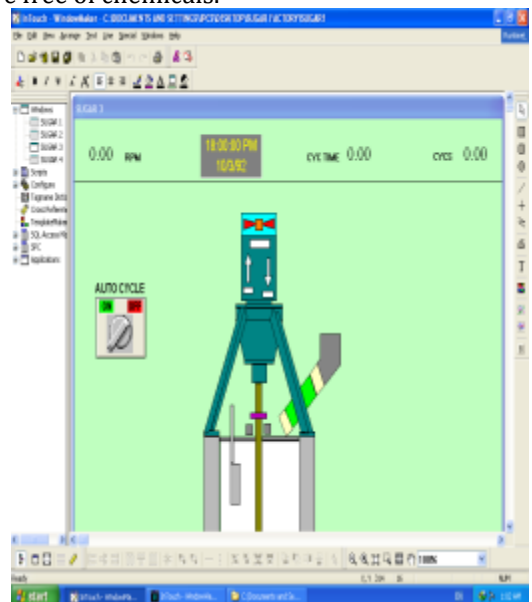


Figure 3. SCADA output

**CONCLUSION:**

Thus the centrifuge control system in sugar washing process can refined the sugar of approx. 1300 kg within 120 seconds. In previous process there are several chemicals used to refine the sugar but in this process there is no need of such chemicals to refine the sugar. Hence this project is useful in refining good quality of sugar. Centrifuge control system in sugar washing process the sugar syrup is processed and extracts the sugar and molasses. The extraction process is carried out by rotating the shaft inside the cylinder which makes the sugar to deposit on the surface of the cylinder. The deposited sugar is removed using plough and filtered. Thus the refined sugar is obtained at the end of the process.

**REFERENCES:**

1. D.K Grover and S.S Grewal , "The Problems of Sugar Industry in India", Vihar Publishers, 1991.
2. D.K. Pant, S.M. Saraswat and Ajay Mishra , "Sugar Industry Diversification for Value Addition", Co-operative sugar, Vol.37, No.5, January 2006.
3. A.H. Dagde (2001), Right Sizing of Manpower in Sugar Industry - A New Theme, Co-operative Sugar, Vol.36, No. 8, April 2005
4. Nevins, J. L., and D. E. Whitney. "Adaptable-programmable assembly systems: an Information and control problem." Proc. IEEE Intercon, PP. 387-406, April 1975.
5. R. H. Anderson, "Programmable automation: The future of computers in manufacturing", Datamation, Vol. 18, pp. 46-52, 1972.
6. Mohamed Endi, Y.Z. Elhalwagy, Attalla hashad., "Three-Layer PLC/SCADA System Architecture in Process Automation and Data Monitoring" 978-1-4244-5586-7/10/C 2010 IEEE.
7. <https://www.bma-worldwide.com/de.html?id=2392&L=1>
8. <http://www.industry.siemens.com/verticals/global/en/food-beverage/references/sugar/pages/default.aspx>
9. <http://www.plantautomation.com/doc/sugar-factory-automation-strategy-0001>
10. <http://www.sugarindustry.com/sugarprocess.htm>
11. [www.wikipedia.com](http://www.wikipedia.com)

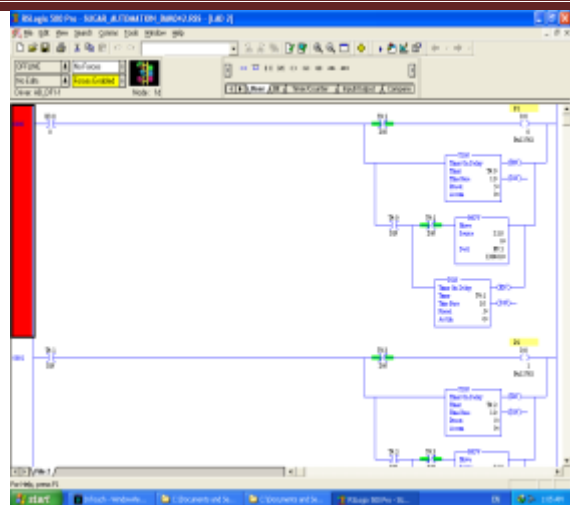


Figure 4 . Screenshot of PLC output

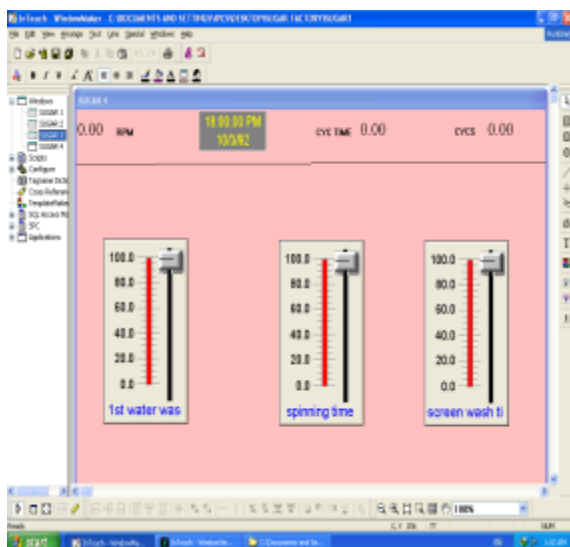


Figure 5 . Screenshot of SCADA output

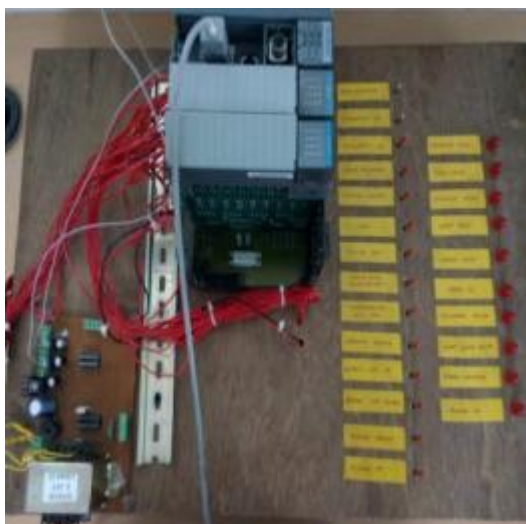


Figure 6. Project kit

# High Frequency AC Link Dual Active Bridge Isolated Bidirectional Dc-Dc Converter for PV Application

DRK. Mahesh & P. Manikya Rao & P. Poushya

Assistant Professors, Malla Reddy College of Engineering, Hyderabad, Telangana, India.

**ABSTRACT:** In this paper, high repeat cooling association two fold dynamic platform separated bidirectional aldc-dc converter for PV application is proposed. The proposed converter beats most of the issues associated with that present open PV converters. Dual active bridge (DAB) converters have been standard in high voltage, low and medium power DC-DC applications, further more a center high repeat interface in solid state transformers. The proposed DAB has the upside of being used as a piece of high walk up/down converters, which over see high voltages, when diverged from normal two-level DABs.

**Keywords:** Bidirectional converters, dc-dc conversion, and dual active bridge.

## I. INTRODUCTION

For the present, power transformation frameworks (PCSs) essentially utilize line-recurrence (LF) transformersto accomplish galvanic detachment and voltage coordinating [1]-[5]. A rapid improvement of appropriated era and vitality stock piling has prompted the expanding prevalence of PCSs as a continually ending key interface [6].

Bethatas it may, massive, substantial, misfortunes, an d boisterous LF transformers impede the effectiveness and influence the thickness of PCSs. Lately, the utilization of high recurrence (HF) transformers setup of conventional LF transformers is thought to be creating a pattern of cutting edge power transformation. Fig.1 demonstrates a similar photograph of 50-Hz LF and 20-kHz HF transformers. The upsides of HF transformers are low volume, light weight, and ease. Further more, high-recurrence join (HFL) PCSs in light of HF transformers can likewise maintain a strategic distance from voltage and current wave form bending brought about by the center immersion of LF transformers. Furthermore, when the exchanging recurrence is over 20 kHz, PCS commotion can be significantly decreased. Particularly, out of sight of fast extend of PCS; HFL-PCSs have wide application prospects.

In the exploration of HFL-PCSs, disengaged bidirectional dc-dc converters (IBDCs) generally serve as the key circuit. By and large, all of IBDCs can be developed from conventional secluded unidirectional dc-dc converters (IUDCs, for example, fly back IUDC can make double fly back IBDC, half-connector push-pull IUDC can form double half-connector push-pull IBDC, and full-connector IUDC can create double dynamic scaffold IBDC.

Actually, other than the IBDCs made out of IUDCs with the same sort, the IUDCs with distinctive sorts like wise can create IBDCs, for example, half-connect IUDC and push-pull IUDC can make a half-scaffold push-pull IBDC in light of the fact that the half-extension and push force structures can withstand high and low-source voltages, separately, so this kind of IBDC can be utilized as a part of the application with a wide voltage extent and a bidirectional force stream.



Fig.1. Comparative photo of 50-Hz LF and 20-kHz HF transformers

Like the order of conventional dc-dc converters in force gadgets, this paper introduces an arrangement of IBDC topology in light of the quantity of switches. The easiest IBDC topology is a double switch structure, for example, double flyback IBDC, double Cuk IBDC, and Zeta-Sepic IBDC. The run of the mill model of three-switch topology is forward-flyback IBDC. Four-switch topologies essentially contain double push-pull IBDC, push-draw forward IBDC, push-pull-flyback, and double half-span IBDC. The commonplace model of five-switch topology is full-extension forward IBDC. The regular model of six-switch topology is half-full connect IBDC. Eight-switch

topology is essentially double dynamic extension IBDC

## II. MODELLING OF PV MODULE

A photovoltaic cell is one which changes over approaching daylight into electric current by method for photoelectric impact. It is fundamentally a p-n intersection manufactured in a wafer. The yield of a PV cell is low and thus these cells are associated in arrangement and parallel to expand the voltage and current levels. Since a PV cell displays nonlinear connection in the middle of voltage and current for differing levels of temperature and Irradiance levels. A sun oriented cell can be demonstrated by utilizing an one diode model, which is the most broadly utilized system. We can likewise a two diode model or a three diode model for displaying a PV cell. In this work, a solitary diode mode is considered. In a some diode demonstrate, a PV cell is displayed as a variable current source in hostile to parallel with a diode, additionally an arrangement and shunt resistance (RS & RP) [4].

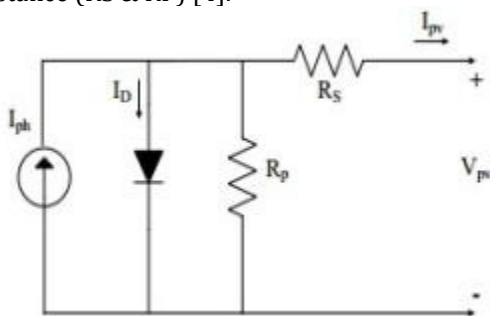


Figure2.The one diode model

The yield of PV cell is given by

$$I = N_p I_{ph} - N_p I_0 \left( \exp \left[ \frac{q(V/N_s + I R_s / N_p)}{k T} \right] - 1 \right) - \frac{V}{R_p}$$

where, I is the present, V is the voltage of the PV module, I<sub>ph</sub> is the photograph current, I<sub>0</sub> is the opposite immersion current, N<sub>p</sub> is the quantity of cells associated in parallel, N<sub>s</sub> is the quantity of cells joined in arrangement, q is the charge of an electron

(1.6\*10<sup>-19</sup>C), k is Boltzmann's consistent (1.38\*10<sup>-23</sup>J/K), A<sub>n</sub> is p-n intersection ideality calculate, (1 < a < 2, a = 1 being the perfect worth), and T is the PV module temperature.

For a sun powered cell, the main produced current is by method for a photograph current which is straightforwardly subject to temperature and also irradiance level given by

$$I_{ph} = [I_{sc} + k_1(T - T_{ref})]G$$

Where I<sub>sc</sub> is the short out current of the PV cell, K<sub>1</sub> is the short out current/temperature coefficient T is the present barometrical temperature and T<sub>ref</sub> is the temperature at ostensible condition (250oC and 1000W/m<sup>2</sup>), G is the present irradiance level. The P-V and I-V attributes of a PV cell are demonstrated in figure 3. The most extreme force is achieved when the cell works at I<sub>mp</sub> and V<sub>mp</sub>.

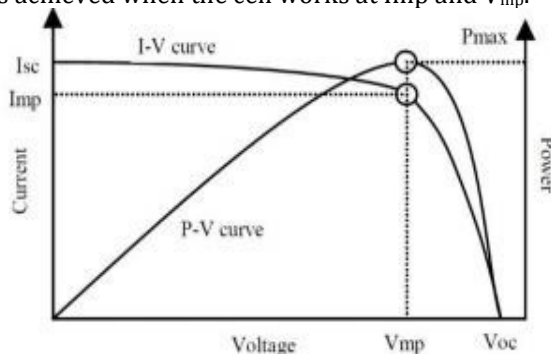


Fig -3: Current-voltage and power-voltage characteristics of a solar cell

The PV module considered for reproduction was Tata TP 250 Series with determinations at Nominal Operating Cell Temperature (NOCT – 20oC & 800 W/m<sup>2</sup>) was viewed as opposed to Standard Test Condition (STC – 25oC & 1000W/m<sup>2</sup>).

## III. PROPOSED CONVERTER

### A. Basic Principle

The far reaching investigations of the operation, outline, and control of DAB-IBDC in consistent state and a limit control plan for DAB-IBDC utilizing the common exchanging surface is available. Examined the brief while scale transient procedures with stage movement control and proposed an arrangement of methods to build framework strength.

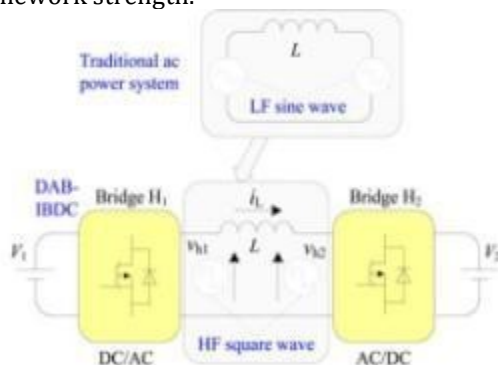


Fig. 4. Basic principles of traditional ac power system and DAB-IBDC.

Fig. 4 demonstrates that like the control of the force transmission in conventional air conditioning force frameworks, the course and

extent of the inductor current  $i_L$  can be changed by conforming the stage move between air conditioning yield square wave voltages  $v_{h1}$  and  $v_{h2}$  of scaffolds  $H_1$  and  $H_2$ , which can control the bearing of force stream and size of DAB-IBDC. The distinction is that the voltages in both sides of the inductor in conventional air conditioning force framework are line-recurrence sinusoidal waves and in DAB-IBDC are high-recurrence square waves. The transmission force models of the customary air conditioning force framework and of DAB-IBDC can be determined as

$$\begin{cases} P_{\text{sin}} = \frac{V_{\text{rms1}} V_{\text{rms2}}}{2\pi f_s L} \sin \phi \\ P_{\text{square}} = \frac{nV_1 V_2}{2\pi^2 f_s L} \phi(\pi - \phi) \end{cases}$$

Where  $V_{\text{rms1}}$  and  $V_{\text{rms2}}$  are the root mean square (RMS) of sinusoidal waves, and  $\phi$  is the stage move between air conditioning voltages. Truth be told, in light of the high-recurrence power transmission, the force thickness and particularity enhance altogether. Subsequently, DAB-IBDC is considered as the center circuit of the HFL-PCSSs pulling in a great deal consideration. Beside these essential qualities, the studies on DAB-IBDC likewise concentrate on transmission power portrayal, dead band impact, and element model.

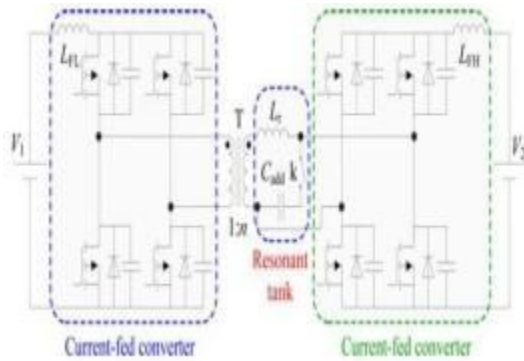
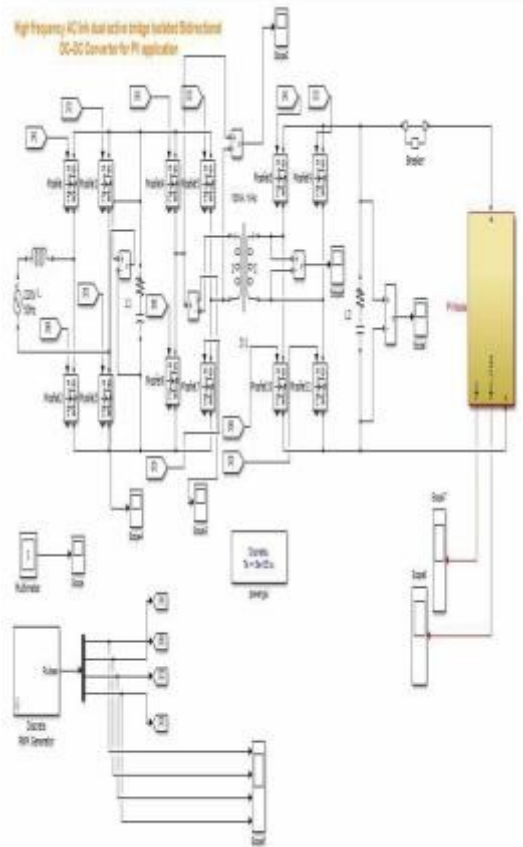


Fig 5. Resonant DAB-IBDC

## VI. SIMULATION RESULTS

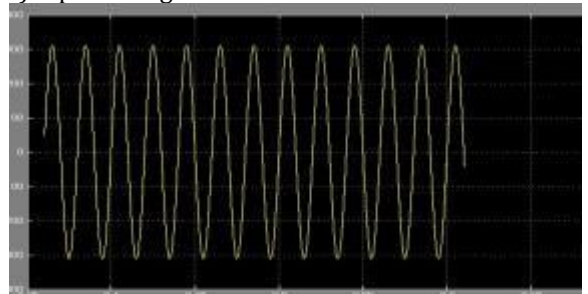
Simulation is performed using MATLAB/SIMULINK software. Simulink library files include inbuilt models of many electrical and electronics components and devices such as diodes, MOSFETS, capacitors, inductors, motors, power supplies and so on. The circuit components are connected as per design without error, parameters of all components are configured as per requirement and simulation is performed.

## SIMULATION CIRCUIT

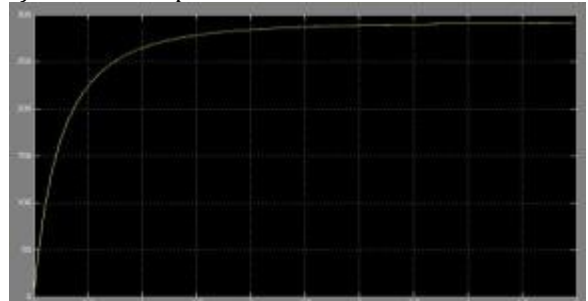


## WAVEFORMS

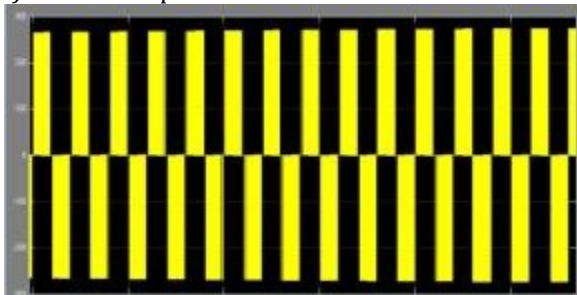
a) Input voltage



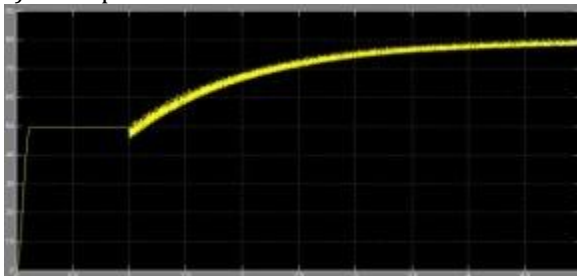
b) Rectifier Output



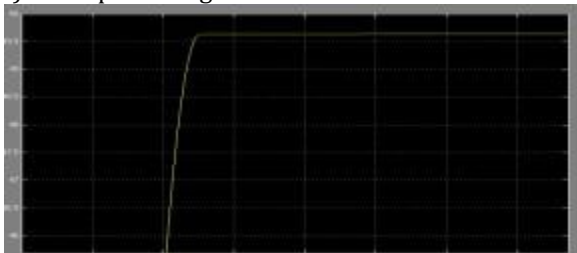
c) Inverter output



d) D Coutput



e) PV output voltage



## V.CONCLUSION

In this paper a high frequency ac link converter with dual active bridge isolated is proposed for a bidirectional dc-dc power converter for PV

application is proposed . Simulation study is carried out using MATLAB/SIMULINK software.

## REFERENCES

1. J. C. Wu and H. L. Jou, "A new UPS scheme provides harmonic suppression and input power factor correction," *IEEE Trans. Ind. Electron.*, vol. 42, no. 6, pp. 629–635, Dec. 1995.
2. P. K. Jain, J. R. Espinoza, and H. Jin, "Performance of a single-stage UPS system for single-phase trapezoidalshaped ac-voltage supplies," *IEEE Trans. Power Electron.*, vol. 13, no. 5, pp. 912–923, Sep. 1998.
3. J. Rodr'iguez, S. Bernet, B. Wu, J. O. Pontt, and S. Kouro, "Multilevel voltage-source-converter topologies for industrial medium-voltage drives," *IEEE Trans. Ind. Electron.*, vol. 54, no. 6, pp. 2930–2945, Dec. 2007.
4. S. Roy and L. Umanand, "Integrated magnetics-based multisource quality ac power supply," *IEEE Trans. Ind. Electron.*, vol. 58, no. 4, pp. 1350– 1358, Apr. 2011.
5. G. Franceschini, E. Lorenzani, and G. Buticchi, "Saturation compensation strategy for grid connected converters based on line frequency transformers," *IEEE Trans. Energy Convers.*, vol. 27, no. 2, pp. 229– 237, Jun. 2012.
6. G. Franceschini, E. Lorenzani, and G. Buticchi, "Saturation compensation strategy for grid connected converters based on line frequency transformers," *IEEE Trans. Energy Convers.*, vol. 27, no. 2, pp. 229– 237, Jun. 2012.
7. R. Huang and S. K. Mazumder, "A soft-switching scheme for an isolated dc/dc converter with pulsating dc output for a three-phase high frequency- link PWM converter," *IEEE Trans. Power Electron.*, vol. 24, no. 10, pp. 2276–2288, Oct. 2009.

## INTEND INNOVATIVE TECHNOLOGY FOR RECOGNITION OF SEAT VACANCY IN BUS

Gudipelly Mamatha<sup>1</sup> & B.Manjula<sup>2</sup> & P.Venkatapathi<sup>3</sup>

<sup>1</sup>M.Tech Scholar, Malla Reddy College of Engineering,Hyderabad,Telangana,India.

<sup>2</sup>Assistant Professors, Malla Reddy College of Engineering,Hyderabad,Telangana,India.

<sup>3</sup>Associate Professor, Malla Reddy College of Engineering,Hyderabad,Telangana,India.

---

**ABSTRACT:** Contemporary comes close to readily available to locate the bus area do not anticipate the seat accessibility in bus when it gets to the boarding factor. In the active globe, waiting on a public transportation without recognition of either seat schedule. An individual waiting on bus needs to know the present seats accessibility of the following readily available bus as well as the offered ability to take a trip. It is worthless to await a bus without expertise of existing readily available capability of bus. The suggested system will certainly give the offered seats when it gets to the individual's terminal. This system could inspire travelers to take a trip in bus instead of investing for cars or taxis. By making use of WIFI component for information interaction objective. That information, openings information will be upgraded. This android system would certainly aid the guests to have a sufficient traveling by capturing the best bus at the correct time with much less initiative.

**Keywords:** Face detection, Haar-like features, Morphological image processing, Contrast limited adaptive histogram equalization

---

### I. INTRODUCTION

By comprehending the future extent of modern technologies offered today we will certainly have a numerous kinds of application and also enhancement of bus stand tracking and also control. Previous deal with bus radar there is an as well substantial. Yet could " To do numerous applications at the very same time in previous job. In bus stand tracking as well as control carries out complete bus stand task on basis of 2 components „ In bus component " as well as „ bus stand component ". Supply accessibility to live info pertaining to bus timetables, Expected Time of Arrival (ETA), Estimated Time of Departure (ETD), and so on, with Display at Bus stands, Self-service Short Messaging Service (SMS) along with the Internet. Showing uninhabited seats and also uninhabited systems for buses in bus stops. Counting of the individuals existing in the bus in bus side as well as counting the uninhabited placements of the system on system side.

Nowadays, most people use public vehicle instead of personal car due to the rising of fuel price and traffic jams. Public company has been developing the system for displaying the position of the passenger vehicle for convenience of customers. However, those systems only indicate the position of the vehicle but not show the availability of seats in the vehicle. Customers will waste a time for waiting the next passenger vehicle and cannot manage the time travel or

activities correctly. If customers know both of the position of the passenger vehicle and vacancy of seats, customers can use the time to other activities before the passenger vehicle arrives. Customers can plan their travel better.

In this research, the seat vacancy identification system is designed by using image processing technique. Webcam is connected with Raspberry Pi 2 in the electric vehicle for detecting the object on vehicle and sending the data to the server via 3G communication. This system use Open Source Computer Vision (OpenCV) to analyze and process the data then calculated the vacancy of the electric vehicle by using the maximum face detection data.

### II. LITERATURE REVIEW AND RELATED THEORY

"Real-Time Integrated CCTV using Face and Pedestrian Detection Image Processing Algorithm for Automatic Traffic Light Transitions", this research deals with the traffic light for pedestrian who wants to cross the road. If the pedestrian cross the road they press the button and wait for traffic light. This system use CCTV instead the button and use image processing for detecting the face of pedestrian. If CCTV detects the face of pedestrian, the system will set the red light to show for 45 second. On the other hand if CCTV does not detect the face, the red light will show for only 30 second. [1] "To Analyze the

Impact of Image Scaling Algorithms on Viola – Jones Face Detection Framework”, this research deals with the Viola – Jones algorithm about the problem from low quality of the image and find the optimum solution from Viola – Jones algorithm. The system uses two methods to scaled image that are window scaling and image scaling. The image scaling has 5 techniques that is Nearest Neighbor, Bi-Linear, Bi-Cubic, Extended Linear, and Piece-Wise Extended Linear. The system uses 5 difference face database for analyzing the performance of 5 different image scaling techniques. The system was developed by using C++, Visual studio 2010, and Open Source Computer Vision (OpenCV). They used confusion matrix that compose of True Positive, False Positive, and False Negative to compute the performance of each technique. From the result, they found that the analysis in format of the window scaling is better than image scaling. [2] “FACE DETECTION USING COMBINATION OF SKIN COLOR PIXEL DETECTION AND VIOLA-JONES FACE DETECTOR”, this research studies the detection of the human skin. It uses a combination of two techniques that are a novel hybrid color models and Viola – Jones algorithms. Its purpose is to identify the object is human or not. The system is designed in MATLAB and use ECU face and skin database to evaluate the accuracy. From the results, this method has high performance more than the other. When use this method with Viola – Jones face detector, it will be more efficient. [3]

#### A. Haar-like features

Haar-like features are a popular technique for detecting the face of human in the present. They are a method that has fast processing and more accuracy. The method is proposed by Paul Viola and Michael Jones in 2001. [4] Algorithms of Haar-like features are separating the image from input image to the sub window and scanning for detecting the face. They use integral image technique for finding the summation of the pixel inside the image, and then use the detector that can change the size and the position for finding the difference of white and black areas. When finish from integral image process, the next step is calling Adaptive Boosting or AdaBoost. This process is the data classification by increasing weight to the classification of a face until the best face detected. Determine is classification by  $i = \{0, 1, 2, 3, \dots, n\}$ , the process starts from . The classification of may be less accuracy. If finish from the process of ,AdaBoost will increase accuracy of the classification and create the new classification that is . This process will do

continuously until the final classification and end the process. The last step is Cascaded Classifier. This step separates the image to sub-window and check the sub-window for finding the face. If a sub-window is not a face, it will reject the sub-window. If the sub-window has a chance of having human face, it will go to the next classifier that increases the weight of classifier. This step will find the face from the sub-window until get the best of face detected.

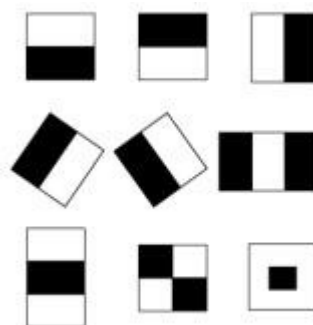


Figure 1: Type of Haar-like features

#### B. Contrast limited adaptive histogram equalization or CLAHE

Contrast limited adaptive histogram equalization or CLAHE is the process for increasing the image quality. This process is developed from adaptive histogram equalization. This method considers the data of histogram equalization in each of pixel of gray scale format. In the first step, this method finds average histogram value of the image. The method uses the histogram value that has higher than the average value to share to all pixels inside the image for equal histogram value. [5]

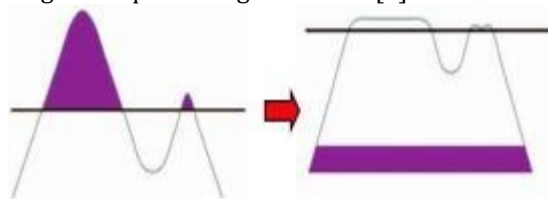


Figure 2: Contrast limited adaptive histogram equalization method



Figure 3: (A) Original image (B) The image from CLAHE process

C. Morphological process

Morphological process is the process for changing shape or structure of the image. The process use matrix data that comprise the binary values 0 and 1 for calculation. It is called structuring element. Morphological process has 2 methods that are dilation and erosion.

Dilation is a technique for adding the edge pixel of object. This technique creates the structuring element (set B), then use structuring element to scan the data of image (set A). When the data of image (set A) has some binary data on the image matching with structuring element (set B), the binary data of the image will change by using  $A \oplus B = \{x \mid \textcircled{\in} \cap A \neq \emptyset\}$ .

Erosion is a technique that is different from dilation technique. It reduces the edge pixel of object by using structuring element (set B) to scan the data of image (set A) same dilation technique. When the data of image (set A) has some binary data on the image matching with structuring element (set B), the binary data of the image will change by using  $A \ominus B = \{x \mid \textcircled{\in} \subseteq A\}$ . [6][7]

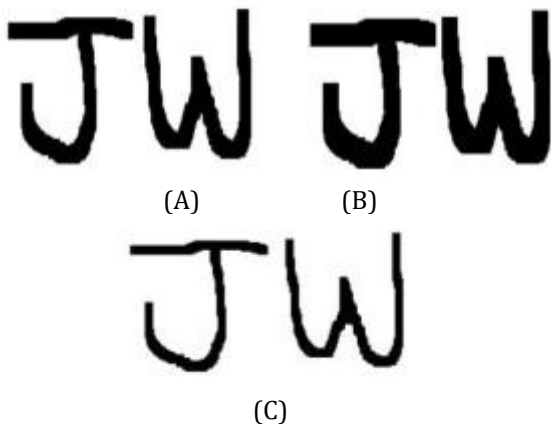


Figure 4: (A) Original image (B) Dilation method (C) Erosion method

III. METHODOLOGY

The devices that include webcam, Raspberry Pi 2 model B, and 3G module are installed in electric vehicle at the top-front of the electric vehicle. When the electric vehicle leaves from the station, the system will capture the image in the passenger seat area (1 image per 1 second) and send to the server by using 3G communication. The server processes the images that receive from Raspberry Pi in electric vehicle by using Open Source Computer Vision (OpenCV).

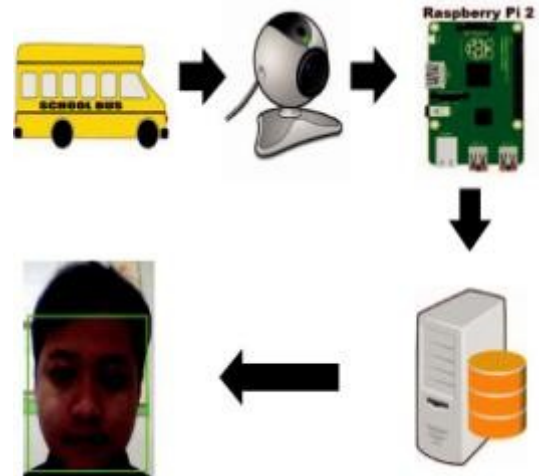


Figure 5: Overview of overall system

The system is divided into two parts. The first part is hardware. It installed and worked on the vehicle. The second part is program on the server. It is used for process the data from hardware. The system work is shown in figure 6.

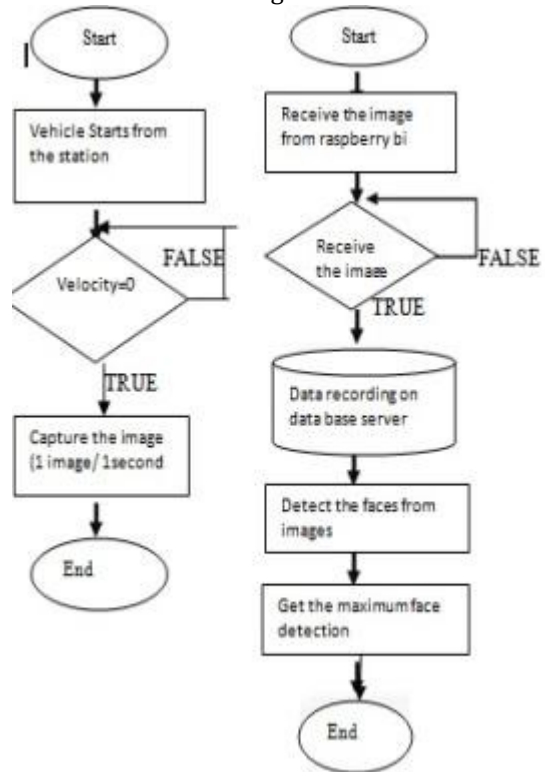


Figure 6: Program flowchart of the system in the vehicle and server

The program has processes to reduce the image noise. It uses method from Open Source Computer Vision (OpenCV). It is shown in figure 7

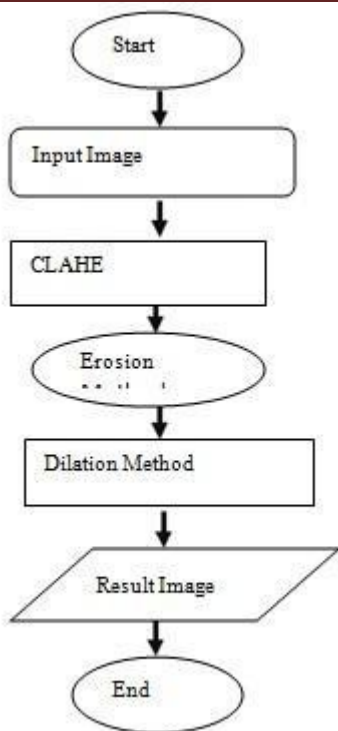


Figure 7: Reducing noise method flowchart

The program use contrast limited adaptive histogram equalization or CLAHE method. This step will adjust the histogram of the image for the appropriate value and change to grayscale format.

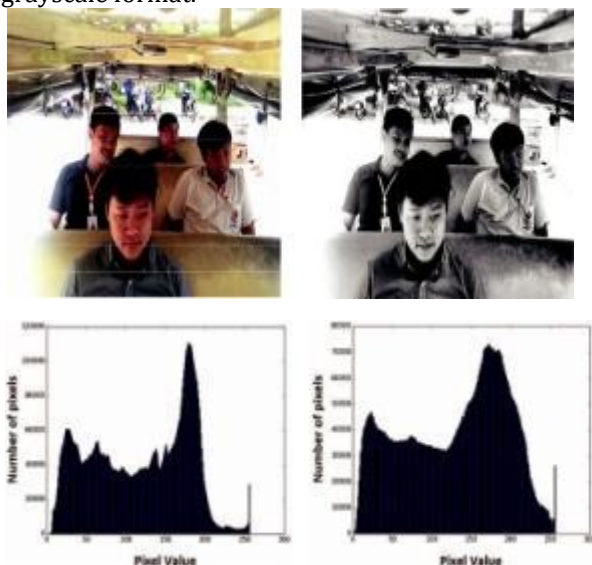


Figure 8: The comparison histogram of original image and the image from CLAHE method

When the system finishes adjusting histogram then the image noise will be reduce by using the morphological process. The image noise is processed by using the erosion method for removing unwanted pixel. Then, the dilation

method applies after the erosion method to increase the edge pixel of the image. The result of the face in the image is clearer when compare with the original image (figure 9).



Figure 9: The comparison of original image and the final image result

In the last process, the system will use Haar-like feature algorithm for finding the passengers faces. The system will detect only the face of human by using the face shape. In each image, the result of passengers face detection is not equal. When the process finish, the system will give only the maximum number of the passenger face from all of the images. Finally, the system will use the maximum number of the face detection to subtract with the number of the electric vehicle seat and show the remaining seat of the electric vehicle.



Figure 10: Example of face detection

*A. Result*

The experiment use different number of passengers and experimental time. Three experiments are conducted. The passengers in electric vehicle are not equal in each round. In each experiment uses different number of images to evaluate the accuracy of face detection in electric vehicle. The result of experiment is shown in table I.

TABLE I.

The number of images	Round 1		Round 2		Round 3		Accuracy (Percent)
	1	2	1	2	1	2	
5	6	4	7	4	8	5	57.33
40	6	5	7	6	8	7	74.00
100	6	5	7	6	8	6	79.19

150	6	5	7	6	8	7	78.96
200	6	5	7	4	8	4	90.65
240	6	5	7	8	8	8	90.66
280	6	5	7	8	8	4	90.69

\* : Number of passengers; Number of passengers detected by face detection technique.

From the result, the number of images has an effect for face detection. If we use fewer images, the program will be low performance and accuracy. The program cannot detect the face because the face of passengers is not clear. This problem consists from environment around the vehicle. It makes the images too light or dark. If the number of image is increases (long capturing time), the movement of passenger face is increase as well. The program can detect the face of the passenger better because the program has a more chance to detect the passengers face from many images.

**IV. CONCLUSION**

Vehicle Seat Vacancy Identification using Image Processing Technique was designed and tested. Webcam and Raspberry Pi were installed in electric vehicle. When the vehicle starts from the station, webcam captured the images and send to the server by using Raspberry Pi and 3G communications. The images were sent completely. From experimental result (Table I), the number of images have a direct impact to the face detection result. If the number of images increases, the accuracy of face detection is increase as well. Because the system will has more chance to detect the passengers face from many images. The noises in images occur from environment inside and outside the vehicle such as the light and face blur. The system improve quality of images by using contrast limited adaptive histogram equalization and morphological process. The system can work well at 200 – 300 images data. It gives 91.67 % accuracy.

**REFERENCES**

1. Cyrel O. Manlises, Jesus M. Martinez Jr., Jackson L. Belenzo, Czarleine K. Perez, and Maria Khristina Theresa A. Postrero, "Real-Time Integrated CCTV Using Face and Pedestrian Detection Image Processing Algorithm For Automatic Traffic Light Transitions", School of Electrical, Electronics and Computer Engineering, Mapua Institute of Technology, 2015
2. Himanshu Sharma, Sumeet Saurav, Sanjay Singh, Anil K Saini, and Ravi Saini, "Analyzing Impact of Image Scaling Algorithms on Viola-

3. Jones Face Detection Framework", Advanced Electronics System, Academy of Scientific and Industrial Research, CSIR-Central Electronics Research Institute, 2015
3. GUAN-CHUN LUH, "FACE DETECTION USING COMBINATION OF SKIN COLOR PIXEL DETECTION AND VIOLA-JONES FACE DETECTOR", Department of Mechanical Engineering, Tatung University, 2014
4. Paul Viola, and Michael Jones, "Rapid Object Detection using a Boosted Cascade of Simple Features", Mitsubishi Electric Research Labs, Compaq Cambridge Research Lab, 2001
5. He, F. Li, L. Yin, H., Huang X., "Transport Monitoring System Based on ZigBee and GPRS" Computer Distributed Control and Intelligent Environmental Monitoring (CDCIEM), 2012 International Conference, pp.178 – 181, 2012.
6. K.Sreedhar, and B.Panlal, "ENHANCEMENT OF IMAGES USING MORPHOLOGICAL TRANSFORMATIONS", International Journal of Computer Science & Information Technology (IJCSIT), Vol 4, No 1, pp. 33-50, Feb 2012
7. Liang, X. Shasha, G. Haitao, Z., "Dynamic transport checking and booking framework in view of ArcGIS Server innovation "Software engineering and Information Processing (CSIP), International Conference , pp.1438 – 1441, 2012.
8. N. Raj and R. K. Sharma, "A High Swing OTA with wide Linearity for design of Self Tuneable Resistor", International Journal of VLSI design & Communication system (VLSICS), Volume 1, No. 3, pp. 1-11, 2010.
9. N. Raj, A.K. Singh, A.K. Gupta, "Modeling of Human Voice Box in VLSI for Low Power Biomedical Applications", IETE Journal of Research, Vol. 57, Issue 4, pp. 345-353, 2011.
10. N. Raj, A.K. Singh, and A.K. Gupta, "Low power high output impedance high bandwidth QFGMOS current mirror", Microelectronics Journal, Vol. 45, No. 8, pp. 1132-1142, 2014.
11. N. Raj, A.K. Singh, and A.K. Gupta, "Low-voltage bulk-driven self-biased cascode current mirror with bandwidth enhancement", Electronics Letters, Vol. 50, No. 1, pp. 23-25, 2014.
12. N. Raj, A.K. Singh, and A.K. Gupta, "Low Voltage High Output Impedance Bulk-driven Quasi-floating Gate Self-biased High-swing Cascode Current Mirror", Circuit System & Signal Processing Journal, Vol. 35, No. 8, pp. 2683-2703, 2015.
13. N. Raj, A.K. Singh, and A.K. Gupta, "High performance Current Mirrors using Quasi-floating Bulk", Microelectronics Journal, Vol. 52, No. 1, pp. 11-22, 2016.
14. N. Raj, A.K. Singh, and A.K. Gupta, "Low Voltage High Performance Bulk-driven Quasi-floating Gate Self-biased Cascode Current Mirror",

- 
- Microelectronics Journal, Vol. 52, No. 1, pp. 124-133, 2016.
15. N. Raj, A.K. Singh, and A.K. Gupta, "Low Voltage High Bandwidth Self-biased High Swing Cascode Current Mirror", Indian Journal of Pure and Applied Physics, Vol. 55, No. 4, pp. 245-253, 2017.
  16. Raj N. and Gupta A. K., "Analysis of Operational Transconductance Amplifier using Low Power Techniques", Journal of Semiconductor Devices and Circuits (STM Journal), Vol. 1, No. 3, pp. 1-9, 2015.
  17. Raj N. and Gupta A. K., "Multifunction Filter Design using BDQFG Miller OTA", Journal of Electrical and Electronics Engineering: An International Journal (EEEIJ Journal), Vol. 4, No. 3, pp. 55-67, 2015.
  18. N. Raj, A.K. Singh, and A.K. Gupta, "Low Power Circuit Design Techniques: A Survey", International Journal of Computer Theory and Engineering, Vol. 7, No. 3, pp. 172-176, 2015.

## OBSERVING OPERATING ACTIVITIES OF WORK VEHICLES BY USING ZIGBEE NETWORK SYSTEM

ASHOK BHUKYA\* & Mr.G.Sanjeev\*\*

\*PG Scholar, Department of Electronics and Communication Engineering, Malla Reddy College of Engineering, Hyderabad,India

\*\*Professor, Department of Electronics and Communication Engineering, Malla Reddy College of Engineering Hyderabad,India.

**ABSTRACT:** Observing activities of working vehicles on a work site, such as a factory, is important in regard to managing the lifetime of vehicles and achieving high operational availability. However, it is a problem that an administrator cannot completely grasp the activities of a working vehicle. Existing systems cannot cover a large area, particularly in an indoor environment. A system is proposed for monitoring operating activities of working vehicles, regardless of whether they are operating indoors or outdoors. The system calculates the activity rate of a vehicle by analyzing the topology of a network configured by the wireless technology ZigBee. In addition, it was experimentally verified that network topology and RSSI can be used to estimate activities of working vehicles.

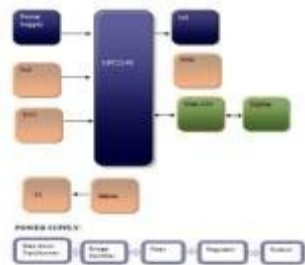
**Keywords:** ZigBee; Sensor Network; Activity; Status;

### 1.INTRODUCTION

**EMBEDDED SYSTEMS:** Each day, our lives become more dependent on 'embedded systems', digital information technology that is embedded in our environment. More than 98% of processors applied today are in embedded systems, and are no longer visible to the customer as 'computers' in the ordinary sense. An Embedded System is a special-purpose system in which the computer is completely encapsulated by or dedicated to the device or system it controls. Unlike a general-purpose computer, such as a personal computer, an embedded system performs one or a few pre-defined tasks, usually with very specific requirements. Since the system is dedicated to specific tasks, design engineers can optimize it, reducing the size and cost of the product. Embedded systems are often mass-produced, benefiting from economies of scale. The increasing use of PC hardware is one of the most important developments in high-end embedded systems in recent years. Hardware costs of high-end systems have dropped dramatically as a result of this trend, making feasible some projects which previously would not have been done because of the high cost of non-PC-based embedded hardware. But software choices for the embedded PC platform are not nearly as attractive as the hardware.

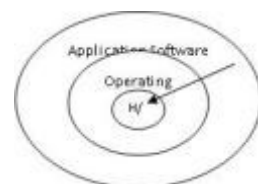
Typically, an embedded system is housed on a single microprocessor board with the

programs stored in ROM. Virtually all appliances that have a digital interface -- watches, microwaves, VCRs, cars -- utilize embedded systems. Some embedded systems include an operating system, but many are so specialized that the entire logic can be implemented as a single program



### 1.Overview of an Embedded System Architecture

Every Embedded system consists of a custom-built hardware built around a central processing unit. This hardware also contains memory chips onto which the software is loaded.



The operating system runs above the hardware and the application software runs above the operating system. The same architecture is applicable to any computer including desktop

computer. However these are significant differences. It is not compulsory to have an operating system in every embedded system. For small applications such as remote control units, air conditioners, toys etc.

**2. ARM LPC2148:** The LPC2141/42/44/46/48 microcontrollers are based on a 16-bit/32-bit ARM7TDMI-S CPU with real-time emulation and embedded trace support, that combine microcontroller with embedded high speed flash memory ranging from 32kB to 512 kB. . For critical code size applications, the alternative 16-bit Thumb mode reduces code by more than 30 % with minimal performance penalty. Due to their tiny size and low power consumption, LPC2141/42/44/46/48 are ideal for applications where miniaturization is a key requirement, such as access control and point-of-sale. Serial communications interfaces ranging from a USB 2.00 Full-speed device, multiple UARTs, SPI, SSP to I2C-bus and on-chip SRAM of 8 kB up to 40 kB, make these devices very well suited for communication gateways and protocol converters, soft modems, voice recognition and low end imaging, providing both large buffer size and high processing power.

Various 32-bit timers, single or dual 10-bit ADC(s),10-bit DAC,PWM channels and 45 fast GPIO lines with upto nine for the board to setup, once the signal is gone, the CPU starts immediately. However, if the reset signal latches wake up timer starts. During this time, the board setup itself. If the reset signal latches longer than the time However, if the reset signal latches shorter than the time taken for the board to setup, once the signal is gone, the board waits for the wake up time to finish its first loop before starting the CPU (See Figure 3). these microcontrollers suitable for industrial control and medical systems nine edge or level sensitive external interrupt pins make

## 2.LITERATURE SURVEY

### 2.1.EXISTING SYSTEM

GPS is a typical way for achieving such positioning; however, it cannot be used in indoor environments because GPS signals are blocked by wallsceilings The Global Positioning System (GPS),originally Navstar GPS,<sup>[1]</sup> is a satellite-based radionavigation system owned by the United StatesUnited States government and operated by the United States Air Force.<sup>[2]</sup> It is a global navigation satellite system that provides geolocationand time information to

a GPS receiver anywhere on or near the Earth where there is an unobstructed line of sight to four or more GPS satellites.<sup>[3]</sup>

### Disadvantage:

It requires vehicle to be in outdoor for correct positioning.

### 2.2.PROPOSED SYSTEM

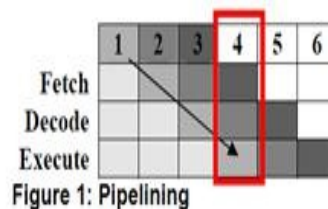
This system utilizes a ZigBee device attached to a working vehicle to observe the activities of the vehicle. The system collects topology and RSSI data from the network built by the ZigBee. These data are used for estimating relative positions of the working vehicles. The activity rate of each working vehicle is calculated by analysing the position information in a time-series manner. Finally, the calculated activity rate of each working vehicle is displayed.

### Advantages:

- 1.No need of external microcomputer since ZigBee has inbuilt one in it.
- 2.The links between the nodes are established with probability of 95%.

### 3.PIPELINING

An instruction cycle has 3 stages:



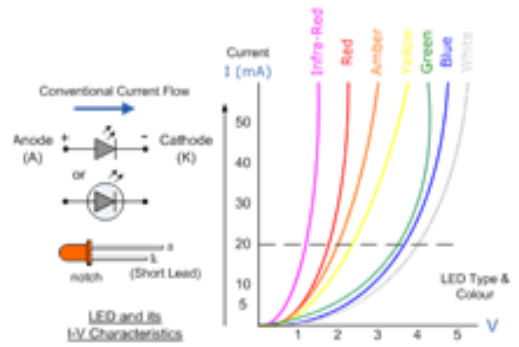
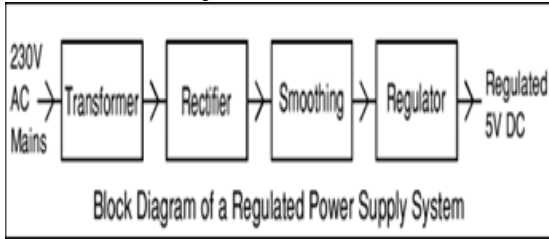
During the execution of the 1st instruction, the 2nd instruction being decode and the 3rd instruction is being fetch. See the Figure 1 below

### RESET AND WAKEUP TIMER:

LPC2148 can be reset in 2 ways; from the RESET button or Watch Dog Timer. taken for the board to setup, once The signal is gone, , the CPU starts immediately wake up timer starts. During this time, the board setup itself. If the reset signal latches longer than the time However, if the reset signal latches shorter than the time taken for the board to setup, once the signal is gone, the board waits for the wake up time to finish its first loop before starting the CPU (See Figure 3).



**4.HARD WRE REQUIRED**



For example a 5v regulated supply:  
 Each of the blocks is described in more detail below:

**Transformer** - steps down high voltage AC mains to low voltage AC.

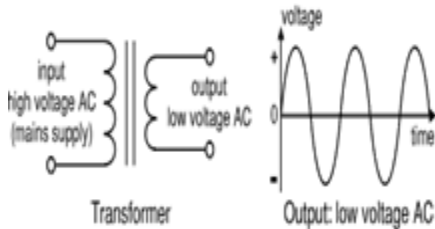
**Rectifier** - converts AC to DC, but the DC output is varying.

**Smoothing** - smoothes the DC from varying greatly to a small ripple.

**Regulator** - eliminates ripple by setting DC output to a fixed voltage.

Power supplies made from these blocks are described below with a circuit diagram and a graph of their output:

**4.1 TRANSFORMER ONLY**



**4.2 LIGHT EMITTING DIODES I-V CHARACTERISTICS**

Before a light emitting diode can "emit" any form of light it needs a current to flow through it, as it is a current dependant device. As the LED is to be connected in a forward bias condition across a power supply it should be Current Limited using a series resistor to protect it from excessive current flow. From the table above we can see that each LED has its own forward voltage drop across the PN-junction and this parameter which is determined by the semiconductor material used is the forward voltage drop for a given amount of forward conduction current, typically for a forward current of 20mA. In most cases LEDs are operated from a low voltage DC supply, with a series resistor to limit the forward current to a suitable value from say 5mA for a simple LED indicator to 30mA or more where a high brightness light output is needed.

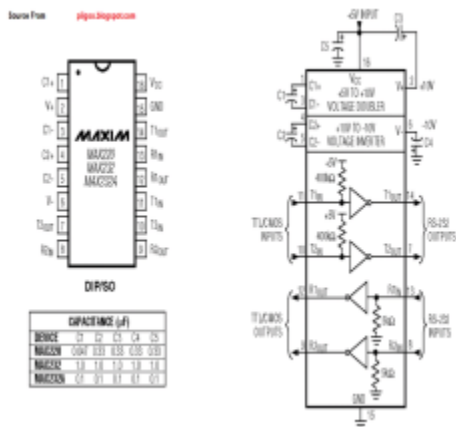
RS232 Line Type & Logic Level	RS232 Voltage	TTL Voltage to/ from MAX232
Data Transmission (Rx/Tx) Logic 0	+3V to +15V	0V
Data Transmission (Rx/Tx) Logic 1	-3V to -15V	5V
Control Signals (RTS/CTS/DTR/DSR) Logic 0	-3V to -15V	5V
Control Signals (RTS/CTS/DTR/DSR) Logic 1	+3V to +15V	0V

Communication can happen right after the association. *Direct addressing* uses both radio address and endpoint identifier, whereas indirect addressing uses every relevant field (address, endpoint, cluster and attribute) and requires that they be sent to the network coordinator, which maintains associations and translates requests for communication. *Indirect addressing* is particularly useful to keep some devices very simple and minimize their need for storage. Besides these two methods, *broadcast* to all endpoints in a device is available, and *group addressing* is used to communicate with groups of endpoints belonging to a set of devices. The receivers reduce RS-232 inputs (which may be as high as  $\pm 25$  V), to standard 5 V TTL levels. These receivers have a typical threshold of 1.3 V, and a typical hysteresis of 0.5 V. The later MAX232A is backwards compatible with the original MAX232 but may operate at higher baud rates and can use smaller external capacitors - 0.1 $\mu$ F in place of the 1.0 $\mu$ F capacitors used with the original device. The newer MAX3232 is also backwards compatible, but operates at a broader voltage range, from 3 to 5.5V..

**PIN DIAGRAM OF MAX232**

Max232 is designed by Maxim Integrated Products. This IC is widely used in RS232 **Communication** systems in which the conversion of voltage level is required to make TTL devices to be compatible with PC serial port

and vice versa. This chip contains charge pumps which pumps the voltage to the Desired Level



MAX232	1	2	3	4	5	6	7	8	9	10	11	12	13	14	15	16
MAX232	1	2	3	4	5	6	7	8	9	10	11	12	13	14	15	16
MAX232	1	2	3	4	5	6	7	8	9	10	11	12	13	14	15	16
MAX232	1	2	3	4	5	6	7	8	9	10	11	12	13	14	15	16

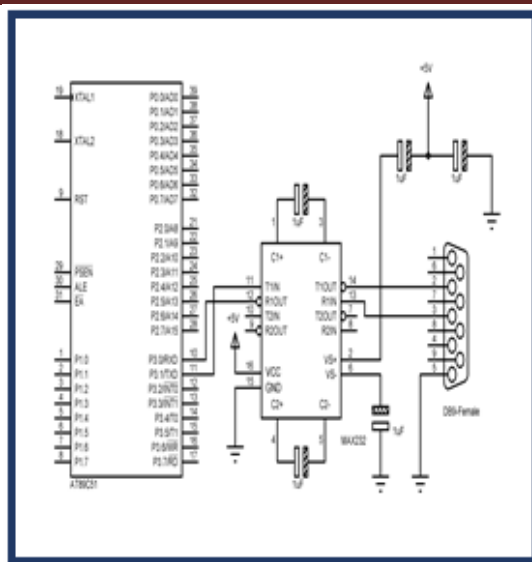
**4.3 TYPICAL APPLICATIONS**

he MAX232(A) has two receivers that convert from RS-232 to TTL voltage levels, and two drivers that convert from TTL logic to RS-232 voltage levels. As a result, only two out of all RS-232 signals can be converted in each direction. Typically, the first driver/receiver pair of the MAX232 is used for TX and RX signals, and the second one for CTS and RTS signals.

**4.4 VOLTAGE LEVELS**

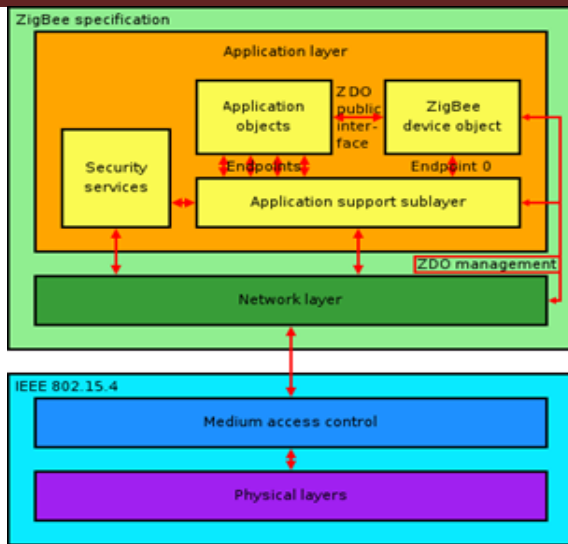
TIA-232 line type and logic level	TIA-232 voltage	TTL voltage to/from MAX232
Data transmission (Rx/Tx) logic 0	+3 V to +15 V	0 V
Data transmission (Rx/Tx) logic 1	-3 V to -15 V	5 V
Control signals (RTS/CTS/DTR/DSR) logic 0	-3 V to -15 V	5 V
Control signals (RTS/CTS/DTR/DSR) logic 1	+3 V to +15 V	0 V

It is helpful to understand what occurs to the voltage levels. When a MAX232 IC receives a TTL level to convert, it changes a TTL Logic 0 to between +3 and +15V, and changes TTL Logic 1 to between -3 to -15V, and vice versa for converting from RS232 to TTL. This can be confusing when you realize that the RS232 Data Transmission voltages at a certain logic state are opposite from the RS232 Control Line voltages at the same logic state. To clarify the matter, see the table below.

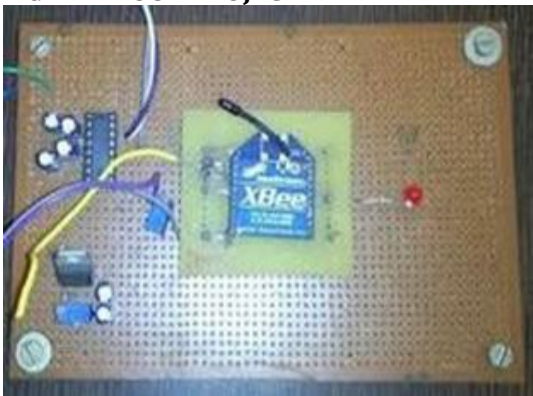


**5. TECHNICAL OVERVIEW**

ZigBee is a low-cost, low-power, wireless mesh network standard. The low cost allows the technology to be widely deployed in wireless control and monitoring applications. Low power-usage allows longer life with smaller batteries. Mesh networking provides high reliability and more extensive range. ZigBee chip vendors typically sell integrated radios and microcontrollers with between 60 KB and 256 KB flash memory. Zigbee is a wireless technology developed as an open global standard to address the unique needs of low-cost, low-power wireless IoT networks. ... The Zigbeestandard operates on the IEEE 802.15.4 physical radio specification and operates in unlicensed bands including 2.4 GHz, 900 MHz and 868 MHz.. Zigbee is not a product, rather it is a protocol developed by the Zigbee alliance, that allows for the universal compatability of devices created by different manufacturers all over the world for use in a wireless home management system (Zigbee 2011). Zigbee's relatively low priced wireless home synchronization specification is carried over the IEEE 802.15.4 architecture (Radmand, unk)



**6. ZIGBEE IN OUR PROJECT**



Typical applications without special security needs will use a network key provided by the trust center (through the initially insecure channel) to communicate. Thus, the trust center maintains both the network key and provides point-to-point security. Devices will only accept communications originating from a key provided by the trust center, except for the initial master key. The security architecture is distributed among the network layers as follows:

1. The MAC sub layer is capable of single-hop reliable communications. As a rule, the security level it is to use is specified by the upper layers.
2. The network layer manages routing, processing received messages and being capable of broadcasting requests. Outgoing frames will use the adequate link key according to the routing, if it is available; otherwise, the network key will be used to protect the payload from external devices.
3. The application layer offers key establishment and transport services to both ZDO and applications.

4. It is also responsible for the propagation across the network of changes in devices within it, which may originate in the devices themselves (for instance, a simple status change) or in the trust manager (which may inform the network that a certain device is to be eliminated from it). It also routes requests from devices to the trust center and network key renewals from the trust center to all devices. Besides this, the ZDO maintains the security policies of the device.

The security levels infrastructure is based on CCM\*, which adds encryption- and integrity-only features to CCM.

Chip vendors/devices include

To become ZigBee certified as a semiconductor company, vendors must ensure their applications are interoperable. Periodic interoperability events verify that devices work with other certified devices.

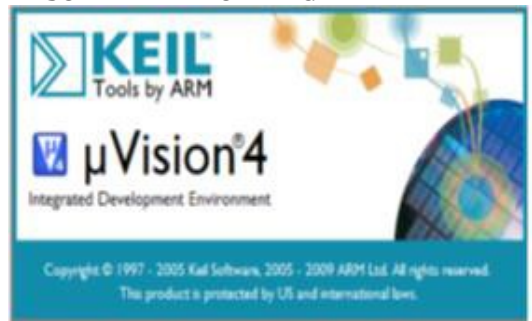
Atmel ATmega128RFA1, AT86RF230/231

- Digi International Xbee XB24CZ7PIS-004
- Ember EM250, EM351, EM357
- Free scale MC13224, MC13226
- Green Peak GP520-GP530-GP540

**KEIL SOFTWARE**

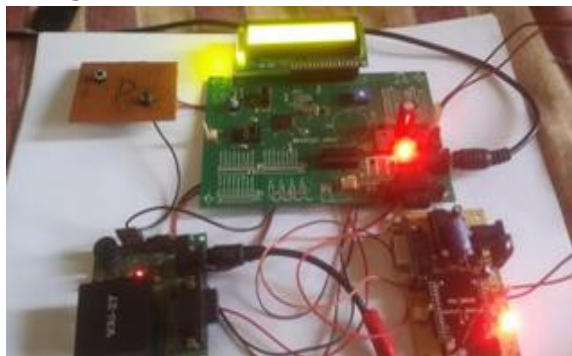
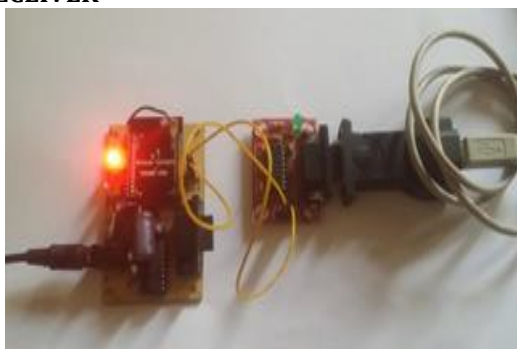
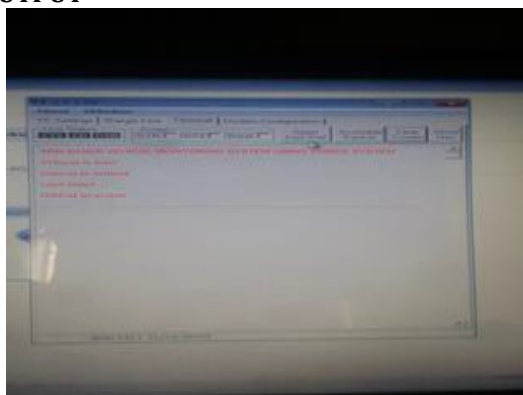
The Keil 8051 Development Tools are designed to solve the complex problems facing embedded software developers. When starting a new project, simply select the microcontroller you use from the Device Database and the µVision IDE sets all compiler, assembler, linker, and memory options for you.

**KEIL SOFTWARE WORKING**



**KIT**

Zigbee is an IEEE 802.15.4-based specification for a suite of high-level communication protocols used to create personal area networks with small, low-power digital radios, such as for home automation, medical device data collection, and other low-power low-bandwidth needs, designed for small scale projects which need wireless connection.

**TRANSMITTER****RECEIVER****OUTPUT****ADVANTAGES**

By this system we can monitor the vehicle working from far distance.

Reduce the man power for machinery.

Saving the time and money.

**APPLICATIONS**

We can use this system in mining area.

In chemical industries.

In dangerous area, prohibited area

And used in industries like glasses making, steel mining etc..

**ACKNOWLEDGMENT**

1.The research in this paper was sponsored by Guangzhou Higher Education Colleges Science and Technology Project(project No.121421312),

Guangdong province industry university research project(Project No. 2013B090600030).

2.This paper is funded by the project of Sichuan provincial science and Technology Department.

Project number:

2017JY0011, 2017GZ0331.

3. This work was supported by the Science and Technology Innovation Commission of Shenzhen under Grants JCY20150324141711695

4. The author wishes to thank Key Laboratory of Shanghai On-line measurement and control technology and all colleagues who provided technical support. This work was supported by the National Science & Technology Pillar Program (Grant No. 2014BAK02B04), the Project of General Administration of Quality Supervision, Inspection and Quarantine of the People's Republic of China(Grant No.2014QK138).

**CONCLUSION**

A system is proposed for monitoring the operating activities of working vehicles, regardless of whether they are operating indoor or outdoor. The proposed system determines the relative positional relationship between the working vehicle from a change in the ZigBee topology and RSSI. The topology is estimated by a combination of response-time estimation and node search (a standard function of ZigBee). It was found that the response time between adjacent devices is 30 ms or less. Based on these experimental results, an algorithm for estimating the patterns of activities of working vehicles was proposed. This algorithm was used for in an experiment on collecting topology data from AGVs. The results of the experiment indicate that the operating activities of each AGV differ according to working hours.

In the future, to grasp the activity of a working vehicle by creating an activity pattern, the proposed system will be evaluated experimentally. In addition, a function for visualizing the activity of working vehicles on a tablet will be implemented. This study was partly supported by SCAT.

**REFERENCES**

1. Frank Vahid /Tony Givargis " embedded system design: A unified hardware and software Introduction",WileyIndian edition ,2002
2. Embedded system architecture - by tammy Noergaard -Elsevier publications,2005.
3. Implementation of the ZigBee Network Layer: Reference Guide (in nesC/TinyOS), Andr&, Cunha
4. Implementation details of the time division beacon scheduling approach for ZigBee

- cluster-tree networks, A Cunha□M Alves.A Koubaa - Ipp Hurray! Research Group, 2007
5. Multicast method in zigbee network□ YJ Lim□ MJLee□XHHu□US - 2009
  6. F. Cuomo, U. Monaco, and F. Melodia, "Routing in ZigBee: Benefits from Exploiting the IEEE 802.15.4 Association Tree," Proc. IEEE I n t'l Conf. Comm. (ICC), June 2007.
  7. S.A. Khan and F.A. Khan, "Performance Analysis of a ZigBee Beaco n Enable Cluster T ree Network," Proc. Int'l Conf. Electrical Eng( I CE E) , Apr. 2009.
  8. J. Han, "Global Optimization of ZigBee Parameter s f o r E n d- to- End Deadline Guarantee of Real-Time Data," IEEE Sensor J., vol. 9, n o . 5 , pp. 512-514, May 2009.
  9. A. Abedi and M. P. da Cunha, "Hybrid wireless communications with high reliability and limited power constraints in noisy environments," in *NASA/CANEUS Fly-by-wireless workshop*, March 2007.
  10. H. Yan, Y. Xu, and Z. Wang, "Wireless sensor network for point positioning a falling rocket projectile in an explosive testing zone," in *2010 Fourth International Conference on Sensor Technologies and Applications (SENSORCOMM)*, July 2010, pp. 317-322.
  11. A. Abedi, "A power efficient coded architecture for distributed wireless sensing," *IET Wireless Sensor Systems Journal*, vol. 1, no. 3, pp. 129-136, Sep. 2011.
  12. Tao Tao.Tong Zhong-hua,Zhang Hui-yi. Depth Analysis of Zig8ee Protocol on Wireless Sensoractuator Network[1]. Energy Procedia,2011,13
  13. Li X, Cheng X, Yan K, et al. A monitoring system for vegetable greenhouses based on a wireless sensor network [1]. *Sensors*, 2010,10(10): 8963-8980.
  14. Balachander, D.,Rao, T. R.,& Mahesh,G. (2013, April). RF propagation investigations in agricultural fields and gardens for wireless sensor communications. In *Information & Communication Technologies (ICT), 2013 IEEE Conference on* (pp. 755-759). IEEE.
  15. CHEN, W. & WAS SELL, I. J. (2012) Energy-efficient signal acquisition in wireless sensor networks: a compressive sensing framework. *Wireless Sensor Systems, IET*, 2(1), 1-8.
  16. Zhang Li. The Application of ZigBee Technology In the Internet of Things[J]. *Network Technology*, 2010, 3(3): 1-5.
  17. Shang Jianbo. Wireless communication technology based on ZigBee and its application[J]. *Information Technology and Informatization* , 2014 (5): 104-105.
  18. Zhan Zhiqiang, Xia Junwen, Wang Yunling, Yu Lei. Measurement Uncertainty Evaluation of Digital Modulation Quality Parameters: Magnitude Error and Phase Error[C]. *MATEC Web of Conferences*. EDP Sciences, 2016, 61.
  19. S. Ferdoush, X. Li. Wireless sensor network system design using Raspberry Pi and Arduino for environmental monitoring applications, *Procedia Computer Science*, Vol.34, 103- 110, 2014.
  20. T. Ming, K. Ota, M. Dong, Z. Qian. AccessAuth: Capacity-aware security access authentication in federatedIoT-enabled V2G networks, *Journal of Parallel and Distributed Computing*, DOI: 10.1016/j.jpdc.2017.09.004, 2017.

#### WEB SITES

- [www.national.com](http://www.national.com)
- [www.atmel.com](http://www.atmel.com)
- [www.atmel.com](http://www.atmel.com)

# VLSI DESIGN OF N x N BIT HIGH PERFORMANCE MULTIPLIER WITH REDUNDANT BINARY ENCODING

BHUVANESWARI K<sup>1</sup> & Dr . R.PURUSHOTHAM NAIK<sup>2</sup> & MOSES CH<sup>3</sup>

<sup>1</sup>M.Tech(ES & VLSI), Department of ECE, Malla Reddy College Of Engineering, Hyderabad, INDIA.

<sup>2</sup>Associate Professor, Department of ECE, Malla Reddy College Of Engineering, Hyderabad,INDIA.

<sup>3</sup>Asst. Professor, Department of ECE, Malla Reddy College Of Engineering, Hyderabad, INDIA.

**ABSTRACT:** Due to its high modularity and carry-free addition, a redundant binary (RB) representation can be used when designing high performance multipliers. The conventional RB multiplier requires an additional RB partial product (RBPP) row, because an error-correcting word (ECW) is generated by both the radix-4 Modified Booth encoding (MBE) and the RB encoding. This incurs in an additional RBPP accumulation stage for the MBE multiplier. In this paper, a new RB modified partial product generator (RBMPPG) is proposed; it removes the extra ECW and hence, it saves one RBPP accumulation stage. Therefore, the proposed RBMPPG generates fewer partial product rows than a conventional RB MBE multiplier. Simulation results show that the proposed RBMPPG based designs significantly improve the area and power consumption when the word length of each operand in the multiplier is at least 32 bits; these reductions over previous NB multiplier designs incur in a modest delay increase (approximately 5%). The power-delay product can be reduced by up to 59% using the proposed RB multipliers when compared with existing RB multipliers.

**Keywords:** Redundant binary, Modified Booth encoding, Redundant binary encoding, Redundant binary Modified partial product generator (RBMPPG), Redundant binary to normal binary converter

## I.INTRODUCTION

DIGITAL multipliers are widely used in arithmetic units of microprocessors, digital signal processors and multimedia. Many algorithms and architectures have been proposed to design high-speed and low-power multipliers [1], [2]. A normal binary (NB) multiplication by digital circuits includes three steps. In the first step, partial products are generated; in the second step, all partial products are added by a partial product reduction tree until two partial product rows remain. In the third step, the two partial product rows are added by a fast carry propagation adder. Two methods have been used to perform the second step for the partial product reduction. A first method uses four-two compressors, while a second method uses redundant binary (RB) numbers [5], [6]. Both methods allow the partial product reduction tree to be reduced at a rate of 2:1.

This paper focuses on the RBPP generator for designing a 2n-bit RB multiplier with fewer partial product rows by eliminating the extra ECW. A new RB modified partial product generator based on MBE (RBMPPG-2) is proposed. In the proposed RBMPPG-2, the ECW of each row is moved to its next neighbour row. Furthermore, the extra ECW generated by the last partial product row is combined with both the two most significant bits

(MSBs) of the first partial product row and the two least significant bits (LSBs) of the last partial product row by logic simplification. Therefore, the proposed method reduces the number of RBPP rows from  $N=4 \times 1$  to  $N=4$ , i.e., a RBPP accumulation stage is saved. The proposed method is applied to 8x8-, 16x16-, 32x32-, and 64x64-bit RB multiplier designs; the designs are synthesized using the Nan-Gate 45 nm Open Cell Library. The proposed designs achieve significant reductions in area and power consumption compared with existing multipliers when the word length of each of the operands is at least 32 bits. While a modest increase in delay is encountered (approximately 5 percent), the power-delay product (PDP) at word lengths of at least 32 bits confirms that the proposed designs are the best also by this figure of merit.

This paper is organized as follows. Section 2 introduces radix-4 Booth encoding. The design of the conventional RBPP generator is also reviewed. Section 3 presents the proposed RBMPPG. This section also demonstrates the adoption of the proposed RBMPPG into various word-length RB multipliers. Section 4 provides the evaluation results of the new RB multipliers using the proposed RBMPPG for different word lengths

and compares them to previous best designs found in the technical literature.

TABLE:1 MODIFIED BOOTH ENCODING SCHEME

$b_{2i+1}$	$b_{2i}$	$b_{2i-1}$	Operation
0	0	0	0
0	0	1	+A
0	1	0	+A
0	1	1	+2A
1	0	0	-2A
1	0	1	-A
1	1	0	-A
1	1	1	0

**II. REVIEW OF BOOTH ENCODING AND RB PARTIAL PRODUCT GENERATOR**

**Radix-4 Booth Encoding**

Booth encoding has been proposed to facilitate the multiplication of two's complement binary numbers [17]. It was revised as modified Booth encoding or radix-4 Booth encoding [18]. The MBE scheme is summarized in Table 1. The multiplier bits are grouped in sets of three adjacent bits. The two side bits are overlapped with neighbouring groups except the first multiplier bits group in which it is {b1, b0, 0}. Each group is decoded by selecting the partial product shown in Table 1, where 2A indicates twice the multiplicand, which can be obtained by left shifting. Negation operation is achieved by inverting each bit of A and adding '1' (defined as correction bit) to the LSB [10], [11]. Methods have been proposed to solve the problem of correction bits for NB radix-4 Booth encoding (NBBE-2) multipliers. However, this problem has not been solved for RB MBE multipliers.

**III. RB PARTIAL PRODUCT GENERATOR**

As two bits are used to represent one RB digit, then a RBPP is generated from two NB partial products [1], [2], [3], [4], [5], [6]. The addition of two N-bit NB partial products X and Y using two's complement representation can be expressed as follows [6]:

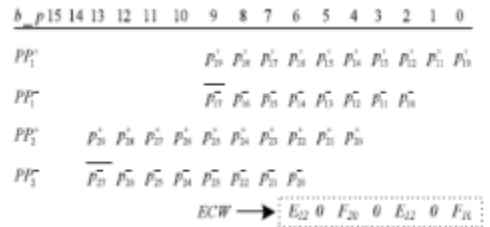
$$\begin{aligned}
 |X + Y = X - Y' - 1 \\
 &= \left( -x_N 2^N + \sum_{i=0}^{N-1} x_i 2^i \right) - \left( -\overline{y}_N 2^N + \sum_{i=0}^{N-1} \overline{y}_i 2^i \right) - 1 \\
 &= -(x_N - \overline{y}_N) 2^N + \sum_{i=0}^{N-1} (x_i - \overline{y}_i) 2^i - 1 \\
 &= (X, Y) - 1,
 \end{aligned}$$

where Y' is the inverse of Y, and the same convention is used in the rest of the paper. The composite number can be interpreted as a RB

number. The RBPP is generated by inverting one of the two NB partial products and adding -1 to the LSB. Each RB digit Xi belongs to the set {1; 0; 1}; this is coded by two bits as the pair.

TABLE 2. RB ENCODING USED IN THIS WORK

$X_i^+$	$X_i^-$	RB digit ( $X_i$ )
0	0	0
0	1	
1	0	1
1	1	0



Conventional RBPP architecture for an 8-bit MBE multiplier(X -, X +). RB numbers can be coded in several ways. Table2 shows one specific RB encoding [6], where the RB digit isobtained by performing Xi - Xi Both MBE and RB coding schemes introduce errors and two correction terms are required: 1) when the NB number is converted to a RB format, -1 must be added to the LSB of the RB number; 2) when the multiplicand is multiplied by -1 or -2 during the Booth encoding, the number is inverted and b1 must be added to the LSB of the partial product. A single ECW can compensate errors from both the RB encoding and the radix- 4 Booth recoding. The conventional partial product architecture of an 8-bit MBE multiplier [5], [6] is shown in Fig. 1, where b\_p represents the bit position generated by using an encoder and decoder (Fig. 2) [10]. An N-bit CRBBE-2 multiplier includes N=4 RBPP rows and one ECW; the ECW takes the form as follows:

$$ECW = E_{(N/4)2^0} F_{(N/4)0} \dots 0 E_{i2^0} F_{i0} \dots 0 E_{12^0} F_{10}, \tag{3}$$

where i represents the ith row of the RBPPs,  $E_{i2^0} \in \{0; 1\}$  and  $F_{i0} \in \{0; 1\}$ . In  $F_{i0}$ , a-1 correction term is always required by RB coding. If  $F_{i0}$  also corrects the errors from the MBE recoding, then the correction term cancels out to 0. That is to say that if the multiplicand digit is inverted and added to 1, then  $F_{i0}$  is 0, otherwise  $F_{i0}$  is -1. The error-correcting digit  $E_{i2}$  is determined only by the Booth encoding:

$$E_{22} = \begin{cases} 0, & \text{no negative encoding} \\ 1, & \text{negative encoding.} \end{cases} \tag{4}$$

As shown in Fig. 1 the first RBPP row, i.e. PP1, consists of the first partial product row PP + and the second partial product row PP-1

$$p_{19}^+ = \overline{p_{18}^+},$$

$$p_{18}^+ = \overline{b_1} \overline{b_0} \cdot 0 + \overline{b_1} b_0 \cdot a_7 + b_1 \overline{b_0} \cdot \overline{a_7} + b_1 b_0 \cdot \overline{a_7}$$

$$= \overline{b_1} b_0 \cdot a_7 + b_1 \overline{a_7}. \tag{6}$$

According to Eq. (2), the sign extension bit p+ 29 is also the inverse of p+ - 1 27 28. The p 17 in PP and the p -in PP - 2 are also negated as p - 17 and p - 27. Eq. (5) and Eq. (6) are further used in the next section when presenting the proposed modified RBPP generator.

#### IV. PROPOSED RB PARTIAL PRODUCT GENERATOR

A new RB modified partial product generator based on MBE (RBMPPG-2) is presented in this section; in this design, ECW is eliminated by incorporating it into both the two MSBs of the first partial product row ( ) and the two LSBs of the last partial product row(PP (N/4)).

##### Proposed RBMPPG-2

Fig. 3 illustrates the proposed RBMPPG-2 scheme for an 8x8-bit multiplier. It is different from the scheme in Fig. 1, where all the error-correcting terms are in the last row. ECW1 is generated by PP1 and expressed as

$$ECW_1 = 0 E_{12} 0 F_{10}. \tag{7}$$

The ECW2 generated by PP2 (also defined as an extra ECW) is left as the last row and it is expressed as:

$$ECW_2 = 0 E_{22} 0 F_{20}. \tag{8}$$

To eliminate a RBPP accumulation stage, ECW2 needs to be incorporated into PP1 and PP2. As discussed in Section 2.2 for Fi0 and as per Table 1, F 20 is determined by

schemes introduce errors and two correction terms are required: 1) when the NB number is converted to a RB format, -1 must be added to the LSB of the RB number; 2) when the multiplicand is multiplied by -1 or -2 during the Booth encoding, the number

is inverted and b1 must be added to the LSB of the partial product. A single ECW can compensate errors from both the RB encoding and the radix-4 Booth recoding. The conventional partial product architecture of an 8-bit MBE multiplier [5], [6] is shown in Fig. 1, where b\_p represents the bit position generated by using an encoder and decoder (Fig. 2) [10]. An N-bit CRBBE-2 multiplier includes N=4 RBPP rows and one ECW; the ECW takes the form as follows: b5; b4; b3 as follows:

$$F_{20} = \begin{cases} -1, & b_5 b_4 b_3 = 000, 001, 010, 011, \text{ or } 111 \\ 0, & b_5 b_4 b_3 = 100, 101, \text{ or } 110. \end{cases} \tag{9}$$

TABLE 3. TRUTH TABLE OF

b7 b6b5	E22F20			
000	0	1	1	0 0
001	0 0	0	0	0 a1 a0
010	0	1	1	a1 a0
011	0 0	0	0	0 a0 0
100	1	0	1	1
101	1 0	1	0	0
110	1	0	1	1
111	0 0	0	0	0 0

As per Table 1, when b5b4b3 = 111, -0 = 0 can be used. Therefore, F20 can be expressed as follows:

$$F_{20} = \begin{cases} -1, & b_5 b_4 b_3 = 000, 001, 010, \text{ or } 011 \\ 0, & b_5 b_4 b_3 = 100, 101, 110, \text{ or } 111. \end{cases} \tag{10}$$

By setting PP + to all ones and adding b1 to the LSB of the partial product, F20 can then be determined only by b5 as follows:

$$F_{20} = \begin{cases} -1, & b_5 = 0 \\ 0, & b_5 = 1 \end{cases} \tag{11}$$

A modified radix-4 Booth encoding and a decoding 19 = p+ 19, Q+ 18 = p+ 18, Q- 21 = p- 21 and Q- 20 = p- 20. 2) When E2 = 1, a 1 is added to p+ 19p+ 18p- 21p- 20. 3) When E2 = -1, a 1 is subtracted from p+ 19p+ 18p- 21p- 20. The relationships between Q+ 19, Q+ 18, Q- 21, Q- 20 and p+ 19, p+ 18, p- 21, p- 20 are circuit for the partial product PP+ 2 are proposed here (Fig. summarized in Table 4. As the two MSBs of PP+ 1 i.e., p+ 19, 4); an extra three input OR gate is then added to the design of [10] (Fig. 2). The three inputs of the additional OR gate are b5, b4, and b3. When b5b4b3 = 111, it

1011	1011	1100	1010
------	------	------	------

is clear that  $b_5 b_4 p_{+18}$  take complementary values as shown in Eq. (5), the operations of adding or subtracting a 1 will never incur in an overflow. Therefore, as per Eq. (15) and Table 4, the logic  $b_3 = 000$ ,  $p_{+2i} = 1$ , and  $PP_{+2}$  is set to all ones. So,  $E_{22}$  and  $F_{20}$  in ECW2 are now determined by  $b_7 b_6 b_5$  without  $b_4$ ;  $b_3$ .

Although the complexity is slightly increased compared with the previous design (Fig. 2), the delay stage remains the functions of  $Q_{+19}$ ,  $Q_{+18}$ ,  $Q_{-21}$ ,  $Q_{-20}$  can be expressed as same. In this work,  $Q_{+19}$ ,  $Q_{+18}$ ,  $Q_{-21}$ , and  $Q_{-20}$  are used to  $21_{20}$  represent the modified partial products.  $q_{-2(-2)}$ , and  $q_{-2(-1)}$  are used to represent the additional partial products that are determined by  $F_{20}$ . As -1 can be coded as 111 in RB format,  $E_{22}$  and  $F_{20}$  can be represented by  $E_2$ ,  $q_{-2}$ ,  $q_{-1}$ , (Fig. 3b) as follows:  $2(-2)$   $2(-1)$

$$E_2 = \begin{cases} E_{22}, & F_{20} = 0 \\ E_{22} - 1, & F_{20} = -1, \end{cases}$$

$$q_{2(-2)} = q_{2(-1)} = \begin{cases} 0, & F_{20} = 0 \\ 1, & F_{20} = -1. \end{cases} \quad (12,13)$$

As per Eq. (11) and Eq. (13),  $q_{-2(-2)}$ , and  $q_{-2(-1)}$  can be also expressed as follows:

$$q_{2(-2)} = q_{2(-1)} = \overline{b_5}. \quad (14)$$

This is further explained by the truth table of  $E_{22}$ ,  $F_{20}$  and  $E_2$ ,  $q_{-2(-2)}$ , and  $q_{-2(-1)}$  (Table 3). Now ECW2 only includes  $E_2$  and  $E_2 \in \{0; 1; -1\}$ ;  $E_2$  can be incorporated into the modified partial products  $Q_{+19}$ ,  $Q_{+18}$ ,  $Q_{-21}$  and  $Q_{-20}$  by replacing  $p_{19}$ ,  $p_{18}$  and  $p_{21}$ ,  $p_{20}$  in multiplier.

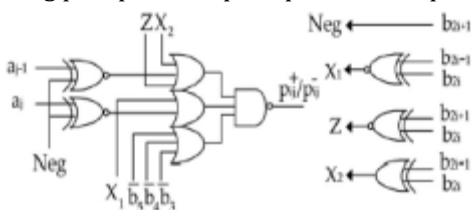


Fig.1. The modified radix-4 booth encoding and decoding scheme for PP+

TABLE 4. TRUTH TABLE OF

			(E2=-1)
0100	0100	0101	0011
0101	0101	0110	0100
0110	0110	0111	0101
0111	0111	1000	0110
1000	1000	1001	0111
1001	1001	1010	1000
1010	1010	1011	1001

the shortest path Fig. 3c. From the truth table,  $E_2$  can be determined by  $b_7 b_6 b_5$  as follows:

$$E_2 = \begin{cases} -1, & b_7 b_6 b_5 = 000, \text{ or } 010 \\ 1, & b_7 b_6 b_5 = 101 \\ 0, & b_7 b_6 b_5 = 001, 011, 100, 110, \text{ or } 111. \end{cases}$$

(15)

So the following three cases can be distinguished:  
 1) When  $E_2 = 0$ ,  $Q_{+19}$ ,  $Q_{+18}$ ,  $Q_{-21}$  and  $Q_{-20}$  remain unchanged as:  $Q_{+19} = p_{+19}$ ,  $Q_{+18} = p_{+18}$ ,  $Q_{-21} = p_{-21}$  and  $Q_{-20} = p_{-20}$ .  
 2) When  $E_2 = 1$ , a 1 is added to  $p_{+19}$ ,  $p_{+18}$ ,  $p_{-21}$ ,  $p_{-20}$ .  
 3) When  $E_2 = -1$ , a 1 is subtracted from  $p_{+19}$ ,  $p_{+18}$ ,  $p_{-21}$ ,  $p_{-20}$ .  
 The relationships between  $Q_{+19}$ ,  $Q_{+18}$ ,  $Q_{-21}$ ,  $Q_{-20}$  and  $p_{+19}$ ,  $p_{+18}$ ,  $p_{-21}$ ,  $p_{-20}$  are summarized in Table 4. As the two MSBs of  $PP_{+1}$  i.e.,  $p_{+19}$ ,  $p_{+18}$  take complementary values as shown in Eq. (5), the operations of adding or subtracting a 1 will never incur in an overflow. Therefore, as per Eq. (15) and Table 4, the logic functions of  $Q_{+19}$ ,  $Q_{+18}$ ,  $Q_{-21}$ ,  $Q_{-20}$  can be expressed as follows

$$Q_{+19}^+ = (b_7 \oplus b_5 + b_7 b_6 b_5) \cdot p_{+19}^+ + \overline{b_7 b_5} \cdot (\overline{p_{+18}^+ + p_{+21}^+ + p_{+20}^+} \oplus p_{+19}^+) + b_7 \overline{b_6 b_5} \cdot (p_{+18}^+ p_{+21}^+ p_{+20}^+ \oplus p_{+19}^+),$$

$$Q_{+18}^+ = (b_7 \oplus b_5 + b_7 b_6 b_5) \cdot p_{+18}^+ + \overline{b_7 b_5} \cdot (\overline{p_{+21}^+ + p_{+20}^+} \oplus p_{+18}^+) + b_7 \overline{b_6 b_5} \cdot (p_{+21}^+ p_{+20}^+ \oplus p_{+18}^+),$$

$$Q_{-21}^- = (b_7 \oplus b_5 + b_7 b_6 b_5) \cdot p_{-21}^- + \overline{b_7 b_5} \cdot (\overline{p_{-21}^- \oplus p_{-20}^-} + b_7 \overline{b_6 b_5} \cdot p_{-21}^- \oplus p_{-20}^-),$$

$$Q_{-20}^- = (b_7 \oplus b_5 + b_7 b_6 b_5) \cdot p_{-20}^- + \overline{b_7 b_5} \cdot \overline{p_{-20}^-} + b_7 \overline{b_6 b_5} \cdot \overline{p_{-20}^-}.$$

(16, 17, 18, 19)

The delay of the RBMPPG-2 can be further reduced by generating  $Q_{+19}$ ,  $Q_{+18}$ ,  $Q_{-21}$ ,  $Q_{-20}$  directly from the multiplicand A and the multiplier B. The relationships between  $p_{+19}$ ,  $p_{+18}$  and A, B have been discussed in Section 2.2 as Eq. (5) and Eq. (6). The relationships between  $p_{-21}$ ,  $p_{-20}$  and A, B are also shown in Table 3 according to the MBE scheme. Therefore,  $Q_{+19}$ ,  $Q_{+18}$ ,  $Q_{-21}$ ,  $Q_{-20}$  can be expressed as follows by replacing  $p_{+19}$ ,  $p_{+18}$ ,  $p_{-21}$ ,  $p_{-20}$  with the multiplicand bits ( $a_i$ ) and the multiplier bits ( $b_i$ ) after simplification:

$$Q_{19}^+ = \overline{b_1 b_0 a_7} + b_1 \overline{a_7} \left( \overline{b_5 \cdot b_7 + b_6 a_0 + b_6 a_1} \right) + \left( \overline{b_1 b_0 a_7} + b_1 \overline{a_7} \right) \cdot b_5 \cdot b_7 \overline{b_6 a_1} \overline{a_0},$$

$$Q_{18}^+ = \overline{b_1 b_0 a_7} + b_1 \overline{a_7} \cdot \left( \overline{b_5 \cdot b_7 + b_6 a_0 + b_6 a_1} + b_5 b_7 \overline{b_6 a_1} \overline{a_0} \right) + \left( \overline{b_1 b_0 a_7} + b_1 \overline{a_7} \right) \cdot \left[ b_5 \cdot (b_7 + b_6 a_0 + b_6 a_1) + b_5 \cdot b_7 \overline{b_6 a_1} \overline{a_0} \right],$$

(20,21)

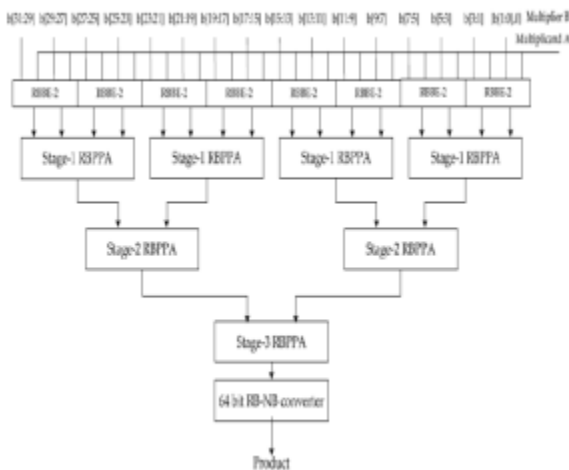


Fig 6. The block diagram of a 64-bit RB multiplier using the proposed RBMPPG-2

The above figure performs multiplication for 64 bit,128 bit and up to N-bits

**V. DESIGN OF RBMPPG-2-BASED HIGH-SPEED RB MULTIPLIERS**

The proposed RBMPPG-2 can be applied to any 2n-bit RB multipliers with a reduction of a RBPP accumulation stage compared with conventional designs. Although the delay of RMPPG-2 increases by one-stage of TG delay, the delay of one RBPP accumulation stage is significantly larger than a one-stage TG delay. Therefore, the delay of the entire multiplier is reduced. The improved complexity, delay and power consumption are very attractive for the proposed design.

A 32-bit RB MBE multiplier using the proposed RBPP generator is shown in Fig. 6. The multiplier consists of the proposed RBMPPG-2, three RBPP accumulation stages, and one RB-NB converter. Eight RBBE-2 blocks generate the RBPP; they are summed up by the RBPP reduction tree that has three RBPP accumulation stages. Each RBPP accumulation block contains RB full adders (RBFAs) and half adders (RBHAs). The 64-bit RB-

NB converter converts the final accumulation results into the NB representation, which uses a hybrid parallel-prefix/carry select adder (as one of the most efficient fast parallel adder designs).

There are four stages in a conventional 32-bit RB MBE architecture; however, by using the proposed RBMPPG-2, the number of RBPP accumulation stages is reduced from 4 to 3 (i.e., a 25 percent reduction). These are significant savings in delay, area as well as power consumption. The improvements in delay, area and power consumption are further demonstrated in the next section by simulation. Table 5 compares the number of RBPP accumulation stages in different 2n-bit RB multipliers, i.e., 8x8-bit, 16x16-bit, 32x32-bit, 64x64-bit multipliers.

TABLE 5. COMPARISON OF RBPP ACCUMULATION STAGES IN RBPP REDUCTION TREE

Methods	64X4X	32X32	16X16	8X8
CRBBE-2	5	4	3	2
RBBE-4[4]	4	3	2	1
Proposed	4	3	2	1

For a 64-bit multiplier, the proposed design has four RBPP accumulation stages; it reduces the partial product accumulation stages; it reduces the partial product accumulation delay time by 20 percent compared with CRBBE-2 multipliers. Although both the proposed design and RBBE-4 have the same number of RBPP accumulation stages, RBBE-4 is more complex, because it uses radix-16 Booth encoding.

**VI. PERFORMANCE EVALUATION**

The performance of various 2n-bit RB multipliers using the proposed RBMPPG-2 is assessed; the results are compared with NBBE-2, CRBBE-2 and RBBE-4 [14] multipliers that are the latest and best designs found in the technical literature. All designs of RB multipliers use the RBFA and RBHA of [7]. An RB-NB converter is required in the final stage of the RB multiplier to convert the summation result in RB form to a two's complement number. It has been shown that the constant-time converter in [7] does not exist [19], [20], [21]. However, there is a carry-free multiplier that uses redundant adders in the reduction of partial products by applying on-the-fly conversion [22] in parallel with the reduction and generates the product without a carry-propagate adder.

A hybrid parallel-prefix/carry-select adder is used for the final RB-NB converter. The NBBE-2 multiplier design uses the same encoder and decoder as shown in Fig.2. Four-two compressors are used in the partial product reduction tree. The extra ECW in the NB multiplier designs is also modified as proposed in [11].

The multiplier designs are described at gate level in Verilog HDL and verified by Synopsys VCS using randomly generated input patterns; the designs are synthesized by the Synopsys Design Compiler using the Nan Gate 45 nm Open Cell Library. In the simulation of each design, a supply voltage of 1.25 V and room temperature are assumed. Standard buffers of a 2X strength are used for both the input drive and the output load. The option for logic structuring is turned off to prevent the tool from changing the structure of the unit cells. The average power consumption is found using the Synopsys Power Compiler with back annotated switching activity files generated from 2,500 random input vectors. Table 6 summarizes the delay, area, power and power-delay product of the NB and RB multiplier designs; the delay, area, power and PDP metrics are compared separately. Consider the delay first; compared with CRBBE- 2, the proposed designs can reduce the delay.

TABLE 6. DESIGN PULSE OF RB MULTIPLIER (USING NAN GATE 45NM OPEN CELL LIBRARY)

Methods	64X4X	32X32	16X16	8X8
CRBBE-2	5	4	3	2
RBBE-4[4]	4	3	2	1
Proposed	4	3	2	1

VII. SIMULATION AND RESULT

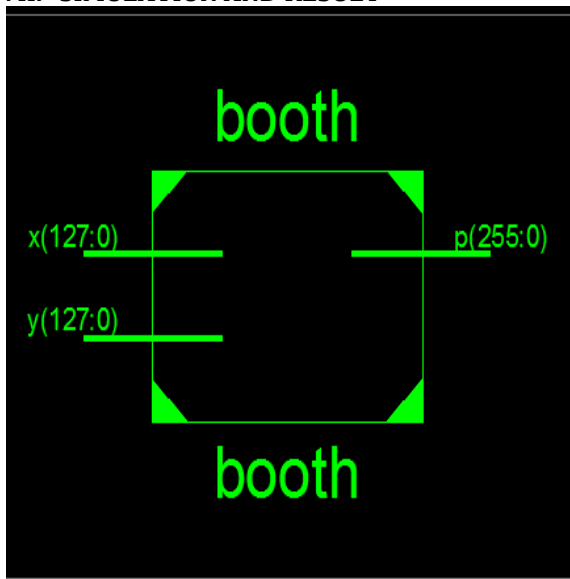


Fig. 3. RTL of the multiplier

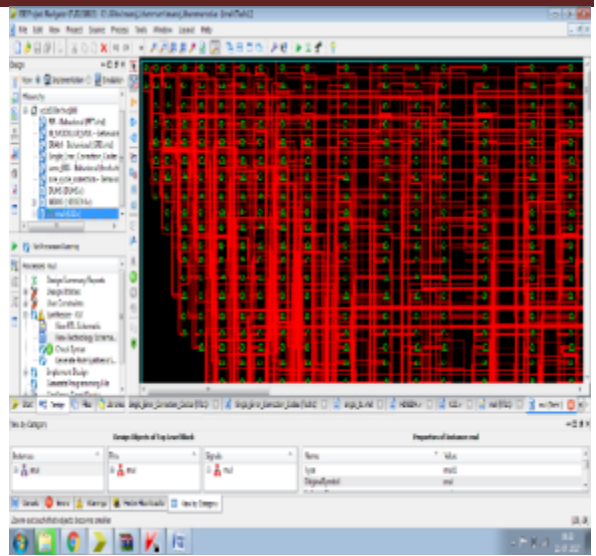


Fig. 4. Internal architecture for Multiplier RTL

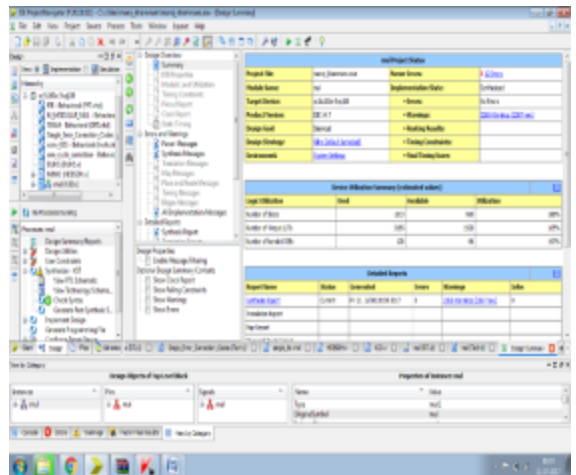


Fig. 5. Multiplier Synthesis report



Fig. 6. Simulation result of NxN bit multiplier

TABLE 7. DEVICE UTILIZATION SUMMARY

Logic Utilization	Used	Available	Utilization
No.Of Slice LUTs	30432	63400	48%
No.Of fully used LUT- FF pairs	0	30432	0%
No.Of bonded IOBs	512	210	243%

### VIII. CONCLUSION

We have proposed a novel recursive decomposition algorithm for RB multiplication to derive high-throughput digit-serial multipliers. By suitable projection of SFG of proposed algorithm and identifying suitable cut-sets for feed-forward cut-set retiming, three novel high-throughput digit-serial RB multipliers are derived to achieve significantly less area-time-power complexities than the existing ones. Moreover, efficient structures with low register-count have been derived for area-constrained implementation; and particularly for implementation in FPGA platform where registers are not abundant. The results of synthesis show that proposed structures can achieve saving of up to 94% and 60%, respectively, of ADPP for FPGA and ASIC implementation, respectively, over the best of the existing designs. The proposed structures have different area-time-power trade-off behaviour. Therefore, one out of the three proposed structures can be chosen depending on the requirement of the application environments. Compare existing method the proposed method is less power consumption, high speed, less time requirement and performance is high.

### REFERENCES

1. I. Blake, G. Seroussi, and N.P. Smart, *Elliptic Curves in Cryptography*, ser. London Mathematical Society Lecture Note Series. Cambridge, U.K.: Cambridge Univ. Press, 1999.
2. N. R. Murthy and M. N. S. Swamy, "Cryptographic applications of brahmaqupta-bhaskara equation," *IEEE Trans. Circuits Syst. I, Reg. Papers*, vol. 53, no. 7, pp. 1565–1571, 2006.
3. L. Song and K. K. Parhi, "Low-energy digit-serial/parallel finite field multipliers," *J. VLSI Digit. Process.*, vol. 19, pp. 149–166, 1998.
4. P. K. Meher, "On efficient implementation of accumulation in finite field over  $GF(2^m)$  and its applications," *IEEE Trans. Very Large Scale*

- Integr. (VLSI) Syst., vol. 17, no. 4, pp. 541–550, 2009.
5. L. Song, K. K. Parhi, I. Kuroda, and T. Nishitani, "Hardware/software codesign of finite field datapath for low-energy Reed-Solomon codecs," *IEEE Trans. Very Large Scale Integr. (VLSI) Syst.*, vol. 8, no. 2, pp. 160–172, Apr. 2000.
6. G. Drolet, "A new representation of elements of finite fields  $GF(2^m)$  yielding small complexity arithmetic circuits," *IEEE Trans. Comput.*, vol. 47, no. 9, pp. 938–946, 1998.
7. C.-Y. Lee, J.-S. Horng, I.-C. Jou, and E.-H. Lu, "Low-complexity bit-parallel systolic montgomery multipliers for special classes of  $GF(2^m)$ ," *IEEE Trans. Comput.*, vol. 54, no. 9, pp. 1061–1070, Sep. 2005. [8] P. K. Meher, "Systolic and super-systolic multipliers for finite field  $GF(2^m)$  based on irreducible trinomials," *IEEE Trans. Circuits Syst. I, Reg. Papers*, vol. 55, no. 4, pp. 1031–1040, May 2008.
8. J. Xie, J. He, and P. K. Meher, "Low latency systolic montgomery multiplier for finite field  $GF(2^m)$  based on pentanomials," *IEEE Trans. Very Large Scale Integr. (VLSI) Syst.*, vol. 21, no. 2, pp. 385–389, Feb. 2013.
9. H. Wu, M. A. Hasan, I. F. Blake, and S. Gao, "Finite field multiplier using redundant representation," *IEEE Trans. Comput.*, vol. 51, no. 11, pp. 1306–1316, Nov. 2002.
10. A. H. Namin, H. Wu, and M. Ahmadi, "Comb architectures for finite field multiplication in  $F_{2^m}$ ," *IEEE Trans. Comput.*, vol. 56, no. 7, pp. 909–916, Jul. 2007.
11. A. H. Namin, H. Wu, and M. Ahmadi, "A new finite field multiplier using redundant representation," *IEEE Trans. Comput.*, vol. 57, no. 5, pp. 716–720, May 2008.
12. A. H. Namin, H. Wu, and M. Ahmadi, "A high-speed word level finite field multiplier in  $F_{2^m}$  using redundant representation," *IEEE Trans. Very Large Scale Integr. (VLSI) Syst.*, vol. 17, no. 10, pp. 1546–1550, Oct. 2009.
13. A. H. Namin, H. Wu, and M. Ahmadi, "An efficient finite field multiplier using redundant representation," *ACM Trans. Embedded Comput. Sys.*, vol. 11, no. 2, Jul. 2012, Art. 31.
14. North Carolina State University, 45 nm FreePDK [wiki \[Online\]. Available: http://www.eda.ncsu.edu/wiki/FreePDK45:Manual](http://www.eda.ncsu.edu/wiki/FreePDK45:Manual)
15. P. K. Meher, "Systolic and non-systolic scalable modular designs of finite field multipliers for Reed-Solomon Codec," *IEEE Trans. Very Large Scale Integr. (VLSI) Syst.*, vol. 17, no. 6, pp. 747–757, Jun. 2009.
16. K. K. Parhi, *VLSI Digital Signal Processing Systems: Design and Implementation*. New York: Wiley, 1999.

17. J. L. Massey and J. K. Omura, "Computational method and apparatus for finite field arithmetic," U.S. patent application, 1984.
18. S. Gao and S. Vanstone, "On orders of optimal normal basis generators," *Math. Comput.*, vol. 64, no. 2, pp. 1227-1233, 1995.
19. A. Reyhani-Masoleh and M. A. Hasan, "Efficient digit-serial normal basis multipliers over GF(2<sup>n</sup>)," *IEEE Trans. Comput.*, vol. 52, no. 4, pp. 428-439, Apr. 2003.
20. A. Reyhani-Masoleh and M. A. Hasan, "Low complexity word-level sequential normal basis multipliers," *IEEE Trans. Comput.*, vol. 54, no. 2, pp. 98-C110, Feb. 2005.
21. N. Raj and R. K. Sharma, "A High Swing OTA with wide Linearity for design of Self Tuneable Resistor", *International Journal of VLSI design & Communication system (VLSICS)*, Volume 1, No. 3, pp. 1-11, 2010.
22. N. Raj, A.K. Singh, A.K. Gupta, "Modeling of Human Voice Box in VLSI for Low Power Biomedical Applications", *IETE Journal of Research*, Vol. 57, Issue 4, pp. 345-353, 2011.
23. N. Raj, A.K. Singh, and A.K. Gupta, "Low power high output impedance high bandwidth QFGMOS current mirror", *Microelectronics Journal*, Vol. 45, No. 8, pp. 1132-1142, 2014.
24. N. Raj, A.K. Singh, and A.K. Gupta, "Low-voltage bulk-driven self-biased cascode current mirror with bandwidth enhancement", *Electronics Letters*, Vol. 50, No. 1, pp. 23-25, 2014.
25. N. Raj, A.K. Singh, and A.K. Gupta, "Low Voltage High Output Impedance Bulk-driven Quasi-floating Gate Self-biased High-swing Cascode Current Mirror", *Circuit System & Signal Processing Journal*, Vol. 35, No. 8, pp. 2683-2703, 2015.
26. N. Raj, A.K. Singh, and A.K. Gupta, "High performance Current Mirrors using Quasi-floating Bulk", *Microelectronics Journal*, Vol. 52, No. 1, pp. 11-22, 2016.
27. N. Raj, A.K. Singh, and A.K. Gupta, "Low Voltage High Performance Bulk-driven Quasi-floating Gate Self-biased Cascode Current Mirror", *Microelectronics Journal*, Vol. 52, No. 1, pp. 124-133, 2016.
28. N. Raj, A.K. Singh, and A.K. Gupta, "Low Voltage High Bandwidth Self-biased High Swing Cascode Current Mirror", *Indian Journal of Pure and Applied Physic*, Vol. 55, No. 4, pp. 245-253, 2017.
29. Raj N. and Gupta A. K., "Analysis of Operational Transconductance Amplifier using Low Power Techniques", *Journal of Semiconductor Devices and Circuits (STM Journal)*, Vol. 1, No. 3, pp. 1-9, 2015.
30. Raj N. and Gupta A. K., "Multifunction Filter Design using BDQFG Miller OTA", *Journal of Electrical and Electronics Engineering: An International Journal (EEEIJ Journal)*, Vol. 4, No. 3, pp. 55-67, 2015.
31. N. Raj, A.K. Singh, and A.K. Gupta, "Low Power Circuit Design Techniques: A Survey", *International Journal of Computer Theory and Engineering*, Vol. 7, No. 3, pp. 172-176, 2015.

# Design of Nano-Calculator Using Quantum Dot Cellular Automata (QCA)

FARHEEN BEGUM & P.VENKATAPATHI

PG Scholar, Associate Professor

Department of Electronic and Communication Engineering, Malla Reddy College of Engineering, Hyderabad, India.

**ABSTRACT:** CMOS technology over junction transistor is a very important contribution in terribly massive Scale Integrated technique for the last 20 years. Quantum Dot Cellular Automata (QCA) brings as a replacement answer to the elemental limits of CMOS technology. This paper could be a proposal of creating Quantum dot cellular automata (QCA) based mostly Nano-calculator. In this Calculator we've simulated four basic operations: addition, subtraction, multiplication and division. QCA is associate degree advance technology that overcomes some limitations of CMOS like change speed. QCA generated circuits operates within the order of THz frequency vary wherever circuits doesn't need any additional power provide for operation.

**Keywords:** Clocksignal; Adder; Subtractor; Multiplier; Demultiplexer; nano Calculator.

## I. INTRODUCTION

Quantum Dot Cellular Automata (QCA) is enforced by quadratic cells within which four potential wells reside in four corners of the cell connected by electron tunnel junctions. within the QCA

cells specifically 2 electrons will reside within the potential wells. because of repulsion of their columbic forces, they occupy 2 opposite corners. so there will be 2 configurations, one for binary zero and another one for binary one. elementary analysis on Quantum dot cellular automata was planned by the authors in [1].

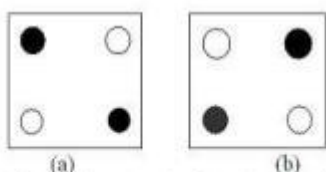


Fig.1. QCA cells with four quantum dots (a) cell with polarization  $p = -1$  (Logic '0') (b) cell with polarization  $p = 1$  (Logic '1')

## II. CLOCKING

The Quantum Dot Cellular Automata based circuits operate in four clock phases such as Switch, Hold, Release and Relax.

In **Switch** phase, extra electrons within a cell are polarized under the influence of neighboring cells. In this phase, a cell attains a definite binary value. Tunnel wants to get closed and potential barrier keeps on rising. In **Hold** phase, the potential barrier is maximum and tunnel gets closed so that electrons do not switch and retain their polarity.

In **Release** phase, the potential barrier keeps on lowering and tunnel tends to get opened. As a result cells lose their polarity. In **Relax** phase, the potential barrier is minimum and tunnel stays open. As a result a cell has no influence on its neighbors. In QCA cells having different colors means that they are under different clocks and having same color means they are under same clock. In QCA, Green refers to clock 0, Violet refers to clock 1, Blue refers to clock 2 and White refers to clock 3. The clocking of is proposed in [1-2].

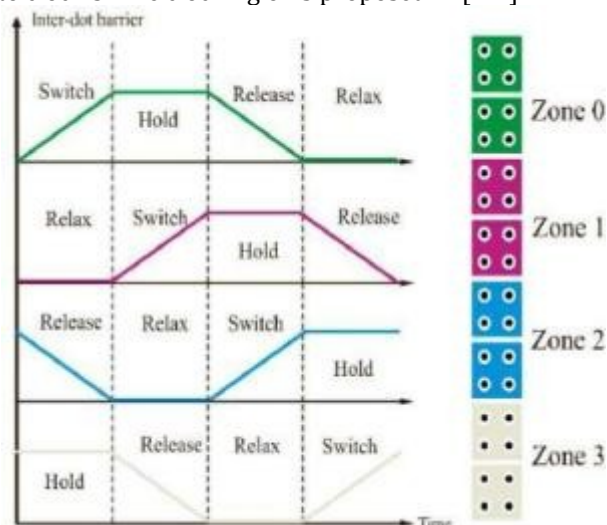


Fig.2 Clocking in QCA

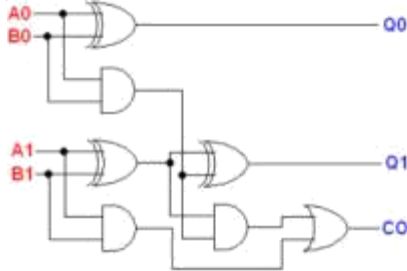
## III. NANO CALCULATOR

The calculator has completely been simulated using QCA technology. As compared to CMOS, QCA has taken miniaturization of hardware devices on a whole new level.

The different parts of the calculator are explained as below:

**A. Adder**

One bit adder has been proposed in [3]. In this paper we have designed a two bit adder using QCADesigner tool [4]. **Figure3(a)** depicts the circuit diagram with two 2-bit binary inputs A0B0



and A1B1, three XOR gates, three AND gates and one OR gate. Q0 and Q1 are the 2-bit binary sum and C0 is the carry. **Figure 3(b)** shows the diagram designed by QCADesigner tool of the adder circuit. Here three clock zones are used to complete a full cycle.

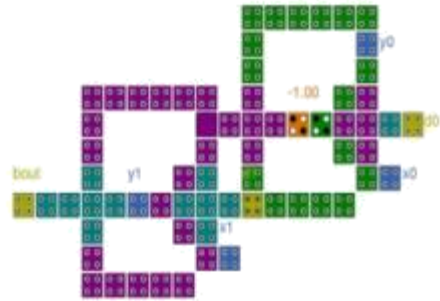


Fig. 3(a) Circuit for 2-bit Adder

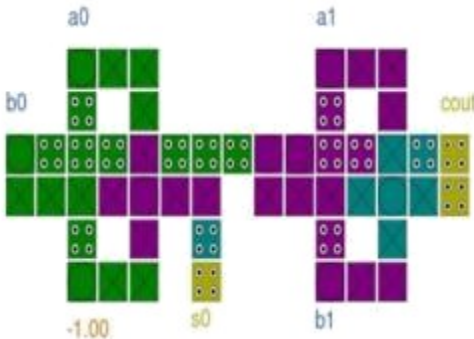


Fig. 3(b) Circuit for 2-bit adder using QCADesigner tool

**B. Subtractor**

Subtractor using QCA technology has been proposed in [5-6]. In this paper a two bit Subtractor is designed using QCA. Figure 3(c) shows the A0B0 and A1B1 are the two 2-bit binary inputs and D0D1 is the difference and C is the carry. XOR, AND and OR gates are used to build this circuit. Figure 3(d) shows the QCA version of the Subtractor circuit. Here three clock zones are used to complete a full cycle.

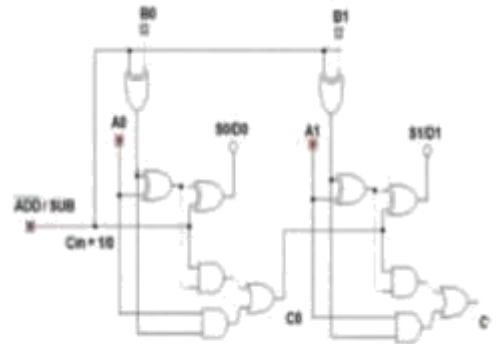


Fig.3(c). Circuit for 2-bit subtractor

**C. Multiplier**

Figure 4(a) shows the Multiplier circuit using A0B0 and A1B1 the two bit binary inputs and C0C1C2C3 is the four bit binary product as output. Here six AND gates and two XOR gates are used to build up this circuit. Figure 4(b) is the QCA version of the multiplier circuit. Here, four clock zones are used to complete a full cycle.

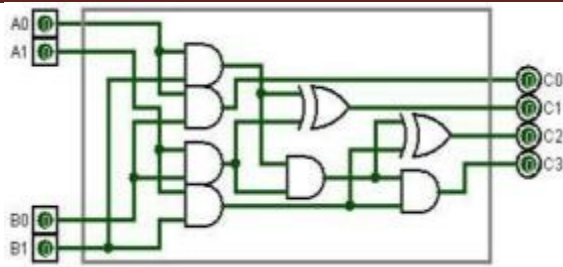


Fig. 4(a) Circuit for 2-bit multiplier

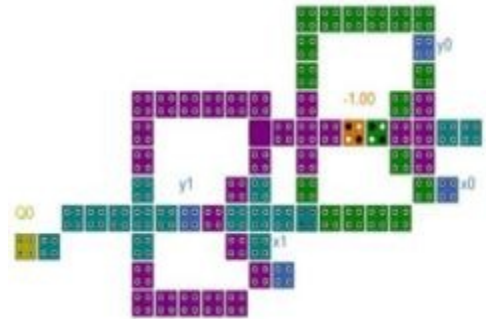


Fig.5(b) Circuit for 2-bit divider in QCA

*E. Demultiplexer*

A 1X4 de-multiplexer is used to integrate the four circuits (Adder, Subtractor, Multiplexer and Divider) into a single circuit to simulate the calculator circuit as a final result. **Figure 6(a)** shows only one input A, four outputs (D0, D1, D2, D3) and two control lines (I0, I1) to build up the DEMUX circuit. **Figure 6(b)** is the QCA based design of the DEMUX circuit. Here, three clock zones are used to complete a full cycle.



Fig.4(b) Circuit for 2-bit multiplier in QCA

*D. Divider*

A two bit divider circuit is shown in **Figure 5(a)** where A0B0 and A1B1 are the two binary inputs. **Figure 5(b)** shows the QCA based circuit design of the divider circuit. Here, three clock zones are used to complete a full cycle.

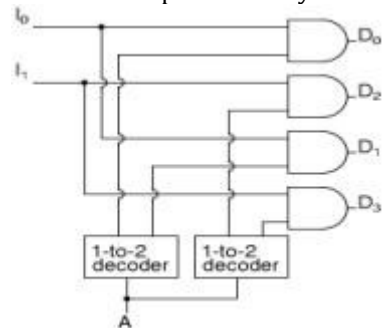


Fig.6 (a) Circuit for 1X4 Demux

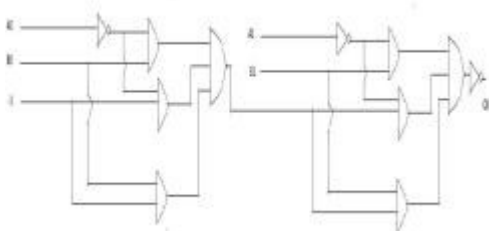


Fig-5(a). Circuit for 2-bit divider

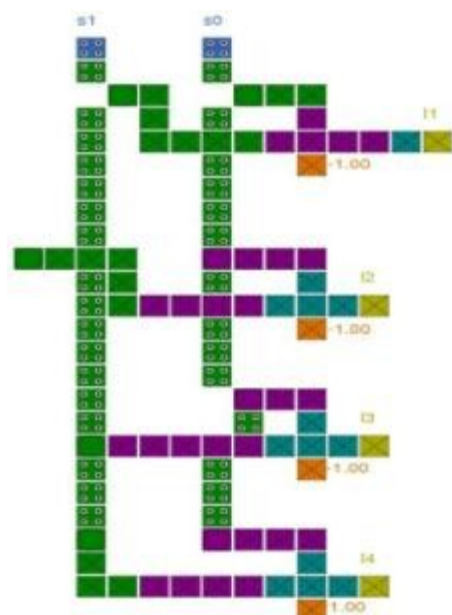


Fig.6 (b) QCA Circuit for 1X4 Demux

**IV. NANO CALCULATOR IN QCA**

Figure 7 refers to the final circuit diagram of the calculator using Quantum dot cellular automata. Here 00 represents adder circuit, 01 represents Subtractor circuit, 10 represents Multiplier circuit and 11 represents divider circuit.

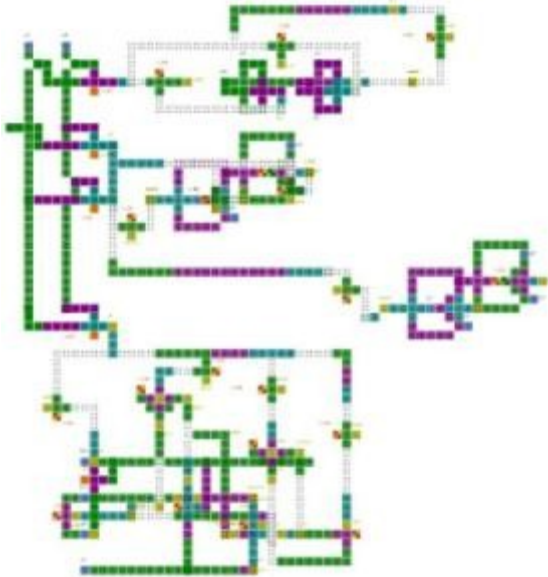


Fig.7 Calculator in QCA

All the designed circuit outputs are shown in the following figures. Figure 8(a) and 8(b) shows the corresponding Adder and Subtractor circuit. Figure 9, 10 and 11 shows the corresponding Multiplier, Divider and Demultiplexer circuit outputs.

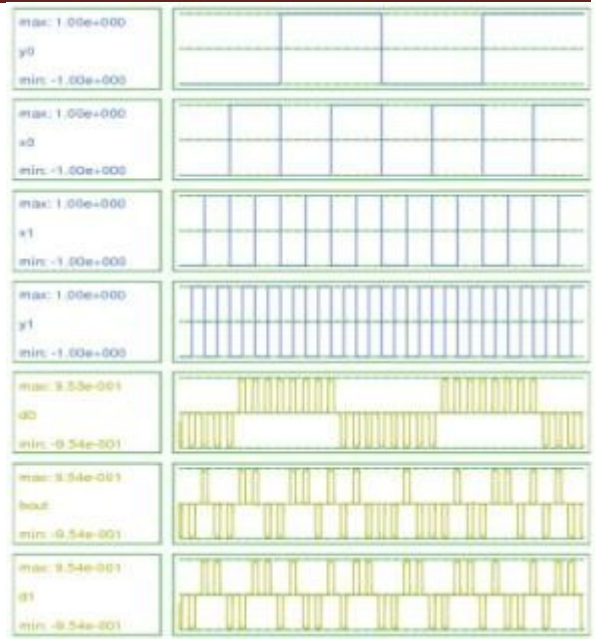


Fig.8 (b) Clocked output of the Subtractor circuit

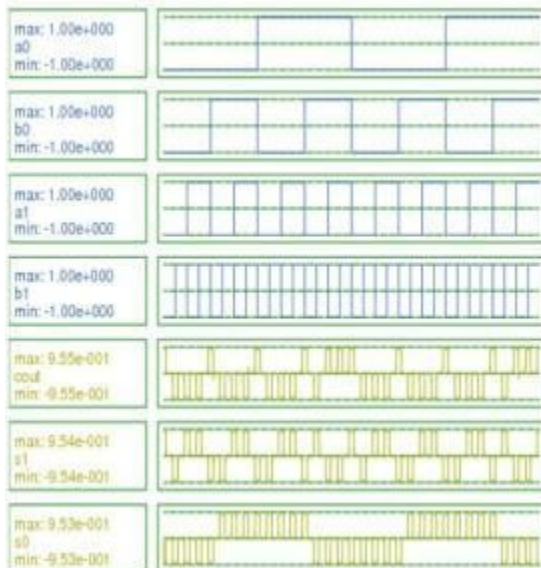


Fig.8 (a) Clocked output of the Adder circuit

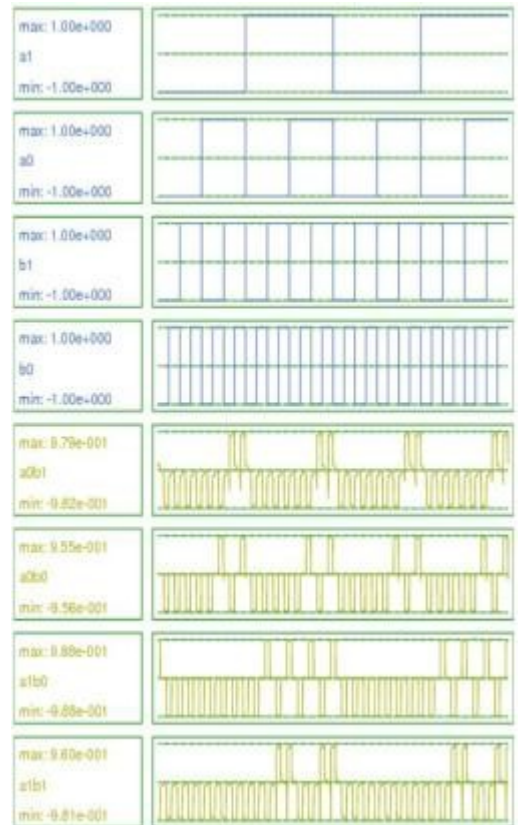


Fig.9 Clocked output of the Multiplier circuit

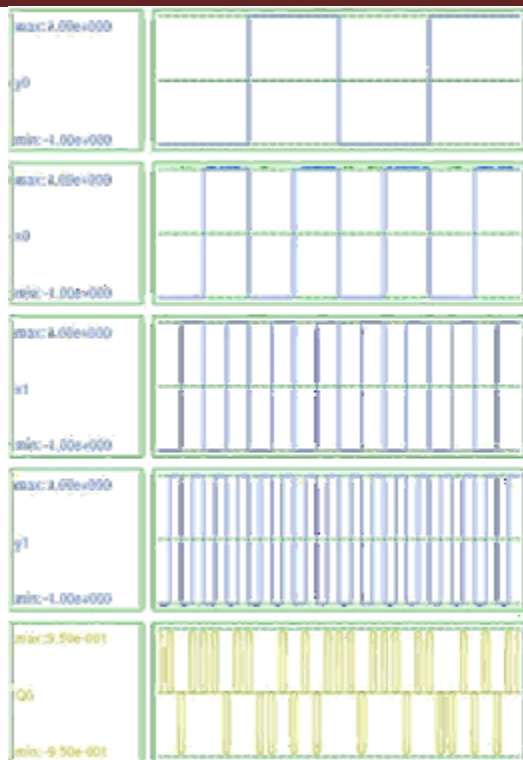


Fig.10 The clocked output of the Divider circuit.



Fig 11.Clocked output of the Demultiplexer circuit

## VI.CONCLUSION

In QCA the semiconductor unit logic is changed to quantum logic. Nano Calculator using this technology may be a new idea wherever single atom in a very quantum dot takes

the management of operations like addition, subtraction, multiplication and division. In future this design is aimed to design and improve the system performance level with additional arithmetic operations compare to existing CMOS design methodology. The calculator designed by QCA technology using QCA Designer is certainly a modification just in case of speed and space consumption over all the opposite shrewd devices.

## REFERENCES

1. C. S. Lent, and P. Tougaw, "A device architecture for computing with quantum dots," *Proceeding of IEEE*, vol. 85-4, pp. 541-557, April 1997.
2. Angsuman Khan, RatnaChakrabarty, "Design of Ring and Johnson Counter in a Single Reconfigurable Logic Circuit in Quantum Dot Cellular Automata", in *International Journal of Computer Science and Technology (IJCST)* Vol. 4. Issue 1. Jan - March, 2013.
3. BibhashSen, AyushRajoria, and Biplab K. Sikdar, "Design of Efficient Full Adder in Quantum-Dot Cellular Automata", *Hindawi Publishing Corporation, TheScientific World Journal*, Article ID 250802, Volume 2013.
4. [www.qcadesigner.com](http://www.qcadesigner.com)
5. Ali NewazBahar, SajjadWaheed ,NazirHossain , Md. Asaduzzaman , " A novel 3-input XOR function implementation in quantum dot-cellular automata with energy dissipation analysis" *Alexandria Engineering journal* ,pp-2,3, 2017.
6. B. Ramesh, M. Asha Rani, "Design of Binary to BCDCode Converter using Area Optimized Quantum DotCellular Automata Full Adder" *International Journal of Engineering (IJE)*, Volume (9) : Issue(4)2015
7. Asaduzzaman, "A novel 3-input XOR function implementation in quantum dot- cellular automata with energy dissipation analysis. Ali NewazBahar,SajjadWaheed,NazirHossain,MdAlexandriaEngineering journal,2017
8. [8] Design of Binary to BCD Code Converter using Area Optimized Quantum Dot CellularAutomata Full Adder. B.Ramesh,M.Asha Rani Internationl Journal of Engineering(IJE),2015
9. N. Raj and R. K. Sharma, "A High Swing OTA with wide Linearity for design of Self Tuneable Resistor", *International Journal of VLSI design & Communication system (VLSICS)*, Volume 1, No. 3, pp. 1-11, 2010.
10. N. Raj, A.K. Singh, A.K. Gupta, "Modeling of Human Voice Box in VLSI for Low Power Biomedical Applications", *IETE Journal of Research*, Vol. 57, Issue 4, pp. 345-353, 2011.
11. N. Raj, A.K. Singh, and A.K. Gupta, "Low power high output impedance high bandwidth

- QFGMOS current mirror”, *Microelectronics Journal*, Vol. 45, No. 8, pp. 1132-1142, 2014.
12. N. Raj, A.K. Singh, and A.K. Gupta, “Low-voltage bulk-driven self-biased cascode current mirror with bandwidth enhancement”, *Electronics Letters*, Vol. 50, No. 1, pp. 23-25, 2014.
  13. N. Raj, A.K. Singh, and A.K. Gupta, “Low Voltage High Output Impedance Bulk- driven Quasi-floating Gate Self-biased High-swing Cascode Current Mirror”, *Circuit System & Signal Processing Journal*, Vol. 35, No. 8, pp. 2683-2703, 2015.
  14. N. Raj, A.K. Singh, and A.K. Gupta, “High performance Current Mirrors using Quasi-floating Bulk”, *Microelectronics Journal*, Vol. 52, No. 1, pp. 11-22, 2016.
  15. N. Raj, A.K. Singh, and A.K. Gupta, “Low Voltage High Performance Bulk-driven Quasi-floating Gate Self-biased Cascode Current Mirror”, *Microelectronics Journal*, Vol. 52, No. 1, pp. 124-133, 2016.
  16. N. Raj, A.K. Singh, and A.K. Gupta, “Low Voltage High Bandwidth Self-biased High Swing Cascode Current Mirror”, *Indian Journal of Pure and Applied Physics*, Vol. 55, No. 4, pp. 245-253, 2017.
  17. Raj N. and Gupta A. K., “Analysis of Operational Transconductance Amplifier using Low Power Techniques”, *Journal of Semiconductor Devices and Circuits (STM Journal)*, Vol. 1, No. 3, pp. 1-9, 2015.
  18. Raj N. and Gupta A. K., “Multifunction Filter Design using BDQFG Miller OTA”, *Journal of Electrical and Electronics Engineering: An International Journal (EEEEIJ Journal)*, Vol. 4, No. 3, pp. 55-67, 2015.
  19. N. Raj, A.K. Singh, and A.K. Gupta, “Low Power Circuit Design Techniques: A Survey”, *International Journal of Computer Theory and Engineering*, Vol. 7, No. 3, pp. 172-176, 2015.

# THE DEVELOPMENT OF A REMOTELY CONTROLLED HOME AUTOMATION SYSTEM FOR ENERGY SAVING

G.Naveen<sup>1</sup> & B.Manjulai<sup>2</sup>

<sup>1</sup>M.Tech Student ,MRCE,Hyderabad

<sup>2</sup>Asst.Prof,Dept of ECE, MRCE,Hyderabad

**ABSTRACT:** *The purpose of this study is to showcase the design and development of a web-enabled home automation system prototype. The unit was developed using low- cost components such as the ubiquitous Arduino microcontroller. One of the features of the developed unit is the ability to monitor the power consumed by electrical loads. The unit also has the ability to control the status of individual loads through the internet using a web-enabled mobile application. This feature enables load management that could contribute to energy saving.*

**Keywords:**

## 1. INTRODUCTION

The aim of this project is focused on the development of a prototype for an internet based home automation system. The focus is to establish a platform that allows communication between the web-enabled mobile application and the microcontroller situated at a remote location anywhere in the world.

### 1.1 BACKGROUND

Over the year's humans have learned to rely on technology, the use of technology has thus developed tremendously over the years. This is evident in the telecommunication stream, previously communication was done face to face or through the postcard or letter. In some cultures, it was tradition to play the drum as a form of communication to warn, invite or express a celebration in the neighboring villages. However, today communication takes place relatively fast, easier and without a lot of hassles through the usage of cell phones. A cell phone's function is not limited to calling and texting; it can be used for various functions. Cell phones have become a necessity in people lives, communication and entertainment are all possible with the smartphones. Automation is the backbone of modern industries, it is the key to global economic growth as it allows for increasing productivity and accuracy by cutting out the human intervention while reducing costs. Home automation is the extension of industrial process automation to households' appliances. Among others home automation may include the remote control of lights (Centralized or individual), air conditioning, security system (remote power monitoring) and other systems

such as those used for entertainment. Home automation provides improved comfort and security, increases energy efficiency and convenience for users. Today automation is introduced in homes through the connectivity of house appliances and smartphones, tablets, and PCs.

### 1.2 PROBLEM STATEMENT

Energy consumption can be measured through its environmental impact and usage; the measure of the amount of power consumed by the load side of an electrical circuit is termed energy consumption. The maximum power that a load can consume is equal to the total power generated by the source minus the power lost in the transmission line. When the load requires more energy than what the source can provide, this becomes a major issue, which results in load shedding and blackouts. Energy consumption is a major issue in the modern world. Inefficient power monitoring and controlling techniques in the households, businesses, and institutions are the main cause of power consumption.

### 1.3 LITERATURE REVIEW

A home automation system is a channel by which homeowners and occupants have remote control over different types of electrical and electronics appliances in their home. The home automation system is the use of robotics and computer technologies to household appliances by defining the home automation as domestics. Energy saving is the advantage that a home automation system gives to all its clients and especially forgetful ones, in that they can

now track energy usage at home or while being away to ensure that unnecessary appliances are turned off as needed to reduce energy consumption [1, 2,3].

Convenience is what makes the internet based home automation interesting in that one does not have to go home and turn ON the geyser and wait for the water to get warm, while still at work one can turn ON the geyser to ensure that once they're home the water is warm enough and ready to be used. This saves time and it is very convenient. While security issues arise, the emphasis is that through surveillance cameras a user can remotely monitor the house. This should monitor incidents of property intrusion. With the home entertainment section, a user can control the distribution of sound throughout the house depending on the room occupancy or control light intensity from the couch while watching an interesting movie.

With an increase in energy consumption and population, there is an inevitable need to conserve energy with the means possible. The major cause of energy consumption is the inability to remotely monitor and control appliances.

The literature found that all authors that web-enabled mobile application used to monitor and control appliances remotely can greatly increase efficient energy usage. While [4] mentioned only two communication protocols (Z-Wave and ZigBee), [5] and [6] speaks about ZigBee, Bluetooth, GSM, and Wi-Fi as possible communication methods that a home automation system can host. To implement the home automation system, [6] in their study present interesting methods that could be used. These methods include phone-based home automation system, Bluetooth-based home automation system, GSM based home automation system, Mixed type home automation system, a wireless control system and ZigBee-based home automation system. The GSM based home automation presented by [4] consists of User with an APP inventor user interface, a GSM network, a GSM modem, an Arduino microcontroller, peripheral devices, relay logics and the appliances to be controlled. The system presented here can be controlled by means of a GSM network, internet, or speech control. Then internet being the best of choice as it enables the system to be controlled from anywhere in the world, then GSM uses SMS-based commands to control the appliances. The user sends text commands to the server which might be a PC, the server then passes the commands to the Control

Unit which in turn controls the appliances. The GSM is used for communication where there is no internet connectivity. The AT (Attention) command are use used by the server to communicate with the GSM modem. The server consists of a web server, database, main control program and speech recognition says the Satish et al. Every appliance node consists of a transmitter, a receiver an I/O device and a controlling unit (Microcontroller). The GSM is used for its high availability, coverage, and security, but it suffers from the SMS costs and the relative dependency of the SMS on the network. Another drawback of GSM based system is that no user interface is given to the user to control the device. The system cannot be customized on devices as it comes preprogramed. The study of [4] described different technologies and home automation systems, the authors focused on describing home automation system based on a security point of view in their study. [7] elaborates on various security weaknesses in existing home automation systems. The challenges in the home automation systems were examined. In their study, [5] considered mobile based home automation, Bluetooth-based home automation system, Dual Tone Multi-Frequency based home automation systems, and internet based home automation system, Short Messaging Service based home automation system. Since the goals of this project aimed an internet-based system, the focus was more on the internet based home automation system and a mobile based home automation system.

Figure 1 presents the diagram of how the sensors, mechanical and electrical devices communicate using the home network through GSM module using a subscriber identity module (SIM). This uses a transducer to convert machine's function into an electrical signal readable by a microcontroller. The signals sent to the microcontroller are analysed, and based on this analysis the microcontroller commands the GSM module to select between one of the three communication methods mentioned above (SMS, GPRS or DTMF) [4].

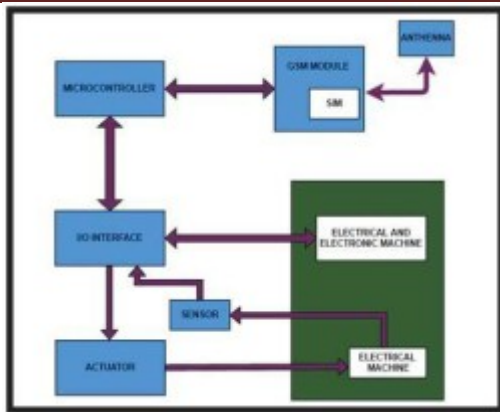


Figure 1: Mobile-based home automation

In this study, the focus was on developing the application to interact with the home automation system, the security issues were only flashlights to consider before marketing the product. Given the time constraints, the focus was first on the minimum deliverables and as time went on, more features were added to the system to make it more interesting that includes a security feature which prompts the users to authenticate themselves before loading the application.

As the literature reveals, a microcontroller is the most popular and most flexible controlling unit used for home automation system. In this project, Microcontroller Systems Design IV was the main subject that helped with implementation. There are currently many challenges that home automation systems have to address. Some of these are reviewed in [7]. In [8] a life cycle assessment is provided for by considering both the benefits and environmental impacts of home automation systems.

**2. SYSTEM DESIGN**

Home automation can be implemented in several ways, there are many possible approaches towards the development of the mobile application and the home automation. In this section, some pertinent approaches were presented together with their advantages and disadvantages. Many factors affect the advantage and disadvantage of a home automation system such as the security, implementation, timeline, cost, the complexity of the system, availability of the component, documentation, and support offered by the manufacturers to list a few. In this section, the focus will be on the security, implementation, and cost while evaluating different approaches. Decentralized home automation system, DTMF Based, GPRS Based, Central controller Based, Mixed Type Home Automation, Internet Based

Home Automation System, Wireless Control System, Phone- Based Home Automation, Bluetooth Based Home Automation, ZigBee Based Home Automation, and GSM Based Home Automation. From this list of home automation system implementation methods, the internet based on a microcontroller as a controlling unit were the choice and the focus of this project.

**2.1 INTERNET BASED HOME AUTOMATION SYSTEM**

A microcontroller is a self-contained system with peripherals, memory and a processor that can be used as an embedded system. Most programmable microcontrollers used today are embedded in other consumer products or machinery including phones, automobiles and household appliances or computer systems. Due to that, another name for a microcontroller is "embedded controller." Some embedded systems are more sophisticated, while others have minimal requirements for memory and programming length and a low software complexity. Input and output devices include solenoids, LCD displays, relays, switches, and sensors for data like humidity, temperature or light intensity or power usage.

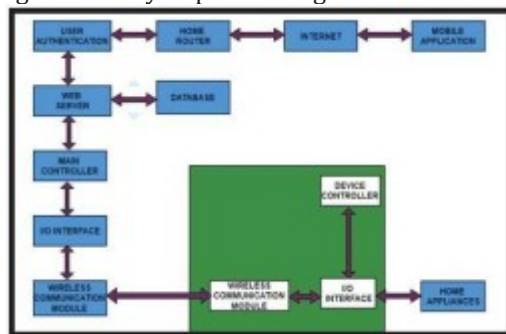


Figure 2: An Internet-based home automation system [4]

Figure 3 below shows a microcontroller based home automation system. The user mobile application interacts with the microcontroller via the web server using the internet protocol. The microcontroller receives commands from the user interface and performs the required tasks based on a controlling algorithm governing the controller. The controller reads devices status and updates this data into the server for the user mobile application. Also, refer to figure 4 in the literature review for a typical internet based home automation system.

The server handles the users and ensures secure communication between the user mobile application and the controlling unit. Once a user is identified, he will then be allowed access to

the controlling interface (Web page). The advantages of using a microcontroller have reduced the size of circuitry, affordability, and increased flexibility. A microcontroller can be used as a substitute for other integrated circuits (ICs). It can also be easily reprogrammed to modify its functionality. The Microcontroller that was used for this project is the Arduino MEGA 2560 R3.

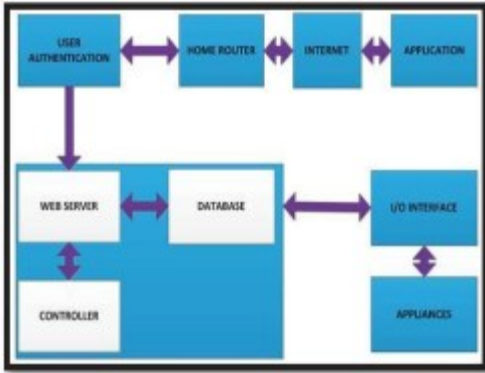


Figure 3: Proposed Home automation (Internet Based home automation with microcontroller)

The downside of this system is its dependency on the mobile connectivity to the internet, if the mobile connectivity is compromised, the user will be unable to remotely monitor and control the home automation system and the limited number of devices depends on the I/O limit of the microcontroller used. A PLC could also be used as a controller for such a system, the PLC is more robust than the microcontroller. The choice of microcontroller controller over the PLC is the cost, and the PLC is not open source, thus making the Arduino microcontroller even the best choice for the system prototyping.

**3. DESIGN METHODOLOGY**  
**3.1 THE WEBSITE**

When related web pages are collected (Including picture and video contents), and if they can be accessed through the same domain name or IP address, and they are published on at least one web server, then the collection is called website. A website as mentioned can be accessed through the World Wide Web (Internet), or on a local area network (LAN) by referencing a Uniform Resource Locator (URL) which is the ID of the website. Web sites are created for many reasons, ranging from entertainment to education, and today websites can be used to control household appliances. An Arduino web server was used to serve as the user interface where the client is presented with user clickable buttons to control the house appliances

and monitor the power consumption. The web page as shown in the figure 9 below is made of two important sections, the energy monitoring section, and the control section. The power gauge was designed using java scripts when the “read power” button is clicked, an http request is generated and sent to the web server requiring the power consumption. The server then responds to the request by supplying the web client with the raw reading on the current sensor.

The controlling section of the user interface consists of buttons, and once clicked they each send a corresponding request to the server, then the server in return turns ON/OFF the appliances associated with the request. The server also updates the web client with corresponding images of the appliance status.

The website was created using HTML, XML, and Java Scripts. When access is granted to a user, the user interface is now available to turn on or off devices, check power consumption, change camera position, adjust light brightness, and check the status of entrances.

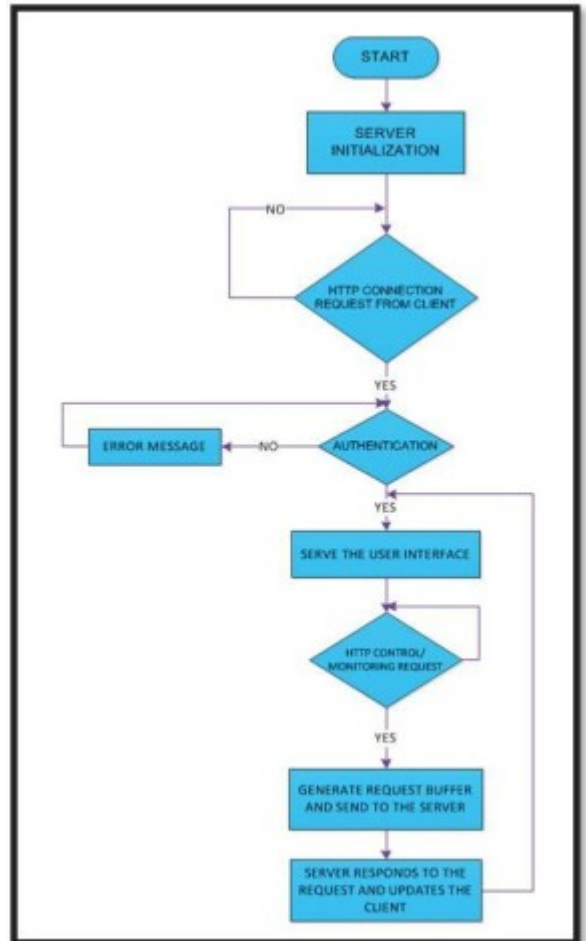


Figure 4: Program Flow-chart

Specific functions are used to generate and send a specific http request to the server depending on the user's request, for instance when the "Read Power" button is clicked, a function called PowerControl is called. This function generates a random number every time is called, it sends a request buffer to the server using the "GET" method. The request buffer consists of a "Get" method, a specific command "Power" and a random number. The random number is used to avoid the browser caching.

To understand the website design, a study of the HTML, XML, CSS, and JS is required.

### 3.3.1 THE HYPERTEXT MARKUP LANGUAGE (HTML)

The Hypertext Markup Language is a standard used to design the look of the web page. It focuses on the graphic, font, color, and hyperlink effects on web pages, and has for building blocks, elements. HTML describes the structure of web pages using markup, tags representing its elements. The web browsers do not display HTML tags, but instead, tags are used to determine how the web page should be displayed.

### 3.3.2 THE EXTENSIBLE MARKUP LANGUAGE (XML)

XML stands for Extensible Markup Language. It is a text-based markup language derived from Standard Generalized Markup Language (SGML). XML tags identify the data and are used to store and organize the data, rather than specifying how to display it like HTML tags, which are used to display the data.

### 3.4 USER INTERFACE (UI)

The user interface interacts a human with a hardware or software, it is the means by which a person controls a hardware device or software application.

The website presents the user with a means to check power consumption, control appliances, camera position and light dimmer control and finally check the status of entrances for intrusion detection. Each section of the user interface is explained as follow:

#### a. THE WATTMETER

The Wattmeter as shown in figure 5 below, was created using the HTML canvas and Java Scripts, the meter was designed to measure up to 30 kW of power. The green color represents a smiling face on the gauge, meaning that the power consumption is good. The yellow color on the gauge represents power consumption range which the user should start worrying about and make plans to reduce it. The red color represents the range of power consumption at which the system automatically switches off appliances.

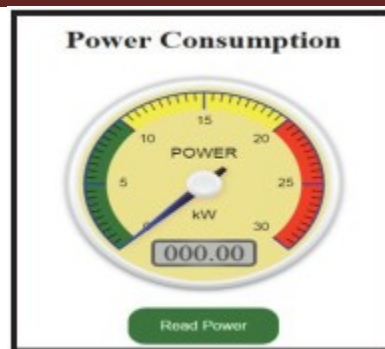


Figure 5: The wattmeter

#### b. APPLIANCE CONTROL

Appliance control as shown in figure 6 below enables a person to turn ON/OFF appliances; a light bulb, a stove, a heater and a tv respectively. The system is designed in such a way that a picture representing the current state of the appliance is updated on the user interface.

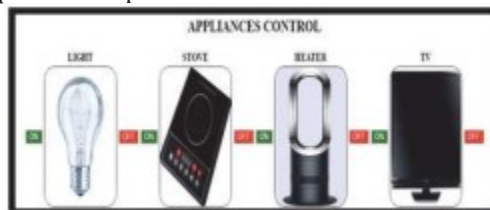


Figure 6: Appliance ON/OFF Control

#### C. CAMERA POSITION AND LIGHT BRIGHTNESS CONTROL

This section of the user interface as shown in figure 7 below presents the user with means to adjust the position of a camera as well as adjust the brightness of a light. The adjustment is accomplished through two sliders.

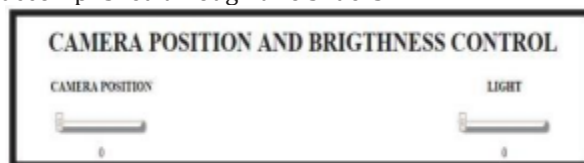


Figure 7: Camera Position and Light BrightnessControl

#### d. INTRUSION DETECTION

The intrusion detection section of the user interface as shown in figure 8 consists of a "CheckEntrance" button, the entrance names, and the entrance status fields.

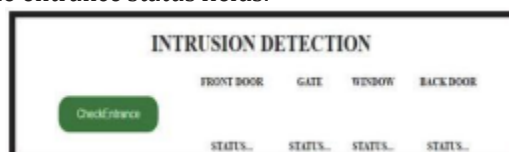


Figure 8: Intrusion Detection

Finally, the complete user interface is a web page that can be accessed via a web browser or using the android web-enabled mobile application created using App Inventor. The android app will be discussed in the next section

### 3.5 THE WEB SERVER

The web server is a dedicated device or computer or program that uses the Hypertext Transfer Protocol (HTTP) to serve a website to the web client as a response to their request.

In this project, the microcontroller was used to serve the website using HTTP on port 25, and it is also the main controller of the system. The web server and controller is made of an Arduino Mega 2560 R3 (controller which is programmed and manages the overall system), Arduino WiFi R3 shield (Allows the controller to have internet connectivity through WiFi modules), and an SD card (Found the WiFi shield and gives the controller the ability to save files and use them when needed) from which the controller serves the system's user interface. The microcontroller hosts the website saved in an SD card, the web server when launched, it serves the website to the internet client requesting for it. Once the website which is a user interface is made available to the user, there are now capable of entering their username and password to have access to the overall system.

## 4. USER INTERFACE

At the completion of this project, the following results were found to be satisfactory and above the minimum deliverables.

It was found in this research that the Arduino UNO does not behave expectedly when the program size is above 56% of its full memory. For this reason, this project's controller was changed to ATmega 2560 to solve the memory issue.

### 4.1 THE WEB USER INTERFACE

Figure 9 below represent the complete user interface, and as explained in the design procedure.

It was found that the calling a function using the "OnLoad" attribute in the HTML code causes the rest of the functions in the code to not execute, for this reason the power gauge does not update automatically and a button was used for its "OnClick" property.



Figure 9: The Complete Web User Interface

### 4.2 THE ANDROID APP

The Android app as shown in figure 10 below loads the web interface shown above and provides the user with a means to remotely control home appliances and monitor the power consumption thereof.

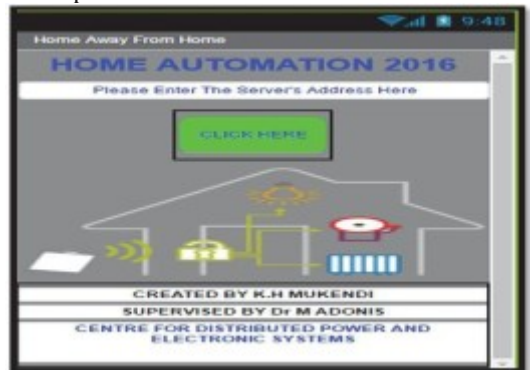


Figure 10: The Mobile Application interface

## 5. CONCLUSION

The paper summarised the design and development of a web-enabled home automation system. A comprehensive literature review was presented that chronicles the impact and technologies used in home automation systems. The system design methodology is also presented. The mobile application design elements are shown. These highlight the user interface and its monitoring and control features. Field trials are to be implemented in the next phase. These trials will involve the gathering of experimental data. The results should show what impact the developed unit operation has on reducing energy

consumption through load management strategies. The additional features of: camera positioning; light brightness control and intrusion detection, have been evaluated in real-time.

## REFERENCES

- Joumaa, H, Ploix, S, Abras, S and De Oliveira, G. "A MAS integrated into Home Automation system, for the resolution of power management problem in smart homes", *Energy Procedia*, Vol. 6, March 2011, pp. 786-794
- Mehdi, G and Roshchin, M. "Electricity Consumption Constraints for Smart-home Automation: An Overview of Models and Applications", *Energy Procedia*, Vol 83, December 2015, pp. 60-68
- Ha, DL, Ploix, S, Zamai, E and Jacomino, M. "A home automation system to improve household energy control, 12th IFAC Symposium on Information Control Problems in Manufacturing, Vol. 39, Issue 3, 2006, pp. 15-20.
- Toshchi, G, Campos, L and Cugnasca, C. "Home automation networks: A survey", *Computer Standards & Interfaces*, Vol. 50, February 2017, pp. 42-54
- Sriskanthan, N, Tan, F and Karande, A. "Bluetooth based home automation system", *Microprocessors and Microsystems*, Vol. 26, Issue 6, August 2002, pp. 281-289
- Abdulrahman, T, Isiwekpeni, O, Surajudeen-Bakinde, N and Otuoze, A. " Design, Specification and Implementation of a Distributed Home Automation System", *Procedia Computer Science*, Vol.94, 2016, pp. 473-478
- Jacobsson, A, Boldt, M and Carlsson, B. "A risk analysis of a smart home automation system", *Future Generation Computer Systems*, Vol. 56, March 2016, pp. 719-733
- Louis, JN, Calo, A, Leiviska, K and Pongracz, E. "Environmental Impacts and Benefits of Smart Home Automation: Life Cycle Assessment of Home Energy Management System", 8th Vienna International Conference on Mathematical Modelling – MATHMOD 2015, Vol. 48, Issue 1, 2015, pp. 880-885
- N. Raj and R. K. Sharma, "A High Swing OTA with wide Linearity for design of Self Tuneable Resistor", *International Journal of VLSI design & Communication system (VLSICS)*, Volume 1, No. 3, pp. 1-11, 2010.
- N. Raj, A.K. Singh, A.K. Gupta, "Modeling of Human Voice Box in VLSI for Low Power Biomedical Applications", *IETE Journal of Research*, Vol. 57, Issue 4, pp. 345-353, 2011.
- N. Raj, A.K. Singh, and A.K. Gupta, "Low power high output impedance high bandwidth QFGMOS current mirror", *Microelectronics Journal*, Vol. 45, No. 8, pp. 1132-1142, 2014.
- N. Raj, A.K. Singh, and A.K. Gupta, "Low-voltage bulk-driven self-biased cascode current mirror with bandwidth enhancement", *Electronics Letters*, Vol. 50, No. 1, pp. 23-25, 2014.
- N. Raj, A.K. Singh, and A.K. Gupta, "Low Voltage High Output Impedance Bulk- driven Quasi-floating Gate Self-biased High-swing Cascode Current Mirror", *Circuit System & Signal Processing Journal*, Vol. 35, No. 8, pp. 2683-2703, 2015.
- N. Raj, A.K. Singh, and A.K. Gupta, "High performance Current Mirrors using Quasi-floating Bulk", *Microelectronics Journal*, Vol. 52, No. 1, pp. 11-22, 2016.
- N. Raj, A.K. Singh, and A.K. Gupta, "Low Voltage High Performance Bulk-driven Quasi-floating Gate Self-biased Cascode Current Mirror", *Microelectronics Journal*, Vol. 52, No. 1, pp. 124-133, 2016.
- N. Raj, A.K. Singh, and A.K. Gupta, "Low Voltage High Bandwidth Self-biased High Swing Cascode Current Mirror", *Indian Journal of Pure and Applied Physic*, Vol. 55, No. 4, pp. 245-253, 2017.
- Raj N. and Gupta A. K., "Analysis of Operational Transconductance Amplifier using Low Power Techniques", *Journal of Semiconductor Devices and Circuits (STM Journal)*, Vol. 1, No. 3, pp. 1-9, 2015.
- Raj N. and Gupta A. K., "Multifunction Filter Design using BDQFG Miller OTA", *Journal of Electrical and Electronics Engineering: An International Journal (EEEIJ Journal)*, Vol. 4, No. 3, pp. 55-67, 2015.
- N. Raj, A.K. Singh, and A.K. Gupta, "Low Power Circuit Design Techniques: A Survey", *International Journal of Computer Theory and Engineering*, Vol. 7, No. 3, pp. 172-176, 2015.

## IOT BASED CHILD SAFETY WEARABLE DEVICE

Poonam Gupta<sup>1</sup> & Ms.P.Anitha<sup>2</sup>

<sup>1</sup>PG scholar, Dept of Electronics and Communication Engineering, Malla Reddy College of Engineering, Hyderabad, India.

<sup>1</sup>Asst. Professor, Dept of Electronics and Communication Engineering, Malla Reddy College of Engineering, Hyderabad, India

**ABSTRACT:** This paper discusses the concept of a smart wearable device for little children. The major advantage of this wearable over other wearable is that it can be used in any cellphone and doesn't necessarily require an expensive smartphone and not a very tech savvy individual to operate. The purpose of this device is to help parents locate their children with ease. At the moment there are many wearables in the market which help track the daily activity of children and also help find the child using Wi-Fi and Bluetooth services present on the device. But Wi-Fi and Bluetooth appear to be an unreliable medium of communication between the parent and child. Therefore, the focus of this paper is to have an SMS text enabled communication medium between the child's wearable and the parent as the environment for GSM mobile communication is almost present everywhere. The parent can send a text with specific keywords such as "LOCATION" "TEMPERATURE" "UV" "SOS" "BUZZ", etc., the wearable device will reply back with a text containing the real time accurate location of the child which upon tapping will provide directions to the child's location on google maps app and will also provide the surrounding temperature, UV radiation index so that the parents can keep track if the temperature or UV radiation is not suitable for the child. The prime motivation behind this paper is that we know how important technology is in our lives but it can sometimes can't be trusted, and we always need to have a secondary measure at hand. The secondary measure used in this project is the people present in the surrounding of the child who could instantly react for the child's safety till the parents arrive or they could contact the parents and help locate them. The secondary measure implemented was using a bright SOS Light and distress alarm buzzer present on the wearable device which when activated by the parents via SMS text should display the SOS signal brightly and sound an alarm which a bystander can easily spot as a sign of distress. Hence this paper aims at providing parents with a sense of security for their child in today's time.

**Keywords:** Children, Arduino, Safety, Wearable.

### 1.INTRODUCTION

The Internet of Things System (IoT) [1] refers to the set of devices and systems that stay interconnected with real-world sensors and actuators to the Internet. IoT includes many different systems like smart cars, wearable devices [2] and even human implanted devices, home automation systems [3] and lighting controls; smart phones which are increasingly being used to measure the world around them. Similarly, wireless sensor networks [4] that measure weather, flood defenses, tides and more. There are two key aspects to the IoT: the devices themselves and the server-side architecture that supports them. The motivation for this wearable comes from the increasing need for safety for little children in current times as there could be scenarios of the child getting lost in the major crowded areas. This paper focusses on the key aspect that lost child can be helped by the people around the child and can play a significant role in the child's safety until reunited with the parents.

Most of the wearables available today are focused on providing the location, activity, etc. of the child to the parents via Wi-Fi [8] and Bluetooth [9]. But Wi-Fi and Bluetooth seem a very unreliable source to transfer information. Therefore it is intended to use SMS as the mode of communication between the parent and child's wearable device, as this has fewer chances of failing compared to Wi-Fi and Bluetooth. The platform on which this project will be running on is the Arduino [10] Uno microcontroller board based on the ATmega328P, and the functions of sending and receiving SMS, calls and connecting to the internet which is provided by the Arduino GSM shield using the GSM network [11]. Also, additional modules employed which will provide the current location of the child to the parents via SMS. The second measure added is SOS Light indicator that will be programmed with Arduino UNO board to display the SOS signal using Morse code. The different modules stay enclosed in a custom designed 3D printed case [12]. In the

scenario, a lost child can be located by the parent could send an SMS to the wearable device which would activate the SOS light feature on the wearable. Therefore alerting the people around the child that the child is in some distress and needs assistance as the SOS signal is universally known as the signal for help needed. Additionally, the wearable comes equipped with a distress alarm buzzer which sets to active by sending the SMS keyword "BUZZ" to the wearable. Hence the buzzer is loud and can be heard by the parent from very considerable distance. Also the parents via SMS can receive accurate coordinates of the child, which can help them locate the child with pinpoint accuracy. Some of the existing work done on these similar lines are for example the low-cost, lightweight Wristband Vital [2] which senses and reports hazardous surroundings for people who need immediate assistance such as children and seniors. It is based on a multi-sensor Arduino micro-system and a low- power Bluetooth 4.1 module. The Vital band samples data from multiple sensors and reports to a base station, such as the guardian's phone or the emergency services. It has an estimated battery life of 100 hours. The major drawback for the Vital band is that it uses Bluetooth as the mode of communication between child and the parent. Since the distance between the two in some cases could be substantial and the Bluetooth just won't be able to establish a close link between the two.

## 2. SYSTEM DESIGN AND ARCHITECTURE

This section discusses the architecture and the design methodologies chosen for the development of the Child Safety wearable device.

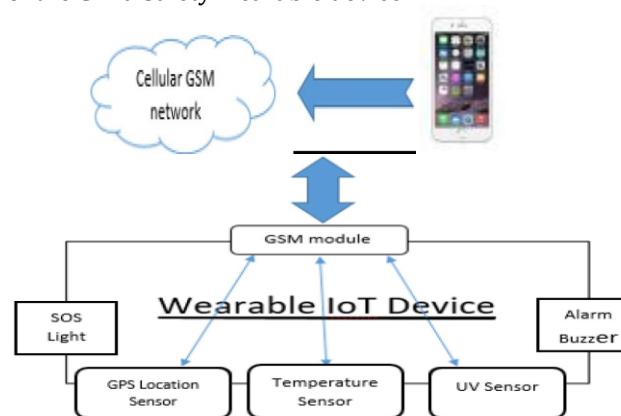


**Fig 1. System overview of the wearable device.**

### A. System Overview

An ATmega328p microcontroller controls the system architecture of the wearable with an Arduino Uno boot-loader. A 5 pin header allows

for power (+3 V) and ground connections as well as providing access to TX, RX, and reset pins of the ATmega328p. The Fig illustrates the architecture of the child safety wearable device, which depicts the various technologies and technological standards used. The system architecture of the wearable is based and controlled by an AT - mega328p microcontroller with an Arduino Uno boot loader. The Arduino Uno collects various types of data from the different modules interfaced to it, such as the GPS module upon being triggered by the Arduino GSM shield. The GSM shield is used as an interface to send the data received by the Arduino Uno via SMS or MMS to a smart phone over GSM/GPRS. The GSM shield functions as a trigger for the Arduino Uno to request data from its various modules. If an SMS text with distinct characters is sent to request the current location or GPS coordinates is sent to the Arduino GSM shield via the user's smartphone, then the GSM shield triggers the Arduino Uno to request the current GPS coordinates. The GSM shield uses digital pins 2 and 3 for the software serial communication with the MIO. Pin2 is connected to the MIO's TX pin and pin 3 to its RX pin. Once the Arduino Uno has received the coordinate information, it will process this information and transfer it over to the GSM shield, which then via SMS sends the coordinates to the user's smart phone. The user can just tap on the coordinates which will open up the default GPS application installed on the phone and will show the user the distance between the child and the user.

### B. Wearable IoT Device

The wearable device, for now, is not built on a SoC model, rather has been proposed using larger components and can later build on the SoC platform once put into manufacture.

The wearable IoT device tasked with acquiring various data from all the different modules connected. It comprises of Arduino Uno based on the ATmega328P microcontroller. It receives the data from its various physically connected modules, anatomizes this data and refines the data in a more user understandable format to the different available user interfaces. The user, therefore, can conveniently view the information on their cell phone. The physical characteristics of the wearable device are proposed to be as a wrist watch which remains placed around the wrist of the child during times when the child is not being accompanied by an adult/parent. For the moment the design is not made compact, since the main focus now has been to show that this concept of smart wearable would be highly impactful for the

safety of children. The wearable system runs on a battery with an output voltage of 5V. In order to maximize power consumption, the wearable device has been programmed to provide G P S and image information only upon request by SMS text via GSM shield.

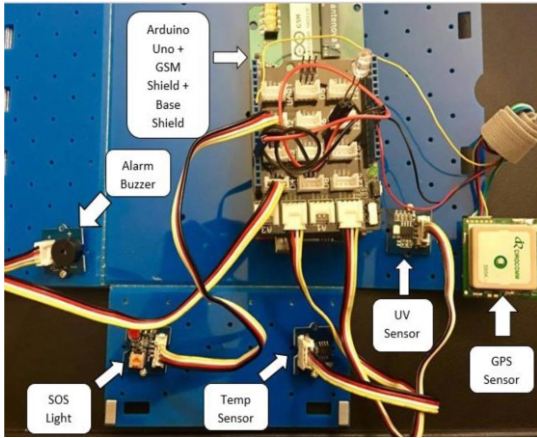
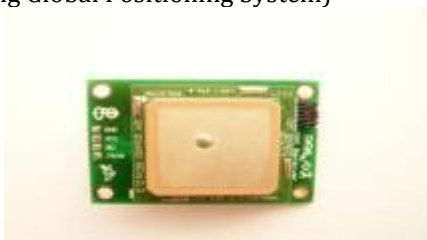


Fig 2. Proposed wearable IoT Device.

### 1) GPS Location Sensor

For determining the real time location of the child Parallax PMB-648 GPS module has been used which communicates with the Arduino Uno through a 4800 bps TTL-level interface. The connections between the Arduino Uno and the GPS module established with three wired connections which enable the Arduino to read the GPS data.

The GPS module receives location information from the various satellites present in the NAVSTAR (American Satellites Timing and Ranging Global Positioning System)



GPS system [1]. It has a low power consumption and size of the only 32x32mm, which is very compact. 20 parallel satellite-tracking channels for fast acquisition and reacquisition. The output received from the GPS module is a standard string information which is governed by the National Marine Electronics Association (NMEA) protocol. To interface the PMB-648 GPS module with the Arduino to provide precise latitude and longitude GPS coordinates, the Tiny GPS library was added into the Arduino IDE. The Yin (red wire) on the PMB-648 GPS module is connected to the 5V pin on the Arduino Uno via jumper cables. Similarly,

the GND (black wire) pin on the GPS module is connected to the GND pin on the Arduino Uno via jumper cables. The TXD (yellow wire) is connected to pin 6 of the Arduino Uno via jumper cables on the breadboard. The pin six on the Arduino Uno is a digital pin which can also be used for PWM (Pulse Width Modulation) applications. Once the SMS trigger text "LOCA nON" is sent from the cell phone of the user, this text is received by the Arduino GSM Shield which in turn triggers the Arduino Uno to execute the GPS code to fetch the current, accurate location of the GPS module. The location output received from the GPS module is in the following format:

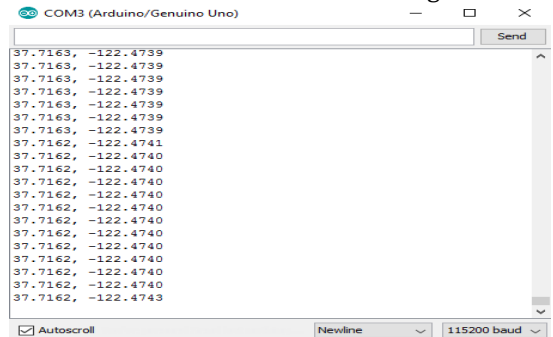
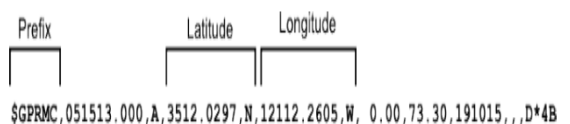


Fig 3. Output received GPS location sensor.

The latitude and longitude coordinates received are stored in variables called "flat" and "flon," which are then called upon when the SMS text received on the GSM module matches with the keyword "LOCA nON." If an SMS text is received which contains none of the pre-programmed keywords, then the Arduino GSM shield automatically deletes the text message and does not reply back the user the with any location details. Once the SMS trigger text "LOCATION" is sent from the smartphone of the user, this text is received by the Arduino GSMShield which in turn triggers the Arduino Uno to execute the GPS code to fetch the current, accurate location of the GPS module. The location output string received from the GPS module is in the following format:

- 1) 220516-Time Stamp
- 2) A-validity- A-ok, V-invalid
- 3) 5133.82-current Latitude
- 4) N-North/South
- 5) 00042.24-current Longitude
- 6) W-East/West
- 7) 173.8-Speed in knots
- 8) 231.8-True course
- 9) 130694-Date Stamp
- 10) 004.2-Variation
- 11) W-East/West
- 12) \*70-checksum





In the scenario, if a child is separated from his/her parents. The parent can locate their child by sounding a very loud alarm on the wearable. To achieve this, grove seed studio buzzer was used, which has a piezoelectric module which is responsible for emitting a strong tone upon the output being set to HIGH. The grove buzzer module is activated upon sending an SMS text with the keyword "BUZZ" from a cell phone. Also, this buzzer works similar to the SOS led by alerting the people nearby with the distressed tone that the child might be lost and is in need of assistance. The buzzer is connected to the D4 digital port of the base shield.

### C. Gateway:

1) Arduino GSM Shield : GSM/GPRS Modem-RS232 is built with Dual Band GSM/GPRS engine-SIM900A, works on frequencies 900/ 1800 MHz. The baud rate is configurable from 9600-115200 through AT command. The onboard Regulated Power supply allows you to connect wide range unregulated power supply . Using this modem, one can make audio calls, SMS, Read SMS, attend the incoming calls and internet ect through simple AT commands.

It transfers the information over to the user via SMS. Arduino provides GSM libraries for GSM module as well as allowing the GSM module to make/receive a call, send/receive SMS and act as a client/server. The GSM module receives 5V power supply directly from the 5V pin connection at the Arduino Uno 5V. The serial communication between the Arduino Uno and GSM module is performed between the serial pins 0,1. The Arduino has been programmed to receive SMS text messages from the parent's cellphone via GSM module. The GSM module will constantly be scanning the received text messages for the specific keywords such as "LOCATION", "TEMPERATURE", "SOS" and "BUZZ".

Its very reliable as the GSM shield is an Arduino produced device, it has the necessary GSM libraries installed into the Arduino IDE interfacing with Arduino Uno. The basic reason for using the GSM shield as the mode of communication over Wi-Fi and Bluetooth was that this wearable was aimed at being accessible to any cellphone user and not necessarily an expensive smartphone user. A user who is technologically challenged can also use it with ease as the technology is made user-friendly.



Fig 5. Gateway: Arduino GSM Shield.

2) Cellphone SMS app interface

For transferring the information over to the user via SMS by using General Packet Radio Service(GPRS) which can provide data rates around 56-114 Kbit/sec an Arduino GSM Shield is used. Arduino provides several libraries such as Ethernet, Wi-Fi for the different Arduino shields. Similarly, they provide GSM libraries for their official GSM shield as well which allows the gsm shield to make/receive a gsm shield to make/receive a call, send/receive SMS and act as a client/server.

### III. RESULTS:

In this section, the experimental tests were performed to detennine the various components of the proposed wearable device.

#### A. GPS Location Sensor

By testing the wearable device multiple times with repeated SMS texts. The GPS location sensor will be able to respond back with precise latitude and longitude coordinates of the wearable device to the user's cellphone, which then the user would click on the received Google maps URL which would, in tum, open the gmaps app or any default browser and display location. In all cases the GPS module is tested, it responds back to the user's cellphone within a minute. The GPS turned out to be so precise with the location that it performed even better than the GPS on an expensive smartphone. As shown in the image below, the GPS module (red bubble) was able to show the current location of the wearable with pinpoint accuracy and also show exactly at which side of the building it is present. Whereas for the smartphone (blue dot) is showing the wearable to be present on the street, which is marginally off

from the exact location. This marginal miss match in the pin-point location of the wearable can turn out to be fatal in a real life scenario, where the parent may be misled to the wrong location of the child. The only drawback that could be stated was, the GSM module could not interpret multiple valid keywords sent in a single message. For example, SMS string sent: LOCA NON TEMPERATURE UV BUZZ SOS; it would not send a reply back to the GSM module.

**B. Temperature and UV sensor:**

Similar to the GPS location sensor, the Temperature, and UV sensors were tested multiple times under different temperatures and higher intensities of sunlight. Both the sensors performed exceptionally well to the test performed. The response time to receive a response back to the keywords "TEMPERATURE" and "UV" was under a minute. Also, the temperature sensor was subjected to higher temperatures and compared with a thermostat reading present in the room which would differ with the sensor reading by +0.2°C to -0.2°C. Also, the UV sensor was measured under different intensities of sunlight. The UV sensor was quick in responding to the changes in the intensity of sunlight. The response time to receive a response back to the keywords "UV" was under a minute as well.

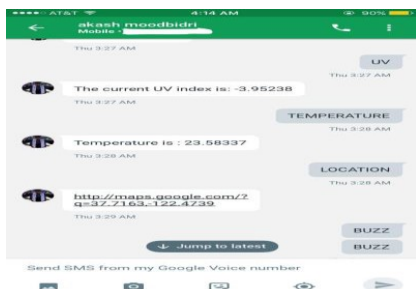


**Fig 7. SMS app screen for UV and Temperature sensor**

**c. SOS Light and Distress Alarm Buzzer:**

The light and buzzer differ from the above sensors in the SMS trigger mechanism. Upon sending an SMS with either "SOS" or "BUZZ," this would trigger the light and buzzer to perform an output function instead of providing measurements back to the user's cellphone such as in the scenario of the other sensors. Upon receiving the correct keywords, the SOS light and Alarm Buzzer would first perform the particular task of flashing the SOS light and sounding a distress alarm which can take a little longer than their respective counterparts. After completion of their respective functions, the response is sent

back to the user' cell phone stating: "SOS Signal Sent" and "Playing Buzzer."

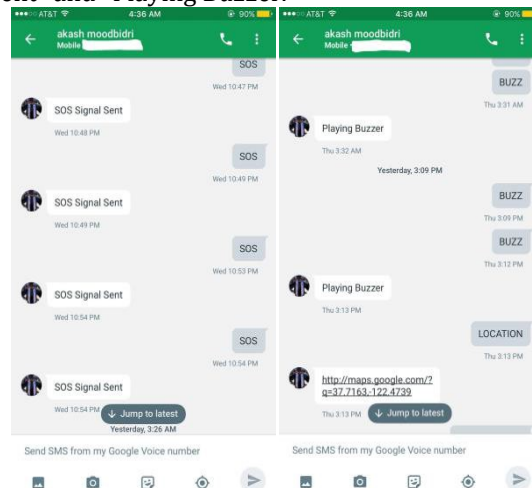


**Fig 8. SMS app screen for Left: SOS Light and Right: Distress alarm buzzer.**

**IV. FUTURE SCOPE**

**1) Camera Module:**

For surveillance of the child's surroundings, to get a clearer picture of the location, this wearable can also contain a camera module incorporated in it. The hardware that could be used would be an Adafruit TTL serial camera. Since the major focus of this wearable project is the GSM module which is a better alternative than Bluetooth, Wi-Fi or ZigBee due to the short range and connectivity issues of these technologies. The red and black wires will be connected directly to +5V and GND respectively to the Arduino Uno board. Whereas for the RX pin which will be used for sending data via Arduino Uno and Arduino GSM board and for the TX pin which will be utilized for receiving incoming data via from the modules. The IOK resistor divider, the camera's serial data pins are 3.3V logic, and it would be a good idea to divide the 5V down so that its 2.5V. Normally the output from the digital 0 pin is 5V high, the way we connected the resistors is so the camera input (white wire) never goes above 3.3V. To talk to the camera, the Arduino Uno will be using two digital pins and a software serial port to talk to the camera. Since the camera or the Arduino Uno do not have enough onboard memory to save snapshots clicked and store it temporarily, therefore an external storage source microSD breakout board will be used to save the images temporarily. The camera works on a standard baud rate of 38400 baud. The camera will be collecting information in the same manner as the GPS module. It will be on standby conserving power waiting for the

particular keyword "SNAPSHOT" to be sent from the user's smartphone to the GSM shield will activate the camera to start clicking a snapshot of the surrounding and save the file temporarily on the external microSD card. After which Arduino Uno will access the saved image from the microSD storage and transfer it to the GSM module which send it to the user via SMS/MMS text.

## 2) Android App:

The idea behind the Android app has been derived from having an automated bot to respond to text message responses from the user. It will provide the user with predefined response options at just the click of a button. The user doesn't need to memorize the specific keywords to send. Also, the bot will be preprogrammed to present the user with a set of predefined keyword options such as "LOCATION," "SNAPSHOT," "SOS," etc. Whereas for the future aspect of this wearable device based on what type sensor is added to it, additional specific keywords could be added such as, "HUMIDITY," "ALTITUDE," etc.

## V. CONCLUSIONS

The child safety wearable device is capable of acting as a smart IoT device. It provides parents with the real-time location, surrounding temperature, UV radiation index and SOS light along with Distress alarm buzzer for their child's surroundings and the ability to locate their child or alert bystanders in acting to rescue or comfort the child. The smart child safety wearable can be enhanced much more in the future by using highly compact Arduino modules such as the LilyPad Arduino which can be sewed into fabrics. Also a more power efficient model will have to be created which will be capable of holding the battery for a longer time.

## VI. REFERENCES

1. B. Dorsemaine, 1. P. Gaulier, 1. P. Wary, N. Kheir and P.Urien, "Internet of Things: A Definition and Taxonomy," Next Generation Mobile Applications, Services and Technologies, 2015 9th International Conference on, Cambridge, 2015, pp. 72-77.
2. H. Moustafa, H. Kenn, K. Sayrafian, W. Scanlon and Y.Zhang, "Mobile wearable communications [Guest Editorial]," in IEEE Wireless Communications, vol. 22, no. 1, pp. 10-11, February 2015.
3. S. Nasrin and P. 1. Radcliffe, "Novel protocol enables DIY home automation," Telecommunication Networks and Applications Conference (ATNAC), 2014 Australasian, Southbank, VIC, 2014, pp. 212-216.
4. F. A. Silva, "Industrial Wireless Sensor Networks: Applications, Protocols, and Standards [Book News]," in IEEE Industrial Electronics Magazine, vol. 8, no. 4, pp. 67-68, Dec.2014.
5. Jun Zheng; Simplot-Ryl, D.; Bisdikian, c.; Mouftah, H.T., "The internet of things [Guest Editorial]," in Communications Magazine, IEEE , vo1.49, no.11, pp.30-31, November 2011 doi:10.1109/MCOM.2011.6069706
6. K. Braam, Tsung-Ching Huang, Chin-Hui Chen, E. Montgomery, S. Vo and R. Beausoleil, "Wristband Vital: A wearable multi-sensor microsystem for real-time assistance via low-power Bluetooth link," Internet of Things (WF-IoT), 2015 IEEE 2nd World Forum on, Milan, 2015, pp. 87-91. doi: 10.1109/WF-IoT.2015.7389032
7. "Digital parenting: The best wearables and new smart baby monitors. The latest smart baby monitors and connected tech for your peace of mind," Tech. Rep., 2015. [Online]. Available: <http://www.wearable.com/parenting/the-best-wearables-babies-smart-baby-monitors>.
8. "WiFi and WiMAX - break through in wireless access technologies," Wireless, Mobile and Multimedia Networks, 2008. IET International Conference on, Beijing, 2008, pp. 141-145.
9. P. Bhagwat, "Bluetooth: technology for short-range wireless apps," in IEEE Internet Computing, vol. 5, no. 3, pp. 96-103, May/June 2001.
10. Y. A. Badamasi, "The working principle of an Arduino," Electronics, Computer and Computation (ICECCO), 2014 11th International Conference on, Abuja, 2014, pp. 1-4.
11. N. Raj and R. K. Sharma, "A High Swing OTA with wide Linearity for design of Self Tuneable Resistor", International Journal of VLSI design & Communication system (VLSICS), Volume 1, No. 3, pp. 1-11, 2010.
12. N. Raj, A.K. Singh, A.K. Gupta, "Modeling of Human Voice Box in VLSI for Low Power Biomedical Applications", IETE Journal of Research, Vol. 57, Issue 4, pp. 345-353, 2011.
13. N. Raj, A.K. Singh, and A.K. Gupta, "Low power high output impedance high bandwidth QFGMOS current mirror", Microelectronics Journal, Vol. 45, No. 8, pp. 1132-1142, 2014.
14. N. Raj, A.K. Singh, and A.K. Gupta, "Low-voltage bulk-driven self-biased cascode current mirror with bandwidth enhancement", Electronics Letters, Vol. 50, No. 1, pp. 23-25, 2014.
15. N. Raj, A.K. Singh, and A.K. Gupta, "Low Voltage High Output Impedance Bulk-driven Quasi-floating Gate Self-biased High-swing Cascode Current Mirror", Circuit System & Signal Processing Journal, Vol. 35, No. 8, pp. 2683-2703, 2015.

16. N. Raj, A.K. Singh, and A.K. Gupta, "High performance Current Mirrors using Quasi-floating Bulk", *Microelectronics Journal*, Vol. 52, No. 1, pp. 11-22, 2016.
17. N. Raj, A.K. Singh, and A.K. Gupta, "Low Voltage High Performance Bulk-driven Quasi-floating Gate Self-biased Cascode Current Mirror", *Microelectronics Journal*, Vol. 52, No. 1, pp. 124-133, 2016.
18. N. Raj, A.K. Singh, and A.K. Gupta, "Low Voltage High Bandwidth Self-biased High Swing Cascode Current Mirror", *Indian Journal of Pure and Applied Physics*, Vol. 55, No. 4, pp. 245-253, 2017.
19. Raj N. and Gupta A. K., "Analysis of Operational Transconductance Amplifier using Low Power Techniques", *Journal of Semiconductor Devices and Circuits (STM Journal)*, Vol. 1, No. 3, pp. 1-9, 2015.
20. Raj N. and Gupta A. K., "Multifunction Filter Design using BDQFG Miller OTA", *Journal of Electrical and Electronics Engineering: An International Journal (EEEIJ Journal)*, Vol. 4, No. 3, pp. 55-67, 2015.
21. N. Raj, A.K. Singh, and A.K. Gupta, "Low Power Circuit Design Techniques: A Survey", *International Journal of Computer Theory and Engineering*, Vol. 7, No. 3, pp. 172-176, 2015.

## **BOOKING SYSTEM OF A VEHICLE PARK USING IOT TECHNOLOGY**

**M.Prudhvi Raj & N.Naresh & Vijayalakshmi Ch**

Department of ECE, Mallareddy College Of Engineering, maisammaguda, India.

**ABSTRACT:** we provide a system for parking reservations and security, maintenance during a exceedingly in a very non-public automobile parking field in an urban metropolis. Our system style is employed to eliminate surplus time conception to search out Associate in nursing empty extract a automobile parking field. By identical sheath, we will conjointly save over seventy five to eighty five % of fuel wastage in an exceedingly automobile lot to check the empty parking slot. The reservation processes square measure happening solely by the user. Therefore the user visit lot exploitation Associate in Nursing humanoid application through an online access and notice the empty parking slot and a reserve parking slot as per their preference. Here we tend to gift the main response to user's reservation action and therefore the driving force will put aside his own seemingly parking slot supported the time and price perform. We've projected a system with multi-processing queuing mechanism (MPQM) to avoid multi-user approach downside (MUAP) throughout the reservation procedure in our perceptive automobile parking booking arrangement supported IOT technology.

**Keywords:** android Application, android Studio, Arduino UNO, internet of Things, Multi-User Approach process (MUAP), QR Code, un hearable sensing element.

### **I. INTRODUCTION**

Now a day's congestion of traffic will increase chop-chop with the increasing growth of population. With relevance the amount of population the usage of cars conjointly exaggerated. Thanks to a lot of usage of automobile the tie up occurred on the road. as a result of the finding of free parking slot takes longer. Hence, we tend to lose a particular amount of your time and created over seventy five to eighty five % of fuel wastage to search out the empty parking extract lot. to resolve this downside, we want a special system within the lot to live empty area and show the knowledge to the folks that searching for the empty area. However, many systems designed antecedently to avoid time wastage in automobile lot.

In the sensible parking allocation and reservation system, a system itself allocates the automobile parking space for each user [1][2].

In this, the system observes the gap between the user and parking areas with the assistance of world positioning system [1]. With this distance mensuration the system calculates the typical time conception for the user getting into the automobile parking space [1]. Then the system allocates the suitable parking slot for the user [1] [3]. Therefore the user could or might not be accepted the allotted automobile parking space [1]. If once the user accepts allotted slot, then the user will able to modification his parking slot [1]

[4]. In our system all the user will able to reserve own seemingly parking spot. therefore there's no restriction between the slot reservation, and user request. Here the user reserves his spot with respect the system framework represented. Here every step of the reservation method is differentiated by DLSSM. MUAP is avoided by special queuing method (MPQM) with the embedded method management unit (EPCU) in our sensible automobile parking system [1].

### **II. LITERATURE SURVEY**

**V. Venkateswaran, N. Prakash, and IJRET [1]:** during this paper, they introduce a special system for sensible parking reservations Associate in Nursing security maintenance in an exceedingly industrial automobile lot in urban surroundings. Here they furnish the main response to user's reservation action and therefore the driving force will reserve his own seemingly parking slot supported the price perform. rather than economical automobile parking we want a special security choices to create our vehicle terribly safe. By this case they need provided a higher security steerage of barrier gate management security system; with the assistance of embedded method management unit (EPCU). There square measure several steps taken to create a reservation with completely different lighting theme mechanism (DLSSM).

**Amir O. Kotb, Yao-Chun Shen, Xu Zhu, Senior Member, IEEE, and Yi Huang, Senior**

Member, IEEE [2]: during this paper, they introduce a brand new sensible parking system that's supported intelligent resource allocation, reservation, and rating. The projected system solves this parking issues by providing secure parking reservations with the bottom potential price and looking time for drivers and therefore the highest revenue and resource utilization for parking managers.

**Yanfeng Geng, Student Member, IEEE, and Christos G. Cassandras, Fellow, IEEE [3]:** during this paper the system assigns Associate in Nursingd reserves an optimum automobile parking space supported the driver's price perform that mixes proximity to destination and parking price.

**Sheelarani, S. Preethi Anand, S. Shamili and K. Sruthi [4]:** during this paper, they projected a wise parking application, wherever users are able to park their vehicles by finding Associate in Nursinging empty automobile parking space through humanoid Application or will even park their vehicles directly through Embedded Hardware. Associate in Nursinging Intelligent Parking System is enforced supported Slot Allotment.

**Hongwei Wang and Wenbo He [5]:** during this paper they we tend to style and implement a image of Reservation-based sensible Parking System (RSPS); that permits drivers to effectively notice and reserve the vacant parking areas. By sporadically learning the parking standing from the sensing element networks deployed in parking tons, the reservation service is affected by the modification of physical parking standing. The drivers will access this cyber-physical system with their personal communication devices.

### III. PROJECTED WORK

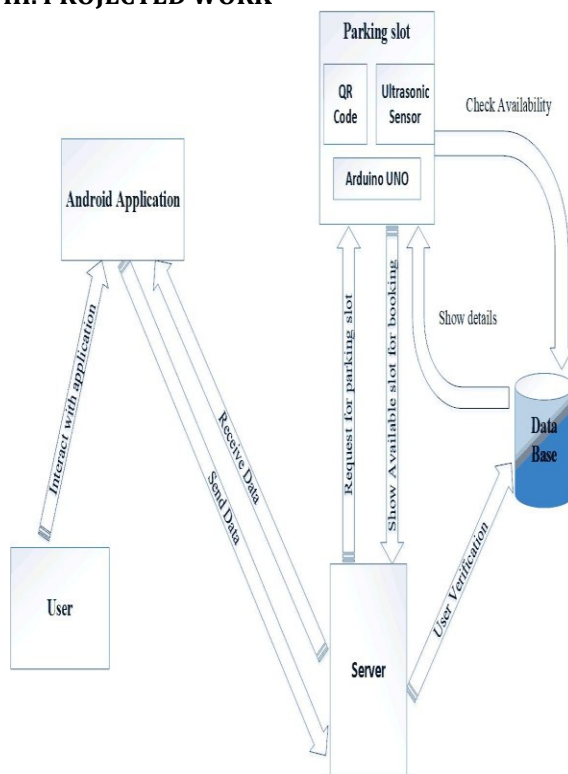


Fig 1. Parking Reservation System style diagram

We square measure progressing to style a system that consists of various modules like server, database, user application and parking slot arrangement. we offer Associate in Nursinging humanoid application to user owing to consistent with Google there square measure one.4 billion active humanoid devices over worldwide. A user should 1st transfer the humanoid application in his humanoid movable. when user should go just one time for registration with specific id (using AADHAR CARD no. or License no.) exploitation the applying. Then registered user info is distributed to the server system and knowledge keep within the information. The parking slot info is additionally keep within the information that is usually updated, and server manages and update this info and keep causation notification to the user when parking slot booking. User will use humanoid application to book specific parking slot at desired area. once user book specific slot, then the server generates QR code and send to the user (Android Application) and therefore the information through server system. With the assistance of QR code user are accessing specific reserved parking slot and park the automobile. At the parking slot there's a mechanism wherever we tend to use Arduino UNO and un hearable sensing element. Arduino is employed for managing un

hearable sensing element and entry gate. The unhearable sensing element is beneficial for detective work the automobile position. once user can scan QR code at the parking slot that point user are charged or pay money for a time length that is user already mention at the slot booking time through humanoid application. In such vital condition or in some new modification is needed for parking system we offer an online website for the Admin user. Admin will manage parking locations and user information through the web site. this method style is incredibly easy, effective, eco-friendly and user friendly.

#### A. Arduino UNO R3:

The Arduino UNO R3 could be a microcontroller board supported the ATmega328 (data-sheet). it's fourteen digital input/output pins (of that half-dozen is used as PWM outputs), half-dozen analog inputs, a sixteen MHz quartz oscillator, a USB affiliation, an influence jack, Associate in Nursing ICSP header, and a button [6]. we tend to square measure exploitation Arduino UNO R3 for dominant entry gate (motor) and unhearable sensing element.

#### B. Android

Humanoid could be a mobile software package developed by Google, supported the UNIX system kernel and designed primarily for bit screen mobile devices like sensible phones and tablets. As of could 2017, humanoid has 2 billion monthly active users, and it's the most important put in base of any software package [7]. Hence, we've determined to make Associate in Nursing humanoid application that is employed for interacting with user and booking parking slot for a particular time length.

#### C. Android Studio

Humanoid Studio is that the official integrated development surroundings (IDE) for Google's humanoid software package, engineered on Jet Brains' IntelliJ plan code and designed specifically for humanoid development [8]. we tend to use humanoid Studio to make Associate in Nursing humanoid Application.

#### D. Apache Felis catus:

Apache Tomcat implements many Java EE specifications, as well as Java Servlets, Java Server Pages (JSP), Java EL, and net Socket, and provides a "pure Java" protocol net server surroundings during which Java code will run [9].

#### E. Ultrasonic Sensor:

It emits Associate in Nursing ultrasound at forty 000 cps, that moves through the air Associate in Nursingd if there's an object or obstacle in its path it'll rebound back to the module [10]. This unbearable sensing element is employed for

detective work the automobile distance from the entry gate.

#### F. Quick Response (QR) Code:

A QR Code could be a two-dimensional barcode that's legible by smart phones. It permits to write in code over 4000 characters in an exceedingly two-dimensional barcode. "QR Code" could be a registered trademark of DENSO WAVE INCORPORATED [11]. we tend to square measure exploitation QR code for identification of a legitimate user at the time of user enter the parking slot.

### IV. FINAL RESULT WITH DESIGN

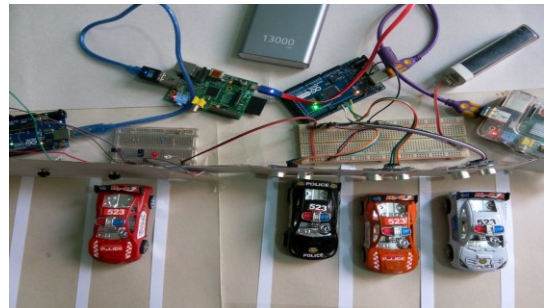


Fig2. Final project design



Fig3. Parking information on mobile for booking vehicle slot

We can verify the parking slots with the help of mobile app

### V.CONCLUSIONS

We have steered a wise automobile parking arrangement to achieve light and economical usage of automobile lot. Basically, this method work consistently detects the non-reserved parking slot and updates the info in server aspect exploitation website that is meant for the distinct lot. the typical time consumption for update the knowledge is incredibly but former systems. we tend to uprise a good parking reservation system wherever the user will reserve their slot exploitation their humanoid application or with the help of Associate in Nursing embedded hardware. this method is economical and helpful in metropolitan cities. this method is applied to

avoid dense traffic within the parking areas like looking malls, theaters, traveller spots and different busy areas, thereby cutting time and therefore the use of the fuel and contamination.

## REFERENCES

- [1] V. venkateswaran, n. prakash, "intelligent approach for smart car parking reservation and security maintenance system", *ijret journal*. vol. 3, pp. 248-251, January 2014.
- [2] <http://esatjournals.net/ijret/2014v03/i02/ijret20140302042.pdf>
- [3] Amir o. kotb; yao-chun shen; xu zhu; yi huang, iparker—a new smart car-parking system based on dynamic resource allocation and pricing". *ieee trans*, 2016. vol. 17, no. 9, pp. 2637 – 2647
- [4] <http://ieeexplore.ieee.org/document/7465828/>
- [5] Yanfeng geng and c.g. cassandras, "new "smart parking" system based on resource allocation and reservations", *ieee trans. intel. trans sys*, vol. 14, pp. 1129-1139, september 2013.
- [6] <http://ieeexplore.ieee.org/iel7/6979/4358928/06492250.pdf>
- [7] p. sheelarani, s. preethi anand, s. shamili and k. sruthi, effective car parking reservation system based on internet of things technologies wcftr'16, 2016.
- [8] <http://ieeexplore.ieee.org/document/7583962/>
- [9] Hongwei wang and wendo he, "a reservation-based smart parking system" 2011.
- [10] <http://ieeexplore.ieee.org/iel5/5888675/5928760/>
- [11] <http://www.trossenrobotics.com/p/arduino-no.aspx>
- [12] [https://en.wikipedia.org/wiki/android\\_\(operating\\_system\)](https://en.wikipedia.org/wiki/android_(operating_system))
- [13] [https://en.wikipedia.org/wiki/android\\_studio](https://en.wikipedia.org/wiki/android_studio)
- [14] [https://en.wikipedia.org/wiki/apache\\_tomcat](https://en.wikipedia.org/wiki/apache_tomcat)
- [15] <http://howtomechatronics.com/tutorials/arduino/ultrasonic-sensor-hc-sr04/>
- [16] [19] N. Raj and R. K. Sharma, "A High Swing OTA with wide Linearity for design of Self Tuneable Resistor", *International Journal of VLSI design & Communication system (VLSICS)*, Volume 1, No. 3, pp. 1-11, 2010.
- [17] N. Raj, A.K. Singh, A.K. Gupta, "Modeling of Human Voice Box in VLSI for Low Power Biomedical Applications", *IETE Journal of Research*, Vol. 57, Issue 4, pp. 345-353, 2011.
- [18] N. Raj, A.K. Singh, and A.K. Gupta, "Low power high output impedance high bandwidth QFGMOS current mirror", *Microelectronics Journal*, Vol. 45, No. 8, pp. 1132-1142, 2014.
- [19] N. Raj, A.K. Singh, and A.K. Gupta, "Low-voltage bulk-driven self-biased cascode current mirror with bandwidth enhancement", *Electronics Letters*, Vol. 50, No. 1, pp. 23-25, 2014.
- [20] N. Raj, A.K. Singh, and A.K. Gupta, "Low Voltage High Output Impedance Bulk-driven Quasi-floating Gate Self-biased High-swing Cascode Current Mirror", *Circuit System & Signal Processing Journal*, Vol. 35, No. 8, pp. 2683-2703, 2015.
- [21] N. Raj, A.K. Singh, and A.K. Gupta, "High performance Current Mirrors using Quasi-floating Bulk", *Microelectronics Journal*, Vol. 52, No. 1, pp. 11-22, 2016.
- [22] N. Raj, A.K. Singh, and A.K. Gupta, "Low Voltage High Performance Bulk-driven Quasi-floating Gate Self-biased Cascode Current Mirror", *Microelectronics Journal*, Vol. 52, No. 1, pp. 124-133, 2016.
- [23] N. Raj, A.K. Singh, and A.K. Gupta, "Low Voltage High Bandwidth Self-biased High Swing Cascode Current Mirror", *Indian Journal of Pure and Applied Physic*, Vol. 55, No. 4, pp. 245-253, 2017.
- [24] Raj N. and Gupta A. K., "Analysis of Operational Transconductance Amplifier using Low Power Techniques", *Journal of Semiconductor Devices and Circuits (STM Journal)*, Vol. 1, No. 3, pp. 1-9, 2015.
- [25] Raj N. and Gupta A. K., "Multifunction Filter Design using BDQFG Miller OTA", *Journal of Electrical and Electronics Engineering: An International Journal (EEEIJ Journal)*, Vol. 4, No. 3, pp. 55-67, 2015.
- [26] N. Raj, A.K. Singh, and A.K. Gupta, "Low Power Circuit Design Techniques: A Survey", *International Journal of Computer Theory and Engineering*, Vol. 7, No. 3, pp. 172-176, 2015.

# An Energy-Efficient Cooperative Spectrum Sensing for Cognitive Radio: A Review

P.Venkatapathi<sup>1</sup>, R Krishna Chaitany<sup>2</sup>, Dr.Habibulla Khan<sup>3</sup>, Dr.S.Srinivasa Rao<sup>4</sup>

Research Scholar<sup>1</sup>, PG Scholar<sup>2</sup>, Professor & Dean (Student Affairs)<sup>3</sup>, Professor & HOD<sup>4</sup>

<sup>1,3</sup>Department of ECE,K LEF, Vijayawada, Guntur District, A.P., INDIA.

<sup>2</sup>Malla Reddy College of Engineering, Hyderabad, Telangana, India

<sup>4</sup>Malla Reddy College of Engineering and Technology, Hyderabad, Telangana, India

---

**ABSTRACT:** Cognitive radio (CR) is a promising solution for improving spectral utilization. Those bands of frequencies which are allocated to primary users (PU) or licensed users, can be used by secondary users (SU) or cognitive users, when PU are not present. Hence, spectrum sensing is necessary to identify the available spectrum and to prevent harmful interference with licensed users. Cooperative spectrum sensing (CSS) is used commonly because spectrum sensing of individual nodes cannot achieve high detection accuracy. The drawback of CSS scheme is that there exists a tradeoff between energy consumption and sensing performance. A more accurate sensing procedure requires minimizing energy consumption without degrading detection performance. In this paper, a survey of various works which aims to maximize the energy efficiency without degrading sensing performance is done.

**Keywords:** primary users; secondary users; cooperative spectrum sensing; energy efficiency; detection performance.

---

## I. INTRODUCTION

Spectrum resources are required for the purpose of communication. The frequency spectrum has been divided into different parts and each part is assigned for specific use. The electromagnetic radio spectrum is a natural resource, the use of which by transmitters and receivers is licensed by governments [1]. The following observations can be made about the spectrum:-

- Some frequency bands in the spectrum are sparsely occupied.
- Some other frequency bands are partially used
- The remaining frequency bands are heavily occupied.

This underutilization of the electromagnetic spectrum leads to spectrum holes or white spaces. A spectrum hole is a band of frequencies assigned to PU, but the band is not being utilized by that user. CR has been proposed to promote the efficient use of spectrum by exploiting the existence of spectrum holes. CR is an intelligent wireless communication system that senses its operational electromagnetic environment and adjusts its radio operating parameters like modulation type, power output, frequency etc to modify system operations such as maximizing throughput, mitigating interference, etc. SUs are the CR entities that uses spectrum

hole. These SUs should not cause any interference to the PU. Hence, it is important to detect the PU correctly.

Spectrum sensing is the key function of CR. It is the process of monitoring the spectrum to detect the presence of PU on a specific channel. If the PU is absent (not utilizing spectrum) then, SU can utilize spectrum. Otherwise, SU cannot use the spectrum. Spectrum sensing techniques include energy detection, matched filter detection, cyclostationary feature detection, waveform detection etc [2]. A matched filter is a linear filter designed to maximize the output signal to noise ratio (SNR) for a given input signal. In matched filter detection technique, an unknown signal is correlated with a time shifted version of impulse response of the matched filter. Cyclostationary feature detection technique is the best method for detecting modulated signal with high levels of noise. PU signal is periodic in nature and hence they will exhibit periodic statistical properties which will not be present in noise and interference. In energy detection technique, sum of square of received signals amplitude is taken. The energy detection method is also called as blind detector because it ignores the structure of the signal. Energy detection is commonly used because it is easy to implement and is less complex. Moreover, prior information about PU is not required as in case of matched filters.

Spectrum sensing by individual nodes suffers from the problem of hidden terminals, multipath fading, noise, shadowing, etc. This will reduce detection performance [3]. Therefore, CSS is used. Here, a parallel fusion sensing architecture is employed. CSS is the process of making final decision (regarding the presence or absence of PU) based on the sensing data collected by SU. In CSS, large number of SUs are employed to detect the channel. This information is passed on to a central entity, called as fusion center (FC). After collecting the sensing result, fusion is performed by FC and a decision is made.

In order to avoid interference and for efficient utilization of spectrum, correct decision should be made. Detection performance can be improved by –

- Increasing the sensing time
- Increasing the number of nodes
- Reducing the transmission distance
- Increasing the number of data samples transmitted to FC

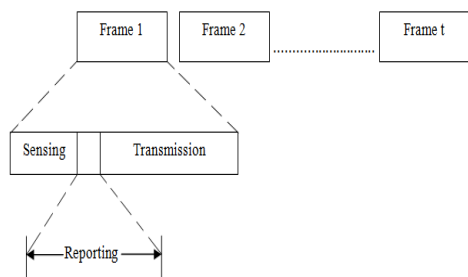


Fig. 1. Time frame architecture

Along with the increase in detection performance, more number of processes will be involved. Hence, more energy will be consumed. As the sensing performance increases, the energy consumption will also increase [4]. In this paper, possible ways of energy saving without compromising sensing performance is discussed.

The rest of this paper is organized as follows. System model is presented in section II. In section III, some of the works which helps in achieving energy efficiency is discussed. Finally, the work is concluded in section IV.

## II. SYSTEM MODEL

Assume that the time is divided into frames and each frame follows a CSS scheme and data transmission. This is illustrated in Fig. 1. Processes involved in each frame [4] are as follows:-

- Single node spectrum sensing and processing
- Delivery of data to the FC

- After collecting data from all the SU, processing and decision making is done by the FC
- Decision circulation among the nodes
- Data transmission by the allowed SU

Only first three processes are involved in spectrum sensing phase. A block level description of this is shown in Fig. 2. Consider a CR network with M SUs, one control channel (channel between SU and FC), one licensed channel (channel between PU and SU) and one FC. Here, each of the SU will be sensing the PU signal. Spectrum sensing can be formulated as a binary hypothesis problem, given by (1) and (2).

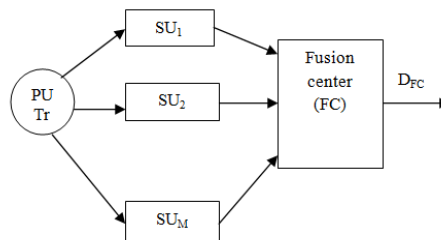


Fig. 2. Cooperative spectrum sensing

$$H_0: y(n) = u(n) \quad (1)$$

$$H_1: y(n) = h(n)s(n) + u(n) \quad (2)$$

where  $H_0$  and  $H_1$  denote the absence or presence of PU on the licensed channel respectively.  $y(n)$  represent received signal at each SU.  $u(n)$  represent noise.  $S(n)$  is the PU signal.  $h(n)$  is the channel gain. PU is said to be present if it belongs to the hypothesis  $H_1$  and is said to be absent if it belongs to the hypothesis  $H_0$ .

First of all, the signal from PU is sampled. Each SU perform spectrum sensing by energy detection technique [3]. In this technique, average of energy content in received sample is taken. Let  $E_i$  denote local statistics of SU  $i$  and is given by (3).

$$E_i = \frac{1}{N_i} \sum_{n=1}^{N_i} |y_i(n)|^2$$

Where  $N_i$  denotes number of samples,  $y_i(n)$  received signal at the  $i$ th SU and  $n = 1, 2, 3, \dots, N_i$ . This sensed information is transmitted by the SU to the FC. FC is responsible for making the final decision. SU can transmit either the data or the decision to the FC.

According to the type of information that SUs transmits to the FC, CSS schemes can be generally categorized into two kinds: soft combination schemes and hard combination schemes [5]. In soft combination scheme, SUs directly send their local statistics which are

energy values of the received signals from the SU to the FC. It includes equal gain combining (EGC) or square law combining (SLC) and maximum ratio combining (MRC). In EGC, estimated energy is sent to FC where they will be added together. This is given in (4).

$$E_{EGC} = \frac{1}{M} \sum_{i=1}^M E_i$$

where  $E_i$  is the energy of the  $i$ th node. Decision is made by comparing EGC with the threshold value. In MRC, Weighted estimated energy is sent to FC where they will be added together. This is given by (5).

$$E_{MRC} = \frac{1}{M} \sum_{i=1}^M W_i E_i$$

where  $W_i$  is the weight of the  $i$ th node and  $E_i$  is the energy of the  $i$ th node. Decision is taken by comparing EMRC with threshold value. On reaching the FC, this estimated energy is compared with a threshold value. PU is said to be present if the estimated energy is greater than the threshold value. In hard combination scheme, SU converts local statistics into one-bit decision, i.e., 0 or 1 implies that a PU is absent or present, respectively. Then, they send these one-bit decisions to the FC. Hard decision fusion rule, includes OR, AND, half voting (HV), majority, and, in general, the K-out-of-N (KN) rule. As per OR rule, the PU is considered to be present, if at least one of the nodes detects the event. For PU detection using AND rule, all the nodes should detect it. In case of HV and majority rules, at least half and more than half of the nodes, respectively, should detect the PU. As per KN rule, the PU is considered to be present if at least K out of N nodes detects it. The cooperative detection probability and false alarm probability for AND, OR and the general KN rules are given by (6), (7) and (8) respectively, where 'x' denotes 'detection' or 'false-alarm' and  $P_{xi}$  denotes the detection or false-alarm probability of the  $i$ th node.

$$Q_{x,AND} = \prod_{i=1}^M P_{xi} \quad (6)$$

$$Q_{x,OR} = 1 - \prod_{i=1}^M (1 - P_{xi}) \quad (7)$$

$$Q_{x,KN} = \sum_{i=k}^M \binom{M}{i} P_x^i (1 - P_x)^{M-i} \quad (8)$$

Two metrics which determine spectrum sensing performance is probability of detection and probability of false alarm. Probability of detection is the probability that the PU is active, and SU detect it successfully. Probability of false alarm is the probability that the PU is not active but the SU detects it to be active. Therefore, detection probability should be maximized to avoid interference, and false alarm probability should be minimized for efficient utilization of spectrum.

### III. ENERGY SAVING METHODS

The authors in [6] proved that there exist an optimal sensing time which gives maximum throughput for the SUs provided the PU is protected. Here, the optimal sensing time is found by solving a concave optimization problem or by exhaustive search algorithm. The throughput is maximized in such a way that probability of false is less than the targeted probability of false alarm. The number of samples collected by the SUs from the PU reduces along with the reduction in sensing time. This helps in reducing the number of processes involved in spectrum sensing. Moreover, the ON time of spectrum sensing sensor reduces and hence battery life of the sensor increases. Optimization of sensing time helps in increasing the data transmission time. Hence, spectrum utilization can be improved. However, sensing period energy consumption is less compared to the energy consumed during transmission of data to the FC. Here, transmission time energy consumption is not considered. As a result, much of the energy cannot be saved using this method.

As the number of nodes increases, sensing performance will also increase. Once the number of cooperative nodes has reached a certain number, detection performance is only marginally increased upon addition of nodes. The number of active nodes should be chosen in such a way that the sensing performance is only marginally improved if an additional sensor is added and is decremented if a sensor is removed. In [7], relay is selected based on residual battery capacity and interference condition. The device is considered to be active only if residual battery capacity is greater than set energy threshold level and interference with the PU is less than the interference threshold level. By using this method battery life of sensors can be saved. Also, the sensors need not be replaced frequently. However, this method will not help in improving spectrum utilization because channel conditions are not considered.

Correct decision can be obtained only if the channel between SU and FC is perfect. But in practice, reporting channel may experience fading which will degrade the performance of CSS. In [8], the authors proposed a cluster based spectrum sensing technique. Here, those SUs which are close to each other are grouped into clusters, so that the channel between any two nodes in the same cluster is perfect. Then, in each cluster, SU with the largest channel gain is selected as the cluster head. Each SU will transmit their local statistics to cluster head. Cluster head will make a cluster decision. Finally, decision made by the cluster head is transmitted to FC, where final decision is made about presence or absence of the PU. As the transmission distance between nodes is reduced only less transmit power, is required. This method reduces the reporting error and hence sensing performance can be improved. On the other hand, computational complexity increases with the increase in number of SUs and an extra energy is consumed due to the exchange of information.

Edward Peh and Ying-Chang Liang in [9] shows that cooperating a certain number of SU with highest PUs signal to noise ratio (SNR) has better performance than cooperating all the SU. Either a targeted probability of detection or probability of false alarm is set. After setting one of the probabilities, the other one is optimised. In order to give PU their desired level of protection, probability of detection is set at a fixed value while false alarm probability is reduced. To have high capacity, probability of false alarm is fixed at a constant value and detection probability is maximized as much as possible. It is shown that by reducing number of nodes probability of false alarm decreases significantly with constant detection probability (under the OR fusion scheme) and probability of detection increases with constant false alarm probability (under the AND fusion scheme). The advantage is that the communication overhead in terms of exchanged messages and processing is reduced. Hence, energy consumption reduces. But variable channel conditions will induce SNR variations. Moreover, each SU instantaneous SNR is needed and it has to be delivered to the FC. Practically, it is difficult to obtain the instantaneous SNR of each node.

In fading channels, the link between the SUs and the FC may not be good. A reporting link selection algorithm between the cooperative node and the FC is done in [10]. Here, nodes are arranged based on decreasing order of their SNR value and the links corresponding to higher SNR value is chosen as the reporting links. Number of

links that has to be chosen depends on the total error rate (sum of miss detection and false alarm probability). Total error rate should be less than the targeted error bound for a given detection threshold. The number of links transmitting its data to the FC reduces and hence, less number of processes is involved in decision making. This reduces the energy consumed by FC. But channel conditions will cause variations in SNR. This may lead to selection of non-reliable links.

In [11], YngveSel'en, Hugo Tullberg, and Jonas Kronander has proposed algorithms to chose nodes which are spatially separated because closely spaced sensor will experience same shadow fading. Here, sensors are selected based on location of sensors and associated uncertainty. In correlation measure based node selection algorithm, it is assumed that all nodes are active and a sensor with largest summed correlation measure (e.g. - Euclidian distance) relative to the other sensors is removed. In iterative partitioning algorithm, sensors that are separated by more than decorrelation distance (minimum distance between sensors that experience uncorrelated shadow fading) from all the present sensors in the active set are chosen. As the number of sensors participating in spectrum sensing reduces battery life time can be improved. A large number of processes are involved in computation of correlation measure. This may increase the complexity. The proposed sensor selection method is good compared to the random sensor selection method.

As the number of SUs increases, larger bandwidth is required for reporting the result to the FC. Therefore the authors in [12] proposed a censoring technique, where only those SUs with enough information are allowed to transmit their data to FC. This is done by setting two thresholds  $\eta_1$  and  $\eta_2$ . If the energy collected by the SU lies between  $\eta_1$  and  $\eta_2$ , then no decision is made and there will not be any data transmission to FC. If the collected energy is greater than  $\eta_2$  then decision H1 is transmitted and if it is less than  $\eta_1$  decision H0 is transmitted to the FC. After censoring, average number of bits transmitted from the SU to the FC is quantized. By reducing the number of bits, number of computations involved in FC reduces. In this method, irrelevant information is not transmitted to the FC. It is showed that a large amount of reduction in sensing bits is possible with a very little performance degradation. If all the SU makes no decision, then the FC will not be able to make any final decision regarding presence or absence of the PU.

Sleeping and censoring scheme is presented in [13]. In sleep mode, each of the radio will switch OFF its spectrum sensing transceiver. In censoring process, only awake nodes, which lie in a particular information region, are allowed to transmit data to FC. Moreover, optimal sleeping and censoring parameters are obtained which minimizes the energy consumption. Also, it provides detection probability greater than the minimum targeted probability of detection and false alarm probability less than maximum permissible probability of false alarm. When prior information about PU is not available, Neyman Pearson setup is followed and when prior information is available Bayesian setup is followed. It was shown that sleeping rate is higher when the sensing and transmission energies are equal and censoring rate is higher when transmission energy is greater than sensing energy. The proposed method helps in reducing the energy consumption significantly. However, in this work it is assumed that all nodes receive same SNR. This is possible only when all users have same distance to the PU.

Another algorithm for node selection is presented in [14]. Here, three methods are proposed for choosing nodes with best detection performance. The three methods are simple counting (SC), partial agreement counting (PAC) and collision detection (CD). In SC algorithm, number of ones (PU present) of each radio during the training period is counted and those CR with the highest count is allowed to cooperate. SC algorithm assumes that all nodes have same targeted false alarm rate. In PAC algorithm, SUs which have highest agreement with the FC is chosen to cooperate in spectrum sensing. The PAC method assumes that the FC has highest performance. This is not possible practically. In CD scheme, it is assumed that absence of PU is the global decision. Then the FC will transmit a channel release message to the SU. On receiving this message it will reply with an acknowledgement. If the FC receives the acknowledgement, the channel is assumed to be error free. This is not possible practically because channel conditions will cause unsuccessful message transmission. The proposed node selection algorithm helps in reducing the energy consumption but performance will decrease if malicious users are present. Moreover, if majority of SUs face bad channel conditions, incorrect decision will be made.

The linear CSS scheme (proposed in [15]) outperforms likelihood ratio test (LRT). The channel between SU and FC will not be ideal.

Therefore, likelihood threshold has to be provided to each of the nodes. This is not possible practically. Here, linear combination weights are provided instead of changing the threshold for each node. The objective of [15] is to maximize the probability of detection while maintaining probability of false alarm below a targeted value.

#### **IV. CONCLUSION**

CR technology has been proposed to make full use of limited spectrum resource. In CR technology, it is essential to make correct decision in order to achieve efficient spectrum utilization and to avoid interference. CSS is an efficient method for making final decision regarding presence or absence of PU. The detection performance depends on a number of parameters like number of cooperative nodes involved in CSS, sensing time, distance and number of samples involved in processing. But all these methods will lead to larger energy consumption. Thus an increase in sensing performance can be achieved only by comprising energy efficiency. A cooperative spectrum sensing algorithm should consume less energy and should ensure high sensing performance in terms of probability of detection and probability of false alarm. In this paper, works which gives high sensing performance is studied. High sensing performance can be achieved by increasing the number of nodes involved in cooperative spectrum sensing, increasing the sensing time, reducing the distance etc. But all these parameters have an optimal value beyond which there won't be much increase in sensing performance. Choosing that optimal value for all the parameters might give an energy efficient system.

#### **REFERENCES**

1. Haykin, Simon. "Cognitive radio: brain-empowered wireless communications." *IEEE journal on selected areas in communications* 23.2 (2005): 201-220
2. Yucek, Tevfik, and HuseyinArslan. "A survey of spectrum sensing algorithms for cognitive radio applications." *IEEE communications surveys & tutorials* 11.1 (2009): 116-130.
3. Ghasemi, Amir, and Elvino S. Sousa. "Spectrum sensing in cognitive radio networks: requirements, challenges and design trade-offs." *IEEE Communications Magazine* 46.4 (2008).
4. Krzysztof Cichon, Adrian Kliks and Hanna Bogucka, "EnergyEfficient Cooperative Spectrum Sensing: A Survey," *IEEE Communications Surveys and Tutorials*, Volume: 18, Issue: 3, Pages-1861 – 1886, April 2016.

5. D. Teguig, B. Scheers and V. Le Nir, "Data fusion scheme for cooperative spectrum sensing in cognitive radio network," in Military Communications and Information Systems conference, IEEE, December 2012.
6. Liang, Ying-Chang, et al. "Sensing-throughput tradeoff for cognitive radio networks." IEEE transactions on Wireless Communications 7.4 (2008): 1326-1337.
7. Bouallegue, Takoua, and KaoutharSethom. "New threshold-based Relay Selection Algorithm in Dual Hop Cooperative Network." Procedia Computer Science 109 (2017): 273-280.
8. "Cluster-based cooperative spectrum sensing in cognitive radio systems." Communications, 2007. ICC'07. IEEE International Conference on. IEEE, 2007.
9. Peh, Edward, and Ying-Chang Liang. "Optimization for cooperative sensing in cognitive radio networks." Wireless Communications and Networking Conference, 2007. WCNC 2007. IEEE. IEEE, 2007.
10. Song, Qingjiao, and WalaaHamouda. "Performance Analysis and Optimization of Multiselective Scheme for Cooperative Sensing in Fading Channels." IEEE Transactions on Vehicular Technology 65.1 (2016): 358-366.
11. Selén, Yngve, Hugo Tullberg, and Jonas Kronander. "Sensor selection for cooperative spectrum sensing." New Frontiers in Dynamic Spectrum Access Networks, 2008. DySPAN 2008. 3rd IEEE Symposium on. IEEE, 2008.
12. Sun, Chunhua, Wei Zhang, and Khaled Ben Letaief. "Cooperative spectrum sensing for cognitive radios under bandwidth constraints." Wireless Communications and Networking Conference, 2007. WCNC 2007. IEEE. IEEE, 2007.
13. Maleki, Sina, Ashish Pandharipande, and Geert Leus. "Energyefficient distributed spectrum sensing for cognitive sensor networks." IEEE sensors journal 11.3 (2011): 565-573.
14. Khan, Zaheer, et al. "On the selection of the best detection performance sensors for cognitive radio networks." IEEE Signal Processing Letters 17.4 (2010): 359-362.
15. Quan, Zhi, Shuguang Cui, and Ali H. Sayed. "Optimal linear cooperation for spectrum sensing in cognitive radio networks." IEEE Journal of selected topics in signal processing 2.1 (2008): 28-40.

## Resource Allocation Strategies in Cognitive Radio Systems:A Survey

P.Rajeshwari<sup>1</sup>, P.Venkatapathi<sup>2</sup>, Dr.Habibulla Khan<sup>3</sup>, Dr.S.Srinivasa Rao<sup>4</sup>

PG Scholar<sup>1</sup>, Research Scholar<sup>2</sup>, Professor & Dean (Student Affairs)<sup>3</sup>, Professor & HOD<sup>4</sup>

<sup>1</sup> Malla Reddy College of Engineering, Hyderabad, Telangana, India

<sup>2,3</sup> K L University, Green Fields, Vaddeswaram, Guntur District, A.P., INDIA.

<sup>4</sup> Malla Reddy College of Engineering and Technology, Hyderabad, Telangana, India

**ABSTRACT:** In this paper, resource allocation and multiple access in cognitive radio (CR) and compressed sensing (CS)-based wireless networks are studied. Energy-efficiency oriented design becomes more and more important in wireless systems, which motivates us to propose a location-aware power strategy for single user and multiple users in CR systems and a CS-based processing in wireless sensor networks (WSNs) which reduces the number of data transmissions and energy consumption by utilizing sparsity of the transmitted data due to spatial correlation and temporal correlation. In particular, the work on location-aware power allocation in CR system gives a brief overview of the existing power allocation design in the literature and unifies them into a general power allocation framework.

**Keywords:** Cognitive radio, energy efficiency, resource allocation, location-aware strategy, OFDM

### INTRODUCTION

In recent years, the design concept of wireless communications is shifting towards energy-efficiency besides capacity and rates, primarily aiming to resolve the escalating overall energy consumption foreseen in the near future. Such a concept is the core component of green communications. Cognitive Radio (CR), thanks to its sensors, is an enabling technology for green communications which enhances the spectrum efficiency and reduces the electromagnetic radiation levels. Compressed sensing (CS), a novel mathematical theory, can also be applied in wireless communication systems to implement green communications. CS acquires a signal of interest indirectly by collecting a relatively small number of observations rather than evenly sampling it at the Nyquist rate which fundamentally changes the traditional digital signal processing in wireless communications and enhances the energy efficiency. Motivated by the benefits of these mentioned technologies, my research work is focused on the sensing and power allocation strategy of CR systems and CS-based wireless sensor networks (WSNs) to hold the promise of green communications.

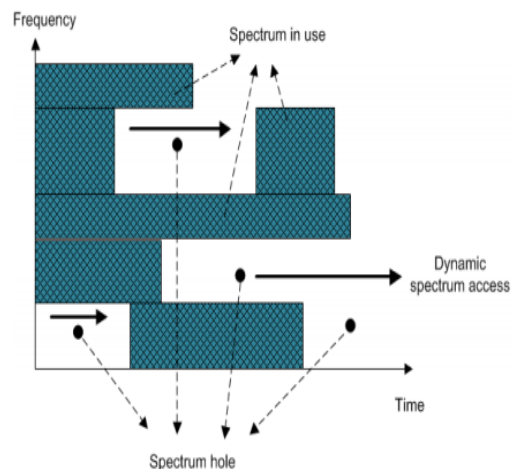


Figure 1.1: Spectrum hole and dynamic spectrum access.

### 1.1 Cognitive Radio

In November 2002, the Federal Communications Commission (FCC) published a report [1] and it shows that spectrum access is a more significant problem than the physical scarcity of spectrum due to the inflexible spectrum regulation policy. In fact, most of the allocated frequency bands are under-utilized: some frequency bands in the spectrum are largely unoccupied most of the time, and some other frequency bands are only partially occupied [2, 3]. This motivates the rise of CR, which is an intelligent wireless communication system that makes use of spectrum according to its surrounding environment to improve spectrum utilization significantly. In a CR system, it is

possible for a SU (not authorized) to utilize the spectrum resource unoccupied by the PU. Basically, a CR is a radio that can dynamically sense the spectrum and make use of the underused spectrum resource in an opportunistic manner by changing its transmitter parameters. As shown in Fig. 1.1, CR opportunistically accesses the unused spectrum, referred to as spectrum holes. The spectrum hole is the frequency resource

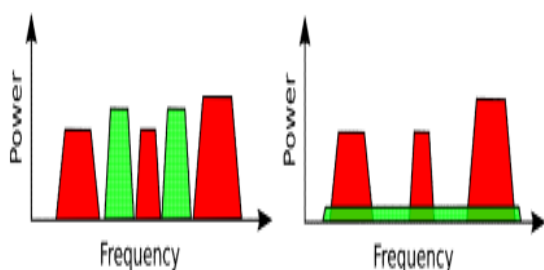


Figure 1.2: Overlay and underlay spectrum access

assigned to PUs, but not being utilized at a particular time or specific geographic location. Spectrum sensing, which monitors the usage of licensed spectra, is a key component required in CR to avoid possible mutual interference between PUs and SUs. There are various spectrum sensing methods, such as matched filter-based detection, energy detection, feature detection, hybrid sensing, cooperative sensing. There exists much research work on spectrum sensing for CR systems, e.g., [4–7]. In [8], the authors give a survey of spectrum sensing methodologies for cognitive radio and an optimal spectrum sensing framework is developed in [7]. Based on the spectrum sensing results, the CR systems need to allocate the spectrum holes to SUs and adopt appropriate transmit power to enhance performance of CR systems meanwhile avoiding harmful interference to PUs. Sensing and power strategy optimization are important research topics in CR systems that hold the promise of advancing green communication. There exist a number of power allocation approaches in the literature. Depending on spectrum policies laid by the primary system, these approaches can be classified as either overlay-based where the SUs can utilize the spectrum only when the PU is absent or underlay-based where the SUs are allowed to share the spectrum with the PU, see Fig. 1.2. The red and green power represent for transmit power of PUs and SUs, respectively. The left figure is for overlay and for the underlay case, appropriate power control has to be incorporated

to avoid unacceptable interference to the primary system.

The rest of this brief introduces the new scheme by first summarizing the parallel filters considered in Section II. Then, in Section III, the proposed scheme is presented. Section IV presents a case study to illustrate the effectiveness of the approach. Finally, the conclusions are summarized in Section V.

## LITERATURE SURVEY

Several solutions have been proposed to handle the RA congestion problem in pioneering works, such as access class barring (ACB) [9–13], extended access barring (EAB) [14], dynamic allocation [15], specific backoff scheme [16], and pull-based scheme [17]. By introducing a separate access class, ACB allows the eNodeB to control the access of UEs separately. Two vital parameters in the ACB method are the barring factor which represents the probability of barring and the backoff factor which indicates the backoff time before retrying random process if the UE fails the ACB check. Many scholars have worked on the dynamic adjustment of the barring factor. In [10], a joint resource allocation and access barring scheme is proposed to achieve uplink scheduling and random access network (RAN) overload control, in which the access barring parameter is adaptively changed based on the amount of available RBs and the traffic load. In [11], two dynamic ACB algorithms for fixed and dynamic preamble allocation schemes are proposed to determine the barring factors without priori knowledge of the number of MTC devices. [9] formulates an optimization problem to determine the optimal barring parameter which maximizes the expected number of MTC devices successfully served in each RA slot. [12] proposes a two-stage ACB scheme to increase access success probability. In the first stage, the UEs use the barring factor broadcast by the eNodeB. The UEs which pass the ACB check are viewed as primary UEs and allowed to select non-special preambles randomly, while the UEs which fail are treated as secondary UEs and select the special preambles. In the second stage, each secondary UE calculates its barring probability independently based on the expected number of secondary UEs. In terms of the backoff factor, [13] compares the performance of uniform backoff (UB) and binary exponential backoff (BEB) algorithms and proposes a new algorithm to adaptively adjust the backoff window size under unsaturated traffic conditions. EAB extends the granularity of the access class to distinguish multiple classes, which has been

introduced in 3GPP standard to throttle the access of Machine Type Communication (MTC) devices [17]. A prioritized random access with dynamic access barring (PRADA) framework is proposed in [14], which optimizes the EAB parameters such as activation time, barring opportunity, and backoff time. PRADA includes two components: pre-allocation of different amount of RA slots for different classes and dynamic access barring (DAB). The average number of successful preambles is observed in each two neighboring RA slots to estimate the RA load. If the RA load is heavy, EAB is triggered and the RA attempts of the UEs with their first preamble transmissions are deferred for a long time. However, there are concerns that EAB may be frequently activated and deactivated since the number of successful preambles drastically varies for bursty RA arrivals. It will result in performance deterioration, for instance, decrease in RA success probability. To guarantee throughput, [15] proposes a game-theoretic framework to dynamically allocate additional RA resources to MTC devices. [16] elaborates a MTC specific backoff scheme which introduces a dynamic backoff indicator assignment algorithm to reduce RA collision probability. The pull-based scheme [17] allows the eNodeB to control network load by dominating the paging operation, where MTC devices will trigger RA process upon receiving a paging message.

The main idea behind aforementioned schemes is to disperse the transmission of the access request to control overload and increase the access probability within a relatively short time. In spite that these approaches can reduce access collision to a certain degree, the retransmission of numerous UEs can again aggravate collision and further increase the access delay. Moreover, several schemes have been developed to mitigate collision and reduce access delay by increasing available RA resources. For example, Thomsen et al. [18] proposes a code-expanded RA scheme which adopts the concept of access code word to increase the amount of available contention resources in the RA process. Moreover, a preamble reuse scheme is proposed in [19], which spatially partitions the cell coverage into multiple regions and reduces the cyclic shift size to generate more preambles. However, the extent of the RA resource increase is limited and severe collision and retransmission are still inevitable.

The RAN overload problem can also be tackled by efficiently utilizing the radio resources for the RA process. In [20], the authors propose a novel random access scheme based on fixed timing

alignment information to reduce collision probability given a large number of fixed-location machine-to-machine (M2M) devices. In the scheme proposed in [21], M2M UEs form coalitions and perform relay transmission with an objective to reduce network congestion. To increase the preamble detection probability, the authors of [22] propose an enhanced RA scheme, in which the eNodeB adopts the transmission time difference to detect the UEs which utilizes the same preamble. Furthermore, the eNodeB creates multiple RARs in response to detected UEs which select the same preamble. However, this scheme fails to consider the limitation on PUSCH resources. With the increase of successfully transmitted preambles, the limited PUSCH resources may be another bottleneck for RA process. In summary, most of existing solutions to improve LTE RA performance mainly focus on controlling traffic or increasing available RA resources. However, the available RA resources are limited. Moreover, the access delay cannot be guaranteed by controlling traffic.

Successive interference cancellation (SIC) enables throughput efficiency enhancements by utilizing collided packets for decoding instead of discarding them [23], which makes it an obvious candidate for alleviating RA congestion problem. evaluates the random access throughput performance of asynchronous code division multiple access (CDMA) systems with interference cancellation receivers. Power randomization is explored to aid iterative receiver processing. Proposes a code-division random access (CDRA) scheme, which adopts specific sets of code words to spread the uplink resources in a non-orthogonal manner among users. The code words assignment scheme allows a random subset of users communicating single bits to the base station (BS). It is worth noting that CDRA uses a convex optimization based multiple user detection algorithm to avoid obtaining the delays and channel state information (CSI) of the users at the BS. Moreover, [23] employ SIC to resolve collisions in the tree (also known as splitting) algorithm to improve random access throughput. These schemes rely on the property of tree algorithm where all packets are retained one-by-one in line with the underlying tree structure. However, this property is not available in LTE RA assumption. There also has been extensive studies on random access networks with SIC-enabled multi-packet reception capabilities. Nevertheless, most of recent works focus on the theoretical analysis of capture probability and power allocation scheme design. Few studies have considered the backoff and

retransmission process in LTE RA procedure. To the best of our knowledge, systematic performance analysis of the SIC- enabled RA process under LTE scenario has not been reported yet. Recently, non-orthogonal multiple access (NOMA) has received many interests. Combined with SIC, NOMA allows simultaneously transmissions of multiple UEs with different powers. Nonetheless, recent studies on NOMA mainly focus on performance analysis of data transmission process. In practical networks such as LTE-A and future 5G networks, the introduction and realization of NOMA and SIC in the random access process could be very challenging. As far as we're concerned, corresponding protocol and mechanism design which is compatible with existing LTE standard has not been reported yet.

### CONCLUSION

This paper has elaborated the role of adaptive resource allocation in CR networks in terms of energy efficiency since energy-efficiency oriented design is more and more important for wireless communications. In comparison between the existing scheme and the proposed resource allocation scheme, we have found that resource allocation by considering spatial information enhances the energy efficiency and avoids unnecessary spectrum sensing

### REFERENCES

1. J. Mitola, "Cognitive radio: an integrated agent architecture for software defined radio," Ph.D. dissertation, 2000.
2. S. Haykin, "Cognitive radio: brain-empowered wireless communications," *IEEE J. Sel. Areas Commun.*, vol. 23, no. 2, pp. 201–220, 2005.
3. Q. Zhao and M. Sadler, B, "A survey of dynamic spectrum access," *IEEE Signal Process. Mag.*, vol. 24, no. 3, pp. 79–89, 2007.
4. A. Ghasemi and E. S. Sousa, "Fundamental limits of spectrum-sharing in fading environments," *IEEE Trans. Wireless Commun.*, vol. 6, no. 2, pp. 649–658, Feb. 2007.
5. L. B. Le and E. Hossain, "Resource allocation for spectrum underlay in cognitive radio networks," *IEEE Trans. Wireless Commun.*, vol. 7, no. 12, pp. 5306–5315, Dec. 2008.
6. X. Zhou, G. Li, D. Li, D. Wang, and A. Soong, "Probabilistic resource allocation for opportunistic spectrum access," *IEEE Trans. Wireless Commun.*, vol. 9, no. 9, pp. 2870–2879, 2010.
7. X. Kang, H. Garg, Y.-C. Liang, and R. Zhang, "Optimal power allocation for ofdm-based cognitive radio with new primary transmission protection criteria," *IEEE Trans. Wireless Commun.*, vol. 9, no. 6, pp. 2066–2075, 2010.
8. G. Bansal, M. J. Hossain, V. K. Bhargava, and T. Le-Ngoc, "Subcarrier and power allocation for OFDMA-based cognitive radio systems with joint overlay and underlay spectrum access mechanism," *IEEE Trans. Veh. Technol.*, vol. 62, no. 3, pp. 1111–1122, Mar. 2013.
9. S. Wang, Z.-H. Zhou, M. Ge, and W. Chonggang, "Resource allocation for heterogeneous cognitive radio networks with imperfect spectrum sensing," *IEEE J. Sel. Areas Commun.*, vol. 31, no. 3, pp. 464–475, Mar. 2013.
10. Y. Tachwali, B. F. Lo, I. F. Akyildiz, and R. Agusti, "Multiuser resource allocation optimization using bandwidth-power product in cognitive radio networks," *IEEE J. Sel. Areas Commun.*, vol. 31, no. 3, pp. 451– 463, 2013.
11. D. Shiung, Y.-Y. Yang, and C.-S. Yang, "Transmit power allocation for cognitive radios under rate protection constraints: a signal coverage approach," *IEEE Trans. Veh. Technol.*, vol. 59, no. 8, pp. 3956–3965, Oct. 2013.
12. J. Zou, H. Xiong, D. Wang, and C. Chen, "Optimal power allocation for hybrid overlay/underlay spectrum sharing in multiband cognitive radio networks," *IEEE Trans. Veh. Technol.*, vol. 59, no. 8, pp. 3956–3965, Oct. 2013.
13. J. Mao, G. Xie, J. Gao, and Y. Liu, "Energy efficiency optimization for OFDM-based cognitive radio systems: a water-filling factor aided search method," *IEEE Trans. Wireless Commun.*, vol. 99, no. 99, pp. 534–539, Oct. 2013.
14. T. Xue, Y. Shi, and X. Dong, "A framework for location-aware strategies in cognitive radio systems," *IEEE Wireless Commun. Letters*, vol. 1, no. 1, pp. 30–33, Feb. 2012.
15. A. G. Marques, L. M. Lopez-Ramos, G. B. Giannakis, and J. Ramos, "Resource allocation for interweave and underlay crs under probability-of-interference constraints," *IEEE J. Sel. Areas Commun.*, vol. 30, no. 10, pp. 1922–1933, Nov. 2012.
16. Y. Song and J. Xie, "Optimal power control for concurrent transmissions of location-aware mobile cognitive radio ad hoc networks," in *Proc. IEEE Global Telecommun. Conf. (Globecom)*, 2009, pp. 1–6.
17. H. Celebi and H. Arslan, "Cognitive positioning systems," *IEEE Trans. Wireless Commun.*, vol. 6, no. 12, pp. 4475–4483, 2007.
18. W. Chee, S. Friedland, and S. H. Low, "Spectrum management in multiuser cognitive wireless networks: optimality and algorithm," *IEEE J. Sel. Areas Commun.*, pp. 421–430, Feb. 2011.
19. J. Wang and D. P. Palomar, "Worst-case robust MIMO transmission with imperfect channel knowledge," *IEEE Trans. Signal Process.*, no. 8, pp. 3086–3100.
20. S. Boyd and L. Vandenberghe, *Convex Optimization*. Cambridge University Press, 2004.

21. W. Yu and R. Lui, "Dual methods for nonconvex spectrum optimization of multicarrier systems," *IEEE Trans. Commun.*, vol. 54, no. 7, pp. 1310–1322, 2006.
22. F. Meshkati, M. Chiang, H. V. Poor, and S. C. Schwartz, "A game-theoretic approach to energy-efficient power control in multicarrier CDMA systems," *IEEE J. Sel. Areas Commun.*, pp. 1115–1129, Jun. 2006.
23. C. U. Saraydar, N. B. Mandayam, and D. J. Goodman, "Efficient power control via pricing in wireless data networks," *IEEE Trans. Commun.*, vol. 50, no. 2, pp. 291–303, Feb. 2002.

## SUPER ACTIVE MATRIX OLED

Y.ROJA RANI<sup>1</sup> & Dr .R.PURUSHOTHAM NAIK<sup>2</sup> & B.SAMATHA<sup>3</sup>

M.Tech(ES & VLSI)<sup>1,3</sup> , Associate Professor<sup>2</sup>

Department of ECE, Malla Reddy College Of Engineering, Hyderabad, INDIA.

**ABSTRACT:** In modern technology, typically use active matrix which contain thin film transistor (TFT's) display. In this TFT's transistor include capacitors that enable individual pixel to active. By using TFT's the active matrix is more efficient than OLED. These active matrices mainly used in mobiles phones i.e., in touch screen for high resolution. But newly Samsung introduced super AMOLED with better brighter screen, low power consumption less sunlight reflection, high resolution and very high-speed refresh rate i.e., speed up the response time. Super AMOLED also called as SAM AMOLED. Samsung adopted diamond PenTile technology for high resolution in mobiles.

**Keywords:** electro luminescence, pixel, pixel per inch, self-emission, thin film transistor.

### I.INTRODUCTION

ACTIVE Matrix Light Emitting diode is a display technology used in mobile as screen. AMOLED describes a specific type of display i.e., thin-film display technology in which organic compounds form the electroluminescent material, and active matrix refers to the technology behind the addressing of pixels. The basic principle behind the working of AMOLED is Electroluminescence. Electroluminescence (EL) is an optical phenomenon and electrical phenomenon in which a material emits light in response to the passage the electric current or by a strong electric field [1]. Electroluminescence is the result of excitation of electrons which releases their energy as photons which produce light [2]. For recombination, electrons and holes may be separated by doping the material to form a p-n junction (in semiconductor electroluminescent devices such as light-emitting diodes) or through excitation by impact of high-energy electrons accelerated by a strong electric field (as with the phosphors in electroluminescent displays) [3]. AMOLED has expresses pure colours when electric current stimulates the relevant pixels. The primary colour matrix is arranged in red, green and blue pixels which are mounted directly to print on board. By using specific colours can improves overall colour contrast. Active-matrix OLEDs (AMOLED) require a thin-film transistor as backplane to switch each and every individual pixel on or off. This layer of organic semiconductor material is situated between two electrodes. Generally, at least one of these electrodes is transparent. AMOLED used in mobiles phones, media players and digital

cameras [5]. OLEDs are light weight, durable, power efficient and ideal for portable applications. According to Samsung, Super AMOLED reflects one-fifth as much sunlight as the first-generation AMOLED. Super AMOLED is part of the Pen tile matrix family, sometimes abbreviated as SAMOLED [6][7].

### II.EXISTING METHOD

Super-AMOLED (Active-Matrix Organic Light-Emitting Diode) displays are AMOLED displays for mobile devices (such as smartphones, wearables) with an integrated touch function. Samsung's latest Super AMOLED displays adopt a new sub pixel arrangement called Diamond shaped Pixel by replacing the previous PenTile scheme. Modern PenTile OLED displays reach very high pixel densities Samsung are using PenTile for high-resolution (over 230 pixels per inch) OLED. In 2012, AMOLED technology used in mobiles, tv screen display and digital display cameras with low power. AMOLED display contains OLED pixel to generate light by integrated on a thin film transistor (TFT) array which controls electric flowing to each individual pixel. These TFT black plane technologies are polycrystalline silicon and amorphous silicon are used in AMOLED's. The first EL introduced by pope and coworker in 1963 from an organic molecule, anthracene and its thickness 10 $\mu$ m - 5mm when a bias of several hundred volts was applied across it. P. S. Vincent achieved bright blue EL from vacuum which was deposited by 0.6 $\mu$ m thickness and its anthracene crystal films applied with bias of less than 100V. The breakthrough was achieved by Tang and VanSlyke in 1987, he made a

bilayer structure by using thermally evaporating with the small molecular weight organic materials. In 1989, Tang developed a laser-dye doped Alq<sub>3</sub> multilayer structure, in which the fluorescent efficiency was increased and the emission color varied from the original green to the dopant emission color. As of 2008, AMOLED technology was used as screen in mobile phones, media players and digital cameras and they continued to make progress for low-power, low-cost. Super-AMOLED displays are AMOLED displays for mobile devices (such as smartphones, wearables) with an integrated touch function. Samsung's latest Super AMOLED displays adopt a new sub pixel arrangement called Diamond shaped Pixel by replacing the previous PenTile scheme. Modern PenTile OLED displays reach very high pixel densities. Samsung are using PenTile for high-resolution (over 230 pixels per inch) OLED. In January, it was reported that Samsung will adopt a new sub pixel scheme that uses diamond sub-pixels.

### III. PROPOSED METHOD

Super AMOLED is Samsung's own version of AMOLED display which is enhanced for a better output [9]. With Super AMOLED display, a phone can be thinner, consume less battery and offer higher contrast and better touch sensitivity among other benefits. Super-AMOLED is identical to AMOLED. Thus, these two technologies are same but there is only one difference in the layer that detects touch called the digitizer or also known as capacitive touchscreen layer. SAM AMOLED is embedded directly into the screen, whereas the entirely separate layer in AMOLED display i.e., on top of the screen [3]. Super-AMOLED displays carry many benefits over AMOLED displays because of the way these layers are designed:

- The device is thinner because the technologies for display and touch are on the same layer.
- Higher contrast, plus the lack of an air gap between the digitizer and the actual screen, yield a crisper with more high vivid display.
- Less power supply is needed for Super-AMOLED screen because it doesn't generate heat as much as older screen technologies. This is due to because the pixels are turned on and off directly therefore not emitting light using power when displaying black.
- The screen is more sensitive to touch.

- Because of many layers light reflection is reduced it makes reading outdoors in bright light easier.
- A higher refresh rate helps to speed up the response time.

### PenTile Technology

PenTile (pen means five) matrix is a family of patented sub-pixel matrix schemes used in electronic device displays and also PenTile is a trademark of Samsung. These subpixel are embedded in the display driver, allowing plug and play compatibility with conventional RGB (Red-Green-Blue) stripe panels. The blue sub-pixel is lower luminous efficiency than the red and green sub-pixels. so, the blue sub-pixels need high current which results faster degradation compared to the red and green sub-pixels. By using PenTile layout can reduce the number of sub-pixels which are needed to create a specified resolution. Most PenTile displays use rectangular grids of alternating green and blue/red pixels. But now Samsung using Diamond Pixel which will give high resolution. In a Diamond Pixel display, there are twice as many green sub-pixels as there are blue and red ones, and the green sub-pixels are oval and small while the red and blue ones are diamond-shaped and larger (the blue sub-pixel is slightly larger than the red one). The diamond shapes were chosen because the sub-pixel packed maximum to achieve the highest possible PPI. The greens are oval shaped because they are squeezed between the larger red and blue ones because green is most efficient OLED emitter when compared to blue which has shortest lifetime.

### TFT and SUPER AMOLED:

TFT (Thin Film Transistor) is used in displays in AMOLED. Super AMOLED technology is more expensive and is used only in high-end flagships, offering a number of benefits. This display technology is more bright and vivid colours and also great battery efficiency with wide viewing angles when lighter displays. Each pixel in the display brighter with less power because it doesn't generate as much heat as older screen technologies. The screen is more sensitive to touch and light reflection is reduced because there aren't as many layers, which makes reading outdoors in bright light easier and also addresses the former's sunlight reflection downside by lowering it to 80%. In effect, it produces brighter and more vivid display regardless of external light intensity [1].

**TABLE 1.COMPARISON OF PARAMETERS**

Display technique	OLED	AMOLE	SAM AMOLED
Technological type	Self-emission of light	Self-emission of light	Self-emission of light
Resolution	4,800 x 3,840	720 x 1280 pixels	1080*2220
Viewing angle	Good	V good	Super good
PPI	1,443PPI	16:9 ratio	18.5:9 ratio (441 PPI)
refresh rate	120Hz	Medium	Higher than AMOLED

**IV.ADVANTAGES AND DISADVANTAGES**

- **Faster:** SAM AMOLED has much better response time than other displays. So, these screens provide us better user experience. By this advantage SAM AMOLED screens in mobile phones
- **High contrast ratio:** High contrast ratio is another advantage of SAM AMOLED
- **Overall display quality:** With deep blacks combined with high contrast then the images displayed on panel are brighter and more vivid than other display techniques.
- **Large Viewing Angle:** Viewing angle is always problem in flat screens but by using SAM AMOLED displays, viewing angle is large than 170 degree because they produce their own light to increases their viewing angle.
- **Flexible:** Today we are getting displays which can bend. This is possible only through SAM AMOLED screens.
- **Durability:** Another advantage of SAM AMOLED is that it is more durable than traditional screens. Their chance of getting broken is comparatively less to LCD screens and other displays.
- **Good for Eyes:** SAM AMOLEDs are eye smoothening. These screens provide better viewing experience because they have high contrast, brightness and color aspects.

**DISADVANTAGES**

- Cost is more

**V.APPLICATIONS**

- The SAM AMOLED are basically used in the touch screens of mobile phones and also used in computers, netbooks, tablet pc.

- AMOLED technology is already made near to eye display like “virtual images” When projected on a head mounted or helmet mounted display, such image appears like an image in a movie theatre or on a computer monitor, but these are very small display near to the eye. Such an image displayed with very high resolution and contract.
- These are used as flat screens in television[2].

**VI.CONCLUSION**

Super Active matrix organic light-emitting diode displays have been considered as potential for the next generation. The flat panel displays of SAM AMOLED in providing wider viewing angle, larger colour gamut by using PenTile technology. These efficiently used in mobile displays. SAM AMOLED continues to make progress towards low power. The screen is more sensitive to touch and higher refresh rate helps speed up the response time.

**VII. FUTURE SCOPE**

Samsung is doing best and developing several next generation display technologies based on OLEDs for display in mobiles, television screen and tab etc. Now Samsung has been developing a foldable OLED device for a long time which may dramatically change in market. The display screen is more sensitive to touch with high resolution. Samsung currently putting a fingerprint sensor, speaker (Sound on Display) and also Haptic capabilities. That increased speed makes ideal for larger, with higher definition display.



Fig.1. Future display of foldable OLED device

## REFERENCES

1. Landauer, Rolf, "Irreversibility and heat generation in the computing process," IBM Journal of Research and Development ,vol.44, no.1.2, pp.261,269, Jan. 2000 doi: 10.1147/rd.441.0261
2. Bennett, C.H., "Logical Reversibility of Computation," IBM Journal of Research and Development , vol.17, no.6, pp.525,532, Nov. 1973doi: 10.1147/rd.176.0525
3. B, Raghu Kanth; B, Murali Krishna; G, Phani Kumar; J, Poornima,"A Comparative Study of Reversible Logic Gates", International Journal of VLSI & Signal Processing Applications, vol.2, Issue 1, Feb 2012, (51- 55), ISSN 2231-3133 ( Online ).
4. Morrison, M.; Ranganathan, N., "Design of a Reversible ALU Based on Novel Programmable Reversible Logic Gate Structures," VLSI (ISVLSI), 2011 IEEE Computer Society Annual Symposium on , vol., no., pp.126,131, 4-6 July 2011doi: 10.1109/ISVLSI.2011.30.
5. Nachtigal, M.; Thapliyal, H.; Ranganathan, N., "Design of areversible single precision floating point multiplier based on operand decomposition," Nanotechnology (IEEE-NANO), 2010 10<sup>th</sup> IEEE Conference on , vol., no., pp.233,237, 17-20 Aug. 2010.
6. John P. Hayes, "Computer Architecture and Organization", McGraw-Hill, 1998. ISBN 10: 0070273553 / ISBN 13:9780070273559
7. Min-Lun Chuang; Chun-Yao Wang, "Synthesis of Reversible Sequential Elements," Design Automation Conference, 2007.ASPDAC'07. Asia and South Pacific , vol., no., pp.420,425, 23-26 Jan.2007 doi: 10.1109/ASPAC.2007.358022
8. Yelekar, P.R.; Chiwande, S.S., "Design of sequential circuit using reversible logic," Advances in Engineering, Science and Management (ICAESM), 2012 International Conference on , vol.,no., pp.321,326, 30-31 March 2012
9. N. Raj and R. K. Sharma, "A High Swing OTA with wide Linearity for design of Self Tuneable Resistor", International Journal of VLSI design & Communication system (VLSICS), Volume 1, No. 3, pp. 1-11, 2010.
10. J N. Raj, A.K. Singh, A.K. Gupta, "Modeling of Human Voice Box in VLSI for Low Power Biomedical Applications", IETE Journal of Research, Vol. 57, Issue 4, pp. 345-353, 2011.
11. N. Raj, A.K. Singh, and A.K. Gupta, "Low power high output impedance high bandwidth QFGMOS current mirror", Microelectronics Journal, Vol. 45, No. 8, pp. 1132-1142, 2014.
12. N. Raj, A.K. Singh, and A.K. Gupta, "Low-voltage bulk-driven self-biased cascode current mirror with bandwidth enhancement", Electronics Letters, Vol. 50, No. 1, pp. 23-25, 2014.
13. N. Raj, A.K. Singh, and A.K. Gupta, "Low Voltage High Output Impedance Bulk-driven Quasi-floating Gate Self-biased High-swing Cascode Current Mirror", Circuit System & Signal Processing Journal, Vol. 35, No. 8, pp. 2683-2703, 2015.
14. N. Raj, A.K. Singh, and A.K. Gupta, "High performance Current Mirrors using Quasi-floating Bulk", Microelectronics Journal, Vol. 52, No. 1, pp. 11-22, 2016.
15. N. Raj, A.K. Singh, and A.K. Gupta, "Low Voltage High Performance Bulk-driven Quasi-floating Gate Self-biased Cascode Current Mirror", Microelectronics Journal, Vol. 52, No. 1, pp. 124-133, 2016.
16. N. Raj, A.K. Singh, and A.K. Gupta, "Low Voltage High Bandwidth Self-biased High Swing Cascode Current Mirror", Indian Journal of Pure and Applied Physic, Vol. 55, No. 4, pp. 245-253, 2017.
17. Raj N. and Gupta A. K., "Analysis of Operational Transconductance Amplifier using Low Power Techniques", Journal of Semiconductor Devices and Circuits (STM Journal), Vol. 1, No. 3, pp. 1-9, 2015.
18. Raj N. and Gupta A. K., "Multifunction Filter Design using BDQFG Miller OTA", Journal of Electrical and Electronics Engineering: An International Journal (EEEIJ Journal), Vol. 4, No. 3, pp. 55-67, 2015.
19. N. Raj, A.K. Singh, and A.K. Gupta, "Low Power Circuit Design Techniques: A Survey", International Journal of Computer Theory and Engineering, Vol. 7, No. 3, pp. 172-176, 2015.

# THE FinFET TECHNOLOGY

B.SAMATHA<sup>1</sup> & Dr .R.PURUSHOTHAM NAIK<sup>2</sup> & Y.ROJA RANI<sup>3</sup>

M.Tech(ES & VLSI)<sup>1,3</sup> , Associate Professor<sup>2</sup>

Department of ECE, Malla Reddy College Of Engineering, Hyderabad, INDIA.

**ABSTRACT:** The Integrated Circuit(IC) is become an integral part in all aspects of Industrial growth and modifying Its Characteristics as per updated technology. The semiconductor industries are emerging with new ideas which goes beyond the Moore's law predictions which predicted that "The number of transistor per chip would quadruple for every three years". But this "Physical law" does not hold forever and gave a final conclusion that "another metric will be needed to chosen to allow the future trend to be mapped and predicted". Even the Moore's law was very old Prediction, Most of the industries comparing the its standards with it .Now a days ,Transistor Technology is going towards the low technology node the reason is there is shrinking the transistor size, automatically its driving performance will be improved. So, this paper is discussing on the new proposed technology architectures of Dual gate and tri gate MOSFET.

**Keywords:** Transistors, Bulk MOSFET,FD- Silicon On Insulator(SOI),3DLithography, High dielectric spacer material/Metal. Gate

## I.INTRODUCTION

### 1. History of Transistor

In view of difficulty in Planar CMOS Technology scaling to preserve an acceptable Gate to Channel control Fin FET Multi gate Devices have been proposed as a Technology option For replacing existing Technology. As devices shrink further, the problems with conventional (planar) MOSFETs are on rise. The electronic industries are designing the chip with a perfect logic and finishing up with fabrication verification tests. But , the major concerns lies in the patterning the wafer(Substrate) as per the requirement that The research in technology of Field Effect Transistor has began several centuries ago[1],[2]. Even the name is given as Transistor, several war time efforts was made for the device to show its originality at the times of "developing age" of Technology. Transistor was named as Surface states Triode, Semiconductor Triode, Crystal Triode, Solid Triode and lotatron prior to the name given as Transistor by John r Pierce. At present , the designing the circuit was made easy by utilizing the resources available to us. So one could imagine ,how old the roots of transistor Technology is and how many inventions and efforts made by the scientists at those times had still stood behind the Ancient Techniques.

1. Prior to the invention of Transistors, there are
2. Devices existed which are 30-40 years ago before the Transistor was invented.
3. The research in technology of Field Effect Transistor has began several centuries ago.

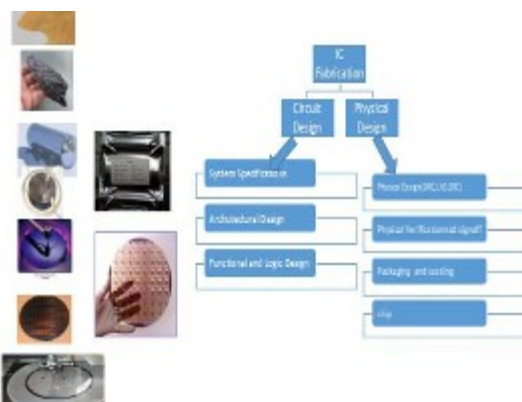


Fig.1. Evolution of Transistor Technologies

At present ,the designing the circuit was made easy by utilizing the resources available to us. So one could imagine how old the roots of transistor Technology is and how many inventions and efforts made by the scientists at those times.

### Methods of designing a chip:

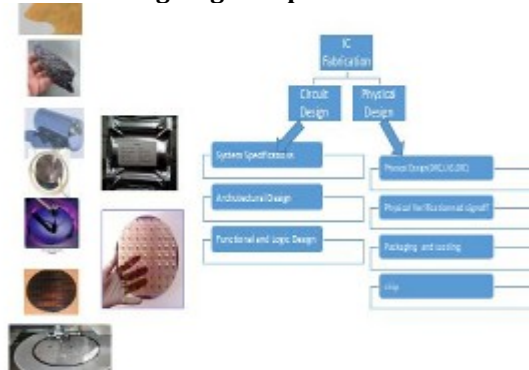


Fig.2. IC Chip Fabrication

A circuit/design which is used in any domain pertained to some common strategies like low cost, high speed, low power consumption, less heat dissipation, small area. In the science, what are scaling issues in Bulk MOSFETS and how they are minimized by using accessed technology like Fin FET[3].

They are given by:

- 1.Short Channel Effect
- 2.Input Thresh hold voltage
- 3.Leakage current.
- 4.DIBL & GIBL
- 5.Hot Carrier Injection(HCI).
- 6.Thermal stability and
- 7.Floating Body Effect

**II.PROPOSED TECHNOLOGY**

In this paper, we are discussing novel device architectures like SOI Tri gate MOSFET with

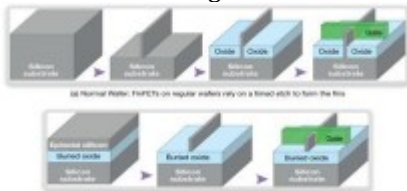


Fig.3. (a).Bulk SOI and Fig(b) Tri gate Fin FETSOI

**Electron Beam Lithography:**

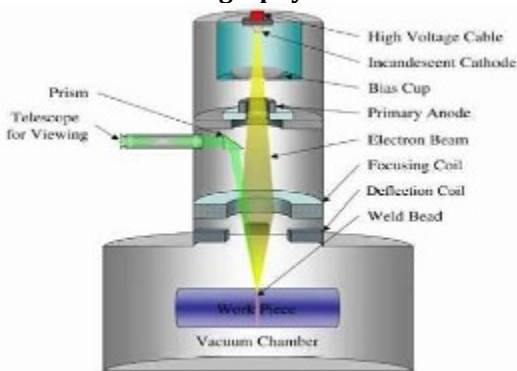


Fig.4.Electron Beam Lithographer

**Power Consumption: 50 to 200 kV, 10<sup>4</sup> kW/mm**

- 1.The next generation Extreme Ultraviolet Ray  $\lambda=13\text{nm}$ ,but this is not going to intersect with 7nm or 10 nm.But the nodes like 45nm, 32nm, 22nm are convenient for the Industries lithography cost is favourable to them.
- 2.But they can't ready to go beyond 22nm.
- 3 .Now the Question is how the industries print the node that is possible with the given lithography.

4. So that technique is called “double patterning technique” which enables future technology node[4].

**Silicon On Insulator(SOI):**

**Fabrication Method:** SIMOX (Separation by implantation of Oxygen).

**Process:**

FD-SOI, is a planar process technology that delivers the benefits of reduced silicon geometries while actually simplifying the manufacturing process.

1. **Initial Silicon:** Wafer A, Wafer B

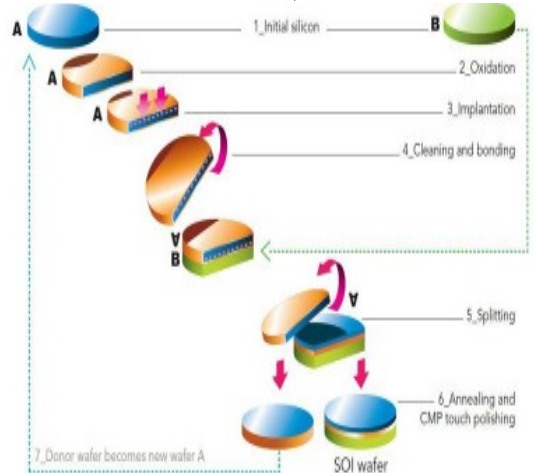


Fig.5.SIMOX method

2. **Oxidation:** Adding molecules, the opposite process to reduction

**Subtractive Fin Method:**

(Etching Silicon into the Fin)

1. Photo Resist material:Silicon Nitride
2. Hard mask: Amorphous Silicon.
3. If we use SiN ,then we don't use top surface of fin for current conduction act as a Bulk Fin FET
4. If we decide to remove Hard Mask, it is commonly forms a Trigate SOI Fin fet

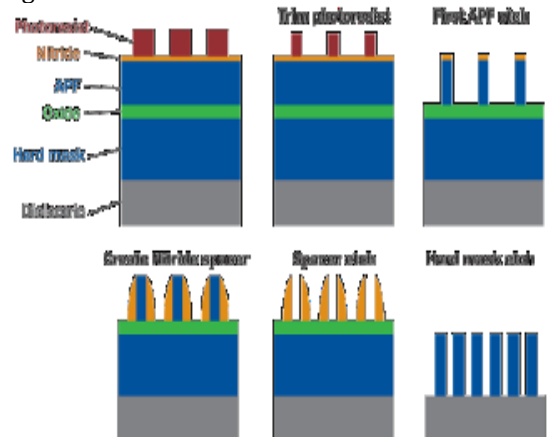


Fig.6. Subtractive Fin Method (Etching fin into silicon)

**High k, Low k Gate materials/Dual k spacers:**

1.Dielectric Constant(k):“It is defined as physical measure of how easily a material can be affected by external electric field”

2.One of the key issues concerning new gate dielectrics is the low crystallization temperature.

3.In planar MOSFETS, we use SiO<sub>2</sub> as insulating dielectric.

4.So, we are chosen for other high k dielectric materials to avoid problems like “Thermal Runaway”[5].

**Dielectric Classification:**

- Dielectric constant of SiO<sub>2</sub> is K=3.9.
- High k Materials:“The materials with k>3.9 are called High k materials
- Examples: N(Nickel), Si(silicon), Al(aluminium), Ta and La have been incorporated into the high-k gate dielectrics, especially HfO<sub>2</sub>-based oxides
- Low K materials:“The materials with K<3.9 are called Low k materials

**Dual K Spacers:**

In This paper ,using HFO<sub>2</sub>/Al<sub>2</sub>O<sub>3</sub> can as dielectric spacer. The reason is given in the

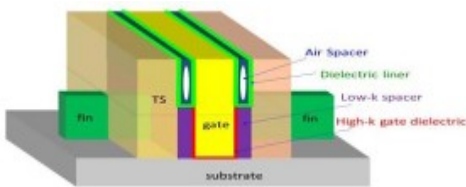


Fig.7. Dielectric and high k gate in Fin FET

The best characteristics of High k material dielectric should have

1. High dielectric constant,
2. large band gap with a favorable band alignment,
3. low interface state density and
4. A good thermal stability.

**High k material is of two types:**

1.Inner High k Spacer(L sp, h k)=HFO<sub>2</sub>

2.Lower High Spacer(L sp, l k)=SiO<sub>2</sub>

High k spacer HFO<sub>2</sub> is introduced for minimizing Tunnelling and for good electric field production then why we introduced l dielectric spacer

**Reason:**

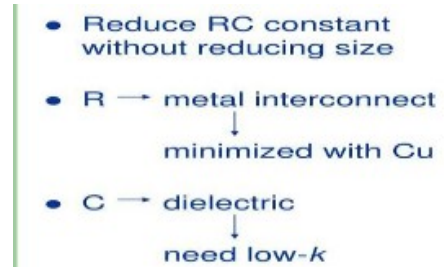
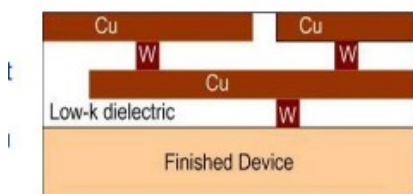


Fig.8.Dual K Spacer

**1.Symmetric Dual K Spacer**

The devices in which the same apply voltage is applied to Entire device

**2.Asymmetric Dual K Spacer**

1. The Devices in which Different Voltage levels can be applied to on a single device

2. Improve the cutoff frequency ( $f_T$ ) and maximum oscillation frequency ( $f_{max}$ ), given the significant reduction of inner fringe capacitance towards drain side.

3. It is due to the shifting of the drain extension’s doping concentration away from The gate edge.

4. Therefore, the asymmetric drain extension Dual -k tri gate Fin FET (AssymmetricDual -k) is a new structure that combines different Dual-k spacers on the source and drain and asymmetric drain extension on a single silicon on insulator (SOI) platform to enhance the almost all analog/RF FOM[6].

**Example: FPGA board**

The Dual k spacer is an attempt to control lateral spread of the electric electric field at gate sidewalls.

Too high or too low high k dielectric is not a correct choice for alternate gate dielectrics.

**Different FinFET Structures:**

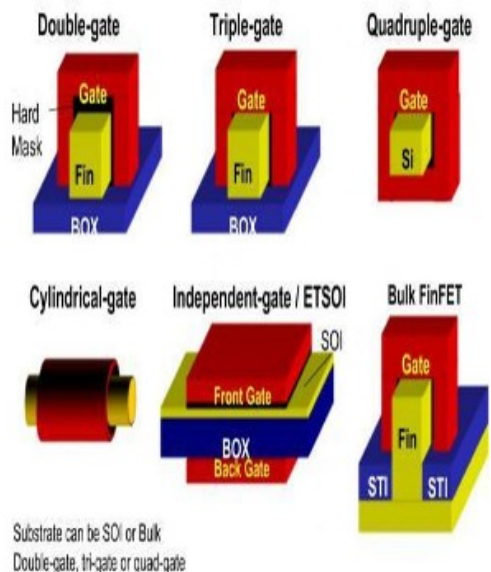


Fig.9. Different FinFET STRUCTURES

**TABLE 1. SPECIFICATIONS OF DIELECTRIC SPACERS FOR FinFET:**

Zirconium Silicate	12
Hafnium silicate	15
Lanthunum Oxide(La2o3)	20-30
Halfnium Oxide	40
Zirconium Oxide(ZrO2)	25
Cesium Oxide (CeO2 )	26
Bismuth Silicon Oxide (Bi4Si2o12)	35-75
Titanium Oxide(TiO2)	30

**III.GENERAL AND V-I CHARACTERISTICS SOI Tri gate FinFET:**

**(a)Sub Threshold Slope:** Sub threshold slope or swing is an important parameter reveals how better the device functions as a switch. The lower the value of SS, the more efficient and rapid the switching speed of the device from[6] the off state to the on state.

Sub thresh hold slope=63.7591 m v/Decade

**(b)Drain to Source Current (Id sat):**

There is an increase in Id sat for SOI TRI-GATE Fin FET when we use High-k dielectric”

**(c)Aspect Ratio (AR) Of Fin:**

$AR = H_{fin} / w_{fin}$

Narrow Fins ensures better SCE immunity. Reduced Paracitic capacitance.

**(d)Fin Width:**

LER, Interface roughness varies with W fin, T ox Variation can be larger if Transistor size less than an atom.

(Effects wavelength and pattern Lithiography . Gm decreases with increase in fin width).

**(e)Effective Oxide Thickness (EOT):**

If Gate thickness is smaller than the dielectric thickness there could be no chance for high leakage current.

**(f)Drain Source off Current (I off):**

One of the biggest challenges faced by MOSFET scaling is high value of off state current or high leakage current resulting in high power consumption. As we use dielectric which can hold sufficient charge which reduces leakage current there by reducing I off current[1].

**SOI Tri Gate FinFET(Input Threshold Voltage)**

- 1.TiN / 1nm

Al2O3/0.8nm SiO2Stack

$V_{th} = 0.304175$

1. TiN/2nm

HFO2/0.8nm SiO2 Stack

$V_{th} = 0.309925V$

2. Tin/3nm

La2O3/0.8nm SiO2 Stack

$V_{th} = 0.312169V$

**IV. COMPARISION BETWEEN FDSOI AND FinFET**

Characteristics	FD SOI	FinFET on Bulk
Performance Metrics	Better	10 % lower performance
Power Metrics	Betterr	100 mv Higher supply Increased variability
Low Power Features	Ultra Powerful Body Biasing Efficient Multiple	Nobody biasing Low efficiency multiple Vt
Design Compatibility	Easy SOC migration from Bulk	New Technology Implementati
Process Integration	Process Integration simple	Complex isprocess

**V. ADVANTAGES OF FinFET**

1. Thresh Hold voltage is controlled without use of heavy doping.
2. Raised Source and Drain on SOI to reduce parasitic capacitance.
3. Good Electro Static Control.
4. The main advantage is Gate burden
5. Over Source and Drain Channels Reduced
6. An ultra thin silicon fin for suppression of ShortChannel Effect.

**VI. APPLICATIONS OF ASSYMMETRIC 8T SRAM FinFET**

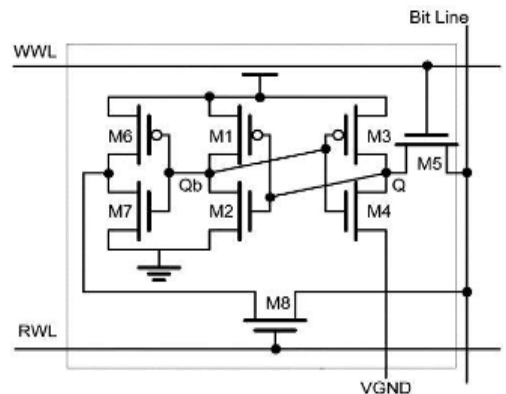


Fig.10. Schematic of a single-ended 8T SRAM cell with asymmetrical cell VGND biasing

SRAM Asymmetric dual structures helps in

1. Maintaining SNM (Static Noise Margin)
2. Adjusting Pull up Ratio Cells Ratio

**TABLE2. CONVENTIONAL 6T SRAM AND FinFET SRAM**

Parameters	Conventional 6T SRAM		FinFET based 6T SRAM	
	Write	Read	Write	Read
Technology	45nm	45 nm	45 nm	45nm
Supply	700 mv	700 mv	700 mv	700 mv
Leakage Current	69 Amps	55Am ps	69Am ps	53Am ps
Leakage Power	7.3 nW	1.7 W	7.5 nW	1.7 W
Delay	20.57 ns	21.7n s	20.55 ns	21.44 ns

**VII. CONCLUSION**

The Transistor Technology has efficient even though the devices shape and parameters are changed by different fabrication steps[9]. The Shrinking technology nodes makes Transistor Technologies more beneficial to future generations.

**VIII. FUTURE SCOPE**

**Extending FinFETS**

Fin FET are on way to modify its characteristics in form of Carbon Nano Tubes. That means we have Silicon channel in form of Tiny Nano wires.

**Structure of Carbon Nanotube Transistor**

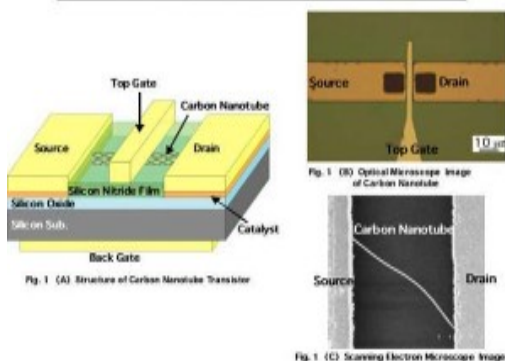


Fig.11. Carbon Nano tube FinFETS

**IX. REFERENCES**

1. Reference: IEEE Prime Asia conference <https://meetings.vtools.ieee.org>
2. Silicon on Insulator Technology(SIMOX) method fabrication. <https://teknogenius.blogspot.com>

3. <https://www.youtube.com> Photo mask lithography for EUV era
4. <https://www.intel.com> High-k, Quantum Mechanical Tunneling and Gate Leakage
5. <https://jnep.sumdu.edu.ua> voltage, current specifications
6. <https://patents.google.com>Dielectrics spacer materials and their relative permiaibilities
7. <https://www.techdesignforums.com/practice/files/2013/05/tdf-snpvff-fdsoi-3lrg.jpg>
8. <https://image.slidesharecdn.com/> / Fin FET Fabrication
9. [https://www.google.co.in/amp/s/www.researchgate.net/post/How\\_are\\_dielectrics\\_classified\\_as\\_high-K\\_and\\_low-K/amp](https://www.google.co.in/amp/s/www.researchgate.net/post/How_are_dielectrics_classified_as_high-K_and_low-K/amp)
10. <http://image.slideserve.com/219809/> Why - low-k-dielectrics are used
11. N. Raj and R. K. Sharma, "A High Swing OTA with wide Linearity for design of Self Tuneable Resistor", International Journal of VLSI design & Communication system (VLSICS), Volume 1, No. 3, pp. 1-11, 2010.
12. N. Raj, A.K. Singh, A.K. Gupta, "Modeling of Human Voice Box in VLSI for Low Power Biomedical Applications", IETE Journal of Research, Vol. 57, Issue 4, pp. 345-353, 2011.
13. N. Raj, A.K. Singh, and A.K. Gupta, "Low power high output impedance high bandwidth QFGMOS current mirror", Microelectronics Journal, Vol. 45, No. 8, pp. 1132-1142, 2014.
14. N. Raj, A.K. Singh, and A.K. Gupta, "Low-voltage bulk-driven self-biased cascode current mirror with bandwidth enhancement", Electronics Letters, Vol. 50, No. 1, pp. 23-25, 2014.
15. N. Raj, A.K. Singh, and A.K. Gupta, "Low Voltage High Output Impedance Bulk- driven Quasi-floating Gate Self-biased High-swing Cascode Current Mirror", Circuit System & Signal Processing Journal, Vol. 35, No. 8, pp. 2683-2703, 2015.
16. N. Raj, A.K. Singh, and A.K. Gupta, "High performance Current Mirrors using Quasi-floating Bulk", Microelectronics Journal, Vol. 52, No. 1, pp. 11-22, 2016.
17. N. Raj, A.K. Singh, and A.K. Gupta, "Low Voltage High Performance Bulk-driven Quasi-floating Gate Self-biased Cascode Current Mirror", Microelectronics Journal, Vol. 52, No. 1, pp. 124-133, 2016.
18. N. Raj, A.K. Singh, and A.K. Gupta, "Low Voltage High Bandwidth Self-biased High Swing Cascode Current Mirror", Indian Journal of Pure and Applied Physic, Vol. 55, No. 4, pp. 245-253, 2017.
19. Raj N. and Gupta A. K., "Analysis of Operational Transconductance Amplifier using Low Power Techniques", Journal of Semiconductor Devices and Circuits (STM Journal), Vol. 1, No. 3, pp. 1-9, 2015.

20. Raj N. and Gupta A. K., "Multifunction Filter Design using BDQFG Miller OTA", Journal of Electrical and Electronics Engineering: An International Journal (EEEEJ Journal), Vol. 4, No. 3, pp. 55-67, 2015.
21. N. Raj, A.K. Singh, and A.K. Gupta, "Low Power Circuit Design Techniques: A Survey", International Journal of Computer Theory and Engineering, Vol. 7, No. 3, pp. 172-176, 2015.

## DESIGN OF BUS TRACKING AND FUEL MONITORING SYSTEM

Vasam shirisha & Dr. P. John Paul

PG Schalar, Professor

Department of ECE, Malla Reddy College Of Engineering, Hyderabad, Telangana, INDIA.

**ABSTRACT:** In today's world, actual record of fuel filled and fuel consumption in vehicles is not maintained. It results in a financial loss. To avoid this we are implementing a microcontroller based fuel monitoring and vehicle tracking system. In this paper, the implementation of embedded control system based on the microcontroller is presented. The embedded control system can achieve many tasks of the effective fleet management, such as fuel monitoring, vehicle tracking. Using GPS vehicle tracking technology Fuel monitoring have been the major problem that most of bus companies looking to solve. This paper developed a bus tracking and monitoring the fuel and speed system to provide a facility for the management requirements by the administrator using GPS and GSM Technology.

**Keywords:** microcontroller, GPS, GSM, fuel level indicator.

### I. INTRODUCTION

The challenges of successful fuel monitoring involve efficient and specific design, and a commitment to implementation of the monitoring project, from data collection to reporting and using results. Tracking is the use of GPS technology to identify, locate and maintain contact reports with one or more fleet vehicles. Implementing real-time vehicle tracking as part of a commercial company's mobile resource management policy is essential for comprehensive operational control driver security and fuel savings. Rising fuel costs constantly challenge fleet operators to maintain movement of vehicles and monitor driver behavior to avoid delaying traffic conditions by either, combining deliveries, reconfiguring routes or rescheduling timetables. This aims to maximize the number of deliveries while minimizing time and distance Fuel monitoring system help the administrator to know the exact amount of fuel content of the bus, so fuel theft could be avoided and administrator could maintain the fuel more efficiently. In addition to that alcohol breath of the driver to sense whether he has drunken or not.



Vehicle tracking system

The design and development of a vehicle tracking and fuel monitoring system especially useful for mining in real-time has been reported in this paper. The system principally monitors vehicle moving and tracking such as position, and speed and subsequently identifies alcohol detection. A lot of vehicle theft occur and accident due to over speed, alcohol drunken by driver .GPS is increasingly being used in vehicle tracking and monitoring services. To resolve the problems like avoid speed and collision, traffic jams ARM processor based vehicle monitoring is implemented as well providing information for the vehicle owner. The system has been designed for ARM processor vehicle tracking and

monitoring will provide effective and real time vehicle location using GPS and GSM. A GPS based vehicle tracking will inform where you vehicle is and where it has been and how long it has been. The system uses geographic positions and time information from the global Positioning Satellites. The system has on board which resides in the vehicle to be tracked and a Base Station that monitor data from the various vehicles.

### BLOCK DIAGRAM

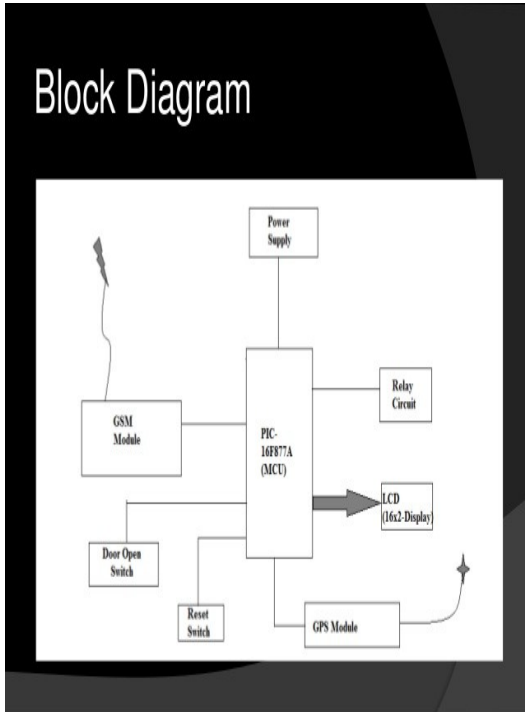


Fig. System block diagram System Overview

### Power Supply:

This section is meant for supplying Power to all the sections mentioned above. It basically consists of a Transformer to step down the 230V ac to 9V ac followed by diodes. Here diodes are used to rectify the ac to dc. After rectification the surface level of nearly any fluid, including water, saltwater, and oils.

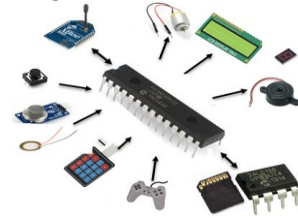
### IV. CONCLUSION

This paper offers a smart design of tracking and monitoring and fuel monitoring system which helps the bus companies to provide high quality of service. This design can provide the location of the busses etc. of the service with an error less than 10m in the case of slow speed and clear environment and the system give the accurate arrival time of the bus and provide the location of the bus in Google map for both user and administrator. This system reduces the waiting time of remote users for bus and provides

bus tracking at any location, management and fuel monitoring obtained rippled dc is filtered using a capacitor Filter. A positive voltage regulator is used to regulate the obtained dc voltage.

### Microcontroller:

This section forms the control unit of the whole project. This section basically consists of a Microcontroller with its associated circuitry like Crystal with capacitors, Reset circuitry, Pull up resistors (if needed) and so on. The Microcontroller forms the heart of the project because it controls the devices being interfaced and communicates with the devices according to the program being written.



### LCD Display:

This section is basically meant to show up the status of the project. This project makes use of Liquid Crystal Display to display / prompt for necessary information.

### GPS modem:

A GPS modem is used to get the signals and receive the signals from the satellites. In this project, GPS modem get the signals from the satellites and those are given to the microcontroller. The signals may be in the form of the coordinates; these are represented in form of the latitudes, longitudes and altitudes.



### GSM modem Section:

This section consists of a GSM modem. The modem will communicate with microcontroller using serial communication. The modem is interfaced to microcontroller using MAX 232, a serial driver. The Global System for Mobile Communications is a TDMA based digital wireless network technology that is used for communication between the cellular devices. GSM phones make use of a SIM card to identify the user's account.

### Fuel level indicator:

The sensor used for measurement of fluid levels is called a level sensor. The sensing probe element

consists of a special wire cable which is capable of accurately sensing.



## REFERENCES

- [1] J. C. Williams, "2012 Sleep in America poll: Transportation workers 'sleep,'" Nat. Sleep Foundation, Arlington, VA, USA, Tech. Rep., 2012.
- [2] T. A. Ranney, E. Mazzae, R. Garrot, and M. J. Goodman, "NHTSA driver distraction research: Past, present, and future," Nat. Highway Traffic Safety Admin., East Liberty, OH, USA, Tech. Rep., 2000.
- [3] R. N. Khushaba, S. Kodagoda, S. Lal, and G. Dissanayake, "Driver drowsiness classification using fuzzy wavelet-packet-based feature extraction algorithm," *IEEE Trans. Biomed. Eng.*, vol. 58, no. 1, pp. 121–131, Jan. 2011.
- [4] Y. Liang, M. L. Reyes, and J. D. Lee, "Realtime detection of driver cognitive distraction using support vector machines," *IEEE Trans. Transp.Syst.*, vol. 8, no. 2, pp. 340–350, Jun. 2007.
- [5] R. I. Hammoud, G.Witt, R. Dufour, A. Wilhelm, and T. Newman, "On driver eye closure recognition for commercial vehicles," *SAE Int. J. Commercial Veh.*, vol. 1, no. 1, pp. 454–463, Apr. 2009.
- [6] T. Moriyama, T. Kanade, J. Xiao, and J. F. Cohn, "Meticulously detailed eye region model and its application to analysis of facial features," *IEEE Trans. Pattern Anal. Mach. Intell.*, vol. 28, no. 5, pp. 738–752, May 2006.
- [7] Y. Dong, Z. Hu, K. Uchimura, and N. Murayama, "Driver inattention monitoring system for intelligent vehicles: A review," *IEEE Trans.Transp. Syst.*, vol. 12, no. 2, pp. 596–614, Jun. 2011.
- [8] D. DeMenthon and L. S. Davis, "Modelbased object pose in 25 lines of code," *Int. J. Comput. Vis.*, vol. 15, no. 1/2, pp. 123–141, Jun. 1995.
- [9] B. D. Lucas and T. Kanade, "An iterative image registration technique with an application to stereo vision," in *Proc. Int. Joint Conf. Artif. Intell.* 1981, pp. 674–679.
- [10] J. Shi and C. Tomasi, "Good features to track," in *Proc. IEEE Conf.Comput. Vis. Pattern Recognit.*, 1994, pp. 593–600.
- [11] G. G. Slabaugh, "Computing Euler angles from a rotation matrix," City Univ. London, London, U.K., Tech. Rep., 1999.
- [12] M. La Cascia, S. Sclaro, and V. Athitsos, "Fast, reliable head tracking under varying illumination: An approach based on registration of texture mapped 3D models," *IEEE Trans. Pattern Anal. Mach. Intell.*, vol. 22, no. 4, pp. 322–336, Apr. 2000.
- [13] N. Raj and R. K. Sharma, "A High Swing OTA with wide Linearity for design of Self Tuneable Resistor", *International Journal of VLSI design & Communication system (VLSICS)*, Volume 1, No. 3, pp. 1-11, 2010.
- [14] N. Raj, A.K. Singh, A.K. Gupta, "Modeling of Human Voice Box in VLSI for Low Power Biomedical Applications", *IETE Journal of Research*, Vol. 57, Issue 4, pp. 345-353, 2011.
- [15] N. Raj, A.K. Singh, and A.K. Gupta, "Low power high output impedance high bandwidth QFGMOS current mirror", *Microelectronics Journal*, Vol. 45, No. 8, pp. 1132-1142, 2014.
- [16] N. Raj, A.K. Singh, and A.K. Gupta, "Low-voltage bulk-driven self-biased cascode current mirror with bandwidth enhancement", *Electronics Letters*, Vol. 50, No. 1, pp. 23-25, 2014.
- [17] N. Raj, A.K. Singh, and A.K. Gupta, "Low Voltage High Output Impedance Bulk- driven Quasi-floating Gate Self-biased High-swing Cascode Current Mirror", *Circuit System & Signal Processing Journal*, Vol. 35, No. 8, pp. 2683-2703, 2015.
- [18] N. Raj, A.K. Singh, and A.K. Gupta, "High performance Current Mirrors using Quasi-floating Bulk", *Microelectronics Journal*, Vol. 52, No. 1, pp. 11-22, 2016.
- [19] N. Raj, A.K. Singh, and A.K. Gupta, "Low Voltage High Performance Bulk-driven Quasi-floating Gate Self-biased Cascode Current Mirror", *Microelectronics Journal*, Vol. 52, No. 1, pp. 124-133, 2016.
- [20] N. Raj, A.K. Singh, and A.K. Gupta, "Low Voltage High Bandwidth Self-biased High Swing Cascode Current Mirror", *Indian Journal of Pure and Applied Physic*, Vol. 55, No. 4, pp. 245-253, 2017.
- [21] Raj N. and Gupta A. K., "Analysis of Operational Transconductance Amplifier using Low Power Techniques", *Journal of Semiconductor Devices and Circuits (STM Journal)*, Vol. 1, No. 3, pp. 1-9, 2015.
- [22] Raj N. and Gupta A. K., "Multifunction Filter Design using BDQFG Miller OTA", *Journal of Electrical and Electronics Engineering: An International Journal (EEEI Journal)*, Vol. 4, No. 3, pp. 55-67, 2015.
- [23] N. Raj, A.K. Singh, and A.K. Gupta, "Low Power Circuit Design Techniques: A Survey", *International Journal of Computer Theory and Engineering*, Vol. 7, No. 3, pp. 172-176, 2015.

# IMPLEMENTATION OF AUTOMATIC DRIVER DROWSINESS ALERT SYSTEM BY USING IOT

Suresh kumar Perumalla<sup>1</sup> & Vijaya Lakshmi Chintamaneni<sup>2</sup>

PG Scholor<sup>1</sup>, Assistant Professor<sup>2</sup>

Department of ECE, Malla Reddy College Of Engineering, Hyderabad, Telangana, INDIA.

**ABSTRACT:** Drowsiness is the reason for many of the road accidents. Manually tracing the drowsy driver isn't an easy task, as a result daily thousands of vehicles are running on the roads therefore we'd like a system that has to come back with each automotive and if it detects the sleepy headed driver it should stop the vehicle now. Additionally to the present if the driving force is slept the vehicle is stopped, and it monitors the heart-beat, Respiration rate and temperature of the driving force and displays it within the digital display. These 3 parameters are terribly important as a result of it shows the body standing of the driving force. These parameters are monitored manually and just in case of emergency the in-charge of the ward calls the doctor.

**Keywords:** LCD display, Temperature sensor, IR Sensor, Pulse Rate Sensor, ARM7 Microcontroller, and IOT (WIFI Module).

## I. INTRODUCTION

Driver sleepiness detection may be an automotive safety technology that helps forestall accidents caused by the driver obtaining drowsy. Varied studies have recommended that around 20% of all road accidents are fatigue-related, up to 50% on bound roads. Some of these systems learn driver patterns and might find once a driver is becoming drowsy. The development of technologies for detecting or preventing sleepiness at the wheel may be a major challenge within the field of accident shunning systems. Due to the hazard that sleepiness presents on the road, ways must be developed for counteracting its affects [4].

The aim of this project is to develop an epitome drowsiness detection system. The main target is going to be placed on coming up system which will accurately monitor the eye flicker rate, heart-beat breath rate and temperature of the driving force. In this project we tend to use sensors to live all these factors. The values measured are going to be sent to the microcontroller wherever the measured values are going to be compared with the reference values. If the values measured don't match with the reference values then the microcontroller can send a signal within the LCD show thereby preventing accidents.

## II. PROPOSED DROWSINESS ALERT UNIT

This is a little system; therefore we will simply plant it on any vehicle. The attention blink detector is fastened to the driving force. The eye blink detector senses the movement of the eyeball.

The detector output is connected to a microcontroller. The automotive engine beginning system is directly controlled by the microcontroller. If the detector detects no output from the detector, as a result there is no movement within the eyeball; it sends the signal to the microcontroller.

The microcontroller straightaway stops the engine or locks it from beginning conjointly offer warning signal and show the rationale in an exceedingly digital display [1].

The system is developed by interfacing a heartbeat sensor, IR sensor and temperature sensor with an ADC that converts the associate degree along readings to digital, thus extracted digital knowledge is processed employing a microcontroller [1]. The reference values of those 3 parameters and therefore the telephone numbers are kept within the microcontroller memory [2].

If anyone of those 3 parameter exceeds the reference price the microcontroller mechanically call the keep variety. The microcontroller used here is arm7 lpc2148, it has an inbuilt ADC and counters, and therefore the counter is employed to count heartbeat, respirator rate and ADC for changing analog temperature to digital.

**III.BLOCK DIAGRAM**

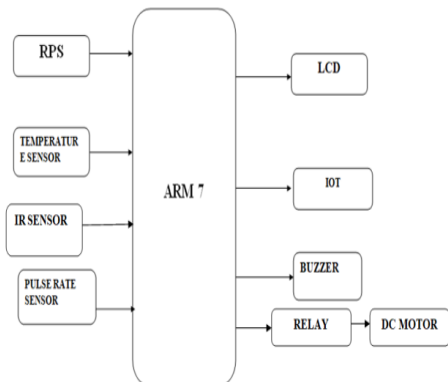


Fig1:project block diagram

**BLOCK DIAGRAM DESCRIPTION:**

**A. Regulated power supply**

Regulated power supply is an electronic circuit that's designed to provide constant DC voltage of predetermined value across load terminals irrespective of AC main fluctuations or load variations

Regulated Power Supply - Block Diagram

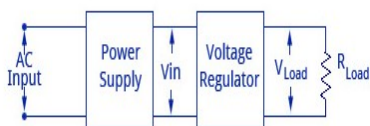


Fig2.power supply block diagram

A regulated power supply basically consists of a normal power supply and voltage regulating device, as illustrated within the figure. The output from a normal power supply is fed to the voltage regulating device that gives the final output. The output voltage remains constant regardless of variations within the ac input voltage or variations in output (or load) current.

The ac voltage typically 230v is associated with the transformer, that means the ac voltage directly down to at first separated by a simple capacitive filter to supply a dc voltage for the most part has some ripple or ac voltage variation. A regulator circuit will utilize this dc input to supply a regulated voltage that not just has a lot of ripple voltage. This voltage regulation is here and there acquired utilizing one of various voltage regulation IC units.

**B. Temperature Sensor**

The LM35 is one sort of typically utilized temperature detecting component which will be utilized to measure temperature with an electrical

o/p near to the temperature (in °C). It will quantify temperature all the more precisely contrast and a thermistor. This sensor produces a high output voltage than thermocouples and won't require that the output voltage is intensified. The LM35 has a output voltage that is corresponding to the Celsius temperature. The scale issue is .01V/°C.

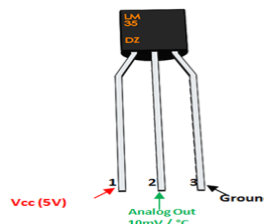


Fig 3.Temperature sensor pin diagram

Pin No	Pin Name	Description
1	Vcc	Input voltage is +5V for typical applications
2	Analog Out	There will be the increase in 10mV for raise of every 1°C. Can range from -1V(-55°C) to 6V(150°C)
3	Ground	Connected to ground terminal of the circuit

Table 1.pin description of Temperature sensor

The uses of LM35 temperature sensor incorporate the accompanying

1. Estimating temperature of a specific situation also, HVAC applications
2. Giving thermal shutdown to a part/circuit
3. Checking Battery Temperature

**C. IR Eye blink Sensor**

An ideal IR eye blink detector should have many vital properties. The sensor was hooked up to the implanted holder and positioned in front of the eye. Throughout eye blink detection, IR light from the led illuminates the eye and mirrored IR light induces an electrical current through the IR photodiode



Fig 4.IR Eye blink Sensor pin diagram

#### D. Pulse Rate Sensor

This pulse sensing element fits over a tip and uses the quantity of infrared reflected by the blood circulating inside to do simply that. when the heart pumps, blood pressure rises sharply, and then will the quantity of infrared from the electrode that gets reflected back to the detector

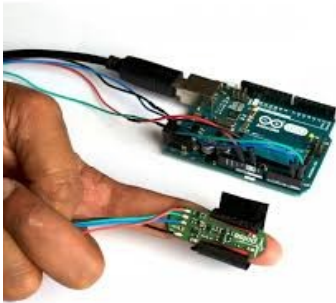


Fig 5. Pulse Rate Sensor

A heart rate monitor is a personal monitoring device that allows one to measure one's heart rate in real time or record the heart rate.



Fig 6. Pulse Rate Sensor pin diagram

The sensing element consists of a brilliant bright red led and light detector. The led has to be super bright because the most light should pass spread in finger and detected by detector. Now, once the heart pumps a pulse of blood through the blood vessels, the finger becomes slightly additional opaque and then less light weight reached the detector. With every heart pulse the detector signal varies. This variation is regenerate to electrical pulse. This signal is amplified and triggered through an amplifier that outputs +5V logic level signal. The output is also indicated by a led that blinks on every heart beat.

#### E. ARM7 Micro-controller

ARM7 LPC2148 Microcontroller Socket is utilized with LPC2148 Pro Development Board. It is an independent board for LPC2148 microcontroller. It has control on reset circuit with MCP130T brownout checking chip and power decoupling capacitors.



Fig 7. ARM7 Micro-controller

These two I/O ports are of 32-bit wide and are given by the 64 pins of the microcontroller. The naming tradition of the I/O pins on the LPC2148 Microcontroller is Pa.bc where 'a' is the quantity of the port i.e. 0 or 1 (as LPC2148 has just two ports) and 'bc' is the quantity of the stick in the port a

#### F. LCD Display

LCD (Liquid Crystal Display) screen is an electronic showcase module and locate an extensive variety of uses. A 16x2 LCD display is exceptionally fundamental module and is ordinarily utilized in different gadgets and circuits. ... A 16x2 LCD implies it can show 16 characters for each line and there are 2 such lines.

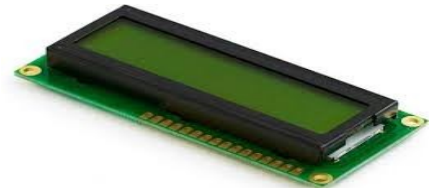


Fig 8. LCD Display

The fluid has a remarkable favourable position of having low power utilization than the LED or cathode beam tube. Fluid precious stone presentation screen deals with the guideline of blocking light as opposed to discharging light. LCD's requires backdrop illumination as they don't radiates light by them.

#### G. IOT (WIFI Module)

An IoT module is a little electronic gadget inserted in objects, machines and things that interface with remote systems and sends and receives information. Once in a while alluded to as a "radio chip", the IoT module contains a similar innovation and data circuits found in cell phones yet without highlights like a display or keypad

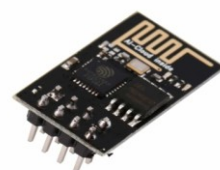


Fig 9. IOT Module

The ESP8266 Wi-Fi Module is an independent SOC with integrated TCP/IP protocol stack that can give any microcontroller access to your Wi-Fi network. The ESP8266 is able to do either facilitating an application or offloading all Wi-Fi networking functions from another application processor

*H. Buzzer*

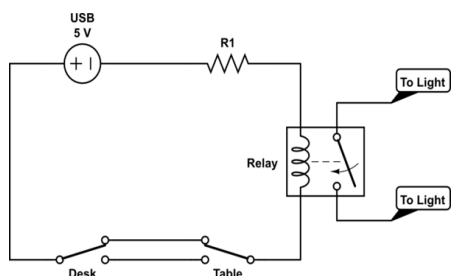
A buzzer is a mechanical, electromechanical, magnetic, electromagnetic, electro-acoustic or piezoelectric sound signalling gadget. A piezo electric buzzer can be driven by a swaying electronic circuit or other sound signal source. A click, signal or ring can show that a button has been squeezed



Fig 10. Buzzer pin diagram

*I. Relay*

Transfers control one electrical circuit by opening and shutting contacts in another circuit.



As relay diagrams appear, when a relay contact is ordinarily open (NO), there is an open contact when the relay isn't invigorated.

*J. DC Motor*

The DC engine is a machine that changes electric energy into mechanical energy in form of pivot

As terminal voltage increments or diminishes, the speed of the associated DC engine additionally increments or diminishes. ... The AC inverter permits a standard induction motor to be worked at any speed, much the same as the DC engine. It does this without brushes. Brushes are the essential support cerebral pain when utilizing a DC engine.

**IV. SIMULATION RESULTS**

Majority of the road accidents are occurring due to driver negligence and

drowsiness, to overcome this we are building a smart embedded system and with the help of sensors we can prevent the accidents by alerting the driver in the conditions like drowsiness/dizziness and abnormal health conditions like sudden heart attack, vehicle locations details are sent to the persons who are connected with the system. In this Project we are using the ARM7 Micro controller as the base operating system, for the operations and results. For this project we have given a power supply using the RPS module, and with the help sensors like eye blink sensor, pulse rate sensor, temperature sensors we can detect the vehicle condition and driver drowsiness and can make decisions accordingly. By using Temperature sensor we can monitor the vehicle engine condition, when the engine is over heated the engine will be automatically off, and a message is sent to persons who are connected to the device with the location details with the help of IOT based wifi module. By using the pulse rate sensor we can monitor the Driver abnormal health conditions. The pulse rate sensor need to wear by the driver, and the pulse counts are monitored, if the pulse rate is not as per the normal range, then a location details are sent to specific persons who are connected with system in the form a message, and ignition is off. Similarly with the eye blink sensor also, the eye blink sensor works as per no of eye blinks driver makes in a specific period of time, and if the count is below the normal range, or the blink rate completely zero, then the vehicle will automatically shuts down and the message will be sent and along with this a buzzer sound is raised in the vehicle whenever the driver is drowsy while driving. Along with above sensors we can also use Alcohol sensor and speed sensor, and a 16X2 LCD display is attached to the system for display purpose, and the information is transferred with the help of a IOT based wifi module.

By this project we can have a continuous monitoring of the driver to prevent the accidents. And if any accidents occurred then the system will send message to the specific persons automatically.

**ADVANTAGES:**

- Multiple users can get the information at same time.
- Data can be stored in cloud.
- Long Distance communications is also possible because of the WIFI Module.

**DISADVANTAGES:**

- Driver Must be connected with the system

- No information is passed if their is connection problem.

## V.CONCLUSION

In this paper, we've reviewed the varied strategies available to see the sleepiness state of a driver. This paper additionally, discusses the varied ways that within which sleepiness is manipulated in a very simulated setting. The planned system is employed to avoid varied road accidents caused by drowsy driving and additionally this method used for security purpose of a driver to caution the driver if any fire accident or any gas leak. This paper involves avoiding accident to unconsciousness through eye blink. Here one eyeblink sensor is mounted in vehicle where if driver lose his consciousness, then it alerts the driver through buzzer to prevent vehicle from accident. The pulse rate sensor and temperature device are used for more safety system within the vehicle. Development of a hybrid microcontroller for a vehicle that additionally consists of an alcohol and temperature detector which can sense if the driver is drunk and wouldn't start the vehicle. a whole study on roadsafety goes to be the following boom for the auto business for it to flourish and survive each human from the danger.

The main advantage of this paper is that the accuracy of using physiological parameters to observe sleepiness is basically high. This helps in preventing most of the road accidents that occur because of fatigue.

## REFERENCES

1. Ralph Oyini M bouna, Seong G. Kong, "Visual Analysis of Eye State and Head Pose for Driver Alertness Monitoring", IEEE, pp.1462-1469, vo1.14, 2013, USA
2. <https://ieeexplore.ieee.org/document/6518125/>
3. ArunSahayadhas, KennethSundaraj, "Detecting Driver Drowsiness Based on Sensors A Review", pp.16937-16953, ISSN 1424-8220, Malaysia 2012
4. [http://scholar.google.co.in/scholar\\_url?url=https://www.mdpi.com/14248220/12/12/16937/pdf&hl](http://scholar.google.co.in/scholar_url?url=https://www.mdpi.com/14248220/12/12/16937/pdf&hl)
5. Anirbandasgupta,anjithgeorge,"A Vision Based System For Monitoring The Loss Of Attention in Automotive
6. <https://ieeexplore.ieee.org/document/6565376>
7. Boon-Giin Lee and Wan-Young Chung,"Driver Alertness Monitoring Using Fusion of Facial Features and Bio-Signals", IEEE Sensors journal, vol. 12, no. 7,2012
8. <https://ieeexplore.ieee.org/document/6166846/>
9. Raoul Lopes, D.J Sanghvi, AdityaShah,"Drowsiness Detection based on Eye Movement, Yawn Detection and Head Rotation", Vol. 2, No.6,2012
10. <http://research.ijais.org/volume2/number6/ijais12450368>
11. Artem A. Lenskiy and Jong-SooLee"Driver's Eye Blinking Detection Using Novel Color and Texture Segmentation Algorithms", International Journal Of Control, Automation, and Systems,pp.317-327, 2012
12. <https://link.springer.com/article/10.1007/s12555-012>
13. Parris, J., et.al, "Face and eye detection on hard datasets," Biometrics (IJCB), International Joint Conference on , vol., no., pp.110, 11-13 Oct. 2011
14. <https://ieeexplore.ieee.org/document/6117593/>
15. N. Raj and R. K. Sharma, "A High Swing OTA with wide Linearity for design of Self Tuneable Resistor", International Journal of VLSI design & Communication system (VLSICS), Volume 1, No. 3, pp. 1-11, 2010.
16. N. Raj, A.K. Singh, A.K. Gupta, "Modeling of Human Voice Box in VLSI for Low Power Biomedical Applications", IETE Journal of Research, Vol. 57, Issue 4, pp. 345-353, 2011.
17. N. Raj, A.K. Singh, and A.K. Gupta, "Low power high output impedance high bandwidth QFGMOS current mirror", Microelectronics Journal, Vol. 45, No. 8, pp. 1132-1142, 2014.
18. N. Raj, A.K. Singh, and A.K. Gupta, "Low-voltage bulk-driven self-biased cascode current mirror with bandwidth enhancement", Electronics Letters, Vol. 50, No. 1, pp. 23-25, 2014.
19. N. Raj, A.K. Singh, and A.K. Gupta, "Low Voltage High Output Impedance Bulk- driven Quasi-floating Gate Self-biased High-swing Cascode Current Mirror", Circuit System & Signal Processing Journal, Vol. 35, No. 8, pp. 2683-2703, 2015.
20. N. Raj, A.K. Singh, and A.K. Gupta, "High performance Current Mirrors using Quasi-floating Bulk", Microelectronics Journal, Vol. 52, No. 1, pp. 11-22, 2016.
21. N. Raj, A.K. Singh, and A.K. Gupta, "Low Voltage High Performance Bulk-driven Quasi-floating Gate Self-biased Cascode Current Mirror", Microelectronics Journal, Vol. 52, No. 1, pp. 124-133, 2016.
22. N. Raj, A.K. Singh, and A.K. Gupta, "Low Voltage High Bandwidth Self-biased High Swing Cascode Current Mirror", Indian Journal of Pure and Applied Physic, Vol. 55, No. 4, pp. 245-253, 2017.
23. Raj N. and Gupta A. K., "Analysis of Operational Transconductance Amplifier using Low Power Techniques", Journal of Semiconductor

- Devices and Circuits (STM Journal), Vol. 1, No. 3, pp. 1-9, 2015.
24. Raj N. and Gupta A. K., "Multifunction Filter Design using BDQFG Miller OTA", Journal of Electrical and Electronics Engineering: An International Journal (EEEEJ Journal), Vol. 4, No. 3, pp. 55-67, 2015.
  25. N. Raj, A.K. Singh, and A.K. Gupta, "Low Power Circuit Design Techniques: A Survey", International Journal of Computer Theory and Engineering, Vol. 7, No. 3, pp. 172-176, 2015.

# OPTIMIZING THE CONVOLUTION OPERATION TO ACCELERATE DEEP NEURAL NETWORKS ON FPGA

GODUGU SWATHI<sup>1</sup> & Mrs. B. MANJULA<sup>2</sup>

PG Student<sup>1</sup>, Assistant Professor<sup>2</sup>

Department of ECE, Malla Reddy College Of Engineering, Hyderabad, Telangana, INDIA.

**ABSTRACT:** As convolution contributes most operations in convolutional neural network (CNN), the convolution acceleration scheme significantly affects the efficiency and performance of a hardware CNN accelerator. Convolution involves multiply and accumulate operations with four levels of loops, which results in a large design space. Prior works either employ limited loop optimization techniques, e.g., loop unrolling, tiling, and interchange, or only tune some of the design variables after the accelerator architecture and dataflow are already fixed. Without fully studying the convolution loop optimization before the hardware design phase, the resulting accelerator can hardly exploit the data reuse and manage data movement efficiently. This paper overcomes these barriers by quantitatively analyzing and optimizing the design objectives (e.g., memory access) of the CNN accelerator based on multiple design variables. Then, we propose a specific dataflow of hardware CNN acceleration to minimize the data communication while maximizing the resource utilization to achieve high performance. The proposed CNN acceleration scheme and architecture are demonstrated by implementing end-to-end CNNs including NiN, VGG-16, and ResNet-50/ResNet152 for inference. For VGG-16 CNN, the overall throughputs achieve 348 GOPS and 715 GOPS on Intel Stratix V and Arria 10 FPGAs, respectively.

**Keywords:** Accelerator architectures, convolutional neural networks (CNNs), field-programmable gate array (FPGA), neural network hardware.

## I. INTRODUCTION

The field-programmable gate arrays (FPGA) are fast becoming the platform of choice for accelerating the inference phase of deep convolutional neural networks (CNNs). In addition to their conventional advantages of reconfigurability and shorter design time over application-specific integrated circuits (ASICs) [20], [21] to catch up with the rapid evolving of CNNs, FPGA can realize low latency inference with competitive energy efficiency (~10–50 GOP/s/W) when compared to software implementations on multicore processors with GPUs [10], [12], [13], [17]. This is due to the fact that modern FPGAs allow customization of the architecture and can exploit the availability of hundreds to thousands of on-chip DSP blocks. However, significant challenges remain in mapping CNNs onto FPGAs. The state-of-the-art CNNs require a large number (>1 billion) of computationally intensive task (e.g., matrix multiplications on large numbers), involving a very large number of weights (>50 million) [4], [5]. Deep CNN algorithms have tens to hundreds of layers, with significant differences between layers in terms of sizes and configurations.

More than 90% of the operations in a CNN involve convolutions [2]–[4]. Therefore, it stands to reason that acceleration schemes should focus on the management of parallel computations and the organization of data storage and access across multiple levels of memories, e.g., off-chip dynamic random access memory (DRAM), on-chip memory, and local registers. In CNNs, convolutions are performed by four levels of loops that slide along both kernel and feature maps as shown in Fig. 1. This gives rise to a large design space consisting of various choices for implementing parallelism, sequencing of computations, and partitioning the large data set into smaller chunks to fit into on-chip memory. These problems can be handled by the existing loop optimization techniques [6], [9], such as loop unrolling, tiling, and interchange. Although some CNN accelerators have adopted these techniques [9], [11], [13], [19], the impact of these techniques on design efficiency and performance has not been systematically and sufficiently studied. Without fully studying the loop operations of convolutions, it is difficult to efficiently customize the dataflow and architecture for high-throughput CNN implementations.

```

for (no = 0; no < Nof; no++) → Loop-4
  for (y = 0; y < Noy; y++)
    for (x = 0; x < Nox; x++) } → Loop-3
      for (ni = 0; ni < Nif; ni++) → Loop-2
        for (ky = 0; ky < Nky; ky++)
          for (kx = 0; kx < Nkx; kx++) } → Loop-1
            pixelL(no; x, y) += pixelL-1(ni; S × x + kx, S × y + ky) × weightL-1(ni, no; kx, ky);
            pixelL(no; x, y) = pixelL(no; x, y) + bias(no);
    
```

Fig. 1. Four levels of convolution loops, where  $L$  denotes the index of convolution layer and  $S$  denotes the sliding stride [15].

Specifically, the main contributions of this paper include the following.

- 1) We provide an in-depth analysis of the three loop optimization techniques for convolution operations and use corresponding design variables to numerically characterize the acceleration scheme.
- 2) The design objectives of CNN accelerators (e.g., latency, memory) are quantitatively estimated based on the configurations of the design variables.
- 3) An efficient convolution acceleration strategy and dataflow is proposed aimed at minimizing data communication and memory access.
- 4) A data router is designed to handle different settings for convolution sliding operations, e.g., strides and zero paddings, especially for highly irregular CNNs.
- 5) A corresponding hardware architecture is designed that fully utilizes the computing resources for high performance and efficiency, which is uniform and reusable for all the layers.
- 6) The proposed acceleration scheme and architecture is validated by implementing large-scale deep CNN algorithms, NiN [3], VGG-16 [4], and ResNet-50/ResNet152 [5] for image recognition [1], on two Intel FPGAs. The proposed accelerators achieve end-to-end inference throughput of 715 GOPS on Arria 10 and 348 GOPS on Stratix V, respectively, using a batch size of 1.

## II. ACCELERATION OF CONVOLUTION LOOPS

### A. General CNN Acceleration System

Recently reported CNN algorithms involve a large amount of data and weights. For them, the on-chip memory is insufficient to store all the data, requiring gigabytes of external memory. Therefore, a typical CNN accelerator consists of three levels of storage hierarchy: 1) external memory; 2) onchip buffers; and 3) registers associated with the processing

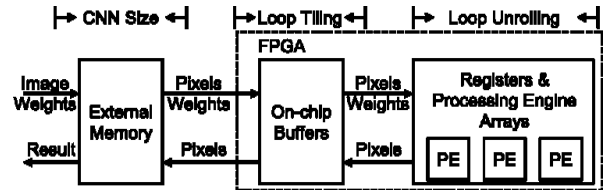


Fig. 2. Three levels of general hardware CNN accelerator hierarchy.

engines (PEs), as shown in Fig. 2. The basic flow is to fetch data from external memory to on-chip buffer, and then feed them into registers and PEs. After the PE computation completes, results are transferred back to on-chip buffers and to the external memory if necessary, which will be used as input to the subsequent layer.

### B. Convolution Loops

Convolution is the main operation in CNN algorithms, which involves 3-D multiply-and-accumulate (MAC) operations of input feature maps and kernel weights. Convolution is implemented by four levels of loops as shown in the pseudocodes in Fig. 1 and illustrated in Fig. 3. To efficiently map and perform the convolution loops, three loop optimization techniques [6], [9], namely, loop unrolling, loop tiling, and loop interchange, are employed to customize the computation and communication patterns of the accelerator with three levels of memory hierarchy.

### C. Loop Optimization and Design Variables

As shown in Fig. 3, multiple dimensions are used to describe the sizes of the feature and kernel maps of each convolution layer for a given CNN. The hardware design variables of loop unrolling and loop tiling will determine the acceleration factor and hardware footprint. All dimensions and variables used in this paper are listed in Table I.

The width and height of one kernel (or filter) window is described by  $(Nkx, Nky)$ .  $(Nix, Niy)$  and  $(Nox, Noy)$  define the width and height of one input and output feature map (or channel), respectively.  $Nif$  and  $Nof$  denote the number of input and output feature maps, respectively. The loop unrolling design variables are  $(Pfx, Pfy)$ ,  $Pif$ ,



number of parallel MAC operations as well as the number of required multipliers ( $P_m$ )

$$P_m = P_{kx} \times P_{ky} \times P_{if} \times P_{ix} \times P_{iy} \times P_{of}$$

2) **Loop Tiling:** Loop tiling is used to divide the entire data into multiple blocks, which can be accommodated in the on-chip buffers, as illustrated in Fig. 8. The loop tiling sets the lower bound on the required on-chip buffer size. The required size of input pixel buffer is  $T_{ix} \times T_{iy} \times T_{if} \times (\text{pixel\_datawidth})$ .

The size of weight buffer is  $T_{kx} \times T_{ky} \times T_{if} \times T_{of} \times (\text{weight\_datawidth})$ . The size of output pixel buffer is  $T_{ox} \times T_{oy} \times T_{of} \times (\text{pixel\_datawidth})$ .

### III. ANALYSIS ON DESIGN OBJECTIVES OF CNN ACCELERATOR

In this section, we provide a quantitative analysis of the impact of loop design variables ( $P^*$  and  $T^*$ ) on the following design objectives that our CNN accelerator aims to minimize.

#### A. Computing Latency

The number of multiplication operations per layer ( $N_m$ ) is

$$N_m = N_{if} \times N_{kx} \times N_{ky} \times N_{of} \times N_{ox} \times N_{oy}$$

Ideally, the number of computing cycles per layer should be  $N_m/P_m$ , where  $P_m$  is the number of multipliers. The number of actual computing cycles per layer is

$$\#\_cycles = \#intertile\_cycles (6)$$

$\times \#intratile\_cycles$  where

$$\#intertile\_cycles = N_{if}/T_{if} \times N_{kx}/T_{kx} \times N_{ky}/T_{ky} \times N_{of}/T_{of} \times N_{ox}/T_{ox} \times N_{oy}/T_{oy} (7)$$

$$\#intratile\_cycles = T_{if}/P_{if} \times T_{kx}/P_{kx} \times T_{ky}/P_{ky} \times T_{of}/P_{of} \times T_{ox}/P_{ox} \times T_{oy}/P_{oy}. (8)$$

#### B. Data Reuse

There are mainly two types of data reuse: spatial reuse and temporal reuse

Having  $P_m$  parallel multiplications per cycle requires  $P_m$  pixels and  $P_m$  weights to be fed into the multipliers. The number of distinct weights required per cycle is

$$P_{wt} = P_{of} \times P_{if} \times P_{kx} \times P_{ky}. (9)$$

If Loop-1 is not unrolled ( $P_{kx} = 1, P_{ky} = 1$ ), the number of distinct pixels required per cycle ( $P_{px}$ ) is

$$P_{px} = P_{if} \times P_{ix} \times P_{iy}. (10)$$

Otherwise,  $P_{px}$  is

$$P_{px} = P_{if} \times ((P_{ix} - 1)S + P_{kx}) \times ((P_{iy} - 1)S + P_{ky}). (11)$$

Note that “distinct” only means that the pixels/weights are from different feature/kernel map locations and their values may be the same. The number of times a weight is spatially reused in one cycle is

$$Reuse_{wt} = P_m/P_{wt} = P_{ix} \times P_{iy}$$

$$(12)$$

(4) here the spatial reuse of weights is realized by unrolling Loop-3 ( $P_{ix} > 1$  or  $P_{iy} > 1$ ). The number of times of a pixel is spatially reused in one cycle ( $Reuse_{px}$ ) is

$$Reuse_{px} = P_m/P_{px}. (13)$$

If Loop-1 is not unrolled,  $Reuse_{px}$  is

$$Reuse_{px} = P_{of} (14)$$

otherwise,  $Reuse_{px}$  is

$$Reuse_{px} = \frac{P_{of} \times P_{kx} \times P_{ky} \times P_{ix} \times P_{iy} ((P_{ix} - 1)S + P_{kx}) ((P_{iy} - 1)S + P_{ky})}{- + \times - +} (15)$$

#### C. Access of On-Chip Buffer

Without any data reuse, the total read operations from on-chip buffers for both pixels and weights are  $N_m$ , as every multiplication needs one pixel and one weight. With data reuse, the total number of read operations from on-chip buffers for weights becomes

$$\#read_{wt} = N_m/Reuse_{wt} (16)$$

and the total number of read operations for pixels is

$$\#read_{px} = N_m/Reuse_{px}. (17)$$

If the final output pixels cannot be obtained within one tile, their partial sums are stored in buffers. The number of write and read operations to/from buffers for partial sums per cycle is  $2 \times P_{of} \times P_{ox} \times P_{oy}$ , where all partial sums generated by Loop-1 ( $P_{kx}, P_{ky}$ ) and Loop-2 ( $P_{if}$ ) are already summed together right after multiplications. The total number of writes/reads to/from buffers for partial sums is

$$\#wr\_rd\_psum = \#\_cycles \times (2 \times P_{of} \times P_{ox} \times P_{oy}). (18)$$

The number of times output pixels are written to on-chip buffers (i.e.,  $\#write_{px}$ ) is identical to the total number of output pixels in the given CNN model. Finally, the total number of on-chip buffer accesses is

$$\#buffer\_access = \#read_{px} + \#read_{wt} + \#wr\_rd\_psum + \#write_{px}. (19)$$

### IV. PROPOSED ACCELERATION SCHEME

The optimization process of our proposed acceleration scheme is presented in this section, which includes appropriate selection of the convolution loop design variables.

#### A. Minimizing Computing Latency

We set variables  $P^*$  to be the common factors of  $T^*$  for all the convolution layers to fully utilize PEs, and  $T^*$  to be the common factors of  $N^*$  to make full

use of external memory transactions. For CNN models with only small common factors, it is recommended to set  $N^*/P^*$  and  $T^*/P^*$  as small as possible to minimize the inefficiency caused by the difference in sizes of CNN models.

### B. Minimizing Partial Sum Storage

To reduce the number and movements of partial sums, both Loop-1 and Loop-2 should be computed as early as possible or unrolled as much as possible. To avoid the drawback of unrolling Loop-1 as discussed in Section IV and maximize the data reuse as discussed in Section III-C, we decide to unroll Loop-3 ( $Pox > 1$  or  $Poy > 1$ ) and Loop-4 ( $Pof > 1$ ). By this means, we cannot attain the minimum partial sum storage, as (9.1) inside Fig. 9.

Constrained by  $1 \leq P^* \leq T^* \leq N^*$ , the second least number of partial sum storage is achieved by (9.2) among (9.2)–(9.9) inside Fig. 9. To satisfy the condition for (9.2), we serially compute Loop-1 and Loop-2 first and ensure the required data of Loop-1 and Loop-2 are buffered, i.e.,  $Tkx = Nkx$ ,  $Tky = Nky$  and  $Tif = Nif$ . Therefore, we only need to store  $Pof \times Pox \times Poy$  number of partial sums, which can be retained in local registers with minimum data movements.

### C. Minimizing Access of External Memory

As we first compute Loop-1 and Loop-2 to reduce partial sums, we cannot achieve the minimum number of DRAM access described in (10.1) and (10.3) inside Fig. 10, where neither the pixels nor the weights are fully buffered for one convolution layer.

Then, the optimization of minimizing the on-chip buffer size while having minimum DRAM access is formulated as  $\min bits\_BUF\_px\_wt$

$$\begin{aligned} \text{s.t. } \#Tile\_px_L &= 1 \text{ or } \#Tile\_wt_L = 1 \\ \text{with } \forall L \in [1, \#CONVs] \end{aligned} \quad (20)$$

where  $\#Tile\_px_L$  and  $\#Tile\_wt_L$  denote the number of tiling blocks for input pixels and weights of layer  $L$ , respectively, and  $\#CONVs$  is the number of convolution layers.  $bits\_BUF\_px\_wt$  is the sum of pixel buffer size ( $bits\_BUF\_px$ ) and weight buffer size ( $bits\_BUF\_wt$ ), which are given by  $bits\_BUF\_px\_wt = bits\_BUF\_px + bits\_BUF\_wt$ . (21)

Both pixel and weight buffers need to be large enough to cover the data in one tiling block for all the convolution layers. This is expressed as  $bits\_BUF\_px$

$$\begin{aligned} &= M \cdot AX(words\_px_L) \times pixel\_datawidth \text{ with} \\ &L \in [1, \#CONVs] \end{aligned} \quad (22) \quad bits\_BUF\_wt = M \cdot AX(words\_wt_L)$$

$$\times weight\_datawidth \text{ with } L \in [1, \#CONVs]$$

(23)

where  $words\_px_L$  and  $words\_wt_L$  denote the number of pixels and weights of one tiling block in layer  $L$ , respectively. These are expressed in terms of loop tiling variables as follows:

$$words\_px_L = Tix_L \times Tiy_L \times Tif_L + Tox_L \times Toy_L \times Tof_L \quad (24)$$

where  $words\_px_L$  is comprised of both input and output pixels. The number of tiles in (20) is also determined by  $T^*$  variables

$$\#Tile\_px_L = Nif_L / Tif_L \times Nox_L / Tox_L \times Noy_L / Toy_L \quad (26)$$

$$\#Tile\_wt_L = Nkx_L / Tkx_L \times Nky_L / Tky_L \times Nif_L / Tif_L \times Nof_L / Tof_L \quad (27)$$

By solving (20), we can find an optimal configuration of  $T^*$  variables that result in minimum DRAM access and onchip buffer size. However, since we have already set  $Tkx = Nkx$ ,  $Tky = Nky$ ,  $Tif = Nif$  as in Section V-B, we can only achieve a suboptimal solution by tuning  $Tox$ ,  $Toy$  and  $Tof$ , resulting in larger buffer size requirement.

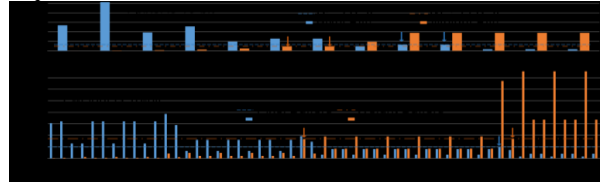


Fig. 9. To guarantee minimum DRAM accesses, either all pixels (blue bars) are covered by pixel buffers (blue dashed lines) or all weights are covered by weight buffers in one layer. Then, we try to lower the total buffer sizes/lines. (a) Pixels and weights distribution of convolution layers in VGG16. (b) Pixels and weights distribution of convolution layers in ResNet-50.

## V. EXPERIMENTAL RESULTS

### A. System Setup

The overall CNN acceleration system on the FPGA chip shown in Fig. 16 is coded in parametrized Verilog scripts and configured by the proposed CNN compiler in [16] for different CNN and FPGA pairs.

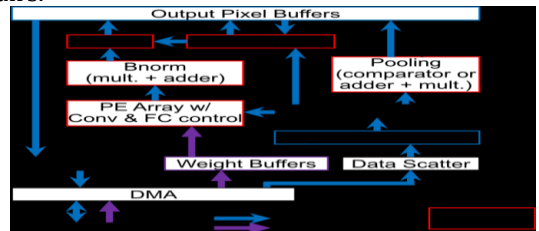


Fig. 10. Overall FPGA-based CNN hardware acceleration system [16].

## B. Analysis of Experimental Results

The performance and specifications of our proposed CNN accelerators are summarized in Table II. In Stratix V and Arria 10, one DSP block can be configured as either two independent 18-bit  $\times$ 18-bit multipliers or one multiplier followed by an accumulator. Since Arria 10 has 1.8 $\times$ more ALMs and 5.9 $\times$ more DSP blocks than the Stratix V we use, larger loop unrolling variables ( $P_{ox} \times P_{oy} \times P_{of}$ ) can be achieved in Arria 10 to obtain  $>2\times$ throughput enhancement than Stratix V.

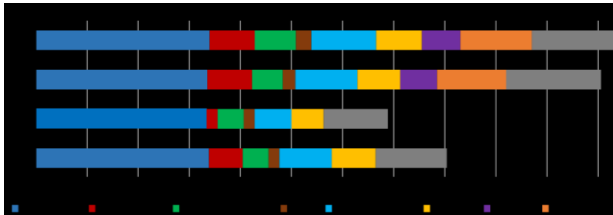


Fig. 11. Logic utilization breakdown of NiN, VGG-16 and ResNet-50/152.

## VI. CONCLUSION

In this paper, we present an in-depth analysis of convolution loop acceleration strategy by numerically characterizing the loop optimization techniques. The relationship between accelerator objectives and design variables are quantitatively investigated. A corresponding new dataflow and architecture is proposed to minimize data communication and enhance throughput. Our CNN accelerator implements end-to-end NiN, VGG-16, and ResNet-50/ResNet-152 CNN models on Stratix V and Arria 10 FPGA, achieving the overall throughput of 348 GOPS and 715 GOPS, respectively.

## REFERENCES

- [1] O. Russakovsky et al., "ImageNet large scale visual recognition challenge," *Int. J. Comput. Vis.*, vol. 115, no. 3, pp. 211–252, 2015.
- [2] A. Krizhevsky, I. Sutskever, and G. E. Hinton, "ImageNet classification with deep convolutional neural networks," in *Proc. Adv. Neural Inf. Process. Syst. (NIPS)*, 2012, pp. 1097–1105.
- [3] M. Lin, Q. Chen, and S. Yan. (Mar. 2014). "Network in network." [Online]. Available: <https://arxiv.org/abs/1312.4400>
- [4] K. Simonyan and A. Zisserman, "Very deep convolutional networks for large-scale image recognition," in *Proc. Int. Conf. Learn. Represent. (ICLR)*, 2015.
- [5] K. He, X. Zhang, S. Ren, and J. Sun, "Deep residual learning for image recognition," in *Proc. IEEE Conf. Comput. Vis. Pattern Recognit. (CVPR)*, Jun. 2016, pp. 770–778.
- [6] D. F. Bacon, S. L. Graham, and O. J. Sharp, "Compiler transformations for high-performance computing," *ACM Comput. Surv.*, vol. 26, no. 4, pp. 345–420, Dec. 1994.
- [7] Y.-H. Chen, T. Krishna, J. S. Emer, and V. Sze, "Eyeriss: An energyefficient reconfigurable accelerator for deep convolutional neural networks," *IEEE J. Solid-State Circuits*, vol. 51, no. 1, pp. 127–138, Jan. 2017.
- [8] Y.-H. Chen, J. Emer, and V. Sze, "Eyeriss: A spatial architecture for energy-efficient dataflow for convolutional neural networks," in *Proc. ACM/IEEE Int. Symp. Comput. Archit. (ISCA)*, Jun. 2016, pp. 367–379.
- [9] C. Zhang, P. Li, G. Sun, Y. Guan, B. Xiao, and J. Cong, "Optimizing FPGA-based accelerator design for deep convolutional neural networks," in *Proc. ACM/SIGDA Int. Symp. Field-Program. Gate Arrays (FPGA)*, Feb. 2015, pp. 161–170.
- [10] C. Zhang, D. Wu, J. Sun, G. Sun, G. Luo, and J. Cong, "Energy-efficient CNN implementation on a deeply pipelined FPGA cluster," in *Proc. ACM Int. Symp. Low Power Electron. Design (ISLPED)*, Aug. 2016, pp. 326–331.
- [11] N. Suda et al., "Throughput-optimized OpenCL-based FPGA accelerator for large-scale convolutional neural networks," in *Proc. ACM/SIGDA Int. Symp. Field-Program. Gate Arrays (FPGA)*, Feb. 2016, pp. 16–25.
- [12] U. Aydonat, S. O'Connell, D. Capalija, A. C. Ling, and G. R. Chiu, "An OpenCL deep learning accelerator on Arria 10," in *Proc. ACM/SIGDA Symp. Field-Program. Gate Arrays (FPGA)*, Feb. 2017, pp. 55–64.
- [13] K. Guo et al., "Angel-Eye: A complete design flow for mapping CNN onto embedded FPGA," *IEEE Trans. Comput.-Aided Des. Integr. Circuits Syst.*, vol. 37, no. 1, pp. 35–47, Jan. 2018.
- [14] Y. Ma, N. Suda, Y. Cao, J.-S. Seo, and S. Vrudhula, "Scalable and modularized RTL compilation of convolutional neural networks onto FPGA," in *Proc. IEEE Int. Conf. Field-Program. Logic Appl. (FPL)*, Aug./Sep. 2016, pp. 1–8.
- [15] Y. Ma, Y. Cao, S. Vrudhula, and J.-S. Seo, "Optimizing loop operation and dataflow in FPGA acceleration of deep convolutional neural networks," in *Proc. ACM/SIGDA Int. Symp. Field-Program. Gate Arrays (FPGA)*, Feb. 2017, pp. 45–54.
- [16] Y. Ma, Y. Cao, S. Vrudhula, and J.-S. Seo, "An automatic RTL compiler for high-throughput FPGA implementation of diverse deep convolutional neural networks," in *Proc. IEEE Int. Conf. Field-Program. Logic Appl. (FPL)*, Sep. 2017, pp. 1–8.
- [17] H. Li, X. Fan, L. Jiao, W. Cao, X. Zhou, and L. Wang, "A high performance FPGA-based accelerator for large-scale convolutional neural networks," in *Proc. IEEE Int. Conf.*

- Field-Program. Logic Appl. (FPL), Aug. 2016, pp. 1-9.
- [18] A. Rahman, J. Lee, and K. Choi, "Efficient FPGA acceleration of convolutional neural networks using logical-3D compute array," in Proc. IEEE Design, Auto. Test Eur. Conf. (DATE), Mar. 2016, pp. 1393-1398.
- [19] M. Motamedi, P. Gysel, V. Akella, and S. Ghiasi, "Design space exploration of FPGA-based deep convolutional neural networks," in Proc. IEEE Asia South Pacific Design Auto. Conf. (ASP-DAC), Jan. 2016, pp. 575-580.
- [20] S. Han et al., "EIE: Efficient inference engine on compressed deep neural network," in Proc. ACM/IEEE Int. Symp. Comput. Archit. (ISCA), Jun. 2016, pp. 243-254.
- [21] L. Du et al., "A reconfigurable streaming deep convolutional neural network accelerator for Internet of Things," IEEE Trans. Circuits Syst. I, Reg. Papers, vol. 65, no. 1, pp. 198-208, Jan. 2018.
- [22] B. Bosi, G. Bois, and Y. Savaria, "Reconfigurable pipelined 2-D convolvers for fast digital signal processing," IEEE Trans. Very Large Scale Integr. (VLSI) Syst., vol. 7, no. 3, pp. 299-308, Sep. 1999.
- [23] Y. Guan et al., "FP-DNN: an automated framework for mapping deep neural networks onto FPGAs with RTL-HLS hybrid templates," in Proc. IEEE Int. Symp. Field-Program Custom Comput. Mach. (FCCM), Apr./May 2017, pp. 152-159.
- [24] X. Wei et al., "Automated systolic array architecture synthesis for high throughput CNN inference on FPGAs," in Proc. ACM the 54th Annu. Design Autom. Conf. (DAC), Jun. 2017, pp. 1-6.
- [25] N. Raj and R. K. Sharma, "A High Swing OTA with wide Linearity for design of Self Tuneable Resistor", International Journal of VLSI design & Communication system (VLSICS), Volume 1, No. 3, pp. 1-11, 2010.
- [26] N. Raj, A.K. Singh, A.K. Gupta, "Modeling of Human Voice Box in VLSI for Low Power Biomedical Applications", IETE Journal of Research, Vol. 57, Issue 4, pp. 345-353, 2011.
- [27] N. Raj, A.K. Singh, and A.K. Gupta, "Low power high output impedance high bandwidth QFGMOS current mirror", Microelectronics Journal, Vol. 45, No. 8, pp. 1132-1142, 2014.
- [28] N. Raj, A.K. Singh, and A.K. Gupta, "Low-voltage bulk-driven self-biased cascode current mirror with bandwidth enhancement", Electronics Letters, Vol. 50, No. 1, pp. 23-25, 2014.
- [29] N. Raj, A.K. Singh, and A.K. Gupta, "Low Voltage High Output Impedance Bulk-driven Quasi-floating Gate Self-biased High-swing Cascode Current Mirror", Circuit System & Signal Processing Journal, Vol. 35, No. 8, pp. 2683-2703, 2015.
- [30] N. Raj, A.K. Singh, and A.K. Gupta, "High performance Current Mirrors using Quasi-floating Bulk", Microelectronics Journal, Vol. 52, No. 1, pp. 11-22, 2016.
- [31] N. Raj, A.K. Singh, and A.K. Gupta, "Low Voltage High Performance Bulk-driven Quasi-floating Gate Self-biased Cascode Current Mirror", Microelectronics Journal, Vol. 52, No. 1, pp. 124-133, 2016.
- [32] N. Raj, A.K. Singh, and A.K. Gupta, "Low Voltage High Bandwidth Self-biased High Swing Cascode Current Mirror", Indian Journal of Pure and Applied Physic, Vol. 55, No. 4, pp. 245-253, 2017.
- [33] Raj N. and Gupta A. K., "Analysis of Operational Transconductance Amplifier using Low Power Techniques", Journal of Semiconductor Devices and Circuits (STM Journal), Vol. 1, No. 3, pp. 1-9, 2015.
- [34] Raj N. and Gupta A. K., "Multifunction Filter Design using BDQFG Miller OTA", Journal of Electrical and Electronics Engineering: An International Journal (EEEIJ Journal), Vol. 4, No. 3, pp. 55-67, 2015.
- [35] N. Raj, A.K. Singh, and A.K. Gupta, "Low Power Circuit Design Techniques: A Survey", International Journal of Computer Theory and Engineering, Vol. 7, No. 3, pp. 172-176, 2015.



Simulation and comparison of proposed coding scheme with previous techniques shown in section V, finally conclusion are made in section VI.

**II. BASIC DEFINITIONS**

1. **Coupling transitions:** Transition of data from 0 → 1 or vice-versa between adjacent bus lines.
2. **Self transitions:** Transition of data from 0 → 1 or vice-versa on bus wire with reference to previous data on it.
3. **Bus width:** Number of bits in data is defined as bus width.

**III. LITERATURE SURVEY AND BUS MODELS**

M. R. Stan and W. P. Burleson proposed that *Bus-Invert* method of coding which became an area of interest in Bus coding for crosstalk [1]. They introduced a concept of inverting the data bits if total number of transitions were more than half of the width of the bus. By doing this the total number of transitions was made less than half. Youngsoo et al introduced modified bus invert coding method [2], called partial Bus invert coding. In this method the whole bus width was not inverted bus a part of it. J.V.R. Ravindra came up with and Low power encoding scheme for data transmission [3]. Saini et al have modified the existing technique with better efficiency [4]. The above approaches have been based on Bus models provided by Chandrakasan [5, 7].

A bus is simply a circuit that connects one part of the circuit to the other. Buses are a typical model for I/O communication. A bus may consist of set of parallel lines with repeaters between them.

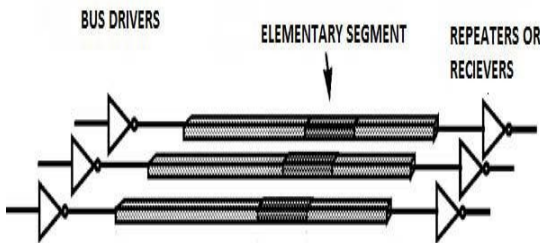


**Fig. 1 – DSM Bus [7]**

For the DSM bus, the distributed line model in terms of RLC [7] as shown is appropriate for describing electrical behavior of the bus.

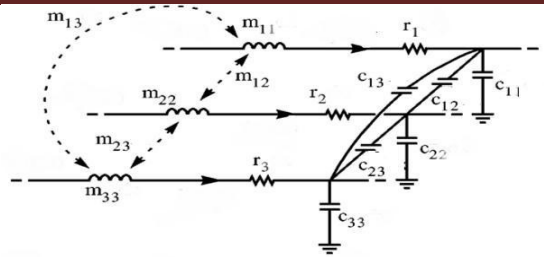


**Fig. 2 – Elementary segments of DSM Bus Lines [7]**

Where  $r_i(x)$  is the serial resistance per unit length of  $i^{th}$  line,  $C_{ii}(x)$  is the capacitance per unit length between the  $i^{th}$  line and ground,  $C_{ij}(x)$  is the capacitance per unit length between the  $i^{th}$  line and  $j^{th}$  line,  $m_{ii}(x)$  is the self inductance per unit length of the  $i^{th}$  line,  $m_{ij}(x)$  is the mutual inductance per unit length between  $i^{th}$  and  $j^{th}$  line.

It is meaningful to consider only the capacitive component of the wire as long as the resistive component of the wire is small and the switching frequencies are in the low to medium range. For on-chip parallel buses, energy is dissipated in charging and discharging parasitic capacitances. The coupling capacitance between the wires dominates the total parasitic capacitance of wires in DSM technologies. Below figure shows the simplified bus energy model [6]:

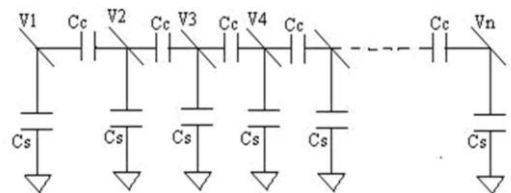


**Fig. 3 – Simple Bus Energy Model [8]**

Where  $C_s$  is the self-capacitance from each bus line to ground and  $C_c$  is the coupling-capacitance between two adjacent bus lines.  $V_1, V_2, \dots$  are the node voltages. Let  $\lambda$  be the capacitance factor which is calculated as [9] the ratio between coupling capacitance to self capacitance. Increase of the capacitance factor leads to the technology scale

**IV. PROPOSED QUADRO CODING TECHNIQUE**

The proposed technique called the Quadro coding technique is based on reducing the number of the transitions occurring on data bus when a new data is to be transmitted. By using the following technique self transitions from 0 → 1 and 1 →

0 can be reduced as new data is sent on the data bus compared to previous data. Let the data be  $n$  bits wide. The developing coding technique is given as follows:

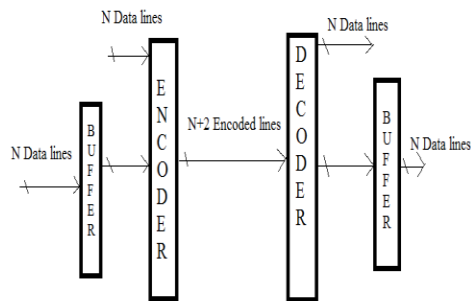


Fig. 4 – Block diagram of complete system

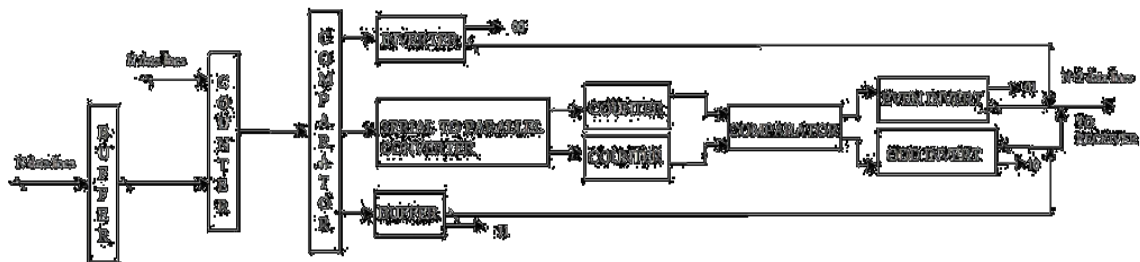


Fig. 5 – Block diagram of Encoder  
 DECODING

**ENCODING**

**STEP 1:** Calculate and compare number of transitions of the present bus data to previous bus data.

To retrieve the data from the encoded data, control bits are recovered from the received data and the following operations are performed according to the control bits.

**STEP 2:** If the number of transitions  $> n/2$  then Invert the data to be sent and append it with '00' as control bits for decoding purpose.

**STEP 3:** If the number of transitions  $\leq n/2$  and  $> n/4$  then Divide the data into even and odd groups.

Odd group :A1,A3,A5,..... Even group:A0,A2,A4,.....  
 Calculate number of transitions between odd group of the present data with the previous data say OGT and number of transitions between even group of present data with the previous data, say EGT.

If  $EGT > OGT$  then Invert the data bits of even group and append it with control bits '01'.

Else  
 Invert the data bits of odd group and append it with control bits '10'.

**STEP 4:** if the number of transitions  $\leq n/4$  then Send the data as it is without any encoding and append it with '11'.

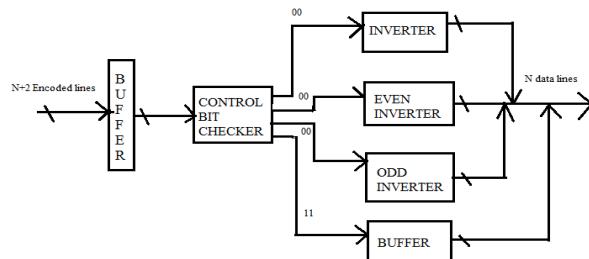


Fig. 6 – Block diagram of Decoder

To retrieve the data from the encoded data, control bits are recovered from the received data and the following operations are performed according to the control bits.

Table I shows operation to be performed on data bits for decoding. Decoding is performed by conversion of an encoded sequence or by dopting exactly opposite sequence of steps of encoding.

TABLE I: DECODING PROCESS EXPLANATION ACCORDING TO THE VALUES OF CONTROL BITS

Control bits	Operation to be performed
00	Invert the received data
01	Invert the data bits of even group
10	Invert the data bits of odd group
11	Data remains same

**V. SIMULATIONS AND RESULTS**

The coding technique provides significant reduction in self transition activity with lesser increase in area overhead. The developing coding technique is found to give significantly better results as compared to previously proposed techniques such as bus invert, partial even/odd invert coding.

To compare the performance of the coding technique with earlier evolved techniques, the power saving factor  $\eta$  [7] is defined as:

$$\eta = \frac{P_{uncoded} - P_{coded}}{P_{uncoded}} \dots \dots \dots (2)$$

Here  $P_{uncoded}$  is the average power consumption of uncoded bus, and  $P_{coded}$  is the average power consumption of power optimized bus scheme. Quadro coding technique is compared with various other techniques evolved earlier is shown in the table below

**Table II** shows comparison of reduction in transition activity of various techniques with proposed coding technique. This table elaborates the total reduction in number of transitions when we use Bus Invert Coding and partial Bus invert coding.

**TABLE II. COMPARISON RESULTS FOR TRANSITION ACTIVITY USING BUS INVERT CODING, PARTIAL INVERT CODING TECHNIQUE.**

Coding Techniques	Data Bus Width	Reduction in transition activity(in %)	Difference in transition activity(in %)
Bus invert coding [1]	8-bit wide	15	21
	16-bit wide	9	14
	32-bit wide	7	8
Partial invert coding [2]	8-bit wide	7	29
	16-bit wide	3	20
	32-bit wide	2	13

**VI. CONCLUSION**

This paper presents a novel coding technique for reducing transition activity in on-chip buses. The technique has been tested on various bus widths and best results are observed for 9 bit bus width, where the transition activity has been reduced by up to 36%. This significant reduction in transition activity results in considerable power saving up to 47%. The power saving varies from 47% to 25% for 8-bit to 32-bit data bus. This technique is

more suitable for shorter length buses as compared to longer buses.

**REFERENCES**

1. M. R. Stan and W. P. Bureson, "Bus-Invert coding for low-power I/O", IEEE Trans. on VLSI, vol. 3, pp. 49- 58, March 1995.
2. Youngsoo Shin, Soo-Ik Chae, and Kiyoung Choi, "Partial Bus-Invert Coding for Power optimization of application-Specific Systems", IEEE Trans. on VLSI, vol. 9, pp. 377-383, April 2001.
3. Ravindra, J. V. R., K. S. Sainarayanan, and M. B. Srinivas. "A novel bus coding technique for low power data transmission." In Proceedings of IEEE Symposium on VLSI Design and Test Conference (VDAT-2005), pp. 263-266. 2005.
4. Saini, Sandeep, and Srinivas B. Mandalika. "A new bus coding technique to minimize crosstalk in VLSI bus." In Electronics Computer Technology (ICECT), 2011 3rd International Conference on, vol. 1, pp. 424-428. IEEE, 2011.
5. Chandrakasan, A. P., S. Sheng, and R. W. Brodersen, "Low-power Digital CMOS Design," IEEE Journal of Solid State Circuits, pp. 473-484, April 1992.
6. Saini, Sandeep, Anurag Mahajan, and Srinivas B. Mandalika. "Implementation of low power FFT structure using a method based on conditionally coded blocks." In Circuits and Systems (APCCAS), 2010 IEEE Asia Pacific Conference on, pp. 935-938. IEEE, 2010.
7. Paul P. Sotiriadis and Anantha P. Chandrakasan, "A Bus Energy Model for Deep Submicron Technology" IEEE Transactions on VLSI systems, vol. 10, No. 3, June 2002.
8. N. Vithya Lakshmi, M. Rajaram, "An octo coding technique to reduce energy transition in low power VLSI circuits", IJRET: International Journal of Research in Engineering and Technology, eISSN: 2319-1163 pISSN: 2321-7308 Volume: 02 Issue: 11 Nov-2013.
9. Sotiriadis, Paul P., and Anantha Chandrakasan. "Low power bus coding techniques considering inter-wire capacitances." Custom Integrated Circuits Conference, 2000. CICC. Proceedings of the IEEE 2000. IEEE, 2000.
10. Ge Chen, Steven Duvall, Saeid Nooshabadi, "An Optimization Strategy for Low Energy and High Performance for the On-chip Interconnect Signalling" ISLPED'09, August 19-21, 2009, San Francisco, California, USA.
11. N. Raj and R. K. Sharma, "A High Swing OTA with wide Linearity for design of Self Tuneable Resistor", International Journal of VLSI design & Communication system (VLSICS), Volume 1, No. 3, pp. 1-11, 2010.

12. N. Raj, A.K. Singh, A.K. Gupta, "Modeling of Human Voice Box in VLSI for Low Power Biomedical Applications", IETE Journal of Research, Vol. 57, Issue 4, pp. 345-353, 2011.
13. N. Raj, A.K. Singh, and A.K. Gupta, "Low power high output impedance high bandwidth QFGMOS current mirror", Microelectronics Journal, Vol. 45, No. 8, pp. 1132-1142, 2014.
14. N. Raj, A.K. Singh, and A.K. Gupta, "Low-voltage bulk-driven self-biased cascode current mirror with bandwidth enhancement", Electronics Letters, Vol. 50, No. 1, pp. 23-25, 2014.
15. N. Raj, A.K. Singh, and A.K. Gupta, "Low Voltage High Output Impedance Bulk- driven Quasi-floating Gate Self-biased High-swing Cascode Current Mirror", Circuit System & Signal Processing Journal, Vol. 35, No. 8, pp. 2683-2703, 2015.
16. N. Raj, A.K. Singh, and A.K. Gupta, "High performance Current Mirrors using Quasi-floating Bulk", Microelectronics Journal, Vol. 52, No. 1, pp. 11-22, 2016.
17. N. Raj, A.K. Singh, and A.K. Gupta, "Low Voltage High Performance Bulk-driven Quasi-floating Gate Self-biased Cascode Current Mirror", Microelectronics Journal, Vol. 52, No. 1, pp. 124-133, 2016.
18. N. Raj, A.K. Singh, and A.K. Gupta, "Low Voltage High Bandwidth Self-biased High Swing Cascode Current Mirror", Indian Journal of Pure and Applied Physics, Vol. 55, No. 4, pp. 245-253, 2017.
19. Raj N. and Gupta A. K., "Analysis of Operational Transconductance Amplifier using Low Power Techniques", Journal of Semiconductor Devices and Circuits (STM Journal), Vol. 1, No. 3, pp. 1-9, 2015.
20. Raj N. and Gupta A. K., "Multifunction Filter Design using BDQFG Miller OTA", Journal of Electrical and Electronics Engineering: An International Journal (EEEIJ Journal), Vol. 4, No. 3, pp. 55-67, 2015.
21. N. Raj, A.K. Singh, and A.K. Gupta, "Low Power Circuit Design Techniques: A Survey", International Journal of Computer Theory and Engineering, Vol. 7, No. 3, pp. 172-176, 2015.

## DESIGN OF POWER AND AREA EFFICIENT APPROXIMATE MULTIPLIERS

B.VIJAYA\* & Dr .R.PURUSHOTHAM NAIK\*\*

M.Tech(ES & VLSI)\*, B.Tech,M.Tech,Ph.D,MISTE\*\*

Department of ECE, Malla Reddy College Of Engineering, Hyderabad, Telangana, INDIA.

**ABSTRACT:** *Inferred preparing can decrease the arrangement multifaceted nature with an extension in execution and power profitability for screw up adaptable applications The proposed gauge is utilized in two varieties of 16-bit multipliers. Mix results reveal that two proposed multipliers achieve control save assets of 72% and 38%, separately, appeared differently in relation to a right multiplier. They have better precision when diverged from existing estimated multipliers. Mean relative botch figures are as low as 7.6% and 0.02% for the proposed assessed multipliers, which are better than the past works. Execution of the proposed multipliers is surveyed with a photo planning application, where one of the proposed models achieves the most astonishing zenith banner to clatter extent.*

**Keywords:** *Approximate computing, error analysis, low error, low power, multipliers.*

### 1.INTRODUCTION:

In applications like multimedia signal processing and data mining which can tolerate error, exact computing units are not always necessary. Research on approximate computing for error tolerant applications is on the rise. Adders and multipliers form the key components in these applications. In [1], approximate full adders are proposed at transistor level and they are utilized in digital signal processing applications. Their proposed full adders are used in accumulation of partial products in multipliers. To reduce hardware complexity of multipliers, truncation is widely employed in fixed-width multiplier designs. Then a constant or variable correction term is added to compensate for the quantization error introduced by the truncated part [2], [3]. Approximation techniques in multipliers focus on accumulation of partial products, which is crucial in terms of power consumption. Broken array multiplier is implemented in [4], where the least significant bits of inputs are truncated, while forming partial products to reduce hardware complexity. The proposed multiplier in [4] saves few adder circuits in partial product accumulation. In [5], two designs of approximate 4-2 compressors are presented and used in partial product reduction tree of four variants of  $8 \times 8$  added multiplier. The major drawback of the proposed compressors in [5] is that they give nonzero output for zero valued inputs, which largely affects the mean relative error (MRE) as discussed later. It overcomes the existing drawback. This leads to better precision. In ,

inaccurate counter design has been proposed for use in power efficient Wallace tree multiplier. A new approximate adder is presented in [10] which is utilized for partial product accumulation of the multiplier. For 16-bit approximate multiplier in [10], 26% of reduction in power is accomplished compared to exact multiplier. Approximation of 8-bit Wallace tree multiplier voltage over-scaling (VOS) is discussed in [11]. Lowering supply voltage creates paths failing to meet delay constraints leading to error. Previous works on logic complexity reduction focus on straightforward application of approximate adders and compressors to the partial products. In this brief, the partial products are altered to introduce terms with different probabilities. Probability statistics of the altered partial products are analyzed, which is followed by systematic approximation. Simplified arithmetic units (half-adder, full-adder, and 4-2 compressor) are proposed for approximation. The arithmetic units are not only reduced in complexity, but care is also taken that error value is maintained low. While systematic approximation helps in achieving better accuracy, reduced logic complexity of approximate arithmetic units consumes less power and area. The proposed multipliers outperform the existing multiplier designs in terms of area, power, and error, and achieve better peak signal to noise ratio (PSNR) values in image processing application. Error distance (ED) can be defined as the arithmetic distance between a correct output and approximate output for a given input. In [12], approximate adders are evaluated and normalized ED (NED) is proposed as a nearly invariant metric

independent of the size of the approximate circuit. Also, traditional error analysis, MRE is found for existing and proposed multiplier designs. The rest of this brief is organized as follows. Section II details the proposed architecture. Section III provides extensive result analysis of design and error metrics of the proposed and existing approximate multipliers. The proposed multipliers are utilized in image processing application.

**2. EXISTING METHOD:**

In applications like sight and sound banner getting ready and data mining which can persevere through error, remedy figuring units are not continually major. They can be supplanted with their construed accomplices. Research on deduced enlisting for screw up tolerant applications is on the rising. Adders and multipliers outline the key fragments in these applications. In [1], inaccurate full adders are proposed at transistor level and they are utilized in cutting edge signal taking care of utilizations. Their proposed full adders are used in social affair of deficient things in multipliers. To diminish hardware multifaceted design of multipliers, truncation is comprehensively used in settled width multiplier designs. Disadvantages of existing system are given underneath

- More Logic multifaceted nature
- More power and more deferral

**3.. PROPOSED ARCHITECTURE**

Implementation of multiplier comprises three steps: generation of partial products, partial products reduction tree, and finally, a vector merge addition to produce final product from the sum and carry rows generated from the reduction tree. Second step consumes more power. In this brief, approximation is applied in reduction tree stage. A 8-bit unsigned 1 multiplier is used for illustration to describe the proposed method in approximation of multipliers. Consider two 8-bit unsigned input operands  $\alpha = \_7$   $m=0 \alpha m 2m$  and  $\beta = \_7n =0 \beta n 2n$ . The partial product  $am, n = \alpha m \cdot \beta n$  in Fig. 1 is the result of AND operation between the bits of  $\alpha m$  and  $\beta n$ . The proposed approximate technique can be applied to signed multiplication including Booth multipliers as well, except it is not applied to sign extension bits.

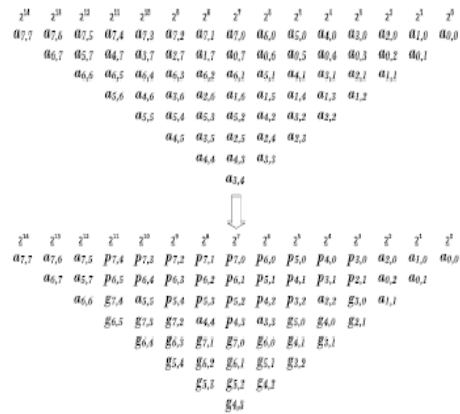


Fig. 1. Transformation of generated partial products into altered partial products

**TABLE I PROBABILITY STATISTICS OF Generate SIGNALS**

m	Probability of the generate elements being				P <sub>err</sub>
	all zero	one 1	two 1's	three 1's and more	
2	0.8789	0.1172	0.0039	-	0.00390
3	0.8240	0.1648	0.0110	0.00024	0.01124
4	0.7725	0.2060	0.0206	0.00093	0.02153

From statistical point of view, the partial product  $am, n$  has a probability of 1/4 of being 1. In the columns containing more than three partial products, the partial products  $am, n$  and  $an, m$  are combined to form *propagate* and *generate* signals as given in (1). The resulting *propagate* and *generate* signals form altered partial products  $pm, n$  and  $gm, n$ . From column 3 with weight 23 to column 11 with weight 211, the partial products  $am, n$  and  $an, m$  are replaced by altered partial products  $pm, n$  and  $gm, n$ . The original and transformed partial product matrices are shown in Fig. 1

$$pm, n = am, n + an, m$$

$$gm, n = am, n \cdot an, m$$

The probability of the altered partial product  $gm, n$  being one is 1/16, which is significantly lower than 1/4 of  $am, n$ . The probability of altered partial product  $pm, n$  being one is  $1/16 + 3/16 + 3/16 = 7/16$ , which is higher than  $gm, n$ . These factors are considered, while applying approximation to the altered partial product matrix

**A. Approximation of Altered Partial Products gm,n**

The accumulation of *generate* signals is done columnwise. As each element has a probability of 1/16 of being one, two elements being 1 in the

same column even decreases. For example, in a column with 4 generate signals, probability of all numbers being 0 is  $(1 - pr)^4$ , only one element being one is  $4pr(1 - pr)^3$ , the probability of two elements being one in the column is  $6pr^2(1 - pr)^2$ , three ones is  $4pr^3(1 - pr)$  and probability of all elements being 1 is  $pr^4$ , where  $pr$  is 1/16. The probability statistics for a number of generate elements  $m$  in each column are given in Table I.

Based on Table I, using OR gate in the accumulation of columnwise generate elements in the altered partial product matrix provides exact result in most of the cases. The probability of error ( $P_{err}$ ) while using OR gate for reduction of generate signals in each column is also listed in Table I. As can be seen, the probability of misprediction is very low. As the number of generate signals increases, the error probability increases linearly. However, the value of error also rises. To prevent this, the maximum number of generate signals to be grouped by OR gate is kept at 4. For a column having  $m$  generate signals,  $\lfloor m/4 \rfloor$  OR gates are used.

**TRUTH TABLE OF APPROXIMATE HALF ADDER**  
**TABLE II**

Inputs		Exact Outputs		Approximate Outputs		Absolute Difference
$x_1$	$x_2$	Carry	Sum	Carry	Sum	
0	0	0	0	0 ✓	0 ✓	0
0	1	0	1	0 ✓	1 ✓	0
1	0	0	1	0 ✓	1 ✓	0
1	1	1	0	1 ✓	1 ✗	1

**TRUTH TABLE OF APPROXIMATE FULL ADDER**  
**FULL ADDER TRUTH TABLE**

Inputs			Exact Outputs		Approximate Outputs		Absolute Difference
$x_1$	$x_2$	$x_3$	Carry	Sum	Carry	Sum	
0	0	0	0	0	0 ✓	0 ✓	0
0	0	1	0	1	0 ✓	1 ✓	0
0	1	0	0	1	0 ✓	1 ✓	0
0	1	1	1	0	1 ✓	0 ✓	0
1	0	0	0	1	0 ✓	1 ✓	0
1	0	1	1	0	1 ✓	0 ✓	0
1	1	0	1	0	0 ✗	1 ✗	1
1	1	1	1	1	1 ✓	0 ✗	1

**B. Approximation of Other Partial Products**

The storing up of other midway things with probability  $1/4$  for am,n and  $7/16$  for pm,n uses deduced circuits. Assessed half-snake, full-snake, and 4-2 blower are proposed for their social event. Carry and Sum are two yields of these assessed circuits. Since Carry has higher weight of matched piece, bungle in Carry bit will contribute more by making botch qualification of two in the yield. Figure is managed with the goal that the

aggregate difference between real yield and induced yield is always kept up as one. In this way Carry yields are approximated only for the cases, where Sum is approximated. In adders and blowers, XOR entryways tend to add to high district and delay. For approximating half-wind, XOR passage of Sum is supplanted with OR entryway as given in (2). This results in a solitary bumble in the Sum figuring as found as a general rule table of estimated half-snake in Table II. A tick check implies that inferred yield matches with reconsider yield and cross stamp implies jumble

Entire =  $x_1 + x_2$   
 Carry =  $x_1 \cdot x_2$  (2)

In the gauge of full-snake, one of the two XOR gateways is supplanted with OR entryway in Sum calculation. This results in botch in last two cases out of eight cases. Carry is balanced as in (3) displaying one goof. This gives more revisions, while keeping up the qualification among exceptional and evaluated a motivator as one. Reality table of harsh full-wind is given in Table III

$W = (x_1 + x_2)$   
 Total =  $W \oplus x_3$   
 Carry =  $W \cdot x_3$  (3)

To keep up irrelevant screw up differentiate as one, the yield "100" (the estimation of 4) for four data sources being one needs to be supplanted with yields "11" (the estimation of 3). For Sum figuring, one out of three XOR entryways is supplanted with OR door. In like manner, to make the Sum identifying with the circumstance where all information sources are ones as one, an additional circuit  $x_1 \cdot x_2 \cdot x_3 \cdot x_4$  is added to the Sum verbalization. This results in goof in five out of 16 cases. Carry is unraveled as in (4). The looking at truth table is given in Table IV

$W_1 = x_1 \cdot x_2$   
 $W_2 = x_3 \cdot x_4$  Sum =  $(x_1 \oplus x_2) + (x_3 \oplus x_4) + W_1 \cdot W_2$   
 Carry =  $W_1 + W_2$  (4)

**TRUTH TABLE OF APPROXIMATE 4-2 COMPRESSOR**

Inputs				Approximate outputs		Absolute Difference
$x_1$	$x_2$	$x_3$	$x_4$	Carry	Sum	
0	0	0	0	0 ✓	0 ✓	0
0	0	0	1	0 ✓	1 ✓	0
0	0	1	0	0 ✓	1 ✓	0
0	0	1	1	1 ✓	0 ✓	0
0	1	0	0	0 ✓	1 ✓	0
0	1	0	1	0 ✗	1 ✗	1
0	1	1	0	0 ✗	1 ✗	1
0	1	1	1	1 ✓	1 ✓	0
1	0	0	0	0 ✓	1 ✓	0
1	0	0	1	0 ✗	1 ✗	1
1	0	1	0	0 ✗	1 ✗	1
1	0	1	1	1 ✓	1 ✓	0
1	1	0	0	1 ✓	0 ✓	0
1	1	0	1	1 ✓	1 ✓	0
1	1	1	0	1 ✓	1 ✓	0
1	1	1	1	1 ✗	1 ✗	1

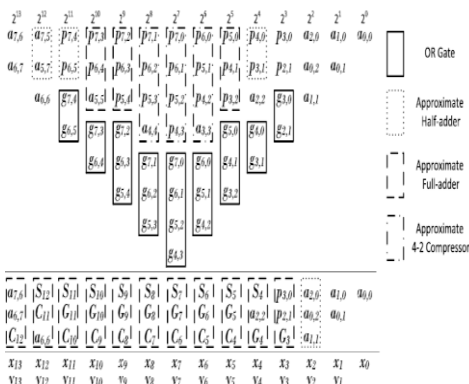


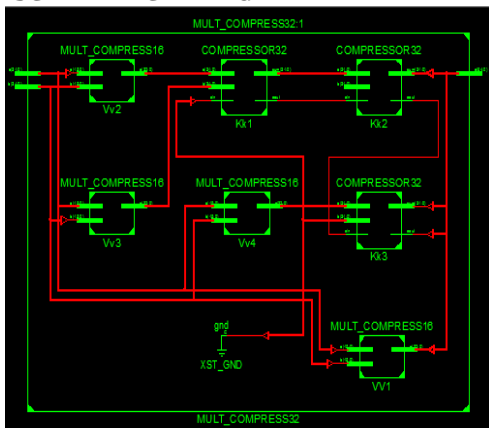
Fig. 2. Reduction of altered partial products

Fig. 2 shows the reduction of altered partial product matrix of  $8 \times 8$  approximate multiplier. It requires two stages to produce sum and carry outputs for vector merge addition step. Four 2-input OR gates, four 3-input OR gates, and one 4-input OR gates are required for the reduction of generate signals from columns 3 to 11. The resultant signals of OR gates are labeled as  $G_i$  corresponding to the column  $i$  with weight  $2i$ . For reducing other partial products, 3 approximate half-adders, 3 approximate full-adders, and 3 approximate compressors are required in the first stage to produce  $S_i$  and  $C_i$  corresponding to column  $i$ . The elements in the second stage are reduced using 1 approximate half-adder and 11 approximate full-adders producing final two operands  $x_i$  and  $y_i$  to be fed to ripple carry adder for the final computation of the result.

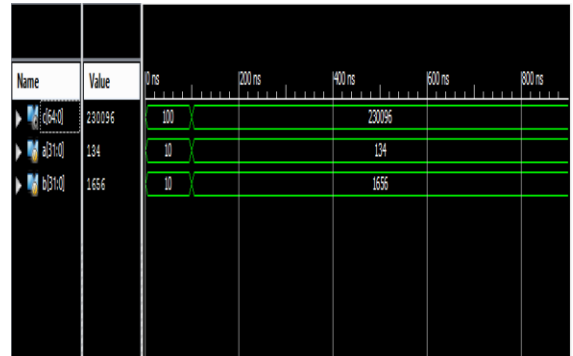
**C. Two Variants of Multipliers**

Two varieties of multipliers are proposed. In the essential case (Multiplier1), estimation is associated in all fragments of partial aftereffects of n-bit multiplier, however in Multiplier2, vague circuits are used in  $n - 1$  smallest enormous segments

**RTL SCHEMATICH DIAGRAM**



**4.RESULTS AND DISCUSSION  
 RTL SIMULATION WAVE FORM:**



**DESIGN SUMMARY:**

Device Utilization Summary (estimated values)			
Logic Utilization	Used	Available	Utilization
Number of Slice LUTs	2692	67400	4%
Number of fully used LUTFF pairs	0	2692	0%
Number of bonded IOBs	129	210	61%

**TIME SUMMARY**

LUT5:I4->0	5	0.097	0.314	Rk2/R2/GC3/G1 (Rk2/R2/s<3>)
LUT5:I4->0	2	0.097	0.299	Rk2/R2/GC7/G1 (Rk2/R2/v<7>)
LUT5:I4->0	3	0.097	0.389	Rk2/R2/GC16/G1 (cout2)
LUT6:I4->0	5	0.097	0.712	Rk3/R1/GC1/G1 (Rk3/R1/q<1>)
LUT6:I0->0	2	0.097	0.688	Rk3/R1/GC3/G (Rk3/R1/s<3>)
LUT6:I1->0	2	0.097	0.299	Rk3/R1/GC7/G3_SWO (M195)
LUT5:I4->0	1	0.097	0.295	Rk3/R1/GC7/G3 (Rk3/R1/GC7/G2)
LUT6:I5->0	1	0.097	0.379	Rk3/R1/GC16/G4_SWO (M177)
LUT6:I4->0	4	0.097	0.707	Rk3/R1/GC16/G4 (Rk3/cout1)
LUT6:I0->0	4	0.097	0.570	Rk3/R2/GC1/G1 (Rk3/R2/q<1>)
LUT6:I2->0	2	0.097	0.688	Rk3/R2/GC6/G11 (Rk3/R2/GC6/G1)
LUT5:I0->0	4	0.097	0.570	Rk3/R2/GC8/G11 (Rk3/R2/GC8/G1)
LUT4:I0->0	1	0.097	0.295	Rk3/R2/GC8/G1 (Rk3/R2/v<8>)
LUT6:I5->0	1	0.097	0.279	Rk3/R2/Mxor_sum<15:1>_12_xc<0>1 (c_61_OBUF)
OBUF:I->0	0.000			c_61_OBUF (c<61>)
-----				
Total		26.335ns	(4.075ns logic, 22.260ns route)	(15.5% logic, 84.5% route)

All approximate multipliers are designed for  $n = 16$ . The multipliers are implemented in verilog and synthesized using Synopsys Design Compiler and a TSMC 65 nm standard cell library at the typical process corner, with temperature 25 °C and supply voltage 1 V. From the Synopsys dc reports, we get area, delay, dynamic power and

leakage power. Multiplier1 all columns, whereas in Multiplier2, approximation is applied in 15 least significant columns during partial product reduction. For the proposed multipliers, the altered partial products are generated and compressed using half-adder, full-adder, and 4-2 compressor structures to form final two rows of partial products. The efficiency of the proposed multipliers is compared with existing approximate multipliers. Inexact compressor design 2 of [5] is used to design compressor based multipliers ACM1, where all columns are approximated and ACM2, where only 15 least significant columns are approximated.

SSM [6] for  $m = 12$  and  $n = 16$  is designed for implementation. PPP design discussed in [7] for  $j = 2$ ,  $k = 2$  is designed and implemented under Dadda tree structure. In [8], the partial product matrix of 16-bit under designed multiplier (UDM) comprises approximate  $2 \times 2$  partial products accumulated together with exact carry save adders. Exhaustive error analysis of the approximate multipliers is done using MATLAB. Exact 16-bit multiplier is designed using Dadda tree structure. Table compares all designs in terms of area, delay, power, power delay product (PDP), and area power product (APP). NED and MRE of the approximate multipliers are listed in Table. If high approximation can be tolerated for saving more power, Multiplier1 and ACM1 are the candidates to be considered. It can be seen that Multiplier1 has better APP, whereas ACM1 has better PDP. However, Multiplier1 has 64% lower NED and three orders of magnitude lower MRE, compared to ACM1. It should be noted that high values of MRE for ACMs are due to nonzero output for inputs with all zeros

### 5.APPLICATION—IMAGE PROCESSING

Geometric mean filter is widely used in image processing to reduce Gaussian noise [13]. The geometric mean filter is better at preserving edge features than the arithmetic mean filter. Two 16-bits per pixel gray scale images with Gaussian noise are considered.  $3 \times 3$  mean filter is used, where each pixel of noisy image is replaced with geometric mean of  $3 \times 3$  block of neighboring pixels centered around it. The algorithms are coded and implemented in MATLAB. Exact and approximate 16-bit multipliers are used to perform multiplication between 16-bit pixels. PSNR is used as figure



(f) 43.0, 0.96 (g) 81.3, 0.45 (h) 73.3, 0.50 (i) 38.8, 0.43 (j) 38.05, 0.76

Fig. 4. (a) Input image-1 with Gaussian noise. Geometric mean filtered images and corresponding PSNR and energy savings in  $\mu J$  using (b) exact multiplier, (c) Multiplier1, (d) Multiplier2, (e) ACM1, (f) ACM2, (g) SSM, (h) PPP, (i) UDM, and (j) VOS.



(a) (b) (c) 36.6, 2.38 (d) 95.1, 1.21 (e) 23.0, 2.56



(f) 51.1, 1.10 (g) 79.7, 0.74 (h) 83.7, 0.58 (i) 37.5, 0.68 (j) 37.34, 0.94

Fig. 5. (a) Input image-2 with Gaussian noise. Geometric mean filtered images and corresponding PSNR and energy savings in  $\mu J$  using (b) exact multiplier, (c) Multiplier1, (d) Multiplier2, (e) ACM1, (f) ACM2, (g) SSM, (h) PPP, (i) UDM, and (j) VOS. The noisy input image and resultant image after denoising using exact and approximate multipliers, with their respective PSNRs and energy savings in  $\mu J$  are shown in Figs. 4 and 5, respectively. Energy required for exact multiplication process for image-1 and image-2 is savings compared to Multiplier1, Multiplier1 has significantly higher PSNR than ACM1. Multiplier2 shows the best PSNR among all the approximate designs. Multiplier2 has better energy savings, compared to ACM2, PPP, SSM, UDM, and VOS. The intensity of image-1 being mostly on the lower end of the histogram causes poor performance of ACM multipliers. As the switching activity impacts most significant part of the design in VOS, PSNR values are affected.

### 6.CONCLUSION:

In this brief, to propose efficient approximate multipliers, partial products of the multiplier are modified using *generate* and *propagate* signals. Approximation is applied using simple OR gate for altered *generate* partial products. Approximate half-adder, full-adder, and 4-2 compressor are proposed to reduce remaining partial products. Two variants of approximate multipliers are proposed, where approximation is applied in all  $n$  bits in Multiplier1 and only in  $n - 1$

least significant part in Multiplier2. Multiplier1 and Multiplier2 achieves significant reduction in area and power consumption compared with exact designs. With APP savings being 87% and 58% for Multiplier1 and Multiplier2 with respect to exact multipliers, they also outperform in APP in comparison with existing approximate designs. They are also found to have better precision when compared to existing approximate multiplier designs. The proposed multiplier designs can be used in applications with minimal loss in output quality while saving significant power and area

## REFERENCES

1. V. Gupta, D. Mohapatra, A. Raghunathan, and K. Roy, "Low-control advanced flag preparing utilizing inexact adders," *IEEE Trans. Comput.-Aided Design Integr. Circuits Syst.*, vol. 32, no. 1, pp. 124–137, Jan. 2013.
2. E. J. Ruler and E. E. Swartzlander, Jr., "Information subordinate truncation plot for parallel multipliers," in *Proc. 31st Asilomar Conf. Signs, Circuits Syst.*, Nov. 1998, pp. 1178–1182.
3. K.- J. Cho, K.- C. Lee, J.- G. Chung, and K. K. Parhi, "Plan of low-blunder settled width adjusted corner multiplier," *IEEE Trans. Large Scale Integr. (VLSI) Syst.*, vol. 12, no. 5, pp. 522–531, May 2004.
4. H. R. Mahdiani, A. Ahmadi, S. M. Fakhraie, and C. Lucas, "Bio-roused uncertain computational squares for effective VLSI execution of delicate figuring applications," *IEEE Trans. Circuits Syst. I, Reg. Papers*, vol. 57, no. 4, pp. 850–862, Apr. 2010.
5. A. Momeni, J. Han, P. Montuschi, and F. Lombardi, "Plan and examination of inexact blowers for duplication," *IEEE Trans. Comput.*, vol. 64, no. 4, pp. 984–994, Apr. 2015.
6. S. Narayanamoorthy, H. A. Moghaddam, Z. Liu, T. Stop, and N. S. Kim, "Energy-effective inexact augmentation for computerized flag preparing and grouping applications," *IEEE Trans. Large Scale Integr. (VLSI) Syst.*, vol. 23, no. 6, pp. 1180–1184, Jun. 2015.
7. G. Zervakis, K. Tsoumanis, S. Xydis, D. Soudris, and K. Pekmestzi, "Outline proficient surmised increase circuits through halfway item aperture," *IEEE Trans. Large Scale Integr. (VLSI) Syst.*, vol. 24, no. 10, pp. 3105–3117, Oct. 2016.
8. P. Kulkarni, P. Gupta, and M. D. Ercegovac, "Exchanging precision for control in a multiplier engineering," *J. Low Power Electron.*, vol. 7, no. 4, pp. 490–501, 2011.
9. C.- H. Lin and C. Lin, "High precision estimated multiplier with blunder revision," in *Proc. IEEE 31st Int. Conf. Comput. Plan*, Sep. 2013, pp. 33–38.
10. C. Liu, J. Han, and F. Lombardi, "A low-control, elite surmised multiplier with configurable halfway mistake recuperation," in *Proc. Conf. Display. (DATE)*, 2014, pp. 1–4.
11. N. Raj and R. K. Sharma, "A High Swing OTA with wide Linearity for design of Self Tuneable Resistor," *International Journal of VLSI design & Communication system (VLSICS)*, Volume 1, No. 3, pp. 1-11, 2010.
12. N. Raj, A.K. Singh, A.K. Gupta, "Modeling of Human Voice Box in VLSI for Low Power Biomedical Applications," *IETE Journal of Research*, Vol. 57, Issue 4, pp. 345-353, 2011.
13. N. Raj, A.K. Singh, and A.K. Gupta, "Low power high output impedance high bandwidth QFGMOS current mirror," *Microelectronics Journal*, Vol. 45, No. 8, pp. 1132-1142, 2014.
14. N. Raj, A.K. Singh, and A.K. Gupta, "Low-voltage bulk-driven self-biased cascode current mirror with bandwidth enhancement," *Electronics Letters*, Vol. 50, No. 1, pp. 23-25, 2014.
15. N. Raj, A.K. Singh, and A.K. Gupta, "Low Voltage High Output Impedance Bulk- driven Quasi-floating Gate Self-biased High-swing Cascode Current Mirror," *Circuit System & Signal Processing Journal*, Vol. 35, No. 8, pp. 2683-2703, 2015.
16. N. Raj, A.K. Singh, and A.K. Gupta, "High performance Current Mirrors using Quasi-floating Bulk," *Microelectronics Journal*, Vol. 52, No. 1, pp. 11-22, 2016.
17. N. Raj, A.K. Singh, and A.K. Gupta, "Low Voltage High Performance Bulk-driven Quasi-floating Gate Self-biased Cascode Current Mirror," *Microelectronics Journal*, Vol. 52, No. 1, pp. 124-133, 2016.
18. N. Raj, A.K. Singh, and A.K. Gupta, "Low Voltage High Bandwidth Self-biased High Swing Cascode Current Mirror," *Indian Journal of Pure and Applied Physic*, Vol. 55, No. 4, pp. 245-253, 2017.
19. Raj N. and Gupta A. K., "Analysis of Operational Transconductance Amplifier using Low Power Techniques," *Journal of Semiconductor Devices and Circuits (STM Journal)*, Vol. 1, No. 3, pp. 1-9, 2015.
20. Raj N. and Gupta A. K., "Multifunction Filter Design using BDQFG Miller OTA," *Journal of Electrical and Electronics Engineering: An International Journal (EEEIJ Journal)*, Vol. 4, No. 3, pp. 55-67, 2015.
21. N. Raj, A.K. Singh, and A.K. Gupta, "Low Power Circuit Design Techniques: A Survey," *International Journal of Computer Theory and Engineering*, Vol. 7, No. 3, pp. 172-176, 2015.

# EFFECT OF DIFFERENT PROCESS PARAMETERS ON THE SYNTHESIS AND CHARACTERIZATION OF CARBON NANOTUBES

Gidla Rabecca Rani

Department of Physics, Malla Reddy College of Engineering, Hyderabad-500100

**ABSTRACT:** Carbon Nanotubes (CNTs) have been of great interest, since their discovery, both from a fundamental point of view and for the future applications. The present work includes the synthesis of Carbon Nanotubes by Arc Discharge Method and the effect of various process parameters during the synthesis. Optimization of the process parameters is necessary for the high yield and good quality of the CNTs with low carbon subsidiary impurities. In the case of synthesis of Multi walled carbon Nanotubes, the study pertains to analysis of the effect of the buffer gas used; the effect of the partial pressure of the buffer gas and effect of shape of cathode on the synthesis of MWCNTs. From the experimental trials, synthesis of MWCNTs seemed to be favorable in Hydrogen atmosphere as the synthesis time of 80 mins in Helium is reduced to 8 mins in Hydrogen. There also appears to be no effect of variation of partial pressure of buffer gas Helium between 300 Torr & 440 Torr on the co-synthesis of SWCNTs & MWCNTs.

**Keywords:** Carbon nanotubes, MWCNTs, Amorphous carbon, Graphite nanoparticles, Arc Discharge.

## 1. INTRODUCTION:

### 1.1 CARBON

[1] Carbon is the lightest member of the IVA family of the periodic table with atomic number 6 and electronic configuration  $1s^2 2s^2 2p^2$ . Its first ionization potential is 11.26V. The atomic weight of C12 = 12.0000 was established by the IUPAC in 1961 as the standard of atomic weights. It is a non-metallic solid which comes under p-block elements of the periodic table. It is a tetravalent compound having four valence electrons to form covalent chemical bonds.

### 1.2 ALLOTROPES OF CARBON

The three relatively well-known allotropes of carbon are amorphous carbon, graphite, and diamond. Once considered exotic, fullerenes are nowadays commonly synthesized and used in research; they include buckyballs (C<sub>60</sub>), carbon nanotubes, carbon nanobuds (C<sub>60</sub> attached to Carbon nanotube wall) and nanofibers. Several other exotic allotropes have also been discovered, such as lonsdaleite, glassy carbon, carbon nanofoam and linear acetylenic carbon.

### 1.3 CARBON NANOTUBES

Carbon nanotubes are extraordinary macromolecules containing only carbon. They are formed by rolling up graphene sheets. Nanotubes are members of the fullerene structural family, which also includes the spherical buckyballs. The ends of a nanotube might be capped with a hemisphere of the buckyball structure.

Carbon nanotubes (CNTs) are one of the most commonly mentioned building blocks of nanotechnology. With one hundred times the

tensile strength of steel, thermal conductivity better than all but the purest diamond, and electrical conductivity similar to copper, but with the ability to carry much higher currents, they seem to be a wonder material.

### 1.3.1 TYPES OF CARBON NANOTUBES AND RELATED STRUCTURES

Carbon Nanotubes are categorized as Single-walled carbon nanotubes (SWCNTs) and Multi-walled carbon nanotubes (MWCNTs). A Single walled carbon nanotube is a rolled up sheet of graphene, which is a planar-hexagonal arrangement of carbon atoms distributed in a honeycomb lattice. Nano tubes can have a single wall (SWNTs) or multiple walls (MWNTs), which consist of several concentric single-walled nanotubes.

### 1.3.2 SYNTHESIS OF CARBON NANOTUBES

There are several techniques for producing single and Multi walled nanotubes. And, all of them have advantages as well as disadvantages. The most established methods are the high temperature techniques, namely arc discharge and laser ablation, as well as chemical vapor deposition.

### THE ARC DISCHARGE METHOD

The carbon arc discharge method, initially used for producing C<sub>60</sub> fullerenes, is the most common and perhaps easiest way to produce carbon nanotubes as it is rather simple to undertake. However, it is a technique that produces a mixture of components and requires separating nanotubes from the soot and the catalytic metals present in the crude product. This method creates nanotubes through arc-vaporisation of two carbon rods

placed end to end, separated by approximately 1mm, in an enclosure that is usually filled with inert gas (helium, argon) at low pressure (between 50 and 700 mbar). A direct current of 50 to 100 A, driven by approximately 20 V creates a high temperature discharge between the two electrodes. The discharge vaporises one of the carbon rods and forms a small rod shaped deposit on the other rod. Producing nanotubes in high yield depends on the uniformity of the plasma arc and the temperature of the deposit form on the carbonelectrode.

## 2. EXPERIMENTALPROCEDURE

### 2.1 SYNTHESIS OF MULTIWALLED CARBON NANOTUBES:

Arc Discharge set up consists of a cylindrical stainless steel chamber with dimensions of 480 mm length and 730 mm diameter. Enclosed in the chamber are two graphite electrodes, a stationary cathode of 75 mm diameter, 20 mm thick, of pure graphite and a movable anode of dimension 15x15x180mm of pure graphite. Fig 1 (a) and (b) shows the Graphite anode bar and the Flat Graphite cathode that are used for the synthesis of Multi walled carbon nanotubes. The chamber and the graphite electrodes are independently water cooled up to 6.5 bar. Each run begins by evacuating the chamber followed by backfilling with buffer gas.

For igniting the arc, the movable graphite anode is made to touch the stationary graphite cathode. Fig 1 (c) shows the plasma arc that is produced inside the chamber, during the process of arcing.

The power supply is set to 40V and the current mayfluctuate between 180 and 742 Amps. An accurate positioning system is employed to maintain a steady feed rate of the movable anode, which canbe instantly adjusted in the range of 0-3 cm min<sup>-1</sup>. The arc current and voltage are monitored automatically and can be precisely controlled by adjusting the output of the arc power supply and the gap between the twodischargingsurfaces. A self-sustained stabilized arc-discharge is established by carefully adjusting the arc-discharge parameters. The anode is continuously sublimated and some of the carbon vapour gets condensed and is deposited on the stationary cathode. The cylindrical cathode deposit grows steadily while the gap between the two surfaces remains constant (about 1 mm). Fig 1 (d) shows the Cathode deposit that is obtained when the synthesis is carried in Helium buffer gas. The remaining carbon vapouris condensed and deposited on the walls of the chamber as soot. After the completion of each run, the chamber is

allowed to cool. Scraping tools are used to remove and collect the soot material that remains affixed to the chamber walls. The cathode deposit which consists of pristine Multi walled carbon nanotubes and other carbonaceous impurities are characterized by a variety of analytical techniques including Field Emission Scanning Electron Microscopy (FE-SEM, S4300SE/N) and Thermo Gravimetric Analysis (TGA, NETZCH STA 449Jupiter).

For the synthesis of Multi walled carbon nanotubes, five production runs were carried out using Helium as buffer gas under the partial pressure of 300 Torr. Details of the production runs mentioned in Table 1. For evaluating the effect of the type of the buffer gas on the synthesis of Multi walled carbon nanotubes, three more production runs were carried out using Hydrogen as buffer gas at partial pressures of 200,350and 500 Torr. Details of the experiments are mentioned in Table 2.

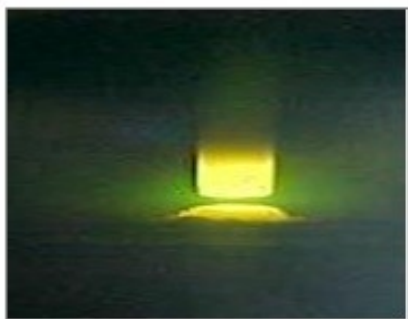
Figure 1 (e) shows the cathode deposit. For evaluating the effect of the shape of cathode on the synthesis of Multi walled carbon nanotubes, five more experiments were carried out using Hydrogen as buffer gas under the partial pressure of 350 Torr. Details of the experiments are mentioned in Table 3. The cup shaped cathode is shown in Figure 1 (f). The time taken for each experiment was 80 min in Helium compared to that of 8 min in Hydrogen.



(a) Graphite Anode bar



(b) Flat graphite cathode



(c) Plasma arcing inside the chamber



(f) Cup shaped graphite cathode  
 Fig 1



(d) Cathode deposit in Helium



(e) Cathode deposit In Hydrogen

**Table 1: Details of the Synthesis of Multi-Walled Carbon Nanotubes in Helium atmosphere at 300 Torr**

Expt.No.	Initial Weight of the anode (Grams)	Cathode deposit (Grams)	Current (Amps)	Voltage (Volts)
1	63.7320	36.801	742-212	40
2	59.8098	31.45	302-220	40
3	60.02	36.7475	456-212	40
4	64.0221	43.982	304-207	40
5	54.0747	25.0405	386-180	40

**Table 2: Details of the Synthesis of Multi Walled Carbon Nanotubes in Hydrogen atmosphere**

Exno	Initial weight of the anode (grams)	Partial pressure of hydrogen (Torr)	Cathode deposit (grams)	Yield, %	Current (Amp)	Voltage (Volts)
1	12.6155	200	3.2048	32	623-465	40
2	47.8436	350	17.999	41	714-305	40
3	32.7046	500	9.0901	34	631-264	40

**Table 3: Comparative study of Multi Walled Carbon Nanotubes synthesized with Flat type cathode and cup Shaped cathode**

Expt. No	Shape of the cathode	Initial weight of the anode (grams)	Partial pressure of hydrogen	Cathode deposit (grams)	Current (Amps)	Voltage (Volts)

			(Torr)			
1	Cup	28.1647	350	10.94	610-406	40
2	Cup	18.55	350	7.8	175-150	30
3	Flat	18.49	350	7.9397	201-145	30
4	Flat	18.2734	350	9.1146	175-110	25
5	Flat	17.6983	500	7.8056	159-120	25

### 3.0 CHARACTERIZATION

The as grown Multi walled carbon nanotubes were characterized by FESEM (Field Emission Scanning Electron Microscope) and the Thermo Gravimetric Analysis (TGA).

#### 3.1 Field Emission Scanning Electron Microscope (FESEM):

The FESEM is very useful tool to observe the nano particles. Under vacuum, electrons generated by a Field Emission Source are accelerated in a field gradient. The beam passes through Electromagnetic Lenses, focusing onto the specimen. As a result of this bombardment different types of electrons are emitted from the specimen. A detector catches the secondary electrons and an image of the sample surface is constructed by comparing the intensity of these secondary electrons to the scanning primary electron beam. Finally the image is displayed on a monitor. This instrument is used for observing sample surfaces at high magnifications.

#### 3.2 TGA: Thermo Gravimetric Analysis:

Thermo Gravimetric Analysis (TGA) is a type of testing that is performed on samples to determine changes in weight in relation to change in temperature. Such analysis relies on a high degree of precision in three measurements: weight, temperature and temperature change. A derivative weight loss curve can be used to tell the point at which weight loss is most apparent. TGA is commonly employed in research and testing to determine characteristics of materials such as polymers, to determine degradation temperatures, absorbed moisture content of materials, the level of inorganic and organic components in materials, decomposition points of explosives and solvent residues. It is also often used to estimate the corrosion kinetics in high temperature oxidation.

### 4.0 RESULTS AND DISCUSSION

#### SYNTHESIS OF MULTI WALLED CARBON NANOTUBES

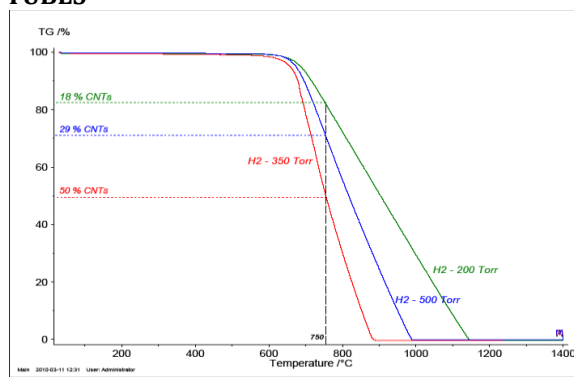


Fig2: TGA of cathode deposits obtained at different partial pressures of Hydrogen

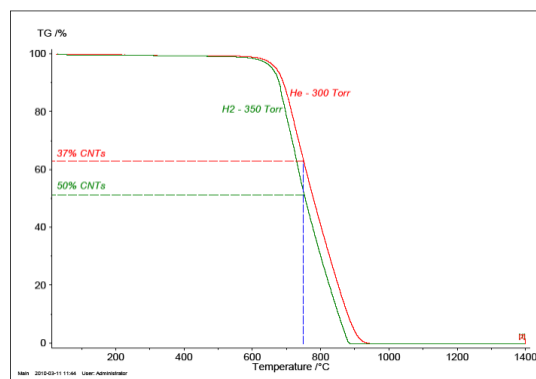
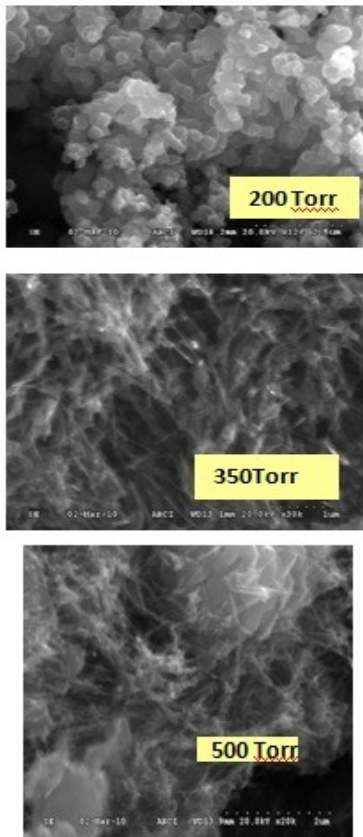


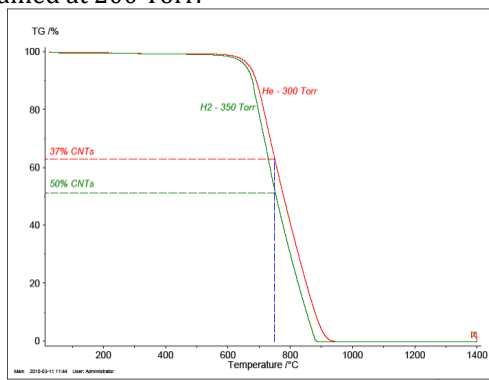
Figure 2 above shows the thermo gravimetric analysis of the cathode deposits obtained in hydrogen atmosphere at different partial pressures of 200 Torr, 350 Torr and 500 Torr. From the TGA Curves, shown in Figure 2, it is observed that the onset of oxidation for MWCNTs synthesized at partial pressure of 200, 350 and 500 Torr commenced at temperature of 600, 550 and 650 deg C respectively. From the above observation, it can be inferred that amorphous carbon does not exist. From the TGA Curves, it is further observed that, MWCNTs, appears to be maximum (~50%) for the deposit obtained at 350

Torr, compared to deposits obtained at 500 Torr (~29%) and 200 Torr (~18%).



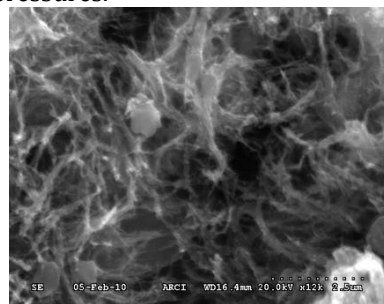
**Fig 3: SEM images of the as synthesized deposits obtained in hydrogen atmosphere**

Fig 3 shows the SEM images of all the three deposits obtained in hydrogen atmosphere at different partial pressures of 200 Torr, 350 Torr and 500 Torr. From the SEM images, maximum amount of MWCNTs are seen in the deposit obtained at 350 Torr. The amount of CNTs is slightly more on the bottom portion of the deposit obtained at 500 Torr. Maximum amount of graphite nanoparticles are seen in the deposit obtained at 200 Torr.

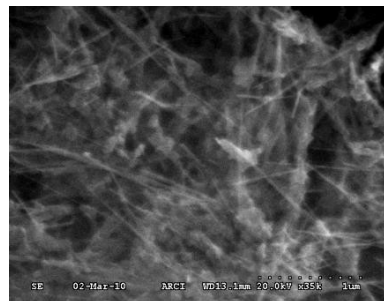


**Fig 4: TGA of the deposits obtained in Helium and Hydrogen atmospheres**

Figure 4 shows the thermo gravimetric analysis of the deposits obtained in helium and hydrogen atmospheres. From the TGA curves shown in figure 4, MWCNTs synthesized in Hydrogen and Helium atmospheres at partial pressure of 350 and 300 Torr respectively, it is observed that more number of MWCNTs are present in the deposit obtained in hydrogen atmosphere (~50%) compared to that obtained in helium atmosphere (~37%). For the purpose of the above comparison, MWCNTs synthesized in Helium atmosphere at partial pressure of 300 Torr is selected based on the earlier experimental results, which established that MWCNTs synthesized at partial pressure of 300 Torr gives better yield of MWCNTs than other partial pressures.



**SEM image of the deposit obtained at 300 Torr of Helium**

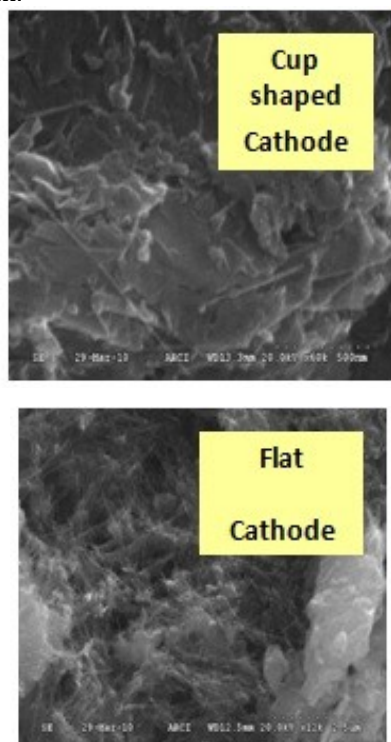


**SEM Image of the deposit obtained at 350 Torr of Hydrogen**

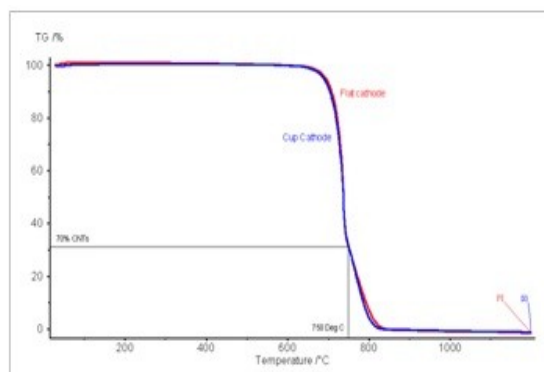
**Fig 5**

Figure 5 shows the SEM images of the deposits obtained in helium and hydrogen atmospheres at partial pressure of 300 and 350 Torr respectively. It is clear that the CNTs are more and amorphous carbon is less in hydrogen atmosphere compared to that in helium atmosphere. Also, the CNTs obtained in helium atmosphere are bent and randomly oriented Whereas, the CNTs have linear orientation and are well distributed, when the synthesis is carried out in Hydrogen atmosphere. Synthesis of MWCNTs is favourable in hydrogen gas because the ionization energy of hydrogen (1312 kJ.mol<sup>-1</sup>) is very less compared to that of helium gas (2372.3 kJ.mol<sup>-1</sup>). Under such conditions, the plasma arc generated in Hydrogen

is of higher quality and the erosion of graphite rod is faster than in Helium. Hence, synthesis time in Hydrogen is 8 mins as compared to synthesis time of 80 mins in Helium. In addition to that, the Thermal conductivity of Hydrogen (0.1805 W.m<sup>-1</sup>.K<sup>-1</sup>) is higher than that of Helium (0.1513 W.m<sup>-1</sup>.K<sup>-1</sup>). Dynamic viscosity of Hydrogen is 0.173 x10<sup>-7</sup> kgf.s/m<sup>2</sup>, where as, the Dynamic viscosity of Helium is 0.394x10<sup>-7</sup> kgf.s/m<sup>2</sup>. density of Hydrogen is 0.08987 kg/m<sup>3</sup>, whereas, density of Helium is 0.1785 kg/m<sup>3</sup>. Higher thermal conductivity accompanied by lower dynamic viscosity and density of Hydrogen enables faster cooling rate of sublimated carbon as compared to Helium.



**Fig.6: SEM images of the deposit synthesized in a cup shaped cathode and on a Flat cathode.**



**Fig7: TGA of the deposits synthesized in a cup shaped cathode and on a Flat cathode**

From the TGA curves shown in figure 7, it is observed that 70% of MWCNTs are present in the deposit, when the synthesis is carried out in a cup shaped cathode and on a Flat cathode. Not much difference could be seen, on comparison.

## 5. CONCLUSIONS

1. Selective growth of both SWCNTs and MWCNTs can be produced within the same arc-discharge run by using appropriate catalyst composition and run conditions, without isolating the tubes of one type from the other.
2. During co-synthesis of SWCNTs & MWCNTs, the as-prepared cathode deposit do not contain the amorphous carbon & catalyst particles which suggests that the wet chemistry may be completely avoided in order to obtain purified MWCNTs from the cathode deposit.
3. Following inferences could be drawn while optimising the parameters, during synthesis of only MWCNTs
  - a) Partial pressure of 350 Torr has given better yield of MWCNTs in Hydrogen atmosphere.
  - a) Better yield of MWCNTs can be obtained in Hydrogen than in Helium.
  - b) No significant improvement in the yield of MWCNTs, with respect to the synthesis in cup-shaped cathode or flat type cathode.
  - c) As-prepared cathode deposit does not contain the amorphous carbon which suggests that further purification is not required.

## REFERENCES

- Chemistry Operations (December 15, 2003). "[Carbon](#)". Los Alamos National Laboratory. Retrieved 2008-10-09[1].
- Walker, J. (1979). "Optical absorption and luminescence in diamond". Reports on Progress in Physics 42: 1605-1659. [Doi: 10.1088/0034-4885/42/10/001](#)
- D.A.Bochvar and E.G.Gal'pern, Dokl.Akad.Nauk.USSR, 209, (610), 1973
- H.W.Kroto, J.R.Heath, S.C.O'Brien, R.F.Curl, and R.E.Smalley, Nature, 318, (162), 1985
- Huhtala, Maria (2002). "[Carbon nanotube structures: molecular dynamics simulation at realistic limit](#)". Computer Physics Communications 146: 30. [doi:10.1016/S0010-4655\(02\)00432-0](#) Dresselhaus, M. S., Dresselhaus, G., and Eklund, P. C., 1996
- Belluci, S. (2005).

- "Carbon nanotubes: physics and applications".  
Phys. Stat. Sol. (c) 2: 34.  
Doi:10.1002/pssc.200460105
- Niyogi, S., Hamon, M. A., Hu, H., Zhao, B.,  
Bhowmik, P., Sen, R., Itkis, M. E., and Haddon,  
R. C., Accounts of Chemical Research, 35, (12),  
2002
- Avouris, P., Chemical Physics, 281, (2-3), 429-  
445, 2002
- Tans, Sander J., Devoret, Michel H., Dal,  
Hongjie, Thess, Andreas, Smalley, Richard E.,  
Geerligs, L. J., and Dekker, Cees, Nature  
(London), 386, (6624), 1997
- Ebbesen, T. W. and Ajayan, P. M., Nature, 358,  
(220-222), 1992
- Journet, C. and Bernier, P., Applied Physics A-  
Materials Science & Processing, 67, (1), 1 S.  
Iijima, Nature ~London! 354, 56 ~1991!.

# PERFORMANCE ANALYSIS OF BOILER IN THERMAL POWER PLANT

P.Papireddy & Dr. S. Ananth & Mr. Vikash Kumar

PG Student, Professor, Assistant Professor

Department of Mechanical Engg. Malla Reddy College of Engineering Maisammaguda, Dhulapally, Kompally, Secunderabad, Telangana-500100, India.

**ABSTRACT:** In India, coal is the dominant source of energy generation. Efficiency of any conventional coal fired unit ranges from 34-38%. This paper presents the efficiency calculation of boiler, turbine and condenser of a 210 MW unit. The study focuses on evaluation of various parameters like dry flue gas loss, wet flue gas loss, moisture in fuel and hydrogen, condenser back pressure, turbine cylinder efficiency, soot formation, etc. and some optimization techniques are mentioned to minimize the same. The benefits of these techniques are considerable fuel saving, emission reduction, heat rate improvement, cost minimization, increased equipment life cycle, etc. Cost analysis through heat rate deviation has been done to determine annual fuel savings. Lastly various critical parameters are mentioned for further improvement of plant performance

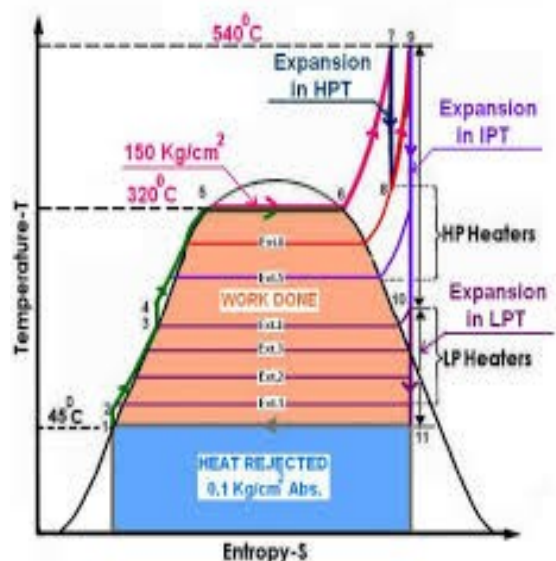
**Keywords:** Coal fired power plant, rankine cycle, boiler efficiency, turbine efficiency, condenser efficiency, heat rate

## I. INTRODUCTION

A boiler is an enclosed vessel that provides a means for combustion heat to be transferred into water until it becomes heated water or steam. The hot water or steam under pressure is then usable for transferring the heat to a process. Water is a useful and cheap medium for transferring heat to a process. When water is boiled into steam its volume increases about 1,600 times, producing a force that is almost as explosive as gunpowder. This causes the boiler to be extremely dangerous equipment that must be treated with utmost care. The process of heating a liquid until it reaches its gaseous state is called evaporation. Heat is transferred from one body to another by means of radiation, which is the transfer of heat from a hot body to a cold body without a conveying medium, convection, the transfer of heat by a conveying medium, such as air or water and conduction, transfer of heat by actual physical contact, molecule to molecule.

**Boiler Specification:** The heating surface is any part of the boiler metal that has hot gases of combustion on one side and water on the other. Any part of the boiler metal that actually contributes to making steam is heating surface. The amount of heating surface of a boiler is expressed in square meters. The larger the heating surface a boiler has, the more efficient it becomes. The quantity of the steam produced is indicated in tons of water evaporated to steam per hour. Maximum continuous rating is the hourly evaporation that can be maintained for 24 hours.

F & A means the amount of steam generated from water at 100°C to saturated steam at 100°C. This condensate is then sent back to boiler through boiler feed pump via low pressure and high pressure heaters.



It works on the principle of modified Rankine cycle. The function of thermal power plant is to generate steam in boiler which is used to drive turbine and generator mounted on the same shaft to produce electricity. The exhaust from low pressure turbine is condensed in condenser and the resultant condensate is extracted through condensate extraction pump.

The CEA in India uses power station heat rate as a proxy for calculating plant efficiency. The heat

rate of a power plant is the amount of chemical energy that must be supplied to produce one unit of electrical energy. Some of the heat rate factors that affect power plant performance are ageing of machine, coal quality, plant load factor, operating margins, initial plant design, etc

The basic purpose of a boiler is to turn water into steam, in this case saturated steam. This operation sounds relatively simple but is actually more complicated. Other components and processes such as the deaerator and economizer are necessary to help the overall operation run more efficiently. The boilers utilized on campus are of the stack drum type, which means there are drums within the boilers stacked one above the other. In these particular boilers there are two drums. The upper drum is called a steam drum and is where saturated steam leaves the boiler. While the lower drum is called the mud drum and is where liquid feed water enters. It is also where sediment carried into the boiler settles. Tubes called risers and down comers are used to connect the two drums.

All of the energy required within the boiler is produced by the combustion of a fuel. The burner acts very similar to the gas stove at home, just more complicated. It is comprised of a wind box, igniter, fuel manifold and/or atomizing gun, observation port and flame safety scanner. Currently the boilers can burn either fuel oil or natural gas. Fluctuating prices of fuel can raise or lower the cost to produce steam. Having the choice between two different fuels gives the option of burning the lower cost fuel.

Operation of the boiler begins with feed water entering the mud drum where it is heated. The combustion of fuel within the furnace provides the required energy which is imparted by a combination of convection and radiation. A two-phase water mixture forms within the riser and begins to ascend to the steam drum due to its decreasing density. Boiling to 100% quality in the tubes is undesirable because water vapour has different heat transfer characteristics than liquid water. This can lead to high wall temperatures and eventual tube burnout. Once it reaches the steam drum the majority of saturated vapour will be removed from the two-phase mixture; there by increasing the remaining mixture's density. The increase in density will initiate its descent in the down comers back to the mud drum. This natural circulation continuously allows for a constant flow of saturated steam exiting the boiler.

Combustion occurs when fossil fuels, such as natural gas, fuel oil, coal or gasoline, react with oxygen in the air to produce heat. The heat from

burning fossil fuels is used for industrial processes, environmental heating or to expand gases in a cylinder and push a piston. Boilers, furnaces and engines are important users of fossil fuels. Fossil fuels are hydrocarbons, meaning they are composed primarily of carbon and hydrogen. When fossil fuels are burned, carbon dioxide (CO<sub>2</sub>) and water (H<sub>2</sub>O) are the principal chemical products, formed from the reactants carbon and hydrogen in the fuel and oxygen (O<sub>2</sub>) in the air. The simplest example of hydrocarbon fuel combustion is the reaction of methane (CH<sub>4</sub>), the largest component of natural gas, with O<sub>2</sub> in the air.

When this reaction is balanced, or stoichiometric, each molecule of methane reacts with two molecules of O<sub>2</sub> producing one molecule of CO<sub>2</sub> and two molecules of H<sub>2</sub>O. When this occurs, energy is released as heat. The combining of oxygen (in the air) and carbon in the fuel to form carbon dioxide and generate heat is a complex process, requiring the right mixing turbulence, sufficient activation temperature and enough time for the reactants to come into contact and combine.

Unless combustion is properly controlled, high concentrations of undesirable products can form. Carbon monoxide (CO) and soot, for example, result from poor fuel and air mixing or too little air. Other undesirable products, such as nitrogen oxides (NO, NO<sub>2</sub>), form in excessive amounts when the burner flame temperature is too high. If a fuel contains sulphur, sulphur dioxide (SO<sub>2</sub>) gas is formed. For solid fuels such as coal and wood, ash forms from incombustible materials in the fuel.

Kumar et al. has used three sides instead of one side roughened duct & found that augmentation in Nu & f was respectively to be 21-86 % & 11-41 %. They also reported augmentation in thermal efficiency of three sides over one side roughened duct to be 44-56 % for varying p/e and 39-51 % for varying e/D<sub>h</sub>.

## **II. METHODOLOGY**

### **Performance of Boiler**

Boiler is an enclosed pressure vessel where heat generated by combustion of fuel is transferred to water to become steam. Boiler efficiency is defined as the heat added to the working fluid expressed as a percentage of heat in the fuel being burnt

#### **Direct Method**

The energy gain of the working fluid (water and steam) is compared with the energy content of the boiler fuel.

$$\eta = \frac{(hg - hf) * Q}{q * GCV} * 100$$

Where,

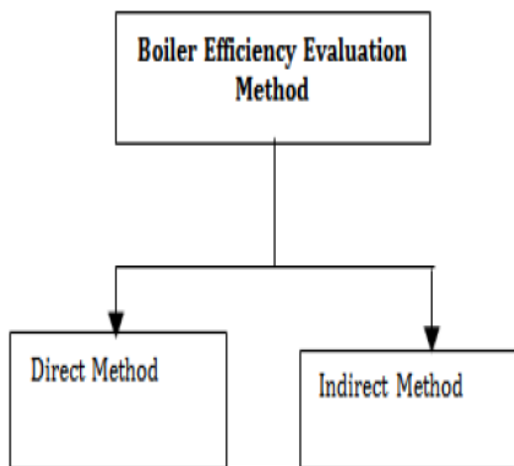
hg- Enthalpy of saturated steam in kCal/kg of steam

hf - Enthalpy of feed water in kCal/kg of water

Q - Quantity of steam generated per hour (Q) in kg/hr.

q- Quantity of fuel used per hour (q) in kg/hr

GCV - gross calorific value of the fuel in kCal/kg of fuel



**Indirect Method or Heat Loss Method:**

The efficiency is the difference between the losses and the energy input.

The main advantage of indirect method is that the errors obtained from this method do not make any major change in the efficiency.

Thus if boiler efficiency is 90% an error of 1% in direct method will result in significant change in efficiency, i.e.

$$90C \pm 0.9 = 89.1 \text{ to } 90.9$$

Whereas in indirect method, 1% error in measurement of losses will result in;

$$\begin{aligned} \text{Efficiency} &= 100 - (10 \pm 0.1) \\ &= 90 \pm 0.1 = 89.9 \text{ to } 90.1 \end{aligned}$$

Accountable losses in coal fired boilers are:

- Heat loss due to dry flue gas as sensible heat (L1)
- Un-burnt losses in bottom ash as carbon (L2).
- Heat loss due to moisture in the coal (L3).
- Heat loss due to moisture from burning of hydrogen in coal (L4).
- Heat loss due to moisture in air (L5).
- Heat loss due to incomplete combustion of carbon (L6)
- Loss due to surface radiation and convection (L7).

$$\begin{aligned} \text{Theoretical air requirement} &= \\ &= \frac{[(11.6 * C) + \{34.8 * (H_2 - O_2/8)\} + (4.35 * S)]}{100} \\ &\text{kg of fuel} \end{aligned}$$

$$\begin{aligned} \text{Excess air supplied} &= \\ &= \frac{O_2\%}{21 - O_2\%} * 100 \end{aligned}$$

Actual mass of air supplied/kg of fuel (AAS)=

$$\left\{1 + \frac{EA}{100}\right\} * \text{Theoretical air}$$

1) Percentage heat loss due to dry flue gas

$$= \frac{m * c_p * (T_f - T_a)}{GCV \text{ of fuel}} * 100$$

Where;

m = mass of dry flue gas in kg/kg of fuel

Cp = Specific heat of flue gas (0.23 kcal/kg 0C)

2) Percentage heat loss due to unburnt carbon in bottom ash =

$$= \frac{\text{Total ash collected / kg of fuel burnt} * GCV \text{ of bottom ash}}{GCV \text{ of fuel}} * 100$$

3) Percentage heat loss due to evaporation of moisture present in fuel

$$= \frac{M * \{584 + c_p * (T_f - T_a)\}}{GCV \text{ of fuel}} * 100$$

Where,

M - kg of moisture in 1kg of fuel

Cp - Specific heat of superheated steam (0.45 kcal/kg)0C

\* 584 is the latent heat corresponding to the partial pressure of water vapour.

4) Percentage heat loss due to evaporation of water formed due to H2 in fuel

$$= \frac{9 * H_2 * \{584 + c_p * (T_f - T_a)\}}{GCV \text{ of fuel}} * 100$$

Where,

H2 - kg of H2 in 1 kg of fuel

Cp - Specific heat of superheated steam (0.45 kcal/kg 0C)

5) Percentage heat loss due to moisture present in air

$$= \frac{AAS * \text{humidity factor} * c_p * (T_f - T_a)}{GCV \text{ of fuel}} * 100$$

Where,  
 Cp – Specific heat of superheated steam  
 (0.45 kcal/kg OC)

6) Percentage heat loss due to incomplete combustion

$$L_6 = \frac{\% \times C \times 5744}{(\% CO + \% CO_2) \times GCV \text{ of coal}} \times 100$$

Where,  
 L5 = % Heat loss due to partial conversion of C to CO  
 CO = Volume of CO in flue gas leaving economizer (%)  
 CO2 = Actual Volume of CO2 in flue gas (%)  
 C = Carbon content kg / kg of fuel

7) Percentage heat loss due to radiation and other unaccounted loss  
 Unaccounted losses include losses from boiler casing to surrounding, loss due to combination of carbon and water, heat carried away in ash, losses due to un-burnt volatile matter, heat loss due to bottom seal water. Radiation loss depends on the effectiveness of the boiler casing insulation.

In a relatively small boiler, with a capacity of 10 MW, the radiation and unaccounted losses could amount to between 1% and 2% of the gross calorific value of the fuel, while in a 500 MW boiler, values between 0.2% to 1% are typical. The loss may be assumed appropriately depending on the surface condition.

Boiler efficiency ( $\eta$ ) = 100 - (1 + 2 + 3 + 4 + 5 + 6 + 7)

**Table1 Losses in boiler by indirect method**

Sl. No.	Heat losses (%)	Design	Corrected
1.	L1	4.46	5.38
2.	L2	0.49	0.63
3.	L3	2.64	2.68
4.	L4	3.49	3.54
5.	L5	0.13	0.16
6.	L6	0.02	0.02
7.	L7	1.21	1.06
	$\eta$ of boiler	87.56	86.53

### Performance of Turbine

**Table 2 Heat rate deviation of different parameters**

Sl. No.	Particulars	Unit	Design	Operation	UHR Loss (Kcal/Kwh)
1.	Partial loading	%		0	0
2.	LPT. Exhaust steam temp Cond. Backpressure	°C Ksc	43.2 0.089	43.5 0.91	-2
3.	D.M. make up	T/Hr		6.25	-11
4.	Final F.W. temp.	°C	247	251.44	0
5.	R.H. spray	T/Hr	0	15.75	-12
6.	Main steam press.	KSC	129	124.57	-9
7.	Main steam temp.	°C	537	533.36	-1
8.	HRH steam temp.	°C	537	537.15	0
9.	oxygen	%	3.5	2.73	0
10.	Fl gas temp. at RAH O/L[Left] Fl gas temp. at RAH O/L[right]	°C °C		146.23 146.57	-8
11.	Turbine cycle eff. Loss (Other than Ageing)	%	0		-18
12.	Carbon in bottom ash	%	2	2.1	0

### Performance of Condenser

Condensers are devices in which cooling water is used to condensate the exhaust steam from the steam turbine.

The primary objective of a condenser is to maintain a very low back pressure on the exhaust side low pressure turbine. This enables the steam to expand to a greater extent which results in an increase in available energy for converting into mechanical work. [Shende M.B. *et al*, 2015]. Following formula is used for calculating condenser efficiency:

Condenser efficiency = rise in temperature of cooling water [Saturation temp corresponding to the absolute pressure in the condenser] - [inlet temp of cooling of water

Steam turbine is a mechanical device that extracts thermal energy from pressurized steam, and converts it to useful mechanical work. The steam turbines are split into three separate stages, High Pressure (HP), Intermediate Pressure (IP) and Low Pressure (LP) stage, which are mounted on the same shaft along with generator. [Kumar *et al*, 2013].

Turbine efficiency is defined as the ratio of mechanical work output in kcal (or KJ) to the total heat available across the turbine in kcal (or kJ) expressed as a percentage.

Following formulas are used for calculating turbine efficiency

1) Total accountable losses + Design heat rate = Unit heat rate

2) Accountable losses of turbine + Design turbine heat rate = Turbine heat rate

3) Turbine cycle efficiency

$$= \frac{860}{\text{turbine heat rate}} * 100$$

**Table 3** Condenser performance parameters

Sl.No.	Particulars	Unit	Design	Operational
1.	Vacuum	Ksc	0.91	0.909
2.	CW O/L Temp	°C	38.4	39.45
3.	CW I/L Temp	°C	30	28.9
4.	LPT Exhaust Temp	°C	43.2	43.5
5.	CW temp. rise	°C	10	10.54

**III. EFFICIENCY CALCULATION**

Step- 1)

DTCHR of 210 MW is 2021 kcal/kwh.

GTCHR=24+2021

= 2045 kcal /kwh

Step-2)

$$\text{Turbine } \eta = \frac{860}{\text{turbine heat rate}} * 100$$

Turbine  $\eta$ = 42.05%

Step -3)

UHR=GTCHR/Boiler Efficiency

=2045/86.53

=2363 kcal/kwh

Step -4)

Condenser  $\eta$

= Rise in cooling water temperature

LPT exhaust temp – Inlet temp. ofc.w

= 0.7219

Step-5)

$$\text{Plant } \eta = \frac{860}{\text{Unit heat rate}} * 100$$

= 35.9%

**IV. COST BENEFIT ANALYSIS**

Heat rate is helpful in determining how efficiently any unit is being operated, as lower is the heat rate higher will be the operational efficiency. For identifying the performance of either any unit or unit equipments, heat rate deviation is used instead of heat rate. This heat rate deviation can be converted into cost for calculating annual fuel cost. Cost calculation using heat rate instead of heat rate deviation is often overlooked in a thermal power plant.

Heat rate deviation in helpful in identifying the problem in any equipment or auxiliary, and its magnitude is helpful in assigning priority level to these problems. Since, heat rate deviations can be converted into cost, it is helpful

in solving the highest priority problems first so as to minimize the amount of fuel consumption.

Cost of heat rate deviation = heat rate deviation\*net generation\* fuel cost

An increase in heat rate results in increasing the fuel consumption whereas any decrease in heat rate results in reduction of fuel requirement for producing a given number of KWH of energy. Heat rate also plays a key role in any purchasing decision, be it fuel, oil, or any equipment, etc.

**Table 4**Cost of heat rate deviation

Sl. No.	Particulars	Unit	UHR Loss (Kcal/kWh)	Cost of heat rate deviation (Rs)
1.	Partial loading	%	0	0
2.	LPT.exhauststeam Temp Cond. backpressure	Deg C Ksc	-2	-34.06
3.	D.M. make up	T/Hr	-11	-187.33
4.	Final F.W. temp.	Deg C	0	0

In above table, cost of heat rate deviation of each parameter has been calculated where,

Net generation= gross generation-auxiliary power consumption

= 195.41MW

Fuel cost = Rs 610/ton or Rs 87.2/106 kcal

-ve sign of heat rate deviation indicates the better performance of plant and +ve sign indicates poor performance of plant.

From table, we get cost of heat rate deviation= Rs - 1038.83

(-) sign indicates the cost saving in fuel.

Annual cost of heat ratedeviation

$$= \text{heat rate fuel cost} * \text{unit rating} * \text{PLF} * \text{hrs in a year}$$

$$= 2452 * \frac{87.2}{10^6} * 210 * 1000 * 1.01 * 8760$$

=Rs 397,266,299.9 /yr

$$= 2452 * \frac{87.2}{10^6} * 210 * 1000 * 1.01 * 8760$$

=Rs 271,399,749.5 /yr

If 1% heat rate is reduced then annual cost of fuel would be

Annual cost of heat rate deviation

$$= 2452 * \frac{87.2}{10^6} * 210 * 1000 * 1.01 * 8760 * 0.01$$

=Rs 3,972,662.99 /yr

Annual cost of heat rate deviation

$$2452 * \frac{87.2}{10^6} * 210 * 1000 * 1.01 * 8760 * 0.69$$

= 2,713,997.49 /yr

This is the annual saving in fuel cost just by 1% improvement in heat rate.

Some the areas where heat rate improvement can result in tremendous improvement of overall heat rate are mentioned below.

- By giving heat rate awareness training to operation staff:- 0.5% to 1%

- Heat rate information availability to plant personnel:- 0.5% to 1.5%
- By proper utilization of controllable losses information by operation staff:- 0.75% to 1%
- By conducting routine testing program at regular intervals:- 0.7% to 2%
- By increasing the routine monitoring of feed water heater performance:- 0.3% to 0.6%
- By optimizing soot blower operation:- 0.7%

Maximum improvement in heat rate ranges from approximately 3 to 5% for this unit. This could save annual cost of fuel from Rs 8,141,992.48 /yr to Rs 13,569,987.48 /yr (for 2015-16 financial year).

## V. DISCUSSION

### Dry flue gas loss optimization

The dry flue gas loss depends on two factors. They are excess air and air heater gas outlet temperature.

### Excess air control

For every 1% reduction in excess air there is approximately 0.6% rise in efficiency. Excess air is monitored by CO<sub>2</sub> and O<sub>2</sub> measurements at air heater inlet.

Air infiltration should be controlled to limit this loss. Various methods like oxygen analyzers, draft gauges and stack damper control can be used to calculate readings of excess air.

### 5.1.2 Air heater gas outlet temperature optimization:-

It should be lowest from overall efficiency point of view, whereas should be high on account of corrosion problem.

For Indian coals having low percentage (approx(0.5%)) of Sulphur, this specified temperature is of the order . A rise in air heater gas outlet temperature reduces boiler efficiency by some of the causes of his gas outlet temperature are lack of soot blowing, high excess air, low final feed water temperature, improper combustion, poor milling, air in leakage before the combustion chamber, etc. Though in the short run, low air heater gas outlet temperature improves efficiency; in the long run it can result in low boiler efficiency because of deposition on its elements and corrosion.

Most obvious cause of low air heater gas outlet temperature is lighting and firing a cold boiler. Its remedy is to bypass the air heater until the gas temperature is high enough to permit normal

operation. It's another reason is air leakage across air heater seals. The rate of air leakage varies with the square root of the differential pressure across the air heater.

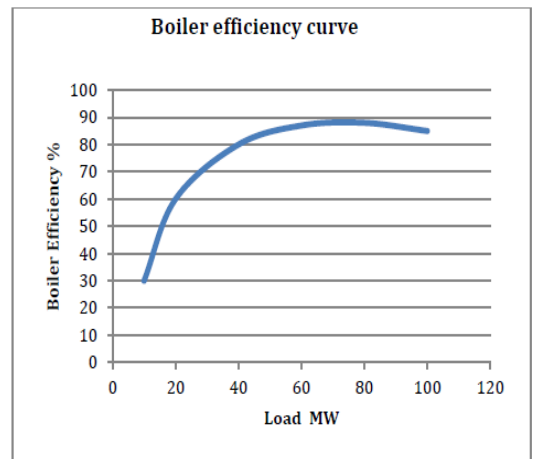
### Wet flue gas loss optimization

Losses due to moisture in fuel, hydrogen in fuel and moisture in combustion air depends on final gas outlet temperature. These losses decrease slightly with fall in boiler output.

Power plant waste heat can be used to remove moisture before pulverization process which can provide heat rate and emission benefits, reduce maintenance cost and it will also be reducing cooling water makeup requirement.

### Carbon in ash loss optimization

This loss depends on the fineness of pulverized fuel, excess air and combustion condition. If combustion is not monitored properly the loss which is normally about 1% may be as high as 4-5%. Some of the causes of high carbon content in ash are coarse grinding, mal adjustment of flame, unequal loading of different mills, incorrect primary air temperature, etc.



### Turbine efficiency optimization

Turbine cylinder efficiency is around 85%, 92% and 80-85% for HP, IP and LPT respectively. Some of the losses that occur in stem path are loss due to solid particle erosion of moving blades, solid particle erosion and roughness of diaphragm blades and damage of the fins of shaft blades.

Optimization of these losses can help in turbine cylinder efficiency improvement. It can be done by taking measures like increasing the turbine exit annulus area, lowering the kinetic energy of the steam as it leaves the last stage blade, steam blowing should be done after boiler Overhauling, Replacement of all Tip Seals, Inter stage & Gland Seals in every capital overhauling, Strict & vigilant control on water chemistry, using additives in feed

water to reduce surface tension due to formation of water droplets, etc.

### Condenser vacuum optimization

Heat loss from thermal power plant is mainly due to heat rejection through the condenser. A difference of 5% in cooling water inlet temperature changes unit heat consumption by around 1%. It can be done by following ways:

- High cooling water inlet temperature leads to higher saturation temperature and corresponding rise in condenser saturation pressure (i.e. lower condenser vacuum) for a design specified cooling water temperature rise and terminal temperature difference. Hence low inlet temperature values must be maintained.

Reduced cooling water flow rate shall increase the cooling water temperature rise, which leads to higher saturation temperature at design terminal temperature difference and corresponding saturation pressure.

Condensate level in the hot well if gets more than design value, will lead to improper heat transfer because it will cover some of the cooling water tubes thereby making them unavailable for condensation.

Internal and external tube deposit causes high terminal temperature difference which can be minimized by on-line condenser tube cleaning and better de-mineralized water quality management respectively.

Air ingress results in poor heat transfer coefficient which increases condensing temperature in order to get heat across air barrier, this makes the vacuum worst. It can be avoided by frequent leak detection test and effective steam sealing of low pressure turbine.

### Steam temperature control

One of the techniques used to prevent excessively high steam temperatures at the inlets to the high pressure and intermediate pressure turbines is to spray liquid H<sub>2</sub>O into the steam. Referred to as attemperating spray, these liquid flows are taken from the turbine cycle and result in an increase in heat rate.

Consequently, attemperating spray flow rates should be the minimum flow rates needed to control steam temperatures to the design levels. If main steam and hot reheat steam were at lower than desired temperatures, while both main steam and hot reheat attemperating sprays were in operation, then it will result in heat rate penalties due to low steam temperatures and to use of attemperation when it was not needed. Thus an upgrade to the steam temperature controls and perhaps repair of leaking flow control valves would be needed to prevent this type of loss.

### Scaling and soot abatement

Factors favoring soot formation are high temperature and shortage of oxygen. Elevated stack temperature indicates soot deposition as well as scaling on the water side. With every 22% C increase in stack temperature, 1% efficiency loss occurs in boilers. Practices like periodic off-line cleaning of radiant furnace surfaces, boiler tube banks, economizers and air heaters are necessary to remove scaling and soot formation.

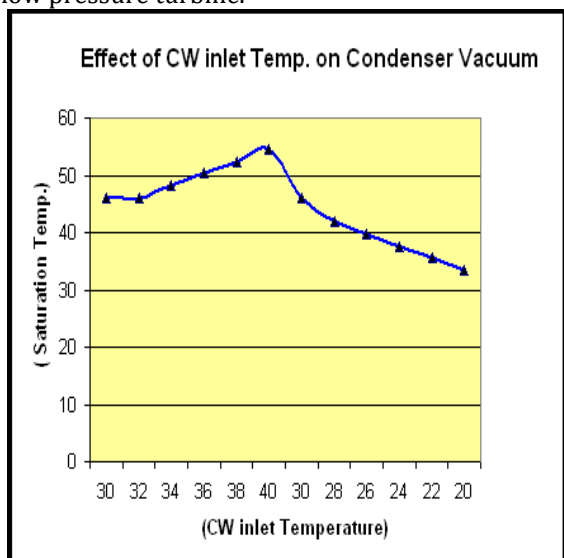
## VI. RESULTS

Following results have been concluded

- 5% change in excess air changes dry flue gas loss by 1%.
- Radiation and convection losses are around 0.4 to 1%
- A difference of 5% in cooling water temperature changes the unit heat consumption by 1%.
- Condenser vacuum should be maintained at 0.89 to 0.9 ksc.
- By combustion optimization heat rate reduction in the range of 0.5% to 1% can be achieved.
- By upgrading steam turbine generators and enhancement of auxiliary component can lead to improvement of 2 to 4%.
- By reducing steam, water and internal leakage heat rate can be improved by 0.5%.

## VII. CONCLUSION

Also following critical parameters must be observed so as to further increase the plant performance:



- Main steam temperature and pressure should be increased
- Re-heater spray should be decreased
- Condenser vacuum should be decreased
- Turbine cylinder efficiency should be increased
- Dry flue gas loss should be decreased
- Un-burnt carbon percentage should be decreased
- Moisture in fuel should be decreased
- Moisture in combustion air should be decreased
- Heat rate should be decreased
- Plant should be operated at full load for maximum efficiency.

### VIII. FUTURE SCOPE

By regular heat rate improvement program, efficiency can be increase to an extent. Following aspects can be further studied to improve plant efficiency. They are-  
Air ingress deteriorates the heat transfer coefficients. There by increasing the condensing temperature in order to get heat across air barrier. This makes the vacuum worse.  
Re heater pressure drop adversely affect the HPT exhaust pressure, thereby affecting the IPT inlet pressure

### IX. REFERENCES

- [1] Dhanre G.T, Dhanre U.T. and Mudafale K, (2014), Review Paper on Energy Audit of a Boiler in Thermal Power Plant, IJSR, vol.2, issue 6, Oct-Nov 2014.
- [2] Kurkiya R and Chaudhary S (2012), Energy Analysis of Thermal Power Plant , International Journal of Science & Engineering Research Volume (IJSER), VOL-3, ISSUE-7, July-2012
- [3] Kumar, C. K. and G. S. Rao (2013). Performance analysis from the energy audit of a thermal power plant, International Journal of Engineering trends and Technology (IJETT), ISSN: 2231-5381.
- [4] Shende M.B, Shinde N. N., Desai S. B.andWagh M.M., (2015), Performance of Thermal Power

- Plant on System Based, IRJET, vol.2, issue.4, july-2015
- [5] Robert J.Tramel (2000), Heat rate improvement guidelines for Indian Power Plants, volume 1, 2United States Tennessee Valley Authority , June 2000
  - [6] Palo Alto (2014), Range and Applicability of heat rate improvements, EPRICA:2014, 3002003457
  - [7] Vinchurkar A.G, Lakhe R.R and Shrivastava R.L (2014). Energy efficiency analysis of thermal plant boilers, IJRME, vol 2,issue 3,May-June-2014.
  - [8] Singh, S. P., Philip G., Singh S.K. (2014), Effect of condenser vacuum on performance of a Reheat Regenerative 210 MW Fossil-Fuel based Power Plants, IJETAE, vol 4,issue 1,Feb-2014.
  - [9] Kumar, V., Prasad, L., Experimental investigation on heat transfer and fluid flow of air flowing under three sides concave dimple roughened duct. International Journal of Mechanical Engineering and Technology (IJMET), Volume 8, Issue 11, November 2017, pp. 1083–1094, Article ID: IJMET\_08\_11\_110.
  - [10] Kumar, V., Prasad, L., Thermal performance investigation of one and three sides concave dimple roughened solar air heaters. International Journal of Mechanical Engineering and Technology (IJMET) Volume 8, Issue 12, December 2017, pp. 31–45, Article ID: IJMET\_08\_12\_004.
  - [11] Kumar, V., Prasad, L., Performance Analysis of three sides concave dimple shape roughened solar air heater, J. sustain. dev. energy water environ. syst., 6(4), pp 631-648, 2018.
  - [12] Kumar, V., Nusselt number and friction factor correlations of three sides concave dimple roughened solar air heater, Renewable Energy 135 (2019) 355-377.
  - [13] Kumar, V., Prasad, L., Experimental analysis of heat transfer and friction for three sides roughened solar air heater, Annales de Chimie - Science des Matériaux, 75-107, ACSM. Volume 41 - n° 1-2/2017.
  - [14] Kumar, V., Prasad, L., Performance prediction of three sides hemispherical dimple roughened solar duct, Instrumentation, Mesure, Métrologie, 273-293 I2M. Volume 17 - n° 2/2018.

## DESIGN OF ABSORPTION REFRIGERATION SYSTEM DRIVEN BY ENGINE EXHAUST GAS FOR VEHICLES

## P.Pavan Kumar & Dr. S. Ananth & Mr. Vikash Kumar

PG Student, Professor, Assistant Professor

Department of Mechanical Engg. Malla Reddy College of Engineering Maisammaguda, Dhulapally, Kompally,  
Secunderabad, Telangana-500100, India

---

**ABSTRACT:** *As we tend to all recognize that absorption refrigeration has no moving elements, Air conditioning is that the method of sterilisation the properties of air (primarily temperature and humidity) to additional favorable conditions. additional usually, air con will talk to any style of technological cooling, heating, ventilation, or medical care that modifies the condition of air. it's a widely known indisputable fact that an outsized quantity of warmth energy related to the exhaust gases from Associate in Nursing engine is wasted. In this thesis, energy from the exhaust gas of an internal combustion engine is used to power an absorption refrigeration system to air-condition an ordinary passenger car. All the required parts for the absorption refrigeration system is designed and modeled in 3D modeling software CREO parametric software. Thermal analysis is done on the main parts of the refrigeration system to determine the thermal behavior of the system.*

**Keywords:** *refrigeration, vapour, absorption, refrigerant, CAD, CREO*

---

### I. INTRODUCTION

Refrigeration is the process of casting off warmness from an enclosed or controlled space, or from a substance, and transferring it to an area in which it's miles unobjectionable. The number one cause of refrigeration is lowering the temperature of the enclosed area or substance after which keeping that decrease temperature as evaluate to surroundings. Cold is the absence of heat, therefore on the way to lower a temperature, one "removes warmness", rather than "including cold." The basic objective of growing a vapour absorption refrigerant system for vehicles is to cool the distance inside the automobile through making use of waste heat and exhaust gases from engine. The air con gadget of motors in these days's world makes use of "Vapour Compression Refrigerant System" (VCRS) which absorbs and gets rid of heat from the interior of the car that's the space to be cooled and in addition rejects the heat to be somewhere else. Now to increase an performance of vehicle past a sure restriction vapour compression refrigerant device resists it because it can't employ the exhaust gases from the engine. The heat required for running the Vapour Absorption Refrigeration System can be obtained from that which is wasted into the atmosphere from an IC engine. G. Vicatos[4] observed that in the exhaust gases of motor vehicles, there is enough heat energy that can be utilized to power an airconditioning system. Once a secondary fluid such as water or glycol is used, the aqua ammonia combination appears to be a good candidate as a working fluid for an absorption car air

conditioning system. In the paper, the waste heat from gas engine turbine can be used as the heat source for the absorption refrigeration system. The experimental analysis showed that performance of the integrated refrigerating system was greatly improved by using the waste heat of gas engine. Colbourne [5] summarized a study analyzing over 50 published technical documents comparing the performance of fluorinated refrigerants and HCs. A significantly higher number of tests showed an increase in performance when using HCs as compared to using fluorinated refrigerants (Colbourne and Suen,)[6]. Similarly, Colbourne and Ritter[7] investigated the compatibility of non-metallic materials with HC refrigerant and lubricant mixtures. They performed experiments in compliance with European standards for the testing of elastomeric materials and ASHRAE material compatibility test standards. Setaro et al. [8] tested and compared the heat transfer and pressure drop through a brazed plate heat exchanger and a tube-and-fin coil for two different refrigerants, R22 and R290 in an air-to water heat pump system. Qin et al. [9] developed an exhaust gas driven automotive air conditioning working on a new hydride pair. The results showed that cooling power and system coefficient of performance increase while the minimum refrigeration temperature decreases with growth of the heat source temperature. System heat transfer properties still needed to be improved for better performance. Koehler et al. [10] designed, built and tested a prototype of an absorption

refrigeration system for truck refrigeration using heat from the exhaust gas. The refrigeration cycle was simulated by a computer model and validated by test data.

**II.COMPONENTS OF AIR COOLED ABSORPTION SYSTEM INTRODUCTION TO CAD AND CREO**

The components are condenser, evaporator in this paper we are designing the condenser and evaporator for that we used cad and creo.

S.N	Engine Type	Power Output (kW)	Waste Heat
1.	Small air cooled diesel engine	35	30-40 % of energy waste loss from IC engines
2.	Water air cooled engine	35-150	
3.	Earth moving machineries	520-720	
4.	Marine applications	150-220	
5.	Trucks and road engines	220	

**A. INTRODUCTION TO CAD**

Computer-aided layout (CAD) is using laptop structures (or workstations) to useful resource within the creation, change, evaluation, or optimization of a layout. CAD software is used to increase the productivity of the fashion designer, enhance the best of design, improve communications through documentation, and to create a database for manufacturing. CAD output is often within the form of digital files for print, machining, or other production operations. The time period CADD (for Computer Aided Design and Drafting) is also used.

Its use in designing digital systems is referred to as electronic design automation, or EDA. In mechanical layout it's far referred to as mechanical design automation (MDA) or computer-aided drafting (CAD), which incorporates the technique of creating a technical drawing with using pc software program.

CAD software for mechanical layout uses either vector-based totally photos to depict the objects of conventional drafting, or might also produce raster portraits showing the overall appearance of designed items. However, it includes greater than simply shapes. As inside the manual drafting of technical and engineering drawings, the output of CAD need to bring statistics, along with substances, approaches, dimensions, and tolerances, consistent with application-unique conventions.

CAD may be used to design curves and figures in two-dimensional (2D) area; or curves, surfaces, and solids in 3-dimensional (3D) space.

**B.INTRODUCTION TO CREO**

PTC CREO, previously known as Pro/ENGINEER, is 3-d modeling software utilized in mechanical engineering, design, production, and in CAD drafting carrier firms. It changed into one of the first 3D CAD modeling applications that used a rule-primarily based parametric gadget. Using parameters, dimensions and features to capture the behavior of the product, it could optimize the improvement product as well as the layout itself.

The name become changed in 2010 from Pro/ENGINEER Wildfire to CREO. It become introduced by using the company who evolved it, Parametric Technology Company (PTC), all through the launch of its suite of design products that consists of programs inclusive of assembly modeling, 2D orthographic perspectives for technical drawing, finite detail analysis and more. PTC CREO says it can provide a more efficient layout experience than different modeling software program due to its unique functions such as the mixing of parametric and direct modeling in one platform. The entire suite of applications spans the spectrum of product development, giving designers alternatives to apply in every step of the manner. The software also has a greater user friendly interface that provides a better revel in for designers. It also has collaborative capacities that make it clean to proportion designs and make changes.

There are limitless advantages to using PTC CREO. We'll check them in this -component series.

First up, the largest advantage is improved productiveness due to its green and flexible design competencies. It changed into designed to be less difficult to use and have functions that allow for design procedures to transport more quickly, making a designer's productivity degree increase. A particular feature is that the software program is available in 10 languages. PTC is aware of they have people from all around the world the usage of their software program, so they offer it in multiple languages so almost all people who wants to use it is able to achieve this.

**C. ADVANTAGES OF CREO PARAMETRIC SOFTWARE**

1. Optimized for model-based totally organizations
2. Increased engineer productivity
3. Better enabled concept layout
4. Increased engineering competencies
5. Increased manufacturing talents
6. Better simulation
7. Design abilities for additive manufacturing

**D. CREO parametric modules:**

- Sketcher
- Part modeling

- Assembly
- Drafting

**E. FINAL DIMENSIONS**

Dimensions of the designed pre-heater  
 Outside Diameter of the tube,  $D_0 = 0.012\text{ m}$   
 Inside Diameter of the tube,  $D_j = 0.01\text{ m}$   
 Length of the tube,  $L = 2\text{ m}$   
 By using comparable calculations additionally findout the

Dimensions of the following Generator  
 It is the place wherein the exhaust gas tube is surpassed  
 via the field and the tube emperature is assumed to be a regular.

Dimensions of the designed generator  
 Outside Diameter of the exhaust gas tube,  $D_0 = \text{zero}.04\text{ m}$   
 Taking interior diameter of the exhaust gasoline tube,  $D_i = \text{zero}.038\text{ m}$   
 Length of the tube required for the desired warmth switch,  $L = 1\text{ m}$

Condenser:  
 Assume circular cross segment of the condenser coil of thickness,  $a = 5\text{ mm}$  & Diameter  $d = 18\text{ mm}$ .  
 Dimensions of the designed condenser  
 Diameter of the tube,  $d = 0.018\text{ m}$  Thickness of the tube,  $a = 0.1/2\text{ m}$  Length of the tube,  $L = 7.40\text{ m}$

Evaporator  
 The evaporator is of circular go segment and should be manufactured from copper tubes to have maximum heat switch from the environment to the refrigerant. The tube is coiled to accommodate it inside the car.

Dimensions of the designed evaporator  
 Outside Diameter of the tube,  $D_0 = \text{zero}.01\text{ m}$   
 Inside Diameter of the tube,  $D_j = 0.008\text{ m}$  Length of the tube,  $L = 6.26\text{ m}$

Absorber  
 Dimensions of the designed absorber  
 Outside diameter of the absorber,  $D_0 = 76\text{ mm}$   
 Total length of the absorber,  $L = 205\text{ mm}$  Outer diameter of the fins,  $D_f = 109\text{ mm}$ , No. Of fins,  $n = 7$

**III. WORKING PRINCIPLE**

Absorption cycles produce cooling and/or heating with thermal input and minimal electric input, by using heat and mass exchangers, pumps and

valves. The absorption cycle is based on the principle that absorbing ammonia in water causes the vapor pressure to decrease. The basic operation of an ammonia-water absorption cycle is as follows. Heat is applied to the generator, which contains a solution of ammonia water, rich in ammonia. The heat causes high pressure ammonia vapor to absorb the solution. Heat can either be from combustion of a fuel such as clean-burning natural gas, or waste heat from engine exhaust, other industrial processes, solar heat, or any other heat source. The high pressure ammonia vapor flows to a condenser, typically cooled by outdoor air. The ammonia vapor condenses into a high pressure liquid, releasing heat which can be used for product heat, such as space heating. The high pressure ammonia liquid goes through a restriction, to the low pressure side of the cycle. This liquid, at low pressures, boils or evaporates in the evaporator. This provides the cooling or refrigeration product. The low pressure vapor flows to the absorber, which contains a water-rich solution obtained from the generator. This solution absorbs the ammonia while releasing the heat of absorption. This heat can be used as product heat or for internal heat recovery in other parts of the cycle, thus unloading the burner and increasing cycle efficiency. The solution in the absorber, now once again rich in ammonia, is pumped to the generator, where it is ready to repeat the cycle [13].

**Vapour absorption refrigeration device**

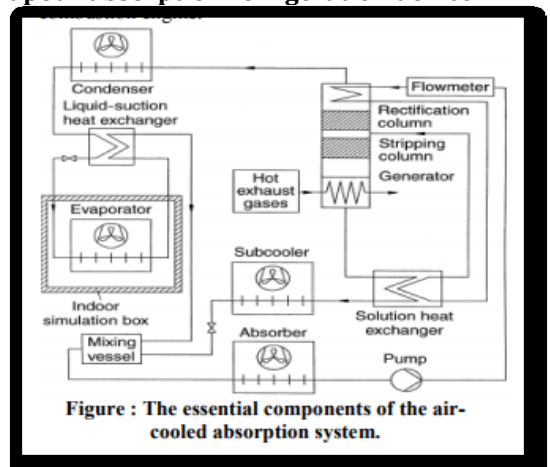


Figure : The essential components of the air-cooled absorption system.

1.	Engine Make	Kirloskar
2.	Engine Type	Single Cylinder
3.	Power	3.7 kW
4.	Speed	1500 rpm
5.	Bore Diameter	80 mm

6.	Stroke Length	110 mm
7.	Room Temperature	29 °C
8.	Exhaust Gas Temperature Range	125°C to 260°C
<b>Table : IC Engine specifications.</b>		

#### IV. LITERATURE REVIEW

**Li-Ting Chen**, 1988, Modified ejector-absorber absorption refrigeration cycle is presented and analyzed. From the results it is observed that a considerable improvement in COP is obtained with the present cycle when compared with that of the conventional cycle[1].

**George Vicatos**, 1995, The author studied the absorption refrigeration system and Heat and Mass correlation and simulate the system and then designed the system. This study has developed a methodology which could be adopted in designing an absorption refrigeration plant, given a refrigeration requirement[2]

**Shiyi Wang**, 1996, In this thesis S Wang designed the system, simulated it at different loads, manufactured it, carried out bench test and road test. In the exhaust gases of motor vehicles, there is enough heat energy which can be utilized to power an air-conditioning system “free” from any energy requirements [3].

**P. Srikhirin et al.**, 2001, This paper provided a literature review on absorption refrigeration technology. A doubleeffect absorption systems using lithium bromide/water seem to be the only high performance system which is available commercially [4].

**J Gryzagoridis et al.**,2008, The theoretical design is verified by a unit that is tested under both laboratory and road-test conditions. The evaluation of the COP, with and without the heat exchanger also proves that unless there is a high purity refrigerant, the effect of the heat exchanger to the generator’s heat is small [5].

**Andre AleixoManzela et al.**, 2010, This work presented an experimental study of an ammonia-water absorption refrigeration system using the exhaust of an internal combustion engine as energy source. Overall, carbon monoxide emission was decreased when the absorption refrigerator was installed in the exhaust gas, while hydrocarbon emissions increased [6].

**Khaled S. AlQdah**, 2011, This work presented an experimental study of an aqua-ammonia absorption system used for automobile

air conditioning system. It is evident that COP strongly depends on working conditions such as generator, absorber, condenser and evaporating the of temperature [7].

**Isaac Mathew Pavoodath**, 2012, In this paper study of absorption refrigeration is done. Such a system would vastly help take of the compressor load of the vehicle engine and would prove a great percentile of power saving for small capacity engines [8].

**Christy V Vazhappilly et al.**, 2013, A breadboard prototype of an absorption system for refrigeration using heat from the exhaust-gases is to be designed, built and tested. The heating coil generator system of absorption refrigeration system has been replaced by plate frame type heat exchanger, there by utilizing the exhaust gases of the IC engine [9].

**Janardhanan.k et al.**, 2014, This work presented a theoretical study of an aqua-ammonia absorption system used for automobile air conditioning system. Using a vapor absorption refrigeration system within an automobile as an air conditioner will not only reduce the fuel consumption of the vehicle while working but will also reduce the environmental pollution [10].

**S. Manojprabhakar et al.**, 2014, This work presented an experimental study refrigeration system, using vapor absorption system. The coefficient of performance of the system is low, that means that the system is expected to use a lot of energy with respect to the cooling it offers [11].

**J.P. Yadav et al.**, 2014, In this paper study of an experimental set up is designed and fabricated. Using heat exchangers, analyzer, and pre-heater the COP of the system further improves. Even by using two evaporators the effectiveness of the system can be increased [12].

**Paul Cedric Agra et al.**, 2014, This paper simulated the performance of the system using waste heat, a Bunsen burner was used which was attached to a propane tank via a rubber hose with a regulator. The small scale model with maximum COP 0.3685 at evaporator temperature 28 degree Celsius was achieved. In order to improve the performance of the system it is suggested to use high concentration of aqua ammonia solution [13].

**S. Thangamohan raja et al.**, 2015, In this paper study of absorption refrigeration is done. The waste heat energy available in exhaust gas is directly proportional to the engine speed and exhaust gas flow rate [14].

**Tambe. Y.D et al.**, 2015, In this paper the more focus was given to the design and manufacturing of the system with 80 cc internal

combustion petrol engine. The experiments conducted on the system, prove that the concept is feasible and could be used for refrigeration in traction and non traction application of engine [15].

**K L Rixon et al.**, 2015, In this paper study, design and fabrication of absorption refrigeration is done and result are obtained accordingly. Using a vapor absorption refrigeration system within an automobile as an air conditioner will not only reduce the fuel consumption of the vehicle but will also provide many other advantages like the efficiency of the engine is not decreased considerably [16].

**N. Chandanareddy et al.**, 2015, In this paper, an overview of utilization of waste heat with a brief literature of the current related research is studied. A maximum power consumption of 42.38 percent is saved using proposed system compared to existing system [17].

**Atishey Mittal et al.**, 2015, In this paper study of comparison of absorption refrigeration and compression refrigeration system is done. Waste heat recovery system is the best way to recover waste heat and saving the fuel [18].

**Dinesh Chandrakar et al.**, 2016, In this paper designing of absorption refrigeration is done and results are obtained. As power output increase, the heat recovered from exhaust gas also increase difficulty may occur when the vehicles at rest or in very slow moving traffic conditions [20].

**Kumar et al.** [14-19] has used three sides instead of one side roughened duct & found that augmentation in Nu & f was respectively to be 21-86 % & 11-41 %. They also reported augmentation in thermal efficiency of three sides over one side roughened duct to be 44-56 % for varying p/e and 39-51 % for varying e/D<sub>h</sub>.

## V.GAPS IDENTIFIED

There are some gaps identified

1.The exhausted waste heat from the running coach engine is well-established by simulation calculation. The calculative results have fine coincidence with the tested data.

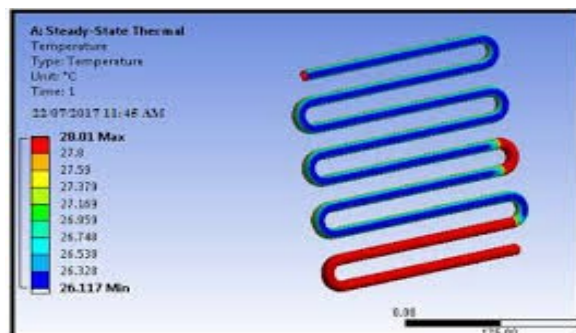
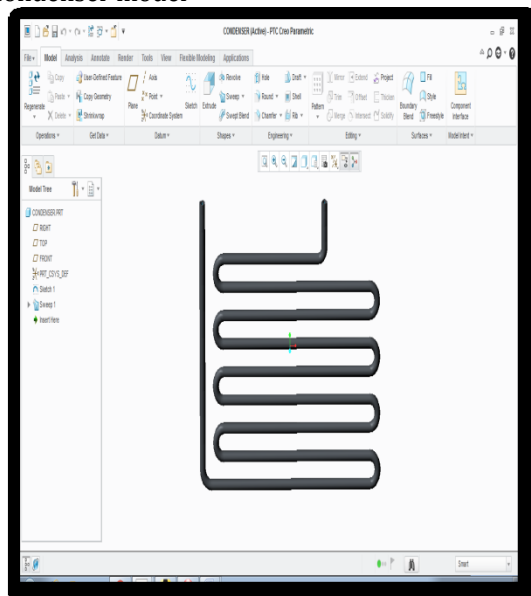
2. On the basis of the quantitative analysis of the exhausted gas parameters, the main devices are determined in the absorption compression hybrid cycle driven respectively by the waste heat of exhaust gases and power from the coach engine. One dimensional steady distribution parameter model in the generator and lumped parameters model in the other heat exchangers are established, for coupling heat transfer in the unt.

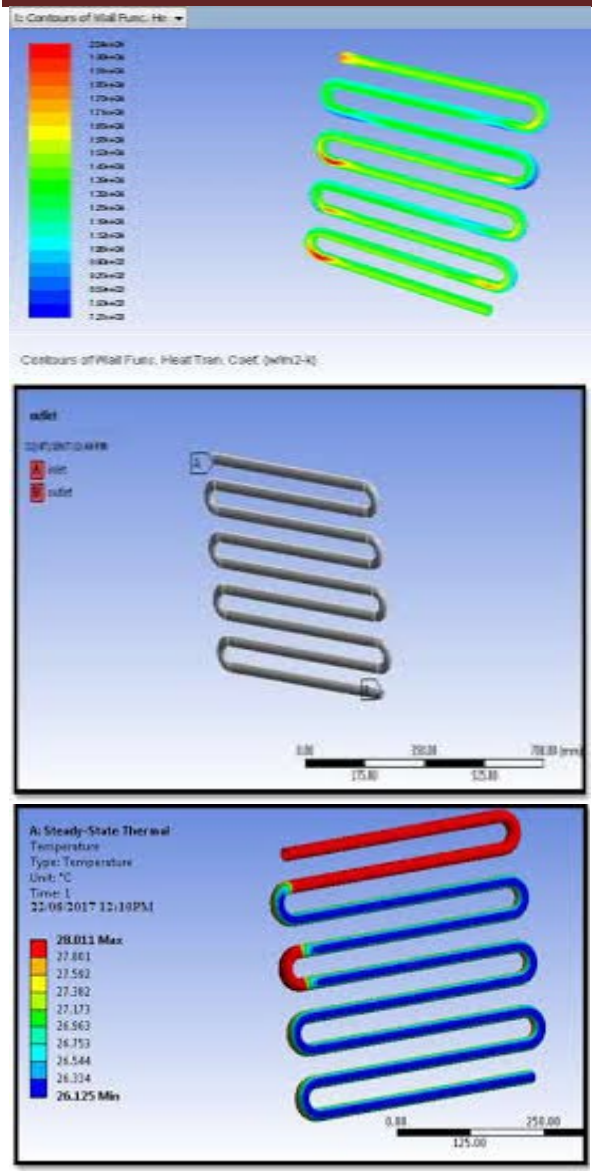
3. The ARSC can completely meet the demand of coach space cooling, when the running speed (u) is greater than 100 km/h; the ARSC together with the CRSC supplies the cooling capacity for the coach, when u is between 40 and 100 km/h; When u is lower than 40 km/h, the ARSC has no cooling effect, and the cooling demand for the coach is fully supplied by the CRSC. The characteristics of the ARSC are analyzed under different ambient temperatures. The performance of the ARSC drops with the rise in ambient temperature.

4. The ACHRC have advantages of meeting coach cooling demands by recovering the waste heat from engine and consuming less fuel oil. The compact and light weight structures are considered to apply into the key devices in the ACHRC

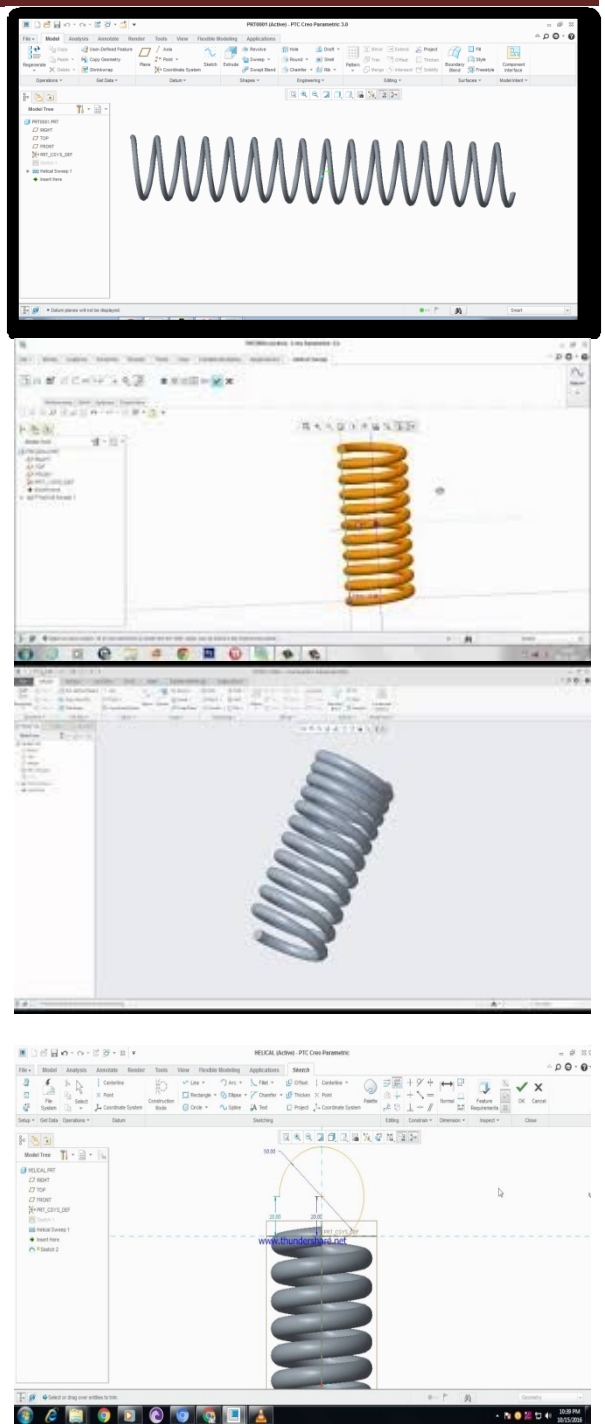
## VI.MODELING OF CONDENSOR AND EVAPORATOR IN CAD AND CREO

Condenser model





Evaporator version



**Advantages**

Uses Engine warmth as supply of energy for this reason enhances the efficiency of engine. Moving parts are handiest within the pump, that's a small detail in the machine therefore operation becomes smooth and also carrying and tearing is decreased. The system works at low evaporator pressures with out affecting the COP of the machine. Environmental friendly, no launch of CFC derivatives. Helps in shielding OZONE layer from

depletion. Helps engine to cool, as it extracts warmth from engine. Low jogging value. Higher engine electricity performance.

## VII.CONCLUSION

1. In the exhaust gases of motor vehicles, there is enough heat energy that can be utilised to power an air-conditioning system. Therefore, if air-conditioning is achieved without using the engine's mechanical output, there will be a net reduction in fuel consumption and emissions.

2. Once a secondary fluid such as water or glycol is used, the aqua-ammonia combination appears to be a good candidate as a working fluid for an absorption car air-conditioning system. This minimises any potential hazard to the passengers.

3. The low COP value is an indication that improvements to the cycle are necessary. A high purity refrigerant would give a higher refrigeration effect, while the incorporation of a solution heat exchanger would reduce the input heat to the generator. The present system has both a reflux condenser and a heat exchanger. However, the reflux condenser is proved inadequate to provide high purity of the refrigerant and needs to be re-addressed. The evaluation of the COP, with and without the heat exchanger also proves that unless there is a high purity refrigerant, the effect of the heat exchanger to the generator's heat is small.

## VIII.REFERENCES

1. Andy Pearson (2008) refrigeration with ammonia and hydro carbons, Int journal of refrigeration, 545-551.
2. I. Horuz (1999) vapor absorption in road transport vehicles, Journal of energy engineering, Vol. 125, No. 2, 48-58
3. Jabnithflame (2011) Development of an A/C system using waste heat of an I.C engine
4. G Victos, J Gryzagoridis & S Wang, "A car air conditioning system based on an absorption refrigeration cycle using energy from exhaust gas of an internal combustion engine", journal of energy in southern Africa, Vol 19, issue 4, November 2008, pp.6-11.
5. Colbourne, D., 2000. An overview of hydrocarbons as replacement refrigerants in commercial refrigeration and air conditioning. Refrigeration Northern Ireland Centre for Energy Research and Technology.
6. Colbourne, D., Suen, K.O., 2000. Assessment of performance of hydrocarbon refrigerants. In: Proceedings of the Fourth IIRGustavLorentzen Conference on Natural Working Fluids, Purdue, USA.
7. Colbourne, D., Ritter, T.J., 2000. Compatibility of Non-Metallic Materials with Hydrocarbon Refrigerant and Lubricant Mixtures. IIF-IIR-

- Commission B1, B2,E1 and E2 - Purdue University, USA
8. Setaro, T., Boccardi, G., Corberan, J.M., Urchueguia, J., Gonzalvez, J., 2000. Comparative study of evaporation and condensation of propane and R22 in a brazed plate heat exchanger and a tube and fins coil. In: Proceedings of the Fourth IIR Gustav Lorentzen Conference of Natural Working Fluids, Purdue, USA, pp.233-238
9. Qin F, Chen J, Lu M, Chen Z, Zhou Y, Yang K. Development of a metal hydride refrigeration system as an exhaust gas-driven automobile air conditioner. Renewable Energy 2007;32:2034-52.
10. Koehler J, Tegethoff WJ, Westphalen D, Sonnekalb M. Absorption refrigeration system for mobile applications utilizing exhaust gases. Heat Mass Transfer 1997;32:333-40.
11. William H Severens and Jullian R. Fellows, Air Conditioning & Refrigeration (Wiley International-1958)
12. Richard G. Jordan and Gayle B. Priester Refrigeration & Air Conditioning (Prentice Hall Of India PvtLtd.,New Delh-1965).
13. A. Mittal, D. Shukla, and K. Chauhan, "A refrigeration system for an automobile based on vapor absorption refrigeration cycle using waste heat energy from the engine", International Journal of Engineering Science and Research Technology, vol. 4, no. 4, 2015.
14. Kumar, V., Prasad, L., Experimental investigation on heat transfer and fluid flow of air flowing under three sides concave dimple roughened duct. International Journal of Mechanical Engineering and Technology (IJMET), Volume 8, Issue 11, November 2017, pp. 1083-1094, Article ID: IJMET\_08\_11\_110.
15. Kumar, V., Prasad, L., Thermal performance investigation of one and three sides concave dimple roughened solar air heaters. International Journal of Mechanical Engineering and Technology (IJMET) Volume 8, Issue 12, December 2017, pp. 31-45, Article ID: IJMET\_08\_12\_004.
16. Kumar, V., Prasad, L., Performance Analysis of three sides concave dimple shape roughened solar air heater, J. sustain. dev. energy water environ. syst., 6(4), pp 631-648, 2018.
17. Kumar, V., Nusselt number and friction factor correlations of three sides concave dimple roughened solar air heater, Renewable Energy 135 (2019) 355-377.
18. Kumar, V., Prasad, L., Experimental analysis of heat transfer and friction for three sides roughened solar air heater, Annales de Chimie - Science des Matériaux, 75-107, ACSM. Volume 41 – n° 1-2/2017.
19. Kumar, V., Prasad, L., Performance prediction of three sides hemispherical dimple roughened solar duct, Instrumentation,

Mesure, *Méetrologie*, 273-293 I2M. Volume 17  
– n° 2/2018.

20. G. Vicatos, "Heat and mass transfer characteristics: Design and optimization of absorption refrigeration machines", PhD

thesis, University of Cape Town, South Africa, 1995.

21. S. Wang, Motor vehicle air-conditioning utilizing the exhaust gas energy to power an absorption refrigeration cycles, University of Cape Town, South Africa, 1996.

## Improvement of an Automobile Radiator using Thermal Analysis

S. Vinay & Dr. A. Karthikeyan & Mr. Vikash Kumar

PG Student, Professor, Assistant Professor

Department of Mechanical Engg. Malla Reddy College of Engineering Maisammaguda, Dhulapally, Kompally, Secunderabad, Telangana-500100, India

**ABSTRACT:** Radiators are used to transfer thermal energy from one medium to another for the purpose of cooling. Radiators are used for cooling internal combustion engines, mainly in automobiles but also in piston engine aircraft, railway locomotives, motorcycles, stationary generating plant. The radiator transfers the heat from the fluid inside to the air outside, thereby cooling the fluid, which in turn cools the engine. Research is being carried out for several decades now, in improving the performance of the heat exchangers, having high degree of surface compactness and higher heat transfer abilities in automotive industry. These compact heat exchangers have fins, louvers and tubes. In this project we are designing a radiator without louver fins and with louver fins. The original radiator has no louver fins, we are modifying that by giving louver fins. 3D model is done in Pro/Engineer.

**Keywords:** Ansys Milling, Taguchi, H13 Steel.

### I. INTRODUCTION

#### A. Introduction to Automobile Radiator

Radiators are heat exchangers used to transfer thermal energy from one medium to another for the purpose of cooling and heating. The majority of radiators are constructed to function in automobiles, buildings, and electronics. The radiator is always a source of heat to its environment, although this may be for either the purpose of heating this environment, or for cooling the fluid or coolant supplied to it, as for engine cooling. Despite the name, radiators generally transfer the bulk of their heat via convection, not by thermal radiation, though the term "convector" is used more narrowly; see radiation and convection, below. The Roman hypocaust, a type of radiator for building space heating, was described in 15 AD. The heating radiator was invented by Franz San Galli, a Polish-born Russian businessman living in St. Petersburg, between 1855 and 1857.

#### B. Radiation and Convection

One might expect the term "radiator" to apply to devices that transfer heat primarily by thermal radiation (see: infrared heating), while a device which relied primarily on natural or forced convection would be called a "convector". In practice, the term "radiator" refers to any of a number of devices in which a liquid circulates through exposed pipes (often with fins or other means of increasing surface area),

Notwithstanding that such devices tend to transfer heat mainly by convection and might logically be called convectors. The term

"convector" refers to a class of devices in which the source of heat is not directly exposed.



Fig.1. Water-air convective cooling radiator.

#### C. Introduction To Pro/Engineer

Pro/ENGINEER, PTC's parametric, integrated 3D CAD/ CAM/CAE solution, is used by discrete manufacturers for mechanical engineering, design and manufacturing. Created by Dr. Samuel P. Geisberg in the mid-1980s, Pro/ENGINEER was the industry's first successful parametric, 3D CAD modeling system as shown in Fig.1. The parametric modeling approach uses parameters, dimensions, features, and relationships to capture intended product behavior and create a recipe which enables design automation and the optimization of design and product development processes. This powerful and rich design approach

is used by companies whose product strategy is family-based or platform-driven, where a prescriptive design strategy is critical to the success of the design process by embedding engineering constraints and relationships to quickly optimize the design, or where the resulting geometry may be complex or based upon equations. Pro/ENGINEER provides a complete set of design, analysis and manufacturing capabilities on one, integral, scalable platform. These capabilities, include Solid Modeling, Surfacing, Rendering, Data Interoperability, Routed Systems Design, Simulation, Tolerance Analysis, and NC and Tooling Design.

Companies use Pro/ENGINEER to create a complete 3D digital model of their products. The models consist of 2D and 3D solid model data which can also be used downstream in finite element analysis, rapid prototyping, tooling design, and CNC manufacturing. All data is associative and interchangeable between the CAD, CAE and CAM modules without conversion. A product and its entire bill of materials(BOM) can be modeled accurately with fully associative engineering drawings, and revision control information. The associativity in Pro/ENGINEER enables users to make changes in the design at any time during the product development process and automatically update downstream deliverables. This capability enables concurrent engineering design, analysis and manufacturing engineers working in parallel and streamlines product development processes. Pro/ENGINEER is an integral part of a broader product development system developed by PTC. It seamlessly connects to PTC's other solutions including Windchill, ProductView, Mathcad and Arbortext. Kumar et al. [19-25] has used three sides instead of one side roughened duct & found that augmentation in Nu & f was respectively to be 21-86 % & 11-41 %. They also reported augmentation in thermal efficiency of three sides over one side roughened duct to be 44-56 % for varying p/e and 39-51 % for varying e/D<sub>h</sub>.

## II. DIFFERENT MODULES IN PRO/ENGINEER

- Part Design
- Assembly
- Drawing
- Sheetmetal
- Manufacturing

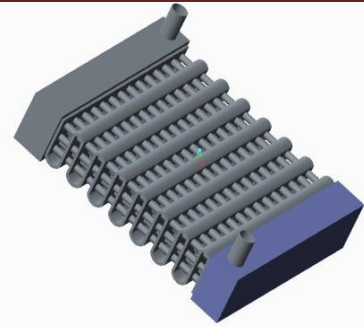


Fig.2. Model of Radiator.

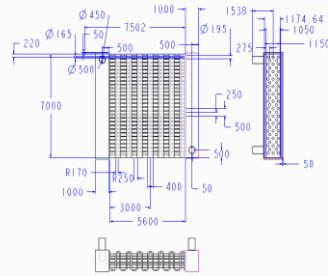


Fig.3. 2D Drawing.

## III. THERMAL ANALYSIS

### A. Without Louver FINS

Set Units - /units,si,mm,kg,sec,k

File- change Directory-select working folder File-Change job name-Enter job name Select element-Solid-20node 90

### B. Material Properties - Aluminum Alloy 6061

Density - 0.0000027 Kg/mm<sup>3</sup> Thermal Conductivity - 180W/mK Specific Heat - 896 J/Kg K

Apply Thermal-Temperature- on Area=353K

Convections - on Area-Film Co-efficient- 0.034 W/mm<sup>2</sup> K Bulk Temperature - 303 K

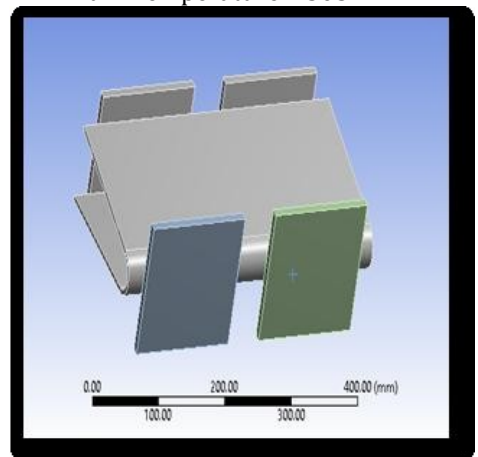


Fig.4. Imported Model.

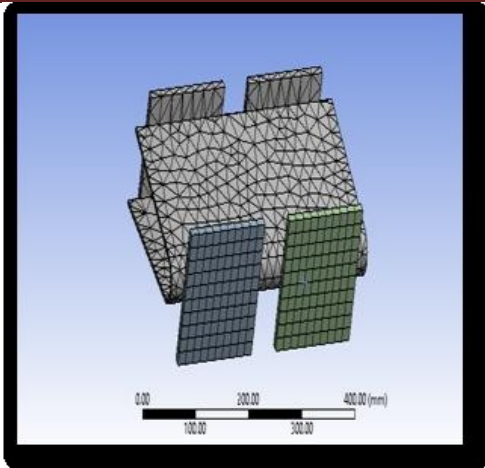


Fig.5. Meshed model.

Material Properties  
Youngs Modulus  
=

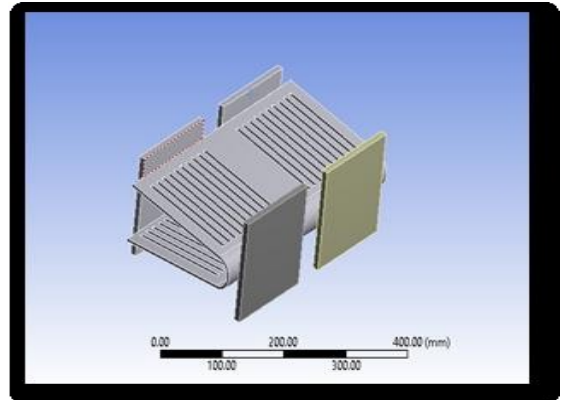


Fig.8. Imported.

### Performance Improvement of an Automobile Radiator using CFD Analysis

#### IV. RESULTS

Results of this paper is as shown in Figs.6 to 12.

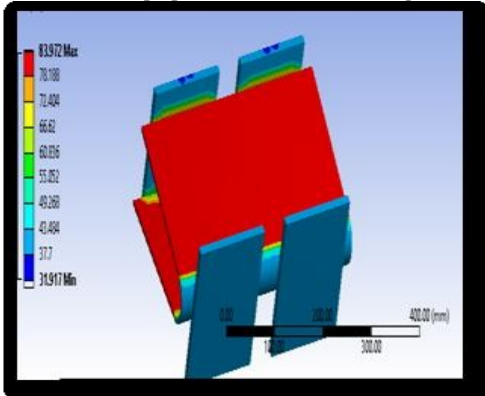


Fig.6. Temperature

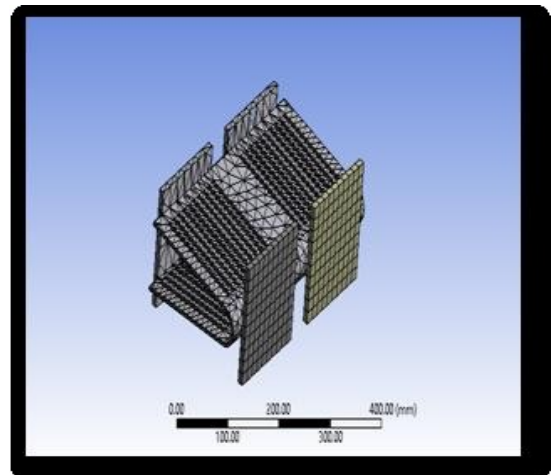


Fig.9. Meshed model.

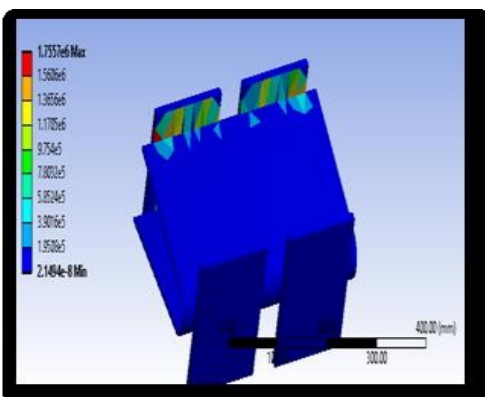


Fig.7. Thermal error.

#### Loads:

Apply Thermal-Temperature- on Area=353K  
Convections – on Area-Film Co-efficient – 0.034  
W/mm<sup>2</sup> K  
Bulk Temperature – 303 K

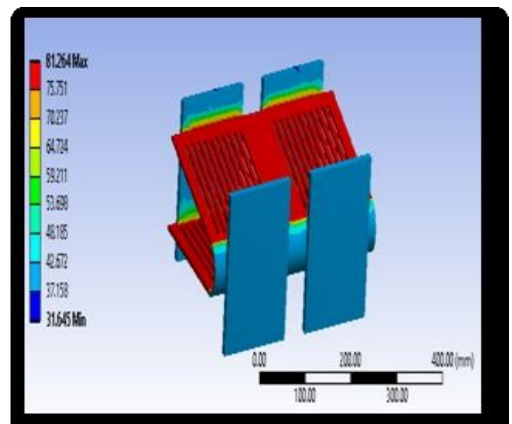


Fig.10. Temperature.

#### A. Heat Flux

With Louver FINS:

Set Units - /units,si,mm,kg,sec,k  
File- change Directory-select  
working folder File-Change job  
name-Enter job name Select  
element-Solid-20node 90

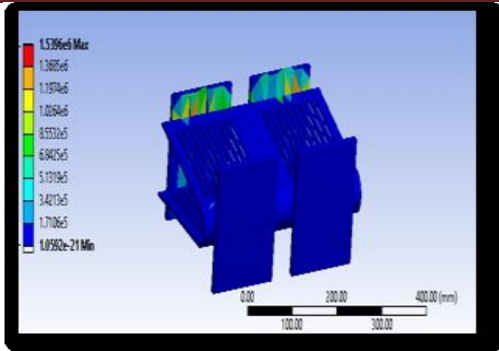


Fig.11. Thermal error

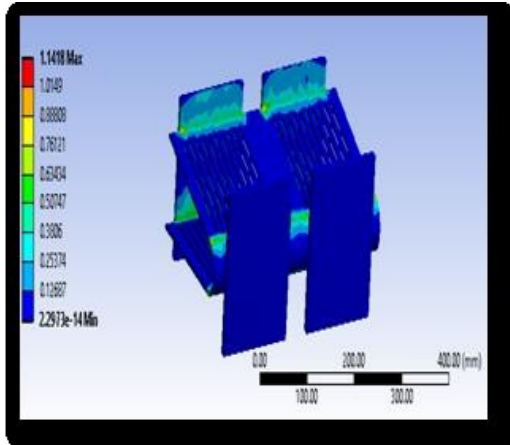


Fig.12. Heat flux.

**B. Results Table CFD Analysis**

**TABLE I: Original Model**

	Mass flow rate (Kg/sec)			
	0.08 kg/sec	0.140 kg/sec	0.210 kg/sec	0.280 kg/sec
Pressure (Pa)	1.56e+01	2.82e+01	4.35e+01	5.94e+01
Velocity (m/s)	1.02e+00	1.77e+00	2.64e+00	3.51e+00
Temperature (K)	3.53e+02	3.53e+02	3.53e+02	3.53e+02
Mass Flow Rate (Kg/S)	1.147e-06	9.8341e-07	2.5331e-07	5.3644e-07
Total Heat Transfer rate at wall (W)	2749	3011	3149	3225

**TABLE II: With Louver FINS**

	Mass flow rate (Kg/sec)			
	0.08 kg/sec	0.140 kg/sec	0.210 kg/sec	0.280 kg/sec
Pressure (Pa)	1.17e+02	2.14e+02	3.37e+02	4.68e+02
Velocity (m/s)	1.44e+00	2.50e+00	3.73e+00	4.94e+00
Temperature (K)	3.53e+02	3.53e+02	3.53e+02	3.53e+02
Mass Flow Rate (Kg/S)	4.616e-06	2.920e-06	2.840e-06	3.069e-06
Total Heat Transfer rate at wall (W)	5961	7463	8346	8872

**TABLE III: Thermal Results**

	With louvers	Without louvers
Temperature (°C)	81.264	83.972
Thermal Error	1.5396e6	1.7557e6
Heat Flux (W/mm <sup>2</sup> )	1.1418	0.98837

**V. CONCLUSION**

In this project a radiator is designed without louver fins and with louver fins. The original radiator has no louver fins, it has been modified by specifying louver fins. 3D model is designed in Pro/Engineer. The analysis tool ANSYS is used to perform CFD analysis on radiator at different mass flow rates. By observing the analysis results, the velocity is increased by 29.16%, pressure is increased by 86.66% and heat transfer rate at walls is increased by 53.88% for the modified model than the original that is the radiator with louvered fins.

performed to analyze the heat transfer rate to determine the thermal flux. The material taken is Aluminum alloy 6061 for thermal analysis. By observing the thermal analysis results, thermal flux is increased by 13.43% for the modified model. So it can be concluded that modifying the radiator model with louver fins yields better results. Ultimately it can be summarized that by providing louvers for the radiator and increasing the louver pitch helped in reducing the pumping power requirements with increase in heat transfer rate. This will help in increasing the power output per unit mass of the radiator. Hence it is recommended to increase the louver spacing for the geometry under consideration.

**VI. REFERENCES**

1. Performance Improvement of a Louver-Finned Automobile Radiator Using Conjugate Thermal CFD Analysis by Junjanna G.C.
2. Performance Investigation of an Automotive Car Radiator Operated With Nanofluid as a Coolant by Durgesh kumar Chavan and Ashok T. Pise Sahin.
3. Heat Transfer Enhancement of Automobile Radiator with TiO<sub>2</sub>/Water Nanofluid by Paresh Machhar, Falgun Adroja.
4. Wolf, I., Frankovic, B., Vilicic, I., A numerical and experimental analysis of neat transfer in a wavy fin and tube heat exchanger, Energy and the Environment (2006) pp.91-101.
5. Wang, C.C., Lo, J, Lin, Y.T. Wei, C.S., Flow visualization of annular and delta winlet vortex generators in fin and tube heat exchanger application, International Journal of Heat and Mass Transfer, 45, (2002), pp.3803-3815.

6. Leu, J.S., Wu, Y.H., Jang, J.Y., Heat transfer and fluid flow analysis in plate-fin and tube heat exchangers with a pair of block shape vortex generators, *International Journal of Heat and Mass Transfer*, 47 (2004), pp. 4327- 4338.
7. Kumar, V., Prasad, L., Experimental investigation on heat transfer and fluid flow of air flowing under three sides concave dimple roughened duct. *International Journal of Mechanical Engineering and Technology (IJMET)*, Volume 8, Issue 11, November 2017, pp. 1083–1094, Article ID: IJMET\_08\_11\_110.
8. Kumar, V., Prasad, L., Thermal performance investigation of one and three sides concave dimple roughened solar air heaters. *International Journal of Mechanical Engineering and Technology (IJMET)* Volume 8, Issue 12, December 2017, pp. 31–45, Article ID: IJMET\_08\_12\_004.
9. Kumar, V., Prasad, L., Performance Analysis of three sides concave dimple shape roughened solar air heater, *J. sustain. dev. energy water environ. syst.*, 6(4), pp 631-648, 2018.
10. Kumar, V., Nusselt number and friction factor correlations of three sides concave dimple roughened solar air heater, *Renewable Energy* 135 (2019) 355-377.
11. Kumar, V., Prasad, L., Experimental analysis of heat transfer and friction for three sides roughened solar air heater, *Annales de Chimie - Science des Matériaux*, 75-107, ACSM. Volume 41 – n° 1-2/2017.
12. Kumar, V., Prasad, L., Performance prediction of three sides hemispherical dimple roughened solar duct, *Instrumentation, Mesure, Métrologie*, 273-293 I2M. Volume 17 – n° 2/2018.

## IMPROVING THE HEAT TRANSFER RATE OF AC CONDENSER BY OPTIMISING THE MATERIAL

Md. Abdul Raheem & Dr. A. Karthikeyan & Mr. Vikash Kumar

PG Student, Professor, Assistant Professor

Department of Mechanical Engg. Malla Reddy College of Engineering Maisammaguda, Dhulapally, Kompally,  
Secunderabad, Telangana-500100, India

**ABSTRACT:** Air conditioning systems have condenser that removes unwanted heat from the refrigerant and transfers that heat outdoors. The primary component of a condenser is typically the condenser coil, through which the refrigerant flows. Since, the AC condenser coil contains refrigerant that absorbs heat from the surrounding air, the refrigerant temperature must be higher than the air. In this thesis heat transfer by convection in AC by varying the refrigerants are determined by CFD and thermal analysis. The assessment is out on an air-cooled tube condenser of a vapour compression cycle for air conditioning system. The materials considered for tubes are Copper and Aluminium alloys 6061 and 7075. The refrigerants varied will be R 22, R 134 and R407C. CFD analysis is done to determine temperature distribution and heat transfer rates by varying the refrigerants. Heat transfer analysis is done on the condenser to evaluate the better material. 3D modeling is done in CREO and analysis is done in ANSYS

**Keywords:**

### INTRODUCTION

In systems involving heat transfer, a condenser is a device or unit used to condense a substance from its gaseous to its liquid state, by cooling it. In so doing, the latent heat is given up by the substance, and will transfer to the condenser coolant. Condensers are typically heat exchangers which have various designs and come in many sizes ranging from rather small (hand-held) to very large industrial-scale units used in plant processes. For example, a refrigerator uses a condenser to get rid of heat extracted from the interior of the unit to the outside air. Condensers are used in air conditioning, industrial chemical processes such as distillation, steam power plants and other heat-exchange systems. Use of cooling water or surrounding air as the coolant is common in many condensers.



### Examples of condensers Applications:

- **Air cooled** – If the condenser is located on the outside of the unit, the air cooled condenser can provide the easiest arrangement. These types of condensers eject heat to the outdoors and are simple to install.

Most common uses for this condenser are domestic refrigerators, upright freezers and in residential packaged air conditioning units. A great feature of the air cooled condenser is they are very easy to clean. Since dirt can cause serious issues with the condensers performance, it is highly recommended that these be kept clear of dirt.

- **Water cooled** – Although a little more pricey to install, these condensers are the more efficient type. Commonly used for swimming pools and condensers piped for city water flow, these condensers require regular service and maintenance.

They also require a cooling tower to conserve water. To prevent corrosion and the forming of algae, water cooled condensers require a constant supply of makeup water along with water treatment.

Depending on the application you can choose from tube in tube, shell and coil or shell and tube condensers. All are essentially made to produce the same outcome, but each in a different way.

- **Evaporative** – While these remain the least popular choice, evaporative condensers can

be used inside or outside of a building and under typical conditions, operate at a low condensing temperature.

Typically these are used in large commercial air-conditioning units. Although effective, they are not necessarily the most efficient.

Prior to beginning your install, make sure you choose a condenser that will provide you with the most efficient use.→→

**LITERATURE REVIEW**

**Balaji Net al [1]**The majority of the research work focused large chillers. But in this paper discusses the single split air conditioning system using instead of air cooling using liquid based cooling. The coolant used in the heat exchanger pure ethylene glycol. Compare the experimental results value of existing system with new modified system. The compressor running time for the pure ethylene glycol based cooling system is less than the existing system. The compressor's running time is reduced from 44 minutes 30 seconds to 33 minutes and 4 seconds. The required indoor temperature of 18°C is reached in 11 minutes 26 seconds earlier. It is evident that the time taken for cooling by the modified system is 25.69 % less than that of the existing split air condition system. Time taken for cooling reduces automatically improve the efficiency of the air conditioning system.

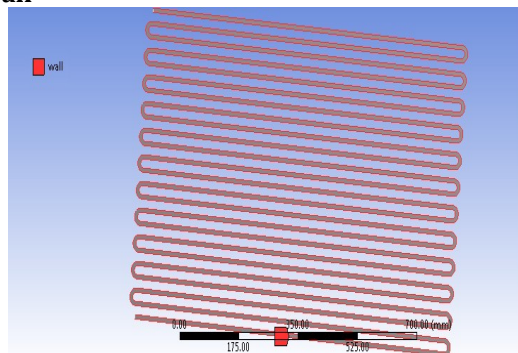
**M. Joseph Stalin et al [2]** As the energy demand in our day to day life escalates significantly, there are plenty of energies are shuffled in the universe. Energies are put in an order of low grade and high grade energies. The regeneration of low grade energy into some beneficial work is fantastic job. One such low grade energy is heat energy. So it is imperative that a significant and concrete effort should be taken for using heat energy through waste heat recovery. This paper concentrates on the theoretical analysis of production of hot water and reduction of LPG occupies most of our condominium for our comforts. An attempt has been taken to recover waste heat rejected by the 1 TR air conditioning systems. For this water cooled condenser is exerted and the water is promulgated by until our desired temperature is acquired. Then the hot water is accumulated in insulated tank for our use. The result of the paper shows that the temperature of hot water, time required for attaining that temperature for the necessary volume of water and the reduction of LPG gas by using hot water is also confabulated. Factors like supply and demand, condenser coil design are pondered and theoretically calculated and the corresponding graphs are drawn. Finally

this could be the surrogate for water heater and it fulfils all the applications of Hot water. Similarly, it could tackle the demand of LPG gas.



Fig – Fluid outlet

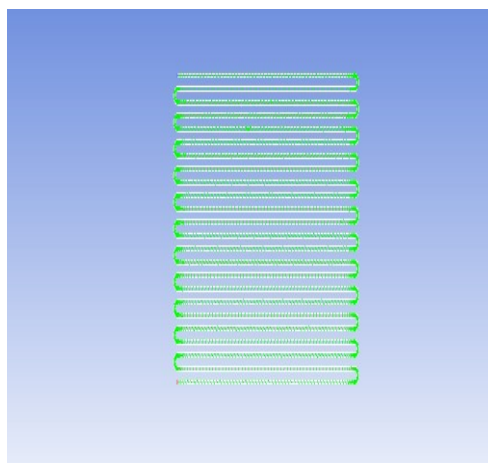
Wall



**File export** → fluent → input file (mesh) → save required name → save.

→→ Ansys → fluid dynamics → fluent → select working directory → ok

→→ file → read → mesh → select file → ok.



General → Pressure based  
 Model → energy equation → on.  
 Viscous → edit → k-epsilon

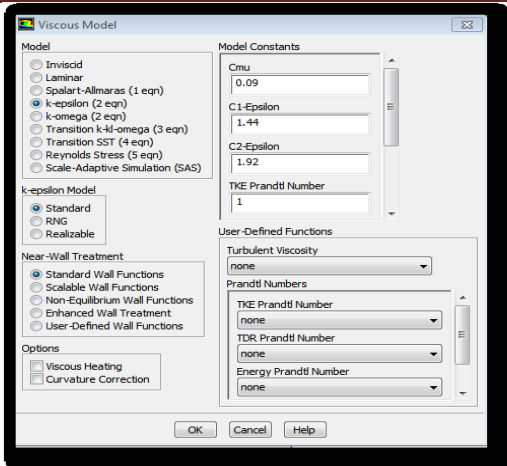


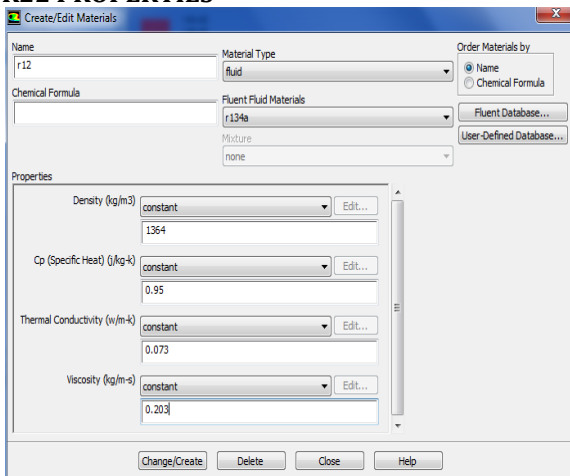
Fig – Viscous Model

Materials → new → create or edit  
 → specify fluid material or specify properties  
 → Ok

**FLUID - R22**

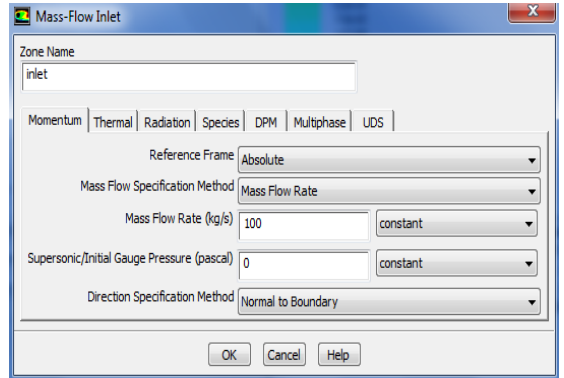
Temperature - T - (°C)	Density - ρ - (kg/m <sup>3</sup> )	Specific Heat Capacity - Cp - (10 <sup>3</sup> J/kg.K)	Thermal Conductivity - k - (W/m K)	Kinematic Viscosity - ν - (10 <sup>-6</sup> m <sup>2</sup> /s)	Prandtl Number - Pr -
-50	1547	0.875	0.067	0.310	6.2
-40	1519	0.885	0.069	0.279	5.4
-30	1490	0.896	0.069	0.253	4.8
-20	1461	0.907	0.071	0.235	4.4
-10	1429	0.920	0.073	0.221	4.0
0	1397	0.935	0.073	0.214	3.8
10	1364	0.950	0.073	0.203	3.6
20	1330	0.966	0.073	0.198	3.5
30	1295	0.984	0.071	0.194	3.5
40	1257	1.002	0.069	0.191	3.5
50	1216	1.022	0.069	0.190	3.5

**R22 PROPERTIES**

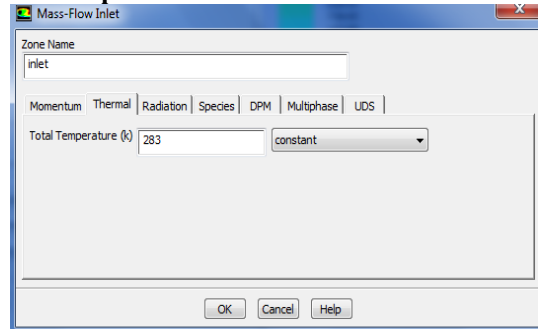


**INLET BOUNDARY CONDITIONS**

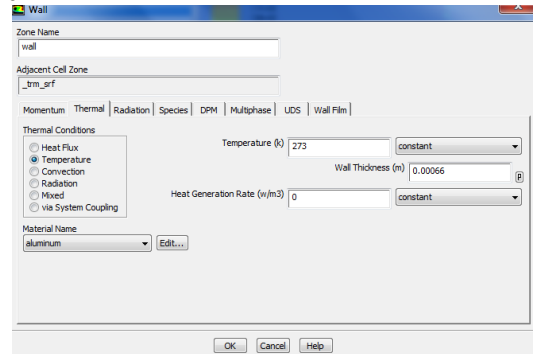
**Inlet**



**Inlet Temperature**

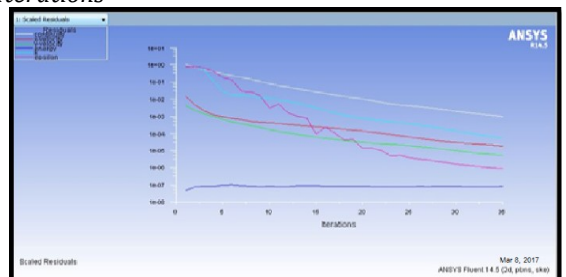


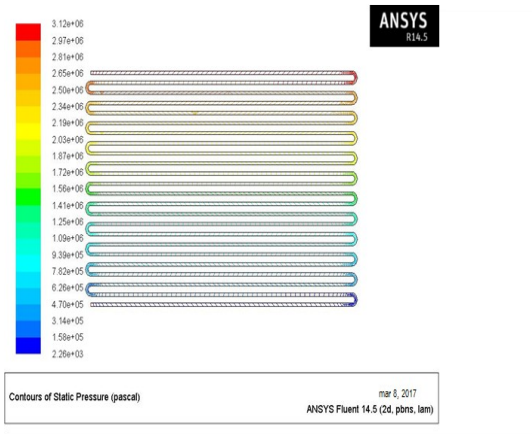
**Wall**



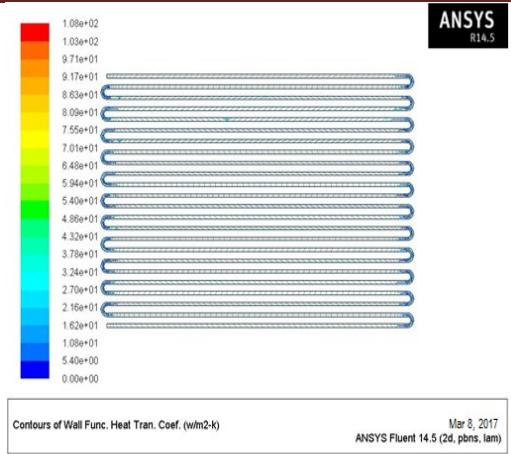
Solution → Solution Initialization → Hybrid Initialization → done  
 Run calculations → no of iterations = 100 → calculate → calculation complete  
 → Results → graphics and animations → contours → setup

**Iterations**

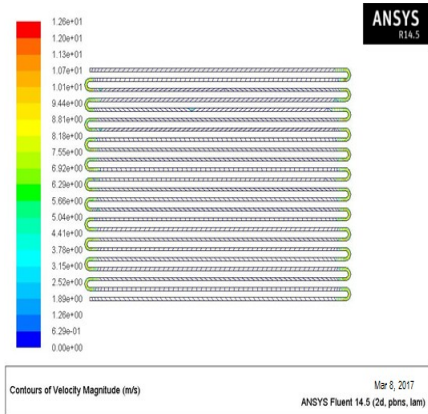




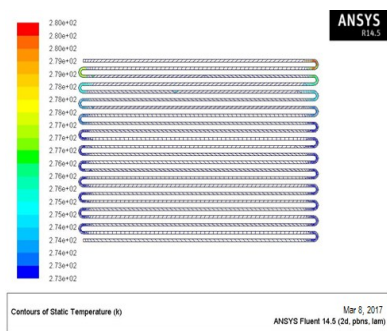
**Contours of Static Pressure**



**Contours of Wall function Heat Transfer Coefficient**



**Contours of Velocity Magnitude**



**Contours of Static Temperature**

**Mass Flow Rate (kg/s)**

inlet	100
interior-trm_srf	-35415.109
outlet	-100.02785
wall	0

Net -0.02784729

**Total Heat Transfer Rate (w)**

inlet	-1439.2496
outlet	2389.7905
wall	-94.993591

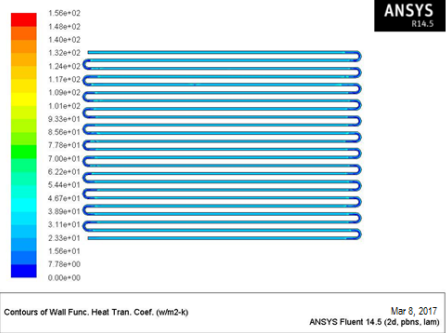
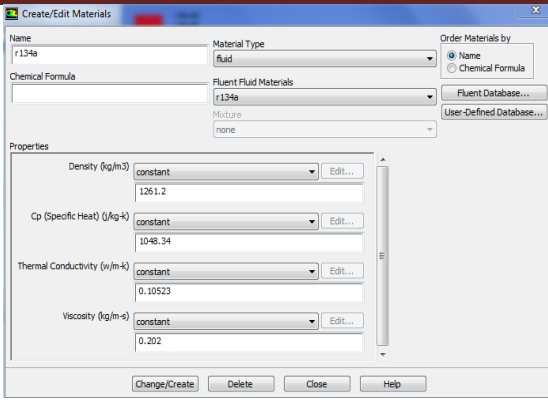
Net 855.549

**FLUID - R134A**

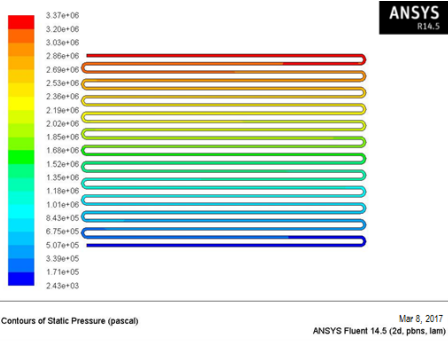
R-134a Properties - SI Units

Temperature (°C)	Absolute Pressure (bar)	Density Liquid (kg/m <sup>3</sup> )	Density Vapor (kg/m <sup>3</sup> )	Enthalpy Liquid (kJ/kg)	Enthalpy Vapor (kJ/kg)	Entropy Liquid (kJ/kgK)	Entropy Vapor (kJ/kgK)
-60	0.15905	1472.0	0.9291	24.491	261.491	0.68772	1.8014
-50	0.29477	1444.9	1.6526	36.302	267.779	0.74358	1.7809
-40	0.51225	1417.0	2.773	48.631	274.066	0.79756	1.76446
-30	0.84379	1388.2	4.4307	61.130	280.324	0.84965	1.75142
-20	1.32719	1358.4	6.7903	73.833	286.513	0.901	1.74113
-10	2.00575	1327.4	10.047	86.777	292.598	0.95095	1.73309
0	2.92769	1295.1	14.433	100.0	298.536	1	1.72684
10	4.14571	1261.2	20.225	113.540	304.276	1.04804	1.72196
20	5.71665	1225.5	27.773	127.437	309.756	1.09613	1.71806
30	7.70132	1187.5	37.517	141.736	314.892	1.14354	1.71473
40	10.1648	1146.7	50.055	156.491	319.676	1.19073	1.71152
50	13.1773	1102.2	66.234	171.778	323.652	1.23794	1.70792
60	16.8156	1052.9	87.346	187.715	326.896	1.28548	1.70325
70	21.1668	996.49	115.564	204.515	328.941	1.33339	1.6965
80	26.3336	928.78	155.130	222.616	329.095	1.38434	1.68585
90	32.4489	838.51	216.595	243.168	325.655	1.43676	1.6692
100	39.7254	649.71	367.064	273.641	309.037	1.5198	1.61465

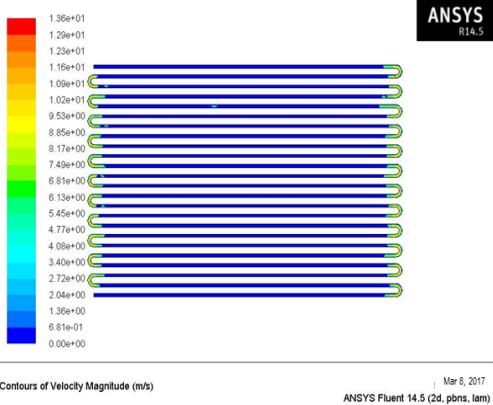
**Properties**



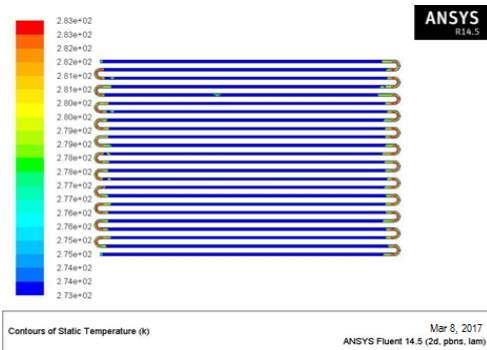
**Contours of Wall Function Heat Transfer Coefficient**



**Contours of Static Pressure**



**Contours of Velocity Magnitude**



**Contours of Static Temperature**

**Mass Flow Rate (kg/s)**

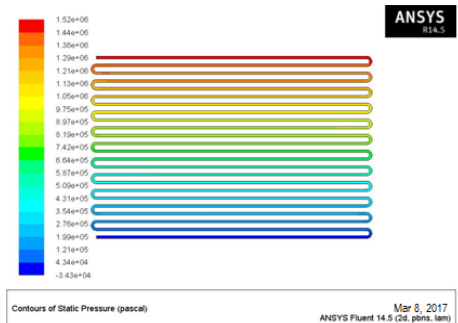
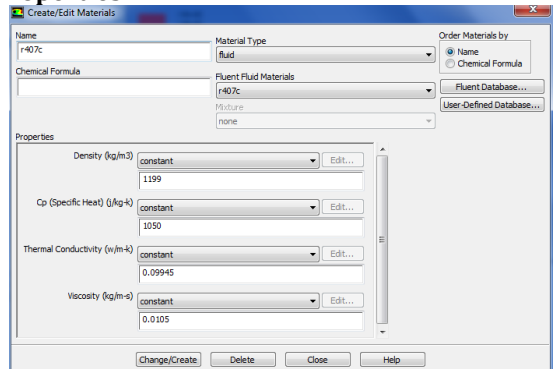
inlet	100
interior-trm_srf	-35416.969
outlet	-99.986626
wall	0
-----	
Net	0.013374329

**Total Heat Transfer Rate (w)**

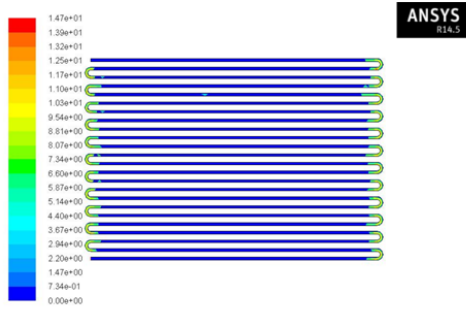
inlet	-1588235
outlet	1600658
wall	-12604.787
-----	
Net	-181.78711

**FLUID - R407C**

**Properties**

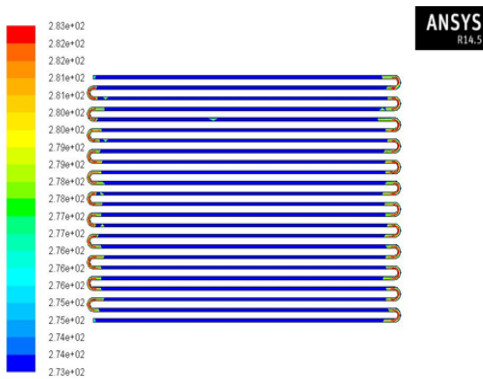


**Contours of Static Pressure**



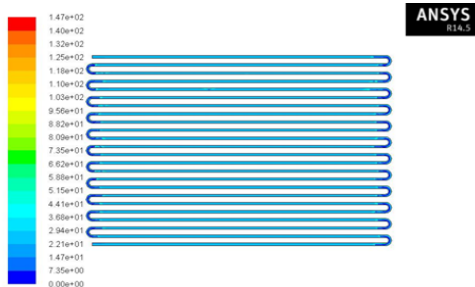
Contours of Velocity Magnitude (m/s) Mar 8, 2017 ANSYS Fluent 14.5 (2d, pbrns, lam)

**Contours of Velocity Magnitude**



Contours of Static Temperature (K) Mar 8, 2017 ANSYS Fluent 14.5 (2d, pbrns, lam)

**Contours of Static Temperature**



Contours of Wall Func. Heat Tran. Coef. (w/m2-K) Mar 8, 2017 ANSYS Fluent 14.5 (2d, pbrns, lam)

**Contours of Wall function Heat Transfer Coefficient**

**Mass Flow Rate (kg/s)**

inlet	100
interior-_trm_srf	-35510.789
outlet	-100.01424
wall	0
Net	-0.01423645

**Total Heat Transfer Rate (w)**

inlet	-1590750
outlet	1602622.8

wall	-11921.454
Net	-48.704102

**THERMAL ANALYSIS**

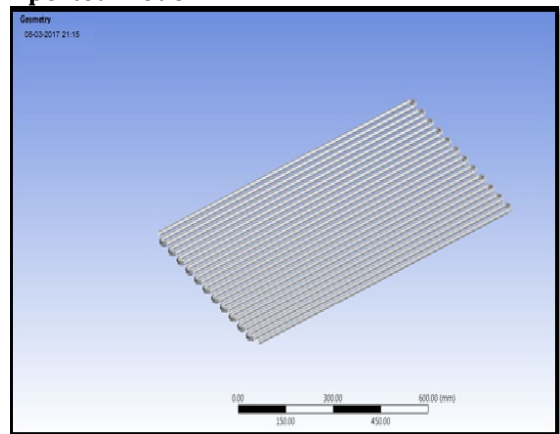
Note : Input for thermal analysis are taken from above CFD results

**MATERIAL – ALUMINIUM 6061**

**FLUID – R22**

Open work bench 14.5>select **steady state thermal** in analysis systems>select geometry>right click on the geometry>import geometry>select IGES file>open

**Imported model**



**ALUMINIUM 6061 MATERIAL PROPERTIES**

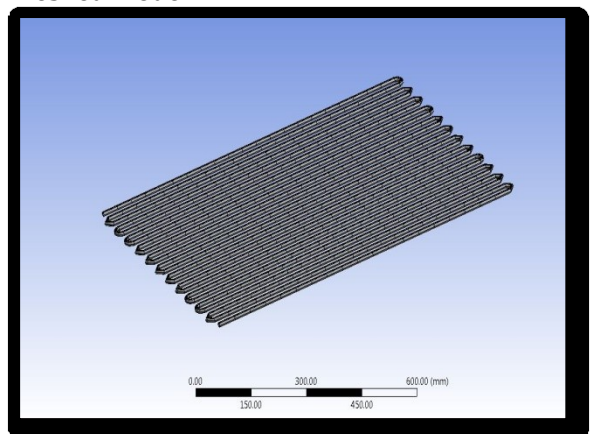
Thermal conductivity of aluminum = 15.1W/mk

Specific heat =356J/Kg K

Density = 0.00000412 Kg/mm<sup>3</sup>

Model >right click>edit>select generate mesh

**Meshed model**



**Boundary conditions**

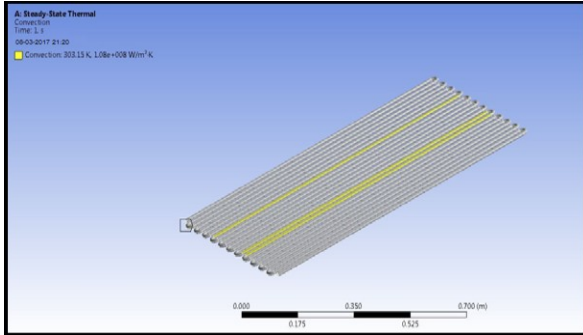
Select steady state thermal >right click>insert>

Select steady state thermal >right click>insert>select heat flux

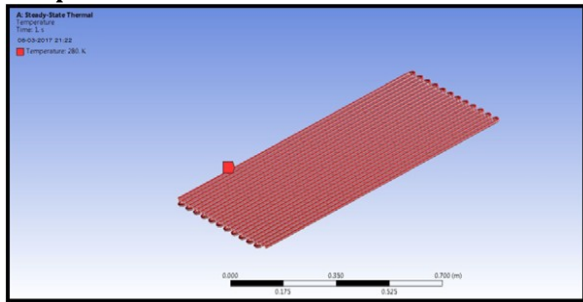
Select steady state thermal >right click>solve

Solution>right click on solution>insert>select temperature

**Convection**

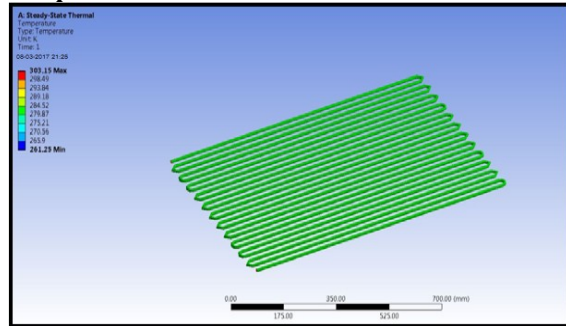


**Temperature**

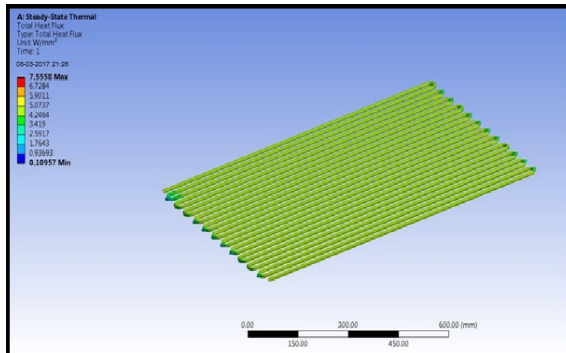


**Results**

**Temperature**

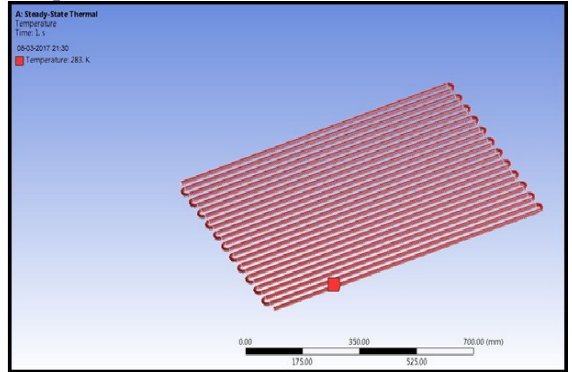


**Heat flux**

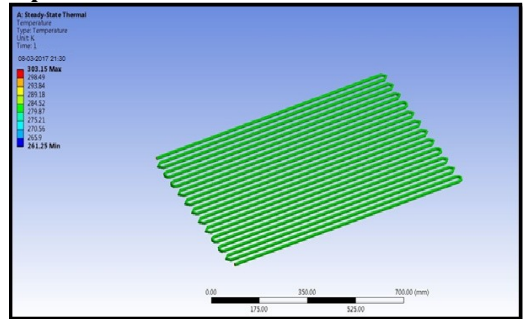


*FLUID - R134A*

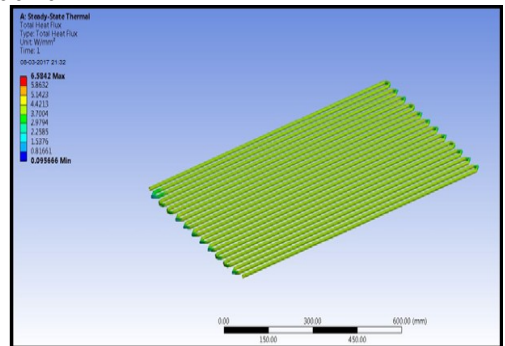
**Temperature**



**Temperature**

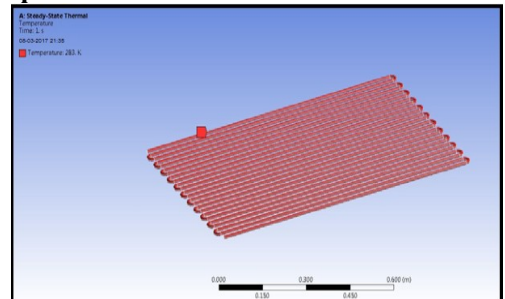


**Heat flux**



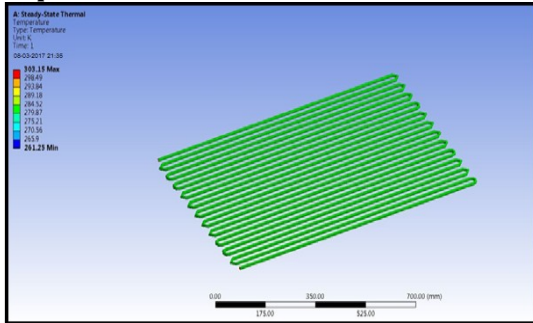
*FLUID - R407C*

**Temperature**

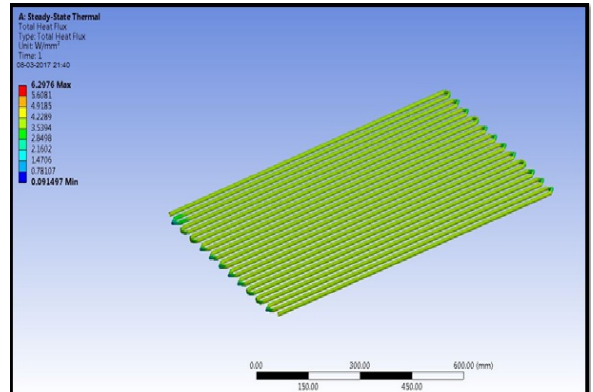


### Temperature

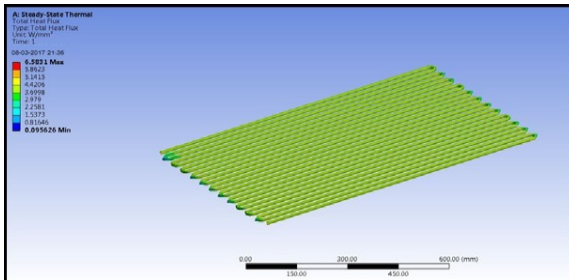
### FLUID - R407C



### Heat flux



### Heat flux



### MATERIAL -COPPER

### FLUID - R22

Thermal conductivity of aluminum = 59.1W/mK

Specific heat =421 J/Kg K

Density = 0.00000771Kg/mm<sup>3</sup>

### MATERIAL -ALUMINIUM 7075

### FLUID - R22

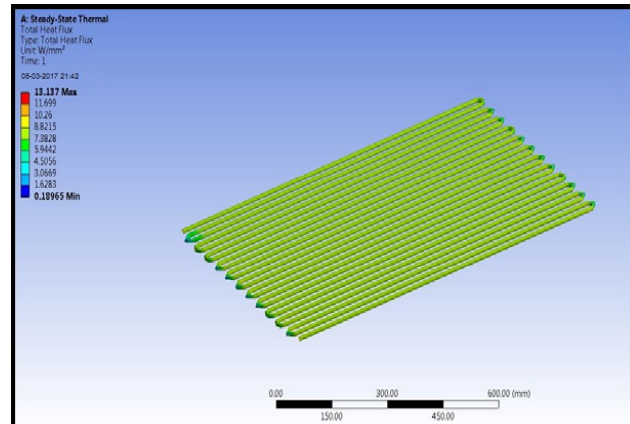
Thermal conductivity of aluminum = 59.1W/mK

Specific heat =421 J/Kg K

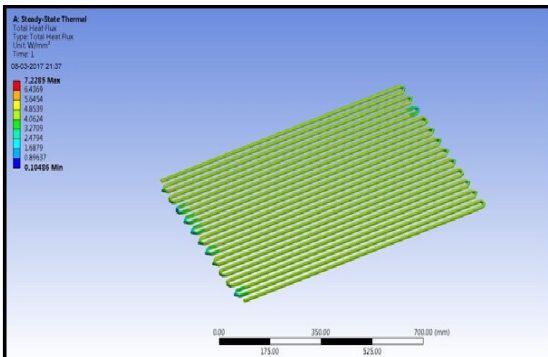
Density = 0.00000771Kg/mm<sup>3</sup>

### Heat flux

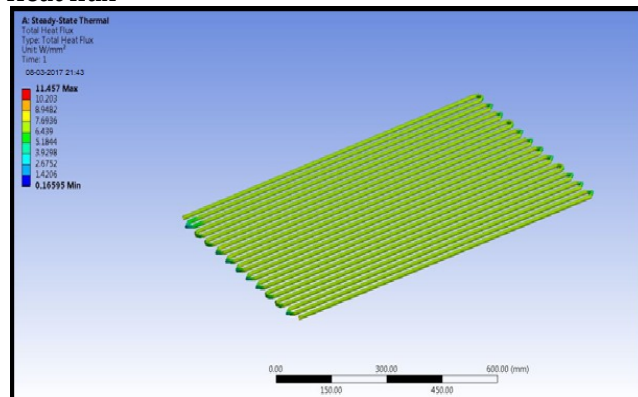
### Heat flux



### FLUID - R134A

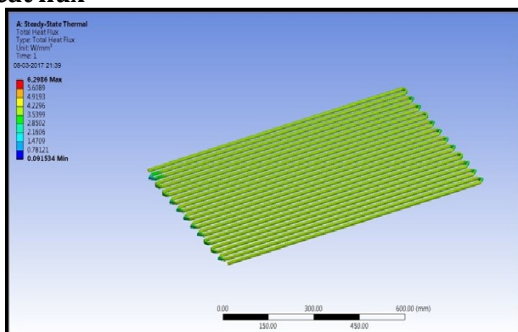


### Heat flux



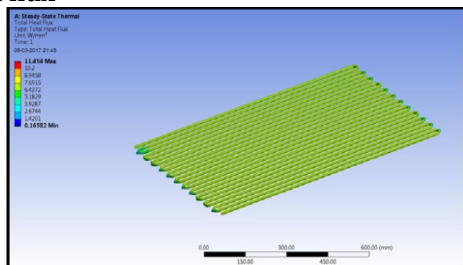
### FLUID - R134A

### Heat flux



**FLUID - R407C**

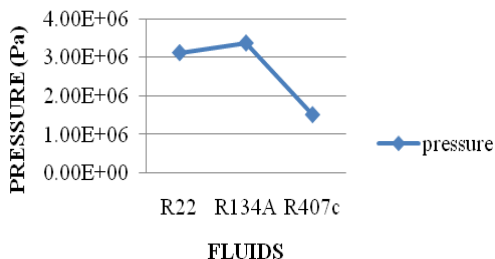
**Heat flux**



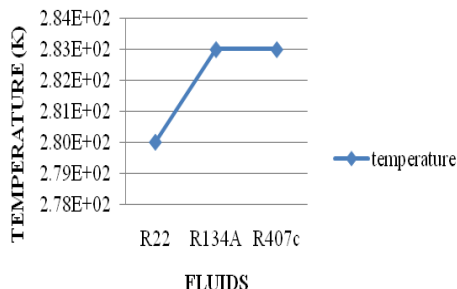
**RESULTS AND DISCUSSION**

CFD ANALYSIS Fluids	Pressure (Pa)	Temperature (K)	Velocity (m/Sec)	Wall Function Heat Transfer Coefficient (W/m <sup>2</sup> -K)	Mass Flow Rate (Kg/Sec)	Total Heat Transfer Rate (W)
<b>R22</b>	3.12e+06	2.80e+02	1.26e+01	1.08e+02	-0.0278429	855.549
<b>R134A</b>	3.37e+06	2.83e+02	1.36e+01	1.56e+02	0.013374329	-181.78711
<b>R407C</b>	1.52e+06	2.83e+02	1.47e+01	1.47e+02	-0.01423645	-48.704102

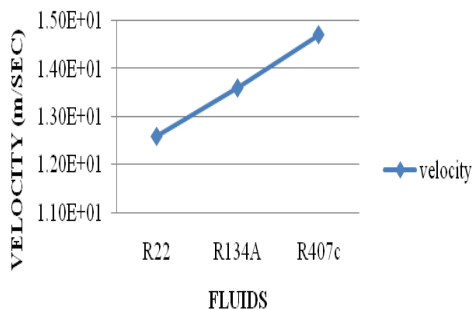
**COMPARISON OF PRESSURE VALUES FOR DIFFERENT FLUIDS**



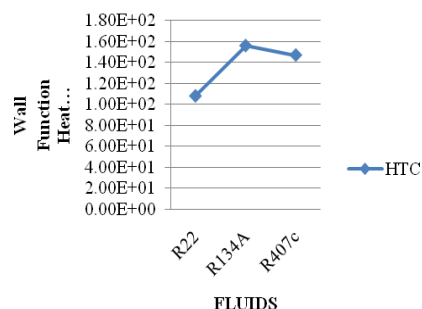
**COMPARISON OF TEMPERATURE VALUES FOR DIFFERENT FLUIDS**



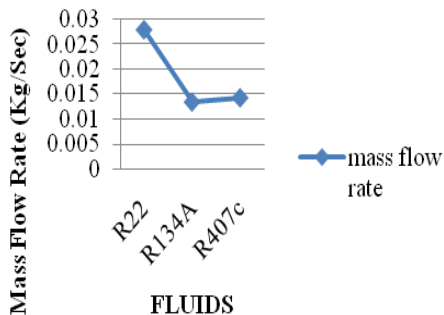
**COMPARISON OF VELOCITY VALUES FOR DIFFERENT FLUIDS**



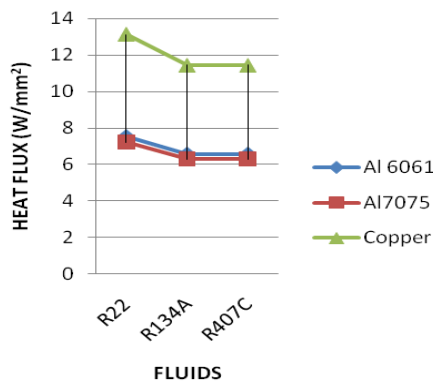
**COMPARISON OF HEAT TRANSFER COEFFICIENT VALUES FOR DIFFERENT FLUIDS**



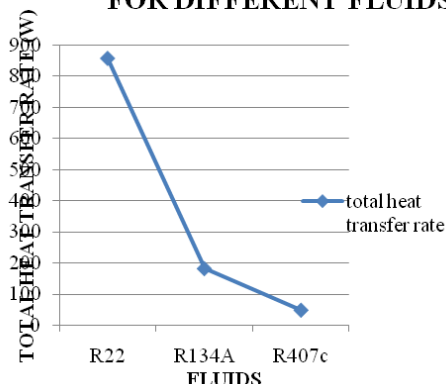
### COMPARISON OF MASS FLOW RATE VALUES FOR DIFFERENT FLUIDS



### COMPARISON OF HEAT FLUX VALUES FOR DIFFERENT FLUIDS AND MATERIALS



### COMPARISON OF HEAT TRANSFER RATE VALUES FOR DIFFERENT FLUIDS



### THERMAL ANALYSIS

Materials	Fluids	Convection (W/m <sup>2</sup> K)	Temperature (°C)	Heat flux (W/mm <sup>2</sup> )
ALUMINIUM 6061	R22	108	303.15	7.5558
	R134a	156	303.15	6.5842
	R407c	147	303.15	6.5831
ALUMINIUM 7075	R22	108	303.15	7.2285
	R134a	156	303.15	6.2986
	R407c	147	303.15	6.2976
COPPER	R22	108	303.15	13.137
	R134a	156	303.15	11.457
	R407c	147	303.15	11.454

### CONCLUSION

In this thesis heat transfer by convection in AC by varying the refrigerants are determined by CFD and thermal analysis. The assessment is out on an

air-cooled tube condenser of a vapour compression cycle for air conditioning system. The materials considered for tubes are Copper and Aluminum alloys 6061 and 7075. The refrigerants varied will be R 22, R 134 and R407C.

CFD analysis is done to determine temperature distribution and heat transfer rates by varying the refrigerants. Heat transfer analysis is done on the condenser to evaluate the better material.

By observing CFD analysis results, the heat transfer coefficient is more when R134A is used and heat transfer rate is more when R22 is used than other fluids. By observing thermal analysis results, the heat flux is more when R22 is used and when material Copper is used. (i.e) The heat transfer rate is more when fluid R134A and material Copper is used.

## REFERENCES

1. Experimental Investigation of Split air Conditioning System by liquid Based Cooling System by Balaji N, Suresh Mohan kumar P
2. EFFICIENT USAGE OF WASTE HEAT FROM AIR CONDITIONER by M. Joseph Stalin, S. Mathana Krishnan, G. Vinoth Kumar
3. Comparitive analysis of an automotive air conditioning systems operating with CO<sub>2</sub> and R134a by J. Steven Brown a, Samuel F. Yana-Motta b, Piotr A. Domanski c
4. Performance Enhancement of Air-cooled Condensers by M. M. Awad , H. M. Mostafa , G. I. Sultan , A. Elbooz
5. S.H. Noie-Baghban, G.R. Majideian, "Waste heat recovery using heat pipe heat Exchanger (HPHE) for surgery rooms in hospitals", Applied Thermal Engineering, Vol. 20, (2000) 1271-1282.
6. P.Sathiamurthi, R.Sudhakaran "Effective utilization of waste heat in air conditioning, Proc. (2003) 13-14.
7. Kumar, V., Prasad, L., Experimental investigation on heat transfer and fluid flow of air flowing under three sides concave dimple roughened duct. International Journal of Mechanical Engineering and Technology (IJMET), Volume 8, Issue 11, November 2017, pp. 1083-1094, Article ID: IJMET\_08\_11\_110.
8. Kumar, V., Prasad, L., Thermal performance investigation of one and three sides concave dimple roughened solar air heaters. International Journal of Mechanical Engineering and Technology (IJMET) Volume 8, Issue 12, December 2017, pp. 31-45, Article ID: IJMET\_08\_12\_004.
9. Kumar, V., Prasad, L., Performance Analysis of three sides concave dimple shape roughened solar air heater, J. sustain. dev. energy water environ. syst., 6(4), pp 631-648, 2018.
10. Kumar, V., Nusselt number and friction factor correlations of three sides concave dimple roughened solar air heater, Renewable Energy 135 (2019) 355-377.
11. Kumar, V., Prasad, L., Experimental analysis of heat transfer and friction for three sides roughened solar air heater, Annales de Chimie - Science des Matériaux, 75-107, ACSM. Volume 41 - n° 1-2/2017.
12. Kumar, V., Prasad, L., Performance prediction of three sides hemispherical dimple roughened solar duct, Instrumentation, Mesure, Métrologie, 273-293 I2M. Volume 17 - n° 2/2018.
13. P. Sathiamurthi, PSS.Srinivasan, design and development of waste heat recovery system for air conditioner, European Journal of Scientific Research ISSN 1450-216X Vol.54 No.1 (2011), Pp.102- 110.
14. N.Balaji, P.Suresh Mohan Kumar, Eco friendly Energy Conservative Single window Air Conditioning System by Liquid Cooling with helical inter cooler ISSN 1450-216X Vol.76 No.3 (2012), pp.455-462
15. S.C.Kaushik, M.Singh. "Feasibility and Refrigeration system with a Canopus heat exchanger", Heat Recovery Systems & CHP, Vol.15 (1995)665 - 673.
16. R.TugrulOgulata, "Utilization of waste-heat recovery in textile drying", Applied

# Thermal performance and analysis of a solar water heating system with heat pipe evacuated tube collector

Md Nizam Raza & Dr. Velmurugan P. & Mr. Vikash Kumar

PG Student, Professor, Assistant Professor

Department of Mechanical Engg. Malla Reddy College of Engineering Maisammaguda, Dhulapally, Kompally, Secunderabad, Telangana-500100, India

**ABSTRACT:** Heat Transfer enhancement used to enhance the heat transfer rate. It is categorized into passive and active methods. Active methods require external power while passive methods do not require any external power to improve the thermohydraulic performance of the system. Passive methods are widely used in both experimental and numerical applications. Passive methods include various components which are located in the fluid flow path such as twisted tapes, coiled wires.

**Keywords:** heat transfer enhancement, coiled wire, thermohydraulic, heat transfer, twisted tape.

## Introduction

Heat transfer enhancement is a process of increasing heat transfer rate and thermohydraulic performance of the system using various methods. Heat transfer enhancement techniques are commonly used in areas such as process industries, heating and cooling in evaporators, refrigerators, radiators, automobiles etc.

Heat transfer enhancement methods are classified into three categories which include active method, passive method, and compound method. Active methods require external power to input the process while passive methods don't require any external power. Two or more active and passive methods can be combined together that is called compound method which is used to produce a higher enhancement.

## Active Techniques

Active techniques are used to enhance the heat transfer rate by using an external power source to adjust the flow field so as to obtain an improvement in thermal efficiency. Providing an external power in most applications is not easy for this reason the use of active techniques is limited.

## Passive techniques

Passive techniques do not require any external power; rather the geometry or surface of the flow channel is modified to increase the thermohydraulic performance of the systems. The inserts, ribs, and rough surface are utilized to promote fluid mixing and turbulence flow, which results in an increment of the overall heat transfer rate.

## Compound technique

A compound technique consists of the combination of more than one heat transfer enhancement method to increase the thermohydraulic performance of heat exchangers. It can be employed simultaneously to generate an augmentation that promotes the performance of the system either of the techniques operating independently.

## Passive technique

### Rough surface

They may be either integral to the base surface or made by placing a roughness adjacent to the surface.

Integral roughness is formed by machining or restructuring the surface. For single phase flow the configuration is generally chosen to promote mixing in the boundary layer near the surface, rather than to increase the heat transfer surface area.

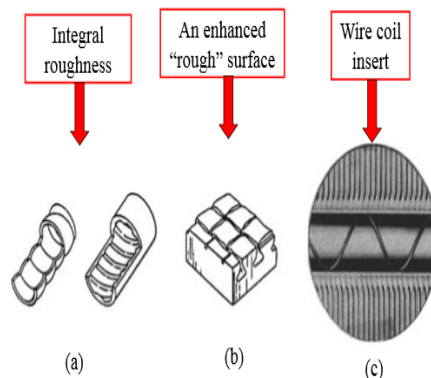


Fig. 1.2 (a) Tube-side roughness for single-phase or two-phase flow, (b) "rough" surface for nucleate boiling, (c) wire-coil insert.

**Extended Surfaces**

They are routinely employed in many heat exchangers.

Thermal resistance may be reduced by increasing the heat transfer coefficient or the surface area of both heat transfer coefficient and surface area. Use of plain fin may provide only area increase. However, formation of a special shape extended surface may also provide increased h.

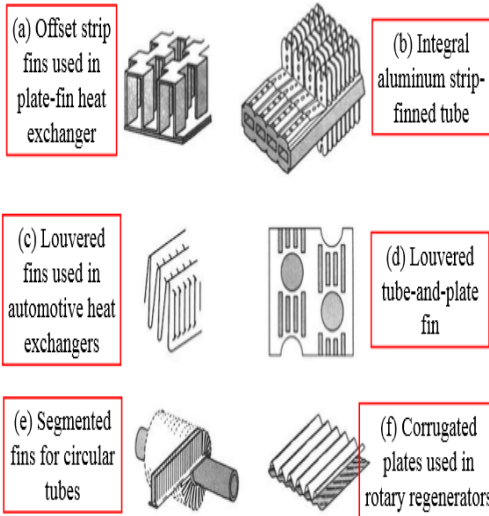
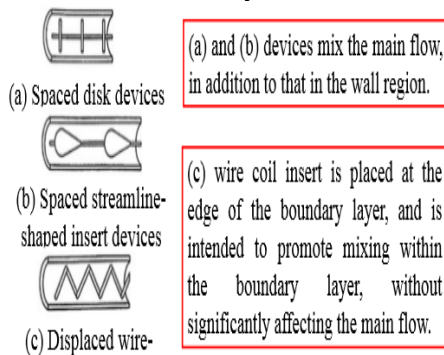


Fig. 1.2 Enhanced surfaces for gases

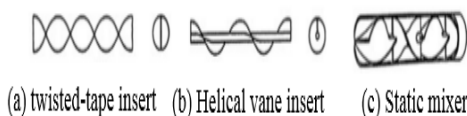
**Displaced inserts**

Displaced insert devices are devices inserted into the flow channel to improve energy transport at the heated surface indirectly.



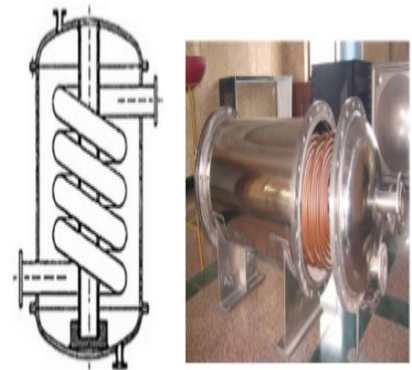
**Swirl flow device**

Swirl flow device include number of geometrical arrangements or tube inserts for forced flow that create rotating or secondary flow.



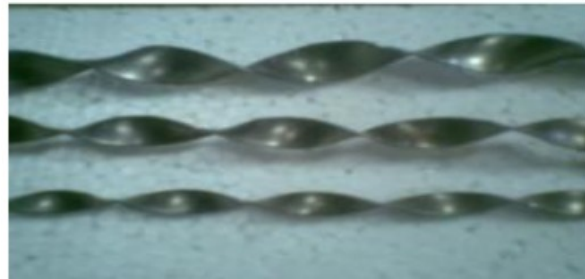
**Coiled tubes**

They may provide more compact heat exchangers secondary flow in the coiled tube produces higher single phase coefficients and improvement in most boiling regimes.



**Twisted tapes**

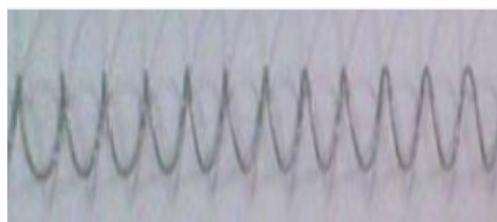
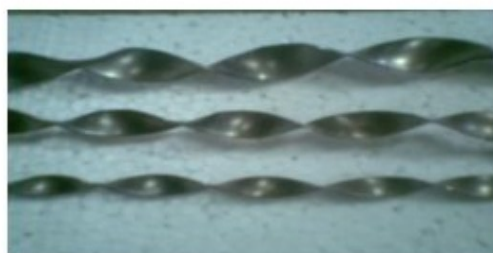
Twisted tapes are the metallic strips twisted using some of the suitable techniques as per the required shape and dimension, which are inserted in the flow to enhance the heat transfer. The twisted tape inserts are most suitable and widely used in heat exchangers to enhance the heat transfer.



Twisted tape inserts increase heat transfer rates with less friction factor. The use of twisted tapes in a tube gives simple passive technique for enhancing the convective heat transfer by making swirl into the heavy flow which disrupting the boundary layer at the tube surface due to rapidly changes in the surface geometry. Which means to say that such type of tapes induce turbulence and swirl flow which induces inside the boundary layer and which gives better results of heat transfer coefficient and Nusselt number due to the changes in geometry of twisted tape inserts. Simultaneously, the pressure drop inside the tube will be increases when using twisted-tape as an insert. For this a many researchers have been done by experimentally and numerically to investigate the desired design to achieve the better thermal performance with less frictional losses. The heat transfer enhancement of twisted tapes inserts depends on the Pitch and Twist ratio.

### Experimental Section

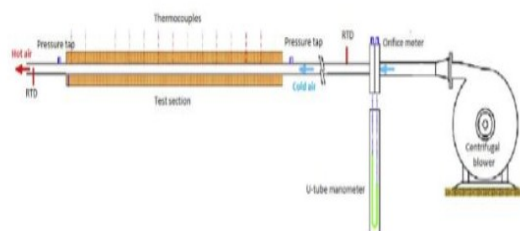
The twisted tapes are made of mild steel and have tape width ( $w$ ) of 10 mm, 15 mm & 20mm. Tape thickness ( $d$ ) of 0.8 mm, and tape length ( $l$ ) of 900 mm. Also a wire coil having pitch of 30 mm is used to generate co-swirl. All tapes were prepared with different twist ratios,  $y/w = 3.5, 2.66$  and  $2.25$  respectively where twist ratio is defined as twist length ( $l$ ) to tape width ( $w$ ). Schematic view of twisted tape & wire coil is shown in Fig. On the other hand, to avoid an additional friction in the system that might be caused the thicker tape. To produce the twisted tape, one end of a straight tape was clamped while another end was carefully twisted to ensure a desired twist length. As shown in Fig these twisted tapes are fixed one by one inside the pipe having wire coil to generate co-swirl



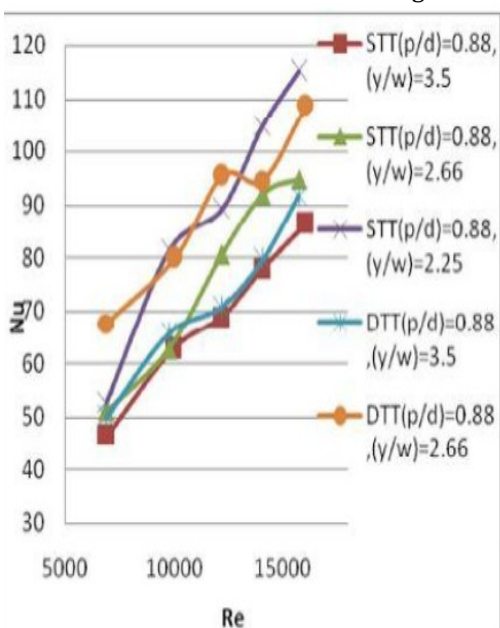
The test section is surrounded by nichrome heating wire, which is wrapped around the test section with a pitch distance of 5 mm. This pitch is good enough to provide a nearly uniform heating on the outer surface of the test section tube. The heating wire was powered by a variable AC power supply. The overall electrical power added to the heating section,  $Q$ , was calculated by measuring the voltage (0–200 V) and the electrical current (0–2 A). To control the convection losses from the test section and other components, foam insulation and glass wool used. Four thermocouples are to be embedded on the test section to measure surface temperature of pipe and two thermocouples are placed in air stream at entrance and exist of test section to measure air temperature. To avoid floating voltage effects, the thermocouple bead is insulated from the electrically heated tube wall surface with a very

thin sheet of mica between the thermocouple and the tube surface so as not to be effected from electricity.

Fig shows the schematic view of experimental set-up.



Experimental results show that the Nusselt number (therefore, the heat transfer coefficient) increases with increasing Reynolds number for the conventional turbulent tube flow. This is the most likely caused by a stronger turbulence and better contact between fluid and heating.



The variations of Nusselt number with Reynolds number for three different twist ratios ( $y/w = 3.5, 2.66, 2.25$ ) with wire coil of pitch ratio ( $p/d = 0.88$ ) shown in figure 6.1. Nusselt number increases with the decrease of twist ratio and the increase of Reynolds number. The highest Nusselt number is achieved for twist ratio ( $y/w = 2.25$ ) and pitch ratio ( $p/d = 0.88$ ).

### Conclusions:

We know the heat transfer enhancement can be done by using treated surfaces, using inserts, using extended surfaces which are the most important passive methods to enhance the heat transfer

The twisted tape inserts are most suitable and widely used in heat exchanger to enhance the heat transfer. Twisted tape inserts increases heat transfer rate with less friction factor. The coiled circular wire should be applied instead of smooth one to obtain higher heat transfer.

### References

1. Prabhakar Ray, Dr. Pradeep Kumar Jhinge, "A review paper on heat transfer rate enhancement by wire coil inserts in the tube", International journal of engineering sciences & research technology (2014), Vol.3(6) pp. 238-243.
2. G. D.Gosavi , S.V.Prayagi and V.S.Narnaware, "Use of perforated fins as a natural convection heat transfer-A Review", International Journal Of Core Engineering & Management (2014),
3. Allan Harry Richard.T.L, Agilan.H, "Experimental Analysis of Heat Transfer Enhancement Using Fins in Pin Fin Apparatus (2015), Vol. 2.
4. Kumar, V., Prasad, L., Experimental investigation on heat transfer and fluid flow of air flowing under three sides concave dimple roughened duct. International Journal of Mechanical Engineering and Technology (IJMET), Volume 8, Issue 11, November 2017, pp. 1083-1094, Article ID: IJMET\_08\_11\_110.
5. Kumar, V., Prasad, L., Thermal performance investigation of one and three sides concave dimple roughened solar air heaters. International Journal of Mechanical Engineering and Technology (IJMET) Volume 8, Issue 12, December 2017, pp. 31-45, Article ID: IJMET\_08\_12\_004.
6. Kumar, V., Prasad, L., Performance Analysis of three sides concave dimple shape roughened solar air heater, J. sustain. dev. energy water environ. syst., 6(4), pp 631-648, 2018.
7. Kumar, V., Nusselt number and friction factor correlations of three sides concave dimple roughened solar air heater, Renewable Energy 135 (2019) 355-377.
8. Kumar, V., Prasad, L., Experimental analysis of heat transfer and friction for three sides roughened solar air heater, Annales de Chimie - Science des Matériaux, 75-107, ACSM. Volume 41 - n° 1-2/2017.
9. Kumar, V., Prasad, L., Performance prediction of three sides hemispherical dimple roughened solar duct, Instrumentation, Mesure, Métrologie, 273-293 I2M. Volume 17 - n° 2/2018.
10. N. C. Kanojiya, V. M. Kriplani, P. V. Walke, "Heat Transfer Enhancement in Heat Exchangers With Inserts: A Review", International Journal of Engineering Research & Technology (2014), Vol. 3
11. Nikhil S Shrikhande, V. M. Kriplani, "Heat Transfer Enhancement in Automobile Radiator using Nanofluids: A Review", International Journal of Engineering Research & Technology (2014), Vol. 3

# ANALYSIS OF HEAT TRANSFER RATE BY VARYING COOLING FLUID FOR ENGINE CYLINDER FINS

Mr.RANJITH AAVULA & Mr.VIKASH KUMAR

M-Tech Student , Professor

Department of Mechanical Engg. Malla Reddy College of Engineering Maisammaguda, Medchal dist.TS

**ABSTRACT:** *The Engine cylinder is one of the major automobile components, which is subjected to high temperature variations and thermal stresses. In order to cool the cylinder, fins are provided on the cylinder to increase the rate of heat transfer. By doing thermal analysis on the engine cylinder fins, it is helpful to know the heat dissipation inside the cylinder.*

*The principle implemented in this project is to increase the heat dissipation rate by using the invisible working fluid, nothing but air. We know that, by increasing the surface area we can increase the heat dissipation rate, so designing such a large complex engine is very difficult. The main purpose of using these cooling fins is to cool the engine cylinder by air.*

*The main aim of the project is to analyze the thermal properties by varying cooling fluid, material and thickness of cylinder fins.*

*Parametric models of cylinder with fins have been developed to predict the thermal behavior. The models are created by the geometry, rectangular and also by varying thickness of the fins for both geometries. Cooling fluids used in this thesis is air, oil. The 3D modeling software used is Pro/Engineer.*

*Thermal analysis is done on the cylinder fins to determine variation in temperature distribution. The analysis is done using ANSYS. Transient thermal analysis determines temperatures and other thermal quantities that vary over time.*

**Keywords:** FINS, CYINDER, AIR, LIQUID-OIL, TEMPARATURE, CFD MODELINS,ANSYS

## Introduction:

Internal combustion engine cooling uses either air or a liquid to remove the waste heat from an internal combustion engine. For small or special purpose engines, air cooling makes for a lightweight and relatively simple system. The more complex circulating liquid-cooled engines also ultimately reject waste heat to the air, but circulating liquid improves heat transfer from internal parts of the engine. Engines for watercraft may use open-loop cooling, but air and surface vehicles must recirculate a fixed volume of liquid.

The main aim of the project is to design cylinder with fins for a 150cc engine, by changing the thickness of the fins, changing the cooling fluid and to analyze the transient thermal properties of the fins. Analyzation is also done by varying the materials of fins. Present used material for cylinder fin body is Aluminum alloy 204 which has thermal conductivity of 110 – 150 w/mk.

Our aim is to change the material for fin body by analyzing the fin body with other materials and also by changing the thickness.

Geometry of fins – Rectangular Thickness of fin – 3mm ,2.5mm

Materials – Aluminum Alloy A204,Al- 6061

Cooling Fluid – Air, Oil

## STEPS INVOLVED IN THE PROJECT:

1. MODELING
2. THEORETICAL CALCULATIONS
3. TRANSIENT THERMAL ANALYSIS

## BASIC PRICIPLE:

Most internal combustion engines are fluid cooled using either air (a gaseous fluid) or a liquid coolant run through a heat exchanger (radiator) cooled by air. Marine engines and some stationary engines have ready access to a large volume of water at a suitable temperature. The water may be used directly to cool the engine, but often has sediment, which can clog coolant passages, or chemicals, such as salt, that can chemically damage the engine. Thus, engine coolant may be run through a heat exchanger that is cooled by the body of water.

Most liquid-cooled engines use a mixture of water and chemicals such as antifreeze and rust inhibitors. The industry term for the antifreeze mixture is *engine coolant*. Some antifreezes use no water at all, instead using a liquid with different properties, such as propylene glycol or a combination of propylene glycol and ethylene glycol. Most "air-cooled" engines use some liquid oil cooling, to maintain acceptable temperatures

for both critical engine parts and the oil itself. Most "liquid-cooled" engines use some air cooling, with the intake stroke of air cooling the combustion chamber. An exception is Wankel engines, where some parts of the combustion chamber are never cooled by intake, requiring extra effort for successful operation.

**Air-cooling**

Cars and trucks using direct air cooling (without an intermediate liquid) were built over a long period from the very beginning and ending with a small and generally unrecognized technical change.

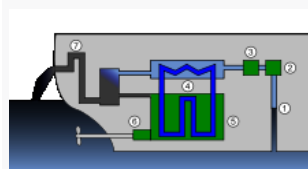
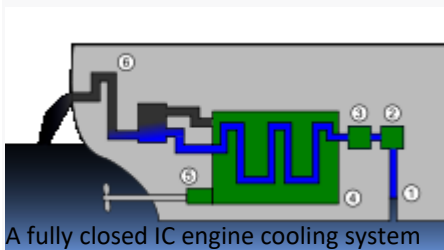
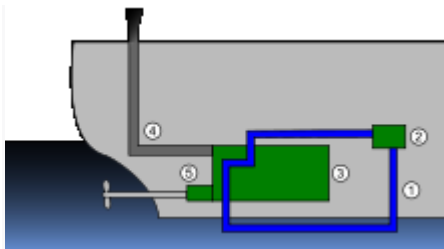
For many years air cooling was favored for military applications as liquid cooling systems are more vulnerable to damage by shrapnel.

Air-cooled engines have may be an advantage from a thermodynamic point of view due to higher operating temperature. The worst problem met in air-cooled aircraft engines was the so-called "Shock cooling".

**Liquid cooling**

*Main article: Radiator (engine cooling)*

Today, most automotive and larger IC engines are liquid-cooled.



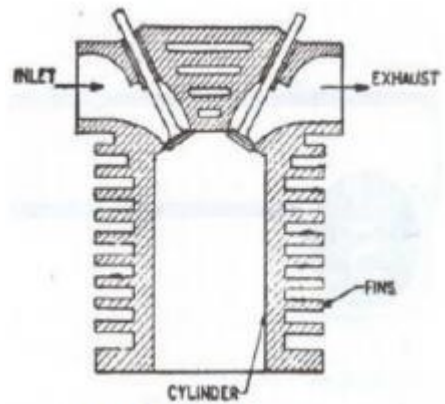
Semiclosed IC engine cooling system

Liquid cooling is also employed in maritime vehicles (vessels). For vessels, the seawater itself is mostly used for cooling. In some cases, chemical coolants are also employed (in closed systems) or they are mixed with seawater cooling.

**Natural Air Cooling:**

In normal cause, larger parts of an engine remain exposed to the atmospheric air. When the vehicles run, the air at certain relative velocity impinges upon the engine, and sweeps away its heat. The heat carried-away by the air is due to natural convection, therefore this method is known as natural air-cooling. Engines mounted on 2-wheelers are mostly cooled by natural air.

As the heat dissipation is a function of frontal cross-sectional area of the engine, therefore there exists a need to enlarge this area. An engine with enlarge area will becomes bulky and in turn will also reduce the power by weight ratio. Hence, as an alternative arrangement, fins are constructed to enhance the frontal cross-sectional area of the engine. Fins (or ribs) are sharp projections provided on the surfaces of cylinder block and cylinder head. They increase the outer contact area between a cylinder and the air. Fins are, generally, casted integrally with the cylinder. They may also be mounted on the cylinder.



Natural air cooling

**Fins:**

A fin is a surface that extends from an object to increase the rate of heat transfer to or from the environment by increasing convection. The amount of conduction, convection, radiation of an object determines the amount of heat it transfers. Increasing the temperature difference between the object and the environment, increasing the convection heat transfer coefficient, or increasing the surface area of the object increases the heat transfer. Sometimes it is not economical or it is not feasible to change the first two options. Adding a fin to the object, however, increases the

surface area and can sometimes be economical solution to heat transfer problems. Circumferential fins around the cylinder of a motor cycle engine and fins attached to condenser tubes of a refrigerator are a few familiar examples.



Fernando Illan simulated the heat transfer from cylinder to air of a two-stroke internal combustion finned engine. The cylinder body, cylinder head (both provided with fins), and piston have been numerically analyzed and optimized in order to minimize engine dimensions. The maximum temperature admissible at the hottest point of the engine has been adopted as the limiting condition. Starting from a zero-dimensional combustion model developed in previous works, the cooling system geometry of a two-stroke air cooled internal combustion engine has been optimized in this paper by reducing the total volume occupied by the engine. A total reduction of 20.15% has been achieved by reducing the total engine diameter  $D$  from 90.62 mm to 75.22 mm and by increasing the total height  $H$  from 125.72 mm to 146.47 mm aspect ratio varies from 1.39 to 1.95. In parallel with the total volume reduction, a slight increase in engine efficiency has been achieved. G. Babu and M. Lavakumar analyzed the thermal properties by varying geometry, material and thickness of cylinder fins.

The models were created by varying the geometry, rectangular, circular and curved shaped fins and also

by varying thickness of the fins. Material used for manufacturing cylinder fin body was aluminum Alloy 204 which has thermal conductivity of 110-150W/mk and also using aluminum alloy 6061 and Magnesium alloy which have higher thermal conductivities. They concluded that by reducing the thickness and also by changing the shape of the fin to curve shaped, the weight of the fin body reduces thereby increasing the efficiency.

After these verifications the effects of parameters such as thickness ratio,  $\alpha$ , dimensionless fin semi thickness,  $\delta$ , length ratio,  $\lambda$ , thermal conductivity

parameter,  $\beta$ , Biot number,  $Bi$ , on the temperature distribution are illustrated and explained.

## LITERATURE SURVEY COOLING SYSTEM OF IC ENGINES

Heat engines generate mechanical power by extracting energy from heat flows, much as a water wheel extracts mechanical power from a flow of mass falling through a distance. Engines are inefficient, so more heat energy enters the engine than comes out as mechanical power; the difference is waste heat which must be removed. Internal combustion engines remove waste heat through cool intake air, hot exhaust gases, and explicit engine cooling.

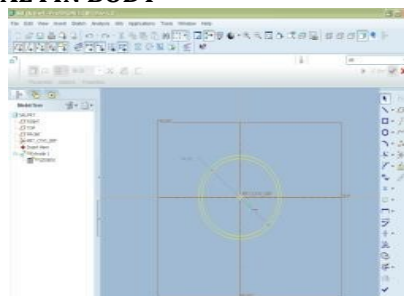
Engines with higher efficiency have more energy leave as mechanical motion and less as waste heat. Some waste heat is essential: it guides heat through the engine, much as a water wheel works only if there is some exit velocity (energy) in the waste water to carry it away and make room for more water. Thus, all heat engines need cooling to operate.

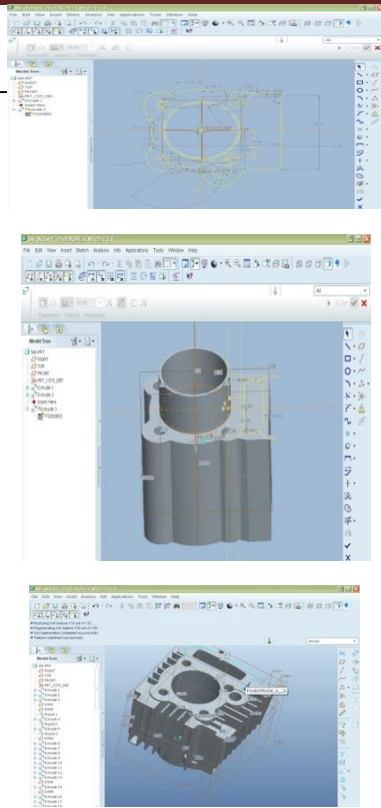
Cooling is also needed because high temperatures damage engine materials and lubricants. Internal-combustion engines burn fuel hotter than the melting temperature of engine materials, and hot enough to set fire to lubricants. Engine cooling removes energy fast enough to keep temperatures low so the engine can survive.

Some high-efficiency engines run without explicit cooling and with only accidental heat loss, a design

called adiabatic. For example, 10,000 mile-per-gallon "cars" for the Shell economy challenge are insulated, both to transfer as much energy as possible from hot gases to mechanical motion, and to reduce reheat losses when restarting. Such engines can achieve high efficiency but compromise power output, duty cycle, engine weight, durability, and emissions.

## MODELS OF CYLINDER FIN BODY ORIGINAL FIN BODY





Thickness  $y=3\text{mm}$   
 $2y=6\text{mm}=0.006\text{m}$

$$m = \sqrt{\frac{hp}{kAc}} = \sqrt{0.266 \times 25}$$

$$kAc = 120 \times 0.00078$$

$$\theta_o = 207.83\text{K}$$

**Heat lost by fin**

$$Q_{\text{fin}} = 132.369\text{W}$$

**Maximum heat transferable by fin when if entire fin at base temperature=862.711**

$$\eta = (Q_{\text{fin}}/Q_{\text{max}}) = (132.36/862.711) \times 100 = 15.3$$

**Effectiveness of fin**

$$\epsilon = 56.56$$

**Effectiveness should be more than 1 THERMAL FLUX CALCULATIONS THICKNESS – 3mm**

Contact area  $A = 1775.62 \text{ mm}^2$  Fin area =  $865.447\text{mm}^2$

Cylinder outside area =  $4436.44\text{mm}^2$

Over all surface area =  $4436.44 + 1775.62 = 6212.06\text{mm}^2$

**Heat flux**

$$\text{Heat flow } q = UA\Delta T$$

$$q/a = 5.9066/6212.06 = 0.0009508 \text{ W/mm}^2$$

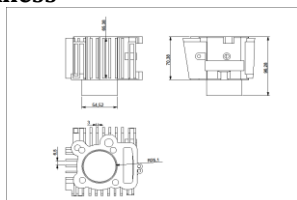
**ALUMINUM ALLOY 6061 – Thickness 2.5mm**

Length of fin  $(L)=130\text{mm}=0.13\text{m}$

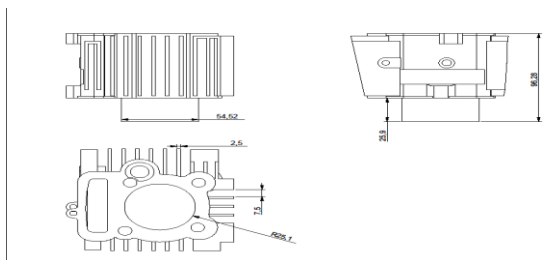
Width of fin  $(b)=130\text{mm}=0.13\text{m}$

Thickness  $y=2.5\text{mm}$

**2D DRAWINGS  
 3mm Thickness**



**mm Thickness**



$$m = \sqrt{\frac{hp}{kAc}} = \sqrt{\frac{0.265 \times 50}{180 \times 0.000325}} = 47.68\text{m}^{-1}$$

$$kAc = 180 \times 0.000325$$

$$\theta_o = 3209.69\text{K}$$

**Heat lost by fin**

$$Q = 8952.64\text{W}$$

**Maximum heat transferable by fin when if entire fin at base temperature**

$$Q_{\text{max}} = 19978.39\text{W}$$

$$\eta = (Q_{\text{fin}}/Q_{\text{max}}) = (8952.64/19978.39) \times 100 = 44.81$$

**Effectiveness of fin**

$$\epsilon = 48$$

**THERMAL FLUX CALCULATIONS  
 THICKNESS-2.5mm**

**Heat flux**

$$\text{Heat flow } q = UA\Delta T$$

$$= 0.001285$$

**COOLING FLUID - OIL**

**ALUMINUM ALLOY 204 – Thickness 3mm**

Length of fin  $(L)=130\text{mm}=0.13\text{m}$  Width of fin

$(b)=130\text{mm}=0.13\text{m}$  Thickness  $y=3\text{mm}$

$$m = \sqrt{\frac{hp}{kAc}} = \sqrt{0.266 \times 50}$$

$$kAc = 120 \times 0.00078 = 11.92 \text{ m}^{-1}$$

$$\theta_o = 273.67\text{K}$$

**Heat lost by fin**

$$Q_{\text{fin}} = 279.65\text{W}$$

**Maximum heat transferable by fin when if entire fin at base temperature**

**CALCULATIONS AND RESULT:  
 HEAT TRANSFER THROUGH FINS  
 COOLING FLUID - AIR**

❖ **ALUMINUM ALLOY 204 – Thickness 3mm**

Length of fin  $(L)=130\text{mm}=0.13\text{m}$

Width of fin  $(b)=130\text{mm}=0.13\text{m}$

$Q_{max}=1135.62W$

$\eta = (Q_{fin}/Q_{max}) = (279.65/1135.62) \times 100 = 24.62$

Effectiveness of fin

$\epsilon = \frac{\text{heat lost with fin}}{\text{heat lost without fin}} = 40$

**Effectiveness should be more than 1**

**ALUMINUM ALLOY 6061 - Thickness 2.5mm**

Length of fin (L)=130mm=0.13m

Width of fin (b)=130mm=0.13m

Thickness y=2.5mm

$m = \sqrt{\frac{hp}{kAc}} = \sqrt{\frac{0.265 \times 50}{180 \times 0.000325}} = 47.68m^{-1}$

$\theta_0 = 3209.69K$

**Heat lost by fin**

$Q = 8952.64W$

**Maximum heat transferable by fin when if entire fin at base temperature**

$Q_{max} = 19978.39W$

$\eta = (Q_{fin}/Q_{max}) = (3209.69/19978.39) \times 100 = 44.81$

**Effectiveness of fin**

$\epsilon = \frac{\text{heat lost with fin}}{\text{heat lost without fin}}$

$\epsilon = \frac{\sqrt{(pk/hA)}}{\sqrt{(2k/hy)}} = \sqrt{\{(2 \times 180)/(50 \times 0.0025)\}} = 48$

**THERMAL FLUX CALCULATIONS**

**THICKNESS - 3mm**

Contact area A = 1775.62 mm<sup>2</sup> Fin area = 865.447mm<sup>2</sup>

Cylinder outside area = 4436.44mm<sup>2</sup>

Over all surface area = 4436.44+1775.62 = 6212.06mm<sup>2</sup>

**Heat flux**

Heat flow  $q = UA\Delta T$

$q/a = 11.813/6212.06 = 0.001901 W/mm^2$

**THICKNESS - 2.5mm**

Contact area A = 1910.85 mm<sup>2</sup> Fin area = 1195.83mm<sup>2</sup>

Cylinder outside area = 4436.44mm<sup>2</sup>

**Heat flux**

Heat flow  $q = UA\Delta T$

$h = q/a = 8.1615/6347.29 = 0.00257 W/mm^2$

**THERMAL ANALYSIS OF FIN BODY**

**COOLING FLUID - AIR**

**ALUMiNUM ALLOY 204 -3mm THICKNESS**

Set Units - /units,si,mm,kg,sec,k

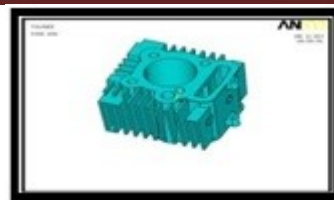
File- change Directory-select working folder File-

Change job name-Enter job name Preferences-Thermal

\preprocessor-Element type-add/edit/delete-

Select Add-Solid 20 node 90

**MODEL IMPORTED FROM PRO/ENGINEER**



Material properties -material Models -Thermal Conductivity -isotropic

**MATERIAL PROPERTIES**

Thermal Conductivity - 120 w/mk Specific Heat - 0.963 J/g °C Density - 2.8 g/cc

**MESHED MODEL**

Select Mesh Tool Icon - Select Smart Size -On Pick All-ok

Select Mesh Tool Window -Select All Areas-pick all

Finite element analysis or FEA representing a real project as a "mesh" a series of small, regularly shaped tetrahedron connected elements, as shown in the above fig. And then setting up and solving huge arrays of simultaneous equations. The finer the mesh, the more accurate the results but more computing power is required

**LOADS**

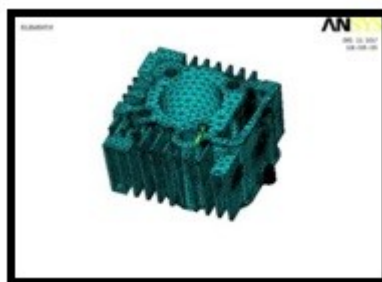
Define Loads -Apply Thermal-Temperature- on Area-Select inside area=5585K

Convections - on Areas (select Remaining areas-Film Co-efficient - 25 W/mmK

Bulk Temperature - 313 K

Solution - Solve - Current LS file - Ok

Select Mesh Tool Window -Select All Areas-pick all



Finite element analysis or FEA representing a real project as a "mesh" a series of small, regularly shaped tetrahedron connected elements, as shown in the above fig. And then setting up and solving huge arrays of simultaneous equations. The finer the mesh, the more accurate the results but more computing power is required

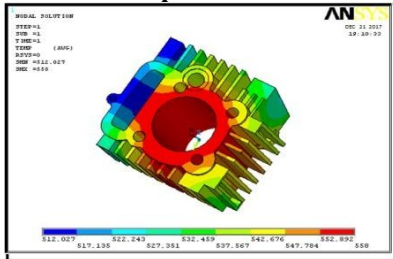
**LOADS**

Define Loads -Apply Thermal-Temperature- on Area-Select inside area=5585K

Convections – on Areas (select Remaining areas-  
 Film Co-efficient – 25 W/mmK  
 Bulk Temperature – 313 K  
 Solution – Solve - Current LS file – Ok

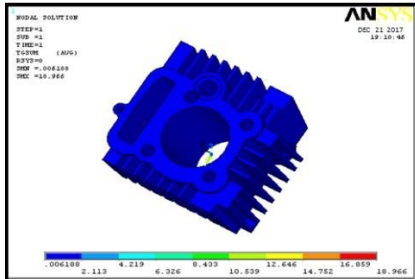
**RESULTS**

**General post processor- contour plot- nodal solution- Nodal Temperature**



According to the contour plot, the temperature distribution maximum temperature at bore because the operating temperature passing inside of the bore. So we applied the temperature inside of the bore and applied the convection to fins. Then the maximum temperature at bore and its distributed to outer surface of the fins.

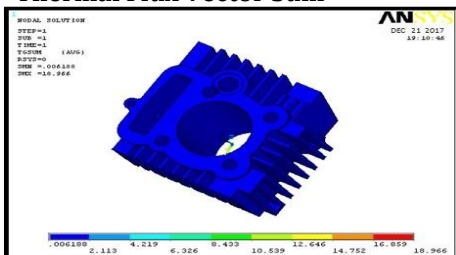
**General post processor- contour plot- Thermal Gradient- Thermal Gradient Vector Sum**



According to the contour plot, the thermal gradient maximum at bore because the operating temperature passing inside of the bore. So we applied the temperature inside of the bore and applied the convection to fins. Then the minimum gradient at fins.

According to the above contour plot, the maximum gradient is 18.966 k/m and minimum gradient is 0.006188 k/m.

**General post processor- contour plot- Thermal Flux – Thermal Flux Vector Sum**



According to the contour plot, the thermal flux maximum at bore because the operating temperature passing inside of the bore. So we applied the temperature inside of the bore and applied the convection to fins. Then the minimum thermal flux at fins.

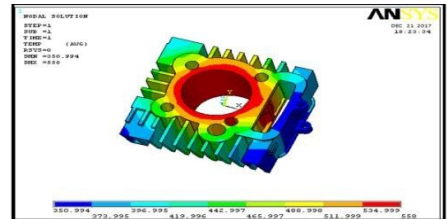
According to the above contour plot, the maximum thermal flux is 18.966 k/m and minimum thermal flux is 0.006188 k/m.

**ALUMINUM ALLOY 6061 – 2.5mm THICKNESS MATERIAL PROPERTIES**

Thermal Conductivity – 180 w/mk  
 Specific Heat – 0.896 J/g °C Density – 2.7 g/cc  
**LOADS**

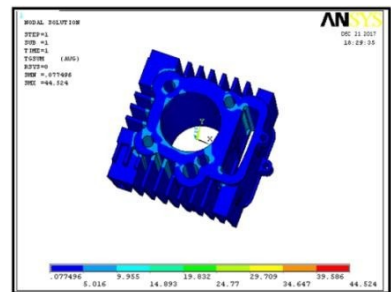
Temperature -558 K  
 Film Coefficient – 50 w/m<sup>2</sup> K Bulk Temperature – 313 K **RESULTS**

**NODAL TEMPERATURE MODEL**



According to the contour plot, the temperature distribution maximum temperature at bore because the operating temperature passing inside of the bore. So we applied the temperature inside of the bore and applied the convection to fins. Then the maximum temperature at bore and its distributed to outer surface of the fins.

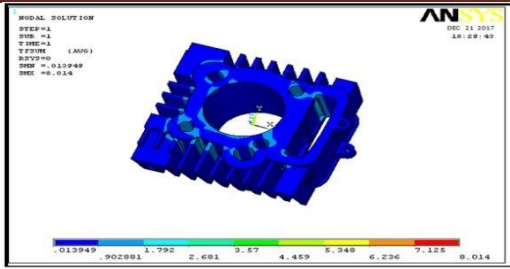
**THERMAL GRADIENT SUM MODEL**



According to the contour plot, the thermal gradient maximum at bore because the operating temperature passing inside of the bore. So we applied the temperature inside of the bore and applied the convection to fins. Then the minimum gradient at fins.

According to the above contour plot, the maximum gradient is 18.966 k/m and minimum gradient is 0.006188 k/m.

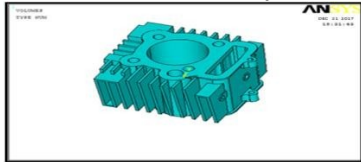
**THERMAL FLUX SUM MODEL**



**THERMAL ANALYSIS OF FIN BODY COOLING FLUID - OIL**

According to the contour plot, the thermal flux maximum at bore because the operating temperature passing inside of the bore. So we applied the temperature inside of the bore and applied the convection to fins. Then the minimum thermal flux at fins. This condition applied all model of Proe

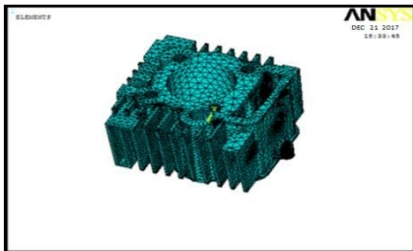
**ALUMINUM ALLOY 204 -3mm THICKNESS MODEL IMPORTED FROM PRO/ENGINEER**



**MATERIAL PROPERTIES**

Thermal Conductivity – 120 w/mk Specific Heat – 0.963 J/g °C Density – 2.8 g/cc

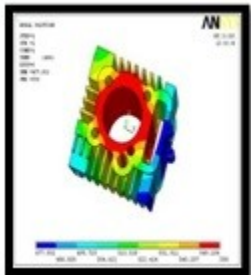
**MESHED MODEL**



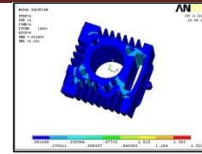
**LOADS**

Temperature -558 K  
 Film Coefficient – 50 w/m<sup>2</sup> K Bulk Temperature – 313 K

**RESULTS**  
 NODAL TEMPERATURE



**THERMAL FLUX SUM MODEL**



maximum thermal flux is 1.522 k/m and minimum thermal flux is 0.001433 k/m.

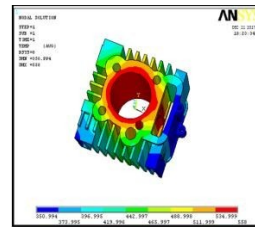
**ALUMINUM ALLOY 6061 – 2.5mm THICKNESS MATERIAL PROPERTIES**

Thermal Conductivity – 180 w/mk  
 Specific Heat – 0.896 J/g °C Density – 2.7 g/cc

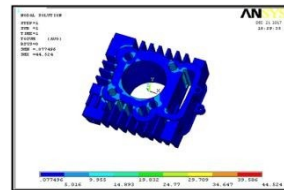
**LOADS**

Temperature -558 K  
 Film Coefficient – 50 w/m<sup>2</sup> K Bulk Temperature – 313 K

**RESULTS**  
 NODAL TEMPERATURE MODEL

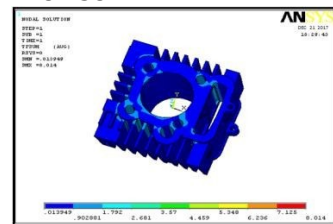


**THERMAL GRADIENT SUM MODEL**



maximum gradient is 44.524 k/m and minimum gradient is 0.077496 k/m.

**THERMAL FLUX SUM**



maximum thermal flux is 8.014 k/m and minimum thermal flux is 0.013949 k/m.

**COOLING FLUID – AIR:**  
**THEORETICAL RESULTS TABLE**

		THICK NESS (mm)	HEA T LOS (W)	EFFECT VENESS	EFFIC ENCY
RECTA NGULA R	AL - 2				
	0	3	132.		
	4		369	56.56	15.35

AL-6061	2.5	135.09	75.89	8.8
---------	-----	--------	-------	-----

**THEORETICAL THERMAL FLUX (W/mm<sup>2</sup>) RESULTS TABLE**

ALLUMINIUM	3mm	2.5mm
OIL	0.001901	0.00257

**THERMAL ANALYSIS RESULTS TABLE**

	Al-204, 3mm	Al-6061, 2.5mm
Nodal Temperature (K)	558	558
Thermal Gradient (K/mm)	18.966	2.694
Thermal Flux (w/mm <sup>2</sup> )	2.276	0.484947

**THEORETICAL THERMAL FLUX (W/mm<sup>2</sup>) RESULTS TABLE**

ALLUMINIUM	3mm	2.5mm
AIR	0.0009508	0.001285

**COOLING FLUID - OIL THEORETICAL RESULTS TABLE**

	THICKNESS (mm)	HEAT LOST (W)	EFFECTIVENESS	EFFICIENCY
RECTANGULAR	3	279.65	40	24.62
	2.5	895.264	48	44.81

**THERMAL ANALYSIS RESULTS TABLE**

	Al-204,3mm	Al-6061,2.5mm
Nodal Temperature (K)	558	558
Thermal Gradient (K/mm)	12.685	44.524
Thermal Flux (w/mm <sup>2</sup> )	1.522	8.014

**CONCLUSION**

In this thesis, a cylinder fin body for a 150cc motorcycle is modeled using parametric software Pro/Engineer. The original model is changed by changing the thickness of the fins. The thickness of the original model is 3mm, it has been reduced to 2.5mm. By reducing the thickness of the fins, the overall weight is reduced Present used material for fin body is Aluminum Alloy 204.. The material for the original model is changed by taking the consideration of their densities and thermal conductivity.

By observing the thermal analysis results, thermal flux is more for Aluminum alloy 6061 and also by reducing the thickness of the fin, the heat transfer rate is increased.

Thermal flux is also calculated theoretically. By observing the results, heat transfer rate is more when the thickness of the fin is 2.5mm.

**FUTURE SCOPE**

The shape of the fin can be modified to improve the heat transfer rate and can be analyzed. The use of Aluminum alloy 6061 as per the manufacturing aspect is to be considered. By changing the thickness of the fin, the total manufacturing cost is extra to prepare the new component.

**REFERENCES**

1. Thermal Engineering by I. Shvets, M. Kondak
2. Kumar, V., Prasad, L., Experimental investigation on heat transfer and fluid flow of air flowing under three sides concave dimple roughened duct. International Journal of Mechanical Engineering and Technology (IJMET), Volume 8, Issue 11, November 2017, pp. 1083-1094, Article ID: IJMET\_08\_11\_110.
3. Kumar, V., Prasad, L., Thermal performance investigation of one and three sides concave dimple roughened solar air heaters. International Journal of Mechanical Engineering and Technology (IJMET) Volume 8, Issue 12, December 2017, pp. 31-45, Article ID: IJMET\_08\_12\_004.
4. Kumar, V., Prasad, L., Performance Analysis of three sides concave dimple shape roughened solar air heater, J. sustain. dev. energy water environ. syst., 6(4), pp 631-648, 2018.

- 
5. Kumar, V., Nusselt number and friction factor correlations of three sides concave dimple roughened solar air heater, *Renewable Energy* 135 (2019) 355-377.
  6. Kumar, V., Prasad, L., Experimental analysis of heat transfer and friction for three sides roughened solar air heater, *Annales de Chimie - Science des Matériaux*, 75-107, ACSM. Volume 41 - n° 1-2/2017.
  7. Kumar, V., Prasad, L., Performance prediction of three sides hemispherical dimple roughened solar duct, *Instrumentation, Mesure, Métrologie*, 273-293 I2M. Volume 17 - n° 2/2018.

## DESIGN AND ANALYSIS OF PRESSURE VESSEL WITH FRP MATERIAL

Sukruthi Priya & P .Ravi Chandra & Mr. V. Ravinder

PG Student, PG Student, Assistant Professor

Department of Mechanical Engg., Malla Reddy College of Engineering Maisammaguda, Dhulapally,  
Kompally, Secunderabad, Telangana-500100, India

**ABSTRACT:** Long life of component is paramount. Today's lot of money is wasted to prevent the component from corrosion. The present project work is aimed at designing pressure vessel using composite material by which it is protected from corrosion and to increase life time.

The present project work aimed at establishing design, analysis and manufacturing process for making pressure vessel with FIBER REINFORCED PLASTIC. Design process consists of implementing FEM for the selection design. Analyzing design is done using CATIA-V5 software.

As the pre component design and development requires use investments in the design of die and break ever number of components to be manufactured is very high. To come out of this problems as to reduce the project cost the advanced FRP based manufacturing technique were adopted to reduce the break ever batch number of components a thorough investigation in the form of pilot project report for the product development.

Present project work is aimed at advanced composite material for the component manufacturing so as to exploit the advantage of failure behavior of FRP for Presents Design and Establishing a Design and Manufacturing Process for the Created Component.

**Keywords:** Pressure vessel, FRP material.

### 1. INTRODUCTION

Composites are able to meet diverse design requirements with significant weight savings as well as "high strength -to-weight ratio" as compared to conventional materials.

Composite material is a material system composed of two or more dissimilar materials, differing in forms and insoluble in each other, physically distinct and chemically inhomogeneous. The resulting product properties are much different from the properties of constituent materials.

Composite are combination of two materials in which one of the materials, called reinforce, is in the form of fiber sheets, or particles, and is embedded in the other materials called matrix. There in forcing material and matrix material ceramic or polymer. Composites are used because overall properties of the composite are superior are used because overall properties of the composite are superior to those of the individual components. For example: polymer ceramic composite have a great modulus than the polymer component, but are not as ceramics.

### 2. LITERATURE REVIEW

#### 2.1 MOISTURE ABSORPTION BEHAVIOR FOR GLASS-FIBER COMPOSITES

Weitzman recently gave a comprehensive review on this subject. In general, the moisture

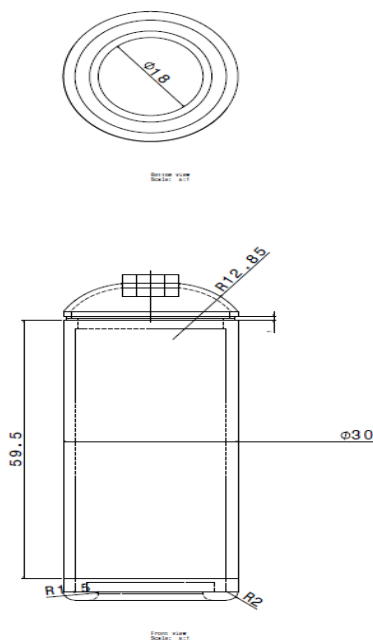
absorption behavior of composite materials can be categorized into several types. Glass fiber reinforced plastic (gfrp) exhibit such behavior under specified conditions. For instance, e-glass/vinyl ester with acryl-silent or epoxy Silone surface treatment follows linear fickian behavior for water absorption up to 80 c .in fact periodic change in the aforementioned environments will results in many such jumps. For example fiber/matrix debones and matrix cracking which is often irreversible? Also an irreversible process causes of leaching out of the material from the bulk following chemical or physical breakdown. Sorption process involving severe circumstances such as elevated temperatures external load and high solvent concentration will often results in behavior. In general the moisture absorption behavior depends on temperature, applied load type of media time and material system and is inseparable from other performance aspects concerning durability.

Moisture absorption will results in development of residual stress plasticizing the resin and accelerate time-dependent behavior .data on visco elastic behavior for pultruded gfrp under the influence of fluid absorption are rare, although there are data on creep-rupture of the material in fluids (i.e., stress corrosion ). As pointed out by some investigators that moisture absorption level in history -dependent, and therefore sorption

behavior under temperature cycles is not the same as under constant humidity and temperature level. However, for pultruded gfrp this kind of data does not exist.

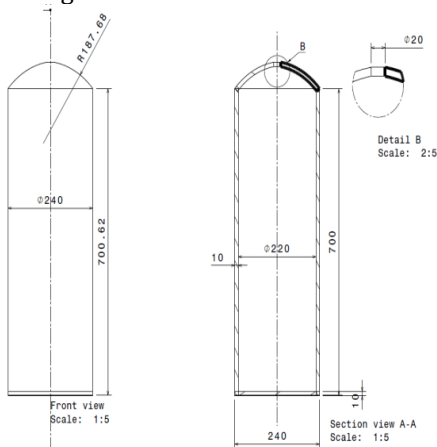
### 3. PROBLEM DESCRIPTION

Proposed design-1:



Design 1 consists of number of grooved profiles. The design was proposed in view of enhancing moment of inertia when comparing to the existing design. But the improving of MOI is sufficient enough as per our expectations. The design 2 has proposed.

Proposed design-2:



Design 2 was better when compared to design1, as the geometrical profile is a almost to a box type cross section. With this considerable

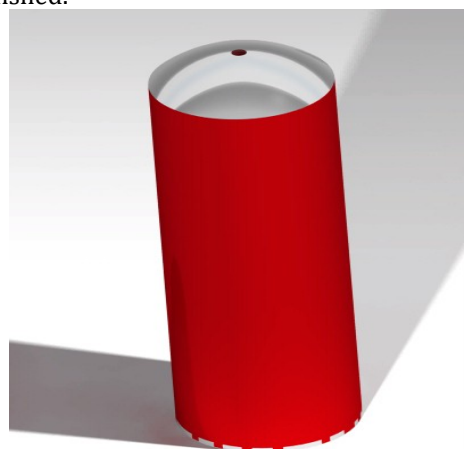
improvement is achieved as per our discussions as we decided to improve the design. Hence design 2 has been selected for fabrication.

### 4. Modelling and Analysis:

Design is a continuous process to better components with improved performance than the existing ones. A new or better component is one which is more economical in all respects such as cost, performances, and aesthetics and so on. The present work also focuses on establishing a manufacturing process suitable for small scale industry in the view of generating new kind of employment. Through consensus the finalized design has been adopted for manufacturing.

In the present work the PVC made oxygen cylinder is studied thoroughly. During this process the design of oxygen cylinder has been studied to FEM analysis making use of ANSYS 13.0 and CATIA-V5 modeling

With simulated loads the stress levels in the structure very high when compare to the yield strength of the component which leads to the failure of the component. The test results were published.



Isometric view of oxygen cylinder

### 5. RESULTS

From the FEM analysis and basic stiffness calculation it is clearly evident from the results that flexural rigidity of the polymer glass reinforced construction with foam core has 51 times greater than compared to PVC Even though the cost of the component is slightly higher than the break even number of components is to produced is very very low, which is the important concern in this project and apart for that the paramount objective to prevent the oxygen cylinder from corrosion.

As the stiffness of the component is 29 times greater than the exiting oxygen cylinder made by

steel. Capacity of FRP oxygen cylinder is comparatively high when compare with the oxygen cylinder manufactured with steel.

Form Break ever analysis it is clearly evident that the large sized batch production is required in case of steel made pressure vessel. The size of the break ever batch number with FRP sandwich construction made it comparable for small scale production. Basic objective of this project is generating a new market with new type of employment opportunities and also to achieve flexibility in design i.e.as per the customer requirements design can be changed design can be introduced very easily and the Break ever size very low.

The product cost is comparatively low and quality of the component is 50 times in view of stiffness is considered As the scope of a product has constraints towards the duration project time the impact energy calculations were not performed definitely the internal energy with stand will be high as the pressure vessel roll is to protect content from the outer atmosphere.

## 6. CONCLUSION

For further improvement, in case strength is to be increased glass epoxy or carbon epoxy and kevel or epoxy based fibers can be utilized for further enhancement and built in color can be achieved by mold design.

## REFERENCES

- 1) An Introduction to Composites Materials by Hull, D. and T.W.Clyne at Cambridge University
- 2) Ashby M.F (1989) on the Engineering design properties of GPS,British plastics federation, London.
- 3) Dingle,M.F.(1987) aligned discontinuous carbon fiber composites.
- 4) ALLEN, H.G., Analysis and Design of Structural Sandwich Panels,Pregamon
- 5) Chawal K (1987) Composite material-science and engineering, Material research and Engineering series by Springer Verlag
- 6) HOLISTER, G.S. & THOMAS, C,F., Fiber Reinforced Materials, Elsevier(1966)
- 7) PLANTEMA, F.J., Sandwich Construction.
- 8) Stanley L. E., S.S. Gharpure, and D. O. Adams (2000). MechanicalProperty Evaluation of Sandwich Panels. International SAMPESymposium and Exhibition, 45(2): 1650-1661.
- 9) Harrington, Ron; Hock Kathy(1991). Flexible Polyurethane Forms, Mildland: The Dow Chemical Company.
- 10) Kumar, V., Prasad, L., Experimental investigation on heat transfer and fluid flow of air flowing under three sides concave dimple roughened duct. International Journal of Mechanical Engineering and Technology (IJMET), Volume 8, Issue 11, November 2017, pp. 1083-1094, Article ID: IJMET\_08\_11\_110.
- 11) Kumar, V., Prasad, L., Thermal performance investigation of one and three sides concave dimple roughened solar air heaters. International Journal of Mechanical Engineering and Technology (IJMET) Volume 8, Issue 12, December 2017, pp. 31-45, Article ID: IJMET\_08\_12\_004.
- 12) Kumar, V., Prasad, L., Performance Analysis of three sides concave dimple shape roughened solar air heater, J. sustain. dev. energy water environ. syst., 6(4), pp 631-648, 2018.
- 13) Kumar, V., Nusselt number and friction factor correlations of three sides concave dimple roughened solar air heater, Renewable Energy 135 (2019) 355-377.
- 14) Kumar, V., Prasad, L., Experimental analysis of heat transfer and friction for three sides roughened solar air heater, Annales de Chimie - Science des Matériaux, 75-107, ACSM. Volume 41 - n° 1-2/2017.
- 15) Kumar, V., Prasad, L., Performance prediction of three sides hemispherical dimple roughened solar duct, Instrumentation, Mesure, Métrologie, 273-293 I2M. Volume 17 - n° 2/2018.

## DESIGN AND CFD ANALYSIS OF HAIR PIN HEAT EXCHANGER AT DIFFERENT NANO FLUIDS

M.Renuka & Dr. Velmurugan P. & Mr. Vikash Kumar

PG Student, Professor, Assistant Professor

Department of Mechanical Engg., Malla Reddy College of Engineering Maisammaguda, Dhulapally, Kompally, Secunderabad, Telangana-500100, India

**ABSTRACT:** Heat exchanger is a device used to transfer heat between one or more fluids. The fluids may be separated by a solid wall to prevent mixing or they may be in direct contact.

In this work, glycerin 40% fluid is mixed with base fluid water(60%) are calculated for their combination properties. The nano fluid is titanium carbide, magnesium Oxide and silver nano particle for weight percentage 0.2%, 0.5%, 0.7% & 1.0%. Theoretical calculations are done determine the properties for nano fluids and those properties are used as inputs for analysis. Hairpin Exchangers are available in single tube (Double Pipe) or multiple tubes within a hairpin shell (Multitude), bare tubes, finned tubes, U-tubes, straight tubes (with rod-thru capability), fixed tube sheets and removable bundle.

3D model of the hair pin heat exchanger is done in CREO parametric software. CFD analysis is done on the hair pin heat exchanger with TiC, MgO & silver nano particle at different weight percentage 0.2%, 0.5%, 0.7% & 1.0%.

**Keywords:** Heat Exchangers , Nano Fluids , CFD , Baffles.

### INTRODUCTION

Heat exchangers are one of the mostly used equipment in the process industries. Heat Exchangers are used to transfer heat between two process streams. One can realize their usage that any process which involve cooling, heating, condensation, boiling or evaporation will require a heat exchanger for these purpose. Process fluids, usually are heated or cooled before the process or undergo a phase change. Different heat exchangers are named according to their application. For example, heat exchangers being used to condense are known as condensers, similarly heat exchanger for boiling purposes are called boilers. Performance and efficiency of heat exchangers are measured through the amount of heat transfer using least area of heat transfer and pressure drop. A better presentation of its efficiency is done by calculating over all heat transfer coefficient. Pressure drop and area required for a certain amount of heat transfer, provides an insight about the capital cost and power requirements (Running cost) of a heat exchanger.

### TUBULAR HEAT EXCHANGERS

A tubular heat exchanger can either consist of a smaller-diameter tube mounted inside a larger diameter tube ("double-pipe exchanger", see Figure 1) or, more commonly, a tube bundle inside a shell ("shell-and-tube exchanger", see Figure 1.1). Thus, heat transfer surfaces are plain or

enhanced tubes. Additionally, shell-and-tube heat exchangers can contain multiple pass tube bundles, i.e., for double-pass we have a bundle of U-tubes, for triple-pass the tubes in the bundle bend twice, etc. Multiple-pass shells are common as well. Baffles, either segmental or doughnut and disc ones, present in the shell direct fluid flow in shell-side, support the tubes, and limit possible tube vibrations.



Figure 1: Countercurrent double-pipe heat exchanger

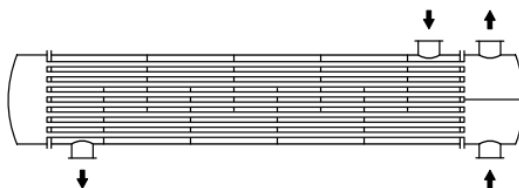


Figure 1.1: Segmentally baffled one-pass shell and two-pass tube shell-and-tube heat exchanger

Flow in shell-side can be improved by suitable adjustments of baffle design as is done in helixchangers (Král et al., 1996) – see Figure 1.2.

Such an arrangement also increases the heat transfer rate vs. pressure drop ratio, reduces leakages (baffle bypass effect), flow-induced vibrations, and limits creation of stagnation zones thus decreasing fouling rate (CB&I Lummus Technology, 2012).

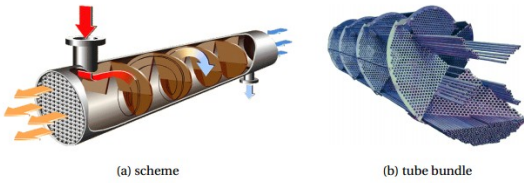


Figure .2. shell-and-tube heat exchanger with helical baffles.

The Helix exchanger: shell-and-tube heat exchanger with helical baffles (CB&I Lummus Technology, 2012, reprinted with permission). Another sub-type of shell-and-tube heat exchangers is the lamella exchanger employing hollow lamellae instead of tubes while no baffle plates are present. This, combined with pure countercurrent and highly turbulent flow, guarantees a high heat transfer rate and low pressure drop (Hewitt et al., 1994, Sec. 4.2.5). It is obvious that a smaller tube diameter will yield higher heat transfer surface area. The lower limit on tube outer diameter, however, is around 20 mm to ensure cleaning can be performed (Hewitt et al., 1994, Sec. 6.2.3). Considering shell-side, the minimum recommended tube pitch is approximately 1.25 times the tube diameter (Hewitt et al., 1994, Sec. 6.2.5). As for thermal expansion, it can be dealt with by using a U-tube bundle, a toroidal expansion joint on the shell, or a floating head. Generally, pure countercurrent flow arrangement is preferred (Hewitt et al., 1994, sec. 3.7). If necessary, heat transfer can be intensified by using twisted tubes (see Figure 2.5), twisted tube inserts, enhanced tube surfaces, etc. Of course, such enhancements should be avoided when fouling is a real possibility. Figure 1.3. Twisted tube

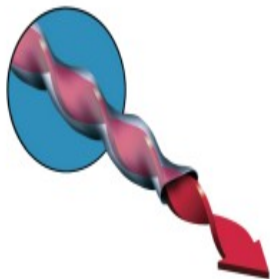


Figure 3. Twisted tube

The above figure (1.3) Twisted tube (Koch Heat Transfer Company, LP, 2012, reprinted with permission); this design is reported to improve shell-side distribution and increase tube-side heat transfer coefficient by 40 % compared to plain tubes.

The advantages of tubular exchangers are the ease of manufacturing and maintenance and the possibility of using tube enhancements. As for disadvantages, these units provide relatively small heat transfer surface area per unit volume.

**Plate Heat Exchangers**

In plate heat exchangers fluids flow alternately between stacked plain or cross-corrugated. Plates that can be sealed and held together in two different ways. Either gasket are placed near the plate edges as shown in Figure 1.2.1 and the stack is held together by a frame or the plates are brazed or welded thus forming a single element. Spiral heat exchangers (see

Figure 1.4) being fundamentally identical, generally contain only two coiled plates.

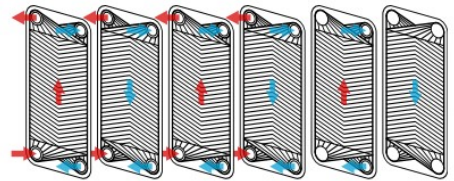


Figure 4: Gasket plates

Flow directions of hot and cold fluids are marked by arrows and gaskets by a thick line (the two rightmost plates are end plates – one for the hot fluid and one for the cold fluid)

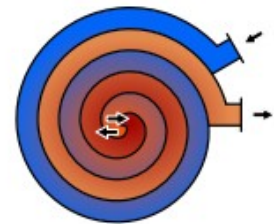


Figure 5 :Cross-section of a spiral heat exchanger

Hot stream inlet and cold stream outlet are near the exchanger axis while cold stream inlet and hot stream outlet are on the outer wall, With plate exchangers we are able to reach very high compactness, that is, a very large Heat transfer area with a small exchanger footprint. Also, heat transfer tends to be more efficient than in shell-and-tube exchangers due to more complex flow passage geometry leading to higher degree of turbulence (Hewitt et al., 1994, Sec. 7.2.1). Since flow arrangement of these heat exchangers can be

considered to be almost pure countercurrent, with a certain Temperature difference we get higher heat duty than for a shell-and-tube exchanger under Equivalent conditions. Alternatively, to get the same heat duty as in case of a shell-and-tube Exchanger a lower temperature difference is necessary.

The gasket plate-and-frame variant is easy to clean and highly scalable – we can easily append additional plates or remove some of the existing ones. These advantages, however, come with the cost of restricted pressure and temperature ranges. Furthermore, we are limited by gasket/fluid compatibility since otherwise the gaskets may deteriorate. Of course, should the plates be brazed or welded together then we get a compact high-pressure and high-temperature heat exchanger capable of working with almost any fluid, but without the added benefits of scalability and easy cleaning. If only one of the fluids is incompatible with the gasket material, partially welded plate exchangers provide a reasonable trade-off between scalability and usability. Here, welded pairs of plates are stacked and sealed with gaskets. The aggressive fluid then flows through the welded pairs while the other, less aggressive fluid flows through gasketed channels. Should both fluids be aggressive, special materials such as graphite, ceramics, or polymers can be employed, but then the pressure and temperature limitations apply again.

Plate-and-shell heat exchangers, consisting of a stack of welded circular cross-corrugated plates fitted into a shell, originate in the concept of a shell-and-tube heat exchanger applied to plate-type exchangers. One of the streams then flows inside the welded plate pairs and the other between these pairs while being directed by shell baffles. Similarly as in case of welded plate heat exchangers, high-pressure and high-temperature streams can be treated in these units. What is more, thermal cycling is not an issue here due to thermal expansion of the plate pack being possible inside the shell. In another but similar type of welded compact heat exchangers, a single plate pack consisting of many large plates welded together is placed into a cylindrical shell.

Plate-fin heat exchangers are built by stacking fins separated by partition plates. Commonly, fins are made of aluminum, steel, or titanium and are plain, serrated perforated array The stack is then welded or brazed together at the edges thus making the exchangers capable of withstanding significant pressures and temperatures.

As for extreme operating conditions (up to 65 MPa and 900 °C; Heatric Ltd., 2012), printed circuit

heat exchangers can be employed. These consist of diffusion-bonded plates with semi-circular flow passages usually between 0.7 and 3.0 mm deep being etched into them (Heatric Ltd., 2012). In this case, various combinations of countercurrent and cross-flow arrangements can be obtained.

Fouling is a serious issue in all the above heat exchangers due to small plate spacing or cross-sectional areas of the flow passages. This must be considered especially if the exchanger cannot be dismantled for cleaning. Other disadvantages of plate-type heat exchangers are the possibility of leakages between plates and relatively high pressure drop (Hewitt et al., 1994, Sec. 8.3.5).

#### **Air-Cooled Heat Exchangers**

Air-cooled heat exchangers, commonly employed e.g. for condensing vapours, have several major advantages. They are cheap and very simple, thus little maintenance is necessary. No intricate piping or pumping system is required and, in most cases, fouling or corrosion do not occur at a significant rate (Hewitt et al., 1994, Sec. 9.2.1). On the other hand, there are disadvantages that must be considered, namely heat transfer coefficient being relatively low and hence these exchangers tend to be larger (Hewitt et al., 1994, Sec. 9.2.2). We must also bear in mind that embedded fans may be noisy and that temperature difference available for cooling may be lower in some locations due to warmer climate.

Figure shows two common arrangements of these exchangers – forced draft and induced draft. In both cases, air passes over tubes in a tube bundle in which cooled fluid is flowing. These arrangements can be either horizontal as shown in the figure, vertical, or inclined. Additionally, tubes may be finned to enhance air-side heat transfer. With induced draft we obtain a more uniform air distribution while with forced draft less electrical power is required by the fan (cooler air has lower density; Hewitt et al., 1994, Sec. 9.3.1.1). If there is no fan then the exchanger works with natural draft – a cooling tower is a typical example of Hairpin heat exchangers utilize true counter-current flow. Unlike multi-pass shell-and-tube designs where correction factors are used to account for inefficiencies resulting from co-current passes, this process maximizes temperature differences between shell side and tube side fluids. When a process calls for a temperature cross (hot fluid outlet temperature is below cold fluid outlet temperature), a hairpin heat exchanger is the most efficient design, with fewer sections and less surface area. Double-pipe heat exchangers utilize a single pipe-within-a-pipe design and are commonly used for high fouling

services such as slurries where abrasive materials are present, and for smaller duties. Standard shell diameters range from 2" (50,8 mm.) to 6" (152,4 mm.). Multi-tube heat exchangers are used for larger duties with standard designs for shell diameters up to 30" (762 mm.) and surface areas in excess of 10,000 ft<sup>2</sup> (930 m<sup>2</sup>) per section. BROWN FINTUBE® range of products includes a variety of unique enhancement devices for different process conditions.

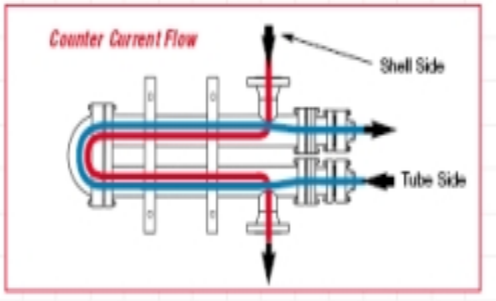


Figure 6 : Hairpin-Style Heat Exchangers

### Hairpin Heat Exchangers

A hairpin design is often more thermally efficient than a traditional shell and tube, which results in a lower up-front cost and lower overall weight. Our experienced designers and engineers can meet any custom cooling requirement.

### CFD ANALYSIS OF HAIR PIN HEAT EXCHANGER

The model is designed with the help of pro-e and then import on ANSYS for Meshing and analysis. The analysis by CFD is used in order to calculating pressure profile and temperature distribution. For meshing, the fluid ring is divided into two connected volumes. Then all thickness edges are meshed with 360 intervals. A tetrahedral structure mesh is used. So the total number of nodes and elements is 6576 and 3344.

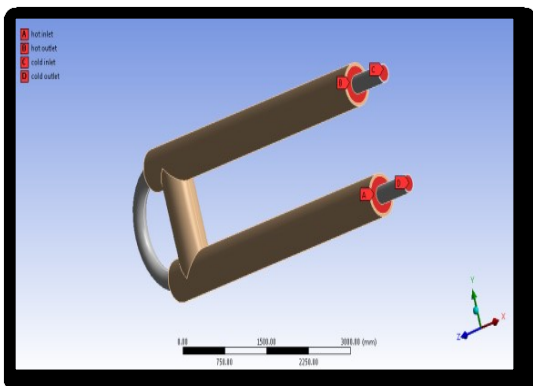


Fig 7 : CFD Flow Analysis of Heat Pin Heat Exchanger

### FLUID- TITANIUM CARBIDE MASS FLOW RATE

Mass Flow Rate	(kg/s)
cold_inlet	0.049999997
cold_outlet	-0.32807603
contact_region-contact_region_3-contact_region_2-contact_region_3-src	-0.55263227
contact_region-contact_region_3-contact_region_2-contact_region_3-trg	0.55263036
contact_region_4-src	0.010181041
contact_region_4-trg	-0.01018121
hot_inlet	0.69999987
hot_outlet	-0.44418025
interior-16	-0.55263025
interior-5	0.010180908
interior-nsbr	-16.106001
wall-14	0
wall-15	0
wall-17	0
wall-18	0
wall-nsbr	0
Net	-0.022250495

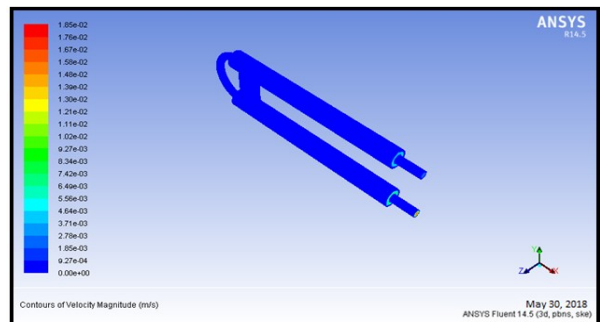
### HEAT TRANSFER RATE

Total Heat Transfer Rate	(w)
cold_inlet	2985.0301
cold_outlet	-70405.109
contact_region-contact_region_3-contact_region_2-contact_region_3-src	0
contact_region-contact_region_3-contact_region_2-contact_region_3-trg	0
contact_region_4-src	0
contact_region_4-trg	0
hot_inlet	150220.63
hot_outlet	-86969.914
wall-14	0
wall-15	0
wall-17	0
wall-18	0
wall-nsbr	0
Net	-4249.3604

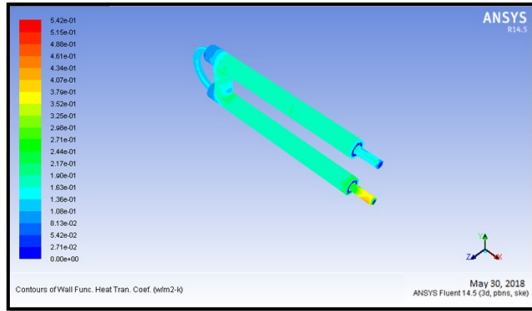
### AT 0.5%

### PRESSURE VELOCITY

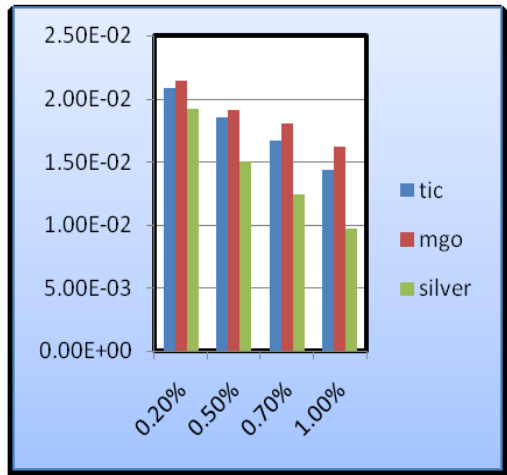
Total Heat Transfer Rate	(w)
cold_inlet	2500.425
cold_outlet	-63756.617
contact_region-contact_region_3-contact_region_2-contact_region_3-src	0
contact_region-contact_region_3-contact_region_2-contact_region_3-trg	0
contact_region_4-src	0
contact_region_4-trg	0
hot_inlet	133404.72
hot_outlet	-73759.672
wall-14	0
wall-15	0
wall-17	0
wall-18	0
wall-nsbr	0
Net	-1501.1453



**HEAT TRANSFER COEFFICIENT**



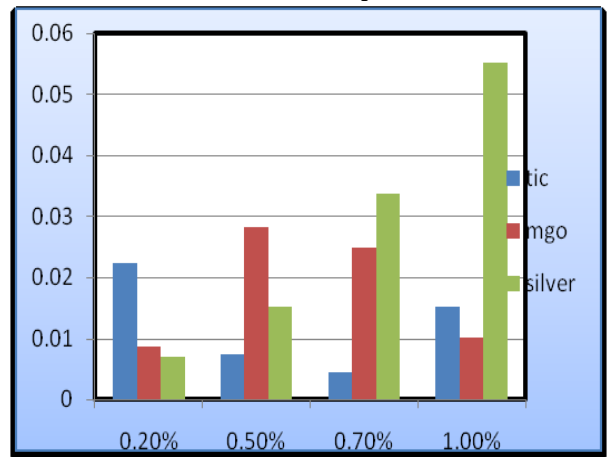
**Velocity plot**



**MASS FLOW RATE**

Mass Flow Rate (kg/s)	
cold_inlet	0.04999997
cold_outlet	-0.33046932
contact_region-contact_region_3-contact_region_2-contact_region_3-src	-0.57151183
contact_region-contact_region_3-contact_region_2-contact_region_3-trg	0.57151026
contact_region_4-src	0.007118477
contact_region_4-trg	-0.007118263
hot_inlet	0.69999987
hot_outlet	-0.42298076
interior-16	-0.57151897
interior-5	0.0071181641
interior_nscr	-16.801451
wall-14	0
wall-15	0
wall-17	0
wall-18	0
wall_nscr	0
Net	-0.007150823

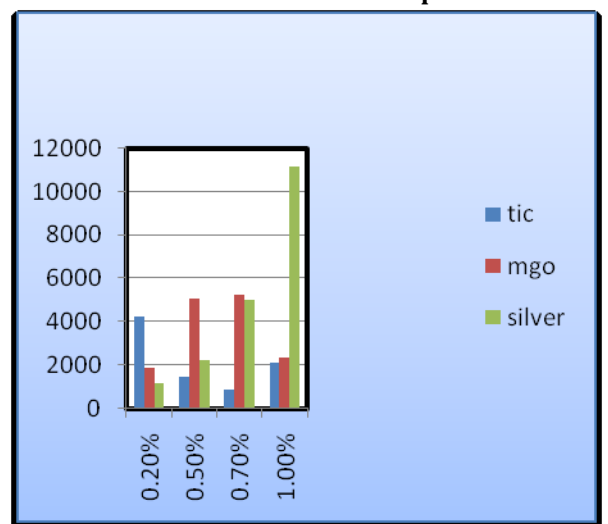
**Mass flow rate plot**



**HEAT TRANSFER COEFFICIENT**

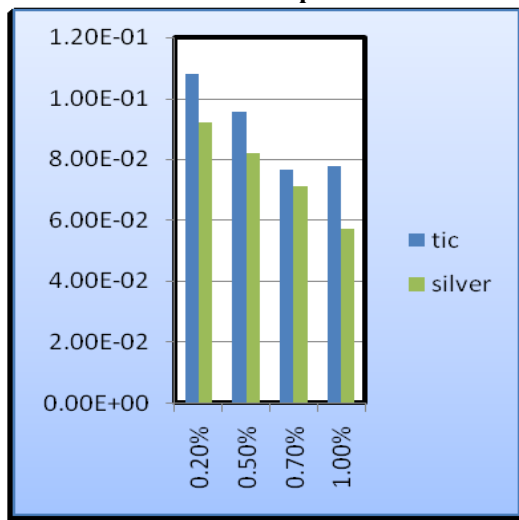
Total Heat Transfer Rate (w)	
cold_inlet	2738.40271
cold_outlet	-66962.672
contact_region-contact_region_3-contact_region_2-contact_region_3-src	0
contact_region-contact_region_3-contact_region_2-contact_region_3-trg	0
contact_region_4-src	0
contact_region_4-trg	0
hot_inlet	141584.45
hot_outlet	-82465.953
wall-14	0
wall-15	0
wall-17	0
wall-18	0
wall_nscr	0
Net	-5086.1448

**Heat transfer coefficient plot**



**Graphs**

**Pressure plot**



**CONCLUSION**

In this paper, glycerin (40%) fluid is mixed with base fluid water (60%) are calculated for their

combination properties. The nano fluid is titanium carbide, magnesium Oxide and silver nano particle for weight percentage 0.2%, 0.5%, 0.7% & 1.0%. Theoretical calculations are done determine the properties for nano fluids and those properties are used as inputs for analysis. Hairpin Exchangers are available in single tube (Double Pipe) or multiple tubes within a hairpin shell (Multitude), bare tubes, finned tubes, U-tubes, straight tubes (with rod-thru capability), fixed tube sheets and removable bundle.

By observing the CFD analysis results the heat transfer rate value more at silver nano particle weight percentage 1.0%. So it can be concluded the silver nano particle nano fluid at weight percentage 0.2% fluid is the better fluid for hair pin heat exchanger.

#### REFERENCES

1. A.O. Adelaja, S. J. Ojolo and M. G. Sobamowo, "Computer Aided Analysis of Thermal and Mechanical Design of Shell and Tube Heat Exchangers", *Advanced Materials* Vol. 367 (2012) pp 731-737 (2012) Trans Tech Publications, Switzerland.
2. Yusuf Ali Kara, Ozbilen Guraras, "A computer program for designing of Shell and tube heat exchanger", *Applied Thermal Engineering* 24(2004) 1797-1805
3. Thundil Karuppa Raj, R., et al: Shell Side Numerical Analysis of a Shell and Tube Heat Exchanger , *Thermal Science* ( 2012), Vol. 16, No. 4, pp. 1165-1174.
4. Hari Haran, Ravindra Reddy and Sreehari, "Thermal Analysis of Shell and Tube Heat ExChanger Using C and Ansys" , *International Journal of Computer Trends and Technology* (2013), vol. 4, Issue 7.
5. Kumar, V., Prasad, L., Experimental investigation on heat transfer and fluid flow of air flowing under three sides concave dimple roughened duct. *International Journal of Mechanical Engineering and Technology (IJMET)*, Volume 8, Issue 11, November 2017, pp. 1083-1094, Article ID: IJMET\_08\_11\_110.
6. Kumar, V., Prasad, L., Thermal performance investigation of one and three sides concave dimple roughened solar air heaters. *International Journal of Mechanical Engineering and Technology (IJMET)* Volume 8, Issue 12, December 2017, pp. 31-45, Article ID: IJMET\_08\_12\_004.
7. Kumar, V., Prasad, L., Performance Analysis of three sides concave dimple shape roughened solar air heater, *J. sustain. dev. energy water environ. syst.*, 6(4), pp 631-648, 2018.
8. Kumar, V., Nusselt number and friction factor correlations of three sides concave dimple roughened solar air heater, *Renewable Energy* 135 (2019) 355-377.
9. Kumar, V., Prasad, L., Experimental analysis of heat transfer and friction for three sides roughened solar air heater, *Annales de Chimie - Science des Matériaux*, 75-107, ACSM. Volume 41 - n° 1-2/2017.
10. Kumar, V., Prasad, L., Performance prediction of three sides hemispherical dimple roughened solar duct, *Instrumentation, Measure, Métrologie*, 273-293 I2M. Volume 17 - n° 2/2018.

# DESIGN AND HEAT TRANSFER ANALYSIS OF A PARABOLIC SHAPED DISH COLLECTOR

N.Sriveni & Dr. Karthikeyan A. & Mr. Vikash Kumar

PG Student, Professor, Assistant Professor

Department of Mechanical Engg., Malla Reddy College of Engineering Maisammaguda, Dhulapally, Kompally, Secunderabad, Telangana-500100, India

**ABSTRACT:** Parabolic dish is a point focusing collector; it is used for the applications, where temperature requirements are very high like in steam generation. The heat gained produces a temperature of between 125 °C to 250 °C and this is used to drive a micro-Steam Turbine or small Stirling Engine that generates electricity. A parabolic dish concentrates only the direct radiation that enters the system parallel to its optical axis.

In this thesis, focuses on solar parabolic dish collector with truncated cone shaped helical coiled receiver made up of copper and coated with nickel chrome at focal point, which is designed and modeled using 3D modeling software Pro/Engineer. The present model has 15 coils for solar receiver. To investigate the performance of the collector, a 20 coiled receiver is also studied. Heat transfer analysis is done on the dish collector by applying different temperatures affecting in a particular day. Comparison is done between the two models.

In this thesis, the CFD analysis is to determine the heat transfer rate, pressure drop, velocity, mass flow rate and heat transfer coefficient for the fluids R134A and R-22 with different tube and coil diameters. Thermal analysis is to determine the temperature distribution and heat flux for copper and aluminum as tube materials.

3D modeling is done pro-engineer and analysis is done in ANSYS software.

**Keywords:** Types of convection, Natural convection, inclined plates, copper material.

## I. INTRODUCTION

A solar dish collector collects heat by absorbing sunlight. A collector is a device for capturing solar radiation. Solar radiation is energy in the form of electromagnetic radiation from the infrared (long) to the ultraviolet (short) wavelengths. The quantity of solar energy striking the Earth's surface (solar constant) averages about 1,000 watts per square meter under clear skies, depending upon weather conditions, location and orientation.



### Flat Plate Thermals

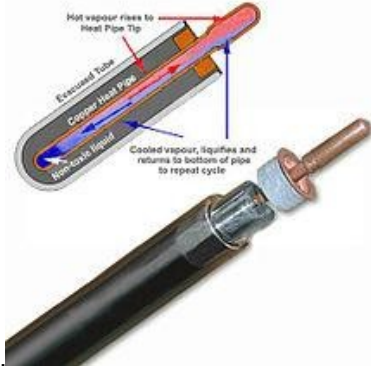
Flat Plate Thermal System for water heating deployed on flat roof Flat-plate Collectors, developed by Hottel and Whilliers in 1950s, are most common type.

They consist (1) a dark flat-plate absorber, (2) a transparent cover that reduces heat losses, (3) a heat-transport fluid (air, antifreeze or water) to remove heat from the absorber, and (4) a heat insulating backing. The absorber consists of a thin absorber sheet (of thermally stable polymers, aluminum, steel or copper, to which a matte black or selective coating is applied) often backed by a grid or coil of fluid tubing placed in an insulated casing with a glass or polycarbonate cover. In water heat panels, fluid is usually circulated through tubing to transfer heat from the absorber to an insulated water tank. This may be achieved directly or through a heat exchanger. Absorber piping configurations include:

- harp – traditional design with bottom pipe risers and top collection pipe, used in low pressure thermosyphon and pumped systems;
- serpentine – one continuous S that maximizes temperature but not total energy yield in variable flow systems, used in compact solar domestic hot water only systems (no space heating role)



Most vacuum tube collectors are used in middle Europe use heat pipes for their core instead of passing liquid directly through them. Direct flow is more popular in China. The heat is transferred to the transfer fluid (water or an antifreeze mix—typically propylene glycol) of a domestic hot water or hydronic space heating system in a heat exchanger called a "manifold".

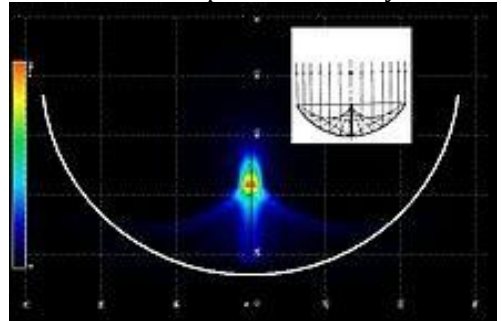


**Glass-glass evacuated tube**

A longstanding argument exists between proponents of these two technologies. Some of this can be related to the physical structure of evacuated tube collectors which have a discontinuous absorbance area. An array of evacuated tubes on a roof has open space between the collector tubes, and vacuum between the two concentric glass tubes of each collector. Collector tubes cover only a fraction of a unit area of a roof. If evacuated tubes are compared with flat-plate collectors on the basis of area of roof occupied, a different conclusion might be reached than if the areas of absorber were compared. In addition, the ISO 9806 standard<sup>[12]</sup> is ambiguous in describing the way in which the efficiency of solar thermal collectors should be measured, since these could be measured either in terms of gross area or in terms of absorber area. Unfortunately, power output is not given for thermal collectors as it is for PV panels. This makes it difficult for purchasers and engineers to make informed decisions.

**Bowl**

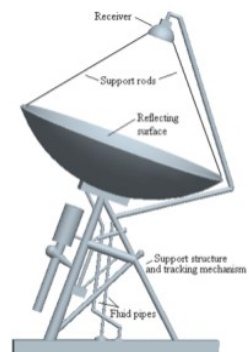
A solar bowl is a type of solar thermal collector that operates similarly to a parabolic dish, but instead of using a tracking parabolic mirror with a fixed receiver, it has a fixed spherical mirror with a tracking receiver. This reduces efficiency, but makes it cheaper to build and operate. Designers call it a *fixed mirror distributed focus solar power system*. The main reason for its development was to eliminate the cost of moving a large mirror to track the sun as with parabolic dish systems.<sup>[17]</sup>



Typical energy density along the 1/2 radius length focal line of a spherical reflector

**PARABOLIC DISH COLLECTOR**

Using parabolic dishes is a well-tested approach to concentrate solar radiation, and was an early experimental tool at many locations worldwide. The optical efficiency of parabolic dishes is considerably higher than that of trough, LFR or power tower systems because the mirror is always pointed directly at the sun, whereas the trough, LFR and power tower have a reduction in projected area due to a frequent low angle of incidence of the solar radiation. A schematic is shown in Figure.



A typical Parabolic dish collector system

**II. LITERATURE REVIEW**

**Design and Analysis of a Parabolic Shaped Solar Dish Collector**

The paper focuses on solar parabolic dish collector with truncated cone shaped helical coiled receiver made up of copper and coated with

nickel chrome at focal point, which is designed and modeled using 3D modeling software Pro/Engineer. The present model has 15 coils for solar receiver. To investigate the performance of the collector, a 20 coiled receiver is also studied. Heat transfer analysis is done on the dish collector by applying different temperatures affecting in a particular day. Comparison is done between the two models. CFD analysis is also done to determine the outlet fluid temperature, mass flow rates etc. Heat transfer analysis and CFD analysis is done by using CFD ANSYS 14.5. Key words: Solar Parabolic Dish Collector; Helical coil receiver collector; 20 Turns; 15 Turns. Heat transfer.

### DESIGN AND DEVELOPMENT OF A PARABOLIC DISH SOLAR WATER HEATER

The design and development of a parabolic dish solar water heater for domestic hot water application (up to 100°C) is described. The heater is to provide 40 litres of hot water a day for a family of four, assuming that each member of the family requires 10 litres of hot water per day. For effective performance the design requires that the solar water heater track the sun continuously, and an automatic electronic control circuit was designed and developed for this purpose.

### DESIGN AND TESTING OF A SOLAR PARABOLIC CONCENTRATING COLLECTOR

This paper is concerned with an experimental study of a simple parabolic trough solar collector tested under the local climatic condition. It presents the collectors' performance and the temperature effective length of the concentrator. A small scale parabolic trough was fabricated with the local available materials using stainless steel sheets as parabolic reflector and galvanized steel pipe as the receiver. As a part of solar technology distribution in Darfur Region, this model is designed erected under the supervision of the Energy Research Center of the University of Nyala (ERCUN).

### Improvements in efficiency of solar parabolic trough

Solar energy is primary source of all type of energy which is present in nature i.e. all the energy derived from it. So, direct utilization of solar energy into useful energy is important. There are so many solar thermal equipments in which concentrating type collector heated the fluid up to 100 to 4000C. It is employed for a variety of applications such as power generation, industrial steam generation and hot water production. Parabolic trough collector is preferred for steam generation because high temperatures can achieve.

### III . PROCEDURE :

Air flow through vertical narrow plates is modeled using CREO design software. The thesis will focus on thermal and CFD analysis with different Reynolds number ( $2 \times 10^6$  &  $4 \times 10^6$ ) and different angles ( $0^\circ, 30^\circ, 45^\circ$  &  $60^\circ$ ) of the vertical narrow plates. Thermal analysis done for the vertical narrow plates by steel, aluminum & copper at different heat transfer

### INTRODUCTION TO CAD

**Computer-aided design (CAD)**, also known as **computer-aided design and drafting (CADD)**, is the use of computer technology for the process of design and design-documentation. Computer Aided Drafting describes the process of drafting with a computer. CADD software, or environments, provide the user with input-tools for the purpose of streamlining design processes; drafting, documentation, and manufacturing processes. CADD output is often in the form of electronic files for print or machining operations. The development of CAD-based software is in direct correlation with the processes it seeks to economize; industry-based software (construction, manufacturing, etc.) typically uses vector-based (linear) environments whereas graphic-based software utilizes raster-based (pixelated) environments.

### INTRODUCTION TO PRO/ENGINEER

Pro/ENGINEER Wildfire is the standard in 3D product design, featuring industry-leading productivity tools that promote best practices in design while ensuring compliance with your industry and company standards. Integrated Pro/ENGINEER CAD/CAM/CAE solutions allow you to design faster than ever, while maximizing innovation and quality to ultimately create exceptional products.

### PRO/ENGINEER WILDFIRE BENEFITS

- Unsurpassed geometry creation capabilities allow superior product differentiation and manufacturability
- Fully integrated applications allow you to develop everything from concept to manufacturing within one application

Pro ENGINEER can be packaged in different versions to suit your needs, from Pro/ENGINEER Foundation XE, to Advanced XE Package and Enterprise XE Package, Pro/ENGINEER Foundation XE Package brings together a broad base of functionality. From robust part modelling to advanced surfacing, powerful assembly modelling and simulation, your needs will be met with this scalable solution. Flex3C and Flex

Advantage Build on this base offering extended functionality of your choosing.

#### DIFFERENT MODULES IN PRO/ENGINEER

- PART DESIGN
- ASSEMBLY
- DRAWING
- SHEET METAL

#### INTRODUCTION TO FINITE ELEMENT METHOD

Finite Element Method (FEM) is also called as Finite Element Analysis (FEA). Finite Element Method is a basic analysis technique for resolving and substituting complicated problems by simpler ones, obtaining approximate solutions Finite element method being a flexible tool is used in various industries to solve several practical engineering problems. In finite element method it is feasible to generate the relative results.

#### General Description of FEM:

To acquire a solution for a continuum problem by FEM, the procedure follows an orderly step by step process. The step- by step procedure is as follows:

**1. Discretization of the Structure:**The first step involves dividing the structure into elements. Therefore suitable finite element should be used to model the structure.

**2. Selection of a proper interpolation or displacement model:** Since the displacement solution is not known exactly for a complex structure under any given load, we assume an approximate solution. The assumed solution must be simple and should satisfy the convergence requirements. In general, interpolation or displacement model should be in polynomial form.

**3. Derivation of element stiffness matrices and load vector:** From the second step, stiffness matrix  $[k^e]$  and load vector  $P^e$  of element  $e$  is solved from either equilibrium conditions or variation principle.

Where  $[k]$  = assembled stiffness matrix.

#### Engineering Applications of Finite Element Method:

Initially FEM method was used for only structural mechanics problems but over the years researchers have successfully applied it to various engineering problems. It has been validated that this method can be used for other numerical solution of ordinary and partial differential equations.

The finite element method is applicable to three categories of boundary value problems:

- Equilibrium or Steady State or Time-Independent problems
- Eigen value problems
- Propagation or transient problems

#### Various applications of FEM:

- Civil Engineering Structures
- Aircraft Structures
- Heat Conduction
- Geomechanics
- Hydraulic and Water Resource Engineering
- Nuclear engineering
- Biomedical Engineering
- Mechanical Engineering
- Electrical Machines and Electromagnetic

#### Advantages of FEA/FEM:

- Non-linear problems are easily solved.
- Several types of problems can be solved with easy formulation.
- Reduces the costs in the development of new products.
- Improves the quality of the end product.

#### Disadvantages of FEA/FEM:

1. Extreme aspect ratios can cause problems.
2. Not well suited for open region problems.

#### ANSYS Software:

ANSYS is an Engineering Simulation Software (computer aided Engineering). Its tools cover Thermal, Static, Dynamic, and Fatigue finite element analysis along with other tools all designed to help with the development of the product. The company was founded in 1970 by Dr. John A. Swanson as Swanson Analysis Systems, Inc. SASI.

#### Benefits of ANSYS:

- The ANSYS advantage and benefits of using a modular simulation system in the design process are well documented. According to studies performed by the Aberdeen Group, best-in-class companies perform more simulations earlier. As a leader in virtual prototyping, ANSYS is unmatched in terms of functionality and power necessary to optimize components and systems.
- The ANSYS advantage is well-documented.

#### Structural Analysis:

Structural analysis is probably the most common application of the finite element method. The term structural (or structure) implies not only civil engineering structures such as ship hulls, aircraft bodies, and machine housings, as well as mechanical components such as pistons, machine parts, and tools.

#### Types of Structural Analysis:

Different types of structural analysis are:

- Static analysis
- Modal analysis
- Harmonic analysis
- Transient dynamic analysis

**Static Analysis:**

Static analysis calculates the effects of steady loading conditions on a structure, while ignoring inertia and damping effects, such as those caused by time varying loads. A static analysis can, however, include steady inertia loads (such as gravity and rotational velocity), and time-varying loads that can be approximated as static equivalent loads (such as the static equivalent wind and seismic loads commonly defined in many building codes).

The kinds of loading that can be applied in a static analysis include:

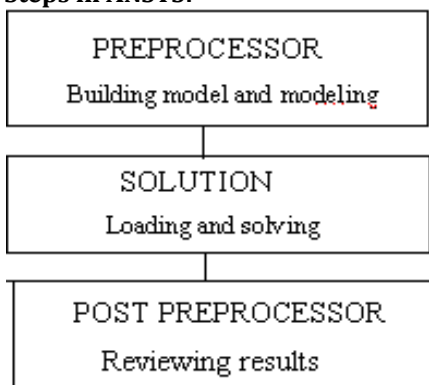
- Externally applied forces and pressures
- Steady-state inertial forces (such as gravity or rotational velocity)
- Imposed (non-zero) displacements
- Temperatures (for thermal strain)

**Overview of steps in a static analysis:**

The procedure for a modal analysis consists of three main steps:

1. Build the model.
2. Apply loads and obtain the solution.
3. Review the results.

**Basic Steps in ANSYS:**



**Pre-Processing (Defining the Problem):** The major steps in preprocessing are given below

- Define key points/lines/ areas/volumes.
- Define element type and material/geometric properties

- Mesh lines/ areas/volumes as required.

**Solution (Assigning Loads, Constraints, And Solving):**

Here the loads (point or pressure), constraints (translational and rotational) are specified and finally solve the resulting set of equations.

**Post Processing:** In this stage, further processing and viewing of the results can be done such as:

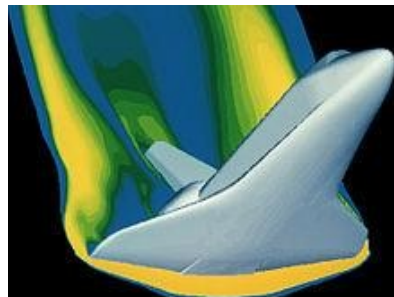
**Advanced Post-Processing:**

ANSYS provides a comprehensive set of post-processing tools to display results on the models as contours or vector plots, provide summaries of the results (like min/max values and locations). Powerful and intuitive slicing techniques allow getting more detailed results over given parts of your geometries.

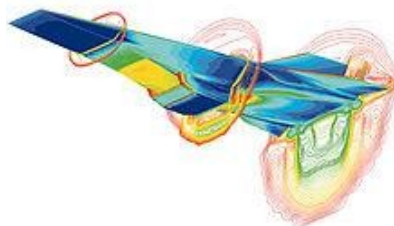
**INTRODUCTION TO CFD**

Computational fluid dynamics, usually abbreviated as CFD, is a branch of fluid mechanics that uses numerical methods and algorithms to solve and analyze problems that involve fluid flows. Computers are used to perform the calculations required to simulate the interaction of liquids and gases with surfaces defined by boundary conditions. With high-speed supercomputers, better solutions can be achieved.

**BACKGROUND AND HISTORY**



A computer simulation of high velocity air flow around the Space Shuttle during re-entry.



A simulation of the Hyper-X scramjet vehicle in operation at Mach-7

The fundamental basis of almost all CFD problems are the Navier–Stokes equations, which define any single-phase (gas or liquid, but not both) fluid flow. These equations can be simplified by removing terms describing viscous actions to yield

the Euler equations. Further simplification, by removing terms describing vorticity yields the full potential equations. Finally, for small perturbations in subsonic and supersonic flows (not transonic or hypersonic) these equations can be linearized to yield the linearized potential equations.

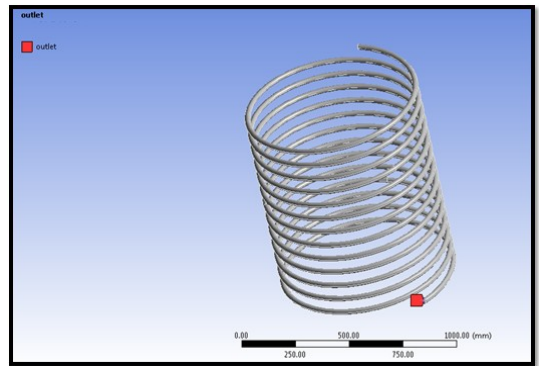
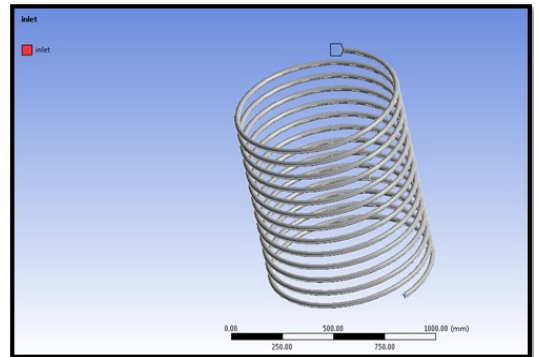
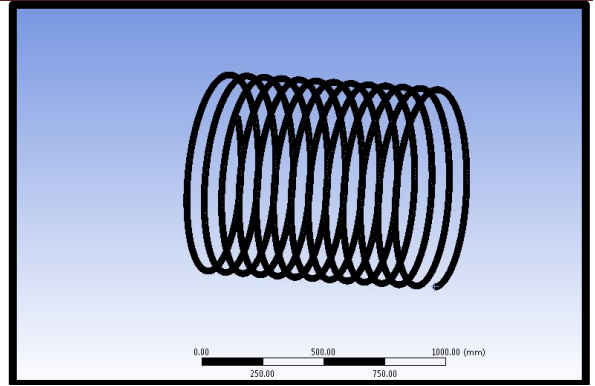
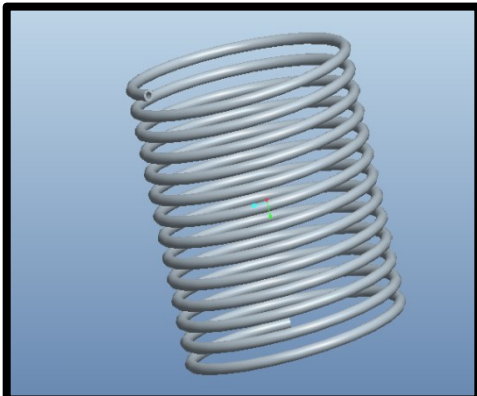
**.Methodology**

In all of these approaches the same basic procedure is followed.

- During preprocessing
  - The geometry (physical bounds) of the problem is defined.
  - The volume occupied by the fluid is divided into discrete cells (the mesh). The mesh may be uniform or non-uniform.
  - The physical modeling is defined – for example, the equations of motion

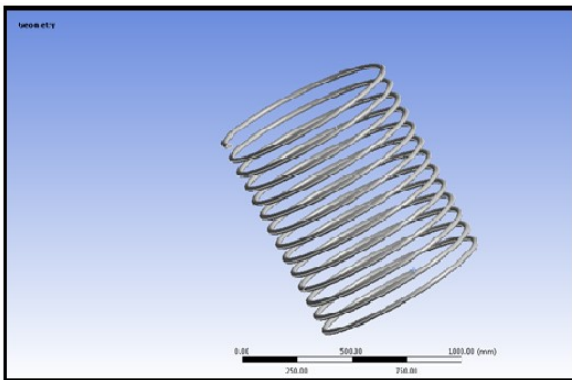
**MODELLING AND ANALYSIS**

**3D MODEL**

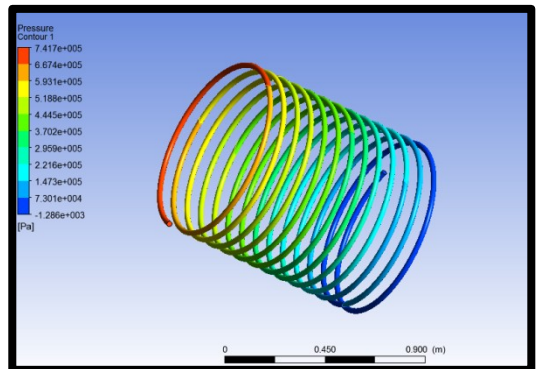


**CFD ANALYSIS OF HELICALLY COILED CAPILLARY TUBES**

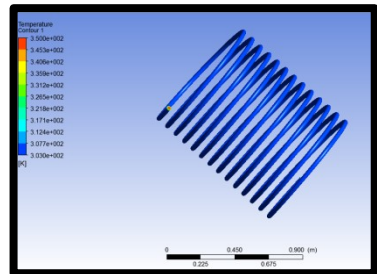
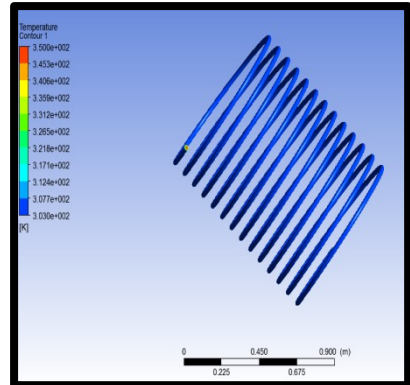
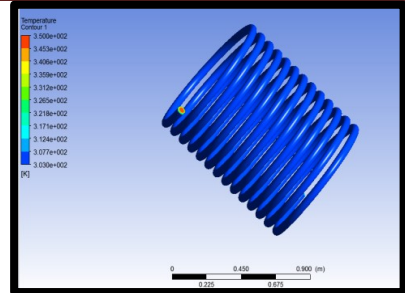
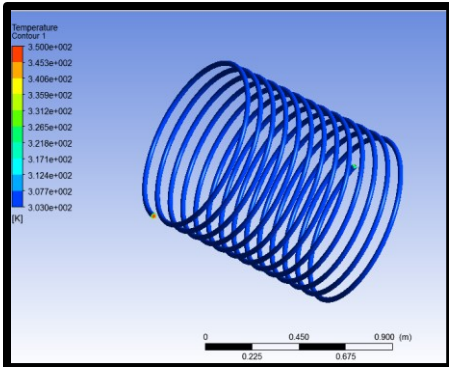
**FLUID - R134A**  
**COIL DIAMETER-25mm**



**PRESSURE**



**TEMPERATURE**



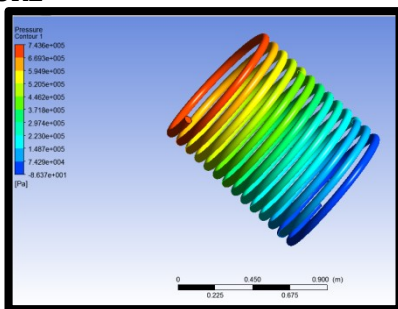
**MASS FLOW RATE**

Mass Flow Rate	(kg/s)
inlet	2.5915148
interior-___msbr	21561.639
outlet	-2.3933501
wall-___msbr	0
<b>Net</b>	<b>0.1981647</b>

**HEAT TRANSFER RATE**

Total Heat Transfer Rate	(w)
inlet	135058.17
outlet	-65275.977
wall-___msbr	-64687.754
<b>Net</b>	<b>5094.4414</b>

**COIL DIAMETER-50mm  
PRESSURE**



**TEMPERATURE**

Mass Flow Rate	(kg/s)
inlet	2.0880271
interior-___msbr	20111.02
outlet	-2.3032918
wall-___msbr	0
<b>Net</b>	<b>-0.29526472</b>

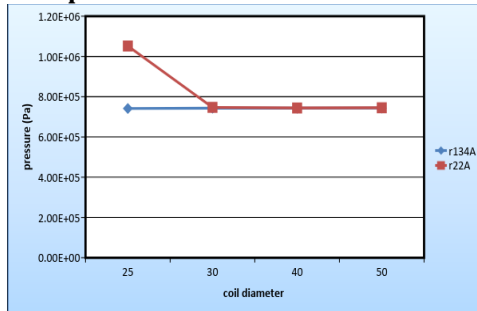
**RESULT TABLES  
CFD ANALYSIS RESULTS**

Fluid	Coil dia. (m)	Pressure (Pa)	Temperature (k)	Mass flow rate (Kg/sec)	Heat transfer rate(w)
R134A	25	7.417e+05	3.50e+02	0.1981647	5094.4414
	30	7.431e+05	3.50e+02	0.088071	4438.2969
	40	7.430e+05	3.50e+02	0.30208788	17768.25
	50	7.436e+05	3.50e+02	1.477181	79467.406
R22A	25	1.052e+06	3.50e+02	0.2952	15173.382
	30	7.471e+05	3.50e+02	0.1247	6491.99
	40	7.440e+05	3.50e+02	0.06250	3696.4023
	50	7.451e+05	3.50e+02	0.58710	30365.797

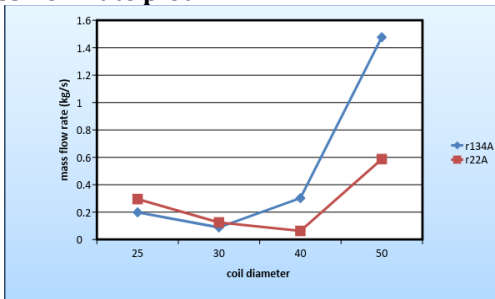
Coil dia. (mm)	Material	Temperature (°C)		Heat flux (w/mm <sup>2</sup> )
		Min.	Max.	
25	Aluminum	31.91	80	1.1332
30		31.184	80	1.1881
40		30.487	80	1.0534
50		30.18	80.123	1.0099
25	Copper	37.25	80	2.1043
30		35.322	80	2.2149
40		32.955	80	1.9819
50		33.0	80.063	1.903

**GRAPHS**

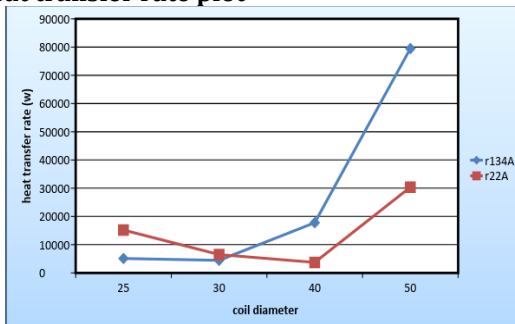
**Pressure plot**



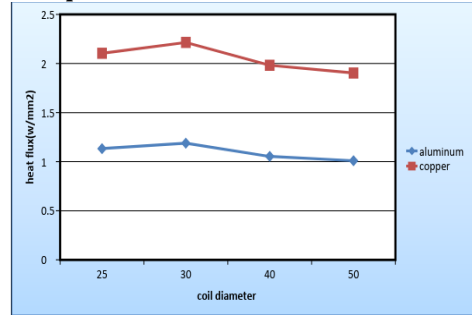
**Mass flow rate plot**



**Heat transfer rate plot**



**Heat flux plot**



**CONCLUSION**

In this thesis, the effects of the relevant parameters on the flow characteristic of R134a and R-22 flowing through adiabatic helical coiled tubes were analytical studied. The helical coiled tubes' diameter, coil diameter, and parameters relating to flow conditions such as inlet pressures and degree of sub cooling were the major parameters investigated.

By observing the CFD analysis the pressure drop value is increased at coil dia. 25mm by the fluid R22A.

By observing the thermal analysis, the Heat flux value is more for copper when we compare with aluminum material.

So we can conclude the copper material and fluid R22A better for capillary tube

**REFERENCES**

1. Coal, oil and natural gas <http://www.thingstalk.net/data/files/dokumenter/fakta-ark/kulolieognaturgas-uk.pdf>
2. Sukhatme S.P. (2007) principles of thermal collection and storage. McGraw Hill, New Delhi
3. Administration, U. E. I., 2010. International energy outlook. Tech. Rep. DOE/EIA-0484(2010), Office of Integrated Analysis and Forecasting, U.S. Department of Energy, Washington, DC.
4. Gunther M., Joemann M. and Csambor S (2010) advanced CSP Teaching Materials, page 09.Germany
5. Garud S.Making solar thermal power generation in india reality overview of technologies, opportunities and challenges, The energy and resources institute(TERI)India, [http://www.aprek.org/files/SolarThermalPowergeneration\\_Final.pdf](http://www.aprek.org/files/SolarThermalPowergeneration_Final.pdf).
6. Valentina A. S., Carmelo E. M., Giuseppe M. G., Miliozzi Adio and Nicolini Daniele (2010) New Trends in Designing Parabolic trough Solar Concentrators and Heat Storage Concrete Systems in Solar Power Plants. Croatia, Italy
7. FOLARANMI, J. (2009) Design, Construction and Testing of a Parabolic Solar Steam Generator. Journal of Practices and

- Technologies ISSN 1583-1078. Vol-14, page 115-133, Leonardo
8. Xiao G. (2007) A closed parabolic trough solar collector. Version 2 Page 1-28
  9. Kumar, V., Prasad, L., Experimental investigation on heat transfer and fluid flow of air flowing under three sides concave dimple roughened duct. International Journal of Mechanical Engineering and Technology (IJMET), Volume 8, Issue 11, November 2017, pp. 1083–1094, Article ID: IJMET\_08\_11\_110.
  10. Kumar, V., Prasad, L., Thermal performance investigation of one and three sides concave dimple roughened solar air heaters. International Journal of Mechanical Engineering and Technology (IJMET) Volume 8, Issue 12, December 2017, pp. 31–45, Article ID: IJMET\_08\_12\_004.
  11. Kumar, V., Prasad, L., Performance Analysis of three sides concave dimple shape roughened solar air heater, J. sustain. dev. energy water environ. syst., 6(4), pp 631-648, 2018.
  12. Kumar, V., Nusselt number and friction factor correlations of three sides concave dimple roughened solar air heater, Renewable Energy 135 (2019) 355-377.
  13. Kumar, V., Prasad, L., Experimental analysis of heat transfer and friction for three sides roughened solar air heater, Annales de Chimie - Science des Matériaux, 75-107, ACSM. Volume 41 – n° 1-2/2017.
  14. Kumar, V., Prasad, L., Performance prediction of three sides hemispherical dimple roughened solar duct, Instrumentation, Mesure, Métrologie, 273-293 I2M. Volume 17 – n° 2/2018.

# NATURAL CONVECTIVE HEAT TRANSFER FROM INCLINED NARROW PLATES

R. Swapna & Dr. T.V. Reddy & Mr. Vikash Kumar

PG Student, Professor (H & S), Vice Principal, Assistant Professor  
Department of Mechanical Engg., Malla Reddy College of Engineering Maisammaguda, Dhulapally,  
Kompally, Secunderabad, Telangana-500100, India

**ABSTRACT:** Natural Convection flow in a vertical channel with internal objects is encountered in several technological applications of particular interest of heat dissipation from electronic circuits, refrigerators, heat exchangers, nuclear reactors fuel elements, dry cooling towers, and home ventilation etc.

In this thesis the air flow through vertical narrow plates is modeled using CREO design software. The thesis will focus on thermal and CFD analysis with different Reynolds number ( $2 \times 10^6$  &  $4 \times 10^6$ ) and different angles ( $0^\circ, 30^\circ, 45^\circ$  &  $60^\circ$ ) of the vertical narrow plates. Thermal analysis done for the vertical narrow plates by steel, aluminum & copper at different heat transfer coefficient values. These values are taken from CFD analysis at different Reynolds numbers.

In this thesis the CFD analysis to determine the heat transfer coefficient, heat transfer rate, mass flow rate, pressure drop and thermal analysis to determine the temperature distribution, heat flux with different materials. 3D modeled in parametric software Pro-Engineer and analysis done in ANSYS.

**Keywords:** Types of convection, Natural convection, inclined plates, copper material.

## I. INTRODUCTION

### Natural Convection

In natural convection, the fluid motion occurs by natural means such as buoyancy. Since the fluid velocity associated with natural convection is relatively low, the heat transfer coefficient encountered in natural convection is also low.

### Mechanisms of Natural Convection

Consider a hot object exposed to cold air. The temperature of the outside of the object will drop (as a result of heat transfer with cold air), and the temperature of adjacent air to the object will rise. Consequently, the object is surrounded with a thin layer of warmer air and heat will be transferred from this layer to the outer layers of air. The temperature of the air adjacent to the hot object is higher, thus its density is lower. As a result, the heated air rises. This movement is called the natural convection current. Note that in the absence of this movement, heat transfer would be by conduction only and its rate would be much lower. In a gravitational field, there is a net force that pushes a light fluid placed in a heavier fluid upwards. This force is called the buoyancy force.

Natural convection is a mechanism, or type of heat transport, in which the fluid motion is not generated by any external source (like a pump, fan, suction device, etc.) but only by density differences in the fluid occurring due to temperature gradients. In natural convection, fluid surrounding a heat source receives heat,

becomes less dense and rises. The surrounding, cooler fluid then moves to replace it. This cooler fluid is then heated and the process continues, forming convection current; this process transfers heat energy from the bottom of the convection cell to top. The driving force for natural convection is buoyancy, a result of differences in fluid density. Because of this, the presence of a proper acceleration such as arises from resistance to gravity, or an equivalent force (arising from acceleration, centrifugal force or Coriolis effect), is essential for natural convection. For example, natural convection essentially does not operate in free-fall (inertial) environments, such as that of the orbiting International Space Station, where other heat transfer mechanisms are required to prevent electronic components from overheating.

### Natural Convection from a Vertical Plate

In this system heat is transferred from a vertical plate to a fluid moving parallel to it by natural convection. This will occur in any system wherein the density of the moving fluid varies with position.

$$Nu_m = 0.478(Gr^{0.25})$$

$$\text{Mean Nusselt Number} = Nu_m = h_m L / k$$

Where

$h_m$  = mean coefficient applicable between the lower edge of the plate and any point in a distance  $L$  ( $W/m^2 \cdot K$ )

$L$  = height of the vertical surface (m)

$k$  = thermal conductivity (W/m. K)

GrashoffNumber =  $Gr =$

$$\frac{gL^3(t_s - t_\infty)}{\nu^2 T}$$

Where

$g$  = gravitational acceleration ( $m/s^2$ )

$L$  = distance above the lower edge (m)

$t_s$  = temperature of the wall (K)

$t_\infty$  = fluid temperature outside the thermal boundary layer (K)

$\nu$  = kinematic viscosity of the fluid ( $m^2/s$ )

$T$  = absolute temperature (K)

## II. LITERATURE REVIEW

In 1972, Aung et al. [12] presented a coupled numerical experimental study. Under isothermal conditions at high Rayleigh numbers their experimental results were 10% lower than the numerical ones. This difference has also been observed between Bodoia's and Osterle's numerical results [8] and Elenbaas' experimental ones [7]. They ascribed the discrepancies to the assumption of a flat velocity profile at the channel inlet.

In 2004, Olsson [17] presented a similar study. He worked on the different existing correlations, including those of Bar-Cohen and Rohsenow, and compared them with experimental results. Finally he proposed some corrected correlations that are valid for a wide range of Rayleigh numbers.

In 1989, Webb and Hill [18] studied the laminar convective flow in an experimental asymmetrically heated vertical channel. They worked on isoflux heating with a modified Rayleigh number (see eq. 13) changing from 500 to 107. Their temperature measurements performed in horizontal direction on the heated wall showed variations of  $\pm 1.5\%$ , and the flow was assumed to be 2D. They studied correlations for local, average and higher channel Nusselt numbers and compared them to previous works ([9], [10] and [11]). Their correlations were calculated for pure convective flow and the radiation losses were estimated and subtracted from the heat input. They found that constants  $C1$  and  $C2$  were strongly dependent on modified Rayleigh numbers below  $Ra_b \_ 105$  but that they were independent for higher Rayleigh numbers. Good agreement was seen between their results for high Rayleigh numbers and the flat plate solution of Sparrow and Gregg [10].

## III. PROCEDURE:

Air flow through vertical narrow plates is modeled using CREO design software. The thesis

will focus on thermal and CFD analysis with different Reynolds number ( $2 \times 10^6$  &  $4 \times 10^6$ ) and different angles ( $0^\circ, 30^\circ, 45^\circ$  &  $60^\circ$ ) of the vertical narrow plates. Thermal analysis done for the vertical narrow plates by steel, aluminum & copper at different heat transfer coefficient values.

Reynolds numbers	Angle of plate	material
$2 \times 10^6$	$0^\circ, 30^\circ, 45^\circ$ & $60^\circ$	Copper
$4 \times 10^6$		aluminum
		steel

## INTRODUCTION TO CAD

Computer-aided design (CAD) is defined as the application of computers and graphics software to aid or enhance the product design from conceptualization to documentation. CAD is most commonly associated with the use of an interactive computer graphics system, referred to as a CAD system. Computer-aided design systems are powerful tools and in the mechanical design and geometric modeling of products and components.

There are several good reasons for using a CAD system to support the engineering design

Function:

- To increase the productivity
- To improve the quality of the design
- To uniform design standards
- To create a manufacturing data base
- To eliminate inaccuracies caused by hand-copying of drawings and inconsistency between
- Drawings

## INTRODUCTION TO CREO

PTC CREO, formerly known as Pro/ENGINEER, is 3D modeling software used in mechanical engineering, design, manufacturing, and in CAD drafting service firms. It was one of the first 3D CAD modeling applications that used a rule-based parametric system. Using parameters, dimensions and features to capture the behavior of the product, it can optimize the development product as well as the design itself.

## ADVANTAGES OF CREO PARAMETRIC SOFTWARE

1. Optimized for model-based enterprises
2. Increased engineer productivity
3. Better enabled concept design
4. Increased engineering capabilities
5. Increased manufacturing capabilities
6. Better simulation
7. Design capabilities for additive manufacturing

## CREO parametric modules:

- Sketcher

- Part modeling
- Assembly
- Drafting

#### ANSYS Software:

ANSYS is an Engineering Simulation Software (computer aided Engineering). Its tools cover Thermal, Static, Dynamic, and Fatigue finite element analysis along with other tools all designed to help with the development of the product. The company was founded in 1970 by Dr. John A. Swanson as Swanson Analysis Systems, Inc. SASI. Its primary purpose was to develop and market finite element analysis software for structural physics that could simulate static (stationary), dynamic (moving) and heat transfer (thermal) problems. SASI developed its business in parallel with the growth in computer technology and engineering needs. The company grew by 10 percent to 20 percent each year, and in 1994 it was sold. The new owners took SASI's leading software, called ANSYS®, as their flagship product and designated ANSYS, Inc. as the new company name.

#### Benefits of ANSYS:

- The ANSYS advantage and benefits of using a modular simulation system in the design process are well documented
- *The ANSYS advantage is well-documented.*
- ANSYS is a virtual prototyping and modular simulation system that is easy to use and extends to meet customer needs; making it a low-risk investment that can expand as value is demonstrated within a company.

#### Structural analysis :

Structural analysis is probably the most common application of the finite element method. The term structural (or structure) implies not only civil engineering structures such as ship hulls, aircraft bodies, and machine housings, as well as mechanical components such as pistons, machine parts, and tools.

#### Types of Structural Analysis:

Different types of structural analysis are:

- Static analysis
- Modal analysis
- Harmonic analysis
- Transient dynamic analysis
- Spectrum analysis
- Bucking analysis
- Explicit dynamic analysis

#### Static Analysis:

Static analysis calculates the effects of steady loading conditions on a structure, while ignoring

inertia and damping effects, such as those caused by time varying loads. Static analysis is used to determine the displacements, stresses, strains, and forces in structural components caused by loads that do not induce significant inertia and damping effects. Steady loading and response are assumed to vary slowly with respect to time.

The kinds of loading that can be applied in a static analysis include:

- Externally applied forces and pressures
- Steady-state inertial forces (such as gravity or rotational velocity)
- Imposed (non-zero) displacements
- Temperatures (for thermal stain)

A static analysis can be either linear or non-linear. All types of non-linearities are allowed-large deformations, plasticity, creep, stress, stiffening, contact (gap) elements, hyper elastic elements, and so on.

#### Over-view of steps in a static analysis:

The procedure for a modal analysis consists of three main steps:

1. Build the model.
2. Apply loads and obtain the solution.
3. Review the results.

#### Basic Steps in ANSYS:

**Pre-Processing (Defining the Problem):** The major steps in pre-processing are given below

- Define key points/lines/ areas/volumes.
- Define element type and material/geometric properties
- Mesh lines/ areas/volumes as required.

The amount of detail required will depend on the dimensionality of the analysis (i.e., 1D, 2D, axis-symmetric, 3D).

**Solution (Assigning Loads, Constraints, And Solving):** Here the loads (point or pressure), constraints (translational and rotational) are specified and finally solve the resulting set of equations.

**Post Processing:** In this stage, further processing and viewing of the results can be done such as:

- Lists of nodal displacements
- Element forces and moments
- Deflection plots
- Stress contour diagrams

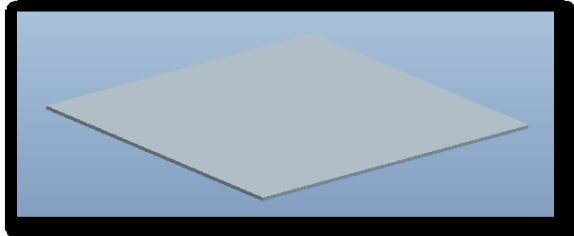
#### Advanced Post-Processing:

ANSYS provides a comprehensive set of post-processing tools to display results on the models as contours or vector plots, provide summaries of the results (like min/max values and locations). Powerful and intuitive slicing techniques allow getting more detailed results over given parts of your geometries. All the results can also be exported as text data or to a

spreadsheet for further calculations. Animations are provided for static cases as well as for nonlinear or transient histories. Any result or boundary condition can be used to create customized charts.

**IV . MODELLING AND ANALYSIS**

**Vertical narrow plate 3D model**



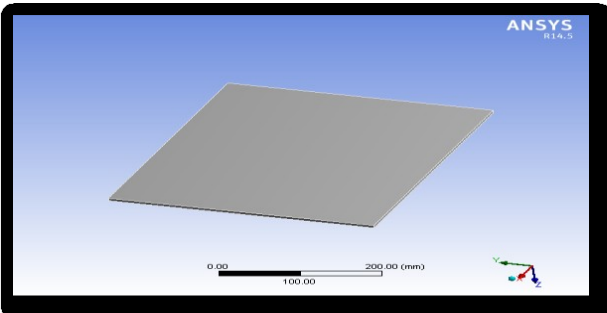
**MATERIAL PROPERTIES OF AIR**

Thermal conductivity =0.024w/m-k

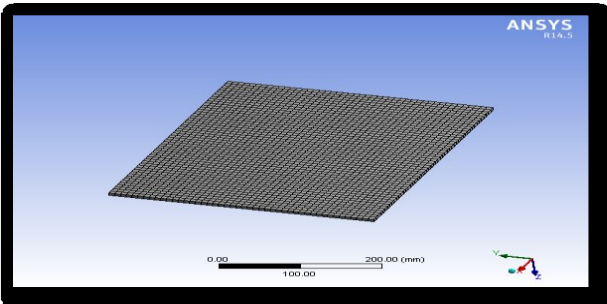
Density =1.225kg/m<sup>3</sup>

Viscosity =1.98×10<sup>-5</sup> kg/m-s

**IMPORTED MODEL**

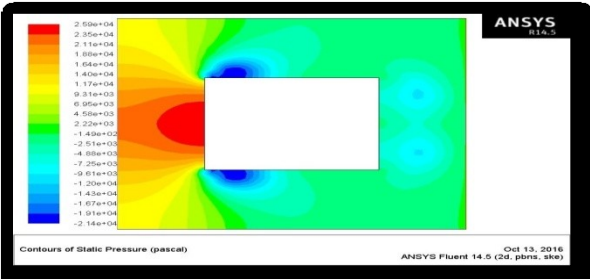


**MESHED MODEL**



**VERTICAL NARROW PLATE AT 0°**

**REYNOLDS NUMBER - 2×10<sup>6</sup>**



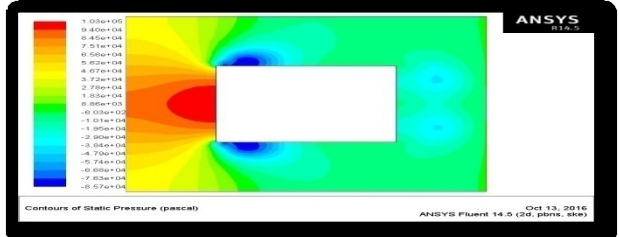
**Mass flow rate**

Mass Flow Rate	(kg/s)
inlet	79.311401
interior_trm_srf	196.93365
outlet	-79.3256
wall_trm_srf	0
Net	-0.014198303

**Heat transfer rate**

Total Heat Transfer Rate	(w)
inlet	5974630.5
outlet	-6031706
wall_trm_srf	0
Net	-57075.5

**REYNOLDS NUMBER - 4×10<sup>6</sup>**



**MASS FLOW RATE**

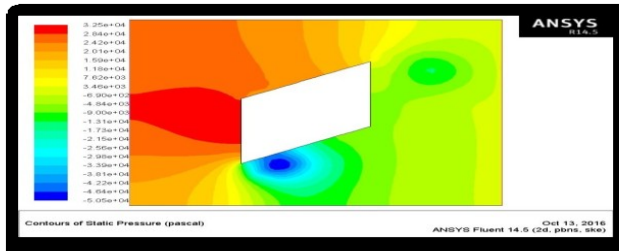
Mass Flow Rate	(kg/s)
inlet	158.63991
interior_trm_srf	393.53253
outlet	-158.66556
wall_trm_srf	0
Net	-0.025650024

**HEAT TRANSFER RATE**

Total Heat Transfer Rate	(w)
inlet	11950556
outlet	-12070637
wall_trm_srf	0
Net	-120081

**VERTICAL NARROW PLATE AT 30°**

**REYNOLDS NUMBER - 2×10<sup>6</sup>**



**Mass flow rate**

Mass Flow Rate	(kg/s)
inlet	99.139221
interior_trm_srf	-54.444607
outlet	-99.00412
wall_trm_srf	0
Net	0.13510132

**Mass flow rate**

Mass Flow Rate	(kg/s)
inlet	99.139221
interior_trm_srf	1081.3646
outlet	-98.893143
wall_trm_srf	0
Net	0.24607849

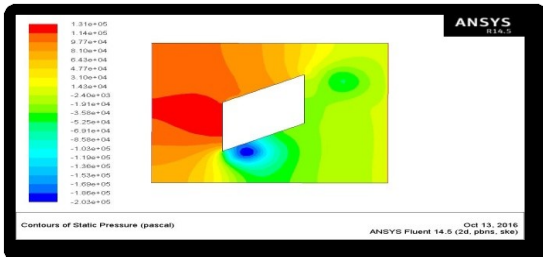
**Heat transfer rate**

Total Heat Transfer Rate	(w)
inlet	1481683.6
outlet	-1479661.3
wall_trm_srf	0
Net	2022.375

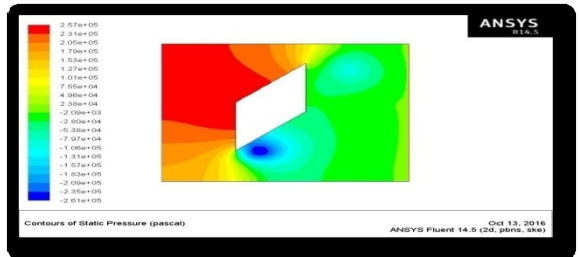
**Heat transfer rate**

Total Heat Transfer Rate	(w)
inlet	1481683.6
outlet	-1478005.8
wall_trm_srf	0
Net	3677.875

**REYNOLDS NUMBER -  $4 \times 10^6$**



**REYNOLDS NUMBER -  $4 \times 10^6$**



**Mass flow rate**

Mass Flow Rate	(kg/s)
inlet	198.29997
interior_trm_srf	-105.51134
outlet	-197.43877
wall_trm_srf	0
Net	0.86120605

**Mass flow rate**

Mass Flow Rate	(kg/s)
inlet	198.29997
interior_trm_srf	2164.0718
outlet	-197.68851
wall_trm_srf	0
Net	0.61146545

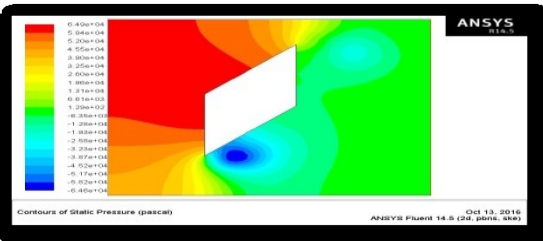
**Heat transferrate**

Total Heat Transfer Rate	(w)
inlet	2963688.3
outlet	-2950814
wall_trm_srf	0
Net	12874.25

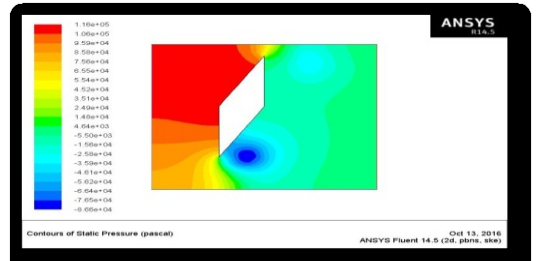
**Heat transfer rate**

Total Heat Transfer Rate	(w)
inlet	2963688.3
outlet	-2954559.3
wall_trm_srf	0
Net	9129

**VERTICAL NARROW PLATE AT  $45^\circ$   
 REYNOLDS NUMBER -  $2 \times 10^6$**



**VERTICAL NARROW PLATE AT  $60^\circ$   
 REYNOLDS NUMBER -  $2 \times 10^6$**



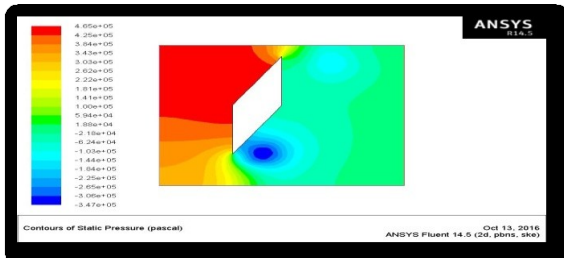
**Mass flow rate**

Mass Flow Rate		(kg/s)
inlet	99.139221	
interior_trm_srf	1325.8466	
outlet	-99.647263	
wall_trm_srf	0	
Net	-0.50804138	

**Heat transfer rate**

Total Heat Transfer Rate		(w)
inlet	1481683.6	
outlet	-1491557.3	
wall_trm_srf	0	
Net	-9873.625	

**REYNOLDS NUMBER -  $4 \times 10^6$**



**Mass flow rate**

Mass Flow Rate		(kg/s)
inlet	198.29997	
interior_trm_srf	2652.6765	
outlet	-199.35345	
wall_trm_srf	0	
Net	-1.0534821	

**Heat transfer rate**

Total Heat Transfer Rate		(w)
inlet	2963688.3	
outlet	-2983982.5	
wall_trm_srf	0	
Net	-20294.25	

**CFD ANALYSIS RESULT TABLE**

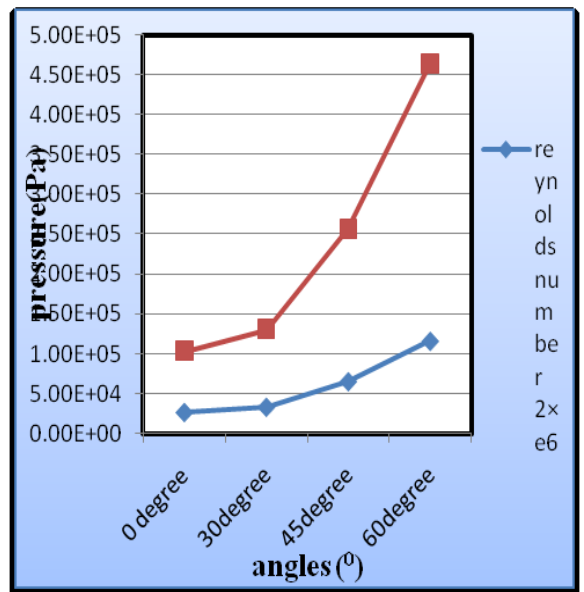
Reynolds number	Models	Pressure (Pa)	Velocity (m/s)	Heat transfer coefficient (w/m <sup>2</sup> -k)	Mass flow rate (kg/s)	Heat transfer rate (W)
$2 \times 10^6$	0°	2.59e+04	2.22e+02	3.14e+02	0.0141983	5707.55
	30°	3.25e+04	2.80e+02	3.39e+02	0.13510132	2022.375

	45°	6.49e+04	3.40e+02	4.06e+02	0.246078	3677.875
	60°	1.16e+05	5.01e+02	4.93e+02	0.50804138	9873.625
	0°	1.03e+05	4.44e+02	5.52e+02	0.02565	1200.81
$4 \times 10^6$	30°	1.31e+05	5.60e+02	5.96e+02	0.86120605	1287.425
	45°	2.57e+05	6.80e+02	7.09e+02	0.611465	9129
	60°	4.65e+05	1.00e+03	8.55e+02	1.05348	2029.425

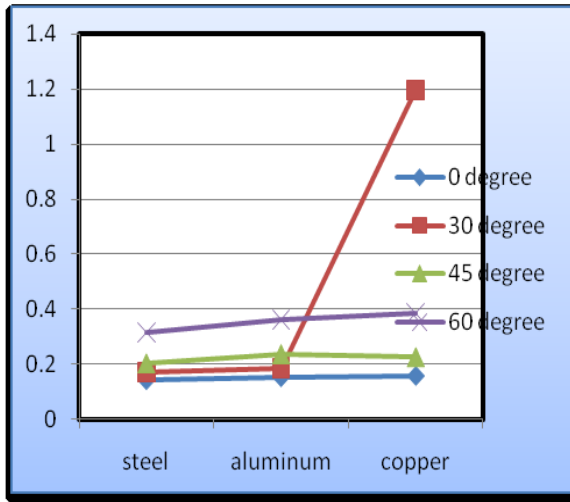
**THERMAL ANALYSIS RESULT TABLE**

Models	Materials	Temperature (°C)		Heat flux (w/mm <sup>2</sup> )
		Max.	Min.	
0°	Steel	343	333.99	0.14103
	Aluminum	343	339.2	0.15159
	Copper	343	341.76	0.15657
30°	Steel	343	331.7	0.17153
	Aluminum	343	338.22	0.18744
	Copper	343	341.41	1.1951
45°	Steel	343	329.74	0.20385
	Aluminum	343	341.08	0.23701
	Copper	343	337.26	0.22608
60°	Steel	343	325.73	0.3144
	Aluminum	343	335.2	0.35993
	Copper	343	340.34	0.38359

**CFD ANALYSIS GRAPHS**



**THERMAL ANALYSIS  
 HEAT FLUX**



**CONCLUSION**

In this thesis the air flow through vertical narrow plates is modeled using CREO design software. The thesis will focus on thermal and CFD analysis with different Reynolds number ( $2 \times 10^6$  &  $4 \times 10^6$ ) and different angles ( $0^\circ, 30^\circ, 45^\circ$  &  $60^\circ$ ) of the vertical narrow plates. Thermal analysis done for the vertical narrow plates by steel, aluminum & copper at different heat transfer coefficient values. These values are taken from CFD analysis at different Reynolds numbers.

By observing the CFD analysis the pressure drop & velocity increases by increasing the inlet Reynolds numbers and increasing the plate angles. The heat transfer rate increasing the inlet Reynolds numbers, more heat transfer rate at  $0^\circ$  angles.

By observing the thermal analysis, the taken different heat transfer coefficient values are from CFD analysis. Heat flux value is more for copper material than steel & aluminum.

So we can conclude the copper material is better for vertical narrow plates.

**REFERENCES**

1. Arpaci, V. S., 1995, "Buoyant Turbulent Flow Driven by Internal Energy Generation," *Int. J. Heat Mass Transfer*, Vol. 38, pp. 2761-2770.
2. Asfia, F. J., and Dhir, V. K., 1994, "An Experimental Study of Natural Convection a Volumetrically Heated Spherical Pool With Rigid Wall," *ASME Paper 94-WA/H7--26*.
3. Cheung, F. B., 1980a, "Heat Source-Driven Thermal Convection at Arbitrary Prandtl Numbers," *J. Fluid Mech.*, Vol. 97, pp. 743-758.
4. Cheung, F. B., 1980b, "The Boundary Layer Behaviour in Transient Turbulent Thermal

5. Convection Flow," *ASME Journal of HEAT TRANSFER* Vol. 102, pp.373-375.
6. Cheung, F. B., 1978, "Turbulent Thermal Convection in a Horizontal Fluid Layer With Time Dependent Volumetric Energy Sources." *AIAA/ASME Thermo physics and Heat Transfer Conf.*,78-HT-6, Palo Alto.
7. Cheung, F. B., 1977, "Natural Convection in a Volumetrically Heated Fluid Layer at High Rayleigh Numbers," *Int. J. Heat Mass Transfer*, Vol. 20, pp.499-506.
8. Cheung, F. B., Shiah, S. W., Cho, D. H., and Tan, M. J., 1992, "Modelling of Heat Transfer in a Horizontal Heat Generating Layer by an Effective Diffusivity Approach," *ASME/HTD*, Vol. 192, pp.55-62.
9. Dinh, T. N., and Nourgalier, R. R., 1997, "On Turbulence Modelling in Large Volumetrically Heated Liquid Pools," *Nucl. Engng. Design*, in press. Fan, T. H., 1996, "Heat Transport Phenomena of Turbulent Natural Convection in a Melt Layer With Solidification," M.S. thesis, The Pennsylvania State University, University Park, PA.
10. Fielder, H. E., and Wile, R., 1970, "Turbulent Freie Konvektion in Einer Horizontalea Flussigkeitss chicht mitt Volumen - Wärmequelle," *Paper NC 4.5, Proc. Fourth Int. Heat Transfer Conf.*, Vol. IV, pp. 1-12.
11. Kumar, V., Prasad, L., Experimental investigation on heat transfer and fluid flow of air flowing under three sides concave dimple roughened duct. *International Journal of Mechanical Engineering and Technology (IJMET)*, Volume 8, Issue 11, November 2017, pp. 1083-1094, Article ID: IJMET\_08\_11\_110.
12. Kumar, V., Prasad, L., Thermal performance investigation of one and three sides concave dimple roughened solar air heaters. *International Journal of Mechanical Engineering and Technology (IJMET)* Volume 8, Issue 12, December 2017, pp. 31-45, Article ID: IJMET\_08\_12\_004.
13. Kumar, V., Prasad, L., Performance Analysis of three sides concave dimple shape roughened solar air heater, *J. sustain. dev. energy water environ. syst.*, 6(4), pp 631-648, 2018.
14. Kumar, V., Nusselt number and friction factor correlations of three sides concave dimple roughened solar air heater, *Renewable Energy* 135 (2019) 355-377.
15. Kumar, V., Prasad, L., Experimental analysis of heat transfer and friction for three sides roughened solar air heater, *Annales de Chimie - Science des Matériaux*, 75-107, ACSM. Volume 41 - n° 1-2/2017.
16. Kumar, V., Prasad, L., Performance prediction of three sides hemispherical dimple roughened solar duct, *Instrumentation, Mesure, Métrologie*, 273-293 I2M. Volume 17 - n° 2/2018.

## Basic Design of An Anthropomorphic Robotic Arm

Pradeep.S<sup>1</sup>, Hari shankar.S.P<sup>2</sup>, Nandha Kumar.M<sup>3</sup>, Rajeshwaran.T<sup>4</sup>, Karthik.V<sup>5</sup>

<sup>1</sup>Assistant professor, Department of Mechatronics Engineering, SNS College of Technology, Coimbatore

<sup>2,3,4,5</sup>UG Student, Department of Mechatronics Engineering, SNS College of Technology, Coimbatore

**ABSTRACT:** The project is concerned with the design and fabrication of writing bot using the Mechatronics system. As per today's status robotics is a key technology in the modern world and it is an emerging technology in the modern world. It is a bot which automatically writes regarding the voice recognized from the user. The physically challenged people suffer a lot to write the exam, in all the possible way the world improves the technology, it is not useful for the physically challenged people. So that this would help the physically challenged people with an anthropomorphic writing bot. The main components of the project are Arduino, servo motor, voice recognition module, and motor drive. Three micro servo motors are employed to manipulate the motion of the end effector. Two servo motors are used to control the movement of the base and joints of the arm. Thus, the voice recognition module is used to recognize the voice. When the user's voice is recognized by the module it sends a command to the Arduino, and then the Arduino control the servo motor according to the voice the bot will write. This task can be used socially like in the field of industries, court and teaching and it can be as well applied for local purposes, commercial enterprise. The benefit of this writing bot gives more accuracy, less cost, and negligible risks to the people and has a diverse scope in future battlefields.

**Keywords:** Arduino, Servo motor, Voice module, Robotic arm

### I. Introduction

In this chapter, technologies in developing a writing bot based on the Mechatronics system are discussed. One of the most functional system of automation is robotics. This robotic system combined with Mechatronics engineering, mechanical engineering, electrical engineering, and computer engineering to form a complete robotic system. The primary feature of this project is speech recognition i.e., Making the system to understand and interpret human voices. Speech recognition is a technology where the system understands the words (irrespective of the meaning) given through speeches. Speech is an ideal method for robotic control and communication. The speech recognition functions individually and independently from the robot's Processor [Central Processing Unit (CPU)]. This has a positive advantage, because it does not occupy the robot's CPU processing power for word recognition. The CPU must merely poll the speech circuit recognition lines occasionally to check if the command has been sent to the robot.

Robotics is an evolving technology where there are many approaches in building a robot and no one can be certain which method or technology may be used in the far future. Robotics is a converging science which employs the advancement of mechanical engineering, material science, sensor fabrication, manufacturing

techniques, and advanced algorithms. The study of robotics will expose an amateur or a professional to hundreds of different fields of study.

Writing bots are robots that implement the writing character of human hand with the help of suitable controlling devices. In the early 1920s, machine recognition came into existence. The first machine to recognize speech to any significant degree was commercially named as Radio Rex. As the developments were made in the field of machine recognition and robotics, many methods are now available to create a writing bot. IoT being one of the most used tools in today's era. Many writing bot are equipped for making it easy accessible by the users.[1]

The writing bots are created with the prime motto of helping the physically challenged people. The physically challenged people face much problems in writing, especially at the time of examinations. The writing robots help the physically challenged people in a much efficient way than the scribe writers. Moreover, the problem for the need of scribe writers during the exam times can be overcome by using the voice-controlled writing robots.

The writing bots provide a good and satisfactory writing quality. Different writing bots have different writing quality and this writing quality depends on the design, components and

the material used for the development of the writing bot.

The word Anthropomorphic is derived from two Greek words Anthropos meaning human and morpheme meaning form. In other words, Anthropomorphic refers to the attribution of human traits, emotions or intention to non-human entities. Since writing is a characteristic subjected only to humans, the writing bots which implement this human character may be called as anthropomorphic writing bots. Anthropomorphic Robot arms are programmable manipulator with similar functions of the human arm. Several kinds of technology prostheses are available for basic function of a human arm. The aim of the project is to develop a robotic arm which helps the physically challenged person to write with the help of voice commands.

## II. OBJECTIVE

- To design and develop a voice-controlled Anthropomorphic Robotic Arm to write exams for the physically challenged.
- To design a robot to achieve a satisfactory writing quality of characters with simple structures

### A. Problem statement

The physically challenged people are unable to write their exam without any human aid.

Lack of Volunteers during the exam times, so that the physically challenged students are unable to focus on exam preparation and also the timetable and the exam venues are decided so late. Older writers are barred because they may know the subject matter better than the candidate and this could result in an unfair advantage. New Writers are mostly busy preparing for their own exams or having personal works. The entire process of documentation is tedious.

## III. literature review

In this paper, a detailed study of existing methodologies has been gained, based on both kinds of literature. [2]M. A. Anusuyadiscussed a review of the speech recognition by a machine. The author says that even when there are many developments in the field of robotics, the accuracy of the automatic speech recognition still remains a challenge for the developers". Her paper stresses the importance of the definition of various types of speech classes, speech representation, feature extraction techniques, speech classifiers, database, and performance evaluation. The paper deals with the basic model of speech recognition, types of speech recognition, application of speech

recognition and problems faced during the ASR design. This paper also suggests the approaches to speech recognition like Acoustic phonetic approach, Pattern recognition approach, approach, and Artificial Intelligence approach. The author has also given a description of Dynamic Time Wrapping, Vector Quantization, feature extraction, and classifiers. The paper discusses the major themes and advances made in the past 60 years of research, so as to provide a technological perspective[3]. Some of the key methods in the development of speech recognition like Hidden Markov Model, DARPA program, Noisy speech recognition etc., were given in a detailed manner.

[4]M. Balaganesh discussed the Robotic arms showing writing skills by speech recognition. The author has given a clear description of the speech recognition software and hardware part. The software part consists of the speech signal, Mel's cepstral coefficient, Dynamic time wrapping and recognition of isolated words. Speech signals refer to the speech sounds produced due to the airflow from the lungs. Mel's coefficient and dynamic time wrapping are the parameters used for speech recognition. The hardware part of the speech recognition consists of MAX 232 interface, PIC 16F628A, and stepper motors. The MAX 232 is an integrated circuit that converts signals from an RS-232 serial port to signals suitable for use in TTL compatible digital logic circuits. The PIC 16F628A is an 18-Pin Flash-based member of the Versatile PIC16CXX family. The author has also given the algorithm for the working of the robotic arm by speech recognition. The microphone is fitted to the robotic arm. The input is given via the microphone which converts the voice into an electrical signal. A PC sound cord transfers this signal to a MATLAB TOOL BOX where the signal acquisition process takes place. The microcontroller unit converts the text signal from the MATLAB toolbox into mechanical action.

*Robotic Motion and Control:*

[5]Oussama Khatib has discussed the motion and force control of robotic manipulators. This paper deals with the control of manipulator motions and active forces based on the operational space formulation. The fundamentals of operational space formulation have been discussed by the author. The end effector motion control, active force control and force control compensator have been given in a detailed manner along with the necessary equations and diagrams. The behavior of the end effector during any impact has also been discussed by the author. The author has highlighted the COSMOS system along with its architecture. The results of using the COSMOS

system along with the other parameters have been given briefly by the author. The author has also added the graph of Contact Force Time Response using Force Sensing Fingers and the graph of Contact Force Time Response using Force Sensing Wrist. The author has concluded that a higher level of performance can only be achieved by a new design of mechanisms based on the requirements of manipulator force control.

[6] Gianluca Massera has discussed Developing a Reaching Behavior in a simulated Anthropomorphic Robotic Arm Through an Evolutionary Technique. The paper deals with an evolutionary technique for developing a neural network-based controller for an anthropomorphic robotic arm with 4 DOF able to exhibit a reaching behavior. The author has given a detailed explanation about the arms reach. The redundancy potentially allows anthropomorphic arms to reach a target point by circumventing obstacles or by overcoming problems due to the limits of the DOF. The author has also compared the robotic arm with the human hand. The sensors used in the robotic arm has also been discussed. The previous attempts of Bianco and Nolfi (2004) to use evolutionary techniques to develop the controller for a robotic arm has also been discussed. The experimental setup and the angles of simulation of the robotic arm have also been given. The author has also highlighted the importance of the neural controller in the robotic arm. The evolutionary algorithm of the robotic arm has also been given in the paper. The results showing the Performance on reaching a fixed target, Performance on reaching a random positioned target along with the suitable diagram has been given by the author.

[7] Thorsten Stein has discussed the Guidelines for the motion control of Humanoid robots: Analysis and Modelling of Human Movements. This paper deals with the analysis of trajectories of limbs and develops guidelines for motion planning based on task-specific characteristics. Also, a new algorithm is provided to compose these elementary models into large models. The author has given information about complex functionalities like humanoid shape, multimodality, ability to learn etc, For the analysis of human movements, the author suggests the concept of motion patterns. The process of data acquisition and processing of human motion data has also been discussed in the paper. The intro and inter-individual variations of the humans along with the graph has been given by the author. The author has also suggested ways for modeling the characteristics of human movements along with the necessary equations.

Classification of phases in human motion and motion control of the humanoid robot has also been discussed by the author.

[8] Veljko Potkonjak has discussed the Redundancy Problem in Writing: From Human to Anthropomorphic Robot Arm. This paper deals with the analysis of the motion of a redundant anthropomorphic arm during the writing. The Distributed Positioning allows a unique solution of the inverse kinematics of redundant mechanisms such as human arm and anthropomorphic robot arm. The paper shows the reasons why the new approach is adopted from the previous results. The author has shown that a strict relationship exists between the form of trajectory and the (tangential) velocity at which it is executed in handwriting. The author has also shown the Seven-DOF's arm in writing task: three for shoulder, two for the elbow, and two for the wrist. The works of previous authors have also been discussed. The author has shown the different angles and working of different joints of the human arm while writing along with the related diagrams and graphs. The model of the arm-hand complex in writing has been discussed briefly by the author along with the required graphs and calculations. The concept of inclination and legibility, which is an important factor to be considered, has been given in a detailed manner by the author.

[9] Tsuneo Yoshikawa has discussed the Analysis and Control of Robot Manipulators with redundancy. This paper deals with the quantitative measurement of manipulability which is applicable to both redundant and nonredundant manipulators. The Control problems of redundant manipulators have also been discussed in this paper. The measure of manipulability has been explained in a detailed manner by the author with the help of calculations and diagrams. Other topics like Subtasks with Order of Priority, Utilization of Redundancy for Optimizing Given Performance Criterion, Singularity Avoidance and Obstacle Avoidance have also been discussed by the author.

#### *Character Recognition:*

[10] Adlina Taufik Syamlan has discussed the Character Recognition for Writing Robot Control Using ANFIS. Image processing, character recognition, path planning, and theta deduction are dealt with in this paper. Letters are restricted to uppercase and in a form of an image. The image is converted into binary, which then letters are separated to form an image matrix. Image matrix will serve as training data for the neural network. Performances of a neural network are evaluated

using test set prepared, to determine the scope of font recognizable using the neural network. The author has discussed the problems like Effect of size in the neural network, Effect of fonts in the neural network, misclassification, and Feature Boundaries in this paper[11].

[12]Salman Yussof has discussed the Algorithm for Robot Writing using Character Segmentation. The paper deals with a flexible algorithm that can allow a robot to write. This algorithm is based on character segmentation, where the main idea is to store character information as segments and the segment information can then be used by the robot to write. The author has developed a sample application using the proposed algorithm to allow a Mitsubishi RV-2AJ robotic arm to write English characters and numbers. The concepts of character segmentation and character storage has been explained in a detailed manner in this paper. The examples of the character table, segment table, and point table have also been added. The implementation of the algorithm along with the block diagram has also been highlighted.

[13]G. Nagydiscussed the Self-Corrective Character Recognition System. The paper deals with a simple statistical categorizer are used to improve recognition performance on a homogeneous data set. This experimental study of the effect of the various parameters in the algorithm is based on ~30 000 characters from fourteen different font styles. The experimental setup and the algorithm of the self-corrective character recognition system have been discussed briefly. The related graphs were very much helpful in analyzing the errors. The tabular column of different machines provided further knowledge on character recognition.

[14]S.Batmavady has discussed about the Segmentation, Recognition and Synthesis of Tamil characters for Robotic Writing. This paper deals with the two important phases namely, recognition of characters and writing of characters. Recognition is done via polynomial fitting. Each character is probed in a graphical sense and equations are obtained. Basic figures like cycloid, circle, spiral, ellipse, etc are studied and their features are utilised in developing equations. The concepts of character recognition like character recognition, feature extraction and character identification has been discussed clearly by the author. For writing, parametric equations and synthesis of characters has been explained clearly in detail along with the related diagrams. The author has concluded that in this robotic writing, pure equations are employed, it is easy to change the size of the characters and change the

direction of characters with minor modifications in the equations.

[15]Herbert Gish discussed about the Segregation of speakers for speech recognition and speaker identification. This paper deals with the method for segregating speech from speakers engaged in dialogs. The method employs a distance measure between speech segments used in conjunction with a clustering algorithm, to perform the segregation. The paper gives detailed information about the distance between speech utterances and theoretical distribution of the distances in a detailed manner along with the related equations. The result of the papers deals with the distributions as a function of duration. The method of segregating speech application in clustering has also been discussed in this paper.

*Arduino Recognition:*

[16]Dr. AbdellatifBabachas discussed the Robot Arms Control with Arduino. The robot arm in this paper has the ability to move in 4 axis directions with 5 servo motors. The robot control is provided by connecting to the Android application via Bluetooth module connected to Arduino Nano microcontroller. Researches have been done by the author and implemented in order to have knowledge about mechanics and software during the operations carried out by the robot arm which is designed to fulfill the tasks determined in accordance with predetermined commands. Arduino Nano microcontroller written in Java language is programmed and servo motor control is provided. The servomotor is preferred in order to be able to perform these operations properly since the motor to be selected must operate precisely and must be at high torque. Thus, it is possible to perform the desired operations by means of the elements located on the Arduino without any circuit construction other than the circuit where the servo motor inputs are located.

[17]KeerthiPremkumar discussed the Smart Phone-Based Robotic Arm Control Using Raspberry Pi, Android, and Wi-Fi. This paper proposes a method for controlling a Robotic arm using an application build in the Android platform. The Android phone and raspberry pi board is connected through Wi-Fi. The android application is the command center of the robotic arm. The program is written in the Python language in the raspberry board. The different data will control the arm rotation. The hardware and software components of the smartphone-based robotic arm along with its architecture has been given in detail by the author. The driver circuit architecture (Raspberry PIE) has been given by the author. The author has concluded that in smartphone

technique, the delay and server problems are reduced as the Wi-Fi is used which is the fastest usage of internet.

*Methodology:*

[18]Boren Li has discussed the Human-like Robotic Handwriting and Drawing. The paper deals with the three strategies of trajectory planning are considered: the basic stroke method, the Bezier Curve method and the non-gradient numerical optimization method. A nonlinear three-link three-dimensional arm, similar to the human arm, tracks the planned trajectories. The feasibility of these methods is demonstrated by simulation. The basic stroke method and the Bezier curve method have been clearly discussed in this paper along with the diagrams and calculations.

[19]Katrin Franke has discussed the Ink-Deposition Model: The relation of writing and ink deposition processes. The paper describes the studies on the influence of physical and biomechanical processes on the ink trace and aims at providing a solid foundation for enhanced signature analysis procedures. Since the robot is able to take up different writing instruments like a pencil, ball pointer fine line pen, the type of inking pen was also varied in the experiments. The methodology includes the synthesis of ink traces and analysis of ink deposition. The related calculations and the graphs were also given in this paper. The author concluded that the better understanding and analytical modeling of the interaction processes of writing movements, physical ink properties, and ink deposition will allow for the design of appropriate algorithms.

[20]Marius-Florin Crainicdiscusses the Secure handwriting using a robot arm for educational purpose. The paper presents a different approach to facilitate and secure the writing of certificates or traditional grade books. This system uses a robot arm, RV-2AJ, which has a pen attached. After the calibration, the robotic arm can write even if the writing surface is on an inclined plane, or the paper is rotated. This system is more secure than the one that uses the ink printer because the movement of the robot arm to reproduce the font on the paper is unique. Another secure element is the embossing stamp. The embossing stamp is created by changing the pen with a needle. The needle creates small closed holes using a pattern in which the information used for writing is encrypted. The author has highlighted the mathematical concepts for the robot calibration with suitable equations. The author has also given the MATLAB algorithm for the robotic arm. The paper has presented another type of handwriting

using a robotic arm. In order to write the pen must gently touch the paper. For this thing, a calibration was made. So by reading 3 points from the writing plane the equation of the plane can be determined and the Z-axis value calculated in order to compensate the writing plane tilt.

[21]Alejandro Acerohas discussed about the Environmental Robustness In Automatic Speech Recognition. This paper deals with the initial efforts to make SPHINX, the CMU spectral estimates across frequencies. The author proposes novel methods based on additive corrections in the cepstral domain. In the first algorithm, the additive correction depends on the instantaneous SNR of the signal. In the second technique, EM techniques are used to best match the cepstral vectors of the input utterances to the ensemble of based on additive corrections in the cepstral domain. The author has given detailed information about the Model of the Environment, SNR-Dependent Cepstral Normalization and Codeword-Dependent Cepstral Normalization. The Codeword-Dependent Cepstral Normalization has been further discussed further which includes MMSE Estimator of the Cepstral Vector, ML Estimation of Noise and Spectral Tilt and Implementation. The related graphs has also been given which was very useful.

*Design:*

[22]Ashraf Elfasakhany has discussed the Design and Development of a Competitive Low-Cost Robot Arm with Four Degrees of Freedom. The paper deals with the design, development, and implementation of a competitive robot arm with enhanced control and stumpy cost. The robot arm is equipped with several servo motors which do links between arms and perform arm movements. The servo motors include encoder so that no controller was implemented. To control the robot we used LabVIEW, which performs inverse kinematic calculations and communicates the proper angles serially to a microcontroller that drives the servo motors with the capability of modifying the position, speed, and acceleration. The robotic design along with the inverse kinematics have been briefed by the author with suitable diagrams and calculations. The selection of components like material to be used, servo motors, end effector selection etc., were also discussed in the paper.

[23]Jamshed Iqbaldiscussed the Modeling and Analysis of a 6 DOF Robotic Arm Manipulator. This paper deals with the kinematic models a 6 DOF robotic arm and analyzes its workspace. the end-effector of the robotic arm can point to the desired coordinates within the precision of  $\pm 0.5\text{cm}$ . The

approach presented in this work can also be applied to solve the kinematics problem of other similar kinds of robot manipulators. The kinematic model, which includes forward, and inverse kinematics has been discussed in a detailed manner by the author along the related calculations. The workspace analysis has also been discussed briefly

Kumar et al. [24-30] has used three sides instead of one side roughened duct & found that augmentation in Nu & f was respectively to be 21-86 % & 11-41 %. They also reported augmentation in thermal efficiency of three sides over one side roughened duct to be 44-56 % for varying p/e and 39-51 % for varying e/D<sub>h</sub>.

**Existing system**

The Existing system is a speech recognizing system. Speech recognition is the process of capturing spoken words using a microphone or telephone and converting them into a digitally stored set of words. The quality of a speech recognizing the system is assessed according to two factors: Its accuracy (Error rate in converting spoken words to digital data) and speed (How well the software can keep up with the human speaker. The Existing methodology is shown in Fig 1

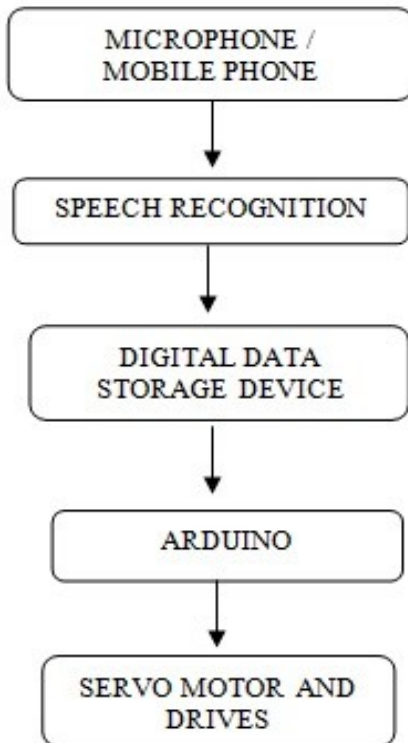


Figure 1

**A. Disadvantage of existing system:**

1. Even the best speech recognition sound in the room (Ex. Television or Radio), the no. of error will be increased.
2. Speech recognition works best if the microphone is close to the user (Ex. In a phone or if the user is wearing a microphone). More distant microphones (Ex. On a table or Wall) will tend to increase the no. of errors. system sometime makes error. If there is a noise or some other
3. In speech recognition system there is a possibility of unauthorized usage. Since this does not depend upon which person is speaking.
4. No password protection.

**Proposed system**

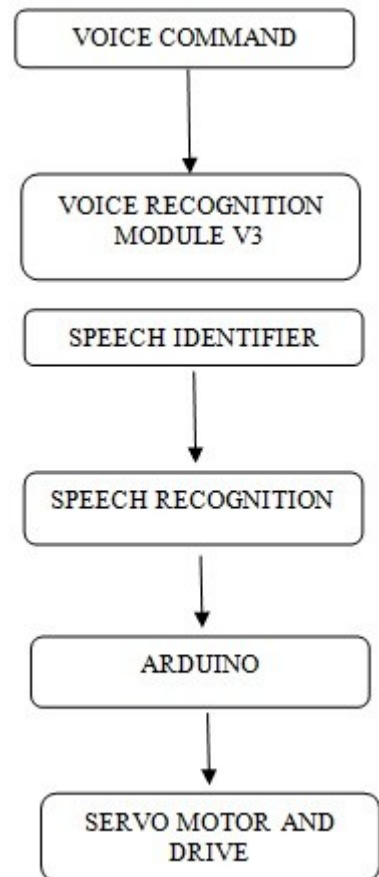


Figure 2 Proposed System

**IV. COMPONENTS**

The selection of materials involves the study of their Characteristics, advantages, availability, cost, user friendly property of components that we want to use.

### A. Selection of components:

The selection of materials involves the study of their Characteristics, advantages, availability, cost, user friendly property of components that we want to use. In our project, we select each and every component, by study thoroughly about them. By proceeding like that only, we have done our selection.

- The software and device chosen to program the execution of our idea is Arduino microcontroller.
- Servomotors
- Elechouse voice recognition module
- Servo motor drive
- Mechanical links for robot arm

The detailed description for selecting components below

### B. Arduino:

The Arduino mega 2560 is a microcontroller board based on the ATmega2560. It has 54 digital input/output pins (of which 14 can be used as PWM outputs), 16 analog inputs, 4 UARTs

(hardware serial ports), a 16MHz crystal oscillator, a USB connection, a power jack, an ICSP header, and reset button. It contains everything needed to support the microcontroller; simply connect it to a computer with a USB cable or power it with an AC-to –DC adapter or battery to get started. The Mega is compatible with most shields designed for the Arduino Duemilanove or Diecimila. The Arduino board is shown in Fig 3

Arduino can sense the environment by receiving input from a variety of sensors and can affect its surroundings by controlling lights, motors, and other actuators. The microcontroller on the board is programmed using the Arduino programming language (based on wiring) and the Arduino development environment (based on processing). Arduino projects can be stand-alone or they can communicate with software on running on a computer (e.g. flash, processing, MaxMSP).



Figure 3 Arduino Mega 2560(www.arduino.cc)

The board can operate on an external supply of 6 to 20 volts. If supplied with less than 7V, however, the 5V pin may supply less than 5V and the board may be unstable. If using more than 12V, the voltage regulator may overheat and damage the board. The recommended range is 7 to 12 volts.

### C. The Five Major Benefits of Using Arduino Starter Kits:

**Inexpensive:** - Arduino boards are relatively inexpensive compared to other microcontroller platforms. The least expensive Version of Arduino module can be assembled by hand, and even the pre-assembled Arduino modules cost less than Rs. 1000.

**Cross platform:** -The Arduino software runs on Windows, Macintosh OSX, and Linux operating systems. Most Microcontrollers systems are limited to windows.

**Simple, clear programming environment:** - The Arduino programming environment is easy-to-use for beginners, yet flexible enough for advanced users to test advantage of as well. For teachers. It's conveniently based on the processing programming environments. So students learning to program in that environment will be familiar with the look and feel of Arduino.

**Open credits and extensible software:** - The Arduino software is published as open credits tools available for extension by experienced programmers. The language can be expanded through C++ libraries, and people wanting to understand the technical details can make the leap from Arduino to the AVR C programming languages on which it's based. Similarly, you can add AVR-C code directly into Arduino program if you want to.

**Open credits and extensible hardware:** - The Arduino is based on Atmel's ATMEGA8 and ATMEGA168 microcontroller. The plans for the modules are published under a creative common license, so experienced circuit designers can make their own version of the module, extending it and improving it. Even relatively inexperienced users can build the breadboard version of the module in order to understand how it works and save money.

### D. DC SERVO MOTOR:

A servo is a device, electrical or mechanical or electro-mechanical, that upon receipt of stimulus or input, will employ feedback for velocity and/or position control, creating a closed loop.

#### Servo Motor:

There are three micro servos are used to control the movement of end effector such as

“pitch” control servo motor, “yaw” control servo motor, and “roll” control servo motor. Pitch servo motor control the up and down movement. Yaw servo motor control the side to side movement. Roll servo motor control the rotating movement. Two servo motors are used to control the movement of joints and base. Thus, the base and joint servo motors control the rotational movement.

*Working Principle of DC Servo Motor:*

A DC servo motor is an assembly of four major components, namely a DC motor, a position sensing device, a gear assembly, and a control circuit. Shown in fig 4.



Figure 0(www. robu.in)

The below figure shows the parts that consisting in RC servo motors in which small DC motor is employed for driving the loads at precise speed and position.

*Internal diagram:*

A DC reference voltage is set to the value corresponding to the desired output. This voltage can be applied by using another potentiometer, control pulse width to voltage converter, or through timers depending on the control circuitry. The dial on the potentiometer produces a corresponding voltage which is then applied as one of the inputs to error amplifier. In some circuits, a control pulse is used to produce DC reference voltage corresponding to desired position or speed of the motor and it is applied to a pulse width to voltage converter. In this converter, the capacitor starts charging at a constant rate when the pulse high. Then the charge on the capacitor is fed to the buffer amplifier when the pulse is low and this charge is further applied to the error amplifier. So the length of the pulse decides the voltage applied at the error amplifier as a desired voltage to produce the desired speed or position. In digital control, microprocessor or microcontroller are used for

generating the PWM pluses in terms of duty cycles to produce more accurate control signals. Thus the internal diagram of servo motor is shown in figure 5.

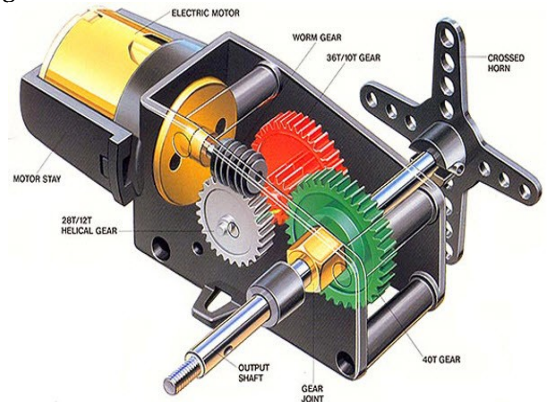


Figure 5 Servo Motor (www. visualgasin.wordpress.com)

The feedback signal corresponding to the present position of the load is obtained by using a position sensor. This sensor is normally a potentiometer that produces the voltage corresponding to the absolute angle of the motor shaft through gear mechanism. Then the feedback voltage value is applied at the input of error amplifier (comparator). The error amplifier is a negative feedback amplifier and it reduces the difference between its inputs. It compares the voltage related to current position of the motor (obtained by potentiometer) with desired voltage related to desired position of the motor (obtained by pulse width to voltage converter), and produces the error either a positive or negative voltage. This error voltage is applied to the armature of the motor. If the error is more, the more output is applied to the motor armature. As long as error exists, the amplifier amplifies the error voltage and correspondingly powers the armature. The motor rotates till the error becomes zero. If the error is negative, the armature voltage reverses and hence the armature rotates in the opposite direction.

*Fundamental characteristics:*

- The motor output torque should be proportional to the voltage applied to it
- The direction of torque developed by the servo-motor should be dependent upon the instantaneous polarity of the control voltage

*Specification:*

- Weight: 55g
- Dimension: 40.7 × 19.7 × 42.9 mm

- Operating Speed (4.8V no load): 20sec / 60 deg
- Operating Speed (6.0V no load): 16sec / 60 deg (no load)
- Stall Torque (4.8V): 10kg/cm
- Stall Torque (6.0V): 12kg/cm
- Operation Voltage: 4.8 - 7.2Volts
- Gear Type: All Metal Gears
- Stable and shock proof double ball bearing design
- Dead band width: 5  $\mu$ s
- Temperature range: 0  $^{\circ}$ C – 55  $^{\circ}$ C.
- Control System: Analog
- Operating Angle: 120degree
- Required Pulse: 900us-2100us

### **E. Why we select the servo motor?:**

There are two types of motors that primarily stand out. These choices are a standard DC motor and a signal-controlled servomotor, both of which have their own advantages and disadvantages. Advantages to the DC motor include a full 360-degree range of motion, one input, and the availability of high torque. However, there are large drawbacks when used in a controlled environment. The largest of these drawbacks is the low precision. The motor is either ON or OFF where speed can be adjusted based on the input. In order to accurately control the position a highly accurate microcontroller will most likely be needed. Another large drawback is the significant cost of higher torque motors.

Advantages to the signal-controlled servos include a lower cost when compared to DC motors, a signal-controlled position, and multiple similarly previous projects to be the starting point of research. Like DC motors, the signal-controlled servos have drawbacks. The largest drawback to servo motors is quickly increasing cost for the increase in torque. Another large drawback is that most stock servo motors only have a 90-degree range of motion. To gain a 180-degree, range of motion additional charges may apply.

In order to keep the low cost, low torque and simplicity high, servo motors were chosen to control the pitch, yaw, and roll of the wrist.

### **F. Servo Control Method:**

Most standard servos have three leads, position power, negative, and signal. The power lead not only acts as the power source for the servo but can also be utilized to turn the servo either on or off. The typical input voltage for power is between 4.8 volts and 6.0 volts. The negative power lead should be common ground.

The signal lead will control the direction of the servo.

The primary method of controlling the servo is to send a pulse-width modulation along the signal lead. This pulse-width modulation signal is a fifty hertz square width, the length of each pulse of the square wave controls how far the servo will rotate. For example, a pulse of 600 microseconds will rotate the servo arm -90 degrees and a 2400 microsecond pulse will rotate the arm positive 90 degrees.

### **G. Open Loop Versus Closed Loop:**

For a servo motor, there is a significant difference in an open loop and closed loop control system. In an Open loop control servo control system, the pulse widths control how far the servo rotate in a specified amount of time. In other words, the length of the pulse width modulation controls how fast the servo rotates, not position. For example, a 600-microsecond pulse may rotate the servo 90 degrees counter-clockwise in 0.15 seconds while a 1000 microsecond pulse may rotate the servo 45-degree counter-clockwise in the same 0.15.

In a close loop servo control system, the length of each pulse controls the position, instead of how fast the servo rotates. For example, a 600-microsecond pulse may rotate the servo to the 90 degrees' counter-clockwise position in 0.15 seconds while a 1000 microsecond pulse may rotate the servo to the 45-degree counter-clockwise position in 0.075 microseconds

Most standard servo motor can only rotate 90 degrees and can be stretched to 180 degrees for an additional cost. These rotational limitations are placed by a potentiometer built into the servo motor. As the potentiometer rotates with the servo, the voltage across the potentiometer changes allowing this voltage change to be used for feedback to control the position. The potentiometer can be disconnected to achieve a full 360-degree continuous rotation, however the feedback to control the position is lost and an external circuit will be required. Since it was specified that the base will rotate below 180 degrees, a continuous rotation is unneeded; this allow for the utilization of the built-in closed loop system.

### **H. Digital versus Analog Servos:**

Like many components in the electronics world, servo motors come in standard analog and digital varieties. Functionally speaking, a digital servo is a standard analog motor with a built-in microprocessor that analysis incoming signals to control the motor. Digital servos have two distinct advantages over their analog counter parts. With

the built-in microprocessor, the servo performance can be better optimized depending on servos function. Also because of the built-in microprocessor, the pulse width modulation sent from the microprocessor operates at a higher frequency than the standard 50Hz used for analog servos. This leads to higher accuracy, smoother acceleration, and the availability to hold higher torque. However, because of the addition of the microprocessor the servo comes with disadvantages. Since the digital servo operates at a higher frequency for higher accuracy, the power consumption also increases. The price of digital servos is also significantly higher than their analog counter parts.

**I. PSU:**

A power supply unit (or PSU) converts mains AC to low voltage regulated DC power for their internal components of a computer. Modern personal computers universally use switched-mode power supplies. Some power supplies have a manual switch for selecting input voltage, while others automatically adapt to the mains voltage. The components that supplies power to a computer. Most personal computers can be plugged into standard electrical outlets. The power supply then pulls the required amount of electricity and converts the AC current to DC current. There are three major kinds of power supplies; unregulated (also called brute force), linear regulated, and switching. A fourth type of power supply circuit called the ripple-regulated, is a hybrid between the "brute force" and "switching" designs and merits a subsection to itself. The PSU board as shown in Fig 6

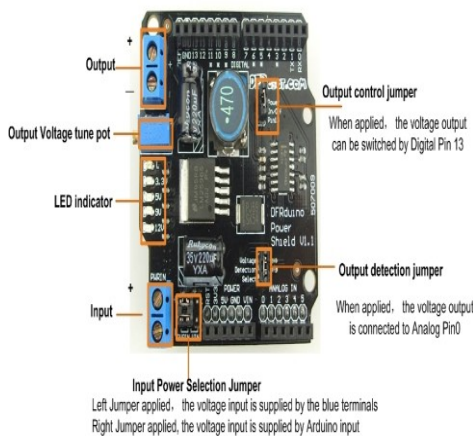


Figure 6 Power Supply Unit(www.robotshop.com)

**J. Voice Recognition Module:**

Voice recognition is a technique that facilitates natural and convenient human machine interface using the voice recognition module. It extracts and analyses voice features of human and

delivered to machine or computer through Mic. Voice recognition technique is classified into many types based on different criteria such as scope of the users, number of words used for recognition, naturalness of speaking. If the voice recognition level is more than 95%, then only the voice recognition is practically used.

**K. Voice recognition module V2:**

Voice recognition module V2 supports 50 commands in all and only 5 commands at the same time. On V2, voice commands are separated into three groups while you training it. And only one group (5 commands) could be imported into recognizer. It means only five voice commands at the same time.

**K. Voice recognition module V3:**

Elechouse voice recognition module (Fig.7) is compact and easy control speaking recognition board. It Arduino compatible. This product is a speaker dependent voice recognition module support up to 80 voice command in all. Maximum seven voice commands could work at same time. Any sound could be trained as a command. User need to train the module first before let it recognizing any voice command.



Figure 7 Elechouse Voice Recognition Module V3 (www.potentiallabs.com)

This board has two controlling ways: serial port (full function), general input things (part of function). General output pins on the board could generates several kinds of waves while corresponding voice command is recognized. On V3, voice commands are stored in large group like a library any seven voice commands in the library could be imported into recognizer. It means seven commands are effective at the same time.

It works under voltage 5.5 volts and less than 40 milliamps. It has both analog and digital interface. In digital interface has five volts TTL level for UART interface and GPIO. In analog interface has 3.5 mm mono channel microphone connector + microphone pin interface. It supports maximum 80 voice commands, it each voice 1500 milliseconds (one or two words speaking). It has

seven voice command at a same time. It supports Arduino library. It is easy to control the UART and GPIO, it has user control general pin output. It accuracy level is 99% under ideal environment.

**L. Why we choose the voice recognition module V3:**

It supports 80 voice commands and are stored in one large group and easy to control the UART, GPIO and recognize seven voice command at same time. It's accuracy level is high compared with V2.

**M. Servo Motor Drive:**

Driving servo motor with the Arduino servo library is pretty easy in servo drive PCA 9685 (Fig 8), but each one consumes a precious pin-not to mention some Arduino processing power. The Adafruit 16 channel 12-bit PWM/servo driver will be drive up to 16 servos over 12C with only 2 pins. The on-board PWM controller will drive all 16 channels simultaneously with no additional Arduino processing overhead. What's more, you can chain up to 62 of them to control up to 992 servos -all with the same two pins.

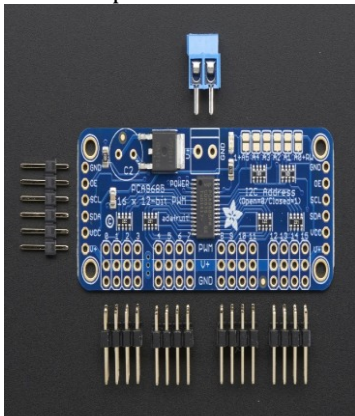


Figure 8 Adafruit PCA9685 Servo Drive  
([www.adafruit.com](http://www.adafruit.com))

The Adafruit PWM/servo driver is the perfect solution for any project that requires a lot of servos.

The pin diagram is shown in fig 9.

**M. Pin outs:**

There are two set of control input pins on either side. Both sides of the pins are identical. Use whichever side you like, you can also easily chain by connecting up two side-by-side.

**M. Power pins:**

GND-This the power and signal ground pin, must be connected.

VCC-This is the logic power pin, connected this to the logic level you want to use for the PCA 9685 output, should be 3 to 5 volts maximum. It also used for the 10 k pullups on SCI/SDA so unless you have your own pullups, have it match the microcontroller's logic level to do.

V+ - this is an optional power pin that will supply distributed power to the servos if your not using for servos you can leave disconnected. It is not used at all by the chips. You can also inject power from the 2-pin terminal block at the top of the board. You should provide 5-6 volt DC if your using servos. If you have to, you can go higher to 12volt DC, but if you mess up and connect VCC to V+ it would damage your board.

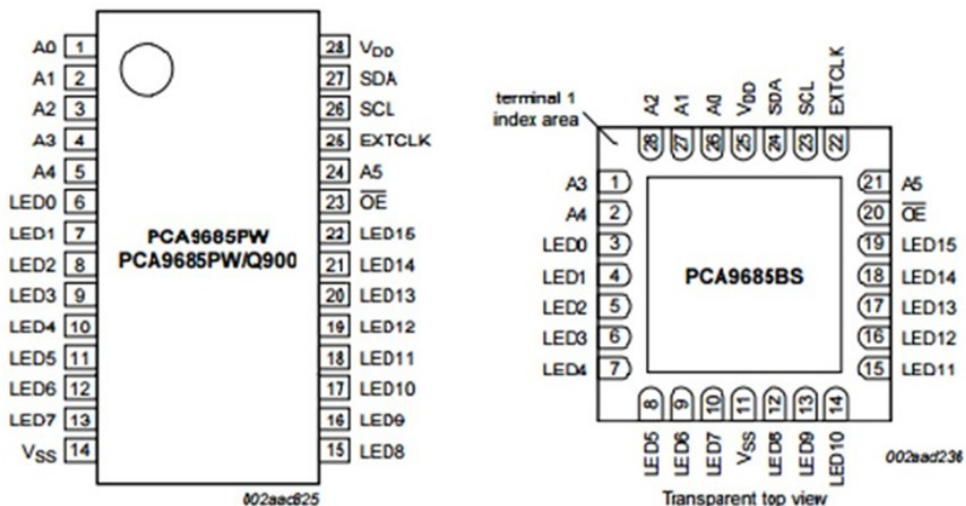


Figure 9 Pin Diagram of PCA9685([www.adafruit.com](http://www.adafruit.com))

The PCA9685 is a 16-channel I2C-bus controlled LED controller optimized for Red/Green/Blue/Amber (RGBA) colour backlighting applications. Each LED output has individual 12-bit resolution (4096 steps) PWM controller with a fixed frequency. The controller operates at a programmable frequency from a typical 24 Hz to 1526 Hz with a duty cycle that is adjustable from 0% to 100% so the LED can be set to output a specific brightness. All outputs are set to the same PWM frequency.

With the PCA9685 as the master chip, the 16-channel 12-bit PWM Servo Driver only needs 2 pins to control 16 servos, thus greatly reducing the occupant I/Os. Moreover, it can be connected to 62 driver boards at most in a cascade way, which means it will be able to control 992 servos in total. The pin diagram is shown in Fig 4.7

#### **Q. Control pins:**

SCL-12c clock pin, connect to your microcontrollers 12C clock line. Can use 3v or 5v logic, and has a weak pullup to VCC

SDA-12Cdata pin, connect to your microcontrollers 12C data line. Can use 3v or 5v logic and has a weak pullup to VCC.

OE-output enable. It can be used to quickly disable all outputs. when this pin is low all pins are enabled. When the pin is high the outputs are disabled.

#### **R. Output Ports:**

There are 16 output ports. Each pot has 3 pins: V+, GND and the PWM output. Each PWM runs completely independently but they must all have the same PWM frequency. There are 220ohm resistors in series with all PWM pins and the output logic is the same as VCC.

After the text edit has been completed, the paper is ready for the template. Duplicate the template file by using the Save As command, and use the naming convention prescribed by your conference for the name of your paper. In this newly created file, highlight all of the contents and import your prepared text file. You are now ready to style your paper; use the scroll down window on the left of the MS Word Formatting toolbar.

#### **Design**

The design of the robotic arm is fully based on the SCARA type. Its full form is "SELECTIVE COMPLIANCE ASSEMBLY ROBOT ARM". It is similar in construction to the jointed arm robot is shown in fig 10, except the shoulder and elbow rotational axis are vertical. It means that the arm is very rigid in a vertical direction and complicated in horizontal direction. Its arm

was rigid in Z the axis pliable in the XY- axes, which allowed it to adapt to holes in the XY-axes.

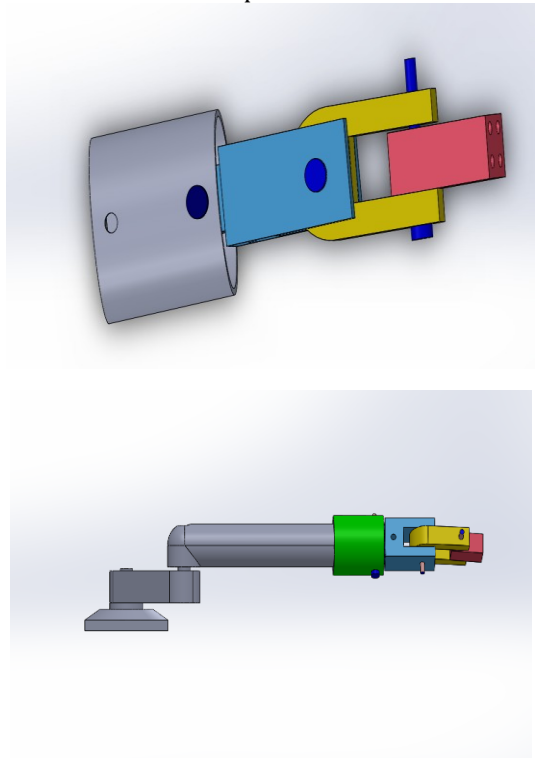


Figure 10 Wrist Design (UP) & Arm (DOWN)

By virtue of the SCARA's parallel-axis joint layout, the arm is compliant in the X-Y direction but rigid in the Z direction, hence the term: selective compliant. This is advantageous for many types of assembly operations, i.e., inserting a round pin in a round hole without binding.

#### **S. Solid Works:**

Solid works software is solid modeling computer aided design (CAD) and computer aided engineering (CAE). Solid works programs for calculations, error, structure, and failure analysis, the premium package is a verifiable autonomous collective. Specifically, SWIFT technology (solid works intelligent future technology) allows the user to automate various time-consuming task and techniques, "diagnosing and resolving problems related to future order, mates, sketch relationship and application of dimensions". Seemingly becoming a trend in a quality CAD software, solid works premium offers a variety of add-ons and additional programming asides from its traditional drawing capabilities. One such program is simulationXpress, a design validation tool that is included within every box of solid works ("how can be design better products using solid works?" 1). This program incorporates real

world physics into an easy functional early detection design flaw widget. Research suggest that solid works is a company on the rise. Engineering placement agencies denote that the demand for solid work tool and skills is over twice that of comparable design pack

### Conclusion

The Anthropomorphic writing bot has been designed in the type of modified SCARA by using the software SolidWorks. The selection of components for the writing bot has also been completed. The ideologies which are like the proposed system are studied carefully and the merits, demerits are taken into consideration. However, the general procedure for taking care of design will need extra caution during the time of implementation.

### REFERENCES

1. Pradeep, S., et al., Iot and its connectivity challenges in smart home, in International Research Journal of Engineering and Technology. 2016. p. 1040-1043.
2. Anusuya, M. and S.K.J.a.p.a. Katti, Speech recognition by machine, a review. 2010.
4. Yasodharan, R., R. Sivabalakrishnan, and P. Devendran, Trusted Routing with an Efficient Certificate Revocation for Mobile Ad Hoc Network.
5. Balaganesh, M., et al. Robotic arm showing writing skills by speech recognition. in Emerging Trends in Robotics and Communication Technologies (INTERACT), 2010 International Conference on. 2010. IEEE.
6. Khatib, O. and J. Burdick. Motion and force control of robot manipulators. in Robotics and Automation. Proceedings. 1986 IEEE International Conference on. 1986. IEEE.
7. Massera, G., A. Cangelosi, and S. Nolfi. Developing a reaching behaviour in a simulated anthropomorphic robotic arm through an evolutionary technique. in Artificial Life X: Proceeding of the Tenth International Conference on the simulation and synthesis of living systems (Cambridge, MA, MIT Press). 2006.
8. Stein, T., et al., Guidelines for motion control of humanoid robots: Analysis and modeling of human movements. 2006. 5: p. 15-30.
9. Potkonjak, V., et al., Redundancy problem in writing: from human to anthropomorphic robot arm. IEEE Trans Syst Man Cybern B Cybern, 1998. 28(6): p. 790-805.
10. Yoshikawa, T. Force control of robot manipulators. in Robotics and Automation, 2000. Proceedings. ICRA'00. IEEE International Conference on. 2000. IEEE.
11. Syamlan, A.T., H. Nurhadi, and B. Pramujati. Character recognition for writing robot control using anfis. in Advanced Mechatronics, Intelligent Manufacture, and Industrial Automation (ICAMIMIA), 2015 International Conference on. 2015. IEEE.
12. Kousalya, T., et al., Study and Implementation of Fault Diagnosis in Induction Motor Using MCSA.
13. Yussof, S., A. Anuar, and K. Fernandez. Algorithm for robot writing using character segmentation. in Information Technology and Applications, 2005. ICITA 2005. Third International Conference on. 2005. IEEE.
14. Nagy, G. and G.J.I.T.o.I.T. Shelton, Self-corrective character recognition system. 1966. 12(2): p. 215-222.
15. Batmavady, S., K. Manivannan, and P.C. Janvier. Segmentation, Recognition and synthesis of tamil characters for robotic writing. in Conference on Computational Intelligence and Multimedia Applications, 2007. International Conference on. 2007. IEEE.
16. Gish, H., M.-H. Siu, and R. Rohlicek. Segregation of speakers for speech recognition and speaker identification. in Acoustics, Speech, and Signal Processing, 1991. ICASSP-91., 1991 International Conference on. 1991. IEEE.
17. Mohamed Ahmed Ghiet, A. and A. Baba, ROBOT ARM CONTROL WITH ARDUINO. 2017.
18. Premkumar, K. and K.G.J. Nigel. Smart phone based robotic arm control using raspberry pi, android and Wi-Fi. in Innovations in Information, Embedded and Communication Systems (ICIIECS), 2015 International Conference on. 2015. IEEE.
19. Li, B., et al. Human-like robotic handwriting and drawing. in Robotics and Automation (ICRA), 2013 IEEE International Conference on. 2013. IEEE.
20. Franke, K. and S. Rose. Ink-deposition model: The relation of writing and ink deposition processes. in Frontiers in Handwriting Recognition, 2004. IWFHR-9 2004. Ninth International Workshop on. 2004. IEEE.
21. Crainic, M.-F., et al. Secure handwriting using a robot arm for educational purpose. in Methods and Models in Automation and Robotics (MMAR), 2014 19th International Conference On. 2014. IEEE.
22. Acero, A. and R.M. Stern. Environmental robustness in automatic speech recognition. in Acoustics, Speech, and Signal Processing, 1990. ICASSP-90., 1990 International Conference on. 1990. IEEE.
23. Elfasakhany, A., et al., Design and development of a competitive low-cost robot arm with four degrees of freedom. 2011. 1(02): p. 47.
24. Iqbal, J., et al., Modeling and analysis of a 6 DOF robotic arm manipulator. 2012. 3(6): p. 300-306.
25. Kumar, V., Prasad, L., Experimental investigation on heat transfer and fluid flow of air flowing under three sides concave dimple

- roughened duct. International Journal of Mechanical Engineering and Technology (IJMET), Volume 8, Issue 11, November 2017, pp. 1083-1094, Article ID: IJMET\_08\_11\_110.
26. Kumar, V., Prasad, L., Thermal performance investigation of one and three sides concave dimple roughened solar air heaters. International Journal of Mechanical Engineering and Technology (IJMET) Volume 8, Issue 12, December 2017, pp. 31-45, Article ID: IJMET\_08\_12\_004.
27. Kumar, V., Prasad, L., Performance Analysis of three sides concave dimple shape roughened solar air heater, J. sustain. dev. energy water environ. syst., 6(4), pp 631-648, 2018.
28. Kumar, V., Nusselt number and friction factor correlations of three sides concave dimple roughened solar air heater, Renewable Energy 135 (2019) 355-377.
29. Kumar, V., Prasad, L., Experimental analysis of heat transfer and friction for three sides roughened solar air heater, Annales de Chimie - Science des Matériaux, 75-107, ACSM. Volume 41 - n° 1-2/2017.

## Domestic Oil Extraction Machine

Anand.M<sup>1</sup>, Manimaran R<sup>2</sup>, Praveen Kumar.M<sup>3</sup>, Sujith Bhrathi.S<sup>4</sup>

<sup>1</sup>Assitant Professor, Department of Mechatronics Engineering,SNS College of Technology,  
Coimbatore, Tamilnadu-641035

<sup>2,3,4</sup>UG-Student, Department of Mechatronics Engineering,SNS college of Technology,  
Coimbatore, Tamilnadu-641035

---

**ABSTRACT:** For years and times, we have been using the Edible oil from various vegetable seeds like coconut, groundnut, mustard and various other seeds. In modern days the oils which we are using are mostly got from the petroleum extract called as paraffin. It is being very unsafe using all extracted from petroleum products which leads to various health problems like cancer, heart problems, paralysis and other problems associated with other health issues. In olden days our ancestors have used the oil extracted from the traditional oil extraction machines. The process of extracting oil from seeds using traditional oil extraction machine requires a large number of seeds to process the oil. It is good being used oil which is been extracted by traditional oil extraction machine and also it gives an assurance that it is been produced only using oil seeds not by any other Petroleum products. The cooking tradition of each and every home mainly depends upon the edible oils without the oil no cooking process could be carried down and also it is not also affordable for every home to have seeds in large numbers to crush seeds that could not be affordable to spend money for oilseeds in a middle-class family where 1kg of oilseeds costs around Rs 100 and daily salary of an individual is Rs 400 per day. But the usage of edible is a mandatory in Indian Cooking style and a person to live.

**Keywords:** Oil expeller, Screw type method, Domestic purpose, Good for health.

---

### Introduction:

For years and times, we have been using the Edible oil from various vegetable seeds like coconut, groundnut, mustard and various other seeds. In modern days the oils which we are using are mostly got from the petroleum extract called as paraffin. It is being very unsafe using all extracted from petroleum products which leads to various health problems like cancer, heart problems, paralysis and other problems associated with other health issues. In olden days our ancestors have used the oil extracted from the traditional oil extraction machines. The process of extracting oil from seeds using traditional oil extraction machine requires a large number of seeds to process the oil. It is good being used oil which is been extracted by traditional oil extraction machine and also it gives an assurance that it is been produced only using oil seeds not by any other Petroleum products.

### Method:

This project deals with a different method of oil extraction by using twin screw expeller mechanically. Mechanical pressing is the most popular method of oil separation from vegetable oilseeds in the world (Mrema& McNulty, 1985). In India, nearly 90% of the total 24 million tonnes of produced oilseeds are crushed using this method. The main reason for popularity of mechanical oil expellers in India as well as in other developing

countries is that these equipments are simple and sturdy in construction, can easily be maintained and operated by semi-skilled supervisors, can be adapted quickly for processing of different kinds of oilseeds, and the oil expulsion process is continuous with product obtained within a few minutes of start of the processing operation.

### System Analysis:

#### Existing System:

The current existing wooden oil extraction machine and other industrial oil expeller machine cost very high and only can be used in large scale operation with a capacity of 10-20kg only. Also, the cost of machine is too expensive so that it can be bought only for professional use and it is large in size also so that it occupies large place. This type of machine is widely used all over places only in industries this wooden oil extraction machine uses 3 phase electricity power supply so that it needs industrial power supply. It has a large size drum so that it is hard to rotate it uses a 35HP gear box at time of carelessness in operating the machine it leads to breakage of bones by misplacing the hand inside the drum. It also comes with wooden drum and Crushing roller which had a drawback makes the oil get expired soon without proper cleaning. The wood has a drawback of breaking down at time of heavy load.

#### Disadvantages in The Existing System:

- 1.The current existing wooden oil extraction machine and other industrial oil expeller machine cost very high
- 2.The system can only be used in large scale operation with a capacity of 10-20kg.

#### **Proposed System:**

This project deals with a different method of oil extraction by using twin screw expeller mechanically. Mechanical pressing is the most popular method of oil separation from vegetable oilseeds in the world (Mrema& McNulty, 1985). In India, nearly 90% of the total 24 million tonnes of produced oilseeds are crushed using this method. The main reason for popularity of mechanical oil expellers in India as well as in other developing countries is that these equipments are simple and sturdy in construction, can easily be maintained and operated by semi-skilled supervisors, can be adapted quickly for processing of different kinds of oilseeds, and the oil expulsion process is continuous with product obtained within a few minutes of start of the processing operation

Extraction efficiency was better with Lot II. Tests also involved preheating the sunflower seeds of Lot II to 50, 60, and 75 °C before extraction. There was a large improvement in expeller capacity and oil output compared to seeds processed at room temperature. One source of renewable energy currently being investigated around the world for use in internal combustion engines is vegetable oil. Oil-type sunflower and the oil obtained from this seed has been shown to be a possible alternative to diesel fuel. If sunflower oil does become a practical alternative energy source, the farmer may not only grow his own fuel source, but also extract the oil from the sunflower seed. Figure 1 shows the steps involved in a small processing system.

Most of the hulls are removed in a large commercial operation because they speed machine wear, contain little oil, and the processed meal with hulls is high in fiber. Extraction efficiency was better with Lot II sunflower seeds than with Lot I sunflower seeds at room temperature (22 °C). Overall expeller capacity and oil output were 40% greater with Lot I than with Lot II sunflower seeds. Preheating the sunflower seeds had a dramatic impact on expeller performance.

This system totally helps all individuals in to this machine in every home. Every machine will be provided at a cheap cost affordable for all peoples. The minimum quantity of seeds required in this machine is 250 Grams to 500 Grams. So that all peoples are affordable in crushing oil and using it for daily needs. Our innovation is going create a

revolution the edible oil industry. Our machine will be placed in all homes like as mixture grinder and other home appliances to extract oil from seeds.

#### **Advantages of proposed system:**

- 1.The proposed system uses domestic motors and other small household size components
- 2.This intern reduces the size and cost of the product and capacity could be reduce to 1-2 kg.

#### **Project Description:**

In olden days our ancestors have used the oil extracted from the traditional oil extraction machines. The process of extracting oil from seeds using traditional oil extraction machine requires a large number of seeds to process the oil. It is good being used oil which is been extracted by traditional oil extraction machine and also it gives an assurance that it is been produced only using oil seeds not by any other Petroleum products.

Speaking in terms of efficiency Expeller processing cannot remove every last trace of liquid (usually oil) from the raw material. A significant amount remains trapped inside of the cake left over after pressing. In most small-scale rural situations this is of little or no importance, as the cake that remains after the oil has been removed finds uses in local dishes, in the manufacture of secondary products, or for animal feed. Some raw materials, however, do not release oil by simple expelling, the most notable being rice bran. In order to remove oil from commodities that do not respond to expelling or to extract the final traces of oil after expelling, it is necessary to use solvent extraction.

The cooking tradition of each and every home mainly depends upon the edible oils without the oil no cooking process could be carried down and also it is not also affordable for every home to have seeds in large numbers to crush seeds that could not be affordable to spend money for oilseeds in a middle-class family where 1kg of oilseeds costs around Rs 100 and daily salary of an individual is Rs 400 per day. But the usage of edible is a mandatory in Indian Cooking style and a person to live.

#### **Conclusion and Result:**

Thus, the proposed system on “Automated Domestic Oil Expeller” is successfully completed its phase I with a complete literature survey. Also, in accordance with the survey made and with the idea on the proposed system the design and the component selection of the product is done and verified successfully.

By adopting this project into use

- Delay will be reduced and process will be speed up.

- The price that is invested can be reduced.

## REFERENCES

- N. Prakash Babu, P. Pandikumar, S., Anti-inflammatory activity of *Albizia lebeck* Benth., an ethnomedicinal plant, in acute and chronic animal models of inflammation: 9 March 2009 *Journal of ethnopharmacology*, 2009 – Elsevier.
- Isaac Bamgboye and A.O.D. Adejumo., Development of a Sunflower Oil Expeller, September, 2007, *Agricultural Engineering International: the CIGR Journal*.
- Soto, R. Chamy, M.E. Zuñiga \* Escuela de., Enzymatic hydrolysis and pressing conditions effect on borage oil extraction by cold pressing., January 2006; *Journal of ethnopharmacology*, 2006 - Elsevier
- Hasan h. ALI dr. Roger fales., Inlet metering pump analysis and experimental evaluation with application for flow control., 12 July 2018, *Renewable Energy*, 2018 – Elsevier.
- Chokchai mueanmas, ruamporn L., Extraction and esterification of waste coffee grounds oil as non-edible feedstock for biodiesel production., 7 september 2018 *Renewable and Sustainable Energy Reviews*, 2009 – Elsevier.
- Lahai koroma, T.B.R. Yormah, L.M. Kamara, G.M.T. Robert., Extraction, utilization, characterization and confirmation of the structure of gorli oil from the dry seeds of the traditional medicinal plant *caloncoba echinata* in sierra leone, Volume 2 issue 8, august 2018, *Journal of ethnopharmacology*, 2009 – Elsevier.
- Adeeko, K. A. and Ajibola, O.O. (1980). "Processing Factors Affecting Yield and Quality of Mechanically Expressed Groundnut Oil". *Journal of British Society of Research in Agricultural Engineering*. Vol.45. No. 1. pp31
- Ajibola, O.O., Eniyemo, S.E, Fasina, O.O and Adeeko, K.A. (1990). Mechanical Expression of Oil from Melon Seeds. *Journal of British Society of Research in Agricultural Engineering*. Vol.45. No. 1. pp 45.
- Akinoso, R., Igbeka, J.C., Olayanju, T. and Bankole, L. (2006). "Modeling of Oil Expression from Palm Kernel (*Elaeis guineensis* Jacq.)". *Agricultural Engineering International: the CIGR Ejournal*. Manuscript FP 05 016. Vol. VIII. October, 2006.
- Canˆeque, V., Velasco, S., Sancha, C., Manzaneres, O., & Souza, O. (1998). Effect of moisture and temperature on the degradability of fiber and on nitrogen fractions in barley straw treated with urea. *Animal Feed Science Technology*, 74, 241–258.
- Berti, M., Wilckens, W., Fischer, S., & Araos, R. (2002). Borage. A new crop for Southern Chile. In J. Janick & A. Whipkey (Eds.), *Trends in new crops and new uses* (pp. 501–505). Alexandria: ASHS Press.
- Bocevskaa, M., Karlovic, D., Turkulov, J., & Pericin, D. (1993). Quality of corn germ oil obtained by aqueous enzymatic extraction. *Journal of American Oils Chemists' Society*, 70, 1273–1277.
- Kumar, V., Prasad, L., Experimental investigation on heat transfer and fluid flow of air flowing under three sides concave dimple roughened duct. *International Journal of Mechanical Engineering and Technology (IJMET)*, Volume 8, Issue 11, November 2017, pp. 1083–1094, Article ID: IJMET\_08\_11\_110.
- Kumar, V., Prasad, L., Thermal performance investigation of one and three sides concave dimple roughened solar air heaters. *International Journal of Mechanical Engineering and Technology (IJMET)* Volume 8, Issue 12, December 2017, pp. 31–45, Article ID: IJMET\_08\_12\_004.
- Kumar, V., Prasad, L., Performance Analysis of three sides concave dimple shape roughened solar air heater, *J. sustain. dev. energy water environ. syst.*, 6(4), pp 631-648, 2018.
- Kumar, V., Nusselt number and friction factor correlations of three sides concave dimple roughened solar air heater, *Renewable Energy* 135 (2019) 355-377.
- Kumar, V., Prasad, L., Experimental analysis of heat transfer and friction for three sides roughened solar air heater, *Annales de Chimie - Science des Matériaux*, 75-107, ACSM. Volume 41 – n° 1-2/2017.
- Kumar, V., Prasad, L., Performance prediction of three sides hemispherical dimple roughened solar duct, *Instrumentation, Measure, Métrologie*, 273-293 I2M. Volume 17 – n° 2/2018.

## Autonomous Swarm Robots

T.Kousalya<sup>1</sup>, K.M. Aarsha Suresh<sup>2</sup>, K.Nivethithaan<sup>3</sup>, Terrin J. Mario Pereria<sup>4</sup>, Dilshad Bin Mohammed Iqbal<sup>5</sup>

<sup>1</sup>Assistant Professor, <sup>2,3,4,5</sup>UG Scholar

Department of Mechatronics Engineering, SNS College of Technology, Coimbatore-35

---

**ABSTRACT:** This paper aims to illustrate and a network of autonomous robots that can work and act together for performing various tasks and operations. Swarm-bots are a collection of mobile robots that can self-assemble and self-organize in order to solve problems that cannot be solved by a single robot. These robots combine the power of swarm intelligence with the flexibility of self-reconfiguration as aggregate swarm-bots can dynamically change their structure to match environmental variations. Swarm robots are more than just networks of independent agents, they are potentially reconfigurable networks of communicating agents capable of coordinated sensing and interaction with the environment. Robots are going to be an important part of the future. In the near future, it may be possible to produce and deploy large numbers of inexpensive, disposable, meso-scale robots. Although limited in individual capability, such robots deployed in large numbers can represent a strong cumulative force similar to a colony of ants or swarm of bees. Various methods of designing and fabrication is done to implement such bots. Once it's a success many of these will be developed for helping and improving the lifestyle of mankind.

**Keywords:** swarm robotics, autonomous robots, robotic communication, machine vision

---

### I. Introduction

AUTONOMUS SWARM ROBOTS: In the 21st Century, robotics has become ubiquitous in all spheres of human activity. Ranging from industry to science to home care. Robots have heralded on of the biggest changes to human life. Robots have taken over hundreds of tasks that humans find either repetitive or dangerous. From industrial welding to space exploration robots have enabled humans to achieve more with less. In industries, robots have completely supplanted humans in various fields including welding, machining etc. The concept of automatons performing dangerous or mundane tasks was even known to the ancient Greeks and Egyptians. In Greek mythology, the legend Cadmus refers to the man who was created of clay and was "breathed into life by man". The most famous of all myths involving artificial humans was that of Pygmalion, in which a sculptor falls in love with a sculpture he had made and brings it to life. The ancient Greek inventor Hero of Alexandria is said to have made the earliest sketches for a fully working model of a mechanical automaton that was said to be powered by steam. But sadly, those sketches were said to have been destroyed when the Library of Alexandria was burned down in 5th Century AD. In China, the fabled metalsmith Yan Shi is said to have designed Mannequins that had the many human-like organs.

Despite the various advances in the field of robotics, robots in the modern day look very utilitarian and less like the robots as depicted in fiction. Modern robots are extremely efficient and fast in various tasks. But these robots tend to be task oriented than being universally i.e. they are made to fulfil one particular task say Welding or Assembly tasks. Modern robots are also employed in wide range of tasks and applications ranging from Education to Industry and Military to Space Exploration. Each robot created is unique and can do the tasks that they were built for in an exceedingly efficient way. Androids as depicted in Science fiction are still a dream, but many researchers are finding ways to make that dream a reality.

Robots in the Information age come in many types and sizes. They range from extremely small such as nano-robots which are very small (typically 1 nanometre across) to automated excavators the size of skyscrapers. The main usage of robots is in industries where the works is quite risky and dangerous.

The main problems faced in robotic systems is the lack of communication among the robots, human intervention needed to carry out tasks, current limitation in software and hardware technology makes the robots primitive.

The solution to this problem can addressed by the concept of swarm robots (Figure 1.1). This has helped us in developing better robots. The

communication among the robots is brought about by using different wireless ways. Some of these wireless communications are:

- Wireless multi-hop communications
- Node mobility
- Networked robots
- Machine-to-machine communications

## II. Literature Review

### ➤ SWARM ROBOTICS

#### 1. Swarm robotics, a review from the swarm engineering perspective

(Manuele Brambilla et al. 2013)<sup>[22]</sup> suggested that swarm robotics as could be an engineering field and that would help to tackle real-world applications. They also noted down the goals which are to be considered for modelling, designing, realizing, verifying, validating, operating, and maintaining a swarm robotic system.

#### 2. Research Advance in Swarm Robotics

(Ying Tan & Zhong-yang Zheng 2013)<sup>[21]</sup> differentiated elaborately between a single robot and a multi-individual robotic system. The descriptive differentiation underlines the advantages of a swarm robotics system. In their paper the main emphasis is about the current research on the swarm robotic algorithms are presented in detail, including cooperative control mechanisms in swarm robotics for flocking, navigating and searching applications.

#### 3. Autonomous Self-Assembly in Swarm-Bots

(Roderich Grob et al. 2005)<sup>[14]</sup> observed the difference in performance of between single robot and of groups of robots self-assembling with an object or another robot. The robustness of the system with respect to different types of rough terrain were also assessed by them.

### ➤ SWARM INTELLIGENCE ALGORITHMS

#### 4. Robots, insects and swarm intelligence

(Amanda J. C. Sharkey 2006)<sup>[15]</sup> The relationships between robots and insects has been explained in two main areas of robotics research i.e., through the behavioral pattern of insects. The development in robotics has been brought by studying the working methodology and characteristics of the insects. It is concluded that bio-robotic modelling and biological inspiration have made important contributions to both insect and robot research, but insects and robots remain separated by the divide between the living and the purely mechanical.

#### 5. Ant Colony Optimization Algorithm for Robot Path Planning

(Michael Brand et al. 2010)<sup>[18]</sup> Path planning is an essential task for the navigation and motion

control of autonomous robot manipulators. The ACO (Ant Colony Optimization) algorithm is an optimization technique based on swarm intelligence. Two different pheromone re-initialization schemes are compared and computer simulation results are presented.

### SPHERICAL ROBOTS

#### ➤ A Literature Review on the Design of Spherical Rolling Robots

(Vincent A. Crossley 2006)<sup>[16]</sup> A spherical robot design is said to be holonomic, which means it can move in any direction. This increases the options for navigating around objects and prevents the robot from getting stuck in corners, but they cannot be over tuned. Stairs and ledges are not an issue for the spherical robots due their features. They have a great capability to recover from collisions with obstacles. This would be useful in a swarm application, where many spheres could be traveling in close proximity, and because of the design they would not interfere with each other's motion. They can be designed to be totally sealed and are also ideal for hazardous environments. The sensors, electronics, and mechanisms are all protected. This makes them capable of functioning in snow, mud, and even water. Spherical robots be assisted or powered by winds. They can also be smaller than wheeled vehicle, and can be made cheaper with fewer parts, or they could even be disposable. Kumar et al. [25-30] has used three sides instead of one side roughened duct & found that augmentation in  $Nu$  &  $f$  was respectively to be 21-86 % & 11-41 %. They also reported augmentation in thermal efficiency of three sides over one side roughened duct to be 44-56 % for varying  $p/e$  and 39-51 % for varying  $e/D_h$ .

## III. SYSTEM DESIGN

In the newly proposed system (*Figure 3.4*), the external shell is not connected to the central axis directly, instead the robot will be connected to the frame enabling the shell to move like a wheel. The use of 1 gyroscope instead of 2 and the use of high torque motors and drives will prevent the unwanted secondary boost. Along with this improvement there will also be a NRF Module will enable communication with other robots and it has an Arduino for automated movement and control. To put differently, the robot can move and interact with other robots on its own.

### Advantages of the Proposed System

- The use of high torque motors will prevent the realignment of the gyroscopes and prevent unwanted boost in torque.

- It is autonomous and can communicate with other robots using nRF204L01 module (Figure 2)
- It is cheap to construct and has a simple design

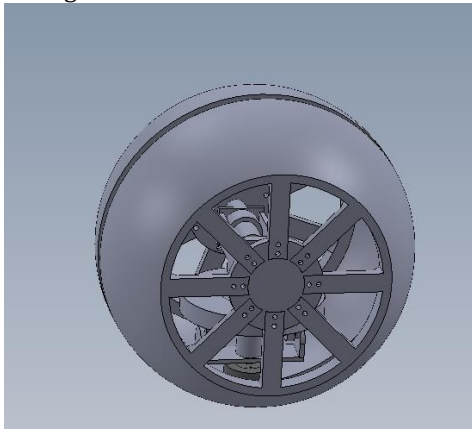


**Fig 1: Proposed Model (Designed using SolidWorks 2016)**

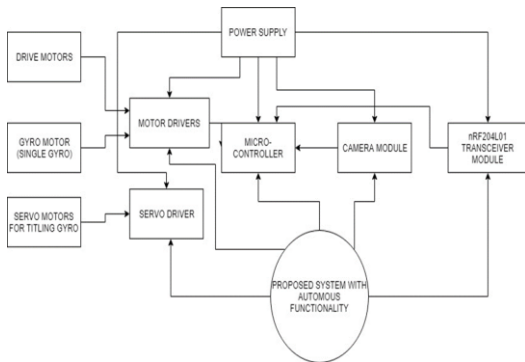


**Fig 2: Block Diagram of Proposed System**

**IV. Design and Construction of the Robot**

Mathematical Calculation was done using the data from the CAD Model to find the Angular Momentum of the Gyro Rotor. So as to verify the selection of the servo motor which is responsible for tilting the spin axis of the gyro-rotor.  
 Moment of Inertia of Gyro Rotor =  $6.58427 \times 10^{-3} \text{ Kgm}^2/\text{sec}$ .

<b>Angular momentum (L)</b>
Formula: $L = I * \omega$ $\omega = 2618 \text{ rad/sec}$ $I = 2.515 \times 10^{-6} \text{ kg.m}^2$ $L = (2.515 \times 10^{-6}) * 2618$
<b>L = <math>6.58427 \times 10^{-3} \text{ Kgm}^2/\text{sec}</math>.</b>
<b>Moment of Inertia (I)</b>

Formula: $I = 1/2 * M * R^2$ $M1 = 200\text{g Or } 0.200\text{kg}$ $R1 = 50\text{mm Or } 0.005\text{m}$ $I1 = 1/2 * M1 * [R1]^2$ $I1 = 1/2 * 0.200 * [0.005]^2$ $I1 = 2.5 \times 10^{-6} \text{ kg.m}^2$	Formula: $I = 1/2 * M * R^2$ $M2 = 30\text{g or } 0.030\text{kg}$ $R2 = 10\text{mm or } 0.001\text{m}$ $I2 = 1/2 * M2 * [R2]^2$ $I2 = 1/2 * 0.030 * [0.001]^2$ $I2 = 1.5 \times 10^{-8} \text{ kg.m}^2$
---	--

**I = I1 + I2**  
**I =  $2.5 \times 10^{-6} + 1.5 \times 10^{-8}$**

**Angular Velocity ( $\omega$ )**

Formula:  $\omega = (\theta_f - \theta_i) * t$   
 $\theta_f = 25000 \times 2\pi$   
 $\theta_i = 0$   
 $t = 60 \text{ sec}$

**$\omega = (25000 * 2\pi) / 60$**   
**=  $2618 \text{ rad/sec}$**

Parameters	Formula	Description
<b>Angular Momentum of Gyro Rotor</b>	$L = I * \omega$	Where, L = angular momentum I = moment of inertia $\omega$ = angular velocity
<b>Moment of Inertia</b>	$I = 1/2 * M * R^2$	Where, M = Mass R = Radius
<b>Angular Velocity</b>	$\omega = (\theta_f - \theta_i) * t$ (in radsec-1)	Where, $\theta_f$ = final angle $\theta_i$ = initial angle t = time

**V. Conclusion**

The Work plan for Project Phase - 1 was followed. The Literature Review and Component Identification was done successfully. Mathematical Calculations and Virtual Simulations were done with positive result. The Prototype was fabricated and was tested, there was some room for improvement to be made with the prototype as the outer hemispherical shell could not be manufactured properly. The prototype functioned successfully other than the earlier mentioned flaw.

**References**

1. Chemel, Brian, Edward Mutschler, and Hagen Schempf. "Cyclops: Miniature robotic reconnaissance system." Robotics and

- Automation, 1999. Proceedings. 1999 IEEE International Conference on. Vol. 3. IEEE, 1999. Rybski, Paul E., Dean F. Hougen, Sascha A. Stoeter, Maria Gini, and Nikolaos Papanikolopoulos.
2. Yim, M., Duff, D.G., Roufas, K.D.: PolyBot: a modular reconfigurable robot. In: Proceedings of the 2000 IEEE International Conference on Robotics and Automation (ICRA 2000). Volume 1, IEEE Press, Piscataway, NJ (2000) 514–520
  3. Castano, A., Shen, W.M., Will, P.: CONRO: Towards deployable robots with inter-robot metamorphic capabilities. *Autonomous Robots* 8 (2000) 309–324
  4. Khosla, P., Brown, B., Paredis, C., Grabowski, B., Navarro, L., Bererton, C., Vandeweghe, M.: Millibot Report. Report on millibot project, DARPA contract DABT63-97-1-0003, Carnegie Mellon University, Pittsburgh, Pennsylvania, USA (2002)
  5. S. Bhattacharya, S.K. Agrawal (Proceedings 2000 ICRA. Millennium Conference. IEEE International Conference on Robotics and Automation. Symposia Proceedings (Cat. No.00CH37065), 06 August 2002, DOI: 10.1109/ROBOT.2000.844763)
  6. Mojabi, Puyan. (Robotics and Automation, 2002. Proceedings. ICRA'02. IEEE International Conference on. Vol. 4. IEEE, 2002)
  7. Sahin, E., Labella T.H., Trianni, V., Deneubourg, J.L., Rasse, P., Floreano, D., Gambardella, L.M., Mondada, F., Nolfi, S., Dorigo, M.: SWARM-BOT: Pattern formation in a swarm of self-assembling mobile robots (2002). In: Proceedings of the IEEE International Conference on Systems, Man and Cybernetics, IEEE Press.
  8. Camazine S, Deneubourg JL, Frank NR, Sneyd J, Theraulaz G, Bonabeau E. Self-organization in biological systems (2003). Princeton: Princeton University Press;.
  9. Groß, R., Dorigo, M.: Cooperative transport of objects of different shapes and sizes. In Dorigo, M., Birattari, M., Blum, C., Gambardella, L.M., Mondada, F., Stützle, T., eds.: Proceedings of ANTS 2004 – Fourth International Workshop on Ant Colony Optimization and Swarm Intelligence. Volume 3172 of Lecture Notes in Computer Science., Springer Verlag, Berlin, Germany (2004) 107–118
  10. Labella, T., Dorigo, M., Deneubourg, J.L.: Efficiency and task allocation in prey retrieval. In Ijspeert, A., Murata, M., Wakamiya, N., eds.: Proceedings of the First International Workshop on Biologically Inspired Approaches to Advanced Information Technology (Bio-ADIT2004). Volume 3141 of Lecture Notes in Computer Science., Springer Verlag, Heidelberg, Germany (2004) 32–47
  11. Labella, T., Dorigo, M., Deneubourg, J.L.: Self-organised task allocation in a swarm of robots. Technical Report TR/IRIDIA/2004-6, Université Libre de Bruxelles, Belgium (2004) To appear in the 7th International Symposium on Distributed Autonomous Robotic Systems (DARS04), June 23-25, 2004, Toulouse, France.
  12. Trianni, V., Nolfi, S., Dorigo, M.: Hole avoidance: Experiments in coordinated motion on rough terrain. In Groen, F., Amato, N., Bonarini, A., Yoshida, E., Kröse, B., eds.: *Intelligent Autonomous Systems 8*, IOS Press, Amsterdam, The Netherlands (2004) 29–36
  13. Sahin E. Swarm robotics: from sources of inspiration to domains of application. In: *Swarm robotics (2005)*, lecture notes in computer science, vol. 3342. Springer. p. 10–20.
  14. Roderich Grob, Michael Bonani, Francesco Mondada, Marco Dorigo (Proceedings of the 3rd International Symposium on Autonomous Minirobots for Research and Edutainment (AMiRE 2005) pg. 314-322.)
  15. Amanda J. C. Sharkey (Artificial Intelligence Review, December 2006, Volume 26, Issue 4, pp 255–268)
  16. Vincent A. Crossley (Pittsburgh, Pa (2006): 1–6.)
  17. Dervis Karaboga, Bahriye Akay (Artificial Intelligence Review, June 2009, Pg. 31:61)
  18. Michael Brand, Michael Masuda, Nicole Wehner, Xiao-Hua Yu (2010 International Conference On Computer Design and Applications, 09 August 2010, DOI: 10.1109/ICCCA.2010.5541300)
  19. Park, G. D., Lee, H., Kim, K. H., & Lee, J. M. ((2011, November). Ubiquitous Robots and Ambient Intelligence (URAI), 2011 8th International Conference on (pg. 511-515). IEEE.)
  20. Chase, R., & Pandya, A. (2012). A review of active mechanical driving principles of spherical robots. *Robotics*, 1(1), 3-23.
  21. Tan, Y., & Zheng, Z. Research Advance in Swarm Robotics (2013). *Defence Technology*, 9(1), 18–39.
  22. M. Brambilla, et al. Swarm Robotics: A Review from a Swarm engineering Perspective (2013), *Swarm Intelligence*, 7(1), 1-41.
  23. Tamer Abukhalil, et al. Survey on Decentralized Modular Swarm Robots and Control Interfaces (2013). *International Journal of Engineering*, 7(2), 44-59.
  24. Micheal Rubenstein et al. Programmable self-assembly in a thousand robot swarm (2014). *Science*, 345, 795-799.
  25. Kumar, V., Prasad, L., Experimental investigation on heat transfer and fluid flow of air flowing under three sides concave dimple roughened duct. *International Journal of Mechanical Engineering and Technology*

- (IJMET), Volume 8, Issue 11, November 2017, pp. 1083-1094, Article ID: IJMET\_08\_11\_110.
26. Kumar, V., Prasad, L., Thermal performance investigation of one and three sides concave dimple roughened solar air heaters. International Journal of Mechanical Engineering and Technology (IJMET) Volume 8, Issue 12, December 2017, pp. 31-45, Article ID: IJMET\_08\_12\_004.
27. Kumar, V., Prasad, L., Performance Analysis of three sides concave dimple shape roughened solar air heater, J. sustain. dev. energy water environ. syst., 6(4), pp 631-648, 2018.
28. Kumar, V., Nusselt number and friction factor correlations of three sides concave dimple roughened solar air heater, Renewable Energy 135 (2019) 355-377.
29. Kumar, V., Prasad, L., Experimental analysis of heat transfer and friction for three sides roughened solar air heater, Annales de Chimie - Science des Matériaux, 75-107, ACSM. Volume 41 - n° 1-2/2017.
30. Kumar, V., Prasad, L., Performance prediction of three sides hemispherical dimple roughened solar duct, Instrumentation, Mesure, Métrologie, 273-293 I2M. Volume 17 - n° 2/2018.

# POULTRY FARM MONITORING AND CONTROLLING USING PLC WITH INTERNET OF THINGS

Mr. A Vishnu<sup>1</sup>, Sheshaghiri N<sup>2</sup>, Joeresh Julius A<sup>3</sup>, Sathish Kumar A<sup>4</sup>, Satharth Noorul Hassan<sup>5</sup>

<sup>1</sup>Assistant professor, Department of Mechatronics Engineering, SNS College of Technology  
<sup>2,3,4,5</sup>Final year student, Department of Mechatronics Engineering, SNS College of Technology

## 1. INTRODUCTION:

The poultry farm is one of the major contributions to the world economy. More than 50 billion chickens are raised annually as a source of food. An average human consumes 70 pound (appx) of chicken in a year. The consumption of the chickens is gradually increasing day by day. According to ICRA's estimate per capita meat consumption is around 3.6 kg per annum which puts total broiler meat market size at Rs.730 billion in terms of retail price. The egg production is at 84 billion eggs translating to a per capita egg consumption of 63 eggs per annum. One of the key roles involved in the development of human civilization is in the area of agriculture. With the continuing increase in the world's population, the demand for food supply is extremely raised. Applying engineering processes to poultry farming may help to maximize the benefit to human kind in terms of cheaper and plentiful availability as well as contribute to the growth of the economy. India is world's second largest emerging economy and along with it has rapidly growing poultry sector. Poultry is one of the fastest growing sectors in India with an average growth rate of 12 % for broiler production per annum. The environment conditions of farms basically affect initial growth of livestock that means there is weight loss in birds, so farmers do not get appropriate weight of birds at the end which is not profitable for farmers. Especially farmers are lagging in field of automation and control conditions of farms. The most of scale poultry farms are situated in rural areas lagging in technology. So, the technology in the poultry automation would result in high production rate and increase in economy of the country. The labor for this humongous sector is a problem faced now a day so we decided to automate the complete process like egg hatching, feeding system, watering system, temperature control, medicine system. So, for this system we have proposed of using a Mitsubishi PLC and a HMI system

collaborated with an IOT system. The PLC system is chosen because the of the input, temperature and life features of the PLC. The whole action can be single handedly controlled by the PLC. The IOT system is enabled for increasing the communication with the poultry owner. The wireless HDMI touch display system is used for continuous monitoring. The whole system can be stopped by using a google assistant voice control system.

Kumar et al. [11-16] has used three sides instead of one side roughened duct & found that augmentation in Nu & f was respectively to be 21-86 % & 11-41 %. They also reported augmentation in thermal efficiency of three sides over one side roughened duct to be 44-56 % for varying p/e and 39-51 % for varying e/D<sub>n</sub>.

## 2. OBJECTIVE

- To provide continuous monitoring and complete automation of the poultry farm which helps to avoid adverse effect on livestock
- Power consumption is being reduced as using of solar panel
- Every updates will be intimated to the user on the system being progressed through SMS.
- Using of Google assistant the entire process is also been controlled.

## 3. EXISTING METHODOLOGY

### 3.1 SYSTEM ANALYSIS

This chapter reviews the system and related studies in the world of poultry, Existing system and The Feature of poultry automation.

### 3.2 EXISTING SYSTEM

In an existing temperature control system the most of the poultry farming uses the traditional method of heating like using boilers to heat up the farm. For the cooling system, water is sprayed inside the farm by using the fogger. Most of the time chicken died with external climatic

conditions, the light or the boilers fixed inside the farm doesn't provide the sufficient heat to a farm. The death rate of chicken is high in the existing method of farming. The shortage of workers is also a problem faced by a poultry owner's. The workers works inside the farm get affected by many diseases and birds as well.

**3.3 DEMERITS IN THE EXISTING SYSTEM**

- i. Death rate of chicken is high
- ii. Efficiency of the current system is very low
- iii. Lack of workers
- iv. Infection for both humans and chickens
- v. Maintaining the temperature is tedious process

**3.4 CHALLENGES FACED BY THE POULTRY INDUSTRY**

Constraints have been identified in the areas of husbandry, feeding and health, availability of inputs, information and credit. The negative effects of the hot climatic conditions of the sub-region have also been a challenge. Adverse effects of excessive exposure to high temperatures include excessive panting, poor growth and development of birds and reduced egg production and size, and lower egg shell quality. It is very disappointing that the poultry industry has been plagued by large imports of day old chickens, eggs and feed despite the availability of local birds which are more sumptuous, nutritious and healthy.

**3.5 DEMERITS OF EXISTING FARMING**

But despite its clear advantages in terms of profitability and affordability, the batter cage system and similar intensive farming techniques also come with disadvantages. Most notably, chickens and hens in intensive poultry farming often suffer from different conditions and pain. A lot of intensively reared chickens suffer from lameness as a result of fast growth, a result of selective breeding and concentrated feed. In addition, the way the cages are designed and as the chickens grow, their droppings accumulate on the floor. When the droppings decompose, ammonia is released. The ammonia then fills the air with unhealthy fumes and this puts chickens at risk of incurring painful blisters, hock burns or ulcerated feet.

**4. METHODOLOGY**

**4.1 PROPOSED SYSTEM**

The labor for this humongous sector is a problem faced now a day so we decided to automate the complete process like egg hatching, feeding system, watering system, temperature control,

medicine system. So for this system we have proposed of using a PLC and a HMI system collaborated with an IOT system. The IOT system is enabled for increasing the communication with the poultry owner. The wireless HDMI touch display system is used for continuous monitoring. The whole system can be stopped by using a Google assistant voice control system.

**4.2 FEATURES OF THE FARM HOUSE AUTOMATION SYSTEM ARE:**

- Automatic lighting
- Climate control
- Fire and smoke detection
- Humidity and moisture control
- Feeder control
- Remote mobile connectivity
- Instant alert system

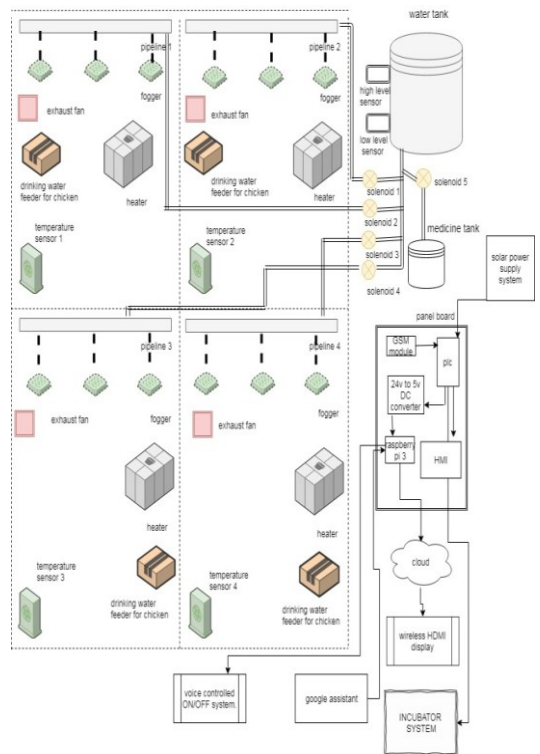


Figure 1 Conceptual diagrams for proposed system

**5. COMPONENTS AND SYSTEM DESIGN**

This section will discuss about the system design and the electronic components that had been used in the system process.

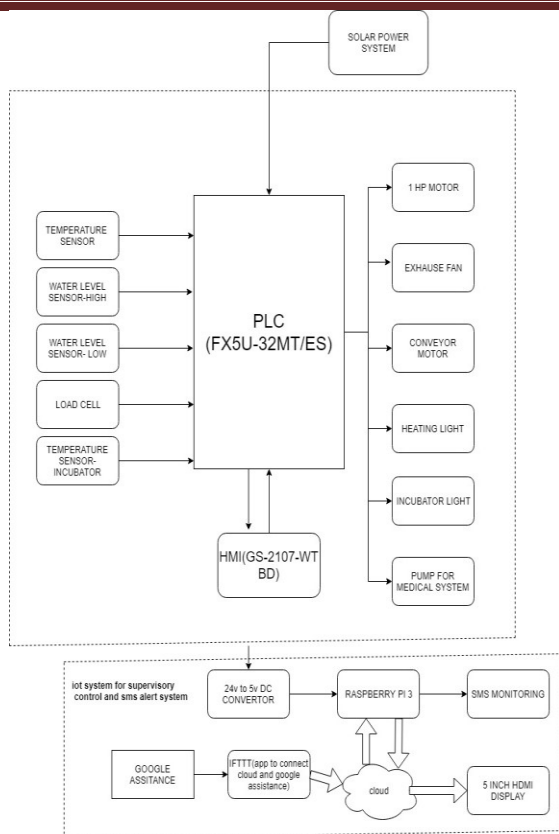


Figure 2 Functional block diagram

## 6. COMPONENTS

### 6.1 TOOLS REQUIRED

1. Languages
  - a. Ladder logic
2. GX WORK3 (fx series plc)
3. ESP8266.
4. F- Series PLC
5. HMI

### 6.2 FX5U-32MT/ES

The first model in the iQ-F series is the FX5U, offering high performance in a compact, cost effective package. The FX5U continues the FX tradition of total flexibility by offering a huge range of new and existing add-on options which further enhance the built-in functions of Ethernet, analogue I/O, data logging, position control, security, communications and networking functions incorporated as standard.

The FX5U will provide users with the ability to specify more powerful systems but with fewer overall components, saving time and cost.

- FX5U CPU base units with very fast processing time
- Versions with up to 256 inputs and outputs

- Expanded input/output area for networks and complex applications
- Can be upgraded by combining with expansion modules
- Built-in SD card slot
- Run/Stop/Reset switch
- Built-in Ethernet port, RS485
- Displays the input and output states via LEDs
- Integrated real-time clock
- Programming software GX Works3

### 6.3 GS-2107-WTBD (HMI)

Mitsubishi Electric GOT2000 HMIs provide the user with a comprehensive range of options to ensure application or process is covered. Comes equipped with a high speed CPU for responsive HMI operation even under high load processes including logging and device data transmission. Supporting a wide variety of communication options including RS232, RS485/422 and Ethernet making this series of HMI very versatile

- Premium processor coupled with expanded memory
- Multi-touch operation
- Wide variety of communication functions to ensure your application is covered
- Double the speed for monitoring & booting of previous generation
- Simplified setup and debugging controls for simple setup
- Supports a wide variety of image formats, including PNG

### 6.4 FR-D720S-255-EC (VFD)

• Simple cabling, the integrated spring clamps connect control and power lines quickly which ensures reliability and simple cabling.

• Easy parameterization software FR-Configuration encourages easy functions such as graphical machine analysis to optimize the drive system.

• An integrated digital dial gives the user direct access to all of the important parameters.

• The integrated four digit LED display monitors and displays current operating values and alarm messages.

• Features a second transistor output which is sink selectable source logic safety input instead of sink logic.

• Directly connect to PLC's instead of safety relays.

• Features a Sensor-less vector control which enables exceptional speed and torque performance.

• Serial interface (RS485) as standard.

• Emergency safe stop input compliant to EN 61800-5-2.

- Maximum short-term overload capacity of 200% for 0.5s.
- Automatically restart after power failures.

### **6.5 MR-JE-20A (SERVO DRIVE)**

- Advance one touch tuning
- Instantaneous power failure override
- Large capacity drive recorder
- Absolute position detection system
- Performance Features;
- SSCNET III/H
- Fast and accurate
- high resolution encoder
- Energy conservation

### **6.6 ESP8266**

The ESP8266 Wi-Fi Module is a self-contained SOC with integrated TCP/IP protocol stack that can give any microcontroller access to your Wi-Fi network. The ESP8266 is capable of either hosting an application or offloading all Wi-Fi networking functions from another application processor. Each ESP8266 module comes pre-programmed with an AT command set firmware, meaning, you can simply hook this up to your Arduino device and get about as much Wi-Fi-ability as a Wi-Fi Shield offers.

The ESP8266 module is an extremely cost effective board with a huge, and ever growing, community. This module has a powerful enough on-board processing and storage capability that allows it to be integrated with the sensors and other application specific devices through its GPIOs with minimal development up-front and minimal loading during runtime. Its high degree of on-chip integration allows for minimal external circuitry, including the front-end module, is designed to occupy minimal PCB area.

## **7. SOFTWARE SPECIFICATION**

### **7.1 GX WORKS 3**

- It is the latest generation of programming and maintenance
- Software offered by Mitsubishi Electric specifically designed for the
- MELSEC IQ-R Series control system.
- It includes many new features such as graphic-based system configuration, integrated motion control setup,
- Multiple language support, providing an intuitive engineering environment solution.

### **7.2 ARDUINO IDE**

The Arduino integrated development environment (IDE) is a cross-platform application (for Windows, macOS, Linux) that is written in the programming language Java. It is used to write

and upload programs to Arduino board. The source code for the IDE is released under the GNU General Public License, version 2. The Arduino IDE supports the languages C and C++ using special rules of code structuring. The Arduino IDE supplies a software library from the Wiring project, which provides many common input and output procedures. User-written code only requires two basic functions, for starting the sketch and the main program loop, that are compiled and linked with a program stub `main()` into an executable cyclic executive program with the GNU toolchain, also included with the IDE distribution. The Arduino IDE employs the program `avrdude` to convert the executable code into a text file in hexadecimal encoding that is loaded into the Arduino board by a loader program in the board's firmware.

### **7.3 BLYNK**

Blynk is a Platform with iOS and Android apps to control Arduino, Raspberry Pi and the likes over the Internet. It's a digital dashboard where you can build a graphic interface for your project by simply dragging and dropping widgets. It's really simple to set everything up and you'll start tinkering in less than 5 mins. Blynk is not tied to some specific board or shield. Instead, it's supporting hardware of your choice. Whether your Arduino or Raspberry Pi is linked to the Internet over Wi-Fi, Ethernet or this new ESP8266 chip, Blynk will get you online and ready for the Internet Of Your Things.

## **9. CONCLUSION**

This project can be adapted to requests formed in the design process, updating the sensor information and reflecting the real factors of environmental poultry farming. Each node has been set to receive the environmental factors (temperature, water level and food level). If any of these observing conditions drops below the predefined threshold, the sensor node will intimate the farmer and automating heating method, filling of water and filling of food takes place. This system will be labor-saving for the farmer and report environmental changes immediately, thereby enabling the farmer to prevent adverse strictly implemented throughout the redaction method and compiled into the feasible machine language once Consequences.

The first set is formed of various sensors dedicated to measure the environmental parameters in the farm building as temperature, humidity, airflow, and others. The sensors are connected to a local control unit that acquires the readings and sends the data. The main controller

receives all the information, processes it, and responds according to predefined algorithms.

## REFERENCES

1. A Few Connectivity Technologies Involved in Internet of Things, Eswar Patnala, Rednam S.S. Jyothi, IJCA Vol. 10, No. 9 Jun 2017 (pp. 167-177).
2. A Study on Internet of Things Service Server Application for Provision of Automatic Service, Am-Suk Oh IJCA Vol. 11, No. 9 Jun 2018 (pp. 25-32).
3. A Dynamic Analysis Tool for Real-time Characteristics Related to Cache Hit-ratio of Real-time Applications, Hyang Yeon Bae IJCA Vol. 10, No. 9 Jun 2017 (pp. 177-190).
4. Sensor Query Control for IoT Data Monitoring, Siwoo Byun IJCA Vol. 11 No Jun 2018 (pp. 109-118).
5. A Poultry Farming Control System Using a ZigBee-based Wireless Sensor Network, Bilal Ghazal, IJCA Vol. 10, No. 9 Jun 2017 (pp. 191-198).
6. A Study on the Control Problem of Driving DC Motor with Very-low speed in Automatic Door System for Home, Hyun-Chang Lee, IJCA Vol. 10, No. 9 Jun 2017 (pp. 199-208).
7. Precise Frost and Ice Detection for Defrost Scheme of Agricultural Refrigerator using Integrated Sensor Module based on Moving Window Method, Ji Hoon Seung, Young Baik Kim, IJCA Vol. 10, No. 9 Jun 2017 (pp. 209-216).
8. A Study of Network Infrastructure based Wireless Network Management Service across the Integrated Heterogeneous Networks, Ronnie D. Caytiles and Byungjoo Park IJCA Vol. 10, No. 9 Jun 2017 (pp. 217-226).
9. Comparative Study of PLC and Arduino in Automated Irrigation System, Mechelle Grace Zaragoza and Haeng-Kon Kim IJCA Vol. 10, No. 6 Jun 2017 (pp. 207-218).
10. Development of HID-Based Motion Recognition Device, Won-Hyuck Choi, Da-Un Kim and Min-Seok Jiev IJCA VOL. 10, No. 8 Jun 2017 (pp. 93-104).
11. Kumar, V., Prasad, L., Experimental investigation on heat transfer and fluid flow of air flowing under three sides concave dimple roughened duct. International Journal of Mechanical Engineering and Technology (IJMET), Volume 8, Issue 11, November 2017, pp. 1083–1094, Article ID: IJMET\_08\_11\_110.
12. Kumar, V., Prasad, L., Thermal performance investigation of one and three sides concave dimple roughened solar air heaters. International Journal of Mechanical Engineering and Technology (IJMET) Volume 8, Issue 12, December 2017, pp. 31–45, Article ID: IJMET\_08\_12\_004.
13. Kumar, V., Prasad, L., Performance Analysis of three sides concave dimple shape roughened solar air heater, J. sustain. dev. energy water environ. syst., 6(4), pp 631-648, 2018.
14. Kumar, V., Nusselt number and friction factor correlations of three sides concave dimple roughened solar air heater, Renewable Energy 135 (2019) 355-377.
15. Kumar, V., Prasad, L., Experimental analysis of heat transfer and friction for three sides roughened solar air heater, Annales de Chimie - Science des Matériaux, 75-107, ACSM. Volume 41 – n° 1-2/2017.
16. Kumar, V., Prasad, L., Performance prediction of three sides hemispherical dimple roughened solar duct, Instrumentation, Mesure, Métrologie, 273-293 I2M. Volume 17 – n° 2/2018.

## HEAT TRANSFER ALONG VERTICAL CHIMNEY

**K. Rajanikanth & Dr. T.V. Reddy & Mr. Vikash Kumar**

PG Student, Professor (H & S), Vice Principal, Assistant Professor  
Department of Mechanical Engg., Malla Reddy College of Engineering Maisammaguda, Dhulapally,  
Kompally, Secunderabad, Telangana-500100, India.

**ABSTRACT:** Chimney, which form the last component of a system using a flue gas such as boiler, play a vital role in maintaining efficiency, draft, etc, of a system and also in minimizing the atmospheric pollution. Steel chimneys are also known as steel stacks. The steel chimneys are made of steel plates and supported on foundation. The steel chimneys are used to escape and disperse the flue gases to such a height that the gases do not contaminate surrounding atmosphere. The hot gases occupy. For the purpose of the structural design of steel the chimney, the height and diameter of chimney. Chimneys are required larger volume than before. The weight of gases per cubic meter becomes less to carry vertically and discharge, gaseous products of combustion, chemical waste gases, and exhaust air from an industry to the atmosphere. In this thesis, chimney materials (concrete used for the design of the chimney. The chimney was considered as a cantilever beam with annular will be designed considering with insulation and without insulation. The Bureau of Indian Standards (BIS) design codes procedures will be the chimney is done in CREO Parametric software and fluid- structural and thermal analysis is done on the chimney in ANSYS software. A simplified model of chimneys with various insulation cross section. 3Dmodel of and carbon epoxy). Static analysis is to determine the deformation, stress and strain for chimney with insulation and without insulation. Thermal analysis to determine the heat flux of the chimney with different materials to different models. CFD analysis to determine the pressure drop, velocity, heat transfer coefficient, mass flow rate and heat transfer rate.

**Keywords:**

### INTRODUCTION

A chimney is a structure that provides ventilation for hot flue gases or smoke from a boiler, stove, furnace or fireplace to the outside atmosphere. Chimneys are typically vertical, or as near as possible to vertical, to ensure that the gases flow smoothly, drawing air into the combustion in what is known as the stack, or chimney effect. The space inside a chimney is called a flue. Chimneys may be found in buildings, steam locomotives and ships. In the United States, the term smokestack (colloquially, stack) is also used when referring to locomotive chimneys or ship chimneys, and the term funnel can also be used. The height of a chimney influences its ability to transfer flue gases to the external environment via stack effect. Additionally, the dispersion of pollutants at higher altitudes can reduce their impact on the immediate surroundings. In the case of chemically aggressive output, a sufficiently tall chimney can allow for partial or complete self-neutralization of airborne chemicals before they reach ground level. The dispersion of pollutants over a greater area can reduce their concentrations and facilitate compliance with regulatory limits.

**RESIDENTIAL FLUE LINERS:** A flue liner is a secondary barrier in a chimney that protects the masonry from the acidic products of combustion, helps prevent flue gas from entering the house, and reduces the size of an oversized flue. Newly built chimneys have been required by building codes to have a flue liner in many locations since the 1950s. Chimneys built without a liner can usually have a liner added, but the type of liner needs to match the type of appliance it is servicing. Flue liners may be clay tile, metal, concrete tiles, or poured in place concrete. Clay tile flue liners are very common in the United States. However, this is the only liner which does not meet Underwriters Laboratories 1777 approval and frequently have problems such as cracked tiles and improper installation. Clay tiles are usually about 2 feet (0.61 m) long, various sizes and shapes, and are installed in new construction as the chimney is built. A refractory cement is used between each tile. Metal liners may be stainless steel, aluminum, or galvanized iron and may be flexible or rigid pipes. Stainless steel is made in several types and thicknesses. Type 304 is used with firewood, wood pellet fuel, and non-condensing oil appliances, types 316 and 321 with coal, and type AL 29-4C is used with non-condensing gas appliances. Stainless steel liners

must have a cap and be insulated if they service solid fuel appliances, but following the manufacturer's instructions carefully. Aluminum and galvanized steel chimneys are known as class A and class B chimneys. Class A are either an insulated, double wall stainless steel pipe or triple wall, air-insulated pipe often known by its genericized trade name Metalbestos. Class B are uninsulated double wall pipes often called B-vent, and are only used to vent non-condensing gas appliances. These may have aluminum inside layer and galvanized steel outside layer. Condensing boilers do not need a chimney. Concrete flue liners are like clay liners but are made of a refractory cement and are more durable than the clay liners. Poured in place concrete liners are made by pouring special concrete into the existing chimney with a form. These liners are highly durable, work with any heating appliance, and can reinforce a weak chimney, but they are irreversible. Designing chimneys and stacks to provide the correct amount of natural draft involves a number of design factors, many of which require iterative trial-and-error methods. As a "first guess" approximation, the following equation can be used to estimate the natural draught/draft flow rate by assuming that the molecular mass (i.e., molecular weight) of the flue gas and the external air are equal. Their training program is available online and in-person, but materials are available to access anytime.

### CHIMNEY POTS, CAPS AND TOPS:

A chimney pot is placed on top of the chimney to expand the length of the chimney inexpensively, and to improve the chimney's [draft](#). A chimney with more than one pot on it indicates that there is more than one fireplace on different floors sharing the chimney. A chimney [cowl](#) is placed on top of the chimney to prevent birds and other animals from nesting in the chimney. They often feature a rain guard to prevent rain or snow from going down the chimney. A metal wire mesh is often used as a [spark arrestor](#) to minimize burning debris from rising out of the chimney and making it onto the roof. Although the masonry inside the chimney can absorb a large amount of moisture which later evaporates, rainwater can collect at the base of the chimney. Sometimes weep holes are placed at the bottom of the chimney to drain out collected water.



A chimney cowl or wind directional cap is a helmet-shaped chimney cap that rotates to align with the wind and prevent a backdraft of smoke and wind back down the chimney.



### A H-style cowl:

An H-style cap (cowl) is a chimney top constructed from chimney pipes shaped like the letter H. (Its image is included in cowl (chimney).) It is an age-old method of regulating draft in situations where prevailing winds or turbulences cause downdraft and backpuffing. Although the H cap has a distinct advantage over most other downdraft caps, it fell out of favor because of its bulky design. It is found mostly in marine use but has been regaining popularity due to its energy-



### History:

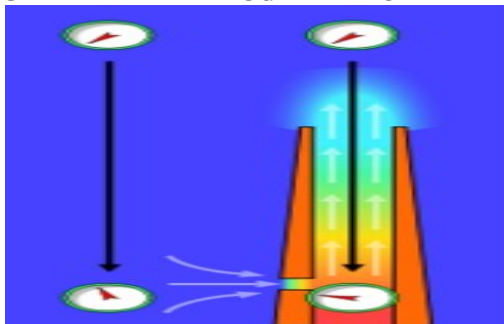


A smoke hood in the Netherlands. Image: Cultural Heritage Agency of the Netherlands

saving functionality. The H-cap stabilizes the draft rather than increasing it. Other downdraft caps are based on the Venturi effect, solving downdraft problems by increasing the updraft constantly resulting in much higher fuel consumption. A chimney damper is a metal plate that can be positioned to close off the chimney when not in use and prevent outside air from entering the interior space, and can be opened to permit hot gases to exhaust when a fire is burning. A top damper or cap damper is a metal spring door placed at the top of the chimney with a long metal chain that allows one to open and close the damper from the fireplace. A throat damper is a metal plate at the base of the chimney, just above the firebox, that can be opened and closed by a lever, gear, or chain to seal off the fireplace from the chimney. The advantage of a top damper is the tight weatherproof seal that it provides when closed, which prevents cold outside air from flowing down the chimney and into the living space—a feature that can rarely be matched by the metal-on-metal seal afforded by a throat damper. Additionally, because the throat damper is subjected to intense heat from the fire directly below, it is common for the metal to become warped over time, thus further degrading the ability of the throat damper to seal. However, the advantage of a throat damper is that it seals off the living space from the air mass in the chimney, which, especially for chimneys positioned on an outside of wall of the home, is generally very cold. It is possible in practice to use both a top damper and a throat damper to obtain the benefits of both. The two top damper designs currently on the market are the Lyemance (pivoting door) and the Lock Top (translating door).

In the late Middle Ages in Western Europe the design of crow-stepped gables arose to allow maintenance access to the chimney top, especially for tall structures such as castles and great manor houses.

**CHIMNEY DRAUGHT OR DRAFT:**



The stack effect in chimneys: the gauges represent absolute air pressure and the airflow is

indicated with light grey arrows. The gauge dials move clockwise with increasing pressure.

Main article: Flue gas stack  
 When coal, oil, natural gas, wood, or any other fuel is combusted in a stove, oven, fireplace, hot water boiler, or industrial furnace, the hot combustion product gases that are formed are called flue gases. Those gases are generally exhausted to the ambient outside air through chimneys or industrial flue gas stacks (sometimes referred to as smokestacks). The combustion flue gases inside the chimneys or stacks are much hotter than the ambient outside air and therefore less dense than the ambient air. That causes the bottom of the vertical column of hot flue gas to have a lower pressure than the pressure at the bottom of a corresponding column of outside air. That higher pressure outside the chimney is the driving force that moves the required combustion air into the combustion zone and also moves the flue gas up and out of the chimney. That movement or flow of combustion air and flue gas is called "natural draught/draft", "natural ventilation", "chimney effect", or "stack effect". The taller the stack, the more draught or draft is created. There can be cases of diminishing returns: if a stack is overly tall in relation to the heat being sent out of the stack, the flue gases may cool before reaching the top of the chimney. This condition can result in poor drafting, and in the case of wood burning appliances, the cooling of the gases before emission can cause creosote to condense near the top of the chimney. The creosote can restrict the exit of flue gases and may pose a fire hazard. Designing chimneys and stacks to provide the correct amount of natural draft involves a number of design factors, many of which require iterative trial-and-error methods. As a "first guess" approximation, the following equation can be used to estimate the natural draught/draft flow rate by assuming that the molecular mass (i.e., molecular weight) of the flue gas and the external air are equal and that the frictional pressure and heat losses are negligible:

where:

- Q** = chimney draught/draft flow rate, m<sup>3</sup>/s
- A** = cross-sectional area of chimney, m<sup>2</sup> (assuming it has a constant cross-section)
- C** = discharge coefficient (usually taken to be from 0.65 to 0.70)
- G** = gravitational acceleration, 9.807 m/s<sup>2</sup>
- H** = height of chimney, m
- T<sub>i</sub>** = average temperature inside the chimney, K

$T_e$  = external air temperature, K.

### Maintenance and problems:



Chimneys on the Parliamentary Library in Wellington, New Zealand.

A characteristic problem of chimneys is they develop deposits of creosote on the walls of the structure when used with wood as a fuel. Deposits of this substance can interfere with the airflow and more importantly, they are combustible and can cause dangerous chimney fires if the deposits ignite in the chimney. Heaters that burn natural gas drastically reduce the amount of creosote buildup due to natural gas burning much cleaner and more efficiently than traditional solid fuels. While in most cases there is no need to clean a gas chimney on an annual basis that does not mean that other parts of the chimney cannot fall into disrepair. Disconnected or loose chimney fittings caused by corrosion over time can pose serious dangers for residents due to leakage of carbon monoxide into the home.[11] Thus, it is recommended—and in some countries even mandatory—that chimneys be inspected annually and cleaned on a regular basis to prevent these problems. The workers who perform this task are called chimney sweeps or steeplejacks. This work used to be done largely by child labour and as such features in Victorian literature. In the Middle Ages in some parts of Europe, a crow-stepped gable design was developed, partly to provide access to chimneys without use of ladders. Iconic non-operational chimney of the Chernobyl reactor #4, preserved as part of the Chernobyl sarcophagus. Masonry (brick) chimneys have also proven to be particularly prone to crumbling during an earthquake. Government housing authorities in cities prone to earthquakes such as San Francisco, Los Angeles, and San Diego now recommend building new homes with stud-framed chimneys around a metal flue. Bracing or strapping old masonry chimneys has not proven to be very effective in preventing damage or injury from earthquakes. It is now possible to buy "faux-brick" facades to cover these modern chimney structures. Other potential problems include:

"spalling" brick, in which moisture seeps into the brick and then freezes, cracking and flaking the brick and loosening mortar seals. shifting foundations, which may degrade integrity of chimney masonry nesting or infestation by unwanted animals such as squirrels, or chimney swifts chimney leaks drafting issues, which may allow smoke inside building issues with fireplace or heating appliance may cause unwanted degradation or hazards to chimney

### Cooling tower used as an industrial chimney

At some power stations, which are equipped with plants for the removal of sulfur dioxide and nitrogen oxides, it is possible to use the cooling tower as a chimney. Such cooling towers can be seen in Germany at the Power Station Staudinger Grosskrotzenburg and at the Power Station Rostock. At power stations that are not equipped for removing sulfur dioxide, such usage of cooling towers could result in serious corrosion problems which are not easy to prevent.

### LITERATURE REVIEW:

**1. Seismic Analysis And Design Of Industrial Chimneys** This paper describes a simplified method that allow obtaining the fundamental period of vibration, lateral displacement, shear force and bending moment through a set of equations, obtaining for all cases studied an error below 10%. The results obtained in this study were applied to a total of 9 real chimneys (4 of steel and 5 of reinforced concrete) built in Chile, with the objective of calibrating founded expressions. During the stage of the analysis, it was verified that the criterion of consistent masses provide better results than the criterion of lumped masses, and as a very important conclusion a discrete analysis of the model in twenty segments of the beam is satisfactory. The most representative variables that define the model with which it is possible to carry out a parametric analysis of the chimney. As important parameters we could refer to: slenderness ratio  $H/D_{inf}$ , radius ratio  $R_{sup}/R_{inf}$ , thickness ratio  $E_{sup}/E_{inf}$  and thickness diameter ratio  $D_{inf}/E_{inf}$ . Later, by varying each one of the chosen parameters several analysis of representative chimneys of this great family, could be carried out. As seismic loads, the spectrums of accelerations recommended by the code of seismic design for structures and industrial installations in Chile, have been considered. Modal responses were combined using the combination rule CQC. In all the cases studied in this investigation, the influence of the P-Δ effect, the

soil structure interaction, and the influence on responses that provoke the inclusion of lining, have been disregarded.

## **2. Analysis Of Self Supported Steel Chimney As Per Indian Standard**

Most of the industrial steel chimneys are tall structures with circular cross-sections. Such slender, lightly damped structures are prone to wind-excited vibration. Geometry of a self supporting steel chimney plays an important role in its structural behaviour under lateral dynamic loading. This is because geometry is primarily responsible for the stiffness parameters of the chimney. However, basic dimensions of industrial self supporting steel chimney, such as height, diameter at exit, etc., are generally derived from the associated environmental conditions. To ensure a desired failure mode design code (IS-6533: 1989 Part 2) imposes several criteria on the geometry (top-to-base diameter ratio and height-to-base diameter ratio) of steel chimneys. The objective of the present study is to justify the code criteria with regard to basic dimensions of industrial steel chimney.

## **3. Analysis of Tall RC Chimney as per Indian Standard Code**

Reinforced chimneys are used in Power plants to take the hot and poisonous flue gas to a great height. They are tall and slender structures, designed mainly to resist the lateral forces like wind and earthquake as well as the thermal stresses of the flue gas. An attempt is done to understand the variation of lateral deflection at the top of the chimney, by varying the height of chimney above 275 m. CED 38:7892 Code of practice for design of reinforced concrete chimney (Third revision of IS 4998:1992 [Part I]) is used for the analysis. The location selected for the study is Bellary in Karnataka. Along wind and temperature are only considered for this study. Sufficient amount of reinforcement is provided to resist the bending moment in the vertical direction and horizontal loops are provided to cater for the horizontal shear and temperature gradient. A total of five models are selected for five different heights and the analysis and design are done. ANSYS software was used to do the analysis. All the models were analyzed and the lateral deflection was calculated.

## **4. Analysis and Computational Study of a High Chimney Tower for Solar Energy**

**Abstract:** A Solar Chimney Power Plant consists of central chimney that is surrounded by a transparent canopy located a few meters above ground level. An analysis of solar chimneys has been developed, aimed particularly to study

stability and structural strength of a model of cylindrical reinforced concrete tower with 500m in tall and 50m in diameter. The design of this tower has several technical challenges. This model is subjected to his own weight, the effects of wind and the pressure due to the flow of air inside the chimney. In this study, the effect of these loads on the stability and strength of the chimney has been examined. The rings stiffened are necessary to prevent ovalisation of the structure. In addition, the influence of various designs of rings-stiffened is taken into consideration in the mechanical behaviour of this tower. Numerical simulation modeling method based on finite element method is adopted using the "Autodesk Robot structural analysis professional" software.

## **5. Nonlinear Dynamic Analysis Of Chimney-Like Towers**

In this study the most important problem i.e. earthquake behaviour of the structures, hysteric behaviour of material and section properties are studied. The significance of this study is mainly concentrated on model simplification that provides sufficient accuracy based on a nonlinear discrete model. Tous power plant chimney is investigated numerically as an example. The nonlinear dynamic analysis essentially needed for seismic assessment in evaluation of actual performance of complicated structures during earthquakes than the damage indices of structure had to be calculated using appropriate damage models.

## **6. Dynamic Soil-Structure Interaction Analysis of Tall Multi-Flue Chimneys Under Aerodynamic And Seismic Force.**

The present paper proposes a semi analytic mathematical model based on which both seismic and aerodynamic response of such a tall chimneys are studied for various soil stiffness and are compared with fixed base conventional method as per UBC 97 (for seismic load) and CICIND (for wind loading). Soil Structure interaction also has an important effect on seismic forces of tall chimneys. Although for tall chimneys rested on firm soil, earthquake loads decreased as a result of increasing in period values, seismic forces may amplify by using different response spectra in calculation. This means that the soil structure interaction effects are reliant on characteristic of the seismic excitation in addition to chimneys properties. JEEVAN T, SOWJANYA G. V (2014)



## INTRODUCTION TO CAD :

**Computer-aided design (CAD)**, also known as **computer-aided design and drafting (CADD)**, is the use of computer technology for the process of design and design-documentation. Computer Aided Drafting describes the process of drafting with a computer. CADD software, or environments, provide the user with input-tools for the purpose of streamlining design processes; drafting, documentation, and manufacturing processes. CADD output is often in the form of electronic files for print or machining operations. The development of CADD-based software is in direct correlation with the processes it seeks to economize; industry-based software (construction, manufacturing, etc.) typically uses vector-based (linear) environments whereas graphic-based software utilizes raster-based (pixelated) environments. CADD environments often involve more than just shapes. As in the manual drafting of technical and engineering drawings, the output of CAD must convey information, such as materials, processes, dimensions, and tolerances, according to application-specific conventions. CAD may be used to design curves and figures in two-dimensional (2D) space; or curves, surfaces, and solids in three-dimensional (3D) objects. CAD is an important industrial art extensively used in many applications, including automotive, shipbuilding, and aerospace industries, industrial and architectural design, prosthetics, and many more. CAD is also widely used to produce computer animation for special effects in movies, advertising and technical manuals. The modern ubiquity and power of computers means that even perfume bottles and shampoo dispensers are designed using techniques unheard of by engineers of the 1960s. Because of its enormous economic importance, CAD has been a major driving force for research in computational geometry, computer graphics (both hardware and software), and discrete differential geometry. The design of geometric models for object shapes, in particular,

is often called *computer-aided geometric design (CAGD)*. Current computer-aided design software packages range from 2D vector-based drafting systems to 3D solid and surface modellers. Modern CAD packages can also frequently allow rotations in three dimensions, allowing viewing of a designed object from any desired angle, even from the inside looking out. Some CAD software is capable of dynamic mathematic modeling, in which case it may be marketed as **CADD** — *computer-aided design and drafting*. CAD is used in the design of tools and machinery and in the drafting and design of all types of buildings, from small residential types (houses) to the largest commercial and industrial structures (hospitals and factories). CAD is mainly used for detailed engineering of 3D models and/or 2D drawings of physical components, but it is also used throughout the engineering process from conceptual design and layout of products, through strength and dynamic analysis of assemblies to definition of manufacturing methods of components. It can also be used to design objects.

## INTRODUCTION TO CREO :

PTC CREO, formerly known as Pro/ENGINEER, is 3D modeling software used in mechanical engineering, design, manufacturing, and in CAD drafting service firms. It was one of the first 3D CAD modeling applications that used a rule-based parametric system. Using parameters, dimensions and features to capture the behavior of the product, it can optimize the development product as well as the design itself. The name was changed in 2010 from Pro/ENGINEER Wildfire to CREO. It was announced by the company who developed it, Parametric Technology Company (PTC), during the launch of its suite of design products that includes applications such as assembly modeling, 2D orthographic views for technical drawing, finite element analysis and more. PTC CREO says it can offer a more efficient design experience than other modeling software because of its unique features including the integration of parametric and direct modeling in one platform. The complete suite of applications spans the spectrum of product development, giving designers options to use in each step of the process. The software also has a more user friendly interface that provides a better experience for designers. It also has collaborative capacities that make it easy to share designs and make changes. There are countless benefits to using PTC CREO. We'll take a look at them in this two-part series. First up, the biggest advantage is increased productivity because of its efficient and flexible design capabilities. It was designed to be

easier to use and have features that allow for design processes to move more quickly, making a designer's productivity level increase. Part of the reason productivity can be increased is because the package offers tools for all phases of development, from the beginning stages to the hands-on creation and manufacturing. Late stage changes are common in the design process, but PTC CREO can handle it. Changes can be made that are reflected in other parts of the process. The collaborative capability of the software also makes it easier and faster to use. One of the reasons it can process information more quickly is because of the interface between MCAD and ECAD designs. Designs can be altered and highlighted between the electrical and mechanical designers working on the project. The time saved by using PTC CREO isn't the only advantage. It has many ways of saving costs. For instance, the cost of creating a new product can be lowered because the development process is shortened due to the automation of the generation of associative manufacturing and service deliverables. PTC also offers comprehensive training on how to use the software. This can save businesses by eliminating the need to hire new employees. Their training program is available online and in-person, but materials are available to access anytime. A unique feature is that the software is available in 10 languages. PTC knows they have people from all over the world using their software, so they offer it in multiple languages so nearly anyone who wants to use it is able to do so.

#### ADVANTAGES OF CREO PARAMETRIC SOFTWARE :

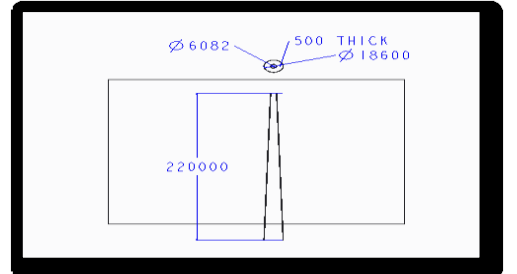
8. Optimized for model-based enterprises
9. Increased engineer productivity
10. Better enabled concept design
11. Increased engineering capabilities
12. Increased manufacturing capabilities
13. Better simulation
14. Design capabilities for additive manufacturing

#### CREO PARAMETRIC MODULES:

- Sketcher
- Part modeling
- Assembly
- Drafting



2D MODEL OF CHIMNEY



#### INTRODUCTION TO FEAL:

Finite element analysis is a method of solving, usually approximately, certain problems in engineering and science. It is used mainly for problems for which no exact solution, expressible in some mathematical form, is available. As such, it is a numerical rather than an analytical method. Methods of this type are needed because analytical methods cannot cope with the real, complicated problems that are met with in engineering. For example, engineering strength of materials or the mathematical theory of elasticity can be used to calculate analytically the stresses and strains in a bent beam, but neither will be very successful in finding out what is happening in part of a car suspension system during cornering. One of the first applications of FEA was, indeed, to find the stresses and strains in engineering components under load. FEA, when applied to any realistic model of an engineering component, requires an enormous amount of computation and the development of the method has depended on the availability of suitable digital computers for it to run on. The method is now applied to problems involving a wide range of phenomena, including vibrations, heat conduction, fluid mechanics and electrostatics, and a wide range of material properties, such as linear-elastic (Hookean) behavior and behavior involving deviation from Hooke's law (for example, plasticity or rubber-elasticity). Many comprehensive general-purpose computer packages are now available that can deal with a wide range of phenomena, together with more specialized packages for particular applications, for example, for the study of dynamic phenomena or large-scale plastic flow. Depending on the type and complexity of the analysis, such

packages may run on a microcomputer or, at the other extreme, on a supercomputer. FEA is essentially a piece-wise process. It can be applied to one-dimensional problems, but more usually there is an area or volume within which the solution is required. This is split up into a number of smaller areas or volumes, which are called finite elements. Figure 1 shows a two-dimensional model of a spanner that has been so divided: the process is called discretisation, and the assembly of elements is called a mesh.

### INTRODUCTION TO ANSYS:

ANSYS is general-purpose finite element analysis (FEA) software package. Finite Element Analysis is a numerical method of deconstructing a complex system into very small pieces (of user-designated size) called elements. The software implements equations that govern the behaviour of these elements and solves them all; creating a comprehensive explanation of how the system acts as a whole. These results then can be presented in tabulated, or graphical forms. This type of analysis is typically used for the design and optimization of a system far too complex to analyze by hand. Systems that may fit into this category are too complex due to their geometry, scale, or governing equations. ANSYS is the standard FEA teaching tool within the Mechanical Engineering Department at many colleges. ANSYS is also used in Civil and Electrical Engineering, as well as the Physics and Chemistry departments. ANSYS provides a cost-effective way to explore the performance of products or processes in a virtual environment. This type of product development is termed virtual prototyping. With virtual prototyping techniques, users can iterate various scenarios to optimize the product long before the manufacturing is started. This enables a reduction in the level of risk, and in the cost of ineffective designs. The multifaceted nature of ANSYS also provides a means to ensure that users are able to see the effect of a design on the whole behavior of the product, be it electromagnetic, thermal, mechanical etc.

### Generic Steps to Solving any Problem in ANSYS:

Like solving any problem analytically, you need to define (1) your solution domain, (2) the physical model, (3) boundary conditions and (4) the physical properties. You then solve the problem and present the results. In numerical methods, the main difference is an extra step called mesh generation. This is the step that divides the complex model into small elements that become solvable in an otherwise too complex

situation. Below describes the processes in terminology slightly more attune to the software.

#### Build Geometry:

Construct a two or three dimensional representation of the object to be modeled and tested using the work plane coordinate system within ANSYS.

#### Define Material Properties:

Now that the part exists, define a library of the necessary materials that compose the object (or project) being modeled. This includes thermal and mechanical properties.

#### Generate Mesh:

At this point ANSYS understands the makeup of the part. Now define how the modeled system should be broken down into finite pieces.

#### Apply Loads:

Once the system is fully designed, the last task is to burden the system with constraints, such as physical loadings or boundary conditions.

#### Present the Results:

After the solution has been obtained, there are many ways to present ANSYS' results, choose from many options such as tables, graphs, and contour plots.

### SPECIFIC CAPABILITIES OF ANSYS:

#### Structural

Static Analysis - Used to determine displacements, stresses, etc. under static loading conditions. ANSYS can compute both linear and nonlinear static analyses. Nonlinearities can include plasticity, stress stiffening, large deflection, large strain, hyper elasticity, contact surfaces, and creep. Transient Dynamic Analysis - Used to determine the response of a structure to arbitrarily time-varying loads. All nonlinearities mentioned under Static Analysis above are allowed. Buckling Analysis - Used to calculate the buckling loads and determine the buckling mode shape. Both linear (eigenvalue) buckling and nonlinear buckling analyses are possible.

#### Thermal:

ANSYS is capable of both steady state and transient analysis of any solid with thermal boundary conditions. Steady-state thermal analyses calculate the effects of steady thermal loads on a system or component. Users often perform a steady-state analysis before doing a transient thermal analysis, to help establish initial conditions. A steady-state analysis also can be the last step of a transient thermal analysis; performed after all transient effects have diminished. ANSYS can be used to determine temperatures, thermal gradients, heat flow rates, and heat fluxes in an object that are caused by

thermal loads that do not vary over time. Such loads include the following:

- Convection
- Radiation
- Heat flow rates
- Heat fluxes (heat flow per unit area)
- Heat generation rates (heat flow per unit volume)

**Fluid Flow:**

The ANSYS/FLOTRAN CFD (Computational Fluid Dynamics) offers comprehensive tools for analyzing two-dimensional and three-dimensional fluid flow fields. ANSYS is capable of modeling a vast range of analysis types such as: airfoils for pressure analysis of airplane wings (lift and drag), flow in supersonic nozzles, and complex, three-dimensional flow patterns in a pipe bend. In addition, ANSYS/FLOTRAN could be used to perform tasks including:

- Calculating the gas pressure and temperature distributions in an engine exhaust manifold
- Studying the thermal stratification and breakup in piping systems
- Using flow mixing studies to evaluate potential for thermal shock
- Doing natural convection analyses to evaluate the thermal performance of chips in electronic enclosures
- Conducting heat exchanger studies involving different fluids separated by solid regions

**COUPLED FIELD:**

A coupled-field analysis is an analysis that takes into account the interaction (coupling) between two or more disciplines (fields) of engineering. A piezoelectric analysis, for example, handles the interaction between the structural and electric fields: it solves for the voltage distribution due to applied displacements, or vice versa. Other examples of coupled-field analysis are thermal-stress analysis, thermal-electric analysis, and fluid-structure analysis. Some of the applications in which coupled-field analysis may be required are pressure vessels (thermal-stress analysis), fluid flow constrictions (fluid-structure analysis), induction heating (magnetic-thermal analysis), ultrasonic transducers (piezoelectric analysis), magnetic forming (magneto-structural analysis), and micro-electro mechanical systems (MEMS).

**Modal Analysis** - A modal analysis is typically used to determine the vibration characteristics (natural frequencies and mode shapes) of a structure or a machine component while it is

being designed. It can also serve as a starting point for another, more detailed, dynamic analysis, such as a harmonic response or full transient dynamic analysis. Modal analyses, while being one of the most basic dynamic analysis types available in ANSYS, can also be more computationally time consuming than a typical static analysis. A reduced solver, utilizing automatically or manually selected master degrees of freedom is used to drastically reduce the problem size and solution time.

**Harmonic Analysis-** Used extensively by companies who produce rotating machinery, ANSYS Harmonic analysis is used to predict the sustained dynamic behavior of structures to consistent cyclic loading. Examples of rotating machines which produced or are subjected to harmonic loading are:

- Turbines
- Gas Turbines for Aircraft and Power Generation
- Steam Turbines
- Wind Turbine
- Water Turbines
- Turbopumps
- Internal Combustion engines
- Electric motors and generators
- Gas and fluid pumps
- Disc drives

A harmonic analysis can be used to verify whether or not a machine design will successfully overcome resonance, fatigue, and other harmful effects of forced vibrations.

**INTRODUCTION TO CFD:**

Computational fluid dynamics, usually abbreviated as CFD, is a branch of fluid mechanics that uses numerical methods and algorithms to solve and analyze problems that involve fluid flows. Computers are used to perform the calculations required to simulate the interaction of liquids and gases with surfaces defined by boundary conditions. With high-speed supercomputers, better solutions can be achieved. Ongoing research yields software that improves the accuracy and speed of complex simulation scenarios such as transonic or turbulent flows. Initial experimental validation of such software is performed using a wind tunnel with the final validation coming in full-scale testing, e.g. flight tests.

**METHODOLOGY:**

In all of these approaches the same basic procedure is followed.

- During preprocessing

- The geometry (physical bounds) of the problem is defined.
  - The volume occupied by the fluid is divided into discrete cells (the mesh). The mesh may be uniform or non-uniform.
  - The physical modeling is defined – for example, the equations of motion + enthalpy + radiation + species conservation
  - Boundary conditions are defined. This involves specifying the fluid behaviour and properties at the boundaries of the problem. For transient problems, the initial conditions are also defined.
  - The simulation is started and the equations are solved iteratively as a steady-state or transient.
  - Finally a postprocessor is used for the analysis and visualization of the resulting solution.
4. Experimental investigation of chimney-enhanced natural convection in hexagonal honeycombs
  5. Theoretical and Applied Mechanics Letters, Volume 4, Issue 3, 2014, Article 032005
  6. Heat transfer enhancement by the chimney effect in a vertical isoflux channel
  7. Kumar, V., Nusselt number and friction factor correlations of three sides concave dimple roughened solar air heater, *Renewable Energy* 135 (2019) 355-377.
  8. Kumar, V., Prasad, L., Performance Analysis of three sides concave dimple shape roughened solar air heater, *J. sustain. dev. energy water environ. syst.*, 6(4), pp 631-648, 2018.
  9. Kumar, V., Prasad, L., Experimental analysis of heat transfer and friction for three sides roughened solar air heater, *Annales de Chimie - Science des Matériaux*, 75-107, ACSM. Volume 41 – n° 1-2/2017.
  10. Kumar, V., Prasad, L., Performance prediction of three sides hemispherical dimple roughened solar duct, *Instrumentation, Mesure, Métrologie*, 273-293 I2M. Volume 17 – n° 2/2018.
  11. Kumar, V., Prasad, L., Experimental investigation on heat transfer and fluid flow of air flowing under three sides concave dimple roughened duct. *International Journal of Mechanical Engineering and Technology (IJMET)*, Volume 8, Issue 11, November 2017, pp. 1083–1094, Article ID: IJMET\_08\_11\_110.
  12. Kumar, V., Prasad, L., Thermal performance investigation of one and three sides concave dimple roughened solar air heaters. *International Journal of Mechanical Engineering and Technology (IJMET)* Volume 8, Issue 12, December 2017, pp. 31–45, Article ID: IJMET\_08\_12\_004.
  13. Kumar, V., Prasad, L., Augmentation in thermal efficiency of three sides over one side concave dimple roughened ducts., *Carbon – Sci. Tech.* 10/3(2018)8-16, ISSN 0974-0546.

### CONCLUSION:

Chimney, which form the last component of a system using a flue gas such as boiler, play a vital role in maintaining efficiency, draft, etc, of a system and also in minimizing the atmospheric pollution. The ease of thermal control by means of air natural convection stimulates the investigation of configurations with the aim at improving the thermal performance. The steel chimneys are used to escape and disperse the flue gases to such a height that the gases do not contaminate surrounding atmosphere. The hot gases occupy. For the purpose of the structural design of steel the chimney, the height and diameter of chimney. Chimneys are required larger volume than before. A chimney, which is an unheated extension of a flow passage, enhances the flow acceleration through buoyancy. It acts like a shroud so that the merged thermal plumes (Thermal boundary layers) inside the pipe are accelerated along the duct without scattering. The height of the chimney determines the acceleration distance of the hot plume, and the heat transfer is enhanced as the flow rate increases.

### REFERENCES:

1. Heat transfer effects of chimney height, diameter, and Prandtl number *International Communications in Heat and Mass Transfer*, Volume 66, 2015, pp. 196-202
2. Enhanced natural convection heat transfer of a chimney-based radial heat sink
3. *Energy Conversion and Management*, Volume 108, 2016, pp. 422-428

# EFFECT OF BIODIESEL BLENDS AND NANO-PARTICLES ON ENGINE PERFORMANCE

Md. Ashfaque Alam & Dr. A. K. Prasad

Research Scholar, Associate Professor,  
Department of Mechanical Engineering, NIT Jamshedpur, Jharkhand-831014, India

**ABSTRACT:** Nanofluids are new kind of colloidal solutions with particle size smaller than one billionth of a meter (1-100 nm) suspended in base fluid to enhance thermophysical properties of diesel. They are used in number of commercial applications like engineering, medical sciences, biotechnology, agriculture, transportation etc. Recently few experimental works using nanosized metallic, non-metallic, organic and mixed particles in base liquid fuel for diesel engine have been widely used. The results are effective due to enhancement in thermo physical and chemical properties of modified fuel. Despite having all superiorities, somewhat unclear and contradictory results are found in literature. Experimental results of different researchers are not generalized so far as to reach at common consensus about this new approach of fuel modification. Keeping all these facts in mind, an attempt is made to summarize the important published work on combustion and stability aspects of nanoparticle laden diesel, biodiesel fuels and their blends, and its effects on fuel and engine overall characteristics with the objective to provide a pathway to conduct further research in this area for utilizing maximum potential of nanoparticle fuel emulsion technology and to provide a promising future fuel for diesel engine.

**Keywords:** Nanoparticles; Diesel; Biodiesel; Emission; Combustion; Stability; Performance

## 1. INTRODUCTION

The diesel engine is one of the preferred prime movers in all the application which are designed to run with diesel fuel. Combustion of diesel fuel is one of the major sources of greenhouse gas emission to the atmosphere resulting in severe environmental problems like global warming and unnatural climate change. Biodiesel has gained popularity as replacement for diesel fuel due to their advantageous properties i.e. biodegradable, non-toxic, eco-friendly, sulphur free, higher oxygen content, etc. and these fuels can be used in the same diesel engine with little or no engine modification [1-2]. It also has the potential to reduce the engine exhaust emission such as carbon monoxide (CO), carbon-di-oxide (CO<sub>2</sub>), hydrocarbons (HC), particulate matters (PM) and smoke. Usage of renewable energy has not been limited to study of Biofuels only. Renewable source of energy like solar energy has found its application in many fields. Kumar and Prasad [3-5] has used three sides instead of one side roughened solar duct & found that augmentation in Nu & f was respectively to be 21-86 % & 11-41 %. They also reported augmentation in thermal efficiency of three sides over one side roughened duct to be 44-56 % for varying p/e and 39-51 % for varying e/D<sub>h</sub>. Kumar 2018 derived correlations for Nusselt number and friction factor applicable for three sides dimple roughened solar duct and studied the effects of three sides concave dimple geometry on artificially roughened solar air heaters [6-8].

### 1.1 Nano particles as fuel additive

Despite having many advantages, diesel engine is known to emit large quantity of pollutants (NO<sub>x</sub>, CO<sub>2</sub>, CO, VOCs, soot, PM, acrolien and formaldehyde) which causes serious health and environmental degradation [9]. According to the IEA (International Energy Agency) the global energy demand is expected to increased by 53% by 2030 [10]. Modifications of fuels by using energetic nano particle as additives, i.e. Nano fuels, are broadly adopted by many researchers to improve the performance with reduction in NO<sub>x</sub> emission of diesel engine. Several researchers have found that nanoparticle inclusion shows better properties over micron size particles such as availability of high reactive surface area responsible for more complete combustion due to reduction in ignition delays [11-12]. Berner et al. [13] indicated that use of nanoparticle helps in effective mixing of components and providing close contact between them, which facilitates diffusion of reactants to the surface and increase their reactivity. Jones et al. [14] investigated the combustion behavior of nanoscale metal and metal oxide particles of aluminum (n-Al and n-Al<sub>2</sub>O<sub>3</sub>) in ethanol. They concluded that during combustion of a stable suspension of n-Al in ethanol, amount of heat released increases almost linearly with n-Al concentration, but that trend was observed only when n-Al concentration was kept above 3%. Guru et

al. [15-16] observed that diesel blended with magnesia additives shows appreciable reduction in flash point, viscosity, freezing point and pollutant emissions. Many researchers have attempted to explore the combustion, ignition and vaporization characteristics of liquid fuel embedded with various micro and nanoscale particles [17], while others have focused their studies on performance and pollution emissions [18]. Initial studies were conducted with micron size metal additives like aluminum (AL), carbon (C), boron (B) etc to explore the burning characteristics of slurry droplets with a high particle loading (40–80%). It was found that few problem like rapid settlement, poor stability and large agglomeration, etc. occurs which requires longer burning time due to slow combustion rates including prolonged ignition delays.

Nanofluid fuels are exceptionally suitable fuel for engine and may find its commercial application in near future. Despite this fact, a limited number of studies are available in public domain. An attempt has been made to consolidate the research findings on the above issues with the objective to make significant contribution towards fundamental understanding of combustion and stability aspects of various nanoparticles inclusion with diesel and biodiesel fuels and its effect on overall diesel engine characteristics.

## 2. RECENT CHANGES IN NANOFLUID FUELS

Nanofluid fuels refer to fuels derived from nanoparticles inclusion which originated from different sources such as metal oxides, non organic materials, ferro material and carbon nanotubes. With continuous improvement in nanoparticle synthesis and preparation method possibilities of producing various nanofluid fuels from different nano- particles are explored. Diesel combustion emits harmful pollutants which are responsible for environmental degradation as well as human health. Biodiesel is considered as viable alternative to diesel. Recently in different combustion studies it was found that like hydrocarbon fuel combustion, metal particles when oxidized releasing large amount of heat, which are even quiet higher than diesel, biodiesel fuels. Beside these, some researchers have attempted to use nanofluid fuels directly in diesel engine to improve ignition and combustion properties of conventional diesel and biodiesels fuel and also investigated its overall effect on engine characteristics [19-20]. Though different nanometallic particles have been proposed (Fe, Al, B etc.) as an additive to various hydrocarbon fuels and biofuels for combustion in conventional engines, few direct combustion studies of nanomaterials have been performed for evaluating the magnitude of heat released by them. Few metal particles like boron due to their high vaporization temperature require addition of iron and aluminum particles which due to its early ignition would rapidly increase the temperature and facilitates the combustion of conventional boron particles [21-22]. Recently researchers are attempting to use combination of different nanoparticles like cerium oxide-zirconium dioxide nanoparticle ( $\text{CeO}_2\text{-ZrO}_2$ ), carbon nanotubes-ceria (CNT-ceria), samarium-doped ceria (SDC) mixed with hydrocarbon fuel as a novel fuel for use in diesel engine [23]. Researchers are trying to produce such nanofluid fuels which should be stable and having long shelf life during storage, having minimum negative health impact and should be technically as well as economically viable for use in commercial applications.

## 3. COMBUSTION ASPECTS OF NANOPARTICLE LADEN FUEL

Due to some desirable combustion feature as high heat of combustion and high energy densities, various metal particles are considered as possible additives for conventional fuels in CI engines. Though very limited theoretical and experimental work is available on combustion aspects of various nanoparticle inclusion with diesel and biodiesel fuels, an effort has been made to review its literature and assimilate the facts related to the combustion, before this it is necessary to take an overview on some important finding of several researches on various aspects of metallic nanoparticle combustion.

### 3.1. Combustion aspects of metallic nanoparticles

Metal particle additives have been used in number of combustion systems which includes nanofluid, gelled propellant [24], thermites and solid propellants [25-26]. The combustion of metal particles are classified as homogeneous (both oxidizer and metal in gaseous phase) and heterogeneous (both oxidizer and metal reaction in condensed phase). Glassman et al. [27] revealed that due to very high boiling point of metal oxides the flame temperature is limited as energy required to decompose the oxide layer is much more than energy actually available for rise in temperature of condensed phase oxide. Levenspiel [28] defined three important processes which control burning rates of metal particles namely; Diffusion of mass through gas phase mixture, Diffusion of mass through oxide layer of the particle and Chemical reactions. Risha et al. [29] have investigated the combustion behavior of nanoaluminum with water and without any gelling agent for different operating pressure, mixture composition and particle size and reported that n-Al water quasi homogenous mixture ignited with linear burning rates. Dreizin et al. [30-33] performed lot of research work

on nanoscale Al combustion in presence of air and oxygen environment during combustion aimed to explore phenomenon of micro explosion and variation in speed of burning droplets at nanoscale metal combustion. Parr et al. [34] in their experimental work on n-Al with post combustion gases of H<sub>2</sub>/O<sub>2</sub>/argon diffusion flame to investigate the ignition temperatures and burning times at stoichiometric mixture ratio found that above 10 μm the combustion process from diffusive controlled process get changes to kinetically controlled process. The author reported that for particle size less than 10 μm, combustion and burning rates are highly temperature dependent. Beckstead et al. [35] proposed a correlation from various experimental data on burning time of aluminum particle combustion considering pressure, temperature, particle size and oxidizer concentration as:

$$t_b = \frac{d_o^{1.8}}{125(X_{O_2} + 0.6X_{H_2O} + 0.22X_{CO_2})} P^{0.3} T^{0.2} \quad (1)$$

where P is pressure, T is surrounding temperature and d<sub>o</sub> is particle diameter. The results obtained from this study show a large deviation from the experimental results considering same parameters for both theoretical and experimental studies. Bazyn et al. [36] performed shock tube experiment on 10 μm aluminum particles in the presence of O<sub>2</sub>, CO<sub>2</sub> and H<sub>2</sub>O in air to study the effect of pressure on combustion time. The authors reported a weak increase in burning rates with H<sub>2</sub>O, CO<sub>2</sub> and decrease in burning rates with O<sub>2</sub> when pressure was increased. The possible explanation for the changed trend in burning times of CO<sub>2</sub>, H<sub>2</sub>O and oxygen is mainly attributed to the availability of two oxygen atoms to react with Al when O<sub>2</sub> molecule diffuses at Al Surface, whereas for H<sub>2</sub>O and CO<sub>2</sub> the available oxygen atom to react with Al is one, thus two times faster diffusion is required with H<sub>2</sub>O and CO<sub>2</sub> to produce same oxygen atoms. Hence kinetics mode dominates O<sub>2</sub> due to presence of more oxygen atoms to Al surface for reaction, whereas for H<sub>2</sub>O and CO<sub>2</sub> diffusion mode is important. Metal properties are regarded as size dependent properties; hence a reduction in particle size increases the chemical reaction due to more participation of surface atoms. Several studies reveal the fact that at nanolength scale various thermo-physical properties shows strong particle size dependence due to large exposed surface areas with enhanced reactivity. Eckert et al. [37] conducted experiments with nanoparticle size ranging from 13 to 40 nm. Similar studies were also performed by Alavi et al. [40] and Puri et al. [38-39] to analyze the melting behavior of n-Al. It was found that the melting temperature of n-Al is highly influenced by particle diameter. The available results depicts a gradual reduction in melting point temperature of metal particles up to 10 nm particle size whereas below this particle size value the melting temperature decreases drastically. This clearly indicates that particle size defines the combustion and ignition mechanism as during small size particle combustion, the burning mechanism of particles are governed by kinetically controlled condition, whereas larger size particles combustion may be governed by diffusion controlled condition. Several researches based on their experimental work have attempted to develop correlations in order to predict the melting and combustion parameters of aluminum as a function of particle size. The important correlation is summarized in Table 1 [37,42-45]. Another prospective candidate considered for fuels and propellant inclusion is boron. It can be found to be best suited for volume limited propulsion, due its highest heating value [46]. It was found from the literature that high vaporization temperature of range of 4000 K and the presence of natural oxide film causes the delay in ignition process plays a very crucial role in combustion of boron systems. Several studies have been conducted to understand the combustion and ignition of boron particles at micron size scale but very limited studies are available on combustion of boron particles at nanoscale. Few experimental studies have been conducted to evaluate the thermal contributions of boron nanoboron particles when mixed with low energy density biofuels. The results revealed that there has been an enhancement in combustion performance of biofuels with faster ignition at lower combustion temperatures, thus releasing large amount of heat during combustion [47-48].

### 3.2. Combustion aspects of various nanoparticle doped liquid fuels

Previous discussion related to combustion aspects of metallic nanoparticles provides the basis for utilizing their possible benefits when dispersed in liquid fuels as an alternative fuel for combustion in diesel engine. Very limited experimental studies on combustion aspects of nanoparticle laden liquid fuels are available in the open literature, and almost no review work is available. In this work key findings of available work on combustion aspects of various nanoparticle doped liquid fuel are summarized. Metal particles are known to have better thermal properties when they are suspended in micro or nanoscale length in different concentration with the base fluids. Several researches in their experimental findings reported a 20% increase in thermal conductivity with a lower particle concentration (< 5%) [49]. The same incremental

trend was observed in the heat transfer coefficient. Based on these above fascinating facts researches are attempting to use these energetic materials with liquid fuels in diesel engine for obtaining better combustion characteristics in terms of higher heating value. In order to gain fundamental understanding of combustion behavior some experimental studies related to single droplet, and some in the bulk base fluid with micro and a nanoscale additives have been performed. Each study has its own significance. Mono droplet combustion studies provide an insight on general burning and vaporization characteristics and how different physical and chemical processes involved in it. Tyagi et al. [50] found that with a very small volume fraction (1–5% by weight) of n-Al and Al<sub>2</sub>O<sub>3</sub> blended with diesel fuel, there has been a significant enhancement in the ignition probability compared to pure diesel fuel. This is due to better radiative heat & mass transfer properties which causes reduction in droplet ignition temperature.

#### 4. EFFECT OF INCLUDING NANOPARTICLES WITH DIESEL BIODIESEL FUEL BLENDS ON ENGINE PERFORMANCE

Among various types of internal combustion engine diesel engine is considered as most prominent and efficient energy conversion device because it directly converts heat into mechanical energy with minimum heat out from the tail pipe as other engines do. Regarding diesel engine this statement is very true that diesel engine performance resembles the performance of workhorse slower, stronger and enduring rather than fiery, fast and high stung. The above features of diesel engine make them the preferred choice for use in commercial applications. As mentioned earlier that with the scarcity of diesel fuel, further with strict environmental norms, biofuels present themselves as an alternative fuel despite some issues such as lower calorific value and inferior cold flow properties etc. as compared to diesel fuel. To overcome this problem, biofuels are modified by adding various nano particles in it, which provides significant improvement in thermo physical properties of biofuels and make them comparable to that of conventional diesel fuel. With the continuous improvement in diesel technology for overall enhancement in engine operating characteristics, researchers are attempting experimental studies on engine performance, emission and combustion parameters which prove to be the real performance indicators. Limited experimental studies have been performed on diesel engine to investigate the engine performance parameters using nanofluid fuels. In this section the discussion have been made to observe the effect of various nanoparticle inclusions with base fuel as diesel, biodiesel and its blend on engine performance parameters such as brake power (BP), brake thermal efficiency (BTE) and brake specific fuel consumption (BSFC).

**Table 1 Developed correlations of aluminum nanoparticle combustion parameters.**

Sr. No	Authors	Parameters	Correlation	Range of Applicability	Terminology
1	Glassman et al. [41]	Time of combustion	$t_{b, diff} = \frac{\rho P d_o^2}{8 \rho_f D \ln(1 + iY_{O, \infty})}$ $t_{b, kin} = \frac{\rho P d_o}{2 MW_p k P X_{O_2}}$	Used to find com. time in diffusion and kinetically controlled com. regime	$t_{b, diff}$ = Combustion time in diffusion controlled region. $d_o$ = initial particle diameter. $t_{b, kin}$ = Combustion time in kinetically controlled region.
2	Ecret et al.[37]	Melting point temperature, latent heat of fusion	$T_m = 97704 - 1920 / D$ $L_{fus} = 14.705 - 177.49 / D$	$13 \leq D < 40 \text{ nm}$ $13 \leq D < 40 \text{ nm}$ Oxide layer thickness 2–5nm	$X_{O, \infty}$ = oxidizer mole fraction. MWp = molecular weight of particle.
3	Jiang et al.[42] Liang et al.[43]	Melting point temperature, latent heat of fusion	$T_m = T_{mb} \exp \left[ \frac{- (2L_{fus} / b)}{3R_u T_{mb}} \right]$ $/ D / 6l - 1$	Based on linde- mann criterion for nearly all nano sized particles	$\rho_p$ = particle density. $\rho D$ = product of gas density & diffusivity. $iY_{O, \infty}$ = oxygen mass fraction in ambient.
4	Zhang et al. [44]	latent heat of fusion	$\frac{L_{fus}(R)}{L_{fus}(b)} = \frac{T_m(R)}{T_m(b)} \left[ 1 - \frac{1}{R / R_u - 1} \right]$	Ro=0.9492, α=1.9186	$T_m$ = melting point Temp. K $L_{fus}$ = latent heat of fusion (kJ/mol)
5	Panda et al. [45]	Vapor pressure	$P_D = P_0 \exp(4\sigma v_1 / k_g T D)$ $P_0 = \exp \left( 13.7 - \frac{36373}{T} \right) \text{ atm}$ $\sigma = 948 - 0.202 T \text{ dyne / cm}$	Vaporization tem. can be calculated iteratively by these three equations at a given ambient pressure & particle diameter	$D$ = particle diameter (nm) $T_{m,b}$ = Bulk melting temperature $L_{fus,b}$ = Bulk heat of fusion $l$ = Length of Al-Al atomic bond. $R_u$ = Universal gas constant. $\alpha$ = Material constant $P_0$ = Vapor pressure. $P_D$ = Vapor pressure over a flat surface. $\sigma$ = Surface tension.

#### 4.1. Effect on brake power

Net power available after the deduction of frictional losses from indicated power is termed as brake power (BP). Kumar et al. [51] performed experimental studies on CeO<sub>2</sub> nanoparticles emulsion fuel for Compression ignition (CI) engine with variable load ranging from 2.1 to 15.9 kg. The authors reported an increase in brake power under all operating conditions when the load on engine increase. All the tests have been conducted at constant engine speed where engine produced equivalent brake power at similar loads. Researchers like Nadem et al. [52] performed experiments on variable speed engine to analyze the effect of engine speed on brake power. It was observed that BP of the engine increases with increase in engine speed, up to certain speed limit, which further depends on engine rating and number of cylinders. In addition to that, a slight increase in BP has been observed with emulsified and nanoparticle mixed biodiesel, diesel fuel blends as compared to diesel fuel alone under same operating conditions. According to them a slight increase in BP, might be due to optimized ignition delay and increase temperatures which causes significant improvement in combustion process and heat release rates. Furthermore with improvement in combustion efficiency of nanofluid fuels a reduction in fuel consumption and emission level leads to the augmentation in the overall efficiency of CI engines. Whereas in an experimental work carried out by Keskin et al. [53] when tested tall oil biodiesel which was doped by Co based additive in a CI engine, reported no appreciable increase in the values of power output and engine torque compared to that of diesel fuel. To have some more insight about nanoparticle mixed diesel, biodiesel fuel blends, Mirzajanzadeh et al. [54] performed experimental work with hybrid nanoparticle of cerium oxide and multiwall carbon nanotubes (MW-CNT) in a diesel biodiesel fuel blend (B5 and B20) on heavy duty 6 cylinder diesel engine. The results revealed that at 1500 rpm and at full load condition there exist a linear relationship between power output and amount of nanoparticle doping levels with diesel biodiesel fuel blend. This trend can be readily viewed from Fig. 1 It is evident from the Fig. 1 that for B5 blend with 30, 60, 90 ppm nanoparticle doping level an increase in 0.58%, 1.79% and 3.52% whereas for B20 blend with 30, 60, 90 ppm an increase in 2.28%, 5.72% and 7.81% was observed in engine power as compared to diesel biodiesel fuel blend without nanoparticles. Fangsuwannrak et al. [55] in their experimental work studied the effect of titanium oxide (TiO<sub>2</sub>) nanoparticle additives with palm biodiesel in an indirect injection diesel engine (IDI). The authors have reported that higher brake power from engine were achieved for any fraction of biodiesel fuel mixed with 0.1% TiO<sub>2</sub> additives as compared to biodiesel fuel without addition of TiO<sub>2</sub> nanoparticles. Further investigations performed with B100-0.1% TiO<sub>2</sub> sample in a speed range of 1600–3000 rpm provides a maximum increment of 1.56% in average brake power. It can be easily seen from Fig. 2 that at all speeds in the range of 1500–4000 rpm the brake power output of the engine increased by adding 0.1% TiO<sub>2</sub> nanoparticles for any fraction of biodiesel fuel blend. Recently an study performed by Ramadhas et al. [56] on theoretical modeling of CI engine performance parameters whose results were further verified by experimental work, provides a effective methodology to model the problem when working with diesel, biodiesel fuels blended with nanoparticles.

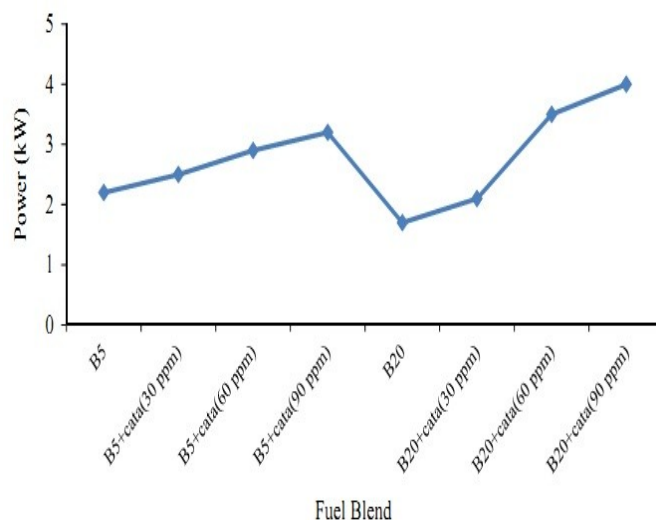


Fig. 1: Variation of maximum power of different fuel blends of (B5-B20) with CeO<sub>2</sub>+MWCNT at full load and at constant speed of 1500 rpm [54].

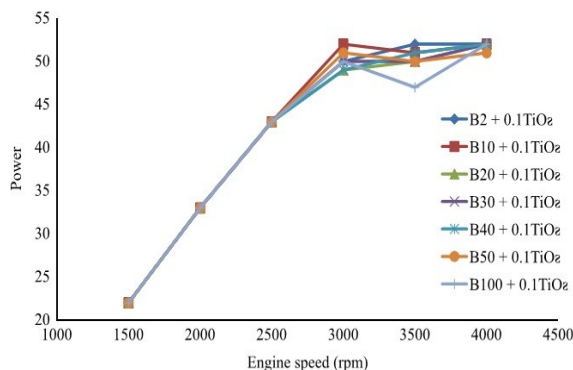


Fig. 2: Variation in brake power of different fuel blends of Palm oil biodiesel (B2-B100) with 0.1TiO<sub>2</sub> for various engine speeds [55].

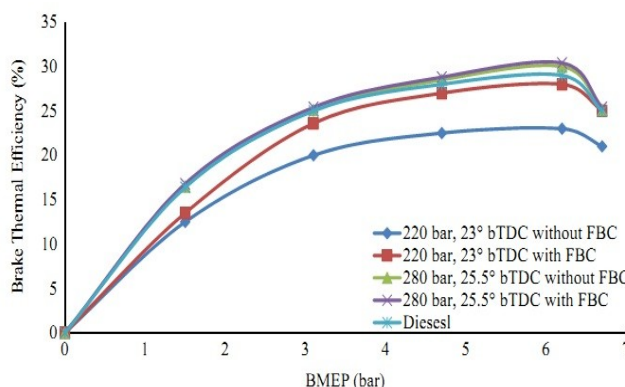


Fig. 3: Variation of brake thermal efficiency with BMEP of different diesel fuel blends with and without FBC [57].

#### 4.2. Effect on brake thermal efficiency

Experimental studies carried out by Kannan et al. [57] with metal based additives FeCl<sub>3</sub> nanoparticles in waste cooking oil biodiesel at different dosing quantities of FeCl<sub>3</sub> nanoparticles within the range of 0.01–0.2 gm (5 mol/L to 50 mol/L). It is evident from the Fig. 3 that at different break mean effective pressures (BMEP), addition of FeCl<sub>3</sub> nanoparticle to biodiesel fuel, gives higher brake thermal efficiency (BTE) as compared to that of biodiesel without FeCl<sub>3</sub>. The available results depicts that, owing to the highly catalytic effect, addition of FeCl<sub>3</sub> nanoparticles to biodiesel fuel, provides enhancement in combustion process which significantly improves the brake thermal efficiency.

### 5. CHALLENGES FACED IN THE FIELD OF BIODIESEL

Due to some inferior physical and chemical properties of biodiesel fuels, addition of different nanoparticles found to be suitable for modifying biodiesel properties and make them comparable with that of diesel fuels. These nanoparticles can be mixed with biodiesel, diesel biodiesel blends without any requirement of engine design modifications. From the overview of available literature in this area, somewhat inconsistent information supported by limited experimental findings along with supply constraints, food security and cost issues hindered their usage as commercial fuel for automobiles and other energy sectors. However some specific issues concerned with the application of nanoparticle blended diesel biodiesel fuel in CI engines must be addressed with utmost care, these are:

1. Colloidal solution of diesel-biodiesel blends with prolonged suspension with various nanoparticles causes agglomeration, settling and precipitation problem. In order to achieve better stability of nano- fluid fuels detailed chemical analysis and identification of more effective surfactant must be required.
2. The addition of nanoparticles to liquid fuels have shown significant effect on drop burning behavior and on bulk fuel combustion characteristics, however the combustion characteristics strongly influenced by the shape and size of nanoparticles.

3. Nanofluids possessed better heat and mass transport properties, which significantly improves the engine performance, emission and combustion characteristics. However due to lack of fundamental understanding of heat transfer and fluid flow behavior of nanoparticles with liquid fuels, it is essential that extensive research work should be carried out in this area to explore its maximum potential.
4. The wear of various engine components (fuel injector assembly, cylinder and piston etc) which deteriorates the performance and life of engine along with other tribological issues arises due to crankcase dilution are rarely reported.
5. Along with theoretical research and experimental methodology adopted by the researchers in order to analyze the performance, emission and combustion characteristics of nanofluid fuels, further studies in this area should be carried out through visual observation approach via Phase Doppler Particle Anemometry (PDPA), high speed imaging techniques (CCD Cameras) and by shadowgraphs.
6. Serious efforts are to be made to evaluate the unknown environmental and health impact issues related to nanofluid fuels. Extensive research should be required in this area before the commercialization of this technology.
7. It is necessary to channelize the research outcomes of this technology with automobile manufacturing industry, to make it viable for commercial applications, thus reduce our dependency on petro-products as fuel for automobiles.

## **6. CONCLUSIONS AND SCOPE FOR FUTURE ASPECTS**

In order to fill the gap in the available relevant literature, the present study provides a detailed overview of some important research work and recent developments in the field of nanofluid fuels which includes the combustion and stability aspects and their potential as reactive additives with diesel and biodiesel blends for use in diesel engine technology. Obvious role of nanoparticles have been found to enhance combustion characteristics of modified diesel fuel which led to the overall improvement in CI engine performance with a significant reduction in engine emissions levels. The major facts that can be drawn from above discussion are summarized as follows.

1. The stability of nanofluid in liquid fuels with reported maximum stability of 7–17 days is of great concern and hinders the use of nanoparticles with diesel biodiesel blended fuels. For highly stable nanofluid fuel solutions the Zeta potential values found to be in the range of 70–60 mV, and operation pH value (O.PH) within the range of 3.5–10.5. Zeta potential values above 70 mV and O.PH below 3.5 provides good stability nanofluid fuels. Further, experimental results revealed that preferred value of surfactant oleic acid as 0.6 vol% in diesel with a nanoparticle loading of 10 ppm are found to provide most stable blend with minimum settling effect.
2. Nanometallic particle additives with diesel biodiesel fuel blends increase the solution viscosity and make them more prone to agglomerations and settling.
3. In most of the previous studies and experimental investigations it was found that metal particles both in micron or nanolength scale when mixed with diesel and biodiesel fuel improves the ignition and combustion behavior.
4. The short ignition delay, better atomization of fuel and high reactive surfaces provides rapid and early start of combustion reactions which in turn gives higher heat release rates and are found to be liable for higher cylinder pressures.
5. The additive effect on nanoparticles with diesel biodiesel fuels sometimes may led to abnormal combustion hence proper selection of above parameters are essentially required for achieving controllable combustion.
6. The application of nanoparticles with biodiesel fuel blend was found to enhance the diesel engine performance in terms of slightly higher engine brake power, higher brake thermal efficiency and lower engine brake specific fuel consumption up to a certain dosage value of nanoparticles, beyond this limit further increase in dosage value does not provide proportional enhancement in the engine performance.
7. The additive effect of nanoparticles with liquid fuel found to lower most of the tail pipe emission like hydrocarbon (HC) emission, smoke levels and CO except NO<sub>x</sub> emissions.
8. CO emission increases with addition of FeCl<sub>3</sub> nanoparticles.
9. The engine NO<sub>x</sub> emissions were found to be higher when nanoparticles are mixed with diesel, biodiesel fuels. Researchers have attempted to trim down the NO<sub>x</sub> level by emulsifying nanoparticle mixed fuel with water which during the combustion of fuel takes sufficient heat for its vaporization

and decreases the peak cylinder temperatures, that ultimately results in the reduced NO<sub>x</sub> emission values.

10. It was also suggested that improving engine design through additional swirling effect produced by providing slots on the piston or by changing the injector nozzle geometry (increasing number of holes in a nozzle) gives high injection pressure, which reduces the fuel droplet diameter and maintains better spray patterns.

#### References:

1. National Policy on Biofuels. A technical report of Ministry of new & renewable energy. Government of India, New Delhi; 2015:1-18.
2. Bhandarkar S. Vehicular pollution, their effect on human health and mitigation measures. *Veh Eng* 2013;1(2):33-40.
3. Kumar, V., Prasad, L., Experimental investigation on heat transfer and fluid flow of air flowing under three sides concave dimple roughened duct. *International Journal of Mechanical Engineering and Technology (IJMET)*, Volume 8, Issue 11, November 2017, pp. 1083-1094, Article ID: IJMET\_08\_11\_110.
4. Kumar, V., Prasad, L., Thermal performance investigation of one and three sides concave dimple roughened solar air heaters. *International Journal of Mechanical Engineering and Technology (IJMET)* Volume 8, Issue 12, December 2017, pp. 31-45, Article ID: IJMET\_08\_12\_004.
5. Kumar, V., Prasad, L., Performance Analysis of three sides concave dimple shape roughened solar air heater, *J. sustain. dev. energy water environ. syst.*, 6(4), pp 631-648, 2018.
6. Kumar, V., Nusselt number and friction factor correlations of three sides concave dimple roughened solar air heater, *Renewable Energy* 135 (2019) 355-377.
7. Kumar, V., Prasad, L., Experimental analysis of heat transfer and friction for three sides roughened solar air heater, *Annales de Chimie - Science des Matériaux*, 75-107, ACSM. Volume 41 – n° 1-2/2017.
8. Kumar, V., Prasad, L., Performance prediction of three sides hemispherical dimple roughened solar duct, *Instrumentation, Measure, Métrologie*, 273-293 I2M. Volume 17 – n° 2/2018.
9. Garg P. Energy scenario and vision 2020 in India. *J Sustain Energy Environ* 2012; 3:7-17.
10. Executive Summary: Short-Term Energy Outlook, Analysis and Projections. A Report of International Energy Agency, OECD/IEA. ([http://www.eia.gov/forecasts/ieo/exec\\_summ.cfm](http://www.eia.gov/forecasts/ieo/exec_summ.cfm)) /; 2014. [Accessed 15.06.16.]
11. Granier JJ, Pantoya ML. Laser ignition of nanocomposite thermites. *Combust Flame* 2004; 138:373-89.
12. Yetter RA, Risha GA, Son SF. Metal particle combustion and nanotechnology. *Proc Combust Inst* 2009; 32:1819-38.
13. Berner MK, Zarko VE, Talawar MB. Nanoparticles of energetic materials, synthesis and properties (Review). *Combust Explos Shock Waves* 2013; 49:625-47.
14. Jones M, Calvin HL, Afjeh A, Peterson GP. Experimental study of combustion characteristics of nanoscale metal and metal oxide additives in biofuel (ethanol). *Nano Express Nanoscale Res Lett* 2011; 6(1):246.
15. Guru M, Koca A, Can O, Cinar C, Sahin F. Biodiesel production from waste chicken fat sources and evaluation with Mg based additive in a diesel engine. *Renew Energy* 2010;35: 637-43.
16. Guru M, Karakaya U, Altıparmak D, Ahcılar A. Improvement of diesel fuel properties by using additives. *Energy Convers Manag* 2002; 43:1021-5.
17. Karmakar S. Energetic Nanoparticles as fuel additives for enhanced performance in propulsion systems. A dissertation for the degree of Doctor of Philosophy, Louisiana State University; 2012.
18. Shaafi T, Velraj R. Influence of alumina Nanoparticles, ethanol and isopropanol blend additive with diesel-soyabean biodiesel blend fuel, combustion, engine performance and emissions. *Renew Energy* 2014; 80:655-63.
19. Aneggi E, de Letitenburg C, Dolcetti G, Trovarelli A. Promotional effect of rare earths and transition metals in the combustion of diesel soot over CeO<sub>2</sub> and CeO<sub>2</sub>-ZrO<sub>2</sub>. *Catal Today* 2006; 114(1):40-7.
20. Zhao S, Gorte RJ. A comparison of ceria and Sm-doped ceria for hydrocarbon oxidation reactions. *Appl Catal* 2004; 277:129-36.
21. Mohan S, Turnov MA, Dreizin EL. Heating and ignition of metallic particles by a CO<sub>2</sub> laser. *J Propuls Power* 2008; 24(2):199-205.
22. Wang N. Boron composite Nanoparticles for enhancement of bio-fuel combustion. A dissertation report. BS, Dalian University of Technology; 2012.
23. Zhao S, Gorte RJ. A comparison of ceria and Sm- doped ceria for hydrocarbon oxidation reactions. *Appl Catal* 2004; 277:129-36.
24. Palaszewski B, Jurns J, Breisacher K, Kearns K. Metalized gelled propellants combustion experiments in pulsed detonation engine. 40thAIAA/ASME/SAE/ASEE Joint Propulsion Conference and Exhibit, Ft. Lauderdale, Florida; 2004.
25. Piercey DG, Klapotke TM. Nanoscale aluminum-metal oxide (thermites) reactions for application in energetic materials. *Cent Eur J Energ Mater* 2010;7(2):115-29.

26. Mench MM, Yeh CL, Kuo KK. Propellant burning rate enhancement and thermal behavior of ultra fine aluminum powder (ALEX). 29th Annual Conference Proceedings of ICT; 29:1-15; 1998.
27. Glassman I, Williams FA, Antaki PA. Physical and chemical interpretation of boron particle combustion. 20th Symposium (International) on Combustion, 20. The Combustion Institute; 1984. p. 2057-64.
28. Levenspiel O. Chemical Reaction Engineering. New York: John Wiley and Sons; 1962.
29. Risha GA, Huang Y, Yetter RA, Yang V. Combustion of aluminum particles with steam and liquid water. 44th AIAA Aerospace Sciences Meeting and Exhibit, Reno, Nevada; 2006.
30. Dreizin EL. Experimental study of stages in aluminum particle combustion in air. *Combust Flame* 1996; 105: 541-56.
31. Dreizin EL. On the mechanism of asymmetric aluminum particle combustion. *Combust Flame* 1999; 117:841-50.
32. Dreizin EL. Effect of phase changes on metal-particle combustion process. *Combust, Explos Shock Waves* 2003; 39:681-93.
33. Dreizin EL. Metal based reactive Nanoparticles. *J Prog Energy Combust Sci* 2009; 35:141-67.
34. Parr T, Johnson C, Hanson-Parr D, Higa K, Wilson K. Evaluation of advanced fuels for underwater propulsion. JANNAF Combustion Subcommittee Meeting, Colorado; 2003.
35. Beckstead MW, Puduppakkam K, Thakre P, Yang V. Modeling of combustion and ignition of solid-propellant ingredients. *Prog Energy Combust Sci* 2007; 33(6):497-551.
36. Bazyn T, Lynch P, Krier H, Glumac N. Combustion measurements of fuel-rich aluminum and molybdenum oxide nano-composite mixtures. *Propellants Explos Pyrotech* 2010; 35:93-9.
37. Eckert J, Holzer JC, Ahn CC, Fu Z, Johnson WL. Melting behavior of nanocrystalline aluminum powders. *Nano Struct Mater* 1993; 2, [407-13].
38. Puri P, Yang V. Effect of particle size on melting of aluminum at nano scales. *J Phys Chem* 2007; 111: 11776-83.
39. Puri P. Multi scale modeling of ignition and combustion of micro and nonaluminum particles. Penn State electronic theses and dissertations for graduate school Thesis. Pennsylvania, USA: Pennsylvania State University; 2008.
40. Alavi S, Thompson DL. Molecular Dynamics simulations of melting of aluminum Nanoparticles. *J Phys Chem* 2006; 110:1518-23.
41. Glassman I, Williams FA, Antaki PA. Physical and chemical interpretation of boron particle combustion. 20th Symposium (International) on Combustion, 20. The Combustion Institute; 1984. p. 2057-64.
42. Jiang Q, Yang CC, Li JC. Melting enthalpy depression of nanocrystals. *Mater Lett* 2002; 56:1019-21.
43. Liang LH, Li JC, Jiang Q. Size-dependant melting depression and lattice contraction of Bi nanocrystals. *Phys. B: Condens Matter* 2003; 334:49-53.
44. Zhang Z, Lu XX, Jiang Q. Finite size effect on melting enthalpy and melting entropy of nanocrystals. *Phys. B: Condens Matter* 1999; 270:249-54.
45. Panda S, Pratsinis SE. Modeling the synthesis of aluminum particles by evaporation-condensation in an aerosol flow reactor. *Nanostruct Mater* 1995; 5:755-67.
46. Kuo KK, Risha GA, Evans BJ, Boyer E. Potential usage of energetic nano-sized powders for combustion and rocket propulsion. *Material Research Society Symposium, Boston, Massachusetts, AA 1.1; 800; 2003.*
47. Natan B, Gany A. Ignition and combustion of boron particles in the flow field of a solid fuel ramjet. *J Propuls Power* 1991; 7(1):37-43.
48. Bellott BJ, Noh W, Nuzzo RG, Girolami GS. Nanoenergetic materials: boron Nanoparticles from the pyrolysis of decaborane and their fictionalization. *J R Soc Chem* 2009:3214-5.
49. Xuan Y, Li Q. Heat transfer enhancement of nanofluids. *Int J Heat Fluid Flow* 2000; 21:58-64.
50. Tyagi H, Phelan PE, Prasher R, Peck R, Lee T, Pacheco JR. Increased hot plate ignition probability for Nanoparticles laden diesel fuel. *Nano Lett* 2008; 8, [1410-6].
51. Kumar A. Effect of cerium oxide nanoparticles on compression ignition engine performance and emission characteristics when using water diesel emulsion. A dissertation report of Thapar University- India; 2014.
52. Nadeem M, Rangkuti C, Anaur K, Haq MRU, Tan IB, Shah SS. Diesel engine performance and emission evaluation using emulsified fuels stabilized by conventional and Gemini surfactants. *Fuel* 2006; 85:2111-9.
53. Keskin A, Metin G, Altıparmak. Influence of metallic based fuel additives on performance and exhaust emissions of diesel engine. *Energy Convers Manag* 2011; 52:60-5.
54. Mirzajanzadeh M, Tabatabaei M, Ardjmand M, Rashidi A, Ghobadian B, Barkhi M, Pazouki M. A novel soluble nano-catalyst in diesel-biodiesel fuel blends to improve diesel engine performance and reduce exhaust emissions. *Fuel* 2015; 139:374-82.
55. Fangsuwannrak K, Triratanasrichai K. Improvements of palm biodiesel, properties by using nano-TiO<sub>2</sub> additive, exhaust emission and engine performance. *Rom Rev Precis Mech Opt Mechatron* 2013; 43:1-8.
56. Ramadhas AS, Jayaraj S, Muraleedharan C. Theoretical modeling and experimental studies on biodiesel-fueled engine. *Renew Energy* 2006; 31, [1813-26].
57. Kannan GR, Karvembu R, Anand R. Effect of metal based additive on performance emission characteristics of diesel engine fuelled with biodiesel. *Appl Energy* 2011; 88, [3694-703].

**Nomenclature**

BD	Barrels/day	DI	Direct injection
Bx	X% volume fraction of biodiesel in a blend of diesel and biodiesel	DLS	Dynamic light scattering
BTE	Brake thermal efficiency	EGR	Exhaust gas recirculation Fbc fuel borne catalyst
BSFC	Brake specific fuel consumption	HRR	Heat release rates
BMEP	Brake mean effective pressure	HC	Hydrocarbon
BTDC	Before top dead centre	IC	Internal combustion engine
2B+Ti	Titanium diboride	CO	Carbon monoxide
CN	Cetane number	CON	Cerium oxide nanoparticles
CI	Compression ignition engine	CNT	Carbon nanotubes

# Application of Optimization Algorithm for Composite Laminate Optimization

A.Karthikeyan<sup>1</sup> & Dr. A.Karthikeyan<sup>2</sup> & Dr.K.Venkatesh Raja<sup>3</sup> & Dr.K.Venkatesh<sup>4</sup>

<sup>1,4</sup>Asso. Prof., Department of Aeronautical Engineering, Excel Engineering College, Tamil Nadu,

<sup>2</sup>Professor, Department of Mechanical Engineering, Malla Reddy College of Engineering, Secunderabad, Telangana State,

<sup>3</sup>Asso. Prof, Department of Mechanical Engineering, VSA Group Of Institutions, Tamil Nadu.

---

**ABSTRACT:** In this project composite laminate optimization code was developed using genetic algorithm in ANSYS APDL code. Now a day's composite material widely used in many industries like aerospace, automobile, marine, structural industries and many more, due to high strength to weight ratio. The main objective of this research is economically use the composite material by optimization techniques. The strength of the Laminated structures is depends upon the fiber angle, thickness, material, sequence of layer and no of layer. To find the optimized combination of above parameter is very difficult by traditional methods, it may struck in to local optimum. To avoid the above difficulties global searching algorithm like genetic algorithm were used.

**Keywords:** Laminate optimization, Genetic algorithm, Structural optimization.

---

## I. INTRODUCTION

Composite materials have received substantial attention as manufacturing materials. Although the high stiffness-to-weight and strength-to-weight properties of composite materials are attractive, their greatest advantage is their ability to be designed to satisfy directional strength and stiffnesses for any particular loading, or multi-loading, of the structure. In laminated composite structures, each ply has its greatest stiffness and strength properties, along the direction, through which the fibers are oriented in. By orienting each layer at different angles, the structure can be designed for a specific loading environment. Along with structural performance and weight, cost is an area of great interest when considering optimization studies in structural design. Obviously, reducing the amount of material required for the structure, minimizes the cost of a laminate composite. However, another method for cost reduction is to allow more than one material in the stacking sequence. Thus, it is possible to use layers of low cost material at locations, in the structure, where performance is less important. In general, the problem of composite laminate stacking sequence optimization has been formulated as a continuous design problem, and solved using gradient based techniques. These methods of solution present several disadvantages: [2] Stacking sequence design often involves design variables, which are limited to small discrete sets of values of ply thickness,

orientation angle or material type, due to manufacturing or cost limitations, therefore, these methods require the transformation of these variables into continuous variables, in order that a solution might be obtained, [3] Converting the continuous solutions back to discrete feasible values, often produces sub-optimal, or even infeasible designs, [4] Composite laminate design problems often have discontinuous objective functions, exhibiting multiple designs with similar performances, involving many local optimum designs. Genetic Algorithms are suitable optimization algorithms for problems with discrete design variables. Its implementation does not require any evaluation of gradients which, together with its easiness of implementation, make it worthwhile investigating. [5] Although, Genetic Algorithms require many function evaluations, which reflect in large computational costs, there are many reported applications of Genetic Algorithms to the design of composite structures. Genetic algorithms have been applied to stacking sequence optimization of composite plates, (Callahan and Weeks, 1992), to stiffened composite panel design (Nagendra et al., 1996), design of laminated composite panels (Hajela, 1990) (Leung and Nevill, 1994) (Fernandes et al., 1998) (Haftka, 1998). The design of optimal composite laminates has been shown to be well suited to the defining characteristics of genetic algorithms. Techniques for improving the efficiency of this methodology

have been explored for several problems using local improvement, memory, migration, and varied selection schemes [13]. For large structures, such as the design of a wing or fuselage, the optimization is divided into smaller, tractable, sub problems using predefined local loads to constrain the optimization [13], [1], [9]. Isolated local optimization results in widely varying stacking sequence orientations between adjacent panels that causes serious manufacturing difficulties and, hence, generates the need for a globally blended solution. [7] Design of a fiber-reinforced composite laminate requires the specification of the stacking sequence, which is defined by the orientation and material type of each ply layer, creating a discrete optimization problem. It is computationally expensive to design an entire wing or fuselage structure with the panels optimized simultaneously. Instead, local panels are commonly optimized for the specified local loads by ignoring the possible continuity of some or all of the layers from one panel to another across the structure [8]. Soremekun et al. [18] introduced multiple elitist selection schemes that by nature aid in discovering alternative designs with similar fitness values. In a standard elitist selection strategy only a single member of a parent population can survive the selection process without being modified and be placed in the child population. [12] In a multiple elitist selection strategy the genetic algorithm allows a greater number of high fitness members to survive the selection process at each generation. Application of GAs for optimization of composite structures was reported by Hajela (1989, 1990). Callahan and Weeks (1992) used a GA to maximize strength and stiffness of a laminate under in-plane and flexural loads. Labossiere and Turkkan (1992) used a GA and neural networks for optimization of composite materials. Haftka, Watson, G'urdal and their coworkers (Nagendra et al., 1992; Le Riche and Haftka, 1993; Nagendra et al., 1993a,b; G'urdal et al., 1994; Le Riche, 1994; Soremekun, 1997) have developed specialized GAs for stacking sequence optimization of composite laminates under buckling and strength constraints. Sargent et al. (1995) compared GAs to other random search techniques for strength design of laminated plates. [10] The applications of GA methods in the field of composite structure optimization include the weight minimization of stiffened panels and shells (Harrison et al., 1995, Nagendra et al., 1996; Kallassy and Marcelin, 1997; Jaunky et al., 1998, Kaletta and Wolf, 2000; Gantovnik et al., 2003b; Kang and Kim, 2005), the strength optimization of plates with open holes

(Todoroki et al., 1995, Sivakumar et al., 1998), the improvement of the energy absorption capability of composite structures (Woodson et al., 1995, Averill et al., 1995; Crossley and Laananen, 1996), [11] the optimization of sandwich-type composite structures (Malott et al., 1996, Kodiyalam et al., 1996; Wolf, 2001; Gantovnik et al., 2002b; He and Aref, 2003; Lin and Lee, 2004), the optimization of dimensional and thermal buckling stability under hygrothermal loads (Le Riche and Gaudin, 1998; Spallino and Thierauf, 2000), the strain energy minimization of laminated composite plates and shells (Potgieter and Stander, 1998), maximizing the fundamental frequency of the laminated composite structure (Sivakumar et al., 1998), the stacking sequence blending of multiple composite laminates (Soremekun et al., 2001, 2002; Adams et al., 2003; Seresta et al., 2004; Adams et al., 2004), the optimization of electromagnetic absorption in laminated composite structures (Matous and Dvorak, 2003), the optimization of composite structures considering mechanical performance and manufacturing cost (Park et al., 2004), the optimization of composite tire reinforcement (Abe et al., 2004), [14] the optimization of composites against impact induced failure (Rahul et al., 2005). A GA is a powerful technique for search and optimization problems with discrete variables, and is therefore particularly useful for optimization of composite laminates. However, to reach an optimal solution with a high degree of confidence typically requires a large number of function evaluations during the optimization search. Performance of GAs is even more of an issue for problems with mixed integer design variables. [15] Several studies have concentrated on improving the reliability and efficiency of GAs. The proposed project is the extension of the study by Kogiso et al. (1994b,a), [16] where, in order to reduce the computational cost, the authors used memory and local improvements so that information from previously analyzed design points is utilized during a search. In the first approach a memory binary tree was employed for a composite panel design problem to store pertinent information about laminate designs that have already been analyzed (Kogiso et al., 1994b). After the creation of a new population of designs, the tree structure is searched for either a design with identical stacking sequence or similar performance, such as a laminate with identical in-plane strains. Depending on the kind of information that can be retrieved from the tree, the analysis for a given laminate may be significantly reduced or may not

be required at all. The second method is called local improvement

## II. GENETIC ALGORITHM OVERVIEW

Genetic algorithms are robust, stochastic and heuristic optimization methods based on biological evolution process. There are several optimization techniques that are used in the context of engineering design optimization. Genetic algorithm is one such technique and is a search strategy based on the rules of natural genetic evolution. The standard genetic algorithm proceeds as follows: an initial population of individuals is generated at random. Every evolutionary step, known as a generation, the individuals in the current population are decoded and evaluated according to some predefined quality criterion, referred to as fitness function. To form a new population (the next generation), individuals are selected according to their fitness. Selection alone cannot introduce any new individuals into the population, i.e. it cannot find new points in the search space. These are generated by genetically-inspired operators, of which the most well known are crossover and mutation. Crossover is performed with crossover probability between two selected individuals. The mutation operator is introduced to prevent premature convergence to local optima by randomly sampling new points in the search space. Genetic algorithms are stochastic iterative processes that are not guaranteed to converge; the termination condition may be specified as some fixed maximal number of generations or as the attainment of an acceptable fitness level.

Kumar et al. [17-22] has used three sides instead of one side roughened duct & found that augmentation in Nu & f was respectively to be 21-86 % & 11-41 %. They also reported augmentation in thermal efficiency of three sides over one side roughened duct to be 44-56 % for varying p/e and 39-51 % for varying e/D<sub>h</sub>.

### Genetic operators

Establishing the GA parameters is very crucial in an optimization problem because they greatly affect the performance of a GA [6]. The genetic algorithm contains several operators, e.g. reproduction, crossover and mutation.

#### (a) Reproduction

The reproduction operator allows individual strings to be copied for possible inclusion in the next generation. After assessing the fitness value for each string in the initial population, only a few strings with a high fitness value are considered in their production. There are many different types of reproduction operators including proportional

selection, tournament selection, ranking selection, etc. In this study, tournament selection is selected, since it has better convergence and computational time compared to any other reproduction operator (Deb, 1999). In tournament selection, two individuals are chosen from the population at random, and then the string which has best fitness value is selected. This procedure is continued until the size of the reproduction population is equal to the size of the population.

#### (b) Crossover

Crossover is the next operation in the genetic algorithm. This operation partially exchanges formation between any two selected individuals. Crossover selects genes from parent chromosomes and creates new offspring.

#### (c) Mutation

This is the process of randomly modifying the string with small probability. Mutation operator changes 1 to 0 and vice versa with a small probability of mutation (P<sub>m</sub>). The need for mutation is to keep diversity in the population. This is to prevent solutions in the population from being trapped in local optima as the problem is solved.

## III. IMPLEMENTATION OF GENETIC ALGORITHM IN ANSYS SOFTWARE

- First create the model in Ansys software or import the model from any modeling software.
- Apply the loading and boundary conditions.
- Then run optimization algorithm in Ansys software
- Automatically Meshing is created and solution is solved in the software .The best result (stress and volume) for each iterations (reproduction, crossover, mutation, addition, deletion and alteration) is stored in separate file.

## IV. OPTIMIZATION ALGORITHM

Composite laminate optimization was carried out for different practical problems with following design variables (no of layers, thickness, material, angle and sequence of layers )

The procedure is given below

#### (a) Reproduction (iteration 1)

In this process laminate design variables are randomly generated and results were stored for different combinations.

#### (b) Crossover (iteration 2)

The best sequence from previous iteration was selected based on high fitness

Fitness[i] = 1-stress[i]/stress [max]

or  
 Fitness[i] = 1-volume[i]/volume [max]  
 In this iteration, laminate sequence were randomly changed from one sequence (parent1) to another sequence (parent2) for producing new sequences (child1 and child2). This concept is applicable for material, angle and thickness sequences.

Sequence1	Sequence2
Before crossover	
1 3 4 2 5	8 7 8
After crossover	
1 3 4 <b>7 8</b>	8 <b>2 5</b>

For example two materials (M1,M2), three thickness(5mm,10mm,15mm) and three angles(0,45,90) were taken for crossover operation

The best sequence1 (parent 1)

Total no layer = 5

Position	1	2	3	4	5
Material	=		M1	M2	M1 M2 M1
Sequence	=		5	5	10 10 15
Thickness	=		45	0	90 90 45
Angle	=				
Sequence					

The best sequence 2 (parent 2)

Total no layer = 5

Position	1	2	3	4	5
Material	=		M2	M2	M1 M1 M1
Sequence	=		5	15	10 5 5
Thickness	=		45	90	45 90 0
Angle	=				
Sequence					

After cross over (child 1)

Total no layer = 5

Position	1	2	3	4	5
Material	=		M1	M2	M1 <b>M1 M1</b>
Sequence	=		5	5	10 <b>5 5</b>
Thickness	=		45	0	90 <b>90 0</b>
Angle	=				
Sequence					

After cross over (child 2)

Total no layer = 5

Position	1	2	3	4	5
----------	---	---	---	---	---

Material	=	M2	M2	M1	<b>M2 M1</b>
Sequence					
Thickness	=	5	15	10	<b>10 15</b>
Sequence					
Angle	=	45	90	45	<b>90 45</b>
Sequence					

The above process is called single point crossover with right side shifting

- Crossover operations are classified into
1. Single crossover with right shifting
  2. Single crossover with left shifting
  3. Single crossover with left to right cross shifting
  4. Single crossover with right to left cross shifting

The best results from above four operations are stored.

(c) Mutation  
 The best sequence from previous iteration was selected based on high fitness. In this process variables are randomly exchange in between the single sequence itself. It is shown in below

Sequence1	
Before Mutation	After Mutation
1 3 4 2 5	1 3 <b>5</b> 2 <b>4</b>

The above process is repeated for all best sequences and result was stored.

(d) Addition  
 The best sequence from previous iteration was selected based on high fitness. In this process variables are added randomly in the best sequence It is shown in below

Sequence1	
Before Addition	After Addition
1 3 4 2 5	1 3 4 2 5 <b>2 3</b>

The above process is repeated for all best sequences and result was stored.

(e) Deletion  
 The best sequence from previous iteration was selected based on high fitness. In this process variables are deleted randomly in the best sequence It is shown in below

Sequence1	
Before Deletion	After Deletion
1 3 4 2 5	1 3 2 5

The above process is repeated for all best sequences and result was stored.

(f) Alteration

The best sequence from previous iteration was selected based on high fitness. In this process variables are altered randomly in the best sequence It is shown in below

Sequence1  
 Before Alteration 1 3 4 2 5  
 After Alteration 1 3 2 2 5

The above process is repeated for all best sequences and result was stored. This is called one generations.

Finally the overall best result from above six operations was plotted and stored. The same process was repeated for 50 numbers of generations. The optimization algorithm is shown in following Fig 1.

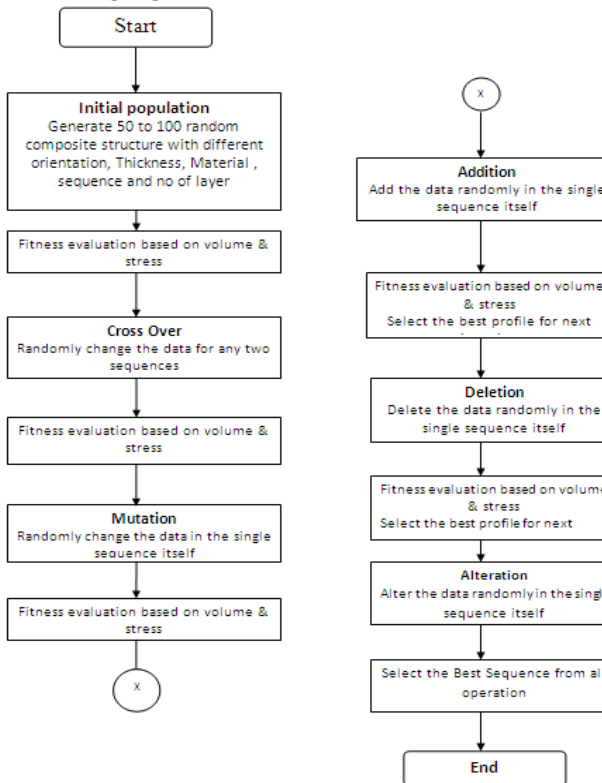


Figure 1. Genetic Algorithm for composite laminate optimization

**V. CASE STUDIES**

Genetic algorithm successfully implemented in following practical problems. The details of the inputs are shown below

1. Number of Material
2. Maximum Number of layer
3. Number of thickness
4. Number of angle
5. Loading & Boundary conditions
6. Model imported / created
7. Number of generations

All problems considered with following material properties  $E_1= 10,000 \text{ N/mm}^2$ ,  $E_2= 10,000 \text{ N/mm}^2$ ,  $E_3= 250,000 \text{ N/mm}^2$ ,  $\mu_{12}=0.25$ ,  $\mu_{23}=0.01$ ,  $\mu_{31}=0.25$ ,  $G_{12}=2000 \text{ N/mm}^2$ ,  $G_{23}=5000 \text{ N/mm}^2$ ,  $G_{31}=5000 \text{ N/mm}^2$ ,  $\rho=7850 \text{ Kg/mm}^3$

**4.1 Plate with hole**

A plate is subjected to biaxial load (1000 N) as shown in Figure 2. Following inputs were used

1. Number of Material =1
2. Maximum Number of layer (N) =8
3. Number of thickness =1 (2mm)
4. Number of angle =2 (45,-45)
5. Number of generations =50

The best results obtained in the 35<sup>th</sup> iteration as shown in below table 1

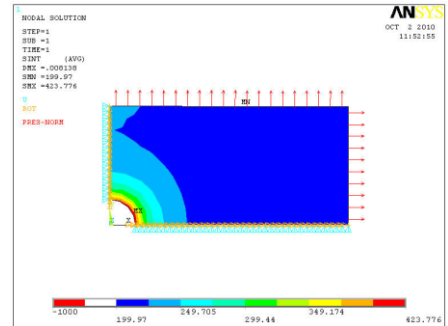


Figure 2a

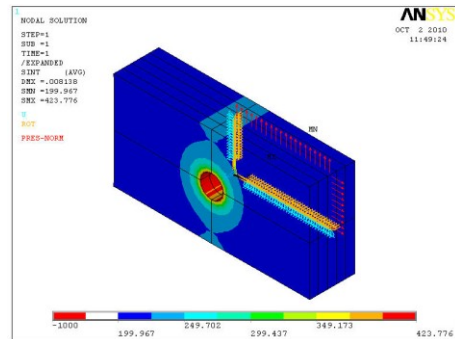


Figure 2b

Figure 2a,b. Optimized stress distribution of plate with hole

**4.2 Bumper with front & side load**

A bumper is subjected to biaxial load (10000 N) as shown in Fig. 3. Following inputs were used

1. Number of Material =1
2. Maximum Number of layer (N) =4
3. Number of thickness =1 (3mm)
4. Number of angle =3 (0,45,90)
5. Number of generations = 50

The best results obtained in the 23<sup>rd</sup> iteration as shown in below table 2.

Table 1. Optimum results at 35<sup>th</sup> iteration

GA operators	Number Of Layer	Material	Thickness	Angle	Stress N/mm <sup>2</sup>	Volume mm <sup>3</sup>
Reproduction	4	1,1,1,1	2,2,2,2	45,-45,-45,45	528.77	10222.43
Cross over	5	1,1,1,1,1	2,2,2,2,2	-45,45,45,-45,-45	423.02	12303.65
Mutation	5	1,1,1,1,1	2,2,2,2,2	-45,45,45,-45,-45	423.02	12303.65
Addition	5	1,1,1,1,1	2,2,2,2,2	-45,45,45,-45,-45	423.02	12303.65
Deletion	5	1,1,1,1,1	2,2,2,2,2	-45,45,45,-45,-45	423.02	12303.65
Alteration	5	1,1,1,1,1	2,2,2,2,2	-45,45,45,-45,-45	423.02	12303.65

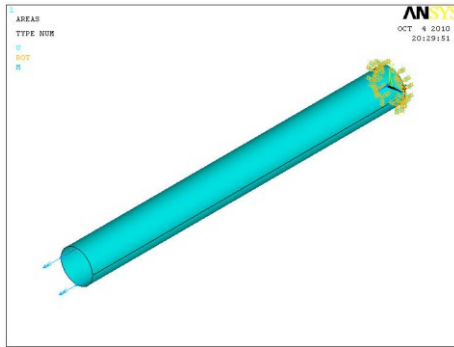


Figure. 3a

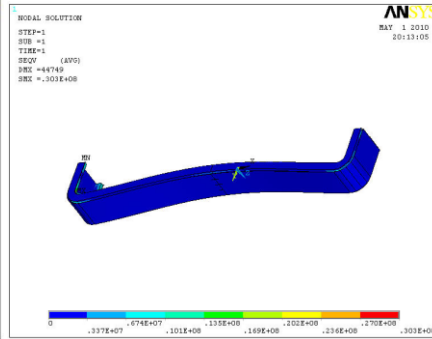


Figure. 3b

Figure 3a,b. Bumper Model and Optimized stress distribution of plate with hole

Table 2. Optimum results at 23<sup>rd</sup> iteration

GA operators	Number Of Layer	Material	Thickness	Angle	Stress N/mm <sup>2</sup>	Volume mm <sup>3</sup>
Reproduction	4	1,1,1,1	3,3,3,3	0,45,90,0	4.567e7	504323.33
Cross over	3	1,1,1	3,3,3	45,0,90	3.03e7	402442.22
Mutation	3	1,1,1	3,3,3	45,0,90	3.03e7	402442.22
Addition	3	1,1,1	3,3,3	45,0,90	3.03e7	402442.22
Deletion	3	1,1,1	3,3,3	45,0,90	3.03e7	402442.22
Alteration	3	1,1,1	3,3,3	45,0,90	3.03e7	402442.22

### 4.3 Hollow Shaft with Twisting Load

A hollow shaft is subjected twisting load of 1000 N as shown in Fig. 4. Following inputs were used

- Number of Material =1
- Maximum Number of layer (N) =6
- Number of thickness =1 (2mm)
- Number of angle =2 (45,-45)
- Number of generations =50

The best results obtained in the 45<sup>th</sup> iteration as shown in below table 3.

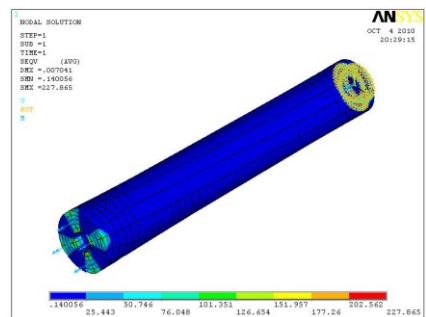


Figure. 4b

Figure 4a,b. Hollow shaft with twisting load and optimum Stress results

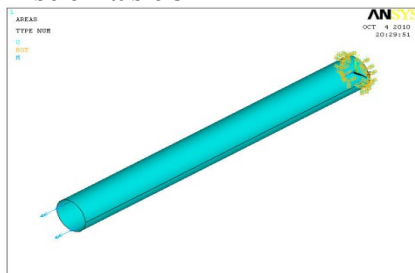


Figure. 4a

Table 3. Optimum results at 45<sup>th</sup> iteration

GA operators	Number Of Layer	Material	Thickness	Angle	Stress N/mm <sup>2</sup>	Volume mm <sup>3</sup>
Reproduction	6	1,1,1,1,1,1	2,2,2,2,2,2	45,-45,45,45,-45,45	354.44	7023432.43
Cross over	5	1,1,1,1,1	2,2,2,2,2	-45,45,-45,45,-45	227.645	6283185.154
Mutation	5	1,1,1,1,1	2,2,2,2,2	-45,45,-45,45,-45	227.645	6283185.154
Addition	5	1,1,1,1,1	2,2,2,2,2	-45,45,-45,45,-45	227.645	6283185.154
Deletion	5	1,1,1,1,1	2,2,2,2,2	-45,45,-45,45,-45	227.645	6283185.154
Alteration	5	1,1,1,1,1	2,2,2,2,2	-45,45,-45,45,-45	227.645	6283185.154

4.4 Plate with bending Load(M<sub>y</sub>)

A plate is subjected to bending load 1000 N in Y axis as shown in Fig. 5. Following inputs were used

Number of Material =1

Maximum Number of layer (N) =4

Number of thickness=1 (2mm)

Number of angle =2 (0,90)

Number of generations =50

The best results obtained in the 33<sup>rd</sup> iteration as shown in below table 4.

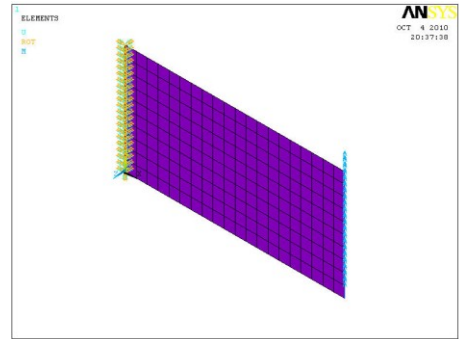


Figure. 5b

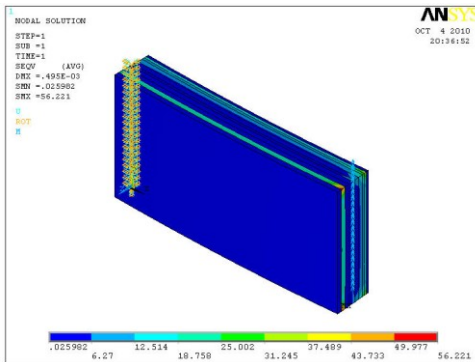


Figure. 5a

Figure 5a,b. Plate with bending load and optimum Stress results

4.5 Box with pressure Load

A Box is subjected to bending load 1000 N as shown in Fig. 6. Following inputs were used

1. Number of Material =1
2. Maximum Number of layer (N)=4
3. Number of thickness =2 (2mm,1mm)
4. Number of angle=2 (0,45)
5. Number of generations=50

The best results obtained in the 40<sup>th</sup> iteration as shown in below table 5.

Table 4. Optimum results at 33<sup>rd</sup> iteration

GA operators	Number Of Layer	Material	Thickness	Angle	Stress N/mm <sup>2</sup>	Volume mm <sup>3</sup>
Reproduction	4	1,1,1,1	2,2,2,2	0,90,90,0	75.33	6750000
Cross over	4	1,1,1,1	2,2,2,2	0,90,0,90	56.221	6250000
Mutation	4	1,1,1,1	2,2,2,2	0,90,0,90	56.221	6250000
Addition	4	1,1,1,1	2,2,2,2	0,90,0,90	56.221	6250000
Deletion	4	1,1,1,1	2,2,2,2	0,90,0,90	56.221	6250000
Alteration	4	1,1,1,1	2,2,2,2	0,90,0,90	56.221	6250000

Table 5. Optimum results at 40<sup>th</sup> iteration

GA operators	Number Of Layer	Material	Thickness	Angle	Stress N/mm <sup>2</sup>	Volume mm <sup>3</sup>
Reproduction	4	1,1,1,1	2,3,2,3	0,45,0,45	208322	10000000
Cross over	4	1,1,1,1	2,3,2,3	0,45,0,45	208322	10000000
Mutation	4	1,1,1,1	2,3,2,3	0,45,0,45	208322	10000000
Addition	4	1,1,1,1	2,3,2,3	0,45,0,45	208322	10000000
Deletion	4	1,1,1,1	2,3,2,3	0,45,0,45	208322	10000000
Alteration	4	1,1,1,1	2,3,2,3	0,45,0,45	208322	10000000

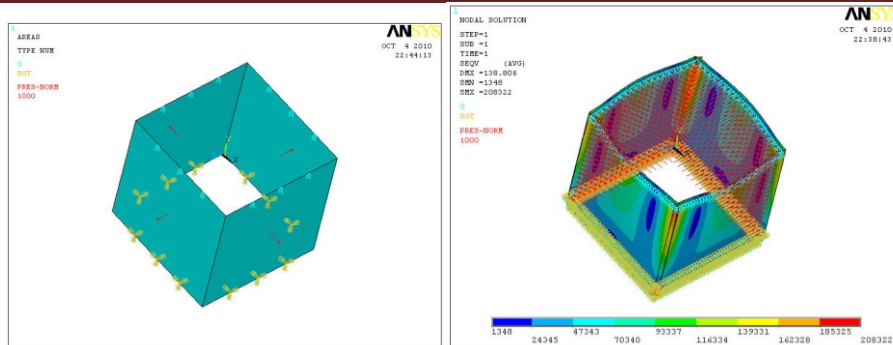


Figure. 6a Figure. 6b

Figure 6a,b. Box subjected to pressure load and optimum Stress results

**CONCLUSION:**

The global optimized genetic algorithm plays major role in composite optimization. The above algorithm can applicable for any type of problems with known loading and boundary conditions. Further the computation time will be reduced by using cluster based optimization i.e many computers simultaneously involved in optimization process. In future this work may extended to failure criteria approach and dynamic problems.

**References**

1. Schmit LA, Farshi B". Optimum laminate design for strength andstiffness". Int J Numer Meth Eng,7(4),519–36, 1973
2. Fukunga H, Vanderplaats GN. "Strength optimization of laminatedcomposites with respect to layer thickness and/or layer orientation angle". Comput Struct 40(6),1429–39, 1991.
3. Adali S, Richter A, Verijenko VE. "Optimization of shear-deformablelaminated plates under buckling and strength criteria". Compos Struct, 39(3–4):,67–78, 1997.
4. Abu-Odeh AY, Jones HL. "Optimum design of composite plates using response surface method", Compos Struct 43(3),233–42, 1998,
5. Park JH, Hwang JH, Lee CS, Hwang W. "Stacking sequence design of composite laminates for maximum strength using genetic algorithms",Compos Struct,52(2):217–31,2001,
6. Sciuva MD, Gherlone M, Lomario D. "Multiconstrained optimization of laminated and sandwich plates using evolutionary algorithms and higher-order plate theories",Compos Struct;59(1),149–54, 2003.
7. Farshi B, Herasati S. "Optimum weight design of fiber composite plates in flexure based on a two level strategy", Compos Struct ,73(4):,95–504. 2006.
8. Muc A, Gurba W. "Genetic algorithms and finite element analysis inoptimization of composite

- structures", Compos Struct ,54(2–3),.275–81 ,2001.
9. Walker M, Smith RE. "A technique for the multiobjective optimisation of laminated composite structures using genetic algorithms and finite element analysis" Compos Struct,62(1),123–8, 2003.
10. Kere P, Lyly M, Koski J. "Using multicriterion optimization for strength design of composite laminates", Compos Struct,62(3–4),329–33, , 2003.
11. Ganguli R, Chopra I. "Aeroelastic optimization of a helicopter rotor with composite coupling", J Aircraft 32(6),1326–34,1995.
12. Ganguli R, Chopra I."Aeroelastic optimization of a helicopter rotor with two-cell composite blades", AIAA J,34(4),835–41, 1996.
13. Ganguli R, Chopra I. "Aeroelastic tailoring of composite couplings and blade geometry of a helicopter rotor using optimization methods"J Am Helicopter Soc, 42(3),218–28. 1997.
14. Murugan MS, Ganguli R. "Aeroelastic stability enhancement and vibration suppression in a composite helicopter rotor", J Aircraft ,42(4),1013–24, 2005.
15. Smith EC, Chopra I. "Formulation and evaluation of an analytical model for composite box-beams", J Am Helicopter Soc 36(3), 23–5, 1991.
16. Ferrero JF, Barrau JJ, Segura JM, Sudre M, Castanie B. "Analytical theory for an approach calculation of non-balanced composite box beams" Thin-Walled Struct , 39(8),709–29, 2001.
17. Kumar, V., Prasad, L., Experimental investigation on heat transfer and fluid flow of air flowing under three sides concave dimple roughened duct. International Journal of Mechanical Engineering and Technology (IJMET), Volume 8, Issue 11, November 2017, pp. 1083–1094, Article ID: IJMET\_08\_11\_110.
18. Kumar, V., Prasad, L., Thermal performance investigation of one and three sides concave dimple roughened solar air heaters. International Journal of Mechanical Engineering and Technology (IJMET) Volume

- 8, Issue 12, December 2017, pp. 31-45, Article ID: IJMET\_08\_12\_004.
19. Kumar, V., Prasad, L., Performance Analysis of three sides concave dimple shape roughened solar air heater, *J. sustain. dev. energy water environ. syst.*, 6(4), pp 631-648, 2018.
  20. Kumar, V., Nusselt number and friction factor correlations of three sides concave dimple roughened solar air heater, *Renewable Energy* 135 (2019) 355-377.
  21. Kumar, V., Prasad, L., Experimental analysis of heat transfer and friction for three sides roughened solar air heater, *Annales de Chimie - Science des Matériaux*, 75-107, ACSM. Volume 41 - n° 1-2/2017.
  22. Kumar, V., Prasad, L., Performance prediction of three sides hemispherical dimple roughened solar duct, *Instrumentation, Mesure, Métrologie*, 273-293 I2M. Volume 17 - n° 2/2018.

# Traveling Salesman Problem for Visiting 10 Tamil Nadu Cities Using Genetic Algorithm

A.Karthikeyan<sup>1</sup> & Dr. A.Karthikeyan<sup>2</sup> & Dr.K.Venkatesh Raja<sup>3</sup> & Dr.K.Venkatesh<sup>4</sup>

<sup>1,4</sup> Asso. Prof., Department of Aeronautical Engineering, Excel Engineering College, Tamil Nadu,

<sup>2</sup> Professor, Department of Mechanical Engineering, Malla Reddy College of Engineering, Secunderabad, Telangana State,

<sup>3</sup> Asso. Prof, Department of Mechanical Engineering, VSA Group Of Institutions, Tamil Nadu.

---

**ABSTRACT:** *The main objective of this paper is to find the shortest path for visiting 10 cities in Tamil Nadu using genetic algorithm. Genetic algorithms are an evolutionary technique that use crossover and mutation operators to solve optimization problems using a survival of the fittest idea. They have been used successfully in a variety of different problems, including the traveling salesman problem. In the traveling salesman problem we wish to find a tour of all nodes in a weighted graph so that the total weight is minimized. The traveling salesman problem is NP-hard but has many real world applications so a good solution would be useful.*

**Keywords:** *Traveling Salesman problem, Genetic algorithm, cites.*

---

## I. INTRODUCTION

The origins of the Traveling salesman problem are unclear. A handbook for Traveling salesmen from 1832 mentions the problem and includes example tours through Germany and Switzerland, but contains no mathematical treatment. Mathematical problems related to the Traveling salesman problem were treated in the 1800s by the Irish mathematician W. R. Hamilton and by the British mathematician Thomas Kirkman. Hamilton's Icosian Game was a recreational puzzle based on finding a Hamiltonian cycle. The general form of the TSP appears to have been first studied by mathematicians during the 1930s in Vienna and at Harvard, notably by Karl Menger, who defines the problem, considers the obvious brute-force algorithm, and observes the non-optimality of the nearest neighbor heuristic. Richard M. Karp showed in 1972 that the Hamiltonian cycle problem was NP-complete, which implies the NP-hardness of TSP. This supplied a scientific explanation for the apparent computational difficulty of finding optimal tours. Great progress was made in the late 1970s and 1980, when Grötschel, Padberg, Rinaldi and other managed to exactly solve instances with up to 2392 cities, using cutting planes and branch-and-bound. In the 1990s, Applegate, Bixby, Chvátal, and Cook developed the program Concorde that has been used in many recent record solutions. Gerhard Reinelt published the TSPLIB in 1991, a collection of benchmark instances of varying difficulty, which has been used by many research groups for

comparing results. In 2005, Cook and others computed an optimal tour through a 33,810-city instance given by a microchip layout problem, currently the largest solved TSPLIB instance. For many other instances with millions of cities, solutions can be found that are provably within 1% of optimal tour.

The Traveling Salesman Problem is well-known among NP-hard combinatorial optimization problems[1]. It represents a class of problems which are analogous to finding the least-cost sequence for visiting a set of cities, starting and ending at the same city in such a way that each city is visited exactly once. The desire of economy, in which least time span or least distance are also significant for a decision maker, ultimately poses TSP as a multi-objective problem. In TSP as a Multi-Objective Combinatorial Optimization Problem, each objective function is represented in a distinct dimension. Of this form, to decide the multi objective TSP in the optimality means to determine the k-dimensional points that pertaining to the space of feasible solutions of the problem and that possess the minimum possible values according to all dimension. The permissible deviation from a specified value of a structural dimension is also considerable because Amna Rehmat, Hina Saeed, Muhammad Shahzad Cheema Pak.j.stat.oper.res. Vol.88 l.III No.2 2007 pp87-98 traveling sales man can face a situation in which he is not able to achieve his objectives completely. There must be a set of alternatives from which he can select one that best meets his aspiration level. Conventional programming approaches does not

deal with this situation however some researches have specifically treated the multi-objective TSP. Fischer and Richter (1982) used a branch and bound approach to solve a TSP with two (sum) criteria. Gupta and Warburton (1986) used the 2- and 3-opt heuristics for the maxordering TSP. Sigal (1994) proposed a decomposition approach for solving the TSP with respect to the two criteria of the route length and bottlenecking, where both objectives are obtained from the same cost matrix. Tung (1994) used a branch and bound method with a multiple labeling scheme to keep track of possible Pareto optimal tours. Melamed and Sigal (1997) suggested an e-constrained based algorithm for bi-objective TSP. Ehrgott (2000) proposed an approximation algorithm with worst case performance bound. Hansen (2000) applied the tabu search algorithm to multi objective TSP. Borges and Hansen (2002) used the weighted sums program to study the global convexity for multi-objective TSP. Jaszkiwicz (2002) proposed the genetic local search which combines ideas from evolutionary algorithms, local search with modifications of the aggregation of the objective functions. Paquete and Stützle (2003) proposed the two-phase local search procedure to tackle bi-objective TSP. During the first phase, a good solution to one single objective is found by using an effective single objective algorithm. This solution provides the starting point for the second phase, in which a local search algorithm is applied to a sequence of different aggregations of the objectives, where each aggregation converts the bi-objective problem into a single objective one. Yan et al (2003) used an evolutionary algorithm to solve multi objective TSP. Angel, Bampis and Gourvès (2004) proposed the dynasearch algorithm which uses local search with an exponential sized neighborhood that can be searched in polynomial time using dynamic programming and a rounding technique. Paquete, Chiarandini and Stützle (2004) suggested a Pareto local search method which extends local search algorithm for the single objective TSP to bi-objective case. This method uses an archive to hold non-dominated solutions found in the search process. There are several practical uses for this problem [2], such as vehicle routing with the additional constraints of vehicle's route, such as capacity of vehicles (Laporte,1992), drilling problems (Onwubolu, 2004), minimize waste (Grafinkel,1977), clustering data arrays (McCormick et al.,1972), X-ray crystallography (Bland et al.,1989), Shot Sequence Generation for Scan Lithography (Shinano et al., 2008) and many others. This problem has also

been used during the last years as a comparison basis for improving several optimization techniques, such as genetic algorithms (Affenzeller, 2003), simulated annealing (Budinich, 1996)), Tabu search (Liu, 2003), local search (Bianchi, 2005), ant colony (Chu, 2004) and Branch and Bound (B&B). The principal types of B&B used to solve the TSP are: The best known Development of an Innovative Algorithm for the Traveling Salesman Problem (TSP) 350 exact algorithms are based on either the B&B method for the Asymmetric TSP (ATSP) (Fischetti et al., 2002) or the Branch and Cut (B&C) method for the Symmetric TSP (STSP) using the double index formulation of the problem (Naddef, 2002). Currently, most algorithms for the TSP ignore high cost arcs or edges and save the low cost ones. In case of the ATSP, the Assignment Problem (AP) is a common choice

## II. OBJECTIVE

The main objective of our project is as follows:

- ✓ To find the shortest path for Tamil Nadu cities.
- ✓ To reduce the time for calculation
- ✓ To search each and every point in the dynamic search space.
- ✓ To get the global optimal solution for the given TSP problem.
- ✓ To accept any type of constraints (fixed constraints & Variable constraints)

## III. GENETIC ALGORITHM

"Survival of the fittest" (On the Origin of Species by means of Natural Selection) Charles Darwin, 1859 A.D[7,8,21]. This thesis studies the problems faced by the Genetic Algorithm in the area of vehicle routing and proposes solutions. The end product of those proposals comes in the form of a standardized model of a Genetic Algorithm for the Vehicle Routing, called the Localized Genetic Algorithm (LGA). A genetic algorithm (GA) is a search technique used in computing to find exact or approximate solutions to optimization and search problems[22]. Genetic algorithms are categorized as global search heuristics. Genetic algorithms are a particular class of evolutionary algorithms (also known as evolutionary computation) that use techniques inspired by evolutionary biology such as inheritance, mutation, selection, and crossover (also called recombination).

Genetic algorithms are used in search and optimization, such as finding the maximum of a function over some domain space.

- In contrast to deterministic methods like hill climbing or brute force complete enumeration, genetic algorithms use randomization.
- Points in the domain space of the search, usually real numbers over some range, are encoded as bit strings, called chromosomes.
- Each bit position in the string is called a gene.
- Chromosomes may also be composed over some other alphabet than {0,1}, such as integers or real numbers, particularly if the search domain is multidimensional.
- GAs are called "blind" because they have no knowledge of the problem.

An initial population of random bit strings is generated.

- The members of this initial population are each evaluated for their fitness or goodness in solving the problem.
- If the problem is to maximize a function  $f(x)$  over some range  $[a,b]$  of real numbers and if  $f(x)$  is nonnegative over the range, then  $f(x)$  can be used as the fitness of the bit string encoding the value  $x$ .

From the initial population of chromosomes, a new population is generated using three genetic operators: reproduction, crossover, and mutation.

- These are modelled on their biological counterparts.
- With probabilities proportional to their fitness, members of the population are selected for the new population.
- Pairs of chromosomes in the new population are chosen at random to exchange genetic material, their bits, in a mating operation called crossover. This produces two new chromosomes that replace the parents.
- Randomly chosen bits in the offspring are flipped, called mutation.

The new population generated with these operators replaces the old population.

- The algorithm has performed one generation and then repeats for some specified number of additional generations.
- The population evolves, containing more and more highly fit chromosomes.
- When the convergence criterion is reached, such as no significant further increase in the average fitness of the population, the best chromosome produced is decoded into the search

space point it represents.

Genetic algorithms work in many situations because of some hand waving called The Schema Theorem.

- Short, low-order, above-average fitness schemata receive exponentially increasing trials in subsequent generations.

Genetic Algorithms are a family of computational models inspired by evolution. These algorithms encode a potential solution to a specific problem on a simple chromosome-like data structures so as to preserve critical information. Genetic algorithms are often viewed as function optimizers, although the range of problems to which genetic algorithm have been applied is quite broad. The basic components of GA are illustrated in the Figure 3.1 gene, chromosome, and population. Usually the chromosome is represented as a binary string. The real trick of GA is on the encoding of problem domain, and the selection of next generation.

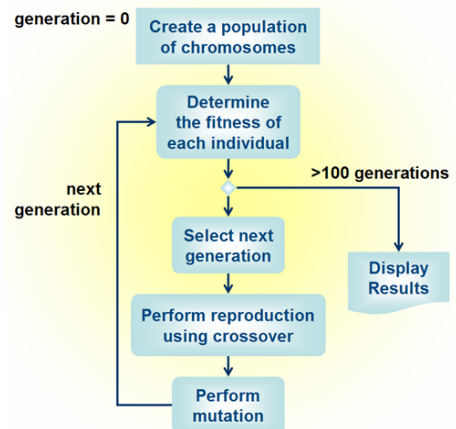


Fig 3.1 Genetic Algorithm flow chart

### 3.1 Input data's for TSP program

1. Distance Matrix for Tamil Nadu cities in the form of 2D array.
2. Number of cities
3. Number of Generations
4. Crossover probability
5. Mutation probability
6. Fixed constraints (Starting cities number)
7. Variable constraints or dynamic constraints

### 3.2 Output results

1. Best sequence (Shortest Route) in Genetic Algorithm with distance in Km.

### 3.3 Sample Inputs for 5 cities problems

- Enter the number of Generations ::>100
- Allow mutation (1:: Yes/2::No) (1:: recommended) ::>1

- Enter the number of fixed constrains : > 1
- Enter the number of fixed in position 1:: > 2
- Enter the number of variable constrains :: > 1

**Set 1**

- Enter the value of constrain 1:: > 4
- Enter the value of constrain 2:: > 5
- Enter the probability of survival (0 to 1) :: > 0.6
- Do you want to apply probabilities (y/n) :: >y
- Enter the probability of cross over (0 to 1) :: >0.8
- Enter the probability of mutation (0 to 1):: >0.8
- Do you the output to be printed (1: yes/2:No) :: >1

**Results from Genetic Algorithm:**

Sequence :: > 24153  
 Distance ::> 718 KM  
 Generation:: > 5<sup>th</sup> Generation  
 Possibility :: > 120  
 Available :: > 105 sequences  
 Solution :: > 47<sup>th</sup> sequences

The program is executed for few numbers of times to get optimal solution having alternate feasible sequences for the same feature. The sequential problem took very few microseconds for the execution of population size of 10; the number of operations are 16; with the probability of survival 0.6. Eight sets of variable constrains and one set of fixed constrains are included in the program (as inputs) with reference to a specific part module

**IV. IMPLEMENTATION OF GENETIC ALGORITHM TO TSP PROBLEMS**

For Example : 5 cites problems  
 General sequence is 1 2 3 4 5  
 Total No of cities N = 5  
 Possible combinations =  $2^{N-1}$   
 $= 2^{5-1}$   
 $= 016$  combinations

**4.1 Reproduction [stage I]**

In reproduction operation city sequence are randomly generated and total distance was calculated for each sequence.

- 13452 [sequence]
- 23154
- 41235
- 32145
- 45123

At least 10 to 20 sequence are generated, this is called initial population. When population size is more, it produces more accurate answers. But it increases computation time.

After generating initial population fitness function was calculated for each sequence

$$f[i] = 1 - d[i]/d[\max]$$

Where

d-distance

i=1,2,.....each sequence

d[ $\max$ ]=max value

Then select the high fitness value [ie. less distance sequence] for next stage

**4.2. Cross over [stage II]**

The best sequence was selected based on high fitness value  $f[i] > 0.7$ . Following are the some of the best sequences

- 32415
- 31245
- 12345
- 32154
- 43215

In crossover operation data's are exchange randomly between any 2 randomly selected sequences. For ex: 32415 and 12345 [parent] are the best sequence selected from above sequences.

After the crossover operation, two new sequences was created by exchanging data's randomly in parents

- 32 | 415 and 12 | 345
- 32 145                  12435 [Childs]

Then distance was calculated for new sequences [Childs].like this 10 to 20 cross over sequence is carried out for all the best sequence Again the Fitness was calculated for each sequence by using following formula.

$$f[ii] = 1 - d[ii]/d[\maxc]$$

Where

d-distance

ii=1,2,.....each sequence

d[ $\maxc$ ]=max value in crossover

Then select the high fitness value [ie less distance] sequence for next stage

**4.3. Mutation**

The best sequence was selected from cross over operation ie fitness value  $f[i] > 0.8$ . Following are the some of the best sequence

- 21345
- 32154
- 42135
- 45231

In mutation operation data exchange randomly in a single sequence. It is shown in following sequence.

Old sequence new sequence  
 21345 31245  
 32154 34152

Then distance was calculated for new sequences. Like this 10 to 20 sequence was created for all the best sequence. Again fitness function is calculated for each sequence by using following formula.

$$f[ii]= 1- d[ii]/d[maxm]$$

Where

d-distance

ii=1,2,.....each sequence

d[maxm]=max value in mutation

Then select the high fitness value [ie less distance sequence in mutation operator. Finally the overall minimum distance ie shortest path was selected from the all operations. This is called one generation.

**Disadvantages of GA**

It generates multiple local minimum

**V. TSP FOR VISITING 10 CITIES**

The main objective of this project is to implement the TSP problem to visit 10 Tamil Nadu cities. The distance (Km) between each cities are given below in table 5.1

Table 5.1.Distance Matrix for 10 Tamil Nadu cities (km)

city	1	2	3	4	5	6	7	8	9	10
1	0	230	354	47	263	247	262	330	181	552
2	230	0	492	183	307	398	400	307	71	689
3	354	492	0	350	225	164	89	321	438	469
4	47	183	350	0	259	252	244	283	134	543
5	263	307	225	259	0	300	133	96	236	531
6	247	398	164	252	300	0	143	322	312	305
7	262	400	89	244	133	143	0	229	346	530
8	330	307	321	283	96	322	229	0	236	627
9	181	71	438	134	236	312	346	236	0	617
10	552	689	469	543	531	305	530	627	617	0

First Row & First Column represent the cities Number & Name of cities are as follows

- 1.Chidambaram,
  - 2.Chennai,
  - 3.coimbatore,
  - 4.Cuddalore,
  - 5.Dharamapuri,
  - 6.Dindugul,
  - 7.Erode,
  - 8.Hosur,
  - 9.Kancheepuram,
  - 10.Kanyakumari,
- Remaining values represents the distance between all cities.

In all case studies 0.8 cross over & mutation probability are considered and test is carried out for 100 iterations.

Shortest route for 10 cities (1.Chidambaram, 2.Chennai, 3.coimbatore, 4.Cuddalore, 5.Dharamapuri, 6.Dindugul, 7.Erode, 8.Hosur, 9.Kancheepuram, 10.Kanyakumari) without any constraints is 7 5 4 8 2 9 1 3 6 10 =1770 KM from genetic algorithm and 10 6 3 7 5 8

2 9 4 1=1324 KM is the best solution in the Simulated Annealing. If city 1 is starting location then 1 4 7 3 5 8 2 9 6 10 = 1696 KM is the best sequence from genetic algorithm and 1 4 9 2 8 5 7 3 6 10 =1324 KM is the best solution in the Simulated Annealing. Like this various cities are fixed as single (1) and multiple (123) starting sequence. The different combinations of sequence for various constraints are shown in table 5.2 and figure 5.1

Table 5.2 Shortest route for 10 cities for No Constraints

Fixed Constraints Staring cities	Best Sequence	Distance(KM)
		GA
No	75482913610	1770
No	10637582941	
No	14928573610	
1	147358296 10	1696
1	149285736 10	
2	241598736 10	1752
2	291485736 10	
3	382941756 10	1880
3	375892416 10	
4	498536712 10	2179
1 2	12461073589	2146
1 2	12948573610	
2 3	238571946 10	2176
2 3	237589416 10	
1 2 3	12376 10 584	2256
1 2 3	123758946 10	
15 10	15 10 673842	2205
15 10	15 10 637842	
10 9 8	10 985241367	2147
10 9 8	10 985736142	
1234	12349685710	2599
1234	12349857610	
12345	12345768910	2782

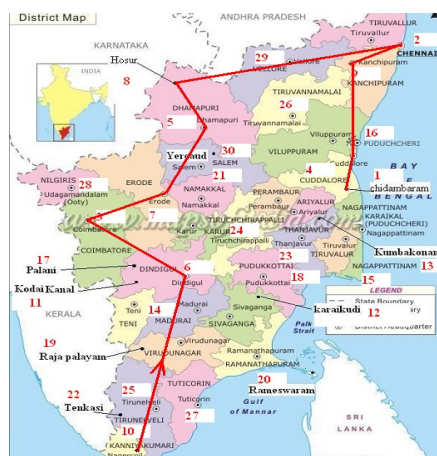


Fig.5.1 a) shortest path for 10 cities 1 4 9 2 8 5 7 3 6 10 =1324KM



Fig.5.1 b) shortest path for 10 cities starting from city 2, 291485736 10 =1369km

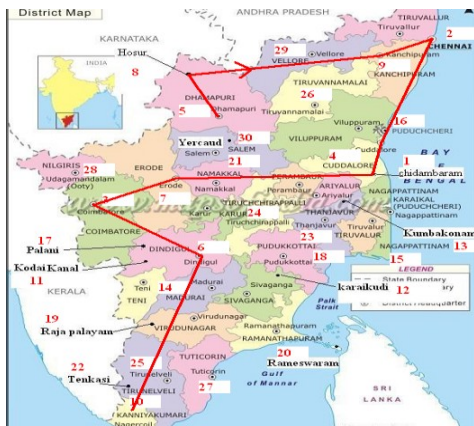


Fig.5.1 c) shortest path for 10 cities starting from city 5, 5 8 9 2 4 1 7 3 6 10=1453 km  
 Fig 5.1 a,b,c Shortest Path for 10 Cities

**VI. CONCLUSION AND FUTURE WORK**

In this paper we have discussed the travelling salesman problem using Genetic Algorithm. Various techniques of genetic algorithm have been discussed in this paper to study travelling salesman problem which is a permutation problem in which goal is to find the shortest path between cities traversing each city at least once. This paper gives a solution to find an optimum route for traveling salesman problem using Genetic algorithm technique for visiting Tamil Nadu cities, in which cities are selected randomly as initial population. The new generations are then created repeatedly until the proper path is reached upon reaching the stopping criteria. The proposed approach can be applied for various advanced network models like logistic network, task scheduling models, vehicle navigation routing models etc. The same approach can also be used for allocation of frequencies in cells of cellular network.

**VII. REFERENCES**

1. ChetanChudasama, S. M. Shah and Mahesh Panchal, "Comparison of Parents Selection Methods of Genetic Algorithm for TSP", International Conference on Computer Communication and Networks (CSI-COMNET), 2011.
2. Dwivedi, TarunaChauhan,SanuSaxena and PrincieAgrawal, "Travelling Salesman Problem using Genetic Algorithm", International Journal of Computer Applications(IJCA), 2012, pp. 25-30.
3. Naveen kumar, Karambir and Rajiv Kumar, "A Genetic Algorithm Approach To Study Travelling Salesman Problem", Journal of Global Research in Computer Science, 2012, Vol. 3, No. (3).
4. Adewole Philip, AkinwaleAdioTaofiki and OtunbanowoKehinde, "A Genetic Algorithm for Solving Travelling Salesman Problem", International Journal of Advanced Computer Science and Applications, 2011, Vol. (2), No. (1).
5. Ivan Brezina Jr.,Zuzana Cickova, "Solving the Travelling Salesman Problem using the Ant colony Optimization", Management Information Systems, 2011, Vol. (6), No. (4).
6. Buthainah Fahren, Al-Dulaimi, and Hamza A. Ali, "Enhanced Traveling Salesman Problem Solving by Genetic Algorithm Technique (TSPGA)", World Academy of Science, Engineering and Technology, 2008, Vol. (14).
7. Rong Yang, "Solving Large Travelling Salesman Problems with Small Populations". IEEE 1997.
8. Chiung Moon, Jongsoo Kim, Gyunghyun Choi ,YoonhoSeo," An efficient genetic algorithm for the traveling salesman problem with precedence constraints", European Journal of Operational Research 140 (2002) 606-617, accepted 28 February 2001.
9. Shubhra Sankar Ray, Sanghamitra Bandyopadhyay and Sankar K. Pal," New Operators of Genetic Algorithms for Traveling Salesman Problem", 2004 IEEE.
10. Lawrence V. Snyder a,\* , Mark S. Daskin , " A random-key genetic algorithm for the generalized traveling salesman problem", European Journal of Operational Research 174 (2006) 38-53, 2005.
11. Milena Karova, Vassil Smarkov, Stoyan Penev," Genetic operators crossover and mutation in solving the TSP problem", International Conference on Computer Systems and Technologies - Comp Sys Tech' 2005.
12. Plamenka Borovska," Solving the Travelling Salesman Problem in Parallel by Genetic Algorithm on Multicomputer Cluster", International Conference on Computer Systems and Technologies - CompSysTech'06
13. Kumar, V., Prasad, L., Experimental investigation on heat transfer and fluid flow of air flowing under three sides concave dimple roughened duct. International Journal of

- Mechanical Engineering and Technology (IJMET), Volume 8, Issue 11, November 2017, pp. 1083–1094, Article ID: IJMET\_08\_11\_110.
14. Kumar, V., Prasad, L., Thermal performance investigation of one and three sides concave dimple roughened solar air heaters. International Journal of Mechanical Engineering and Technology (IJMET) Volume 8, Issue 12, December 2017, pp. 31–45, Article ID: IJMET\_08\_12\_004.
  15. Kumar, V., Prasad, L., Performance Analysis of three sides concave dimple shape roughened solar air heater, J. sustain. dev. energy water environ. syst., 6(4), pp 631-648, 2018.
  16. Kumar, V., Nusselt number and friction factor correlations of three sides concave dimple roughened solar air heater, Renewable Energy 135 (2019) 355-377.
  17. Kumar, V., Prasad, L., Experimental analysis of heat transfer and friction for three sides roughened solar air heater, Annales de Chimie - Science des Matériaux, 75-107, ACSM. Volume 41 – n° 1-2/2017.
  18. Kumar, V., Prasad, L., Performance prediction of three sides hemispherical dimple roughened solar duct, Instrumentation, Mesure, Métrologie, 273-293 I2M. Volume 17 – n° 2/2018.

## WEAR BEHAVIOUR OF ALUMINIUM MATRIX COMPOSITES

Vijayakumar.K

Lecturer, Department of Mechanical Engineering, TPEVR Government Polytechnic College,  
Vellore- 632002, Tamilnadu.

**ABSTRACT:** Aluminium based metal matrix composites have low density, relatively low price, available in large quantities, superior strength to weight ratio and corrosion resistance. So it is extensively used in automotive and aerospace industries for drums, brake callipers, disc brake rotors, transmission casing, connecting rods and oil pumps, where adhesive wear are predominant in these components. For adhesive wear, the influence of applied load, sliding speed, wearing surface hardness, reinforcement content and morphology are critical parameters in relation to the wear rate encountered by the material. The reinforcements added to an alloy lead to variation in properties and improve the composite wear resistance. In this present work, it is to fabricate and study the wear behaviour of Aluminium matrix composites. Aluminium alloy reinforced with B<sub>4</sub>C particles with various weight percentage will be fabricated their wear behaviour will be studied using computerized Pin-on-disc wear testing machine.

**Keywords:** Adhesive wear, Pin-on-disc, wear parameters, Aluminium Matrix Composites (AMCs).

### 1. INTRODUCTION

Today searches in finding new materials superior than the conventional ones have an increasing demand. In these studies, Aluminium Matrix Composites (AMCs) have gained great attention especially in the industries such as aviation, space and automotive. Recently, AMCs have been used for the automobile products, such as engine piston, cylinder liner, brake drum, brake disc due to their light weight, high strength, high specific modulus, low co-efficient of thermal expansion and good wear resistance properties. An important issue in the production of Metal Matrix Composites (MMCs) is the chemical compatibility between the matrix and the reinforcement, particularly when using liquid metal process. Casting of MMCs is an attractive processing method since it is relatively inexpensive and offers a wide selection of materials and processing conditions. But poor wetting between Al and B<sub>4</sub>C below 1100°C means that it is difficult to produce Al - B<sub>4</sub>C composites by mixing particles into the liquid phase. In order to enhance the wettability of ceramics and improve their incorporation behaviour into Al metals, particles are often heat treated or coated.

Therefore, K<sub>2</sub>TiF<sub>6</sub> flux is used in order to increase the wetting between Al and B<sub>4</sub>C and facilitate the incorporation of B<sub>4</sub>C particles into molten aluminium. To avoid insufficient reaction phase at the interface and to lower the processing cost, no additional processes except the traditional casting method were used in this study.

### 2. EXPERIMENTAL PROCEDURE

#### 2.1 MATERIAL SELECTION

Material has been selected based on the properties, cost and application. The boron carbide particles are added as reinforcement with Aluminum cast alloy to improve the wear characteristics of the composite material.

Matrix Phase : ALUMINUM ALLOY LM25

Reinforcement : BORON CARBIDE (B<sub>4</sub>C)

#### 2.1.1 SPECIFICATION OF ALUMINIUM ALLOY LM 25

Table 1 Chemical Composition of Aluminium Alloy LM 25

Contents	Chemical composition
Copper (Cu)	0.01
Silicon (Si)	6.86
Magnesium (Mg)	0.37
Iron (Fe)	0.159
Nickel (Ni)	< 0.001
Tin (Sn)	< 0.005

Zinc (Zn)	0.01
Titanium (Ti)	0.02
Lead (Pb)	< 0.002
Aluminum (Al)	Balance

### 2.1.2 APPLICATIONS OF ALUMINIUM ALLOY LM 25

- Used in Automobile engine blocks and liner.
- Hydraulic cylinders and pressure vessels.
- Intricate components
- In Automotive braking system.

### 2.1.3 BORON CARBIDE (B<sub>4</sub>C)

Boron Carbide is a extremely hard ceramic material. Boron Carbide is one of the hardest materials known, ranking third behind diamond and cubic boron nitride. It is the hardest material produced in tonnage quantities. Boron carbide powder is mainly produced by reacting carbon with B<sub>2</sub>O<sub>3</sub> in an electric arc furnace, through carbo – thermal reduction or by gas phase reactions. For commercial use B<sub>4</sub>C powders usually need to be milled and purified to remove metallic impurities.

### 2.1.4 PROPERTIES OF B<sub>4</sub>C

- Extreme hardness
- Difficult to sinter to high relative densities without the use of sintering aids.
- Good chemical resistance
- Good nuclear properties
- Low density
- Light weight
- Erosion resistance

**Table 2 Typical Properties of Boron Carbide**

Density (g / cm <sup>3</sup> )	2.52
Melting Point (°C)	2445
Hardness (Knoop 100g) (Kg / mm <sup>2</sup> )	2900-3580
Fracture Toughness (MPa.m <sup>-1/2</sup> )	2.9-3.7
Young's Modulus (GPa)	450-470
Electrical Conductivity (at 25°C) (S)	140
Thermal Conductivity (at 25°C) (W/m.K)	30-42
Thermal Expansion Co – eff. X 10 <sup>-6</sup> (°C)	5
Thermal neutron capture cross section ( barn)	600

### 2.1.5 APPLICATIONS OF BORON CARBIDE (B<sub>4</sub>C)

- Used as an abrasive in polishing and lapping applications
- Used for dressing diamond tools.
- Ceramic tooling dies applications.
- Used for precision tool parts.

## 2.2 PROCESSING OF THE COMPOSITE

Liquid state fabrication of Metal Matrix Composites involves incorporation of dispersed phase into a molten matrix metal, followed by its Solidification. In order to provide high level of mechanical properties of the composite, good interfacial bonding (wetting) between the dispersed phase and the liquid matrix should be obtained. The simplest and the most cost effective method of liquid state fabrication is Stir Casting. Stir Casting is a liquid state method of composite materials fabrication, in which a dispersed phase ( ceramic particles, short fibers) is mixed with a molten matrix metal by means of mechanical stirring. The liquid composite material is then cast by conventional casting methods and may also be processed by conventional Metal forming technologies.

Stir Casting is characterized by the following features:

- Content of dispersed phase is limited (usually not more than 30 Vol.%)
- Distribution of dispersed phase throughout the matrix is not perfectly homogeneous.
- There are local clouds (clusters) of the dispersed particles ( fibers).

- There may be gravity segregation of the dispersed phase due to a difference in the densities of the dispersed and matrix phase.
- The technology is relatively simple and low cost.

### 2.3 WEAR TEST

A pin-on-disc test apparatus was used to investigate the dry sliding wear characteristics of the fabricated AMCs. ASTM G99 – 05 a standard test method for wear testing using a pin-on-disc apparatus was followed. The wear specimen (pin) of 6 mm diameter and 40 mm height was machined from the cast AMC samples. The disc material was chosen as AISI 4140 (EN 19) steel alloy. The disc specimen of 55 mm diameter and 10 mm thickness was cut from the steel rod and heat treated to achieve the hardness of 55 HRC. The contact surfaces of the pin and disc material were surface grinded and polished metallographically in order to achieve the surface roughness of 0.8 μm or below. Surface roughness was ensured using contact surface roughness tester SurfCorder SE3500 and the R<sub>a</sub> values are found to be less than 0.8 μm. During the test the pin was pressed against the rotating counter part by applying the load. LVDT on the lever arm helps determine the wear at any point of time by monitoring the movement of the arm. Applied load helps to maintain the pin in contact with the disc. This movement of the arm generates a signal which is used to determine the maximum wear and the coefficient of friction is monitored continuously as wear occurs. The initial weight of the pin material is measured in a single pan electronic weighing machine with least count of 0.0001 g. After running through a fixed sliding distance the specimen was removed, cleaned with acetone, dried and weighed to determine the weight loss due to wear. The difference in the weight measured before and after the test gave the sliding wear of the composite specimen and then the volume loss was calculated.

### 3. RESULTS AND DISCUSSION

The experimental plan is designed to find the factors influencing the wear process to achieve the minimum wear rate and maximum coefficient of friction. The experiments were developed by involving the following factors, sliding speed, sliding distance, load and weight percentage reinforcement of the material. These parameters are helpful in determining the composite performance.

**Table 3 Results of AMCs**

Sl. No	Sliding speed (m/s)	Sliding Distance (m)	Load (N)	% reinforcement	Wear rate (mm <sup>3</sup> /m)	COF
1	1.5	1000	15	Base Alloy	0.002217161	0.4065
2	1.5	1000	30	Base Alloy	0.00339448	0.3811
3	1.5	1000	45	Base Alloy	0.003699875	0.3334
4	2.0	1000	15	Base Alloy	0.004077313	0.4045
5	2.0	1000	30	Base Alloy	0.001889111	0.3672
6	2.0	1000	45	Base Alloy	0.004087481	0.3372
7	1.5	1000	15	3	0.002355	0.4568
8	1.5	1000	30	3	0.002973514	0.3929
9	1.5	1000	45	3	0.003854201	0.3437
10	2.0	1000	15	3	0.003476429	0.4451
11	2.0	1000	30	3	0.003350712	0.4040
12	2.0	1000	45	3	0.00380004	0.4445
13	1.5	1000	15	6	0.0020522	0.4735
14	1.5	1000	30	6	0.002272276	0.4513
15	1.5	1000	45	6	0.003402355	0.4032
16	2.0	1000	15	6	0.004108788	0.4631
17	2.0	1000	30	6	0.003412572	0.4235
18	2.0	1000	45	6	0.002272722	0.3912
19	1.5	1000	15	9	0.001859952	0.5336
20	1.5	1000	30	9	0.002616557	0.4812
21	1.5	1000	45	9	0.003347977	0.4436
22	2.0	1000	15	9	0.001861809	0.5032
23	2.0	1000	30	9	0.002246064	0.4712
24	2.0	1000	45	9	0.002981587	0.4335

Figure 1 Wear Rate Vs Load

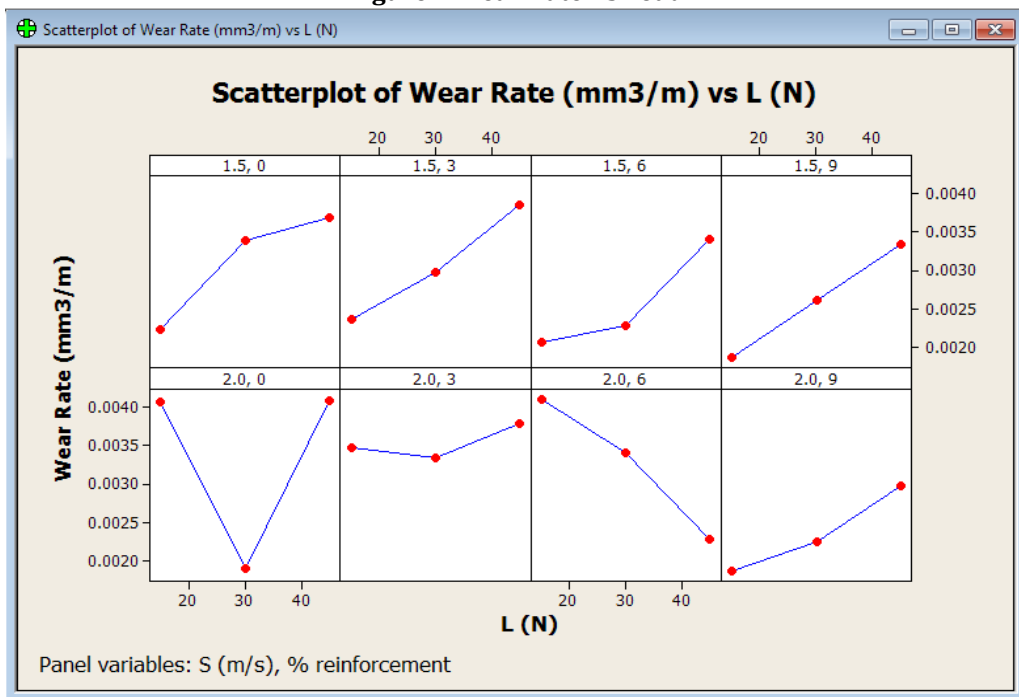
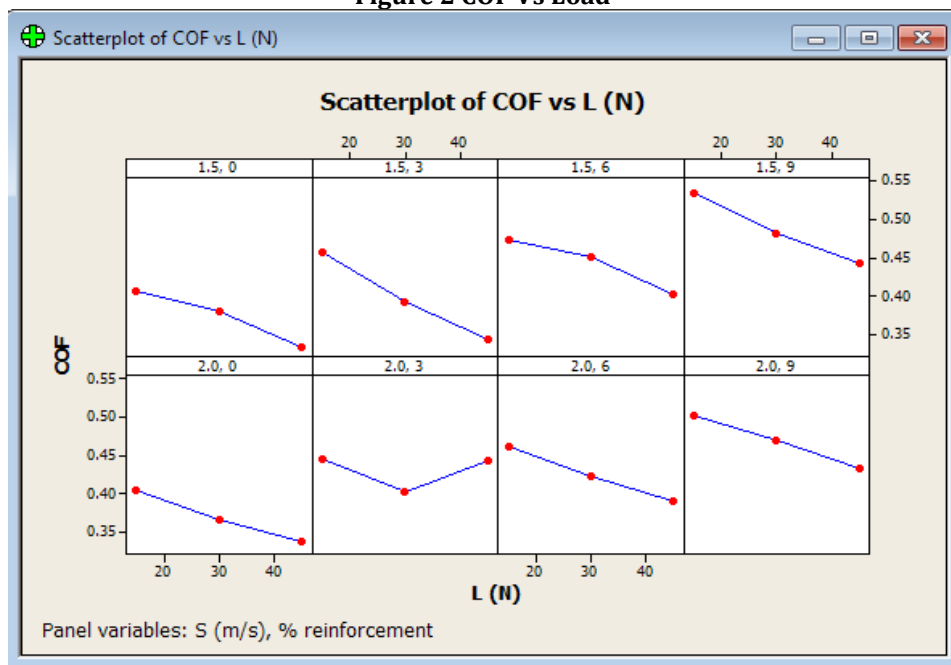


Figure 2 COF Vs Load



#### 4. CONCLUSION

The experimental study reveals following conclusions:

1. For a given load, the cumulative wear volumes of composites and pure aluminium pins increase linearly under dry sliding
2. The wear rate increases linearly with the increase in normal load
3. The average co-efficient of friction decreases with increase in load in both pure aluminium and composites. However the composites show a higher co-efficient of friction than that observed in pure aluminium

## REFERENCES

1. Topcua, H.O Gulsoyb, N. Kadioglu, A.N. Gulluoglu, (2009) 'Processing and mechanical properties of B<sub>4</sub>C reinforcement Al matrix composites', Journal of Alloys and Compounds, Vol.482 pp.516-521
2. GursoyArslan, AyseKalemtas, (2009) Processing of silicon carbide – boron carbide – aluminum composites, 'Journal of the European Ceramic Society, Vol.29, pp.473-480.
3. Surappa.M.K., (2003) 'Aluminum matrix composites: Challenges and opportunities' ,Sadhnan, Vol.28, Parts 1& 2 pp. 319-334.
4. Shorowordi K.M., Laoui. T, Haseeb A.S.M.A, Celis J.P., Froyen .L, (2003) 'Microstructure and interface characteristics of B<sub>4</sub>C, SiC and Al<sub>2</sub>O<sub>3</sub> reinforced Al matrix composites: a comparative study' , Journal of Materials Processing Technology, Vol.142,pp. 738-743.
5. R.Ipek (2005) 'Adhesive wear behavior of B<sub>4</sub>C and SiC reinforced 4147 Al matrix composites (Al/ B<sub>4</sub>C – Al/SiC)' , Journal of material processing technology, Vol.162-163,pp.71-75.
6. Hashim.J.,L.Looney, M.S.J. Hashmi, (1999) Metal matrix composites: production by the stir casting method' , Journal of Materials Processing Technology Vol. 92-93 pp. 1-7
7. Ramachandra.M., K. Radhakrishna, 'Effect of reinforcement of flyash on sliding wear, slurry erosive wear and corrosive behavior of aluminum matrix composite', Wear Vol.262 pp.1450-1462.
8. Deuis.R.L.,C.Subramanian& J.M. Yellupb, 'DRY SLIDING WEAR OF ALUMINUM COMPOSITES -A REVIEW' , Composites Science and Technology, Vol.57,pp.415-435.
9. Pasto.A.E., D.N Braski, T.R. Watkins, W.D. Porter, E. Lara- Curzio, S.B.McSpadden, (1999) Characterization techniques for composites and other advanced materials', Composites: Part B, Vol.30, pp.631-646
10. Kok.M., K.O zdin, (2007) 'Wear resistance of aluminum alloy and its composites reinforced by Al<sub>2</sub>O<sub>3</sub> particles'. Journal of Materials Processing Technology, Vol. 183, pp.301-309
11. Sathyabalan, P.V. Selladurai and P.Sakthivel (2009) ANN Based Prediction of Effect of Reinforcements on Abrasive Wear Loss and Hardness in a Hybrid MMC', American J. of Engineering and Applied Sciences 2 (1) pp. 50-53
12. Shorowordi.K.M., A.S.M.A Haseeb, J.P. Celis, (2006) 'Tribo-surface characteristics of Al- B<sub>4</sub>C and Al-SiC composites worn under different contact pressures', Wear, Vol.261, pp.634-641
13. Hosking.F.M., F.Folgar Portillo, R.Wunderlin T,R. Mehrabian, (1982) Composites of aluminium alloys: fabrication and wear behaviour', Journal Of Materials Science, Vol. 17 pp. 477 – 498
14. IsilKerti, FatihToptan, (2008) 'Microstructural variations in cast B<sub>4</sub>C reinforced aluminium matrix composites (AMCs)', Materials Letters, Vol.62pp. 1215-1218
15. Kumar, V., Prasad, L., Experimental investigation on heat transfer and fluid flow of air flowing under three sides concave dimple roughened duct. International Journal of Mechanical Engineering and Technology (IJMET), Volume 8, Issue 11, November 2017, pp. 1083–1094, Article ID: IJMET\_08\_11\_110.
16. Kumar, V., Prasad, L., Thermal performance investigation of one and three sides concave dimple roughened solar air heaters. International Journal of Mechanical Engineering and Technology (IJMET) Volume 8, Issue 12, December 2017, pp. 31–45, Article ID: IJMET\_08\_12\_004.
17. Kumar, V., Prasad, L., Performance Analysis of three sides concave dimple shape roughened solar air heater, J. sustain. dev. energy water environ. syst., 6(4), pp 631-648, 2018.
18. Kumar, V., Nusselt number and friction factor correlations of three sides concave dimple roughened solar air heater, Renewable Energy 135 (2019) 355-377.
19. Kumar, V., Prasad, L., Experimental analysis of heat transfer and friction for three sides roughened solar air heater, Annales de Chimie - Science des Matériaux, 75-107, ACSM. Volume 41 – n° 1-2/2017.
20. Kumar, V., Prasad, L., Performance prediction of three sides hemispherical dimple roughened solar duct, Instrumentation, Measure, Métrologie, 273-293 I2M. Volume 17 – n° 2/2018.

## **THERMAL ANALYSIS OF VARIOUS FRICTION SURFACING MATERIALS USING ANSYS**

**Sivanesh A R & Aravind Kumar R & Arivazhakan.D & Ananth.S**

Department of Mechanical Engg , Sri Ranganathar Institute of Engineering and Technology,  
Coimbatore, India

---

**ABSTRACT:** Surface engineering techniques are increasingly being used in manufacturing industries to extend the life of components. Friction surfacing is an advanced process of great potential, especially in the field of repair and reclamation of worn and damaged components. The temperature field of consumable rod in friction surfacing, as a kind of thermal processing technology, is an important factor in the successful implementation of the process. In this paper, the heat source model of various consumable rods (Aluminum, Brass, and Zinc) is coated on low carbon steel using friction surfacing process. And we do analysis for each component using ANSYS. From the obtained results we identify the best suitable material for low carbon steel combination.

**Keywords:** Friction surfacing, Temperature field, Thermal analysis

---

### **I. INTRODUCTION**

Friction surfacing is an advanced technique in surface modification. Its typical process is illustrated in Fig. 1 in which a consumable-rod rotates at a high spindle speed. The symbol  $n$  represents rotations per minute, and a certain axial force  $F$  is applied on the consumable-rod from the top to allow the consumable-rod to press against the substrate tightly. As a result, intense friction heat is produced from the friction generated at the rubbing surface between the substrate and the consumable-rod. Later, the contact end of the consumable rod becomes plasticized, and the preheating phase is then accomplished. The substrate begins to move relative to the consumable-rod at traverse speed  $v$ , and the coating material transfers from the end of the consumable-rod to the substrate to form a coating.

Due to its advantages, such as its clean, high efficiency, and good qualities, friction surfacing has become a potential “green” manufacturing technology. It opens up a new area of repair and reclamation of worn and damaged components. In fact, the technique has attracted a number of researchers in the recent decade.

With friction surfacing employed primarily in the field of engineering, most studies conducted on it have focused on its technical characteristics. Vitanov and co-workers (Vitanov et al., 2000, 2001; Vitanov and Voutchkov, 2005) developed a neurofuzzy model-based decision support system to speed up the parameter selection process[1][8]. Verevkin et al. (2003)

calculated the parameters of friction surfacing regimes on the basis of mathematical modeling[2]. Batchelor et al. (1996) attempted to identify the feasibility of various consumable materials (aluminum, zinc and brass) on substrates under, studied the effects of metal type on friction surfacing. Studied the interfacial phenomena during the friction surfacing of low carbon steel[3].

Apart from technical characteristics, many studies dwelled on identifying the mechanisms of the process. Bedford et al.(2001) discussed the mechanism of auto-hardening of the surfacing layer in friction surfacing[4]. Fukakusa (1996, 1997) put forward the concept of real rotational contact plane in friction surfacing, together with in friction welding[5]. The surfacing materials transferred from the consumable rod to the substrate does not pass through the whole rotational plane, but only the center of the rotational plane, that is called real rotational contact plane.

Focus on the utilization of aluminum zinc and brass bars for the coating layer employed hollow rods composed of to get uniformly distributed M.M.C. coatings. Coated aluminum, zinc and brass bars onto substrate (low carbon), and studied the effects of surfacing conditions on the structure and mechanical properties of both the monolayer and multilayer. In the present study, thermal analysis was employed to simulate the consumable-rod's temperature field. The temperature field in friction surfacing, especially of the consumable-rod, is considered an important

element in analyzing the process' mechanism and in the proper choice of key process parameters. The result from this study can provide theoretical guidance in analyzing the feasibility and choosing key parameters in similar endeavors.

**II. EXPERIMENTAL**

The experimental apparatus is modified based on a driller, wherein the substrate's motion relative to the consumable-rod is achieved by moving the working platform of the driller.

Temperatures at certain points of the consumable-rod were measured using a thermocouple. The temperature distribution up to preheat at the consumable-rod were distributed evenly along the axial side with of the interval of 10mm. The temperature of the point at the rubbing surface was measured through the method referred to as "semi-thermal couple" (Du et al., 1996)[6].

The experimental work on micro friction surfacing was conducted by adapting a friction surfacing machine for the purpose. The rotational speed (rpm), the feed rate of mechtrode ( $V_z$ ) and the traverse rate of the substrate ( $V_x$ ) were the essential machine input parameters[7]. The normal force which is set directly on dedicated machines (for friction surfacing) was represented by the feed rate  $V_z$  of the mechtrode because of the specific requirements of the friction surfacing machine. Normal force ( $F_n$ ) and substrate temperatures at specific locations were the measurable in process parameters. And temperature distribution of mechtrode is the process output that measured. The substrate geometry and its dimensions (mm) are shown in Fig. 1.

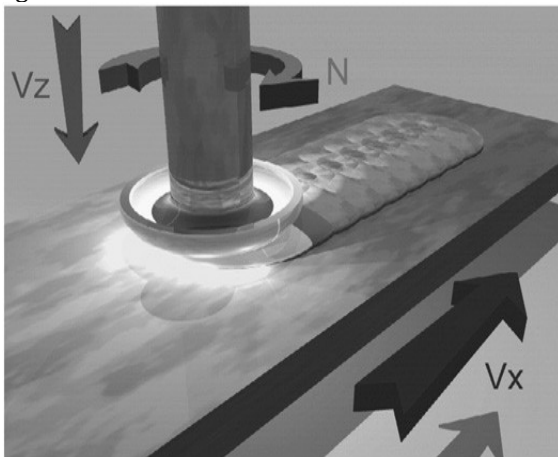


FIG.1. Friction Surfacing Process

**III. COUPLED FIELD ANALYSIS**

**A. MATERIAL OF ALUMINIUM**

*a) Meshed with load model*

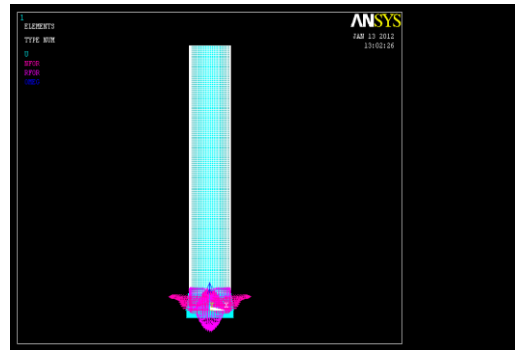


FIG.2. Al. material Meshed with load model

*b) Deformed shape only*

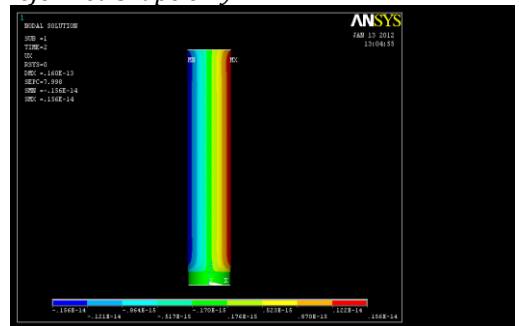


FIG.3. Al. material Deformed shape only

*c) Deformed with un-deformed shape*

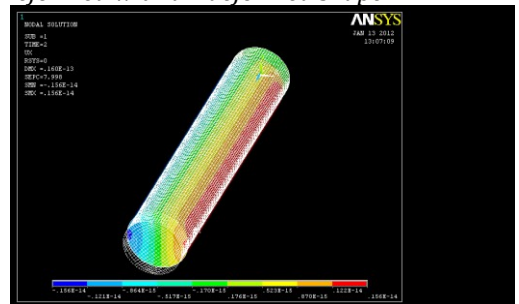


FIG.4. Al. material Deformed with un-deformed shape

**B. MATERIAL OF ZINC**

*a) Meshed with load model*

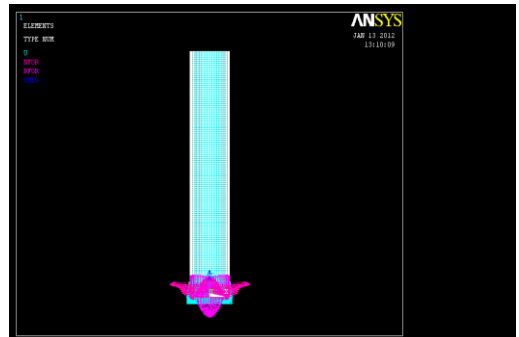


FIG.5. Zn. material Meshed with load model

b) Deformed shape only

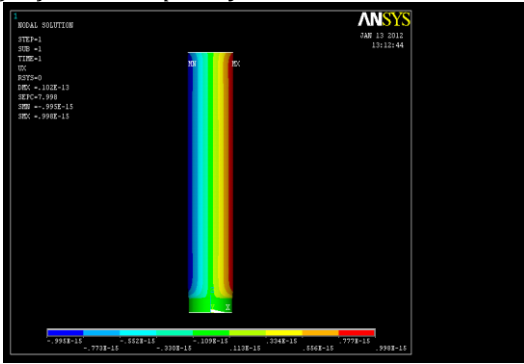


FIG.5. Zn. material Deformed shape only

c) Deformed with un-deformed shape

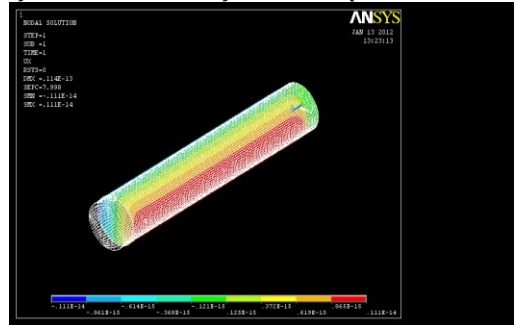


FIG.9. Brass material Deformed with un-deformed shape

c) Deformed with un-deformed shape

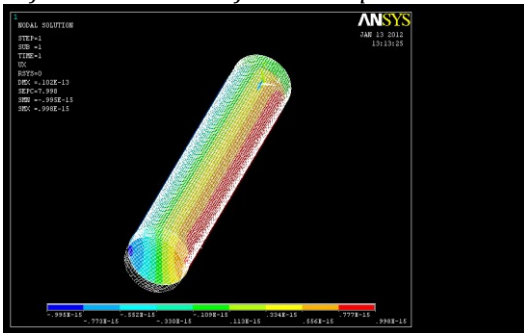


FIG.6. Zn. material Deformed with un-deformed shape

IV. DESIGN CALCULATION

Power (or) heat flux =  $2\pi nrt/60$

Torque (t) =  $(\pi/16) \times fs \times d^3$

$t/j = g\theta/l = \tau/r$

Torque = force x distance (or) length

t = torque

n = speed

g = young's modulus

l = length

r = radius

fs = shear stress

j = polar moment of inertia

C. MATERIAL OF BRASS

a) Meshed with load model

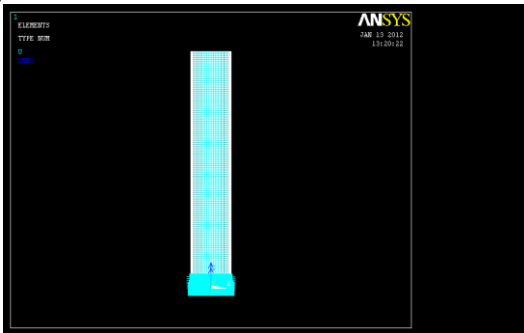


FIG.7. Brass material Meshed with load model

V. THERMAL ANALYSIS

A. Temperature distribution in Aluminium

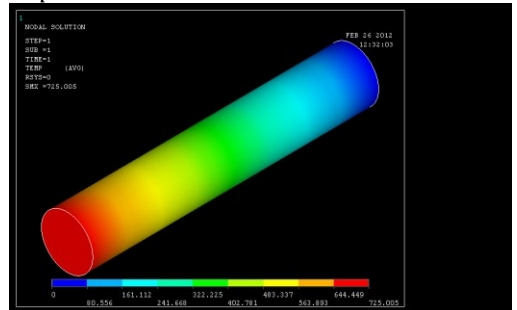


FIG.10. Temperature distribution in Aluminium

B. Temperature distribution in Zinc

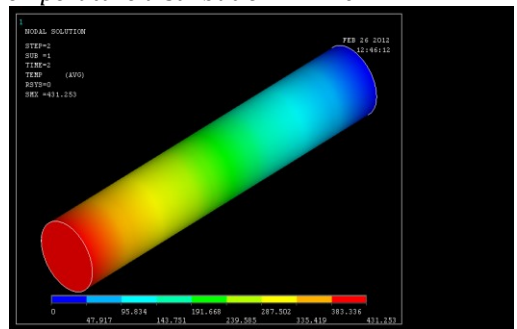


FIG.11. Temperature distribution in Zinc

b) Deformed shape only

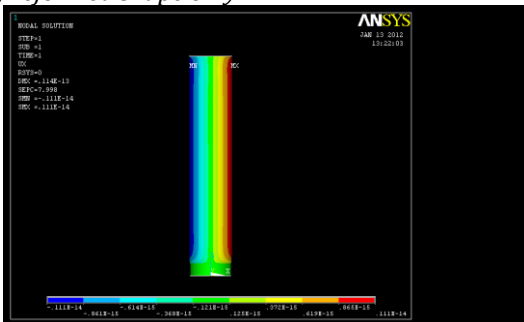


FIG.8. Brass material Deformed shape only

C. Temperature distribution in Brass

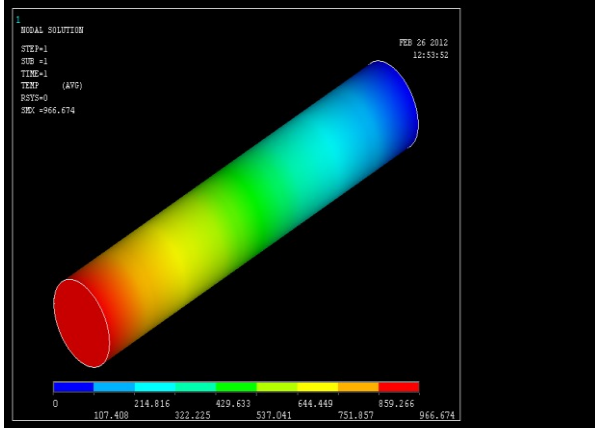


FIG12. Temperature distribution of Brass Material

VI. OPTIMIZATION OF SPEED

TABLE 1. Process parameters of various materials

MATERIALS	OPTIMIZED SPEED (RPM)	TEMPERATURE RANGE (°C)
ALUMINIUM	1500	644.44 - 725.00
ZINC	450	383.33 - 431.25
BRASS	1000	859.26 - 966.67

VII. DIMENSION OF MATERIALS

Substrate (low carbon steel)  
 Length=150 mm  
 Breath=100 mm  
 Thickness=18 mm  
 Consumable rod or mechtrode (Al, B, Zn)  
 Length=100 mm  
 Diameter=18 mm

VIII. MELTING POINT OF MATERIALS

Low carbon steel = (1464-1536°C)  
 Al = 660°C  
 B = 940°C  
 Zn = 419°C

IX. CONCLUSION

- Based on the existing research work we have studied the friction surfacing process. From that we have selected three mechtrode (aluminium, brass and zinc) with the friction surfacing process which done on low carbon steel substrate.
- Finally analysis results to identify the best suitable material for low carbon steel combination.

- Finally zinc is the best suitable material for low carbon steel combination in friction surfacing process

X. REFERENCES

- H. Khalid Rafi, et al. "Friction surface tool steel (H13) coating on low carbon steel: A study on the effects of process parameters on coating characteristics and integrity" Surface and Coatings Technology 205 (2010) 232-242.
- Xuemei Liua,\*, Junshan Yaob, Xinhong Wanga, Zengda Zoua, Shiyao Qua " Finite difference modeling on the temperature field of consumable-rod in friction surfacing" journal of materials processing technology 209 (2009 ) 1392-1399.
- V.I. Vitanov,et al " Application of response surface methodology for the optimization of micro friction surfacing process" Surface & Coatings Technology 204 (2010) 3501-3508.
- H. Khalid Rafi , G.D. Janaki Ram, G. Phanikumar, K. Prasad Rao " Micro structural evolution during friction surfacing of tool steel H13" Materials and Design (2010).
- Mehmet Eroglu "Boride coatings on steel using shielded metal arc welding electrode: Microstructure and hardness. Surface & Coatings Technology" 203 (2009) 2229-2235.
- X. M. Liu , Z.D. Zou , S.Y.Qu" Finite Difference Modeling on The Temperature Field of Substrate in Friction Surfacing" Second International Conference on Computer Modeling and Simulation (2010)
- M.L.Herring,J.I.Mardel, B.I.fox "The effect of material selection and manufacturing process on the surface finish of composites" journal of material processing technology 210(2010)926-940.
- V.I.Vitanov,N.Javaid "investigation of the thermal field in micro friction surfacing" surface & coating technology 204 (2010) 2624-2631.
- Kumar, V., Prasad, L., Experimental investigation on heat transfer and fluid flow of air flowing under three sides concave dimple roughened duct. International Journal of Mechanical Engineering and Technology (IJMET), Volume 8, Issue 11, November 2017, pp. 1083-1094, Article ID: IJMET\_08\_11\_110.
- Kumar, V., Prasad, L., Thermal performance investigation of one and three sides concave dimple roughened solar air heaters. International Journal of Mechanical Engineering and Technology (IJMET) Volume 8, Issue 12, December 2017, pp. 31-45, Article ID: IJMET\_08\_12\_004.
- Kumar, V., Prasad, L., Performance Analysis of three sides concave dimple shape roughened solar air heater, J. sustain. dev. energy water environ. syst., 6(4), pp 631-648, 2018.
- Kumar, V., Nusselt number and friction factor correlations of three sides concave dimple

- roughened solar air heater, Renewable Energy 135 (2019) 355-377.
13. Kumar, V., Prasad, L., Experimental analysis of heat transfer and friction for three sides roughened solar air heater, Annales de Chimie - Science des Matériaux, 75-107, ACSM. Volume 41 - n° 1-2/2017.
14. Kumar, V., Prasad, L., Performance prediction of three sides hemispherical dimple roughened solar duct, Instrumentation, Mesure, Métrologie, 273-293 I2M. Volume 17 - n° 2/2018.

## CHANGING TRENDS AND GROWTH OF SORGHUM IN SELECTED DISTRICTS OF TAMILNADU – INDIA

Mrs. M. Jayashree<sup>1\*</sup> & Dr. E.G. Wesely<sup>2</sup>

<sup>1\*</sup>Assistant Professor of Botany, Sri Sarada College for Women (Autonomous), Salem, Tamil Nadu

<sup>2</sup>Assistant Professor of Botany, Arignar Anna Government Arts College for Men, Namakkal,

**ABSTRACT:** Sorghum, commonly known as Jowar or cholam is the most important cereal crop in the world after wheat, rice, maize and barley. It is found in the arid and semi-arid parts of the world, due to its feature of being extremely drought tolerant. This study was conducted to examine growth trends in area, production, and productivity of major cereal crop sorghum in selected districts of Tamil Nadu, viz., Salem, Dharmapuri and Namakkal in India, over the period of 2010-2015. The data used for the study were collected from the annual season and crop report of Tamil Nadu, from each District Statistics Office. The trend analysis in the time series of area, production and productivity would be helpful to make future plans and to take appropriate decisions to safeguard the situation for the sustainability in food production and future food security. Drastic reduction was observed in the production and area of cultivation of cereal crop Jowar in Tamil Nadu. Shifting of farmer's focus toward the horticultural and plantation crops may be the main cause for negative trend in the production of major cereal crops. Linear, exponential, and logarithmic model observing trend in production, productivity and area under the cultivation of cholam were used for the trend analysis. In this study, the selected districts showed positive gradual increase trends in the production and area under the cultivation, over the subsequent years. This shows we have to shift our focus and switched on the more remunerative crops along with major cereal crops than with horticultural and plantation crops.

**Keywords:** Area, Production, Productivity, Growth trends, Sorghum, Tamilnadu.

### INTRODUCTION

Agriculture play an important role in the overall economic and social well being of the country. Though the share of the agricultural sector in the GDP is declining, it still accounts for nearly 16.1 percent and remains one of the biggest sector after services. India ranks second worldwide in farm output. Agriculture's contribution to GDP has steadily declined from 1951 to 2011, yet it is still the largest employment source and a significant piece of the overall socio - economic development of India. Crop yield per unit area of all crops has grown since 1950, due to the special emphasis placed on agriculture in the five - year plans and steady improvements in irrigation, technology, application of modern agricultural practices and provision of agricultural credit and subsidies since the Green Revolution in India.

India is the second largest rice (paddy) and wheat producing country in the world, next only to china [1, 2] as of FAO). Major cereal crops grown in India are wheat, paddy, sorghum, maize, bajra, barley, ragi. As on date the cultivation of these crops account to around 975.19 lakh hectare of land and a total production of 238.739 million tonnes (Department of Agriculture and Cooperation, Ministry of Agriculture, Government of India). India is not only the largest producer of

cereal as well as largest exporter of cereal products in the world. The huge demand for cereals in the global market is creating an excellent environment for the export of Indian cereal products. India occupy the major share in India's total cereals export with 64.40% during the year 2014-15. Whereas, other cereals including wheat represent 35.60% share in total cereals exported from India during this period [3].

More than ninety percent of high yielding varieties are for irrigated ecosystem and very few improved varieties are available for rainfed ecosystem; which constitutes more than sixty percent of cultivated rice areas in the country. The complex ecological situation of rainfed ecosystem consisting of upland, shallow low land, semi-deep water and deep water conditions is one of prime reasons for low productivity.

Present investigation is an endeavour to search out the progress achieved in Jowar despite the agroclimatic setbacks in Tamil Nadu. As these crops are important to the state. The study is undertaken to have a close look on trends of area, production and productivity of these crops in different agroclimatic regions of Tamil Nadu. Lastly, the study seeks to provide the basis for the future investigation and for developing a programme for higher production.

In view of the prevailing situation in cereals in Tamil Nadu, this paper aims to investigate the following objectives – viz., to study the trend and growth rate in area, production and productivity of this major cereal crop in different agroclimatic regions of Tamil Nadu, to project the expected area and production of Jowar by 2025 and to suggest Policy implication based on the analysis.

**MATERIALS AND METHODS**

The study is carried out in three districts of Tamil Nadu viz, Dharmapuri, Namakkal and Salem. Dharmapuri is situated in the North Western corner of Tamil Nadu and is bounded by Eastern Ghats on the east with the total geographical area of 4497.77Km<sup>2</sup> which 3.46% of Tamil Nadu. Namakkal is located close to Kolli Hills which is the part of the Eastern Ghats with the total are of 3,368.21Km<sup>2</sup>. Salem is the fifth largest city in Tamil Nadu by population and cover 91.34Km<sup>2</sup> and is the center place of the Southern region connecting the states of Tamil Nadu and Kerala and solution part of Karnata states. The share of cultivators and agricultural labourers of these districts are comparatively higher to the state proportion.

The data used for the study is entirely based on secondary source from annual season and crop report of Tamil Nadu, from each District Statistics Office. The study covers 5 years from 2010-2015. Various analytical tools and procedures used to determine empirically the changes, trends and variations in area, production and productivity and relative contributions to the changes in the production of Jowar in these three agroclimatic regions were studied.

**RESULTS AND DISCUSSION**

An attempt has been made to analyse the collected data in the light of objectives in an established sequence.

A discussion has been carried out at different aspects, i.e. absolute and relative changes in area, production and productivity of major cereal crops, their trends and growth rates.

For measuring the absolute change in area, production and productivity. Absolute change can be carried out by the base and end year of the concerned period. These years (beginning and end) may be exceptionally good/bad and will give a distorted picture of the change. Therefore, it was considerable proper to take an average of three years, base and end of a particular period. Absolute change in area, production and yield are carried out by the formula:

$$\text{Absolute change} = Y_n - Y_o$$

Where,

Y<sub>n</sub> = Mean value (area, production and productivity) for the last ending.

Y<sub>o</sub> = Mean value (area, production and productivity) for the first base ending.

The absolute change have been worked out for three agroclimatic regions and absolute change fails to depict a comparative change among the variables and therefore, in addition to absolute change, has also been included in the present study.

$$\text{Relative change} = Y_n - Y_o / Y_o \times 100$$

This measure has been worked out for the variables, for which absolute change has been worked out, as shown in Table 1.

**Table 1: Absolute and Relative change in area, production and productivity of Jowar in different agroclimatic regions Tamil Nadu, India**

District	Area				Production				Yield / Kg ha			
	Current Period	Base Period	Absolute Change	Relative Change (%)	Current Period	Base Period	Absolute Change	Relative Change (%)	Current Period	Base Period	Absolute Change	Relative Change (%)
Dharmapuri	17365	15696	1,669	10.633	45461	12545	32,916	262.383	2617	799	1818	2275.344
Namakkal	85992	19800	66,192	334.303	160096	13817	146,279	10.586	1861	698	1163	116.618
Salem	47452	20702	26,750	129.214	85010	19459	65,551	336.867	1792	940	852	90.638

As shown in the Table 1 and in the bar diagram (Figure 1) the absolute and relative changes in the area three different agroclimatic regions we have studied, revealed an increasing trend over the last five years. In the case of Area, it may be noted that

from the table that there has been a tendency to bring more areas under cultivation in all the three districts of Tamil Nadu, with the little least percentage of relative change observed at Dharmapuri.

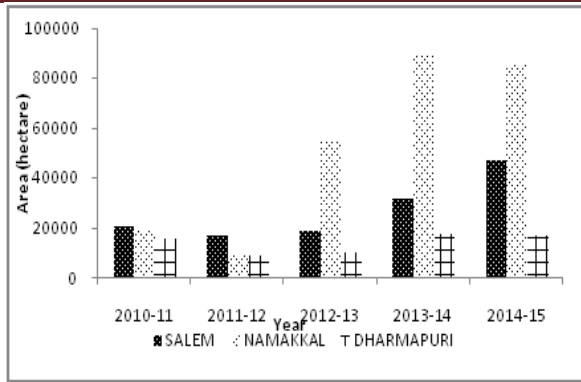


Figure 1. Area under the cultivation of sorghum from 2010-2015.

In case of production (Figure 2) the data showed that, all the agroclimatic regions reported an increasing trend overall. Any how we could see there is downfall in the production at Namakkal district when compare to Dharmapuri and Salem which revealed that though there is gradual increase in the area of cultivation, the production ratio is limited might be due to various climatic factors and soil parameters.

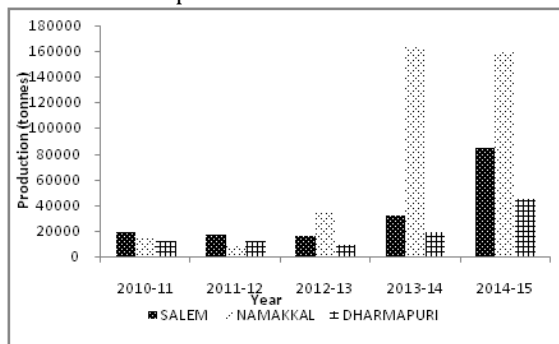


Figure 2. Production of sorghum from 2010-2015.

In all the three district, the state of yield has gone up considerably over the years. All the three parameters - area, production and productivity, when compared shows a continuous constant increase and hence can be concluded that although area and production is high, yield is the responsible factor for the increase in production (Figure 3).

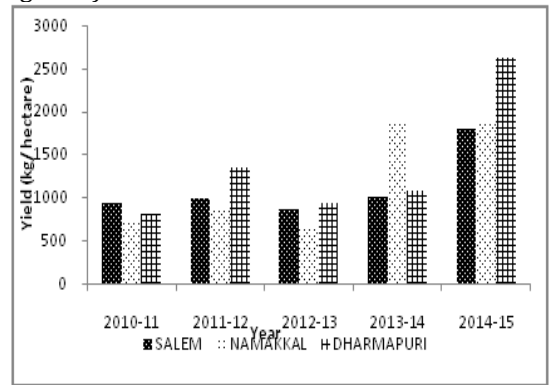


Figure 3. Yield of sorghum from 2010-2015.

The trends in the term of area, production and total productivity of different crops has been analysed by several scientists and researchers in different places throughout the world [4 - 8]. The agricultural area, production and productivity data set when plotted over times scale on the other axis

requires application of different statistical curve fitting techniques to get a smooth

Table 2. Trend analysis of sorgham.

trend that can be useful for meaningful interpretation of the data set [9, 10]. Summary of trend analysis of Jowar over the five years in the three different agroclimatic regions were shown in the Table 2.

	AREA	PRODUCTION	YIELD
<b>Salem</b>			
Linear	$y = 6775.6x + 6935.6$ $R^2 = 0.7244$	$y = 14595x - 9798.1$ $R^2 = 0.6241$	$y = 335.2x + 350.2$ $R^2 = 0.5211$
Exponential	$y = 12845e^{0.2258x}$ $R^2 = 0.7229$	$y = 9303e^{0.3574x}$ $R^2 = 0.6695$	$y = 724.19e^{0.1317x}$ $R^2 = 0.5076$
Logarithmic	$y = 14103\ln(x) + 13758$ $R^2 = 0.507$	$y = 29887\ln(x) + 5368.8$ $R^2 = 0.4228$	$y = 727.01\ln(x) + 659.69$ $R^2 = 0.396$
<b>Namakkal</b>			
Linear	$y = 21122x - 11597$ $R^2 = 0.8387$	$y = 44850x - 58072$ $R^2 = 0.8063$	$y = 332.4x + 187$ $R^2 = 0.7216$
Exponential	$y = 8203.8e^{0.5129x}$ $R^2 = 0.7025$	$y = 3831.2e^{0.7865x}$ $R^2 = 0.8279$	$y = 467.19e^{0.2735x}$ $R^2 = 0.6908$
Logarithmic	$y = 49652\ln(x) + 4227.3$ $R^2 = 0.7487$	$y = 101782\ln(x) - 20977$ $R^2 = 0.6708$	$y = 746.37\ln(x) + 469.55$ $R^2 = 0.5877$
<b>Dharmapuri</b>			
Linear	$y = 1191.4x + 10471$ $R^2 = 0.215$	$y = 7239.6x - 1907.8$ $R^2 = 0.6022$	$y = 335.2x + 350.2$ $R^2 = 0.5211$
Exponential	$y = 10454e^{0.0861x}$	$y = 6787.1e^{0.2998x}$	$y = 649.11e^{0.2137x}$

	$R^2 = 0.1909$	$R^2 = 0.6$	$R^2 = 0.5327$
Logarithmic	$y = 1807.4\ln(x) + 12314$	$y = 14757\ln(x) + 5681.5$	$y = 727.01\ln(x) + 659.69$
	$R^2 = 0.0799$	$R^2 = 0.4042$	$R^2 = 0.396$

It has been observed from the given Bar diagram Figure 1, for the trend analysis, revealed that the area under cultivation of crop Jowar is considerably increasing from the base year 2010-2011 to 2014-2015 except in the year 2011-2012 in all the three districts. Anyhow area under cultivation in Namakkal is exponentially greater when compared to Salem and Dharmapuri. However the area of cultivation in Dharmapuri shows least value of linear trend of  $R^2 = 0.215$  when compared to  $R^2 = 0.8387$  and  $R^2 = 0.7244$  at Namakkal and Salem respectively.

In the case of production it was observed that, there was considerable decrease over the years from 2010-2013 in all the three districts and increased exponentially greater in Namakkal in the year 2013-2014 and 2014-2015 with the value of  $R^2=0.8279$  over  $R^2=0.6695$  and  $R^2=0.6$  in Salem and Dharmapuri respectively.

The productivity of the Bar diagram revealed that there was a considerable increase over the years from 2010-2015 gradually in all the three agroclimatic regions. In the trend analysis for area, production, productivity, it was observed that linear and exponential trend showed the best fitted model with reasonable  $R^2$  values for all the three districts when compared to logarithmic model with the least fitting of all the three models for Dharmapuri.

### Conclusion and Recommendations

Based on the results of the study, it was concluded that there was a significant decrease in area devoted to sorghum cultivation per annum and a significant increase in productivity per annum for the crop for the period 1993-2004. Both the processes of decrease in area and increase in productivity were slow. However, the rate of decline in area would be doubled by the next 46.3 years from 2004 and the rate of increase in productivity would be doubled in the next 19.38 years would be doubled beginning from 2004. It was suggested that the process of decline in area should be reversed through expansion of area devoted to sorghum cultivation. This could be achieved through increased sensitization and mobilization of the local farmer on the need to bring back use such land area that were put

to fallow. The process of increase in productivity should be enhanced through increased use of advisory services and provision of input supports to the farmers engaged in the cultivation of sorghum.

### References

- [1] FAO (2003). Trade Reforms and Food Security -Conceptualizing the Linkages, Corporate Document Repository, Food and Agriculture Organization of the UN, Rome. :<http://www.fao.org/docrep/005/y4671e/y4671e06.htm>.
- [2] FAO. 2013, FAO of the United Nations, <https://en.wikipedia.org> Kachroo et al. (2013). Study on Growth and Instability of Maize in Jammu and Kashmir. Economic Affairs 58(1): 21-28.
- [3] Agricultural statistics at a Glanceagri@ nic.in APEDA. 2015 Cereals, apeda. gov.in
- [4] Ahmad, I. M., Samuel, E., Makama, S. A. and Kiresur, V. R. (2015). Trend of area, Production and Productivity of major cereals: India and Nigeria Scenario. Research Journal of Agriculture and Forestry Sciences. Vol. 3(2), 10-15.
- [5] Ali, S., Badar, N. and Fatima, H. (2015). Forecasting Production and Yield of Sugarcane and Cotton Crops of Pakistan for 2013-2030. Sarhad Journal of Agriculture. Vol. 31(1), 1-9
- [6] Malhi, R. D. K and Kiran, G. S.(2015). Analysis of trends in area, production and yield of important crops of India. International Journal of Agronomy and Agricultural Research. Vol. 7(1), 86-92.
- [7] Maneesh, P. and Deepa, N. R.(2016). Trend Analysis of Area, Production and Productivity of Rice in Kerala in the Context of Food Security. International Journal of Agricultural Research and Review. Vol.4(8), 538-546
- [8] Choudhury, A. and Jones, J. (2014). Crop yield prediction using time series. Journal of Economic and Economic Education Research, Vol. 15, 53-68.
- [9] Samuel E. and Patil B.(2013). Trend analysis of area, production and productivity of major cereals in Ethiopia, International Journal of Agricultural Economics and management. Vol. 3(2), 19-27.
- [10] MaiKasuwa M.A. (2013).Trend Analysis of Area and Productivity of Sorghum in Sokoto State, Nigeria, European Scientific Journal, June, 2013 Edition, 9(16).

## **COLOR IMAGE RETREIVAL SYSTEM USING FUZZY SIMILARITY MEASURE**

**Poornima N<sup>1</sup> & Aravind Kumar R<sup>2</sup> & Sivanesh A R<sup>3</sup>**

<sup>1</sup>Department of Science and Humanities , Sri Ranganathar Institute of Engineering and Technology  
Coimbatore, India

<sup>2,3</sup>Department of Mechanical Engg , Sri Ranganathar Institute of Engineering and Technology  
Coimbatore, India

---

**ABSTRACT:** *Image retrieval has important practical applications in database management, medical, and computer applications etc. For the purpose of effectively retrieving more similar images from the digital image databases, this work uses the color distributions and the mean value to represent the global characteristics of the image. The comparison of image retrieval result between RGB feature vector and hue feature vector in token of image characteristics is taken. The similarity measure is calculated by hue feature vector which is not sensitive to elimination and saturation change and the size of hue vector is reduced on the premise that the retrieval result is not affected. As the experimental results indicated, the proposed technique indeed outperforms other schemes.*

**Keywords:** *Pattern Recognition, Image Retrieval, Similarity Measure.*

---

### **I. INTRODUCTION**

Color image retrieval and classification are very important in the field of image processing. Image retrieval methods are mainly based on color, texture and shape of image. This chapter gives the concept of pattern recognition and its applications in color image and the need for color image retrieval using fuzzy system. Pattern recognition is concerned with the classification of objects into categories, especially by machine. Image analysis deals with the processing and analysis of images. Many pattern recognition systems are designed to classify or analyze images. Pattern recognition is concerned with the automatic detection or classification of objects or events.

A pattern is an entity, vaguely defined, that could be given a name, e.g., fingerprint image, handwritten word, human face, speech signal, DNA sequence [3]. Pattern recognition is the study of how machines can observe the environment, learn to distinguish patterns of interest, make sound and reasonable decisions about the categories of the patterns.

The measurements or properties used to classify the objects are called features and types or categories into which they are classified are called classes. Most pattern recognition tasks are first done by humans and automated later it can be defined as a process of identifying structure in data by comparisons to known structure, the known structure is developed through methods of classification [3]. Two of the main forms of pattern recognition are classification and regression. In

classification problems, data are collected and given discrete class labels. In a regression problem, on the other hand, data labels are typically continuous values, not categorical.

### **II. IMAGE RETREIVAL**

Many images on the world wide web confronts the users with new problems. Images are a fundamental part of our daily communication. The German saying "Ein Bild sagt mehr als tausend Worte" (literally: "A picture says more than a thousand words.") reflects this. The huge amount of pictures digitally available is not manageable by humans any more [2]. A person searching for a picture in a database of 100 images will probably find the search quite fast by just viewing the images or small versions of the images (thumbnails). If a thousand, ten thousand, or even more images are involved, the task becomes boring and interminable. Computers might be able to help here in the same way as they already do for searching text documents. A well-established example for text retrieval is the Internet search engine Google. Entering some keywords often helps finding related documents from the vast amount of documents available on the Internet. Google also offers a possibility to search for images, but the way the search is performed does not always lead to satisfactory results.

A broad variety of applications requires searching for images, in medical applications many images are produced and a physician might search for similar images to learn about

treatments of former patients and their outcomes. Image retrieval is the task of searching for images from an image database [2]. The query to the database can be of various types,

Query-by-text: The user gives a textual description of the image he is looking for. Query-by-sketch: The user provides a sketch of the image she is looking for. Query-by-example: The user gives an example image similar to the one he is looking for. In image retrieval the similarity between two sets of features, extracted from the database image and the query image has been used as a match measure. The match measure has been used to retrieve those regions present in a database of images, which are similar to the query image.

### III. NECESSITY OF COLOR IMAGE RETRIEVAL

Color image retrieval and classification are very important in the field of image processing, As a hotspot in image processing, image retrieval and classification are very important. Image retrieval methods are mainly based on color, texture, shape and semantic-image [8]. Color features are among the most important features used in image database retrieval. Due to its compact representation and low complexity, fuzzy similarity measure is the most commonly used technique in measuring color similarity of images. These features are independent of specific domain and can be used in general systems of retrieval images. The color feature is the first and one of the most widely used visual features in image retrieval and indexing. The most important advantages of color feature are power of representing visual content of images, simple extracting color information of images and high efficiency, relatively power in separating images from each other, relatively robust to background complication and independent of image size and orientation.

For image matching, features are extracted which may be shape features, texture features, or color features. Thus, a database is formed and for each image in the database, image features are found out. Another image, called the query image, is taken as the input image whose features are also found out. Then, the features of the query image are allowed to match with the features of the images in the database [5,8]. One important criterion for testing the efficacy of search and retrieval is that the features of the query image should almost be there in the images of the database.

### IV. COLOR SPACE

Color is a sensation created in response to excitation of our visual system by electromagnetic radiation

known as light. Color is the perceptual result of light in the visible region having wavelength in the region of 400nm to 700nm incident upon the retina of human eye. A color can be specified by a tri-component vector. The set of all colors form a vector space called color space.

#### RGB Color space

For representing colors several color spaces can be used. A color space is a specification of a coordinate system and a subspace within that system where each color is represented by a single point [6]. Color is perceived by humans as a combination of tristimuli i.e., R(red), G(green) and B(blue) which are usually called three primary colors. In hardware devices like monitors and digital cameras RGB color space is used. It is based on Cartesian coordinate system.

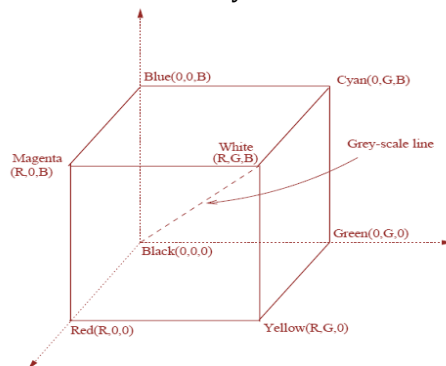


Fig 1 RGB color space using the Cartesian coordinate system

The above Fig 1 represents the RGB color space using the Cartesian coordinate system.

#### HSI Color space

The HSI color model represents every color with three components Hue (H), Saturation (S), Intensity (I). The HSI color space is very important and attractive color model for image processing applications because it represents color similarly how the human eye senses colors. The Hue component describes the color itself in the form of an angle between  $[0,360]$  degrees. 0 degree mean red, 120 means green, 240 means blue, 60 degrees is yellow, 300 degrees is magenta. The Saturation component signals how much the color is polluted with white color. The range of the S component is  $[0,1]$ . The Intensity range is between  $[0,1]$  and 0 means black, 1 means white. It is a nonlinear transformation of the RGB color space.

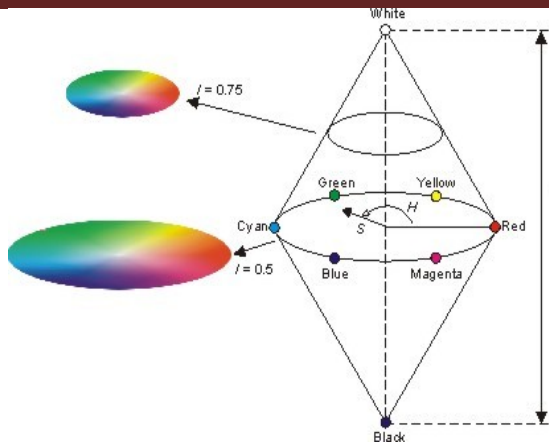


Fig 2 intensity approaches

As the above Fig 2 shows, hue is more meaningful when saturation approaches 1 and less meaningful when saturation approaches 0 or when intensity approaches 0 or 1. Intensity also limits the saturation values.

Fuzzy logic starts with and builds on a set of user-supplied human language rules. The fuzzy systems convert these rules to their mathematical equivalents. This simplifies the job of the system designer and the computer, and results in much more accurate representations of the way systems behave in the real world. Additional benefits of fuzzy logic include its simplicity and its flexibility. Fuzzy logic can handle problems with imprecise and incomplete data, and it can model nonlinear functions of arbitrary complexity.

### V. SIMILARITY MEASURE

Similarity measure is a quantity that reflects the strength of the relation between two objects or features. This chapter mainly focuses on similarity measure and the purpose of finding similarity measure and the comparison between the existing measure and proposed measure for pattern data sets.

Similarity is quite difficult to measure. It is a quantity that reflects the strength of the relation between two objects or features [10]. The similarity between two features A and B is usually denoted as  $S(A,B)$ . It has a normalized range of 0 to 1. Measuring similarity of features endorse to

- 1) Distinguish one object from another
- 2) Group them based on their similarity
- 3) Grouping may also give more efficient organization and ratio of information
- 4) Predict the behavior of new object.

The concept of similarity is fundamentally important in almost every scientific field. For example, in mathematics, geometric methods for assessing similarity are used in studies of

congruence, as well as in allied fields such as trigonometry. Topological methods are applied in fields such as semantics. Fuzzy set theory has also developed its own measures of similarity, which find application in areas such as management, medicine and meteorology. An important problem in molecular biology is to measure the sequence similarity of pairs of proteins.

Similarity is a core element in achieving an understanding of variables that motivate behavior and mediate affect. It also played a fundamentally important role in psychological experiments and theories. For example, in many experiments people are asked to make direct or indirect judgments about the similarity of pairs of objects [7]. A variety of experimental techniques are used in these studies, but the most common are to ask subjects whether the objects are the same or different, or to ask them to produce a number, between say 1 and 7, that matches their feelings about how similar the objects appear. The concept of similarity also plays a crucial but less direct role in the modeling of many other psychological tasks. This is especially true in theories of the recognition, identification, and categorization of objects, where a common assumption is that the greater the similarity between a pair of objects, the more likely one will be confused with the other. Similarity also plays a key role in the modeling of preference and liking for products or brands, as well as motivations for product consumption.

### RGB index

There are three statistical histograms representing one pictures feature. The first is color attribute RED histogram, the second is color attribute GREEN histogram and the last is color attribute BLUE histogram [11]. The statistical index is,

$$U_i = \{V_{ir}, V_{ig}, V_{ib}\}$$

Where,

$$V_{ir} = \{x_{ir1}, x_{ir2}, x_{ir3}, \dots \dots \dots x_{ir128}\}$$

$$V_{ig} = \{x_{ig1}, x_{ig2}, x_{ig3}, \dots \dots \dots x_{ig128}\}$$

$$V_{ib} = \{x_{ib1}, x_{ib2}, x_{ib3}, \dots \dots \dots x_{ib128}\}$$

The difference between picture i and picture j

$$r_{ij} = \sum_{k=1}^{128} |x_{irk} - x_{jrk}|$$

under the RED attribute is

The difference between picture i and picture j under the GREEN attribute is

$$g_{ij} = \sum_{k=1}^{128} |x_{igk} - x_{jgk}|$$

The difference between picture i and picture j under the BLUE attribute is

$$b_{ij} = \sum_{k=1}^{128} |x_{ibk} - x_{jbk}|$$

The similarity measure of two pictures is,

$$ij = \frac{r_{ij} + g_{ij} + b_{ij}}{3}$$

The image retrieval method using fuzzy similarity measure is compared with the existing measures [11]. The images are fetched from the database and their degree of similarity is calculated with the query image.

Table 1 Query image Similarity

SNO	IMAGE	Xiaojuan based similarity method	Fuzzy distance based similarity method
1		0.7093	0.72
2		0.4101	0.1699
3		0.6547	0.5428
4		0.6492	0.5673
5		0.7275	0.72
6		0.7083	0.72
7		0.5379	0.2980
8		0.8222	1

The plot of these images are listed below

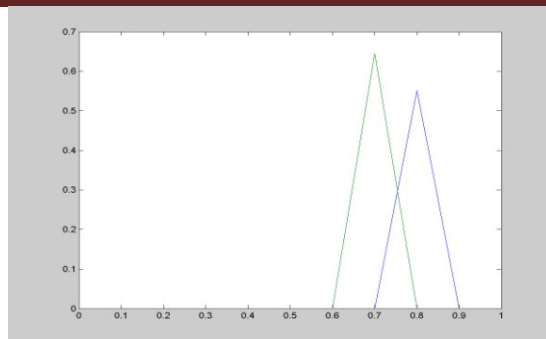


Fig 3.Similarities between Xiaojuan and Fuzzy method of image 1

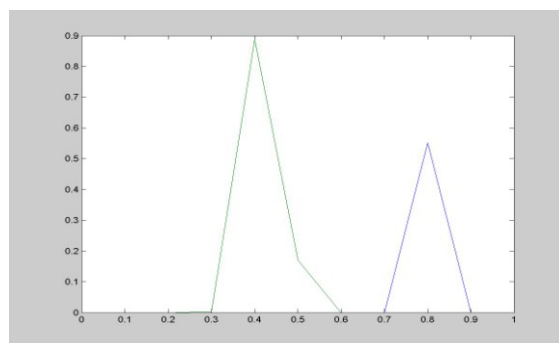


Fig 4.Similarities between Xiaojuan and Fuzzy method of image 2

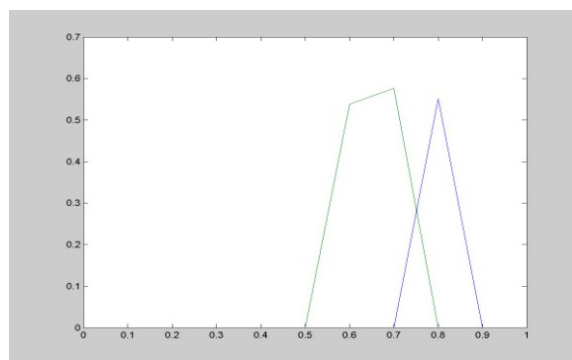


Fig 5.Similarities between Xiaojuan and Fuzzy method of image 3

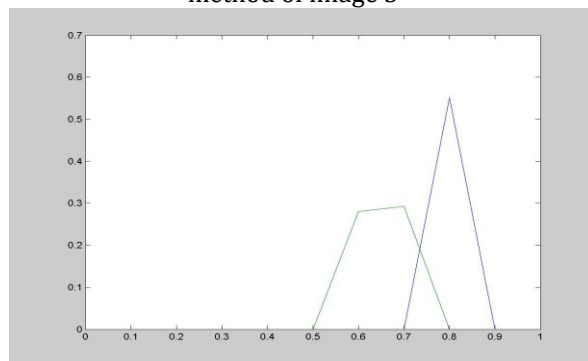


Fig 6.Similarities between Xiaojuan and Fuzzy method of image 4

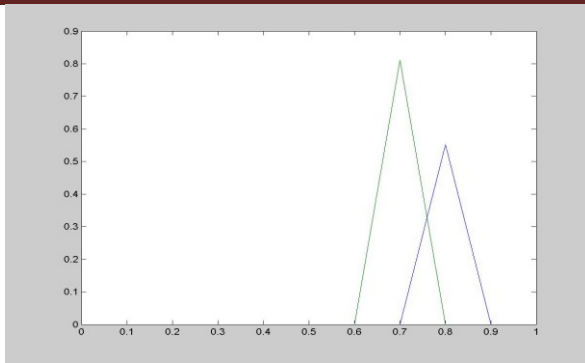


Fig 7.Similarities between Xiaojuan and Fuzzy method of image 5

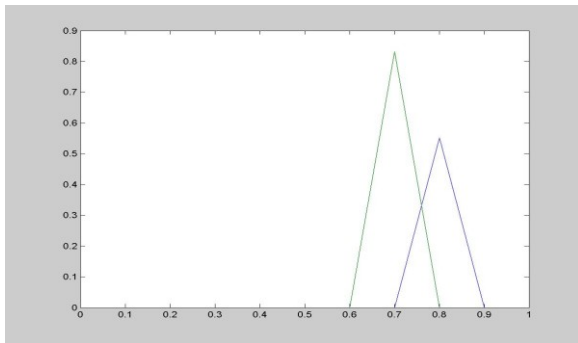


Fig 8.Similarities between Xiaojuan and Fuzzy method of image 6

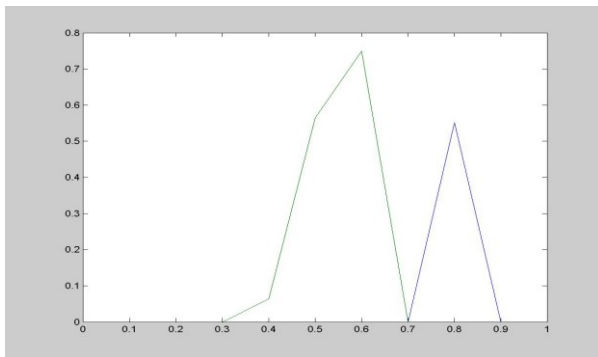


Fig 9.Similarities between Xiaojuan and Fuzzy method of image 7

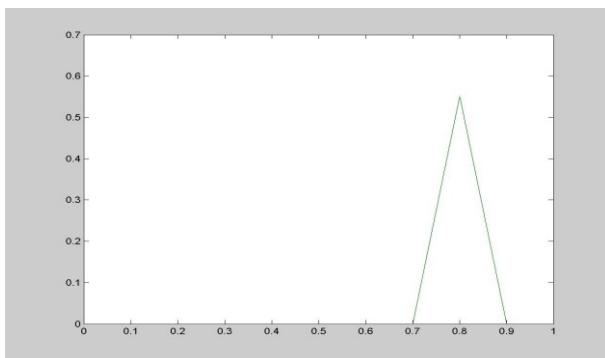


Fig 10.Similarities between Xiaojuan and Fuzzy method of image 8

## VI. COMPARISON

From the Table 5.2, Im 8 is same as that of query image so the degree of similarity should be 1, which is true in the case of fuzzy distance based similarity method but Xiaojuan based similarity method fails to identify the 100% similarity. Also Im 2, is found to be dissimilar with the query image, the degree of similarity is found to be very low in fuzzy distance based similarity method, but the Xiaojuan based similarity method provides a high measure.

Hence it reveals that the fuzzy distance based similarity method provides better similarity when compared with the existing method [9,11]. The experimental results show that idea which takes the fuzzy similarity measure for the method of image retrieval is found to be reasonable and effective.

## VII. CONCLUSION

- Based on the existing research work we have studied the color image retrieval method. This is done using fuzzy similarity measure. The similarity measure is calculated by hue feature vector. The measure greatly reduces the influence of inaccurate measure and provides a very intuitive quantification.
- The results obtained by the proposed method reflect the significance of fuzzy representation rather than the crisp definition

## VIII. REFERENCES

1. Timothy J.Ross, Fuzzy Logic with Engineering Applications, McGraw - Hill, 1997.
2. William K.Pratt, Digital Image Processing, John Wiley and Sons Publications, Third Edition,2001.
3. Earl Gose, Richard Johnsonbaugh, Steve Jost, Pattern Recognition and Image Analysis, Prentice Hall of India, Third Edition,2002.
4. Rafael C.Gonzalez, Richard E.Woods, Digital Image Processing, Prentice Hall of India, Second Edition,2005.
5. Nachtegeal.M, Van der Weken.D, De Witte.V, Schulte.S, Melaange.T, Kerre.E.E, "Color Image Retrieval using Fuzzy Similarity Measures and Fuzzy Partitions", Image Processing, ICIP 2007, IEEE International Conference on, Vol-6, pp. VI-13-VI-16, 2007.
6. Gwangwon Kang, Junguk Beak, Jongan Park, "Features Defined by Median Filtering on RGB Segments for Image retrieval", Computer Modeling and Simulation, EMS '08 Second UKSIM European Symposium on, pp. 436-440, 2008.
7. Jeong- Yo Ha, Gye- young Kim, Hyang-II Choi, "The Content-Based Image Retrieval Method

- Using Multiple Features”, Networked Computing and Advanced Information management. NCM’08. Fourth International Conference on, Vol-1, pp.652-657,2008.
8. Yu Xiaohong, Xu Jinhua, “The Related Techniques of Content-Based Image Retrieval”, Computer Science and Computational Technology. ISCSCCT '08. International Symposium on, vol.1, pp.154-158,2008.
  9. Zhangyan Xu, Shichao Shang, Wenbin Qian, Wenhao Shu “A method for fuzzy risk analysis based on the new similarity of trapezoidal fuzzy numbers”, Expert Systems with Applications, Vol-37, pp. 1920–19270, 2010.
  10. B.Sridevi and R.Nadarajan, “Fuzzy Similarity Measure for Generalised Fuzzy Numbers”, Int.J. Open Problems Compt. Math, Vol-2,No-2, June 2009.
  11. Xiaojuan Ban, Xiaolong Lv, and Jie Chen, “Color Image Retrieval And Classification Using Fuzzy Similarity Measure And Fuzzy Clustering Method”, IEEE Conference on Decision and Control, 2009.
  12. John Yen, Reza Langari, Fuzzy Logic-Intelligence, Control and Information, Pearson Education, 2011.
  13. Gerasimos Louverdis and Ioannis Andreadis, “Soft Morphological Color Image Processing: A Fuzzy Approach”, [med.ee.nd.edu/MED11/pdf/papers/t7-032.pdf](http://med.ee.nd.edu/MED11/pdf/papers/t7-032.pdf).
  14. Kumar, V., Prasad, L., Experimental investigation on heat transfer and fluid flow of air flowing under three sides concave dimple roughened duct. International Journal of Mechanical Engineering and Technology (IJMET), Volume 8, Issue 11, November 2017, pp. 1083–1094, Article ID: IJMET\_08\_11\_110.
  15. Kumar, V., Prasad, L., Thermal performance investigation of one and three sides concave dimple roughened solar air heaters. International Journal of Mechanical Engineering and Technology (IJMET) Volume 8, Issue 12, December 2017, pp. 31–45, Article ID: IJMET\_08\_12\_004.
  16. Kumar, V., Prasad, L., Performance Analysis of three sides concave dimple shape roughened solar air heater, J. sustain. dev. energy water environ. syst., 6(4), pp 631-648, 2018.
  17. Kumar, V., Nusselt number and friction factor correlations of three sides concave dimple roughened solar air heater, Renewable Energy 135 (2019) 355-377.
  18. Kumar, V., Prasad, L., Experimental analysis of heat transfer and friction for three sides roughened solar air heater, Annales de Chimie - Science des Matériaux, 75-107, ACSM. Volume 41 – n° 1-2/2017.
  19. Kumar, V., Prasad, L., Performance prediction of three sides hemispherical dimple roughened solar duct, Instrumentation, Mesure, Métrologie, 273-293 I2M. Volume 17 – n° 2/2018.

## Investigation of Design, Analysis and Manufacturing of GFRP composite leaf spring by VARTM process

P. Manuneethi Arasu<sup>1\*</sup> & A. Karthikeyan<sup>2</sup> & R.Venkatachalam<sup>3</sup>

<sup>1</sup>Department of Mechanical Engineering, KSR College of Engineering, Tiruchengode, Tamil Nadu.

<sup>2</sup>Department of Mechanical Engineering, Malla Reddy College of Engineering, Hyderabad, India

<sup>3</sup>Department of Automobile Engineering, KSR College of Engineering, Tiruchengode, Tamil Nadu.

---

**ABSTRACT:** *Even though many destructive methods are available to identify the quality of the material specimen but the same quality may not reflect in real time product. Analyses of specimen are cost effective compare to destruction testing method. In this paper, strength of the composite structure is analysed and the product is manufactured by advance VARTM method compare to traditional hand layup method. As the result Vacuum-Assisted Resin Transfer Moulding (VARTM) gives low void and high material bonding property compare to other composite specimen's mainly due to 52% of fibre volume fraction which is suitable for automobile structural application.*

**Keywords:**

---

### Introduction

Mild steel (MS) is the widely used material for past years due to very low cost but weight of the material is very high so that fuel economy also gradually increased, even though aluminium are used in higher end car for light weighting but the cost become higher. Current day's carbon fibre reinforced composite widely used in automobile leaf spring due to their high stiffness and high strength compare to their weight ratio. Baker and Rials [1] reported that even though carbon fibre shows twice the strength of steel compare to their weight but the cost is five time the cost of steel so that product cost also increased tremendously. Current researchers highly focusing on new type of FRP reinforced material such as E- Glass fibre for composite material which are already using in boat, transport and aerospace industry.

Developing technology results in different manufacturing technique for composite manufacturing. In this paper Vacuum-Assisted Resin Transfer Moulding (VARTM) is used instead of traditional hand layup process. HyunKim et al. [3] investigated that vacuum process of manufacturing shoes high mechanical property compare to traditional method of manufacturing. In addition to that VARTM method is cost effective and low investment cost compare to other manufacturing methods [4,5]. In this study, hand layup and VARTM method of manufactured FRP composites are compared with existing MS and AL metals for replacing option. Most of the paper are highly focusing on the optimization and design of the material but very few papers are focusing on the manufacturing method replacement technique [6- 8]. In this paper, GFRP are manufactured by hand layup and VARTM processed specimens are compares and analysed and better product are manufactured.

### 3. Manufacturing process of fibre reinforced composites

Composite material quality not only depends on materials but also depends on manufacturing technique by varying fibre volume fraction  $V_f$ . In this paper, simple traditional hand lay-up composite products are at room temperature shown in Fig.1 but recent researchers are focusing on Vacuum assist resin transfer moulding (VARTM) are widely used to achieve high  $V_f$ . For this manufacturing process primarily starts with applying PVA (Poly Vinyl Alcohol) the release agent on the surfaces of the mould. Then the fabrics were pre-impregnated with the matrix material and by hand layup method resin is applied manually. For VARTM method, polyester resin is injected inside the vacuum bag by using vacuum pump at 25Psi pressure as shown in Fig.2. In this paper Isothalic polyester resin, accelerator and catalyst are mixed at the ratio of 1:0.025:0.015 and are injected inside the product. After 1 to 2h, laminate are remove from the mould and cured at room temperature for 24 h. in this paper, All the fibre laminates were made with 10-28 plies by varying position of glass fiber static sequence. The fibre volume fraction are calculated by equation 1 and 2 and are tabulated in table 1.



**Fig 1.** Fabrication process by Hand layup,

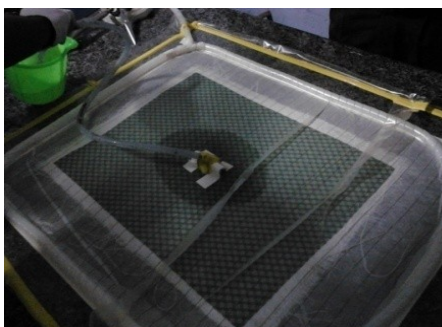


**Fig. 2.** VARTM setup with resin flow

**Fibre volume fraction**

**Equation 1:**  $V_f = (v_f/v_m)$

**Equation 2:**  $V_f + V_m = 1$

$V_f$  represent total volume fraction of fibre,  $v_f$  is volume of fibre and  $v_m$  is volume of matrix and  $V_m$  is total volume fraction of matrix the volume fraction of hand layup and VARTM and their static sequence are tabulated in Table1.

Composite material	Fibre orientation	Fibre volume fraction	Flow time (min)	Curing time (min)	Thickness
GFRP- Hand Layup	0/45/90/90/45/0	0.42	30	30	3
GFRP- VARTM	0/45/90/90/45/0	0.52	40	30	2.9

**Discussion and Analysis**

From Table 1 it shows that fibre/ polyester based composite component gives comparatively high fibre volume fraction compare to hand layup method. low cost than other composite. By the result it has been processed for design by using Pro-Engineering software and the analysis is done by Mat\_54/55 Enhanced composite in ANSYS Explicit Dynamics. Coefficients of stiffness, friction, and tensile property are considered for references by keeping the default values in the software for composite option. The design and analysis of the leaf spring as shown in figure 3 and 4.

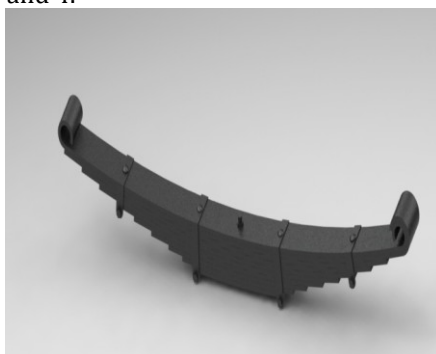


**Fig: 3:** Pro- Engineering design of leaf spring

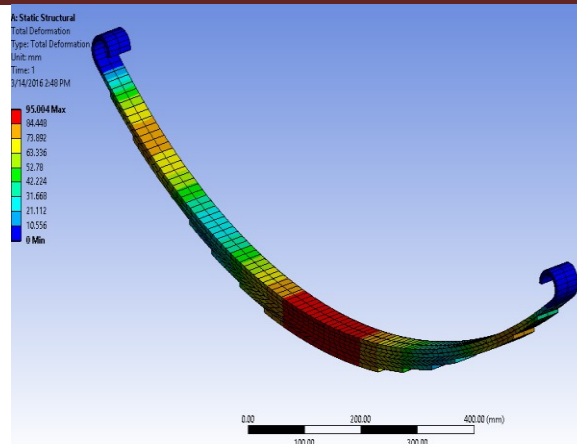


**Fig 4:** Analysis of composite leaf spring

The result shows that high stress is mainly happened in centre of the leaf spring. By this result manufacturing method can be rebuilt by applying more number of glass fibres at the middle of the leaf spring compare to other region. But when the composite is manufactured by hand layup method the void formation will form micro crack which break entire leaf spring. To avoid this issue VARTM method is highly suitable for leaf spring manufacturing

### **Composite fabrication**

By the result the composite leaf spring is manufactured by VARTM process method and the product are cured for 24 hours and the specimen are conducted for test in future research. the composite leaf spring are as shown in figure 5.



**Fig 5:** Leaf spring manufactured by VARTM process

### **Conclusion**

In this paper investigated the two different composite manufacturing process that are traditional hand layup process and VARTM process. VARTM process specimen's shows high volume fraction of 52% so the material quality will be high compare to hand layup process. From the analysis the leaf spring has very high stress formation in middle of the specimen so more glass fibre is implemented when the product is manufactured. Hand layup shows void in specimens so for leaf spring micro crack formation is high by this reason VARTM leaf spring is manufactured with high quality

### **Reference**

1. Darren A. Baker and Timothy G. Rials "Recent advances in low-cost carbon fiber manufacture from lignin" *Journal of applied polymer* vol. 130, no. 2, (2013), pp. 713-728.
2. G. Bogoeva-Gaceva , M. Avella , M. Malinconico , A. Buzarovska , A. Grozdanov , G. Gentile and M. E. Errico "Natural fiber eco-composites" vol. 28, no. 1, (2007), pp. 98-107
3. H.Ku, H.Wang, N.Pattarachaiyakooop and M.Trada "A review on the tensile properties of natural fiber reinforced polymer composites" *Composites Part B: Engineering*, vol. 42, no. 4, (2011), pp. 856-873.
4. Jong-HyunKim, Dong-JunKwon, Pyeong-SuShin, Yeong-MinBeak, Ha-SeungPark, K. LawrenceDeVries and Joung-ManPark "Interfacial properties and permeability of three patterned glass fiber/epoxy composites by VARTM" *Composites Part B: Engineering*, vol. 148, no. 1, (2018), pp. 61-67.

5. Acheson, Pavel Simacek and Suresh G.Advani "The implications of fiber compaction and saturation on fully coupled VARTM simulation" *Composites Part A: Applied Science and Manufacturing*, vol. 35, no. 2, (2004), pp. 159-169
6. Vishwanath R, I. Basil and Kuang Ting Hsiao "Effects of vacuum pressure, inlet pressure, and mold temperature on the void content, volume fraction of polyester/e-glass fiber composites manufactured with VARTM process" *Journal of composite material*, vol. 45, no. 26, (2011).
7. SalimBelouettar, CarlosKavka, BorekPatzak, HeinKoelman, Gast.Rauchs, GaetanoGiunta, AngelaMadeo, SabrinaPricl and AliDaouadji "Integration of material and process modelling in a business decision support system: Case of composelector H2020 project" *Composite Structures*, vol. 204, no. 1, (2018), pp. 778-790.
8. Gulur siddaramanna, shiva shankar and sambagam vijayarangan "mono composite leaf spring for light weight vehicle design, end joint analysis and testing" *materials science*, vol. 12, no. 3, (2006).
9. Kumar, V., Prasad, L., Experimental investigation on heat transfer and fluid flow of air flowing under three sides concave dimple roughened duct. *International Journal of Mechanical Engineering and Technology (IJMET)*, Volume 8, Issue 11, November 2017, pp. 1083–1094, Article ID: IJMET\_08\_11\_110.
10. Kumar, V., Prasad, L., Thermal performance investigation of one and three sides concave dimple roughened solar air heaters. *International Journal of Mechanical Engineering and Technology (IJMET)* Volume 8, Issue 12, December 2017, pp. 31–45, Article ID: IJMET\_08\_12\_004.
11. Kumar, V., Prasad, L., Performance Analysis of three sides concave dimple shape roughened solar air heater, *J. sustain. dev. energy water environ. syst.*, 6(4), pp 631-648, 2018.
12. Kumar, V., Nusselt number and friction factor correlations of three sides concave dimple roughened solar air heater, *Renewable Energy* 135 (2019) 355-377.
13. Kumar, V., Prasad, L., Experimental analysis of heat transfer and friction for three sides roughened solar air heater, *Annales de Chimie - Science des Matériaux*, 75-107, ACSM. Volume 41 – n° 1-2/2017.
14. Kumar, V., Prasad, L., Performance prediction of three sides hemispherical dimple roughened solar duct, *Instrumentation, Mesure, Métrologie*, 273-293 I2M. Volume 17 – n° 2/2018.

# Effect of Geometrical and Roughness Parameters on Artificially Roughened Solar Air Heater

Ahmad Kamal Hassan & Dr. Mohammad Emran Khan & Dr. M. Muzaffarul Hasan

<sup>1,3</sup>Research Scholar, Department of Mechanical Engg., Jamia Millia Islamia, New Delhi, India

<sup>2</sup>Professor, Department of Mechanical Engg. Faculty of Engg. and Tech., Jamia Millia Islamia, New Delhi, India

**ABSTRACT:** Artificial roughness employed on the absorber plate of SAHs is the most effective method to augment the rate of heat transfer to flowing fluid in the roughened duct of solar air heater. Artificial roughness provided is of various forms like ribs, dimples, baffles, wire mesh, delta winglets, etc. The objective of this paper is to analyze the various roughness geometries used on absorber plate in order to improve the heat transfer and friction characteristics. Augmentation in heat transfer for roughened SAHs is obtained by destroying laminar sub-layer in the vicinity of the absorbing surface. However, this gain is accomplished at the expense of increase in pressure drop. The main aim of this paper is to determine the optimum roughness geometry parameter at which maximum heat transfer is obtained at minimum frictional losses.

**Keywords:** Solar air heater, Artificial roughness, roughness pitch, roughness height

## 1. INTRODUCTION

Solar air heaters works on solar thermal technology in which the energy from the sun is captured by an absorbing medium and used to heat air. Solar air heating is a renewable energy heating technology used to heat or condition air for buildings or process heat applications. It is typically the most cost-effective out of all the solar technologies, especially in commercial and industrial applications, and it addresses the largest usage of building energy in heating climates, which is space heating and industrial process heating [34]. The value of heat transfer coefficient and heat capacity for air is low which reduces the heat transfer rate and thus increases the heat loss to the surroundings. A large number of researchers have used solar air heaters of different configurations to remove these drawbacks associated with solar air heaters to better serve the purpose of air heating [35]. Simple flat plate collector is the simplest and most commonly used type of collector. It is composed of one, two or three glazing over a flat plate which is backed by insulation. In flat plate collectors, the area absorbing the solar radiation is the same as the area capturing solar radiation. The collector are oriented towards the equator facing north in the southern hemisphere and facing south in the northern hemisphere [21]. Different types of artificially roughened solar collectors used are shown in Fig. 1.

### 1.1 Artificially roughened solar air heaters

In order to attain higher convective heat transfer coefficient, turbulent flow at the heat transfer surface is required. The artificial roughness has been used extensively for the enhancement of forced convective heat transfer coefficient in solar air heaters. It is found that the use of artificial roughness on heat transferring surface breaks the viscous sub-layer in the proximity of the surface. However, creating turbulence requires energy that comes from the fan or the blower. Hence, it is desirable to create the turbulence very close to the surface only where the heat transfer takes place and the core of the flow is not disturbed to avoid excessive losses. This can be achieved by using roughened surfaces on the air side. Use of artificial roughness seems to be an attractive proposition for improving the heat transfer coefficient [55]. The artificial roughness is one of the most effective methods considering heat transfer coefficient enhancement with limited frictional losses. Several investigators have used different geometries of artificial roughness on the underside of the absorber plate to study the augmentation of heat transfer with corresponding increase in the pumping power. The major thermal resistance in a solid-fluid interaction is due to the formation of a boundary layer and efforts for enhancing heat transfer have been directed towards artificially destroying or disturbing the boundary layer [56]. In order to attain higher heat transfer co-efficient, it is

desirable that the flow at the heat transferring surface is to be made turbulent. However, excessive turbulence leads to increase power requirement from the fan or blower to make the air flow through the duct. It is therefore desirable that the turbulence must be created only in the region very close to the heat transferring surface i.e. laminar sub-layer only. To minimize the friction losses, special care should be taken while selecting the dimension for the roughness geometries like height of the roughness element should be kept small in comparison with the duct dimensions. This has been achieved by active, passive or some combination of active and passive methods.

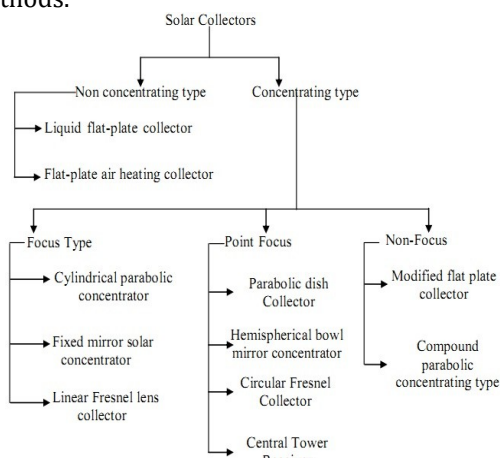


Fig. 1. Different types of solar collectors

### 1.2 Active methods

These methods require additional external energy. Some of the most commonly used active methods are mentioned below:

- (i) Mixing or scrubbing of the fluid from the heat transferring surface by mechanical means.
- (ii) Vibrating or rotating the hot surface which causes the boundary layer thickness to decrease significantly.
- (iii) Flow subjected to acoustic waves of 1 Hz to ultrasonic frequency.
- (iv) Suction of heated fluid through porous surface.

### 1.3 Passive methods

In case of the passive techniques, the direct input of external power is not required. They generally use surface or geometrical modifications to the flow channel, or incorporate an insert, material, or additional device. The artificial roughness is one of passive techniques of enhancement of heat transfer. In this technique, the surface is modified by using different types of roughness that promotes turbulence in the flow field, primary in

single phase flow and does not increase the area of heat transferring surface. These include:

- (i) Use of extended heat transfer surfaces.
- (ii) Use of swirl flow devices such as twisted tap inserts to create rotating flow.
- (iii) Turbulence promoters or roughened heating surfaces to reduce the thickness of the laminar sub-layer or to break the laminar sub-layer.

## 2. ANALYSIS OF ARTIFICIALLY ROUGHENED SURFACE

An extensive experimental study of turbulent flow of fluids in rough pipes with various degrees of relative roughness heights ( $e/D_h$ ) with a range of Reynolds number from 600 to  $10^6$  was carried out by Nikuradse [57]. The roughness was obtained by sand grains cemented to the walls of the pipes. It was found that the friction factor decreases as Reynolds number increases. Based on the law of wall similarity, a correlation for friction factor for flow over sand grain roughness was developed. His data, covering a wide range of roughness heights were correlated by the friction similarity function as given below:

$$f = 2 \left[ A + B \ln \left( V^* e / \bar{u} \right) - 2.456 \ln \left( 2e / D_h \right) \right]^{-2} \quad (1)$$

where, 'A' and 'B' are parameters depending upon the regimes of flow discussed below and ' $\bar{u}$ ' is the mean velocity. The term  $V^*$  is the friction velocity, defined mathematically as:

$$V^* = \sqrt{(\tau_o / \rho)} \quad (2)$$

where, ' $\tau_o$ ' is the wall shear stress and ' $\rho$ ' is the density of the flowing fluid.

Here, a term called Roughness Reynolds number ( $e^+$ ) is defined as given below:

$$e^+ = V^* / (e / \bar{u}) \quad (3)$$

The roughness Reynolds number ( $e^+$ ) defined in terms of  $e/D_h$ , Re, f and is expressed as follows:

$$e^+ = \text{Re} (e / D_h) \sqrt{f / 2} \quad (4)$$

Eq. (1) can be rewritten as:

$$f = 2 \left[ A + B \ln (e^+) - 2.456 \ln (2e / D_h) \right]^{-2} \quad (5)$$

The law of wall similarity was proposed by Nikuradse by correlating his experimental data for different roughened tubes is as follows:

$$U^+ = \frac{\bar{u}}{V^*} = 2.5 \ln\left(\frac{Y}{e}\right) + A$$

(6)  
 He found that a plot of parameter “A” as a function of  $\log(V^* e / \bar{u})$  is very similar to the curve for the resistance law obtained by plotting

$$\left(\frac{1}{(2/f)^{0.5}}\right) + 2 \log(2e / D_h) \text{ vs. } (V^* e / \bar{u})$$

From this the value of “A” was deduced as:

$$A = \sqrt{\frac{2}{f}} + 2.5 \ln\left(\frac{2e}{D_h}\right) + 3.75$$

(7)  
 Thus,

$$A = U^+ - 2.75 \ln\left(\frac{Y}{e}\right) = \sqrt{\frac{2}{f}} + 2.5 \ln\left(\frac{2e}{D_h}\right) + 3.75$$

(8)  
 The non-dimensional parameter “A” is named differently by different investigators as the roughness parameter by (Han et al.) [58] or momentum transfer function (Han et al.) [59] or roughness function (Lau et al.) [60] and is commonly denoted by R ( $e^+$ ). The relation for R ( $e^+$ ) is given as:

$$R(e^+) = \sqrt{\frac{2}{f}} + 2.5 \ln\left(\frac{2e}{D_h}\right) + E$$

(9)  
 where, E is geometric parameter and depends on the configuration of the duct. The value of ‘E’ was reported by Nikuradse as 3.75 for pipe.

The plot of the roughness function, R ( $e^+$ ), against roughness Reynolds number ( $e^+$ ) obtained by Nikuradse is shown in Figure. 2.1 The three flow regions shown in Figure 2.2 are explained as under:

**2.1 Hydraulically Smooth Flow ( $0 < e^+ < 5$ )**

In this flow region of low surface roughness, there is no effect of roughness on the friction factor. The values of the friction factor coincide with those for a smooth pipe for all values of relative roughness height ( $e/D_h$ ). Nikuradse [1952] correlated the measured of pressure loss data in this regime in the form of R ( $e^+$ ).

$$R(e^+) = 5.5 + 2.5 \ln(e^+)$$

(10)

**2.2 Transitionally Rough Flow ( $5 \leq e^+ \leq 70$ )**

In transition zone, the surface roughness becomes noticeable and increase in friction factor with increase in roughness Reynolds number ( $e^+$ ) can be observed. This zone reveals that the resistance factor depends on the Reynolds number and relative roughness height. The roughness height ( $e$ ) and the projection extends through the boundary layer creates vortices which produce an additional loss of energy. Increase in the roughness Reynolds number, the projections passing above the viscous sub-layer increases due to reduced viscous sub-layer thickness with increase in Reynolds number. With increase in the roughness Reynolds number the energy loss is high.

**2.3 Fully Rough Region ( $e^+ > 70$ )**

In fully rough region, the roughness Reynolds number attains a constant value and roughness function is independent of the roughness Reynolds number. Energy loss due to the vortices attains a constant value and an increase in the roughness Reynolds number no longer increases the friction factor.

Law of the wall as proposed by Nikuradse has been represented in Figure. 2.2 which depicts dimensionless velocity ( $U^+$ ) as a function of dimensionless distance ( $Y^+$ ). The different zones of the velocity profile are represented as under:

$$U^+ = Y^+, \text{ for laminar sub-layer, } 0 < Y^+ < 5 \quad (11)$$

$$U^+ = 5.0 \ln Y^+ - 3.5, \text{ for buffer zone, } 5 \leq Y^+ < 30 \quad (12)$$

$$U^+ = 2.5 \ln Y^+ + 5.5, \text{ for turbulent zone, } Y^+ > 30 \quad (13)$$

The different flow regimes velocity profile and law of wall similarity for flow under rough surface as observed by Nikuradse is shown in Figure 2.1 and 2.2 respectively.

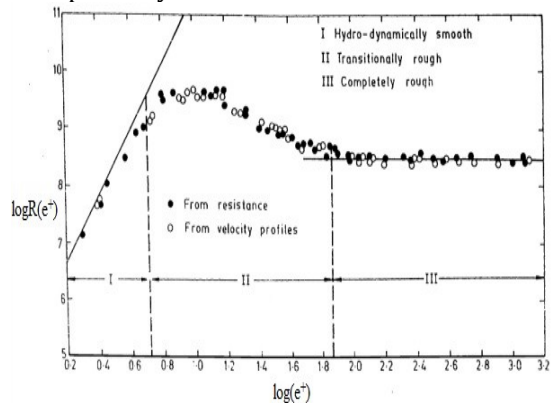


Fig. 1 Relation between roughness function R ( $e^+$ ) and roughness Reynolds number

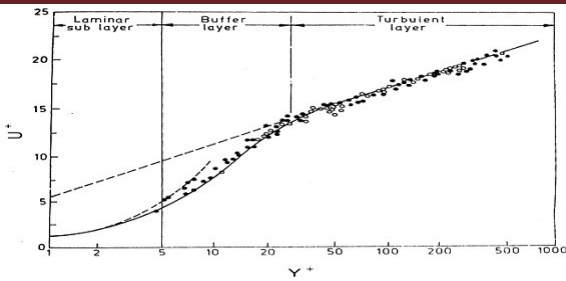


Fig. 2 Velocity profile for flow in circular smooth tubes at high Reynolds number

Fig. 2.3 shows the flow patterns downstream of a rib as the rib height and pitch are changed. Separation occurs at the rib, forming a widening free shear layer which reattaches 6-8 rib heights downstream from the separation point. For value of relative roughness pitch less than 10, the reattachment will not occur thus reducing the heat transfer. While, an increase in roughness pitch beyond 10 also results in decreasing the enhancement, Prasad and Saini [61]. Therefore there exists an optimum arrangement of pitch and height that will result in maximum heat transfer enhancement.

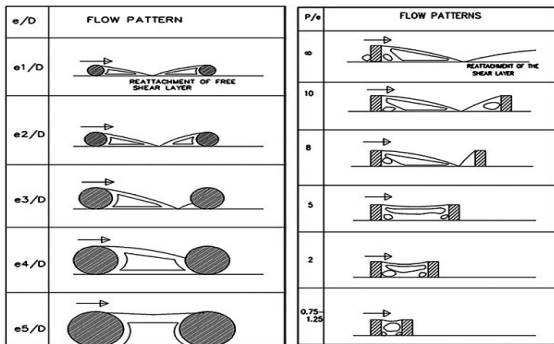


Fig. 3 Effect of rib height and pitch on flow

Prasad and Mullick [62] suggested the use of artificial roughness in the form of small diameter wires in a solar air heater to improve the thermal performance of the collector. Gupta et al. [63-64] investigated the friction factor and heat transfer characteristics of the inclined wires used as the artificial roughness as shown in Fig. 2.4. The investigated parameters are relative roughness height in the range of 0.018 to 0.052, aspect ratio in the range of 6.8 to 11.5, angle of attack varies from 40° to 90° and flow Reynolds number ranges from 3000 to 18000. They reported that angle of attack of 60° produces maximum heat transfer where as the angle of attack of 70° showed the highest friction factor.

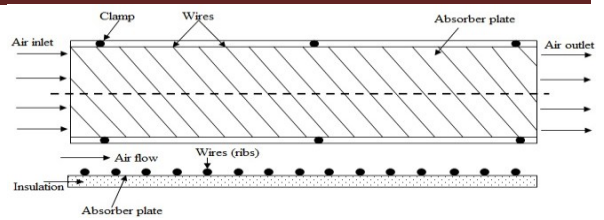


Fig. 4 Roughened absorber plate with inclined wire (Gupta et al. [1997])

Han et al. [65] investigated the effect of rib pitch to height ratio, and rib height to equivalent hydraulic diameter on friction factor and heat transfer coefficient for Reynolds number range of 7,000 to 90,000, relative roughness pitch range of 10 to 40, and relative roughness height range of 0.021 to 0.063 as shown in Fig. 2.5 (a to i). He found that the maximum values of friction factor and the Stanton number occur at a relative roughness pitch of 10. Both the average friction factor and Stanton number increased with increasing relative roughness height.

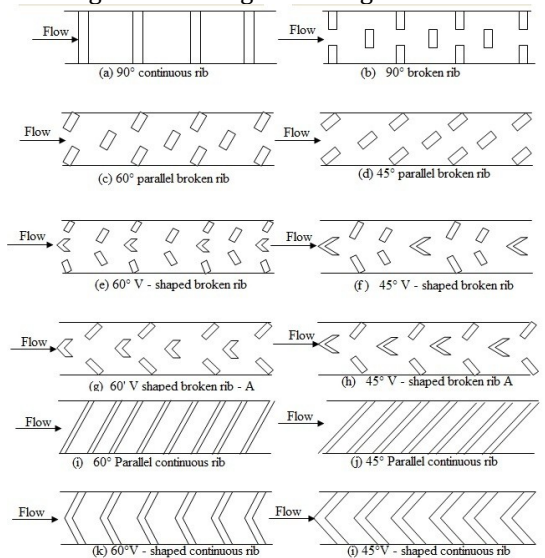


Fig. 5 Top view of rib configuration

Prasad and Saini [61] develops an empirical correlations for heat transfer coefficient and friction factor for a solar air heater duct artificially roughened by small diameter wires of various relative roughness heights ranging from 0.020 to 0.033 and relative roughness pitch varying from 10 to 20 for Reynolds numbers range between 5000 to 50,000. The results showed that the average friction factor and Nusselt number increased with increase in relative roughness height. The average Nusselt number of the roughened duct was about 2.10, 2.24 and 2.34 times than that of the smooth duct for relative roughness height of 0.020, 0.027 and 0.033 respectively. The average friction factor of the

roughened duct was about 3.08, 3.67, and 4.26 times than that of the smooth duct. The increase in the average Nusselt number and average friction factor for relative roughness pitch of 10, 15 and 20 in the roughened duct was about 2.38, 2.14, 2.01 and 4.25, 3.39. Solar energy can be used to supply energy demand in the form of thermal energy (solar thermal systems) as well as in the form of electricity (solar photovoltaic systems). The important applications of solar energy are: Water heating, Space heating and cooling, Solar cooking, Solar crop drying, Solar distillation, Solar refrigeration, Green houses, Solar power (Electric) generation, Solar furnace, Solar water pumping etc. In order to make the solar energy utilization economically viable, its efficient collection and conversion to thermal energy at the absorber surface are very essential. The most important component of solar energy utilization system is the solar collector.

### 3. PERFORMANCE OF SOLAR AIR HEATER DUCT

#### 3.1. Thermal performance

Thermal performance of SAH duct is expressed as the convective heat transport between the absorber and the working medium i.e. air (Fig. 1). The thermal efficiency of a typical SAH duct is low due to low value of convective heat transfer coefficient ( $h$ ) due to laminar sub-layer formation close to the absorber plate. The rate of useful energy gain by the air flowing through SAH duct may also be calculated by using the following equation [7]:

$$Q_u = \dot{m}C_p(T_o - T_i) = hA_p(T_{pm} - T_{fm}) \quad (14)$$

Nusselt number for a smooth duct can be obtained by Dittus-Boelter Equation [8]:

$$Nu = 0.023 Re^{0.8} Pr^{0.4} \quad (15)$$

The heat transfer coefficient ( $h$ ) can be increased by the application of artificial roughness on the air flow side of absorber plate and thereby cause increase in the thermal efficiency given by [9].

$$\eta_{th} = \frac{Q_u}{IA_c} \quad (16)$$

#### 3.2. Hydraulic performance

The air flowing through the SAH duct undergoes frictional losses and hence accounts for the extra energy in form of mechanical power that has to be supplied to the blower to circulate air properly in the duct. The hydraulic performance for the fully

developed turbulent flow can be represented by friction factor which is given by:

$$f = \frac{\Delta p_d D_h}{2\rho L v_d^2} \quad (17)$$

Further using above equations mechanical power can be computed by [10]:

$$P = \frac{\dot{m} \Delta p_d}{\rho} \quad (18)$$

A basic layout of solar flat plate collector is depicted below [11]:

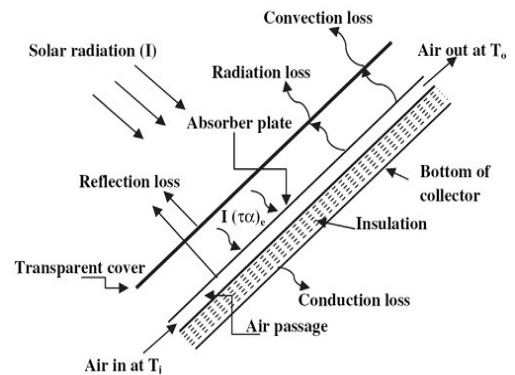


Fig. 6 Basic layout of solar flat plate collector

#### 3.3. Thermo-hydraulic performance

The overall enhancement in the performance of a roughened SAH duct can be determined by considering thermal and hydraulic characteristics simultaneously in contrast to the SAH with smooth duct. A thermohydraulic performance parameter given by [7] is used to compare the roughened and smooth surfaces in terms of Nusselt number and friction factor ratios. Therefore, thermohydraulic performance of a SAH is determined by [12]:

$$\eta_{thp} = \frac{(Nu / Nu_s)}{(f / f_s)^{1/3}} \quad (19)$$

### 4. CONCEPT OF ARTIFICIAL ROUGHNESS

In conventional flat plate SAH's the laminar sub layer has to be disturbed for enhancing the heat transfer by inducing turbulence adjacent to the absorber plate surface. This can be effectively done by the employment of artificial ribs on the air flow side of the absorber. However, the use of artificial roughness may result in high pressure loss due to friction and hence more power requirements for pumping of fluid [13-16]. For the

investigation of the effect of artificial roughness elements, SAH is usually modeled as rectangular channel with one wall comprising ribs on the air flow side while other three walls are kept smooth. The provision of roughness has extended to three walls instead of one wall as used by most of the researchers [17-18].

The key geometrical factors used to characterize the geometry of artificial roughness includes the rib height, rib pitch, inclination, rib cross-section etc. and flow parameter namely Reynolds number. The influence of these parameters on thermal and hydraulic performance of SAH duct is discussed below:

#### 4.1. Effect of rib height ( $e$ ).

The viscous sub layer breaks due to presence of ribs which creates local wall turbulence and enhances the rate of heat transfer. If the ribs project beyond the viscous sub-layer thickness, this will increase the turbulence and heat transfer rate, consequently there will be high friction losses. Prasad & Saini reported that the optimum thermo hydraulic performance will be achieved where roughness height is slightly higher than the transition sub-layer thickness [19].

#### 4.2. Effect of rib pitch ( $p$ ).

The air flow pattern in the inter-rib region is affected with the change in the rib pitch. Reattachment occurs only if the rib elements are separated properly. For effective use of the ribs, the flow should separate and reattach in the inter-rib space; and then again separate. It may be noted that the flow reattachment followed with attached flow is not desirable as it results in re-formation of the laminar sub-layer in the attached length. The pitch of the roughness elements is expressed in non-dimensional form as ratio of pitch to height ratio ( $p/e$ ) [20].

#### 4.3 Effect of rib cross section.

The flow pattern close to the roughened absorber plate also depends on the cross-section of the rib whereas the re-attachment profile also varies among different cross-sections. Circular cross-section has low heat transfer properties as compared to square, triangular or trapezoidal cross-Section [20]. Whereas the pressure drop is lower in circular rib as there is more streamlined flow in contrast to square or triangular ribs which has sharp edges. Other cross-sections like chamfered, L-shaped, trapezoidal etc. were also investigated but generally circular or square cross-section rib is preferred as these provide better thermohydraulic performance and are easily available avoiding machining complications.

#### 4.4. Effect of inclination.

Apart from the effect of rib height and pitch, the parameter that has been found to be most influential is the angle of attack ( $\alpha$ ) of the flow with respect to the rib position. It is to be pointed out that whereas the two fluid vortices upstream and downstream of a transverse rib are essentially stagnant relative to the mainstream flow which raises the local fluid temperature in the vortices and wall temperatures near the rib resulting in low heat transfer. The vortices move along the rib to subsequently join the main stream i.e. the fluid enters at the leading end of the rib and comes out near the trailing end as shown in Fig. 2.41. The moving vortices bring the cooler channel fluid in contact with leading end, raising heat transfer rate while at the trailing end heat transfer is relatively low [21].

#### 4.5 Effect of Reynolds number ( $Re$ ).

The influence of Reynolds number on the flow pattern is illustrated in Fig. 6. At lower Reynolds number, the reattachment distance is relatively large and the flow reattached length is thereby small. The region before the reattachment point comprises low heat transfer rate and is maximum at the reattachment point and drops along the reattached length. So, it can be evidently seen from the Fig. 6 that the reattachment profile changes with the increasing Reynolds number and reattachment distance keeps on decreasing. The flow re-circulation zone behind the rib decreases in the region before the reattachment point. Thus, the low heat transfer region behind the rib is reduced which results in enhancement in overall heat transfer.

Table 1 shows the various roughness geometries and the range of operating and flow parameters used by researchers.

## 5. DISCUSSIONS

Applications of solar energy, most prominent renewable source available, are likely to expand in near future. The conversion of solar energy involves heat exchange process which makes it essential to design more efficient heat exchanger. The artificial rib roughness method is generally preferable for enhancement of heat transfer by breaking laminar sub-layer near the absorbing surface. Numerous rib roughness geometries employed in solar air heaters have been investigated till now (Table 1). Started with the simplest transverse ribs [11,12], the other forms like inclined ribs [18], v-shaped ribs [21] and arc shaped ribs [30-32] were investigated experimentally. Arc shaped ribs offered lower friction penalty as compared to others. Apart from these geometries, investigation has also been

made on other geometries like broken transverse ribs [15], inclined ribs with gap [19], dimple shaped elements [42], expanded metal mesh [20], chamfered ribs [13], s-shaped ribs [35], broken arc ribs [32], w-shaped ribs [37,38], discrete v-down ribs [27,28]. All these investigations reported the thermal performance enhancement with some increase in pumping requirements. Prasad and Mullick [11] initiated the concept of artificial roughness using small diameter wires on the absorber surface on one wall aimed to enrich the thermal performance of the SAH. The wire diameter of 0.84mm,  $e/D = 0.019$  and  $P/e = 12.7$  were the parameters used in this study. The outcome of this study reported the enhancement in the efficiency from 62% to 72% at  $Re = 40,000$ . Prasad and Saini [12] explored the influence of small wires applied as roughness elements on the absorber plate to study their effect on thermal and friction factor performance in fully developed region. The study was carried out for  $P/e = 10, 15$  and  $20$ ,  $e/D = 0.020, 0.027$  and  $0.033$  and Reynolds number ranging  $5000-50,000$ . They concluded that with the increase in  $e/D$ , both Nusselt number and friction factor increase, but the rate of heat transfer enhancement diminishes while the rate of friction factor increase was almost even. The application of rib roughness reported the enhancement of the Nusselt number and friction factor as 2.38 and 4.35 times over a smooth duct. The optimum values of  $P/e$  and  $e/D$  were found to be 10 and 0.027 respectively. The study also suggests that rib height must be equal to laminar sub-layer thickness.

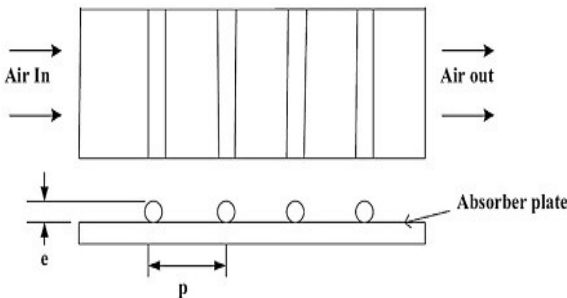


Fig. 7 Transverse rib roughness used by Prasad and Saini

Karwa et al. [13] carried out an experimental study to determine the influence of chamfered ribs applied in transverse direction as artificial roughness for predicting the thermo-hydraulic performance of the roughened SAH duct

Table 1: Different roughness geometry used by different researchers

Authors	Roughness element	Reynolds No.	Non-dimensional parameters and values		
			$p/e$	$e/D_h$	Other parameters
Prasad and Saini	Transverse ribs	5000	10-20	0.02-0.033	
Saini and Saini	Expanded metal mesh	1900-13,000	15	0.012-0.039	$W/H=1, 1, L/e=25-71.87$
Gupta et al.	Small diameter transverse rib	4000-18,000	10	0.02-0.05	$\alpha = 60^\circ$
Karwa et al.	Machined Ribs	3000-20,000	4.5-8.5	0.014-0.032	$d/w=0.167-0.5, W/H=5.87$
Bhagoria et al.	Wedge shaped ribs	3000-18000	10	0.015-0.033	$\Phi=8-15$
Sahu and Bhagoria	Broken integral transverse ribs	3000-12,000	6.67-20	0.0338	$W/H=8$
Jaurker et al.	Rib and groove combination		4.5-10	0.018-0.0363	$g/p=0.3-0.7$
Karmare and Tikekar	Wire ribs-grid shape	3600-17,000	12.5-36	0.035-0.044	$\alpha = 60^\circ, l/s=1.72-1$
Varun et al.	Inclined and transverse wire	2000-14,000	10	0.030	
Saini and Verma.	Dimple protrusions	2000-17,000	8-12	0.018-0.037	
Layek et al.	Chamfered compound rib	3000-21000	10	0.03	$\alpha = 5^\circ-30^\circ, g/p=0.5$
Karmare et al.	Metal grit rib	17,000-40,000	15-17.5	0.035-0.044	$l/s=1.72$
Kumar et al.	Discretized W-shape rib	3000-15,000	10	0.0168-0.0338	$\alpha = 30^\circ-75^\circ, W/H = 8$

Bopche and Tandle	U shaped rib	3800-18,000	6.67-57.14	0.0186-0.03986	$\alpha = 90^\circ$
Hans et al.	Multiple V shape rib	2000-20000	6-12	0.019-0.043	$\alpha = 30^\circ-75^\circ$ W/w = 1-10
Lanjewar et al.	W shaped rib	2300-14,000	10	0.018-0.03375	$\alpha = 30^\circ-75^\circ$ W/H = 8
Lanjewar et al.	W shape with different orientations	2300-14,000	10	0.03375	$\alpha = 30^\circ-75^\circ$ W/H = 8
Sethi et al.	Dimple shape in arc shape	3600-18,000	10-12	0.021-0.036	
Kumar et al.	Multi V shape with gap rib	2000-20,000	6-12	0.022-0.043	$\alpha = 30^\circ-75^\circ$ W/w = 1-10
Yadav et al.	Circular protrusion in arc shape	3600-18,100	12-24	0.015-0.03	$\alpha = 45^\circ-75^\circ$ W/H = 11

(Fig. 8). The parameters range were taken as duct aspect ratio from 4.8 to 12,  $e/D$  from 0.0141 to 0.0328,  $P/e$  from 4.5 to 8.5, Rib chamfer angle from  $-15^\circ$  to  $18^\circ$  and  $Re$  from 3000 to 20,000. The augmentation in Stanton number and friction factor was highest at the chamfer angle of  $15^\circ$  and was of the order of 2 and 3 times respectively.

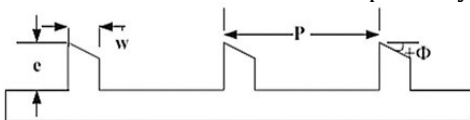


Fig. 8. Chamfered Rib roughness geometry by Karwa et al.

Verma and Prasad [14] experimentally evaluated the outcome of the application of transverse wires in SAH duct in actual outdoor conditions and studied its optimum performance. The investigation range of Reynolds number from 5000 to 20,000,  $P/e$  from 10 to 40, roughness Reynolds number from 8 to 42 and  $e/D$  from 0.01 to 0.03 were investigated. Maximum thermo-hydraulic performance of 71% has been obtained at roughness Reynolds number of 24.

Sahu and Bhagoria [15] investigated the thermal performance of roughened SAH duct using broken transverse rib arrangement as shown in Fig. 9. Investigation was done for  $Re$  from 3000 to 12,000,  $P/e$  from 10 to 30 and  $e/D = 0.0338$ .

Nusselt number attained its maximum value at  $P/e$  of 10 and after that it decreases. The heat transfer coefficient of the roughened absorber plate was 1.25-1.4 times higher than the smooth plate.

Yadav and Bhagoria [17] performed a 2-D investigation on equilateral triangular section transverse rib (Fig. 10) by using CFD code ANSYS FLUENT 12.1. Parameters ranges were taken as  $P/e$  from 7.14 to 35.71,  $e/D$  from 0.021 to 0.042 and Reynolds number from 3800 to 18,000. Maximum improvement in Nusselt number of 3 times and friction factor enhancement of 3.56 times over the smooth duct was obtained corresponding to the  $p/e$  of 7.14, Reynolds number of 15,000 and  $e/D$  of 0.042.

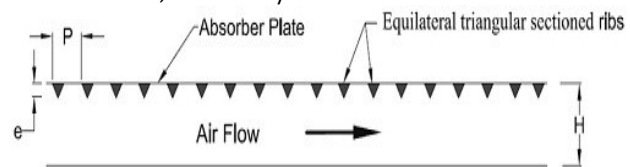


Fig. 9. Equilateral triangular sectioned ribs used by Yadav and Bhagoria

Gupta et al. [18] presented a study on the application of the inclined circular transverse ribs (Fig. 11.) as artificial roughness to investigate the fluid flow characteristics of a roughened SAH duct. The study encompassed the range of Reynolds number from 3000 to 18,000, duct aspect ratio from 6.8 to 11.5,  $e/D$  from 0.018 to 0.052, and fixed  $P/e = 10$ . The study reported the maximum augmentation in Nusselt number and friction factor as 1.8 and 2.7 times of smooth duct at  $\alpha = 60^\circ$  and  $e/D = 0.033$ . Further the best thermohydraulic performance of roughened duct was obtained at  $e/D = 0.033$  corresponding to  $Re = 14,000$ . The authors also studied the performance of Stanton number in transitional flow and fully developed flow. Stanton number was seen to be increasing up to  $Re = 12,000$  and thereafter it decreased.

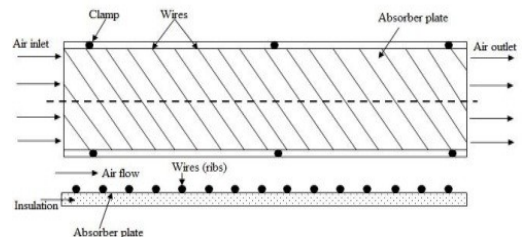


Fig. 10. Roughened absorber plate with inclined wire used by Gupta et al.

Aharwal et al. [19] performed experimentation on a SAH duct with square cross-section inclined ribs with a gap (Fig. 12). The duct has a  $W/H = 5.84$ ,  $P/e = 10$ ,  $e/D = 0.0377$ , and  $\alpha = 60^\circ$ . The gap width ( $g/e$ ),

gap position ( $d/w$ ) and Reynolds number was varied in the range of 0.5–2, 0.1667–0.667 and 3000–18,000 respectively. The maximum augmentation of Nusselt number and friction factor over the smooth duct was 2.59 and 2.87 times respectively. The thermo-hydraulic performance parameter was obtained for the  $g/e = 1.0$  and  $d/w = 0.25$ .

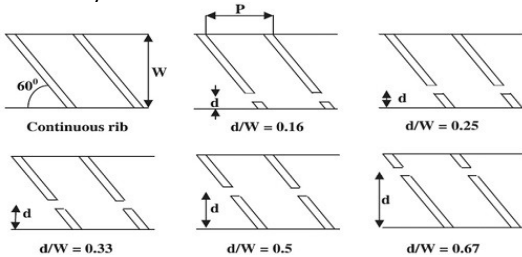


Fig. 11. Inclined transverse ribs with gap used by Aharwal et al.

Saini and Saini [20] determined the performance of a SAH duct roughened with expanded metal mesh geometry (Fig. 13). As an alternative to transverse ribs, authors suggested the use of commercially available metal matrix which can be easy to fix on absorber plate. They investigated the effect of roughness parameters viz.  $L/e$  from 25 to 71.87,  $S/e$  from 15.62 to 46.87,  $e/D$  from 0.12 to 0.039 and  $Re$  from 1900 to 13,000. The highest Nusselt number was attained at  $L/e = 46.87$  and  $S/e = 25$  at  $\alpha = 61.9^\circ$ . The friction factor was registered maximum corresponding to  $\alpha = 72^\circ$  for  $L/e = 71.87$ . The maximum enhancement in heat transfer coefficient was 4 and 5 times respectively over the smooth duct.

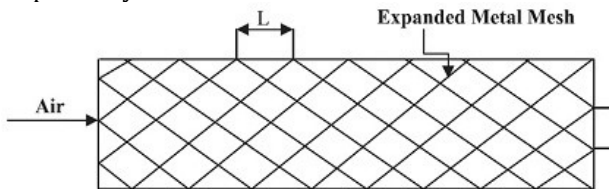


Fig. 12. Expanded metal mesh geometry used by Saini and Saini

Hans et al. [22] presented a study of multiple V-ribs roughness (Fig. 15) considering the parameters as Reynolds number from 2000 to 20,000,  $e/D$  from 0.019 to 0.043,  $P/e$  from 6 to 12,  $\alpha$  from  $30^\circ$  to  $75^\circ$  and  $W/w$  from 1 to 10. The investigation revealed that with the increase in  $W/w$ , heat transfer attains maximum value at  $W/w$  of 6 and is lower on both sides. Nusselt number and friction factor enhancement was attained as 6 and 5 times that of smooth duct.

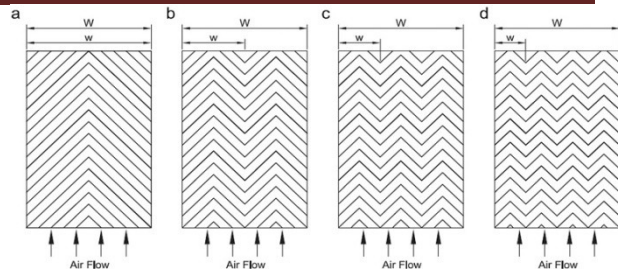


Fig. 13. Multiple V-rib roughness used by Hans et al.

Saini and Saini [30] evaluated the performance of SAH duct roughened with arc shaped wires as rib elements as shown in Fig. 20. Heat transfer coefficient and friction factor were studied for Reynolds number from 2000 to 17,000,  $e/D$  from 0.0213 to 0.0422 and  $\alpha/90$  from 0.3333 to 0.6666. The application of arc shaped roughness geometry resulted in the maximum Nusselt number improvement of 3.80 and friction factor boost of 1.75 times corresponding to parameters as  $\alpha/90 = 0.3333$  and  $e/D = 0.0422$ .

Yadav et al. [31] employed arc shaped dimple roughness (Fig. 21) for parameter range as  $Re$  from 3600 to 18,100,  $P/e$  from 12 to 24,  $e/D$  from 0.015 to 0.03 and  $\alpha$  from  $45^\circ$  to  $75^\circ$ . They found that the maximum boost in Nusselt number and friction factor was 2.89 and 2.93 times respectively for the  $e/D = 0.03$ ,  $P/e = 12$ , and  $\alpha = 60^\circ$ .

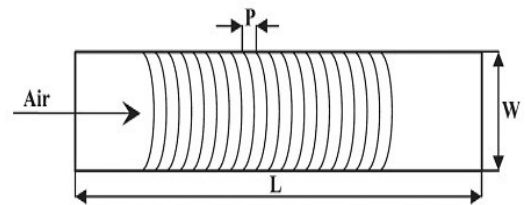


Fig. 14. Arc shaped roughness used by Saini and Saini

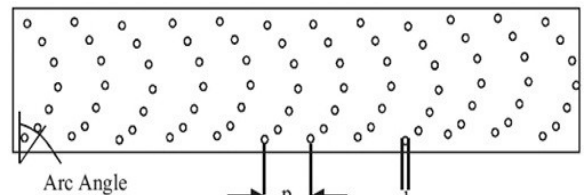


Fig. 15. Arc shaped dimple roughness used by Yadav et al.

Pandey et al. [35] carried out study on multiple arc ribs with gap (Fig. 24) used as roughness in SAH absorber plate. The investigation considered rib parameters as  $P/e$  from 4 to 16,  $e/D$  from 0.016 to 0.044,  $W/w$  from 1 to 7,  $\alpha$  from  $30^\circ$  to  $75^\circ$ ,  $d/x$  from 0.25 to 0.85 and  $g/e$  from 0.5 to 2.0.

The maximum increment found in heat transfer was 5.85 and pumping power increment was 4.96 times at  $P/e=8$ ,  $W/w=5$ ,  $g/e=1$ ,  $d/x=0.65$  and  $e/D=0.044$  at  $Re=21,000$ .

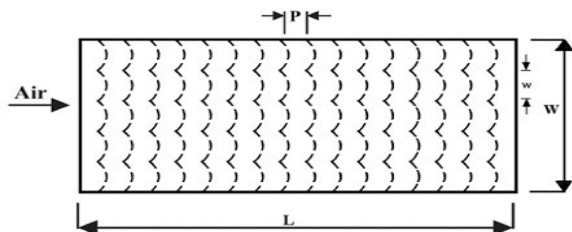


Fig. 16. Multiple broken arc rib used by Pandey et al.

Kumar et al. [36] studied the influence of the arc shape wire ribs arranged in ‘S’ shape on the heat transfer and friction factor characteristics of solar air heater as shown in Fig. 25. The experimentation considered  $Re$  from 2400 to 20,000 and rib parameters as  $P/e$  from 4 to 16,  $e/D$  from 0.022 to 0.054,  $W/w$  from 1 to 4 and  $\alpha$  from  $30^\circ$  to  $75^\circ$ . Experimentation shows the maximum enhancement in Nusselt number and friction factor of 4.64 and 2.71 times over the smooth duct at  $W/w=3$ ,  $P/e=8$  and  $\alpha=60^\circ$ .

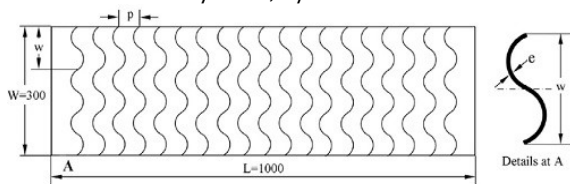


Fig. 17. S- shaped ribs arrangement used by Kumar et al.

Thakur et al. [33] performed 2-D computational simulations of SAH duct roughened with hyperbolic ribs as shown in Fig. 33. The investigation encompassed the parameter range as  $e=0.5-2\text{mm}$  and  $P=10-20\text{mm}$ . The optimum thermohydraulic performance of the order of 2.16 was achieved for  $e=1\text{mm}$  and  $P=10\text{mm}$  at  $Re=6000$ . Performance of hyperbolic rib was compared with rectangular, triangular and semicircular rib geometries and was found to be best among all up to  $Re=10,000$ .

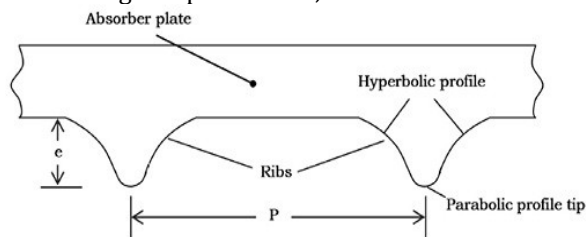


Fig. 18. Hyperbolic rib geometry used by Thakur et al.

## 6. CONCLUSIONS

Applications of solar energy, most prominent renewable source available, are likely to expand in near future. The conversion of solar energy involves heat exchange process which makes it essential to design more efficient heat exchanger. The artificial rib roughness method is generally preferable for enhancement of heat transfer by breaking laminar sub-layer near the absorbing surface. Numerous rib roughness geometries employed in solar air heaters have been investigated till now (Table 1). Started with the simplest transverse ribs [11,12], the other forms like inclined ribs [18], v-shaped ribs [21] and arc shaped ribs [30–32] were investigated experimentally. Arc shaped ribs offered lower friction penalty as compared to others. Apart from these geometries, investigation has also been made on other geometries like broken transverse ribs [15], inclined ribs with gap [19], dimple shaped elements [42], expanded metal mesh [20], chamfered ribs [13], s-shaped ribs [35], broken arc ribs [32], w-shaped ribs [37,38], discrete v-down ribs [27,28]. All these investigations reported the thermal performance enhancement with some increase in pumping requirements. Creation of gap in the rib have shown improved performance over the continuous rib. Further the ribs in multiples such as multiple v-ribs [22], multiple arc ribs [33–35] have resulted in remarkable enhancement in heat transfer coefficient. Economically, the wire fixation method is the most feasible method among other methods; as it does not involve any machining operations and is simple. But it may be a tedious task in large scale production. Therefore, a suitable geometry of artificial roughness must be selected which is not only easily available, but should also be simple to fix on the absorber plate and also offers substantial augmentation in heat transfer coefficient at low pumping power penalty. For better understanding and optimizing of the heat transfer and flow mechanism, attempt have been made to study the effect of various influencing roughness and flow parameters on the thermal and hydraulic performance of solar air heater through the flow visualization. Attempt have been made towards understanding the in-depth flow phenomena related to the heat transfer process. This may be beneficial for the further improvement in this field as the specific locations in the solar air heater can be targeted for improvement in the future.

In this article, a comprehensive review of different rib roughness geometries reported for

conventional solar air heater has been conducted. Effect of various shapes and size of artificial ribs are reported in literature. Substantial heat transfer enhancement has been achieved using ribs of various design accompanied by some pressure losses. Heat transfer and friction characteristics and the correlations reported by the investigators have been summarized. Computational Fluid Dynamics (CFD) analysis has been carried out to visualize and study the effect of various geometrical and flow parameters for the optimum design of solar air heater. Based on the comprehensive literature survey, the following conclusions have been drawn:

1. Application of artificial rib roughness improves the thermo-hydraulic performance of conventional solar air heater. The rib roughness improves the thermal performance due to breaking of laminar sub layer. The friction factor penalty is small as the flow is disturbed in the laminar sub layer only.
2. The thermal and fluid flow characteristics of numerous rib roughness geometries have been investigated for various roughness parameters viz., relative rib pitch, relative rib height, relative rib width, attack angle etc. For most rib geometries, the thermo-hydraulically optimum values of relative rib pitch ( $P/e$ ), relative rib height ( $e/D$ ), relative rib width ( $W/w$ ) and attack angle ( $\alpha$ ) have been reported to be 10, 0.043, 6 and  $60^\circ$  respectively.
3. The thermohydraulic performance of inclined ribs is better than transverse ribs due to creation of secondary flow cells. The V-shape ribs further improve the thermo-hydraulic performance due to more number of secondary flow cells. The arrangement of ribs in multiples, such as multiple V, multiple arc, further enhance the thermohydraulic performance.
4. A gap in rib of the order of rib height substantially improves the thermohydraulic performance of roughened duct. The improvement in Nusselt number in the range of 1.1–1.3 times and pumping power penalty of 1–1.4 times were reported due to introduction of gap.
5. The maximum augmentation in heat transfer and pumping power was 6.74 and 6.37 times for multiple V-ribs with gap, which is followed by multiple V-ribs

with augmentation of 6 and 5 times respectively.

6. From thermo-hydraulic considerations, the arc arrangement has lesser pressure losses than V arrangement, which may be due to curved secondary flow and consequently results in better thermohydraulic performance. Therefore, multiple arc ribs and multiple arc ribs with gap are recommended for better overall thermo-hydraulic performance.

#### FUTURE SCOPE

For future developments, experimental approach used for the analysis of rib roughened SAH duct should be accompanied with Computational Fluid Dynamics (CFD) method which provides fast, non-expensive and in-depth analysis for the optimization of SAH's. More studies can be conducted using sun tracking systems and reflectors. Double pass solar air heaters should be investigated using artificial rib roughness as very few studies are reported in this aspect. Compound heat transfer enhancement techniques may be employed for further improvement in thermal performance of SAH's. Combined with the surface enhancement methods, other reported methods in literature viz. selective coatings, arched or corrugated absorber plate, fluid additive methods can be tested in future for combined heat transfer enhancement in solar air heaters.

#### REFERENCES

1. Duffie, J. A., Beckman, W. A., Solar Engineering Thermal Processes, John Wiley, New York, 1991.
2. Gawande VB, Dhoble AS, Zodpe DB, Chamoli S. A review of CFD methodology used in literature for predicting thermo-hydraulic performance of a roughened solar air heater. *Renew Sustain Energy Rev* 2016; 54:550–605.
3. Sharma SK, Kalamkar VR. Computational fluid dynamics approach in thermo-hydraulic analysis of flow in ducts with rib roughened walls – a review. *Renew Sustain Energy Rev* 2016; 55:756–88.
4. Alam T, Kim M-H. A critical review on artificial roughness provided in rectangular solar air heater duct. *Renew Sustain Energy Rev* 2017; 69:387–400.
5. Yadav, A.S., Bhagoria, J.L., A CFD based thermo-hydraulic performance analysis of an artificially roughened solar air heater having equilateral triangular sectioned rib roughness on the absorber plate. *International Journal of Heat and Mass Transfer* 70 (2014) 1016–1039.
6. Tiwari, R.C., Kumar, A., Gupta, S.K., Sootha, G.D., Thermal performance of flat-plate solar collectors manufactured in India. *Energy*

- Conversion and Management, Volume 31, Issue 4, 1991: 309-313.
7. Sethi, M., Varun, Thakur, N.S., Correlations for solar air heater duct with dimpled shape roughness elements on absorber plate. *Solar Energy*. 2012; 86: 2852–61.
  8. Karwa, R., Chitoshiya, G., Performance study of solar air heater having v-down discrete ribs on absorber plate. *Energy* 2013; 55:939–55.
  9. Patil, A.K., Saini, J.S. and Kumar, K., 2011, Effect of Gap Position in Broken V rib Roughness Combined with Staggered Rib on Thermohydraulic Performance of Solar Air Heater, *Green*, Vol. 1 (4), 329–338.
  10. Singh, I., Singh S., A review of artificial roughness geometries employed in solar air heaters, *Renewable and Sustainable Energy Reviews* 92 (2018) 405–425.
  11. Prasad, B.N., Saini, J.S., "Thermohydraulic optimization of artificially roughened solar air heaters", *Proc. NSC, Solar Energy Society of India, Hyderabad (India)*, 1988.
  12. Verma S.K., Prasad B.N., Investigation for the optimal thermohydraulic performance of artificially roughened solar air heaters, *Renewable Energy*, Vol. 20, 9-36, 2000.
  13. Bopche, S.B., Tandale, M.S., Experimental investigations on heat transfer and friction characteristics of a turbulators roughened solar air heater, *International Journal of Heat and Mass Transfer*, Vol. 52 (11-12), 2834-2848, 2009.
  14. Lanjewar, A., Bhagoria, J.L., Sarviya, R.M., Heat transfer and friction in solar air heater duct with W-shaped rib roughness on absorber plate, *Energy*, Vol. 36, 4531-4541, 2011.
  15. Kumar, A., Saini, RP, Saini, JS., 2012, Experimental investigation on heat transfer and fluid flow characteristics of air flow in a rectangular duct with Multi V-shaped rib with gap roughness on the heated plate, *Solar Energy*, Vol. 86, pp. 1733–49.
  16. Singh, I., Singh, S., A review of artificial roughness geometries employed in solar air heaters, *Renewable and Sustainable Energy Reviews* 92 (2018) 405–425
  17. Kumar, V., Prasad, L., Experimental investigation on heat transfer and fluid flow of air flowing under three sides concave dimple roughened duct. *International Journal of Mechanical Engineering and Technology (IJMET)*, Volume 8, Issue 11, November 2017, pp. 1083–1094, Article ID: IJMET\_08\_11\_110.
  18. Kumar, V., Prasad, L., Thermal performance investigation of one and three sides concave dimple roughened solar air heaters. *International Journal of Mechanical Engineering and Technology (IJMET)* Volume 8, Issue 12, December 2017, pp. 31–45, Article ID: IJMET\_08\_12\_004.
  19. Prasad B.N., Saini J.S., Effect of artificial roughness on heat transfer and friction factor in a solar air heater, *Solar Energy*, Vol. 41(6), 555–560, 1988.
  20. Hans VS, Saini RP, Saini JS. Performance of artificially roughened solar air heaters-a review. *Renew Sustain Energy Rev* 2009; 13: 1854–69.
  21. Alam, T., Kim, M.H., A critical review on artificial roughness provided in rectangular solar air heater duct. *Renewable and Sustainable Energy Reviews* 69 (2017) 387–400.
  22. Taslim, M.E., Li T., Krecher D.M, Experimental heat transfer and friction in channels roughened with angled, V-shaped and discrete ribs on two opposite walls, *Transactions of ASME Journal of Turbo-machinery*, Vol. 118, 20-28, 1996.
  23. Gupta, D., Solanki, S. C., Saini, J. S., 1997, Thermohydraulic performance of solar air heaters with roughened absorber plates. *Solar Energy*, Vol. 61, pp. 33–42.
  24. Gupta, D., Solanki, S.C. and Saini, J.S., 1993, Heat and fluid flow in rectangular solar air heater ducts having transverse rib roughness on absorber plate, *Solar Energy*, Vol. 51, pp. 31-37.
  25. Han, J.C., Zhang, Y.M. and Lee, C.P., 1991, Augmented heat transfer in square channels with parallel, crossed, and V shaped angled ribs, *Trans. ASME Journal of Heat Transfer*, Vol. 113, pp. 590-596.
  26. Saini, S.K. and Saini, R.P., 2008, Development of correlations for Nusselts number and friction factor for solar air heater with roughened duct having arc-shaped wire as artificial roughness, *Solar Energy*, Vol. 82, pp. 1118-1130.
  27. Tanda, C., 2004, Heat transfer in rectangular channels with transverse and V-shaped broken ribs, *International Journal of Heat and Mass Transfer*, Vol. 47, pp. 229-243.
  28. Aharwal, K.R., Gandhi, B.K., Saini, J.S., 2008, Experimental investigation on heat transfer enhancement due to a gap in an inclined continuous rib arrangement in a rectangular duct of solar air heater, *Renewable Energy*, Vol. 33, pp. 585-596.
  29. Saini, R.P., Verma, J., 2008, Heat transfer and friction correlations for a duct having dimple shape artificial roughness for solar air heater, *Energy*, Vol. 33, pp. 1277-1287.
  30. Prasad K., Mullick S.C., Heat transfer characteristics of a solar air heater used for drying purposes, *Applied Energy*, Vol. 13, 83-93, 1985.
  31. Prasad B.N., Saini J.S., Effect of artificial roughness on heat transfer and friction factor in a solar air heater, *Solar Energy*, Vol. 41(6), 555–560, 1988.
  32. Karwa, R., Solanki, S. C. and Saini, J. S., Heat transfer coefficient and friction factor correlation for the transitional flow regime in

- rib-roughened rectangular duct, *Int. Journal of Heat and Mass Transfer*, Vol. 42, pp. 1597-1615, 1999.
33. Sahu MM, Bhagoria JL. Augmentation of heat transfer coefficient by using 90° broken transverse ribs on absorber plate of solar air heater. *Renew Energy* 2005; 30:2057–73.
  34. Yadav, A.S., Bhagoria, J.L., A CFD based thermo-hydraulic performance analysis of an artificially roughened solar air heater having equilateral triangular sectioned rib roughness on the absorber plate. *International Journal of Heat and Mass Transfer* 70 (2014) 1016–1039.
  35. Hans VS, Saini RP, Saini JS. Heat transfer and friction factor correlations for a solar air heater duct roughened artificially with multiple v-ribs. *Sol Energy* 2010; 84:898–911.
  36. Yadav S, Kaushal M, Varun, Siddhartha. Nusselt number and friction factor correlations for solar air heater duct having protrusions as roughness elements on absorber plate. *Exp Therm Fluid Sci* 2013; 44:34–41.
  37. Pandey NK, Bajpai VK, Varun. Experimental investigation of heat transfer augmentation using multiple arcs with gap on absorber plate of solar air heater. *Sol Energy* 2016; 134:314–26.
  38. Kumar, V., Prasad, L., Experimental investigation on heat transfer and fluid flow of air flowing under three sides concave dimple roughened duct. *International Journal of Mechanical Engineering and Technology (IJMET)*, Volume 8, Issue 11, November 2017, pp. 1083–1094, Article ID: IJMET\_08\_11\_110.
  39. Kumar, V., Prasad, L., Thermal performance investigation of one and three sides concave dimple roughened solar air heaters. *International Journal of Mechanical Engineering and Technology (IJMET)* Volume 8, Issue 12, December 2017, pp. 31–45, Article ID: IJMET\_08\_12\_004.
  40. Kumar, V., Prasad, L., Performance Analysis of Three-sides Concave Dimple Shape Roughened Solar Air Heater, *J. sustain. dev. energy water environ. syst.*, 6(4), pp 631–648, 2018.
  41. Kumar, V., Nusselt number and friction factor correlations of three sides concave dimple roughened solar air heater, *Renewable Energy* 135, (2019), 355-377.
  42. Kumar, V., Prasad, L., Experimental analysis of heat transfer and friction for three sides roughened solar air heater, *Annales de Chimie - Science des Matériaux*, 75-107, ACSM. Volume 41 – n° 1-2/2017.
  43. Kumar, V., Prasad, L., Performance prediction of three sides hemispherical dimple roughened solar duct, *Instrumentation, Mesure, Métrologie*, 273-293 I2M. Volume 17 – n° 2/2018.